Nonperturbative Quantum Dynamics on the de Sitter Geometry

and

Diffeomorphism-invariant Observables

Dissertation

zur Erlangung des akademischen Grades
doctor rerum naturalium
(Dr. rer. nat.)

JG|U

vorgelegt

dem Fachbereich für Physik, Mathematik und Informatik
der Johannes Gutenberg-Universität Mainz

Renata Ferrero
geboren am 21. August 1995 in Rom, Italien

Mainz, den 26. April 2023

Renata Ferrero
Institut für Physik (THEP)
Johannes Gutenberg-Universität Mainz
Staudingerweg 7
55128 Mainz

D77 / Dissertation der Johannes Gutenberg-Universität Mainz

ABSTRACT. In Quantum Gravity functional integral approaches attempt to give meaning and nonperturbatively evaluate the sum over histories represented by the gravitational path integral. A variant of this approach proceeds indirectly by re-constructing the sought-for functional integral in the continuum limit from the solution of an appropriate Functional Renormalization Group (FRG) equation. This line of thought is at the core of the Asymptotic Safety scenario, in which the UV completion of Quantum Gravity is realized via a non-trivial fixed point of the FRG flow.

In the first Part of this thesis, we investigate nonperturbative and geometrical aspects of quantum dynamics in de Sitter spacetime, an Einstein space of Lorentzian signature which may be used to model the observed accelerated expansion of the Universe. In this part, three novel lines of research are established. Firstly, we examine the geometrical and dynamical contents of the Renormalization Group (RG) flow in a broader context, such as in connection with a new variant of the AdS/CFT correspondence. Thereby Quantum Einstein Gravity is explored by solving its scale-dependent effective field equations and embedding the family of emerging 4-dimensional de Sitter spacetimes into a single 5-dimensional manifold. Remarkably, we find that there exist only two possible such 5D spacetimes, namely AdS_5 and dS_5. Secondly, we investigate the consequences of nonperturbative, Background Independent quantization of gravity on the geometry of de Sitter by means of a newly introduced spectral flow method. A first important result reveals the dynamical thinning out of the effective degrees of freedom in the UV, which is at the heart of Asymptotic Safety. Furthermore, evidence is found for a dynamical fragmentation of the effective quantum spacetime in disjoint, sub-horizon size patches. Thirdly, we construct scattering amplitudes in curved spacetime, reflecting the geometric properties of de Sitter spacetime in a novel and nontrivial way. In a fully covariant formalism, we compute the scattering potential of a graviton-mediated scattering process involving two very massive scalars at tree level. On Hubble-size scales the potential yields a repulsive force; this can be attributed to the expansion of the de Sitter Universe. Beyond the horizon, the potential vanishes identically.

The second Part of this thesis is devoted to a detailed discussion, and actual computation of physical observables in Quantum Gravity. We analyze the special symmetries of gravity, and we perform the first computations of scale-dependent relational observables in asymptotically safe gravity. First, inspired by the modeling of a physical coordinate scaffolding, we construct general effective dynamics for diffeomorphisms of spacetime. Second, we develop the formalism towards the use of running relational observables within Asymptotic Safety: we introduce RG-dependent couplings associated to the observables, and in the spirit of the composite operator formalism, we derive a new flow equation for these observables. We investigate their scale dependence by computing their critical exponents, carrying out the analysis both in the standard and in the minimal essential renormalization scheme. The (small) quantum corrections encoded in the critical exponents represent universal quantities which can be compared to results from other approaches to Quantum Gravity.

Contents

x

List of Acronyms

ADM Arnowitt–Deser–Misner

AdS anti-de Sitter

AS Asymptotic Safety

BRST Becchi–Rouet–Stora–Tyutin

CDT Causal Dynamical Triangulations

CFT Conformal Field Theory

CMBR Cosmic Microwave Background Radiation

COM Cutoff mode

DM Dark Matter

dRGT de Rham–Gabadadze–Tolley

dS de Sitter

EAA Effective Average Action

EDT Euclidean Dynamical Triangulations

EFT Effective Field Theory

EH Einstein–Hilbert

EMT energy-momentum tensor

EOM equation of motion

ERGE Exact Renormalization Group Equation

ERG Exact Renormalization Group

FLRW Friedmann–Lemaître–Robertson–Walker

FRGE Functional Renormalization Group Equation

FRG Functional Renormalization Group

GEAA Gravitational Effective Average Action

GFP Gaussian fixed point

GR General Relativity

IR infrared

LQG Loop Quantum Gravity

MOND Modified Newtonian Dynamics

NGFP non-Gaussian fixed point

NLSM Nonlinear Sigma Model

QCD Quantum Chromodynamics

QED Quantum Electrodynamics

QEG Quantum Einstein Gravity

QFT Quantum Field Theory

QuadG Quadratic Gravity

RG Renormalization Group

SM Standard Model

UV ultraviolet

CHAPTER 1

Introduction

1.1. The need for Quantum Gravity

The first step towards a quantum theory of gravity can be dated back to 1899, when Max Planck introduced a set of "scales", the Planck mass, time, and length. However, Planck himself was unaware of what he had started: during this period, the theories of Quantum Field Theory (QFT) and General Relativity (GR) had not yet been developed. At Planck's time the search for Quantum Gravity had not yet started and it was not foreseeable what a challenge it would represent for future physicists [1–3].

A few months after Albert Einstein published his seminal papers on the theory of General Relativity [4–7], he noted that [8]:

> Gleichwohl müßten die Atome zufolge der inneratomischen Elektronenbewegung nicht nur elektromagnetische, sondern auch Gravitationsenergie ausstrahlen, wenn auch in winzigem Betrage. Da dies in Wahrheit in der Natur nicht zutreffen dürfte, so scheint es, daß die Quantentheorie nicht nur die Maxwellsche Elektrodynamik, sondern auch die neue Gravitationstheorie wird modifizieren müssen.

Einstein was questioning the possibility of a unification of Planck's quantum theory with his newly developed theory of Gravitation.

Some years later three attempts at a theory of Quantum Gravity had been initiated: Rosenfeld [9], Pauli and Fierz [10] aimed to a formulation of Quantum Gravity in analogy with quantum electrodynamics; Bronstein [11, 12] and Solomon [13] aimed at a full quantization of the (non)linear gravitational equations and the generalization to the case of an absent background metric; van Dantzig [14] treated GR as an intrinsic macroscopic theory, e.g. as an emergent theory arising as a limit of an underlying theory.

Generalizing Feynman's covariant quantization of quantum electrodynamics to non-Abelian gauge theories was the program outlined by DeWitt [15–17]. He made a number of important progresses: he introduced the background field method in order to represent the effective action as a gauge invariant functional of the fields and to connect the counterterms and all possible ultraviolet (UV) divergences of scattering amplitudes at a fixed loop expansion: he included ghost fields to compensate the effect of unphysical

polarizations in loop corrections; and he developed invariant regularization techniques, as the dimensional regularization, for instance.

As for the gravitational field, 't Hooft and Veltman [18] were the first to apply these techniques, in 1974: they showed that, within quantum General Relativity, pure gravity has a finite S-matrix at one loop order, but as soon as matter, i.e., scalar fields, are added, higher curvature counterterms are needed. In 1985 Goroff and Sagnotti [19–21] showed that in pure gravity higher curvature counterterms are required at two loop order. This was the final result proving that quantum General Relativity is not renormalizable as a perturbative quantum field theory, and that it cannot be treated along the lines of Yang–Mills theory at the quantum level.

A theory of Quantum Gravity is expected to be instrumental in an improved understanding of Nature, from the biggest to the smallest structures in the Universe. For example, we can describe the motion of planets and stars and the structure of spacetime with the classical theory of gravity. However, if we zoom into smaller and smaller scales and eventually come across single atoms, General Relativity no longer applies. Along the journey into the microscopic, starting from that point on we need quantum physics. Considering the electromagnetic interaction, in order to account for the structure of atoms and the electromagnetic field itself, also the latter has to be treated according to the laws of quantum mechanics and it turns out to be composed of elementary entities called photons.

Moreover, since Maxwell's theory is Lorentz invariant, a proper description of photons and their interactions implied the development of special relativistic quantum mechanics: this is how Quantum Electrodynamics (QED) started. It was the first example of a Quantum Field Theory, and led to surprisingly precise predictions. Later on it was understood that the weak and nuclear interactions could be described by (quantum) Yang–Mills theories (Quantum Chromodynamics (QCD)), which are non-Abelian generalizations of QED.

So now we have at hand two types of extremely successful theories, which are based on widely different conceptual foundations and mathematical tools. They describe phenomena occurring at widely different scales: sub-atomic distances for QFT, and macroscopic to cosmic distances for GR. As long as we stay within the respective regimes, these theories are perfectly adequate and in accord with the present experiments and observations. However, it seems unlikely that the status quo is the ultimate theory. Rather, one would expect a more uniform description of all interactions to be possible, which likely means that gravity also has to be subjected to the laws of quantum mechanics.

After a relativistic quantum theory had been introduced, the task would have been to develop the next part of the theory, that is, to unify quantum theory, special relativity and the theory of gravitation into a single consistent framework. The yet to be developed theory of Quantum Gravity was supposed to provide a satisfactory description of the structure of spacetime even near the Planck scale, where general relativistic and quantum effects are believed to be equally relevant. This was the motivation for the search for a theory of Quantum Gravity [22–24].

(1) How might one approach then the construction of a theory of Quantum Gravity? One possible path consists in starting from General Relativity, which has to characterize the classical limit of every quantum theory of gravity. In fact, while Newtonian gravity has been tested experimentally to sub-millimeter length scales [25–28], General Relativity fails near spacetime singularities, where no physics can be described. For example, GR does not tell what happens at the center of a black hole or at the beginning of our universe, the cosmological singularity called Big Bang. In extreme astrophysical or cosmological situations the notion of a classical, smooth spacetime breaks down. Hence General Relativity is an incomplete theory, and so the hope is that we shall be able to understand and resolve the related open problems by analyzing in detail its failures.

Furthermore, in modern cosmology, based on General Relativity as an effective field theory on large scales, current cosmological data suggest, the existence of a dark sector in addition to the Standard Model, which should constitute 95% of the total content of the Universe. In the general relativistic picture of the world the spacetime-versus-matter distinction breaks down to some extent. In General Relativity, the metric, i.e., the gravitational field, has acquired properties that have been characteristic of matter from Descartes to Feynman: it satisfies differential equations, it carries energy and momentum, and it can act on, and be acted upon by other forms of energy and momentum. Therefore, in order to explain Dark Matter (DM), modifications of gravity could be a possible avenue if they give rise to an appropriately modified gravitational field equation, that mimics DM in the Universe.

(2) From a more theoretical stance, there are some fundamental features of classical General Relativity which we want its quantum version to inherit. One such feature is Background Independence [29–32]: no particular spacetime (such as Minkowski space) should be given a privileged status. Rather, the geometry of spacetime should be determined dynamically.

In fact, among all fundamental forces in Nature, gravity is exceptional: it is encoded in the very geometry of spacetime. Therefore, this geometry presumably should make its appearance at a fundamental level of the sought-for quantum theory.

Moreover, from a quantum field theoretic point of view there are further fundamental features that a quantum theory of gravity should have, such as unitarity and renormalizability. Formulating the quantum theory of gravity in an ordinary QFT framework could be attempted by studying the quantum excitations around a given classical background metric. However, this results in a perturbatively non-renormalizable theory [18, 19] with questionable predictive power at high energy, or none at all.

The simultaneous disentanglement of all these issues of different nature and origin is very arduous. For instance, the direct perturbative approaches which dominated the field in the first years ignored the Background Independent nature of gravity. They assumed that the spacetime can be considered as a continuous, flat, smooth, and fixed background geometry, and the quantum gravitational field can be treated as a quantum field on this background. In this setting, using standard perturbation techniques, one finds that a scattering amplitude calculated from the Einstein–Hilbert action diverges: the resulting Quantum Gravity turned out to be non-renormalizable.

(3) Moreover, these problems appear hard also because there are very few observations to guide us [33]. Thanks to experimental improvements and astronomical observations, more and more extreme scale regimes can be reached both on the quantum and the macroscopic side. De facto, Newtonian gravity has been tested experimentally down to sub-millimeter scales [25]: GR makes successful predictions on large scales, from the very largest cosmic scales (10^{26} m) down to the scale of the solar system (10^{10} m). Furthermore, on scales of the order of kilometers, quantum effects have to be taken into account in the description of the physics of neutron stars [34]. On the other side, subatomic collider experiments at the LHC observe quantum effects on scales from around 10^{-20} m up to 1 m in molecular physics experiments [35, 36]. In experimental astroparticle physics we have already observed particles with energies only six orders of magnitude away from the Planck scale of about 10^{19} GeV, or $(10^{-35}$ m$)^{-1}$ [37].

However, it may be possible to circumvent the problem of the enormous separation of scales: there are also indirect experimental tests of Quantum Gravity. Fortunately, the cosmos provides another playground to test gravity, for it contains many objects that combine heavy and small properties and thus involve large curvature deformation of spacetime. Furthermore, the gravitational interaction is in a sense isolated from the other interactions, which are smeared out on cosmological scales. For instance, supernovae observations or lensing effects due to massive black holes are good candidates to study the effect of strong spacetime deformations.

A standard example are the imprints of Quantum Gravity that could be traced thanks to the highly precise measurements of the Cosmic Microwave Background Radiation (CMBR) [38, 39]: the CMBR photons in the observable Universe left over from

the Big Bang have a total entropy of about 10^{90} bits. In a discrete model for Quantum Gravity this entropy can be derived by evaluating the information content carried by each physical constituent [40]. As a further example, through the detection of gravitational waves we may find answers about the field content of the classical (effective) theory, including tensor modes [41].

Further indirect experimental signs can be obtained from the computation of scattering amplitudes. Treating gravity as an Effective Field Theory (EFT), scattering processes will give rise to contributions of different nature, both classical and quantum [42]. Scattering amplitudes in flat spacetime have been applied to understand diverse aspects of gravity. A classic result is the construction of the Newtonian potential from the scattering amplitude in the tree-level Born approximation. Furthermore, the most exciting recent application is to calculate new quantities of interest to the gravitational-wave community [43].

In the following section we review the currently available approaches towards Quantum Gravity.

1.2. THE PANORAMA

Each approach to Quantum Gravity starts from different assumptions, privileging one of the main requirements for a well-defined theory, and then attempting to comply with all remaining aspects. In order to quantize the gravitational field one, has to design something new. For instance, if one starts from a perturbative framework keeping renormalizability, then one has to increase the number of symmetries. On the other hand, when starting from a nonperturbative standpoint, instead, one may have to establish a new mathematical toolbox which has the potential of being compatible with Background Independence [44].

In order to cure the UV divergences of gravity, new gravitational interactions can be taken into account, which might become relevant only at high energies. Examples often involve new symmetry principles, for example, conformal symmetry. Another option is to couple gravity to specific matter content, which can represent a finite or an infinite reservoir of particles or quantum states.
A consistent perturbative approach to Quantum Gravity that tries to unify all interactions is perturbative *String Theory*. This approach introduces new symmetries such as supersymmetry by adding an infinite tower of massive particles, which amounts to requiring extra dimensions. This would provide the required ultraviolet completion. In

this picture, gravity is not quantized directly, but emerges from the theory via interactions of closed strings at low energies.

In [45] Maldacena conjectured that string theory on an anti-de Sitter (AdS) background can be described by a Conformal Field Theory (CFT) on the boundary of the AdS space. This is a duality conjecture, and its most popular application is realized on an AdS$^5 \times \mathbb{S}^5$ background with an $N = 4$ Super-Yang—Mills theory on the boundary. Furthermore, the AdS/CFT correspondence can be considered as a concrete realization of the holographic principle.

Another class of approaches towards Quantum Gravity can be divided into various main subclasses following different guiding principles. We present them with examples of concrete realizations of these principles.

(1) Other fundamental variables. Some theories question whether the metric is the fundamental field to be quantized. This leads to various formulations of gravity based on different fundamental variables. For example *Canonical Quantum General Relativity* or *Loop Quantum Gravity (LQG)* [44, 46, 47] introduces new variables, holonomies and fluxes for directly dealing with gravitational interactions. It is based on a nonperturbative formulation that proposes the existence of a minimal length scale in configuration space. The standard formulation is based on canonical quantization of General Relativity theory in four spacetime dimensions. LQG is manifestly Background Independent. It focuses on an inherent notion of quantum discreteness of spacetime which is derived rather than postulated. Among its successes is a certain UV finiteness result and a promising path integral formulation (spin foams).

(2) Nonperturbative renormalizability. Gravity is perturbatively non-renormalizable, but there is evidence that it should be nonperturbatively renormalizable.[1] Accordingly, the formulation of the theory should be nonperturbative from the beginning. Concrete realizations require the existence of an ultraviolet non-Gaussian fixed point (NGFP) characterized by a finite number of coupling constants that determine all other coefficients appearing along the renormalization group trajectory.

Asymptotic Safety [49–51], in metric gravity also known as Quantum Einstein Gravity (QEG), requires the existence of an ultraviolet fixed point. The most commonly employed tool to prove the existence of such a fixed point is the FRG. In the case of QEG, the FRG takes the metric as the carrier field of the gravitational degrees of freedom, and the pertinent effective action functionals are required to depend on the metric in a diffeomorphism-invariant way.

This method it is the subject of the present thesis, and more details will be provided in later chapters.

---

[1]In a paper entitled "Renormalizing the Non-renormalizable" Gawedzki and Kupiainen used a $1/N$-expansion to prove the non-perturbative renormalizability of the Gross–Neveu model in three dimensions [48].

(3) Spacetime discreteness [52, 53]. It can be assumed that the gravitational metric, and hence its underlying spacetime, is not a continuum. Instead, spacetime can be considered as discrete (lattice gravity), which introduces a cutoff of the order of the Planck length in the theory (for instance, discrete *Regge calculus* [54]). The discrete nature of spacetime is expected to cure the UV divergences.

Euclidean Dynamical Triangulations (EDT) or its Lorentzian counterpart, *Causal Dynamical Triangulations (CDT)* [55–57] are such discrete approaches to gravity. In its usual formulation, CDT assumes GR with a positive cosmological constant as the bare action in the path integral. Its dynamical variables are a set of piecewise flat manifolds and a collection of gluing rules that constrain configuration space in the path integral. The UV finiteness relies on the possibility of finding an ultraviolet critical point and a continuum limit.

Another (discrete) example are *Causal sets* [58, 59]. In this approach one postulates that at the most fundamental level, spacetime is discrete, with the spacetime continuum replaced by locally finite causal set of spacetime points, equipped with a proto-causality ordering. The discreteness is encoded in the local finiteness.

(4) New formulations of Quantum Field Theory. There are debates whether new formulations of QFT or gauge theory exist (for instance, axiomatic QFT, algebraic QFT, or non-geometric formulations) that will more easily accommodate dynamical and arbitrary background geometries [60].

Non-commutative geometry [61] generalizes the notion of Riemannian geometry to non-commutative geometry in terms of a non-commutative algebra, a Dirac operator and a Hilbert space; gravity and matter emerge from it using the algebra as an input.

(5) Manifest canonical covariance. The covariant canonical approaches try to combine the advantages of manifest covariance on one side and a well-defined quantization procedure on the other. Among these approaches there are the *covariant phase space methods* [62], *multisymplectic ansätze* [63] or the *history bracket formulation* [64].

Remarks: It has to be stressed that among all these frameworks there exist attempts to implement and/or derive modifications of General Relativity at low energies. Examples include *Higher derivative gravity* [65, 66] and similar modifications of classical gravity. These modifications have to be relevant within bounds set by observations, as General Relativity appears to be a correct description in the infrared (IR).

At this stage another remark is in order: in some of the presented approaches, for computational ease the models have been built in Euclidean signature. In some cases, it is assumed that performing an analytical continuation should reproduce the Lorentzian results; for some other approach, a Lorentzian setting is required from the beginning.

Generally, *Lorentzian signature* and the associated causal properties represent one of the main pillars for a quantum theory of gravity. In this thesis we will perform the first investigations in the field in a curved maximally symmetric Lorentzian geometry, such as de Sitter (dS) spacetime.

In the next section, we are going to characterize the approach adopted in this thesis by discussing the three key features of Quantum Gravity, which we will prioritize, namely Background Independence, diffeomorphism invariance, and nonperturbative renormalizability.

1.3. Background Independence, diffeomorphism invariance and nonperturbative renormalizability

(1) Background Independence. Conceptually, the most severe difficulty one encounters when dealing with a quantum theory of gravity, one which is not shared by any conventional matter field theory, is the requirement of Background Independence [29, 31, 47, 49]. In [24] A. Ashtekar asserted:

> The new strategy is to free oneself of the background spacetime that seemed indispensable for formulating and addressing physical questions; the goal is to lift this anchor and learn to sail the open seas.

At this stage it is important to distinguish between the principle of "Background Independence", with capital letters, and the "background independence". The latter, written with small letters, refers more simply to the independence of some physical quantity with respect to the background field. Instead, the principle of Background Independence requires that *none of the theory's ingredients, predictions and assumptions should depend on any given fixed metric. On the contrary physical metrics are self-consistently resulting from the dynamics of the Quantum Gravity.*

In perturbative GR one writes the quantum metric operator as a sum consisting of a background piece and a perturbation piece around it, obtaining a graviton QFT on a fixed (usually flat) background. Subsequently, perturbation theory breaks Background Independence at every finite order. Such attempts end up in a mathematical disaster: a non-renormalizable theory [18–20] with questionable predictive power [67].[2]

In principle, one can restore Background Independence by summing up the entire perturbation series. However, this turns out to be very arduous task.

---

[2]Various authors have argued in the EFT framework that even theories with an infinite number of relevant parameters can be predictive [42, 68, 69].

Moreover, perturbation theory is not always a good approximation in a non-empty neighborhood of a given expansion point. For an illustration, consider the example in [70]: if one starts with a free particle and adds a perturbation potential of the harmonic oscillator form $\omega^2 q^2$, the exact energy levels of the system are well known to be discrete. By treating the system perturbatively, starting from the free particle, it would be extremely hard to track the discrete spectrum displayed by the "nonperturbatively" quantized harmonic oscillator.

The modern approaches towards Quantum Gravity have incorporated the desideratum of Background Independence in two essentially different ways [24, 44, 71]:

(1) *Approaches which literally do not employ a gravitational background in any way.* Here one tries to define the theory, and work out its implications, without ever employing a background metric or a similar non-dynamical structure. This is the path taken in LQG and the discrete approaches to Quantum Gravity, for instance. However, this path seems very hard, if not impossible, to realize it in a continuum field theory.

(2) *Approaches which self-consistently fix a gravitational background by invoking the fundamental dynamical laws.* One takes advantage of an arbitrary classical background metric at the intermediate steps of the quantization but verifies at the end that no physical prediction depends on which metric was chosen. This background field method is at the heart of the continuum-based gravitational average action approach, which we shall employ in our investigation of Asymptotic Safety.

In this thesis, we will follow the second avenue, the dynamical determination of a self-consistent background.

(2) Diffeomorphism invariance. Gravity is a gauge theory and transforms covariantly under gauge transformations realized by spacetime diffeomorphisms. It is expected, hence, that in Quantum Gravity as well all interactions must transform under this common symmetry group, the 4-dimensional diffeomorphism group. This property renders the definition of local observables particularly striking. However, de facto, we are able to perform measurements of local fields, and along this thesis, we will show how to construct a model for diffeomorphism-invariant observables.

(3) Nonperturbative formulation. In this thesis we adopt a nonperturbative formulation, namely in two respects: first, no expansion in powers of the carrier fields (e.g., metric fluctuations $h_{\mu\nu}$) has to be performed, second, no expansion in small couplings is invoked. As we shall discuss, Asymptotic Safety is very likely to render this theory nonperturbatively renormalizable then.

Ultimately, we advocate an approach to Quantum Gravity that takes over the following successes of classical General Relativity:

(1) The carrier of the physical degrees of freedom is the metric field $g_{\mu\nu}$.
(2) The theory is diffeomorphism-invariant.
(3) The theory complies with the principle of Background Independence.

In other words, the natural language of Quantum Gravity turns out to be diffeomorphism-invariant and nonperturbative, keeping Background Independence as a guiding principle at every stage of the construction of the theory.

1.4. STRUCTURE OF THIS THESIS

This thesis is divided into three main parts.

(1) Each part begins with an introductory survey, in which the main techniques employed and results are presented. We embed the respective research area into the broader Quantum Gravity arena and display the bibliographical state of the art.

Thereafter, in the opening of the single sections, we report an executive summary about the content of the specific investigation, including relevant technical details.

The main sections are composed of the author's original publications, with the exception of the first, mostly introductory part.

Finally, the last chapter of each part, in case this part includes new research results, represents a summarizing chapter and contains a discussion on the results, including them into a broader research context.

The last chapter of this thesis represents a global summary and an overall outlook. We will relate the investigations performed in the thesis to the questions raised in the Introduction and present an overview of the progress made in each Part.

The last Part is devoted to a number of Appendices.

(2) The contents of the various parts can be briefly outlined as follows:

Part I of this thesis gives a comprehensive introduction of the Asymptotic Safety Program. In this approach to Quantum Gravity, the notion of renormalization is defined via the Functional Renormalization Group Equation (FRGE), which is constructed in Chapter 3. The regularized, at all scales well-defined path integral for Quantum Gravity is related to a solution to this equation. We will mainly focus on the RG flow of QEG, focusing on the single-metric "Einstein–Hilbert truncation". We will discuss its solutions on Euclidean and Lorentzian self-consistent backgrounds. Finally, in Chapter 4 the new developments within the FRG framework are outlined.

Part II is based on the author's publications [72–76] (from now on referred to as [RF1], [RF2], [RF3], [RF4], [RF5]), and analyzes the nonperturbative aspects of quantum gravitational phenomena on a dS geometry using different techniques.

In Chapter 7 (**Project (II.A)**) and Chapter 8 (**Project (II.B)**) we construct the scale-dependent effective dS spacetimes implied by the FRG in 4-dimensional Quantum Einstein Gravity.

In **Project (II.A)** we propose a new "geometrization" of the RG trajectories, embedding the family of emerging 4-dimensional spacetimes into a single 5-dimensional manifold, which thus encodes the complete information about all scales. The investigation is performed in both Euclidean and Lorentzian signature; in the latter case the 5D picture of the resulting picture is interpreted as a novel kind of "AdS/CFT correspondence".

Project (II.B) is devoted to the scale-dependent effective geometry of the de Sitter solution. We employ a novel approach whose essential ingredient is a modified spectral flow of the metric dependent d'Alembertian. This allows us to identify the scale-dependent field modes that represent the degrees of freedom that define the effective field theory at the respective scale.

In Chapter 9 (**Project (II.C)**) we study how the quantum properties of dS spacetime might be uncovered through the computation of scattering amplitudes on this spacetime. We introduce a new technique to compute the gravity-mediated scattering of two massive scalar particles in dS spacetime.

Part III deals with the problem of defining diffeomorphism-invariant observables in Quantum Gravity. Because of this very special symmetry of gravity, observables may be defined "relationally". This Part is based on the author's publications [77, 78] (from now referred to as [RF6] and [RF7]).

In Chapter 12 (**Project (III.A)**) we construct a new model for the dynamics of diffeomorphisms, describing relational observables and cosmological solutions. In Chapter 13 (**Project (III.B)**), we compute the RG flow of relational observables in asymptotically safe gravity, deriving the equation for the flow of the relational effective action.

Finally, **Part IV** contains the Appendices. In Appendix A, Appendix B, Appendix C, and Appendix D we establish the basic mathematical background needed for the calculations performed in the FRG approach to Quantum Gravity.

In Appendix E we summarize the main properties of maximally symmetric spacetimes, especially of dS space. This collection of results is particularly relevant for **Part II**; it also contains a number of new results.

Appendix F comprises the intermediate steps in the computation of the propagator in a constantly curved spacetime.

Appendix G discusses the properties of the dynamical diffeomorphisms (Chapter 12) and compares them with different models.

Finally, Appendix H contains the details of the computation of the flow of the relational observables from Chapter 13.

1.5. THE AUTHOR'S CONTRIBUTION

Most of the new results presented in this thesis are based on the author's research publications [RF1]-[RF7]. The results in the author's publication [79] ([RF8]) have not been included in this thesis.

At the beginning of each chapter, it will be stated whether the chapter contains new research results and if so where they are taken from. In particular, the author of this thesis has contributed to the publications as follows:

[RF1] R. Ferrero and M. Reuter. "Towards a Geometrization of Renormalization Group Histories in Asymptotic Safety". In: *Universe* 7.5 (2021), p. 125. arXiv: 2103.15709 [hep-th].

and

[RF2] R. Ferrero and M. Reuter. "On the possibility of a novel (A)dS/CFT relationship emerging in Asymptotic Safety". In: *JHEP* 12 (2022), p. 118. arXiv: 2205.12030 [hep-th].

These two publications introduce a novel procedure for the geometrization of RG trajectories. We analyze the options for a geometrization in a Euclidean and a Lorentzian setting. One of the main results of these papers is that the picture of a certain "(A)dS/CFT correspondence" emerges from the RG flow, thanks to its Asymptotic Safety. The framework has been proposed by M. Reuter; he also made the first steps towards the first illustrative realizations. The investigation about the possible geometrizations and the analyses about the global geometric structure were performed by the author. Thereby, she discovered several surprising connections, such as the global geometric properties related to the specific RG trajectory, and the realization of the novel (A)dS/CFT correspondence. The crucial numerical test reported in Figure 7.1 and Figure 7.2 was performed by the author (by means of the computer algebra system `Mathematica`).

[RF3] R. Ferrero and M. Reuter. "The spectral geometry of de Sitter space in asymptotic safety". In: *JHEP* 08 (2022), p. 040. arXiv: 2203.08003 [hep-th].

This paper continues a novel research line within Asymptotic Safety established by C. Pagani and M. Reuter [80, 81] briefly before the author started her PhD project. This new approach exploits the spectral properties of the scale-dependent kinetic operators appearing in Asymptotic Safety in the case of Euclidean signature.

In this paper we generalized the spectral analysis to Lorentzian spacetimes, which involvees a number of essentially new aspects. Concretely we applied the analysis to the dS spacetimes. A main result of this paper is the thinning out of degrees of freedom in the UV regime. The other main result is the emergent picture of the dS universe, consisting of a collection of 3-dimensional coherent patches, which can be individually described by the effective action occurring along the RG flow. This investigation was performed by the author, gaining expertise on the representation theory of non-compact Lie groups. The author made essential use of the little known, non-standard properties of the special functions associated to such representations. All conclusions presented in the paper were drawn in joint discussions.

[RF4] R. Ferrero and C. Ripken. "De Sitter scattering amplitudes in the Born approximation". In: *SciPost Phys.* 13 (2022), p. 106. arXiv: 2112.03766 [hep-th].

and

[RF5] R. Ferrero and C. Ripken. "Quadratic gravity potentials in de Sitter spacetime from Feynman diagrams". In: *JHEP* 08 (2023), p. 199. arXiv: 2212.08052 [hep-th].

These publications introduce a new framework for the computation of scattering amplitudes in dS spacetime. The method itself had been initiated by C. Ripken. He also made the first step towards the evaluation of the propagator in dS background, sharing with the author his expertise in the usage of the tensor manipulation package xAct for Mathematica. The author proposed the evaluation of the amplitude in an adiabatic expansion. She performed the necessary tensor manipulations and numerical evaluation of the scattering potential in parallel with C. Ripken. The extension towards higher derivative gravity and its implications was obtained in joint discussions.

[RF6] R. Ferrero and R. Percacci. "Dynamical diffeomorphisms". In: *Class. Quant. Grav.* 38.11 (2021), p. 115011. arXiv: 2012.04507 [gr-qc].

This paper arose from the continuation of work that had started already during the author's Master thesis with Prof. R. Percacci. The model for dynamical diffeomorphisms was proposed by R. Percacci. The author studied its dynamical and kinematical properties, connecting the model to relational observables and cosmological models.

[RF7] A. Baldazzi, K. Falls, and R. Ferrero. "Relational observables in asymptotically safe gravity". In: *Annals Phys.* 440 (2022), p. 168822. arXiv: 2112. 02118 [hep-th].

This paper represents the natural attempt to combine the knowledge of the author about relational observables and about the essential FRG formalism within an Asymptotic Safety scenario. The main link was obtained in joint discussion with K. Falls. The numerical evaluations were performed (via `Mathematica`) together with A. Baldazzi.

Part I

Asymptotic Safety: Functional Renormalization Group and Quantum Gravity

CHAPTER 2

Introduction and Survey of Part I

The preparatory **Part I** is devoted to the construction of the gravitational Effective Average Action and its flow utilized in **Part II** and in **Part III**. It consists of the explicit construction of the FRGE and its application to the gravitational Effective Average Action (EAA), as well as the presentation of the main approximate solutions. Moreover, we present novel developments in the field, such as a new *essential renormalization group scheme* and the application of the FRGE to the *renormalization of composite operators*. The presentation of this part is tuned to introduce the main ingredients which will be required in the rest of this thesis.

(1) Renormalization Group. As discussed in the Introduction, in Quantum Gravity the effective action presents ultraviolet and infrared divergences. Consequently, a common procedure is to readjust each bare divergent contribution (for instance infinities appearing in Feynman diagrams) by a suitable counterterm to a give a "renormalized" quantity: this was the early stage of the perturbative renormalization procedure. The numerical values of the renormalized quantities have to be determined by experiments. However, in quantized General Relativity it turns out that there should be infinitely many such renormalized parameters: gravity is perturbatively non-renormalizable [19, 20].

The interpretation of the procedure of "removing infinities" has changed with the inception of the renormalization group. In this context coupling constants have to vary and their variation is described by the so-called renormalization group equations: a scale is introduced in order to determine the measurements of physical quantities. The renormalization group equations relate different coupling constants at different scales (typically momentum or cutoff scales).

(1a) The derivation of the scaling properties of interacting theories was first performed, at a perturbative level, by Callan [82] and Symanzik [83, 84]. They studied the behavior of the renormalized proper vertex functions under a change of the renormalized mass. In the process of renormalization, a mass scale μ must be chosen. Depending on it, the field is rescaled by a constant and as a result the bare coupling constant g is correspondingly shifted to the renormalized coupling constant. Of physical importance are the renormalized n-point functions $G^{(n)}(x_1, x_1, \cdots, x_n; \mu, g)$ computed from Feynman diagrams. For a given choice of renormalization scheme, the computation

of this quantity depends on the choice of the mass, which affects the shift in the coupling. The so-called *Callan–Symanzik equation* relates these shifts. At one-loop order of perturbation theory the equation reads

$$\left(\mu \frac{\partial}{\partial \mu} + \beta(g) \frac{\partial}{\partial g} + n\gamma \right) G^{(n)}(x_1, x_1, \cdots, x_n; \mu, g) = 0 \qquad (2.1)$$

where $\beta(g)$ is the beta function and γ encodes the scaling of the wave function renormalization of the field. It is important to remark at that stage, that here only the finitely many beta functions that are related to the relevant couplings are considered.

(1b) In the 1990s, another, much more general type of RG was developed. The final purpose was the description of a path in theory space connecting the fundamental UV theory with its full effective description: Knowing the effective action Γ and the cutoff scale Λ of the theory, one could directly compute the variation with respect to the cutoff $\Lambda \frac{d\Gamma_\Lambda}{d\Lambda}$. It turned out that this functional is finite and provides all the beta functions of the theory [85]. This construction turned out to be closely related to the renormalization group concept formulated in quantum and statistical field theory which combines functional methods with the renormalization group idea by Wilson [86, 87]. The central idea of the renormalization group à la Wilson[1] is that the quantum fluctuations in the path integral can be integrated out progressively. Concretely, the integration in the path integral is performed dividing the integral into several integration steps, each step corresponding to a certain "momentum shell" of quantum fluctuations. This procedure leads to the control of the change of measurements of physical quantities by smoothing or averaging out microscopic details when going to a lower resolution. Additionally, in order to obtain the corresponding Green's functions from which all physical observables are to be calculated, an integration of the low momentum quantum fluctuations has to be carried out.

Wilson's notion of renormalization was originally based on the construction of a scale-dependent *bare* action, the *Wilson action*. This action is defined iteratively in such a way that lowering the cutoff scale amounts to integrating out those modes in the functional integral whose momenta are contained in the next momentum shell, giving rise to a new action defined at the new scale. The variation of Wilson's action with respect to the cutoff is then governed by an *Exact Renormalization Group Equation (ERGE)*. In comparison to the Callan–Symanzik approach, here the ERGE allows a determination of the complete functional which amounts to completely "solving" the theory in question.

From a practical point of view, using the Wilson action as the fundamental object has the disadvantage that extracting physical information requires performing the remaining functional integration (over all modes modes down to momentum zero) in

---

[1]Wilson was himself inspired by the discrete spin-block averaging procedure by Kadanoff [88].

order to obtain the corresponding effective action. On the other hand, working with a scale-dependent *effective* action would be more suitable for computations and physical intuition, in particular in the framework of gauge theories. It is exactly for this purpose that the Effective Average Action was introduced.

(1c) In the 90's, an alternative way to regularize the path integral and implement the Exact Renormalization Group had been developed. Its main purpose was to perform an alternative manipulation of the path integral. Exploiting the language of functional integrals, based on this intuition a new method had been established: the FRG, and its related FRGE or *Wetterich equation*. Instead of computing the running of the scale-dependent bare action à la Wilson, a concrete implementation of the FRGE uses as its key tool a scale-dependent version of the effective action, the Effective Average Action (EAA) [50, 85, 89–93]. Additionally, in contrast to the perturbative approach to the renormalization group it is possible to implement the underlying RG idea already at the level of the EAA, fully independently of the bare action.[2]

The functional RG gives rise to a nonperturbative differential equation for the EAA. Notably, this equation enforces the occurrence of an IR regularization cutoff and has a structure, such that the IR regularization implicates the UV regularization as well. The FRGE admits solutions that are predictive, such that only a finite set of parameters to be taken from experiment are required. Importantly, these solutions are well-defined both in the IR and UV. This nonlinear equation defines RG trajectories on theory space, a manifold containing all possible invariants compatible with the required symmetries and field content, from which only those that emanate from a suitable UV fixed point are physical relevant. The position of this fixed point defines the fundamental theory, which is thus a prediction of the formalism instead of a mere input. Especially compelling is that such solutions do exist in theories that are otherwise perturbatively non-renormalizable. In fact, for Quantum Gravity the existence of the UV fixed point was proven by M. Reuter [95] in the so-called Einstein–Hilbert truncation. Nowadays there are strong indications for the existence of such a nonperturbative solutions, even for higher truncation orders.

(2) Asymptotic Safety. In the EAA approach the search for a Quantum Field Theory of gravity is guided by the *Asymptotic Safety conjecture*. Proposed by S. Weinberg [96], it employs a generalized notion of renormalizability which goes beyond the standard perturbative ones. The key requirement is the existence of a non-trivial UV fixed point of the FRGE. Crucially, this trajectory has to have a finite number of relevant directions. This makes the Asymptotic Safety scenario predictive, i.e., the relevant couplings correspond to the number of free parameters of the theory that must be fixed by experiment.

---

[2]In principle, when implementing an UV regularization, one can reconstruct a bare action that then depends on the chosen UV regularization scheme. However, this procedure is not required for the FRGE [94].

Moreover, classical General Relativity is recovered as an effective description in the IR, and the bare action emerges from the fixed point condition and is thus a prediction rather than an input. The Asymptotic Safety program then becomes very concrete: It focuses on the search for a UV-finite trajectory in theory space with an UV fixed point, from which the UV-finite trajectories originate.

From a technical point of view, the FRGE turns out to be a system of infinitely many coupled ordinary differential equation for the scale-dependent couplings. In order to perform such searches for a UV fixed point, approximations of the FRGE are needed. In order to iteratively attack this differential system, the idea is to project this equation onto a subset of field monomials, which is denoted a *truncation*.

(3) Quantum Einstein Gravity. In Quantum Einstein Gravity QEG the physical field content is given by the equivalence classes of Riemannian metrics under the action of the diffeomorphism group. This results in a theory space spanned by all diffeomorphism-invariant operators depending on a dynamical metric. In the pioneering works [95, 97] a first truncation of QEG based on a metric field content and diffeomorphism symmetry was studied for the Einstein–Hilbert functional. The promising result of the existence of a UV fixed point, hence the evidence of the Asymptotic Safety conjecture, has been consolidated since then in various truncations and modifications [67, 98–175].

We stress that QEG *is not a quantization of classical General Relativity*: its bare action corresponds to a non-trivial fixed point of the RG flow and is therefore a prediction rather than an ad hoc input.

(4) Background Independence. Promoting General Relativity to the quantum level is a very difficult task, since most of the methods available in the construction of standard quantum field theories on flat space turned out to be inapplicable [29–31, 44, 176]. One of the reasons is that gravity is special because it relates the geometry of spacetime (its base space) with the structure of its gauge group and thus renders the geometry as the mediating gauge field. Hence, Background Independence, the requirement that the formulation should be independent on any background geometry, is central to all constructions of quantum theories of gravity. Different approaches trying to circumvent these difficulties brought to light hidden generalized concepts that only become relevant when gravity enters the game. A conservative approach to Quantum Gravity and thus to a complete theory is realized in Asymptotic Safety.

In this context Background Independence is realized by analyzing the dynamics of the fluctuations which depend on the environment they are placed in, the background metric for instance. It is crucial to know if there exist special backgrounds in which the fluctuations are particularly 'tame' such that, for vanishing external source, they amount to only small oscillations about a stable equilibrium, with a vanishing expectation value. Such distinguished backgrounds are referred to as *self-consistent* since, if

we pick one of those, the expectation value of the field does not get changed by any violent field excitation. From this point of view, Background Independence is realized dynamically through the principle of self-consistence of the solutions of the effective equations of motion.

(5) Euclidean vs. Lorentzian. The FRG is a machinery for nonperturbative QFT that has found applications in areas as diverse as solid-state physics, QCD, and Quantum Gravity. However, it is primarily used in Euclidean signature. For certain applications, however, this standard framework does not convincingly capture the physics situation one seeks to model. For instance, for the purpose to study QFT on cosmological backgrounds, it might be crucial to take into account the signature. In fact, cosmological spacetimes in general do not admit a satisfactory notion of Wick rotation. Furthermore, solving the flow equations often makes use of a technology, the heat kernel expansion, whose application to Lorentzian signature operators is mathematically dubious. Consequently, the signature of spacetime represents one of the principal obstacles preventing a straightforward realistic physical interpretation of the picture emerging from Asymptotic Safety.

In [177] a first investigation of Lorentzian gravity was performed in a 3+1 split setting. For a fixed truncation the resulting Lorentzian renormalization group flow turned out almost identical to the one obtained in the Euclidean case. Furthermore, there is also a reason of principle for giving preference to the Euclidean signature in the functional RG context: In the Euclidean case, the momentum-square of the fluctuations to be integrated out is positive semi-definite. Hence, concerning the order in which different fluctuation modes are integrated out along the RG flow, there exists an almost canonical choice: high momentum first, low momentum later. On the contrary, in Lorentzian spacetimes, there exists no distinguished ordering of the modes that would enjoy a similarly canonical status: The question which arises is how to treat separately, parallelly and distinctively spacelike and timelike modes.

A possible approach consists in relating a hypothetical Lorentzian flow equation and its solutions to their Euclidean analogs by some sort of analytic continuation, like a Wick rotation [178–180]. Such a relationship would lead to significant constraints on the "correct" integration scheme. However, we shall not follow this route here, since in Quantum Gravity the (standard form of the) Wick rotation is not available, see however refs. [181, 182]. Another recent approach is a purely spatial coarse graining that would leave time dependencies untouched [183]. For a different, but likewise state-sensitive approach, see ref. [184].

In order to bypass the ordering problem, in this thesis we prefer to think of the piecemeal integrating out of modes, literally, as a procedure of performing the basic (regularized) path integral in a stepwise fashion, rather than solving a flow equation.

The advantage of the integral formulation is that after expanding the integration variable, the field in the desired basis of field space the actual integration gives us direct access to the individual basis modes.

Composite operators

One of the main critiques addressed to Asymptotic Safety [185, 186] lies in the fact that it does not yet make contact with quantum-gravitational observables, and does not furnish information about the renormalization behavior of geometric operators. In fact, these cannot be extracted from the EAA alone.

(1) Observables in gravity (i.e., classical or Quantum Gravity) are challenging to construct because they are required to be invariant under diffeomorphism transformation [15, 22, 187, 188]. Hence, in order to construct diffeomorphism-invariant observables, they should for example be constructed as the integral over spacetime of some scalar density.

Inevitably, one is forced to deal with some sort of non-locality. As a first qualitative example, we can illustrate with the following observable [189]: Consider the correlation function of two operators $\mathcal{O}_1$ and $\mathcal{O}_2$ [190, 191]

$$G(r) = \frac{1}{\text{vol}[g]} \int \mathrm{d}^d x \sqrt{g(x)} \int \mathrm{d}^d y \sqrt{g(y)} \, \mathcal{O}_1(x) \, \mathcal{O}_2(y) \, \delta(r - \ell_g(x,y)) \,, \qquad (2.2)$$

where $\text{vol}[g]$ is the volume of the manifold and $\ell_g(x,y)$ the geodesic length. Importantly, this observable depends on the geodesics length which is a non-local operator. However, in practice it turns out to be impossible to include this kind of geometric observables as operators within a truncation in the FRGE.

Moreover, in a theory of Quantum Gravity, it is rather natural to ask how geometric quantities, such as the volume of some submanifold, behave at the quantum level [192, 193]. Such geometric properties are crucial for the comparison of different approaches to Quantum Gravity, especially for the comparison of continuum-based with discrete approaches.

(2) Within the EAA formalism, all these approaches have a common feature: they require information about operators which usually are not taken into account in a truncated EAA, at any realistic level of complexity. For instance, it is hard to imagine a truncation ansatz for the gravitational EAA to contain information on the geodesic distance of two given points on the spacetime manifolds.

In order to obtain information regarding an arbitrary operator in a quantum field theoretic framework one can couple it to an external source so that it can be inserted

into correlation functions by taking functional derivatives with respect to the source. This formalism goes under the name of the *composite operator formalism*. It allows to define, and compute correlation functions of not only elementary fields, but also of more complicated local operators at a given spacetime point.[3]

One of the main tasks of this thesis is to investigate the composite operator formalism and its application within the framework of the EAA.

To these purposes, initial investigations to gain knowledge about the scaling behavior of such composite operators have been performed in [134, 194]. Importantly, in the fixed point regime scale invariance is realized, and one expects the observable (2.2) to scale as $G \sim r^{-\Delta}$, where Δ represents a universal scaling dimension.

Starting from the seminal paper [195], C. Pagani developed a formalism to include composite operators in the EAA framework and discussed a method which allows to identify the scaling properties of the composite operators at the fixed point: this was the first appearance of the *composite operator flow equation*.

Essential Renormalization Group Scheme

The RG provides a framework to iteratively perform a *change of integration variables* with the purpose of describing physics at different length scales. This, in practice, translates into a flow in a space spanned by the couplings which parameterize all possible interactions between the physical degrees of freedom. However, this mathematical description might present unphysical redundancies.

(1) Our mathematical descriptions of natural phenomena can contain superfluous information which does not correspond to any description of Nature. This follows since we always have the basic liberty to re-express the set of dynamical variables in terms of a new, simpler, set. In this respect, our mathematical models are said to belong to two equivalence classes: two models are considered to be physically equivalent if they are related by a change of variables. Natural phenomena are therefore described by an equivalence class of effective theories rather than a specific model. However, in practice, in order to test our models against experiment, we would like to find those models that reduce the computational effort needed to compute physical observables.

In the RG context this translates into the fact that theory space is divided into equivalence classes. As a consequence, we do not have to compute the flow of all

---

[3]The introduction of composite operators is unavoidable also in many other cases. For example, let us consider the correlation function between metric operators at different points in the vielbein formalism. In this case the metric itself is a composite operator which can be meaningfully defined only via a suitable regularization and renormalization procedure over and above the usual renormalization of couplings in the EAA.

coupling constants, but instead, we only need to compute the flow of the so-called *essential couplings*, which are those appearing in the expression for physical observables. Changing the other coupling constants, known as the *inessential couplings*, amounts to moving within an equivalence class: inessential couplings are those couplings for which a change in their value can be reabsorbed by a change of variables. Hence, instead of computing their flow, one is free to specify the values of all inessential couplings. The most common example of an inessential coupling is the one related to a simple linear rescaling or renormalization of the dynamical variables, namely the wave function renormalization. Beyond this, there are a number of different inessential couplings related to more general, nonlinear changes of variables.

Being able to identify the inessential coupling and avoiding computing their flow has then the advantage that one can automatically disentangle the physical information from the unphysical content encoded. Such a possibility has been advocated independently by G. Jona-Lasinio [196] and by S. Weinberg [197]. A perturbative approach had been put forward in [198], while the first nonperturbative realization within the Exact Renormalization Group (ERG) framework was performed for the first time in 2021 [199].

(2) In this paper A. Baldazzi, R. Ben Alì Zinati and K. Falls have implemented the *essential renormalization scheme*, that scheme for which one only needs to compute the running of the essential couplings, having specified renormalization conditions that determine the values of the inessential couplings as functions of the former. One of their most prominent results regards the fact that at a fixed point, redundant perturbations are automatically discarded [200]. This makes essential schemes a preferred tool to access only the necessary, essential physical content.

There is a particular simple essential scheme, referred to as the *minimal essential scheme*. In this scheme, all the inessential couplings are set to zero at every scale along the flow. At this stage some remarks are in order:

(1) Having a scheme of this type at hand provides practical advantages as well as a clearer physical picture of renormalization.

(2) On the practical side, a major improvement compared to the standard one is the fact that the form of the propagator maintains a simple form along the flow.

(3) Conceptually, the essential scheme may also lead to a better understanding of the equivalence of quantum field theories and the universality of physics models at the critical points [201–206].

(3) Along the same line A. Baldazzi and K. Falls applied the same scheme to Quantum Gravity [175]. The potential existence of inessential couplings in the context for gravity

was already pointed out in [49, 50, 121, 207]. However, in the attempts to find a suitable fixed point for all gravitational couplings included in higher order approximations, a discussion of the incorporation of field reparameterizations into the RG equations was missing. This was performed for the first time in [175] incorporating field reparameterizations in the gravitational RG equations which allow us to eliminate the inessential couplings from the flow equations.

A. Baldazzi and K. Falls considered the universality class of QEG. In particular, there is a shift of emphasis to the physical degrees of freedom and the physical essential couplings will bring our investigation of Asymptotic Safety closer to the original formulation by S. Weinberg.

Plan of Part I

Chapter 3 begins with the general setup for the construction of the FRGE, describing its application to QEG, and introducing the Asymptotic Safety scenario for Quantum Gravity. In order to regularize IR divergences of the path integral, we add a scale-dependent cutoff action ΔS_k to the action of the gravitational path integral, which will play the role of an infrared cutoff. This cutoff action suppresses the integration of momentum eigenmodes below a scale k^2. Following in a parallel fashion the formal definition of the standard effective action, from the regularized gravitational path integral one can derive a scale-dependent effective action, called the Effective Average Action.

The main feature of the Effective Average Action is that this functional, denoted Γ_k it fulfills the Functional Renormalization Group Equation

$$k\partial_k \Gamma_k = \frac{1}{2} \operatorname{Tr} \left[(\Gamma_k^{(2)} + \mathcal{R}_k)^{-1} \, k\partial_k \mathcal{R}_k \right] , \tag{2.3}$$

which we are going to explain in Chapter 3. The operators $\Gamma_k^{(2)}$ and $\mathcal{R}_k$ represent the Hessian obtained by applying two functional derivatives to the EAA and the cutoff action, respectively. The cutoff action itself serves as an infrared regulator of the (gravitational) path integral, the flow equation is well-defined and regular in the UV as well: The scale derivative $k\partial_k \mathcal{R}_k$ vanishes in the infrared and the UV, regulating the traces on the right hand side of (2.3).

In this way, the problem of defining and computing the path integral can be formally replaced by the investigation of solutions to the FRGE. In gravity the equation is defined on the space of all diffeomorphism-invariant functionals of the fields. These define the *theory space*. From a technical point of view, the FRGE turns out to be a system of infinitely many coupled ordinary differential equation for the scale-dependent couplings. If there exist a trajectory in the space of all couplings that is well-defined for

all values of k, the underlying theory is said to be fully renormalized and *asymptotically safe*. Crucially, this trajectory has to be embedded in a certain finite-dimensional hypersurface of theory space. This makes the Asymptotic Safety scenario predictive, i.e., the finite dimension of this hypersurface corresponds to the number of free parameters of the theory that must be fixed by experiment. The Asymptotic Safety program then becomes very concrete: It focuses on the search for a UV-finite trajectory in theory space with an UV fixed point, from which the UV-finite trajectories originate.

In order to perform such searches for a UV fixed point, approximation schemes for the FRGE are needed. To find approximative solutions one usually truncates the theory space, studying the equation on a reduced space spanned by finitely many basis functionals. We shall present the main approximative solution of the functional renormalization group equation of metric gravity, the single metric Einstein–Hilbert truncation. We will exploit the result of this truncation in the rest of this thesis, particularly in **Part II**. The term "Einstein–Hilbert truncation" refers to the 2-dimensional truncation of theory space that is spanned by the functionals $\int \mathrm{d}^d x \sqrt{g}$ and $\int \mathrm{d}^d x \sqrt{g} R$. This ansatz is parameterized by two dimensionless, scale-dependent constants, Newton's constant $g(k)$ and the cosmological constant $\lambda(k)$. In four spacetime dimensions it turns out that the flow of their RG equations possess a UV fixed point.

Furthermore, we discuss a special class of self-consistent backgrounds which are determined by the solution of the effective equation of motion of the Einstein–Hilbert truncation: the running Einstein spaces. Importantly, these self-consistent backgrounds are equally valid in the Euclidean and the Lorentzian version of our setting.

In Chapter 4, we present two recent developments in the utilization of the FRGE. Both of them are preparations for the renormalization of relational observables in Chapter 13 of **Part III**. In fact, relational observables can be treated as composite operators. We will perform a renormalization of these observables in two schemes: the standard and the essential scheme.

In the first part of Chapter 4, we discuss how to renormalize composite operators O_k (i.e., operators built from basic field monomials) via the functional renormalization group. It allows to define, and actually compute correlation functions of not only elementary fields, but also of more complicated local operators at a given spacetime point It is possible to renormalize bare composite operators by coupling them to arbitrary sources ε, and incorporating them into the gravitational path integral. It is rather straightforward to derive the composite operator functional renormalization group equation. This flow equation has a double-layer structure: it consists of the renormalized composite operators on the left, and the EAA on the right. By invoking a scaling argument we can identify the anomalous dimension matrix describing the scaling dimensions of the composite operators in the UV, i.e., in the fixed point regime.

In the second part of Chapter 4, we present a new renormalization group scheme, the *essential scheme*. In general, during the renormalization process all field monomials compatible with the postulated symmetries of the theory space are generated. However, not all operators are associated to essential couplings, i.e., couplings that appear in physical quantities. Some of the couplings are inessential, meaning that they can be removed by field redefinitions. Hence, a second source of RG scale k-dependence can be introduced, which takes into account the freedom to perform field reparameterization along the flow. The effective action then satisfies then a generalized flow equation which takes into account the k-dependent field reparameterizations. Two important facts have to be emphasized: from this new equation one recovers the same structure of the FRGE equation (2.3) and this equation makes explicit that the RG flow can be reinterpreted as a frame transformation. In order to solve the complete flow, a particular renormalization scheme can be chosen, which sets to zero all the inessential couplings: the minimal essential scheme. Finally, we are going to apply the minimal essential scheme to Einstein–Hilbert gravity.

Seeking a construction of observables within the Asymptotic Safety scenario later in Chapter 13, we set up a general formalism to evaluate the scaling of the relational observables, inspired by the well-established composite operator flow equation. We evaluate their scaling dimensions at the fixed point, both in the standard renormalization group scheme and in the essential scheme.

CHAPTER 3

RG flow of Quantum Einstein Gravity and Asymptotic Safety

Executive summary. We review the explicit construction of the Effective Average Action and its related flow equation, i.e., the type of functional renormalization group equation used in Quantum Gravity. On these grounds, we explain the concept of Asymptotic Safety and its relevance for the nonperturbative renormalizability of gravity. We outline an approximation scheme for the effective average action, the Einstein–Hilbert (EH) truncation, and prove Asymptotic Safety within this ansatz. We classify the solutions of the functional renormalization group equation provided by the single metric EH truncation. Finally, in this approximation, we present a family of self-consistent backgrounds.

What is new? The main contents of this chapter is taken from the literature. The discussion around the Lorentzian self-consistent backgrounds has been taken from a publication of the author.

Partially based on: Reference [RF3].

Plan of this Chapter. In this chapter, we are going to introduce the general idea of the Effective Average Action, and we will describe the functional renormalization group equation upon which it can be constructed. In spirit similar to Wilson's exact RG equations, we emphasize that the FRG approach based upon the EAA has also clear differences from the Wilsonian exact RG.

For simplicity's sake, we will start with the application to a scalar field in rigid flat spacetime. Subsequently, in Section 3.4 we will extend it to gravity.

In order to clarify the concept, we start by formally constructing the Effective Average Action by means of functional integrals. Instead of using a sharp momentum cutoff to split the functional integration into two domains, one use smooth regulator functions, producing essentially the same effect but in a continuous way. Different choices of these functions are possible. These lead to different renormalization group equations, whose solutions share the feature that they relate bare actions describing the same quantum system with different cutoff scales.

3.1. EFFECTIVE AVERAGE ACTION

In this section we introduce the concept of the Effective Average Action [90, 95, 208–210] in the simplest context: scalar field theory on flat d-dimensional Euclidean space $\mathbb{R}^d$.

3.1.1. *The construction for scalar fields*

The central idea of the EAA is to produce a modification of the partition function by integrating out high momentum modes and simultaneously suppress low momentum modes. For a real scalar field ϕ, on Euclidean $\mathbb{R}^d$ this is achieved by the addition of a scale-dependent IR "cutoff functional" $\Delta S_k[\phi]$ in the exponent of the integrand, leading to the definition of the modified partition function

$$Z_k[J] = \int \mathcal{D}\hat{\phi} \exp\left(-S[\hat{\phi}] - \Delta S_k[\hat{\phi}] + \int \mathrm{d}^d x J(x)\hat{\phi}(x)\right) . \tag{3.1}$$

Here J is an external source, and S denotes the bare action. The mode suppression term is characterized by a momentum scale k in the following way:

$$\Delta S_k[\hat{\phi}] = \frac{1}{2} \int \mathrm{d}^d x \, \hat{\phi}(x)\mathcal{R}_k(-\Box)\hat{\phi}(x) . \tag{3.2}$$

It is required that the cutoff kernel $\mathcal{R}_k$ acts as an infrared cutoff. For this purpose it has to have a functional form, such that it leaves the high momentum modes unaffected, i.e., they will be integrated out in the partition function, while it generates a mass-like contribution for the IR modes.

The profile of the function $\mathcal{R}_k(-\Box)$, i.e., $\mathcal{R}_k(p^2)$ in a momentum basis is arbitrary and only has to satisfy certain requirements in the limits $p^2 \gg k^2$ and $p^2 \ll k^2$:

$$\mathcal{R}_k(p^2) \approx \begin{cases} k^2 & \text{for} \quad p^2 \ll k^2 \\ 0 & \text{for} \quad p^2 \gg k^2 \end{cases} . \tag{3.3}$$

The first condition leads to a suppression of the small-momentum modes by a mass-like IR cutoff; the second guarantees that the large-momentum modes are integrated out in the usual way. How $\mathcal{R}_k(p^2)$ interpolates between these two regimes is a matter of calculational convenience. An example is the exponential cutoff $\mathcal{R}_k(p^2) = p^2[\exp(p^2/k^2) - 1]^{-1}$, but other choices are possible (see [49] for other cutoffs and their applications).

The partition function Z_k associated to the one parameter family of bare actions $S + \Delta S_k$ gives rise to the generating functional $W_k[J] = \ln Z_k[J]$. The next steps toward the definition of the Effective Average Action are similar to the standard procedure. One defines the (k-dependent) field expectation value $\phi = \langle\phi\rangle = \delta W_k/\delta J$ and computes

the Legendre transform of $W_k[J]$ with respect to $J(x)$, at fixed k. If the functional relationship $\phi = \phi[J]$ can be solved for the source to yield $J = J_k[\phi]$, it assumes the form

$$\tilde{\Gamma}_k[\phi] = \int \mathrm{d}^d x \, J_k[\phi](x)\phi(x) + W_k[J_k[\phi]] \,. \tag{3.4}$$

Finally, subtracting the cutoff term ΔS_k we arrive at the definition of the EAA Γ_k:

$$\Gamma_k[\phi] = \tilde{\Gamma}_k[\phi] - \Delta S_k[\phi] = \int \mathrm{d}^d x \, J_k[\phi](x)\phi(x) + W_k[\phi] - \Delta S_k[\phi] \,. \tag{3.5}$$

The EAA is closely related to a generating functional for correlators of field averages, hence its name. From the EAA it is possible to directly compute all the (k-dependent) Green's functions of the quantum theory by functional differentiation of Γ_k, i.e., without any additional functional integration.

At the nonperturbative path integral level it suppresses the long-wavelength modes by a factor $\exp\left(-\frac{1}{2}k^2 \int \mathrm{d}^d x \, \phi^2\right)$. In perturbation theory, the ΔS_k-term leads to the modified propagator $(p^2 + m^2 + \mathcal{R}_k(p^2))^{-1}$, which equals $(p^2 + m^2 + k^2)^{-1}$, for $p^2 \ll k^2$. Thus, when computing loops with this propagator, k^2 acts indeed as a conventional IR cutoff if $m^2 \ll k^2$.

The EAA (3.5) has some particularly useful properties:

(1) It represents the scale-dependent version of the standard effective action Γ. In the UV limit $k \to \infty$, it approaches the bare action $\Gamma_{k\to\infty} \to S$.

(2) It satisfies the exact integro-differential equation:

$$
\begin{aligned}
e^{-\Gamma_k[\phi]} = \int \mathcal{D}\hat{\phi} \, \exp\Bigg\{ &-S[\hat{\phi}] + \int \mathrm{d}^d x \sqrt{\bar{g}}(\hat{\phi} - \phi)\frac{\delta}{\delta\phi}\Gamma_k[\phi] \\
&-\frac{1}{2}\int \mathrm{d}^d x \sqrt{\bar{g}}(\hat{\phi} - \phi)\mathcal{R}_k(\hat{\phi} - \phi)\Bigg\} \,.
\end{aligned}
\tag{3.6}
$$

(3) It satisfies the exact FRGE [208]

$$k\partial_k \Gamma_k[\phi] = \frac{1}{2}\mathrm{Tr}\left[(\Gamma_k^{(2)} + \mathcal{R}_k)^{-1} k\partial_k \mathcal{R}_k\right] \,, \tag{3.7}$$

where Tr comprises a functional trace that includes an integration over space-time, $\Gamma_k^{(2)}$ represents the Hessian of the effective average action with respect to the fields.

The FRGE (3.7), often referred to as Wetterich's equation, has a number of convenient properties:

(a) It is fully nonperturbative, no approximation is required for its derivation. In fact, the RHS can be rewritten in a style reminiscent of a one-loop expression:

$$k\frac{\partial}{\partial k}\Gamma_k = \frac{1}{2}\frac{D}{D\ln k}\mathrm{Tr}\,\ln\left[\Gamma_k^{(2)} + \mathcal{R}_k\right] \tag{3.8}$$

Here the scale derivative $\frac{D}{D \ln k}$ acts only on the k-dependence of $\mathcal{R}_k$, not on $\Gamma_k^{(2)}$. The Tr $\ln(\cdots) = \ln \det(\cdots)$ expression in (3.8) differs from a standard one-loop determinant in two ways: it contains the Hessian of the actual effective action rather than that of the bare action S and it has a built-in IR regulator $\mathcal{R}_k$. These modifications make (3.8) an exact equation.

(b) The trace involved is UV finite (because of the presence of $k\partial_k \mathcal{R}_k$ on the RHS).

(c) The trace involved is IR finite (because of the appearance of $\mathcal{R}_k$ in the denominator).

(4) When treated as a classical action, Γ_k can provide an EFT description of quantum physics involving typical momenta near k.

3.1.2. *Generalization to all types of fields*

Historically, the first application of the construnction of the EAA had been performed for scalar field theories and their potential interactions [208]. Right afterwards, it has been applied to scalar QED [210], abelian gauge theories [209, 210] and Yang–Mills gauge theories [90]. In 1996 M. Reuter [95] realized for the first time the construction of a EAA in a gravitational context.

The form of the EAA and its related FRGE is in fact fully generalizable to all types of fields and possesses the same structural setting. There are some technical details, especially related to gauge theories:

(1) The generalization to **Yang–Mills theory** requires a gauge-invariant construction of the EAA, i.e., introducing the notion of a covariant derivative, a gauge-fixing term;

(2) Furthermore, the **Gravitational Effective Average Action (GEAA)** also has to comply with the requirement of Background Independence.

Implementing these additional properties within the EAA framework leads to a deformed notion of "averaging". However, for the following geometrical analysis of the RG flow generated by the FRGE these details are unimportant. We are going to address them later on when constructing the Gravitational Effective Average Action.

3.2. THE GENERAL (GEOMETRIC) SETTING

(1) Theory space. The first step toward setting up the concrete form of the FRGE consists in fixing the space of functionals over which the equation is supposed to be defined. It has become customary to refer to this space comprising, in a sense, all action functionals that are possible in principle, as the *theory space* $\mathcal{T}$. To describe it, we shall be slightly more general than in the previous subsection and consider an arbitrary set of fields denoted collectively by $\phi(x)$.

Then the corresponding theory space consists of all effective action functionals $A :$ $\phi \to A[\phi]$ depending on this set, possibly subject to certain symmetry requirements. So the theory space $\{A[\phi]\}$ is fixed once the field content and the symmetries are fixed.

The theory space contains in particular the bare action, S, the standard effective action Γ, and Effective Average Actions Γ_k for all scales on a completely equal footing. Concretely one may take theory space to contain all functionals that occur in a derivative expansion, i.e., arbitrary field monomials, integrated over spacetime, consisting of any number of fields and derivatives of any order which act on them in all ways possible.

(2) Basis on theory space. Assuming that one can expand the elements of theory space in basis functionals P_i:

$$A[\phi] = \sum_{i=1}^{\infty} U^i P_i[\phi] , \tag{3.9}$$

where the U^i are the *generalized couplings*. The basis $\{P_i[\phi]\}$ will include both local field monomials and nonlocal invariants, and we may use the generalized couplings $\{U^i\}$ as local coordinates on $\mathcal{T}$. More precisely, the theory space is coordinatized by the subset of *essential couplings*, i.e., those coordinates which cannot be absorbed by a field reparameterization.

From the geometric point of view, the FRGE for the EAA, i.e., (3.7) generalized for an arbitrary set of fields, defines a vector field β on theory space. The integral curves along this vector field are the *RG trajectories* $k \to \Gamma_k$ parameterized by the scale k. They start, for $k \to \infty$, at the bare action S and terminate at the ordinary effective action at $k = 0$. The natural orientation of the trajectories is from higher to lower scales k, the direction of increasing coarse graining.

Expanding Γ_k as (3.9):

$$\Gamma_k[\phi] = \sum_{i=1}^{\infty} U^i(k) P_i[\phi] , \tag{3.10}$$

the trajectory $k \mapsto \Gamma_k$ is described by infinitely many running couplings $k \mapsto \{U^i(k)\}$. The system of coupled equations which is generated when inserting (3.9) into eq.(3.7) consists of *infinitely many* differential equations. This is in sharp contradistinction to
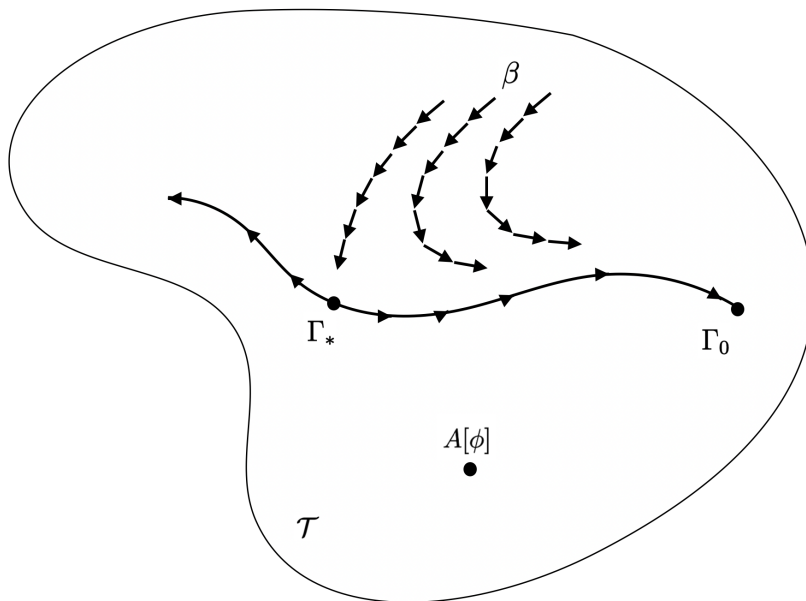
FIGURE 3.1. Illustration of theory space $\mathcal{T}$ and its structures: by definition, the theory space contains all action functionals $A[\phi]$ which can be constructed from a given field content and obey the desired symmetries. Conventionally, all arrows point towards a lower coarse-graining scale, i.e., in the direction of integrating out fluctuation modes. The theory space comes with a vector field, the beta functions β. The curves of this vector field (RG trajectories) are exemplified by the black solid curve. As an example, we consider a trajectory which emanates from a fixed point Γ_* with one UV-repulsive and one UV-attractive eigendirection. The endpoint of the RG trajectory at $k = 0$ coincides with the effective action Γ_0.

the perturbative equations of Callan [82] and Symanzik [83]. In standard field theory terminology one would refer to "bare" parameters $U^i(k = \infty)$ and to "renormalized" parameters $U^i(k = 0)$.

Since any point in theory space, i.e., any admissible functional, can be expanded as a linear combination as in (3.9), then we can derive the scale derivative of the couplings $\{U_i(k)\}$ as follows. The RG flow (3.7) in the basis dependent component form basis reads:

$$k\partial_k \sum_{i=1}^{\infty} U^i(k) P_i[\phi] = \frac{1}{2} \operatorname{Tr}\left[\left(\sum_{i=1}^{\infty} U^i(k) P_i^{(2)}[\phi] + \mathcal{R}_k\right)^{-1} k\partial_k \mathcal{R}_k\right]. \qquad (3.11)$$

The RHS of this equation is an extremely complicated functional of ϕ. However, the theory space, by its very definition, contains all functionals that could possibly be produced by those algorithms, it follows that the ϕ-dependence of $\frac{1}{2}\operatorname{Tr}[\cdots]$ can be

expanded in the basis $\{P_i[\phi]\}$:

$$\frac{1}{2}\mathrm{Tr}[\cdots] = \sum_{i=1}^{\infty} b^i(U^1, U^2, \cdots ; k) P_i[\phi] \, . \tag{3.12}$$

Here the *beta functions* b^i arise expanding the trace on the RHS of the FRGE in terms of $\{P_i[\phi]\}$ and comparing the coefficients multiplying the same operator $P_i[\phi]$.

We would like to work with dimensionless variables in order to avoid rescaling of physical lengths. If the coupling U^i has canonical dimension d_i we define the corresponding dimensionless coupling $u^i(k) = U^i(k)k^{-d_i}$:[1] Since the P_i are linearly independent, then the scale dependence of the EAA is completely determined by (infinitely many) β-functions describing the RG running of the dimensionless couplings:

$$k\partial_k u^i = \beta^i(u^1, u^2, \cdots ; k) \, . \tag{3.13}$$

Here, the βs represent the associated dimensionless β-*functions* of the coupling constants implied by the projected FRGE. At this point, RG trajectories $k \mapsto \big(u^i(k)\big) \equiv u(k)$ are represented by arrays of theory space coordinates. Eq.(3.13) represents an autonomous system of coupled differential equations: they have no explicit dependence on k and define a time-independent vector field on theory space.

(3) RG flow and trajectories. The integral curves of this vector field, $k \mapsto \Gamma_k$, are the RG *trajectories*, and the pair $\{\mathcal{T}, \beta\}$ is called the RG *flow*.

(4) Complete trajectories. In this language, the basic idea of renormalization can be understood as follows. The boundary of theory space is meant to separate points with coordinates $\{u^i, i = 1, 2, \cdots\}$ with all the essential couplings $\{u^i\}$ well-defined, points with undefined, divergent couplings. The basic task of renormalization theory consists in constructing a *complete RG trajectory*, i.e., a trajectory which lies entirely within theory space. It neither leaves theory space (that is, develops divergences) in the $k \to \infty$ limit nor in the $k \to 0$ limit. Every such trajectory defines one possible quantum theory.

(5) Fixed points. The consistent $k \to \infty$ behavior can be ensured by performing the limit $k \to \infty$. The fixed point is a zero of the vector field $\beta \equiv (\beta^i)$, i.e., $\beta^i(u_*) = 0$ for all $i = 1, 2, \cdots$. The running of the RG trajectories stops completely at the fixed point. As a result, one can 'use up' an infinite amount of RG time near/at the fixed point if one bases the quantum theory on a trajectory which runs into such a fixed point. This construction ensures that in the UV limit the trajectory ends at an 'inner point' of theory space giving rise to a well-behaved action functional. Thus, we can be sure that,

---

[1]By definition, $U^i(k) \equiv k^{d_i} u^i(k)$, where d_i denotes the canonical mass dimension $[U^i] = -[P_i] \equiv d_i$, whence $[u^i] = 0$.

for $k \to \infty$, the trajectory does not develop pathological properties such as divergent couplings. The resulting quantum theory is 'safe' from unphysical divergences.

(6) Linearization about a fixed point. The expansion at linear order the RG equations (3.13) around the fixed point u_* is governed by the Jacobi matrix $\mathcal{B}$

$$k\partial_k u^i(k) = \sum_j \mathcal{B}^i{}_j (u^i(k) - u^i_*) \tag{3.14}$$

The Jacobi matrix, denoted also *stability matrix*, is defined as

$$\mathcal{B}^i{}_j(u_*) \equiv \partial_j \beta^i(u_*) , \tag{3.15}$$

If the eigenvectors of $\mathcal{B}$ form a basis, then a solution to (3.14) reads:

$$u^i(k) = u^i_* + \sum_I C_I V^i_I \left(\frac{k_0}{k}\right)^{\theta_I} . \tag{3.16}$$

Here k_0 is a fixed scale, the C_Is are the constants of integration that can be expressed in terms of the initial conditions, and the V_Is are the eigenvectors of the Jacobi matrix with associated negative eigenvalues $-\theta_I$, i.e.:

$$\sum_j \mathcal{B}^j{}_i V^I_j = -\theta_I V^I_i \tag{3.17}$$

Since $\mathcal{B}$ is not symmetric in general the θ^Is are not guaranteed to be real. In any case, we assume that the eigenvectors form a complete system. Its eigenvalues θ_I are called *critical exponents*[2] or *scaling exponents*. Furthermore, the stability matrix can be decomposed according to

$$\mathcal{B}_{ij}(u_*) = -d_i \delta_{ij} + B_{ij}(u_*) , \tag{3.18}$$

where $\mathcal{B}^i{}_j(u_*) = \frac{\partial}{\partial u_i} b_j(u_*)$. The first part represent the canonical mass dimension of the couplings, such that in the end we are left with the quantum corrections to the classical scaling of the coupling at the fixed point, also denoted as *anomalous dimension*. B is therefore called the *anomalous dimension matrix*. For instance, assuming that $B(u_*)$ is a fully diagonalizable matrix and can be diagonalized by a matrix A, then we can write

$$\sum_{l,m} A_{il} \mathcal{B}_{lm}(u_*) A^{-1}_{mj} = -\theta_i \delta_{ij} = -(d_i + \eta_i)\delta_{ij} , \tag{3.19}$$

where the $\{-\eta_i\}$ are the eigenvalues of the diagonalized anomalous dimension matrix B.

We can now classify the "eigendirection" V^I. When lowering k, when flowing from the UV towards the IR along a trajectory, a basis vector is said to be:

---

[2]The reason of this name is due to the fact that when the renormalization group is applied to critical phenomena (second-order phase transitions) the traditionally defined critical exponents are related to the θ^I's in a simple way [211].

(1) *relevant*, if $\mathrm{Re}\,\theta_I > 0$, meaning that the component $u^i(k) - u_*$ grows in the direction of the IR;

(2) *irrelevant*, when $\mathrm{Re}\,\theta_I < 0$, i.e., the coupling shrinks towards the IR;

(3) *marginal*, if $\mathrm{Re}\,\theta_I = 0$, the coupling stays constant at linear order.

So "relevant" is synonymous to "growing under downward evolution", and "irrelevant" means "get damped under downward evolution" from the UV to the IR.

According to this classification, at the fixed point we can decompose the tangent space of theory space in relevant, irrelevant and marginal subspaces that are spanned by the set of the eigenvectors of every couplings. In particular, we discussed how the relevant directions play a special role because these determine the UV critical hypersurface $\mathcal{S}_{\mathrm{UV}}$.

From this analysis a classification of fixed point can be performed:

(1) A fixed point is called *Gaussian* (Gaussian fixed point (GFP)) if its critical exponents agree with the canonical mass dimensions of the corresponding operators:
$$\theta^i = d^i \tag{3.20}$$
Usually this amounts to the trivial fixed point values $u^i_* = 0$ for all couplings and hence $B(u_* = 0) = 0$.

(2) A *non-Gaussian fixed point* (NGFP) is a fixed point which is interacting or non-trivial, i.e., a fixed point whose critical exponents differ from the canonical ones:
$$\theta^i \neq d^i \quad \text{for at least one } i. \tag{3.21}$$
Usually this requires $u^i_* \neq 0$ for at least one coupling.

(7) UV critical surface. If $u^i(k)$ is to describe a trajectory in $\mathcal{S}_{\mathrm{UV}}$, $u^i(k)$ must approach u^i_* in the limit $k \to \infty$ and therefore we must set $C_I = 0$ for all I with $\mathrm{Re}\,\theta^I < 0$. Hence the dimensionality Δ_{UV} of the UV critical hypersurface equals the number of $\mathcal{B}$-eigenvalues with a negative real part, i.e., the number of θ^I's with $\mathrm{Re}\,\theta^I > 0$. The corresponding eigenvectors span the tangent space to $\mathcal{S}_{\mathrm{UV}}$ at the NGFP. If we lower the cutoff for a generic trajectory with all C_I nonzero, only Δ_{UV} relevant parameters corresponding to the eigendirections tangent to $\mathcal{S}_{\mathrm{UV}}$ grow, while the remaining irrelevant couplings pertaining to the eigendirections normal to $\mathcal{S}_{\mathrm{UV}}$ decrease:
$$\dim \mathcal{S}_{\mathrm{UV}} = \# \text{ (relevant directions)} \tag{3.22}$$
Thus near the NGFP a generic trajectory is attracted towards $\mathcal{S}_{\mathrm{UV}}$.

(8) Universality of the critical exponents. An important property of the critical exponents θ_I is that at the exact, un-truncated level they do not depend on the cutoff scheme, i.e., on the operator $\mathcal{R}_k$. They are universal quantities [200].

As an immediate consequence, when we decompose the tangent space in relevant, marginal, and irrelevant subspaces the respective dimensionalities of those subspaces are likewise universal. In conclusion, also the defining property of a fixed point (3.20) or (3.21) is a coordinate-independent statement.

(9) Scaling vs. redundant operators. F. Wegner proved [200] that, at a fixed point of the RG, there are critical exponents that are entirely scheme-dependent (associated to *redundant operators*) and exponents which are not scheme-dependent (related to *scaling operators*).

(1) A *redundant operator* is equivalent to an infinitesimal change of a field variable (see the connection to the so called *inessential* couplings in Chapter 4). Wegner proved order by order in perturbation theory in the couplings that couplings associated to redundant operators have no consequence on the physics and can be set to zero.

RG eigenvalues for redundant operators also depend on the choice of the renormalization group scheme and indeed, by appropriate design of the flow equation. Therefore there is no invariant meaning to the classification in terms of relevant or irrelevant when applied to redundant operators.

(2) On the contrary, renormalization group eigenvalues for *scaling operators* have universal characteristics of the continuum field theory.

One of the most prominent novel results regards the fact that at a fixed point, redundant perturbations can be automatically discarded [175], by a minimal essential renormalization scheme (see Chapter 4).

3.2.1. *Cutoff vs. normalization scale*

Geometrically speaking a truncation of theory space means neglecting all the components of the vector field arising in the FRGE that were not in the subspace of the initial truncation. The vector field is projected onto the subspace of the truncation: the resulting trajectories won't coincide with the exact trajectories. The difference appears exactly in the error in the predictions of the running couplings that we get by truncating the theory space. In any case, producing an approximation of the exact RG flow the running of the coupling constants will inherit the nonperturbative nature of the FRGE.

The system (3.13) will have many solutions in general and the question arises how to label and classify them. Since RG trajectories never cross, we can label every trajectory by the point $u(k)|_{k=\mu} \equiv u_{\text{ren}}$ which it visits when k equals a certain finite normalization scale μ. Thus, in dimensionful terms, say, the trajectory $k \mapsto u^i(k)$ which belongs to the "renormalized couplings" u^i_{ren} is parametrized more explicitly by a function $\mathcal{U}^i(k; u_{\text{ren}}, \mu)$

satisfying $U^i(k) = \mathcal{U}^i(k; u_{\text{ren}}, \mu)$ for all $k \geq 0$, and $\mathcal{U}^i(\mu; u_{\text{ren}}, \mu) = \mu^{d_i} u^i_{\text{ren}} \equiv \bar{u}^i_{\text{ren}}$. At the level of actions,

$$\Gamma_k^{(u_{\text{ren}}, \mu)}[\varphi] = \sum_i \mathcal{U}^i(k; u_{\text{ren}}, \mu) \, P_i[\varphi] \,. \tag{3.23}$$

Here the pair (u_{ren}, μ) serves as an identifier for the specific trajectory in question. However, u_{ren} and μ are not independent: When changing μ, we must also change the point $u_{\text{ren}} \equiv u_{\text{ren}}(\mu)$ if the trajectory is to stay the same. This condition, $\frac{\mathrm{d}}{\mathrm{d}\mu}\mathcal{U}^i(k; u_{\text{ren}}(\mu), \mu) = 0$, is expressed by the Callan–Symanzik-type equation

$$\left[\mu \frac{\partial}{\partial \mu} + \sum_j \beta^j(u_{\text{ren}}) \frac{\partial}{\partial u^j_{\text{ren}}} \right] \mathcal{U}^i(k; u_{\text{ren}}, \mu) = 0 \,, \tag{3.24}$$

and a similar one for the full action:

$$\left[\mu \frac{\partial}{\partial \mu} + \sum_j \beta^j(u_{\text{ren}}) \frac{\partial}{\partial u^j_{\text{ren}}} \right] \Gamma_k^{(u_{\text{ren}}, \mu)}[\varphi] = 0 \,. \tag{3.25}$$

The relation (3.25) holds true for the standard effective action at $k = 0$ in particular. It amounts to the statement that *no physics may depend on the value which we have chosen for the normalization scale μ.*

3.3. Asymptotic Safety with the Effective Average Action

(1) Complete RG trajectories. In the previous section we discussed how the scale dependence of an action is encoded in a running of the coupling constants $\{U^i(k)\}$ (or their dimensionless version $\{u^i(k) = k^{-d_i} U^i(k)\}$) that parametrize the action. This gives rise to a *trajectory* in the underlying theory space, describing the evolution of an action functional with respect to the scale k. *The construction of a consistent QFT amounts to finding a complete RG trajectory. In particular it can be infinitely extended to the UV, having a well-defined limit $\Gamma_{k \to \infty}$.*

This limit must give rise to a QFT which respects all basic physical principles which we consider indispensable (like Background Independence, etc.).

(2) Weinberg's conjecture. In his seminal paper [96], S. Weinberg formulated a conjecture about the existence of the infinite cutoff limit in quantum gravity, which became known as the *Asymptotic Safety Scenario*. His initial proposal advocated Asymptotic Safety as a mechanism which renders physical scattering amplitudes finite (but non-vanishing) at energy scales exceeding the Planck scale. Applied to a QFT Weinberg's conjecture consists of two parts which read as follows:

(1) The theory space contains a non-trivial fixed point, and this fixed point has a low-dimensional UV critical hypersurface.

(2) All complete RG trajectories are contained in $\mathcal{S}_{\text{UV}}$.

In [95] this conjecture was translated in the EAA language: if both (1) and (2) are true, a given trajectory has an acceptable UV limit, and hence signals the existence of a nonperturbatively renormalizable field theory, if and only if its endpoint in the UV is given by the non-trivial fixed point of the RG flow. This behavior is exactly what gave rise to the name "Asymptotic Safety".[3]

If from the FRGE a complete trajectory can be found, such that the IR fixed point is continuously connected with the well-defined UV limit (the RG flow has to give raise to an UV fixed point), then this entails a well-defined description of a QFT. Thereby the existence of a fundamental theory is strictly correlated to the existence of complete RG trajectories of the EAA (which of all possible trajectories is realized in nature can be determined only through measurements). In this frame also the notion of renormalizability acquires another meaning compared to the perturbative setting. The corresponding renormalizability question must be whether the space of all action functionals, which is usually defined as the *theory space* $\mathcal{T}$, contains UV fixed point(s) and complete trajectories stemming from those fixed point(s).

This property of the FRGE, providing a complete "solution of the theory", is in sharp contradistinction to the various types of RG equations used in perturbation theory. They are finite in number and control only the coupling constants related to "renormalizable interactions". In fact, perturbation theory can give only a partial answer here, identifying only the perturbatively renormalizable actions. Therefore, the amount of information encapsulated in the solutions to their RG equations is insufficient to fully determine the effective action Γ. However, many potentially interesting physical systems lie beyond the scope of perturbation theory. Hence an appropriate notion of *nonperturbative renormalizability* is needed.

As a matter of fact, the FRG setup for the EAA does not rely on the smallness of the couplings, asymptotically safe theories can be considered nonperturbatively renormalizable.

Summarizing, the *Asymptotic Safety Conjecture* claims the existence of an appropriate fixed point of the RG flow. This is defined as a point in theory space u_*^i where the running of all dimensionless couplings stops, i.e., functions: $\beta_j(u_*^i) = 0$ for every j. An additional requirement, is that this fixed point must have a finite number of relevant directions. If one defines the UV fixed points' critical surface to consist of all points in theory space which are pulled into the fixed point for increasing RG scale k,

---

[3]In fact, Asymptotic Freedom (well-known from QCD) is a realization of this idea restricted to the case where the underlying fixed point is the Gaussian one.

then essentially the second key hypothesis underlying Asymptotic Safety is that only trajectories lying entirely within the UV critical surface of an appropriate fixed point can be infinitely extended and thus define a fundamental QFT.

(3) Predictivity. Furthermore, asymptotically safe theories are highly predictive as infinitely many parameters are fixed by a finite number of measurements. This becomes manifest if one considers that asymptotically safe theories must have a finite dimensional UV critical surface: For instance, if the UV critical surface has the finite dimension n, it is sufficient to perform only n measurements in order to uniquely identify Nature's RG trajectory. Once the n relevant couplings are measured, the requirement for Asymptotic Safety fixes all other couplings since the latter have to be adjusted in such a way that the RG trajectory lies within the UV critical surface.

Asymptotically safe theories are intended to constitute fundamental QFTs which remain consistent and predictive even at high momentum scales. This distinguishes them from Effective Field Theories, which require an increasing number of coupling constants at high momenta that are in no way constrained theoretically and therefore must be taken from experiments. On the other hand, Asymptotic Safety can "tame" this infinitely many undetermined constants and reduce them to just a few parameters that must be extracted from experiments.

3.3.1. *Truncations*

Up to this point, our construction did not involve any approximation. However, when it comes to solving the FRGE and the system of infinitely many differential equations we clearly must resort to some kind of approximation. An obvious possibility is perturbation theory in one or several couplings which are assumed small; in this way one could recover the RG equations of perturbative renormalization theory, for instance [212, 213].

The method we adopt here, the method of truncated theory spaces, has the essential advantage that it can yield *nonperturbative approximate solutions*. They can go beyond the realm of perturbation theory by summing up contributions from all orders of the small coupling expansion or the loop expansion, for instance. Such solutions might even depend on the small parameters in which perturbation theory is trying to expand in a *non-analytical* way so that at any finite order perturbation theory is "blind" to the corresponding contributions.

(1) Truncated RG flow. The idea is now to truncate the sum of monomials in (3.9) to an ansatz spanning an N-dimensional subspace only

$$\Gamma_k[\phi] = \sum_{i=1}^{N} U^i(k) P_i[\phi] \, . \tag{3.26}$$

When we insert this truncation ansatz in the flow equation (3.7) we obtain

$$k\partial_k \sum_{i=1}^{N} U^i(k)P_i[\phi] = \frac{1}{2} \operatorname{Tr}\left[\left(\sum_{i=1}^{N} U^i(k)P_i^{(2)}[\phi] + \mathcal{R}_k \right)^{-1} k\partial_k \mathcal{R}_k \right], \qquad (3.27)$$

The projected RG flow is described by a set of differential equations for the couplings $\{U^i(k)\}$. They arise as follows. Let us assume we expand the ϕ-dependence of $\frac{1}{2}\operatorname{Tr}[\cdots]$ (with the ansatz for $\Gamma_k[\phi]$ in (3.26) inserted) in a basis $\{P_i[\phi]\}$ of the full theory space which contains the $\{P_i[\phi]\}$'s spanning the truncated space as a subset. Note, however, that in general the Trace on the RHS of (3.27) will give rise to monomials which are not contained in our truncated theory space. Consequently, when projecting the system of equation, we set to zero all the prefactors multiplying those contributions, and we equate the coefficients of the remaining monomials P_i on both sides of (3.27).

(2) Derivative expansion. A natural ordering principle for the interaction terms entering into the Effective Average Action is provided by their number of derivatives. The space $\mathcal{T}$ contains all functionals that can occur in a derivative expansion, i.e., arbitrary field monomials, integrated over spacetime, consisting of any number of fields and derivatives of any order which act on them in all ways possible.

3.3.2. *The Asymptotic Safety Program*

(1) The Program. The Asymptotic Safety Program a way of dealing with the latter conjecture. This may be thought of as a systematic search strategy which identifies physically acceptable theories as compared with the unacceptable ones plagued by short distance singularities. Note that the existence of a fixed point allows the asymptotically safe trajectories to stay in its vicinity for an infinitely long RG time.

Accordingly, the Program furnish a systematic way to search for physically acceptable theories (and their associated actions) free of divergences in the UV. Geometrically speaking, and using the dimensionless language, these actions constitute a *complete RG trajectory.*

(2) Asymptotic Safety and the EAA. As we shall see, the framework of the Effective Average Action is well suited to test the Asymptotic Safety Conjecture in a self-contained manner: it is the *systematic search for a theory space $\mathcal{T}$, supporting appropriate NGFP(s).* In the EAA framework, they amount to the steps in Figure 3.2.

Following the scheme in Figure 3.2, we will use a fixed point of the RG flow in order to control the $k \to \infty$ limit of the complete RG trajectories.

After a preparation in the previous sections we are now in the position to outline the key idea of nonperturbative renormalizability and Asymptotic Safety in gravity. In
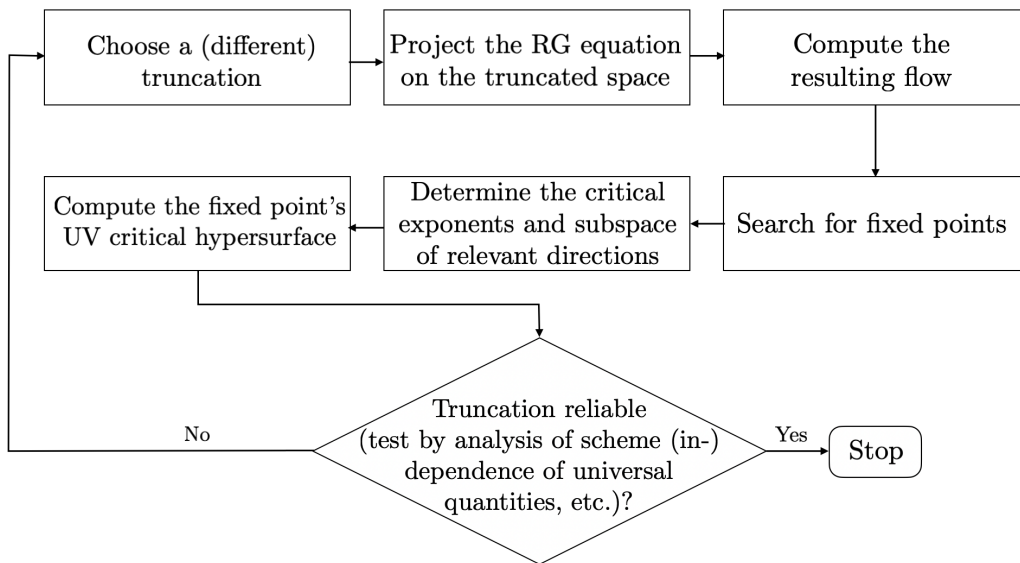
FIGURE 3.2. Algorithmic procedure to test Asymptotic Safety within the EAA framework.

the first instance, we will consider what is special about gravity and how this particular property can comply with the FRG setup for the GEAA.

3.4. GRAVITATIONAL EFFECTIVE AVERAGE ACTION AND ITS FRGE

In the previous section we emphasized that for non-gravitational theories, given a theory space, the form of the FRGE and, as a result, the vector field $\boldsymbol{\beta}$, are basically completely fixed, so that the RG flow and in particular its fixed point structure can be studied without any further input. In the case of gravity, however, it is much harder to make this program work in a concrete way. In this section we are going to discuss the new problems which arise specifically in Quantum Gravity when one tries to develop a renormalization group framework by following the route sketched previously that led to the Effective Average Action.

3.4.1. *The desideratum: Background Independence*

(1) The FRG will turn out particularly suitable for the analysis of Quantum Gravity. The theory of Quantum Gravity we are aiming at should be being compatible with the principle of Background Independence [29–31, 44, 176] (see the discussion in Section 1.3). As in classical GR, no special metric should play a distinguished role. There is *no rigid a priori background* such as flat spacetime available: Spacetime has to be

studied and explained, much more than postulated. Technically speaking, this means that the metric-structure of spacetime has to be kept fully dynamical.

This requirement is what distinguishes a quantum theory of gravity from any other theory. In a rather profound way. the requirement of Background Independence goes beyond the traditional setting of Quantum Field Theory of matter systems on Minkowski space whose conceptual foundations heavily rely on the availability of a non-dynamical Minkowski spacetime as a background structure. In this regard, the correct realization of Background Independence continue to represent a not-yet addressed challenge for many theories of Quantum Gravity.

(2) Many more problems arise when one tries to apply the familiar concepts and calculational methods of quantum field theory to the metric itself without introducing a rigid background structure. Some of them are conceptually deep while others are of a more technical nature. A typical difficulty shows up when one tries to conceive an appropriate notion of a functional renormalization group in the realm of Quantum Gravity. In QFT on a rigid background spacetime typical regularization schemes which are used to make the calculations well-defined both in the IR and the UV make essential use of the metric provided by this background spacetime. In the absence of an intrinsically given metric this procedure fails: There is neither a natural, physically motivated way of choosing the basis of field modes, nor is it clear how to discriminate between IR and UV modes and to fix the order in which the individual modes belonging to some basis of field modes should be integrated out.

(3) However, there is a strategy to implement Background Independence that benefits of the fact that all the general concepts and technical tools of conventional background-dependent QFT are applicable. In fact, one parameterizes the quantum metric as $g_{\mu\nu} = \bar{g}_{\mu\nu} + h_{\mu\nu}$ around an arbitrary background $\bar{g}_{\mu\nu}$. Subsequently, one quantizes the fluctuation $h_{\mu\nu}$ in essentially the same way one would quantize a matter field in a classical spacetime with metric $\bar{g}_{\mu\nu}$. This procedure goes under the name of *background field technique*. Thus, in a sense, the Background Independent quantization of gravity amounts to its quantization on all possible backgrounds simultaneously: $\bar{g}_{\mu\nu}$ is never specified concretely.

Note that we are not implying a perturbative expansion here; $h_{\mu\nu}$ is not supposed to be small in any sense.

We distinguish at this point between the principle of "Background Independence" with capital letters introduced above and the background independence. This latter, with small letters, refers more simply to the independence of some physical quantity with respect to the background field. The background field technique in gravity was first introduced in [17, 214], where for a certain type of gauge fixing the effective action was expressed as a gauge-invariant functional of its fields. Within the EAA approach

to Yang–Mills theory a gauge-covariant (Becchi–Rouet–Stora–Tyutin (BRST)) coarse graining was implemented by M. Reuter and C. Wetterich in 1993 [90, 209].

(4) In 1996 M. Reuter introduced the Gravitational Effective Average Action which combines the advantages of the EAA with the requirements of Background Independence and general coordinate invariance demanded by gravity.

Technically, by using the background field method, Background Independence becomes not manifest during the intermediate steps. Nevertheless, it can be reestablished dynamically at the end. The implementation of Background Independence was developed along three steps:

(1) An arbitrary background is fixed.
(2) The dynamical degrees of freedom are quantized on this background.
(3) The background is re-adjusted in such a way that it becomes *self-consistent*, meaning that the expectation value of the fluctuation vanishes, i.e., $\langle h \rangle_{\text{self-consistent background}} = 0$.

In this way the background is determined dynamically (see Section 3.6).

3.4.2. *Quantum Einstein Gravity*

The FRGE furnishes an alternative way of studying QFT and we can forget about the derivation of the equation from the merely formal functional integral and use the FRGE as the primary tool to calculate the effective action and to define a QFT.[4]

(1) In this approach, the only input data to be fixed at the beginning are, first, the kinds of quantum fields carrying the theory's degrees of freedom, and second, the underlying symmetries. This information determines the stage the RG dynamics takes place on, the theory space, consisting of all possible action functionals that respect the prescribed symmetry. A prime example is given by the theory space of *Quantum Einstein Gravity*.

We are going to denote by *Quantum Einstein Gravity* (QEG), the quantum field theory whose dynamical degrees of freedom are carried by $g_{\mu\nu}$ and whose principal symmetry is diffeomorphism invariance.

(2) In this section we describe in detail the Effective Average Action for gravity, focusing mostly on those aspects that are different from the scalar case. The metric field $g_{\mu\nu}$

---

[4]Given the fact that the functional path integral is ill-defined and make sense only in the presence of an UV cutoff, we would like to find out for which measure and bare actions S the limit of an infinite UV cutoff can be taken consistently. Tackling the so-called *reconstruction problem*, i.e., the problem of finding a UV regularized functional integral, which, has a mathematically well-defined continuum limit and, at the same time reproduces a given RG trajectory, considerable technical and conceptual issues arise [215].

lives on a given spacetime manifold with a fixed topological class and smooth differential structure.

The first step consists in splitting the quantum metric according to

$$\hat{g}_{\mu\nu} = \bar{g}_{\mu\nu} + \hat{h}_{\mu\nu} \, , \tag{3.28}$$

where $\bar{g}_{\mu\nu}$ is a fixed, but unspecified, background metric and $\hat{h}_{\mu\nu}$ are the quantum fluctuations around this background which are not necessarily small. This allows the formal construction of the gauge-fixed (Euclidean) gravitational path integral

$$\int \mathcal{D}\hat{h} \, \mathcal{D}\hat{\xi}^\nu \, \mathcal{D}\hat{\bar{\xi}}_\nu \, \exp\left\{ -S[\bar{g} + \hat{h}] - S_{\mathrm{gf}}[\hat{h}; \bar{g}] - S_{\mathrm{ghost}}[\hat{h}, \hat{\xi}, \hat{\bar{\xi}}; \bar{g}] - \Delta S_k[\hat{h}, \hat{\xi}, \hat{\bar{\xi}}; \bar{g}] \right\} \tag{3.29}$$

Here $S[\bar{g} + \hat{h}]$ is a generic action, which depends on $g_{\mu\nu}$ only, while the background gauge fixing $S_{\mathrm{gf}}[\hat{h}; \bar{g}]$ and ghost contribution $S_{\mathrm{ghost}}[\hat{h}, \hat{\xi}, \hat{\bar{\xi}}; \bar{g}]$ contain $g_{\mu\nu}$ and $\hat{h}_{\mu\nu}$ in such a way that they do not combine into a full $g_{\mu\nu}$.

Remark. A remark concerning the notations we use for the EAA might be in place here. The functionals in (3.29) are distinguished by the "semicolon" notation. This notation helps to keep track of the dependence of the dynamical fields, which is non-trivial because of the splitting (3.28). We can also express the action in terms of the "comma" notation as

$$S\left[\hat{h}, \hat{\xi}, \hat{\bar{\xi}}; \bar{g}\right]\bigg|_{h=g-\bar{g}} = S\left[\hat{g}, \bar{g}, \hat{\xi}, \hat{\bar{\xi}}\right] \, . \tag{3.30}$$

Furthermore, we take $S_{\mathrm{gf}}[\hat{h}; \bar{g}]$ to be a gauge fixing 'of the background type' [216], i.e., it is invariant under diffeomorphisms acting on both $\hat{h}$ and $\bar{g}$. Clearly there exist many possible gauge-fixing terms. A convenient choice which has been employed in practical calculations is the background version of the harmonic coordinate condition [17]:

$$\mathcal{F}_\mu{}^{\alpha\beta}[\bar{g}] = \left[\delta_\mu^\beta \bar{g}^{\alpha\gamma} \bar{\nabla}_\gamma - \beta_{\mathrm{gf}} \bar{g}^{\alpha\beta} \bar{\nabla}_\mu \right] \qquad F_\mu = \sqrt{2}\kappa \mathcal{F}_\mu{}^{\alpha\beta}[\bar{g}] \hat{h}_{\alpha\beta} \, . \tag{3.31}$$

in the action for the corresponding Faddeev–Popov ghosts

$$S_{\mathrm{gh}}[\hat{h}, \hat{\xi}, \hat{\bar{\xi}}; \bar{g}] = -\frac{1}{\kappa} \int \mathrm{d}^d x \, \hat{\bar{\xi}}_\mu \bar{g}^{\mu\nu} \frac{\partial F_\nu}{\partial \hat{h}_{\alpha\beta}} \mathcal{L}_\xi (\bar{g}_{\alpha\beta} + \hat{h}_{\alpha\beta}) \, , \tag{3.32}$$

where $\mathcal{L}$ is the Lie derivative and $\kappa \equiv (32\pi\bar{G})^{-1/2}$. Accordingly, the gauge-fixing term takes the form:

$$S_{\mathrm{gf}} = \frac{1}{2\alpha_{\mathrm{gf}}} \int \mathrm{d}^d x \sqrt{\bar{g}} \bar{g}^{\mu\nu} F_\mu F_\nu \, . \tag{3.33}$$

The key ingredient in the construction of the EAA is the coarse graining term $\Delta S_k[h, \xi, \bar{\xi}; \bar{g}]$. It is quadratic in the fluctuation field,

$$\Delta S_k[h, \xi, \bar{\xi}; \bar{g}] = \frac{\kappa^2}{2} \int \mathrm{d}^d x \, \sqrt{\bar{g}} \, \hat{h}_{\mu\nu} \mathcal{R}_k^{\mathrm{grav} \, \mu\nu\rho\sigma}(-\Box) \hat{h}_{\rho\sigma} + \sqrt{2} \int \mathrm{d}^d x \, \sqrt{\bar{g}} \, \hat{\bar{\xi}}_\mu \mathcal{R}_k^{\mathrm{gh}}(-\Box)\hat{\xi}^\mu \, , \tag{3.34}$$

Now we promote the integral (3.29) with the source term in order to define a generating functional

$$S_{\text{source}} = -\int d^d x \ \sqrt{\bar{g}} \left\{ t^{\mu\nu}\hat{h}_{\mu\nu} + \bar{\sigma}_\mu \hat{\xi}^\mu + \sigma^\mu \hat{\bar{\xi}}_\mu + \mathcal{L}_\xi(\bar{g}_{\mu\nu} + \hat{h}_{\mu\nu}) + \tau_\mu \hat{\xi}^\nu \partial_\nu \hat{\xi}^\mu \right\} \quad (3.35)$$

where we introduced the sources $t_{\mu\nu}$ for $\hat{h}_{\mu\nu}$, $\bar{\sigma}_\mu$ for $\hat{\xi}^\mu$ and σ^μ for $\hat{\bar{\xi}}_\mu$ The two additional sources $\beta^{\mu\nu}$ and τ_μ couple to the BRST variation of $\hat{h}_{\mu\nu}$ and ξ^μ. This leads to a generating functional having the following dependencies

$$W_k \left[t^{\mu\nu}, \sigma^\mu, \bar{\sigma}_\mu; \beta^{\mu\nu}, \tau_\mu; \bar{g}_{\mu\nu}\right] \equiv W_k \left[J; J_{\text{BRST}}; \bar{g}_{\mu\nu}\right] \quad (3.36)$$

We see that, in addition to the sources, W_k also functionally depends on the background metric. Moreover, functional derivatives of W_k with respect to J and J_{BRST} generate the expectation values of the dynamical fields and BRST variations, respectively:

$$h_{\mu\nu} = \langle \hat{h}_{\mu\nu} \rangle = \frac{1}{\sqrt{\bar{g}}} \frac{\partial W_k}{\partial t_{\mu\nu}} \ , \xi^\mu = \langle \hat{\xi}^\mu \rangle = \frac{1}{\sqrt{\bar{g}}} \frac{\partial W_k}{\partial \bar{\sigma}_\mu} \ , \bar{\xi}_\mu = \langle \hat{\bar{\xi}}_\mu \rangle = \frac{1}{\sqrt{\bar{g}}} \frac{\partial W_k}{\partial \sigma^\mu} \quad (3.37)$$

Note that the expectation value of the full metric:

$$g_{\mu\nu} = \langle \hat{g}_{\mu\nu} \rangle = \bar{g}_{\mu\nu} + h_{\mu\nu} \ , \quad (3.38)$$

and to consider Γ_k as a functional of $g_{\mu\nu}$ rather than $h_{\mu\nu}$:

$$\Gamma_k \left[h, \xi, \bar{\xi}; \beta, \tau; \bar{g}\right] \Big|_{h=g-\bar{g}} = \Gamma_k \left[g, \bar{g}, \xi, \bar{\xi}; \beta, \tau\right] \quad (3.39)$$

The "semicolon variant" emphasizes the point of view that the fluctuations of the metric, h, may be regarded as matter-like excitations on a classical spacetime with metric $\bar{g}$. Instead, the "comma variant" makes it explicit that the EAA suffers from an extra $\bar{g}$-dependence over and above the one that combines with h to build up a full metric $g = \bar{g} + h$.

The k-derivative with $h_{\mu\nu}$ and the ghosts coupled to the appropriate sources, provides the starting point for the construction of the functional renormalization group equation for $\Gamma_k[g, \bar{g}, \xi, \bar{\xi}; \beta, \tau]$.

The flow equation can then be divided as:

$$k\partial_k \Gamma_k \left[h, \xi, \bar{\xi}; \bar{g}\right] = \frac{1}{2}\text{Tr}\left[\left(k\partial_k \hat{\mathcal{R}}_k\right)_{hh} \left(\Gamma_k^{(2)} + \hat{\mathcal{R}}_k\right)^{-1}_{\bar{h}h}\right]$$
$$- \frac{1}{2}\text{Tr}\left[\left(k\partial_k \hat{\mathcal{R}}_k\right)_{\xi\bar{\xi}} \left\{\left(\Gamma_k^{(2)} + \hat{\mathcal{R}}_k\right)^{-1}_{\bar{\xi}\xi} - \left(\Gamma_k^{(2)} + \hat{\mathcal{R}}_k\right)^{-1}_{\xi\bar{\xi}}\right\}\right] \ , \quad (3.40)$$

The resulting FRGE turns out to be a suitable tool to investigate the RG flow of gauge theories in a completely covariant approach. As previously sketched out, combining the methods of the FRGE with the background field formalism and applying it to metric gravity (including a suitable gauge-fixing term) yields the effective average

action $\Gamma_k[g, \bar{g}, \xi, \bar{\xi}]$, the primary tool for investigating the gravitational RG flow at the nonperturbative level. It is a functional of the dynamical metric g and the ghost fields ξ and $\bar{\xi}$, but it also has an extra $\bar{g}$-dependence.

(3) Most standard FRG analyses rely on *single-metric truncations*, obtained by projection onto such invariants that depend on $g_{\mu\nu}$ alone. During the computation of the flows this approximation amounts to identifying background and dynamical metric, $\bar{g} = g$ but only after the second functional derivative appearing in the FRGE has been taken. For "Bi-metric" studies distinguishing the dynamical metric $g_{\mu\nu}$ and the background metric $\bar{g}_{\mu\nu}$ for the Einstein–Hilbert truncation we refer to [217].

(4) On account of the large number of independent field components in gravitational theories, RG computations are particularly complicated. Thus, one has to approximate the exact flow by reducing the basis to a finite subset, truncating theory space. For QEG with the aid of computer algebra systems it has been possible to extend these truncations up to order 71 in the Ricci curvature [218] and computations of the infinite dimensional $f(R)$-truncation have been carried out [186, 219].

3.5. The Einstein–Hilbert flow

A first truncation consists in keeping the classical ghost terms but neglecting their action. This leads to the reduced flow equation

$$k\partial_k \Gamma_k\left[h, \xi, \bar{\xi}; \bar{g}\right] = \frac{1}{2}\mathrm{Tr}\left[\frac{k\partial_k \hat{\mathcal{R}}_k^{\mathrm{grav}}}{\Gamma_k^{(2)}[g, \bar{g}] + \hat{\mathcal{R}}_k^{\mathrm{grav}}}\right] - \mathrm{Tr}\left[\frac{k\partial_k \hat{\mathcal{R}}_k^{\mathrm{gh}}}{\mathcal{M}[g, \bar{g}] + \hat{\mathcal{R}}_k^{\mathrm{gh}}}\right] \qquad (3.41)$$

where $\mathcal{M}[g, \bar{g}]$ is the Faddeev–Popov operator obtained from varying (3.32):

$$\mathcal{M}[g, \bar{g}]^\mu{}_\nu = \bar{g}^{\mu\rho}\bar{g}^{\sigma\lambda}\bar{\nabla}_\lambda\left(g_{\rho\nu}\nabla_\sigma + g_{\sigma\nu}\nabla_\rho\right) - 2\beta_{\mathrm{gf}}\bar{g}^{\rho\sigma}\bar{g}^{\mu\lambda}\bar{\nabla}_\lambda g_{\sigma\nu}\nabla_\rho \,. \qquad (3.42)$$

Furthermore, here we shall employ the harmonic gauge which fixes $\beta_{\mathrm{gf}} = 1/2$. Concretely, in this way we pull out the classical gauge-fixing and ghost actions S_{gf} and S_{gh} from Γ_k, and also assume that the coupling to the BRST variations has the same form as in the bare action for all k.

The remaining functional Γ_k depends on both $g_{\mu\nu}$ and $\bar{g}_{\mu\nu}$. Performing the decomposition

$$\Gamma_k[g, \bar{g}] = \bar{\Gamma}_k[g] + \hat{\Gamma}_k[g, \bar{g}]$$
$$\bar{\Gamma}_k[g] = \Gamma_k[g, g] \qquad (3.43)$$
$$\hat{\Gamma}_k = \Gamma_k - \bar{\Gamma}_k \,,$$

we can separate the restriction of Γ_k on the diagonal, $\bar{\Gamma}_k[g]$, from the remaining off-diagonal term $\hat{\Gamma}_k$. It is to be stressed out that, by definition, $\hat{\Gamma}_k$ vanishes whenever its two

arguments are equal, i.e., $\hat{\Gamma}_k[g, g] = 0$. Furthermore, $\hat{\Gamma}_k$ contains quantum corrections to the gauge-fixing term, which also will vanish on the background $\bar{g} = g$.

At this stage $\Gamma_k[g, \bar{g}]$ is still a general bi-metric functional: it depends on two independent metrics g and $\bar{g}$. For a first analysis we restrict the truncation ansatz to the so-called single-metric truncations in which one either sets $\hat{\Gamma}_k[g, \bar{g}]$ to zero exactly (or at most allows it to be of the same form as S_{gf}, even if with a different prefactor $\hat{\Gamma}_k \propto S_{\mathrm{gf}}$). In this way, the only scale dependence in the EAA enters via the functional $\bar{\Gamma}_k[g]$.

Thus far, a determination of the scale dependence of these running constants by solving the flow equation within a single-metric ansatz is possible. The full truncation ansatz then reads

$$\Gamma_k[g, \bar{g}] = \bar{\Gamma}_k[g] + \hat{\Gamma}_k + S_{\mathrm{gf}} , \tag{3.44}$$

with $\hat{\Gamma}_k \propto S_{\mathrm{gf}}$. The projection onto the Einstein–Hilbert action had been first studied by [95, 97]:

$$\Gamma_k = \frac{1}{16\pi G(k)} \int \mathrm{d}^d x \sqrt{g}(R - 2\Lambda(k)) + \text{gauge fixing} + \text{ghosts} , \tag{3.45}$$

which consists of the classical Einstein–Hilbert action with running couplings, Newton's gravitational constant $G(k)$ and the cosmological constant $\Lambda(k)$. This represents the simplest single-metric truncation.

Explicitly, the *Einstein–Hilbert truncation* amounts to the choice:

$$\bar{\Gamma}_k[g] = \frac{1}{16\pi G(k)} \int \mathrm{d}^d x \sqrt{g}\Big(- R(g) + 2\Lambda(k)\Big)$$

$$\hat{\Gamma}_k[g, \bar{g}] = \alpha_{\mathrm{gf}}\Big(\frac{\bar{G}}{G(k)} - \frac{1}{\alpha_{\mathrm{gf}}}\Big) S_{\mathrm{gf}}[g - \bar{g}; \bar{g}] \tag{3.46}$$

where α_{gf} is the gauge-fixing parameter that occurs in the prefactor of the gauge-fixing term (3.33) and $\bar{G}$ denotes the k-independent reference value of the Newton's constant.

The first equation in (3.46) is the generalization of the classical Einstein–Hilbert action, which now is k-dependent, while the second one entails the possibility to change the gauge sector by introducing a non-vanishing $\hat{\Gamma}_k$ proportional to the classical S_{gf}.[5] After all, the chosen $\hat{\Gamma}_k$ replaces the constant gauge-fixing parameter α_{gf} in the prefactor of the original S_{gf} by the scale-dependent ratio $G(k)/\bar{G}$. However, $S_{\mathrm{gf}}[h; \bar{g}]$ is bilinear in the fluctuation $h = g - \bar{g}$, so still bi-metric. Hence, by the single-metric hypothesis, the scale dependence of its coefficient is assumed to be negligible, and to have small impact on $\bar{\Gamma}_k$, and consequently on $G(k)$ and $\Lambda(k)$. In conclusion, it is consistent in the single-metric ansatz to neglect this effect.

---

[5]This particular choice for $\hat{\Gamma}_k$ is motivated by algebraic simplifications.

With the above ansatz, the calculation of the RG flow of $G(k)$ and $\Lambda(k)$ will be simplest if one adopts a special member of the family of gauges in (3.32): There is a special choice of β_{gf} and α_{gf} which simplifies the algebra: we are free to choose $\beta_{\text{gf}} = \frac{1}{2}$, which corresponds to the standard harmonic gauge, and in addition to fix the gauge-fixing parameter to be $\alpha_{\text{gf}} = 1$.

It is convenient to relate the running Newton's constant to its fixed reference value $\bar{G}$ by means of the following dimensionless function $Z_N(k) = \bar{G}/G(k)$, such that

$$G(k) = \frac{\bar{G}}{Z_N(k)} \, . \tag{3.47}$$

Exploiting the single-metric ansatz, one can perform contractions with the full metric or with the fluctuations. Hence we can write $\mathcal{F}_\mu^{\alpha\beta} g_{\alpha\beta} = \mathcal{F}_\mu^{\alpha\beta} h_{\alpha\beta}$ in the gauge-fixing term, and the complete Einstein–Hilbert truncation ansatz then assumes the following form:

$$\Gamma_k[g,\bar{g}] = \frac{1}{16\pi\bar{G}} Z_N(k) \int \mathrm{d}^d x \sqrt{g}\Big(2\Lambda(k) - R(g)\Big) + \frac{Z_N(k)}{32\pi\bar{G}} \int \mathrm{d}^d x \sqrt{\bar{g}}\bar{g}^{\mu\nu} \mathcal{F}_\mu^{\alpha\beta} g_{\alpha\beta} \mathcal{F}_\nu^{\rho\sigma} g_{\rho\sigma} \, . \tag{3.48}$$

At this stage, the setup to compute the flow of $Z_N(k)$ and $\Lambda(k)$ is set.

3.5.1. *Evolution of Newton's constant and the cosmological constant*

Under the trace appearing in the reduced FRGE we need the second functional derivative of Γ_k. This leads to a quadratic form in the field fluctuations. In order to partially diagonalize the quadratic form we decompose the fields as the sum of a traceless tensor and a trace part (we refer the reader to Appendix D).

The differential equations for $Z_N(k)$ and Λ_k are obtained by comparing the coefficients of $\int \mathrm{d}^d x \sqrt{g}$ and $\int \mathrm{d}^d x \sqrt{g} R$ on both sides of the evolution equation at $g_{\mu\nu} = \bar{g}_{\mu\nu}$. For this purpose, we may insert an arbitrary family of metrics $\bar{g}_{\mu\nu}$ that is general enough to identify the terms and to distinguish them from higher-order terms in the derivative expansion, such as $\int \mathrm{d}^d x \sqrt{g} R^2$ or $\int \mathrm{d}^d x \sqrt{g} \nabla_\mu \nabla_\nu R$. These terms might for instance arise on the RHS of the FRGE. Usually, one exploits the freedom of choosing $\bar{g}$ by assuming it to be a maximally symmetric space.

The RHS of the flow equation involves then traces of functions of the covariant Laplacian acting on traceless symmetric tensors, scalars and vectors. Because we need only the zeroth and the first order in the curvature scalar we can expand in R and evaluate the traces by taking advantage of the heat kernel expansion (see Appendix C).

For all these intermediate steps we refer the reader to Appendix C and Appendix D.

Finally, defining the *anomalous dimension* related to the running Newton's constant as:

$$\eta_N(\lambda(k), g(k)) = -k\partial_k \ln Z_N(k) \,, \tag{3.49}$$

where we introduced the *dimensionless variables*

$$g(k) \equiv k^{d-2} = k^{d-2} Z_N(k)^{-1}\bar{G} \,,$$
$$\lambda(k) \equiv k^{-2}\Lambda(k) \,, \tag{3.50}$$

from (D.37) in Appendix D we can obtain the full *Einstein–Hilbert flow*:

$$k\partial_k g(k) = [(d-2) + \eta_N(\lambda(k), g(k))]\, g(k) \,,$$

$$k\partial_k \lambda(k) = -(2 - \eta_N(k))\lambda(k) + \frac{1}{2}g(k)(4\pi)^{1-d/2} \times$$
$$\times \left[2d(d+1)\Phi^1_{d/2}(-2\lambda(k)) - 8d\Phi^1_{d/2}(0) - d(d+1)\eta_N(k)\tilde{\Phi}^1_{d/2}(-2\lambda(k)) \right] \,. \tag{3.51}$$

Here the Φ and the $\tilde{\Phi}$ represent the so-called threshold functions introduced and discussed further in Appendix D, see (D.29).

The system (3.51) involves the anomalous dimension, η_N. From the projected FRGE it is obtained in the form

$$\eta_N(k) = \frac{g(k)\, B_1(\lambda(k))}{1 - g(k)\, B_2(\lambda(k))} \,, \tag{3.52}$$

with

$$B_1(\lambda(k)) = 32\pi \left(\frac{1}{4\pi}\right)^{d/2} \left[\frac{d(d+1)}{24}\Phi^1_{d/2-1}(-2\lambda(k)) - \frac{d(d-1)}{4}\Phi^2_{d/2}(-2\lambda(k)) \right.$$
$$\left. - \frac{d}{6}\Phi^1_{d/2-1}(0) - \Phi^2_{d/2}(0) \right] \,,$$

$$B_2(\lambda(k)) = 32\pi \left(\frac{1}{4\pi}\right)^{d/2} \left[-\frac{d(d+1)}{48}\tilde{\Phi}^1_{d/2-1}(-2\lambda(k)) + \frac{d(d-1)}{8}\tilde{\Phi}^2_{d/2}(-2\lambda(k)) \right] \,. \tag{3.53}$$

In $d = 4$ using the sharp cutoff introduced in Appendix D and the evaluation of the threshold functions in eq.(D.33), we obtain the following explicit RG equations [49]:

$$k\partial_k \lambda(k) = -(2 - \eta_N(k))\lambda(k) - \frac{g(k)}{\pi}\left[5\ln(1 - 2\lambda(k)) - 2\zeta(3) + \frac{5}{2}\eta_N \right] \,,$$

$$k\partial_k g(k) = (2 + \eta_N(k))g(k) \,, \tag{3.54}$$

$$\eta_N(k) = -\frac{2g(k)}{6\pi + 5g(k)}\left[\frac{18}{1 - 2\lambda(k)} + 5\ln(1 - 2\lambda(k)) - \zeta(2) + 6 \right] \,.$$

We can now display a number of typical RG trajectories obtained by numerically integrating the flows equations (3.54).

One can solve the resulting coupled differential equations numerically, obtaining the *phase portrait* of the involved coupling constants (see Figure 3.3). It was first obtained in [220] using the so called optimized cutoff (introduced in Appendix C), which has the advantage that all threshold functions can be evaluated analytically (see Appendix D).

The RG flow is indeed seen to be dominated by two fixed points: the Gaussian fixed point at $g_* = \lambda_* = 0$, and the non-Gaussian fixed point with $g_* > 0$ and $\lambda_* > 0$ (the so-called *Reuter fixed point*). There exist three types of trajectories emanating from the non-Gaussian fixed point: trajectories of Type Ia and Type IIIa which run towards negative and positive cosmological constant, respectively, and a single trajectory of Type IIa (also known as the *separatrix*), which hits the Gaussian fixed point for $k \to 0$.

Writing down the linearized renormalization group flow of the coupling constants $\lambda(k)$ and $g(k)$ in the vicinity of the Gaussian fixed point, one finds [97]

$$\lambda(k) = \alpha_1 \frac{\Lambda_0}{k^2} + \alpha_2 \varpi G_0 k^2 + \cdots$$
$$g(k) = \alpha_2 G_0 k^2 + \cdots \, ,$$

(3.55)

where α_1 and α_2 are constants of integration allowing to adjust the solution to given initial conditions, ϖ is a numerical constant of $O(1)$, and the infrared values $\Lambda_0 \equiv \Lambda(k = 0)$ and $G_0 \equiv G(k = 0)$ are constants of integration whose values select a specific RG trajectory in the 2D theory space. Following the parametrization in eq.(3.55), we can classify the three Types of trajectories and their asymptotic behavior:

Type	Sign of α_1	Asymptotic behavior when k $\to$ 0
Type Ia	$\alpha_1 < 0$	α_1-contribution dominates; $\lambda(k) \to -\infty$
Type IIa	$\alpha_1 = 0$	α_2-contribution dominates; $\lambda(k) \to 0$
Type IIIa	$\alpha_1 > 0$	α_1-contribution dominates; $\lambda(k) \to +\infty$

TABLE 3.1. Renormalization group flow of $\lambda(k)$ in the vicinity of the trivial fixed point, depending on the sign of α_1.

We discussed how within Asymptotic Safety, the fixed point can be also interacting or non-Gaussian. A possible scenario for Quantum Gravity is then supplied by the existence and the analysis of such a non-Gaussian fixed point.

The next sections in this chapter have been assembled from the author's publication [RF3].
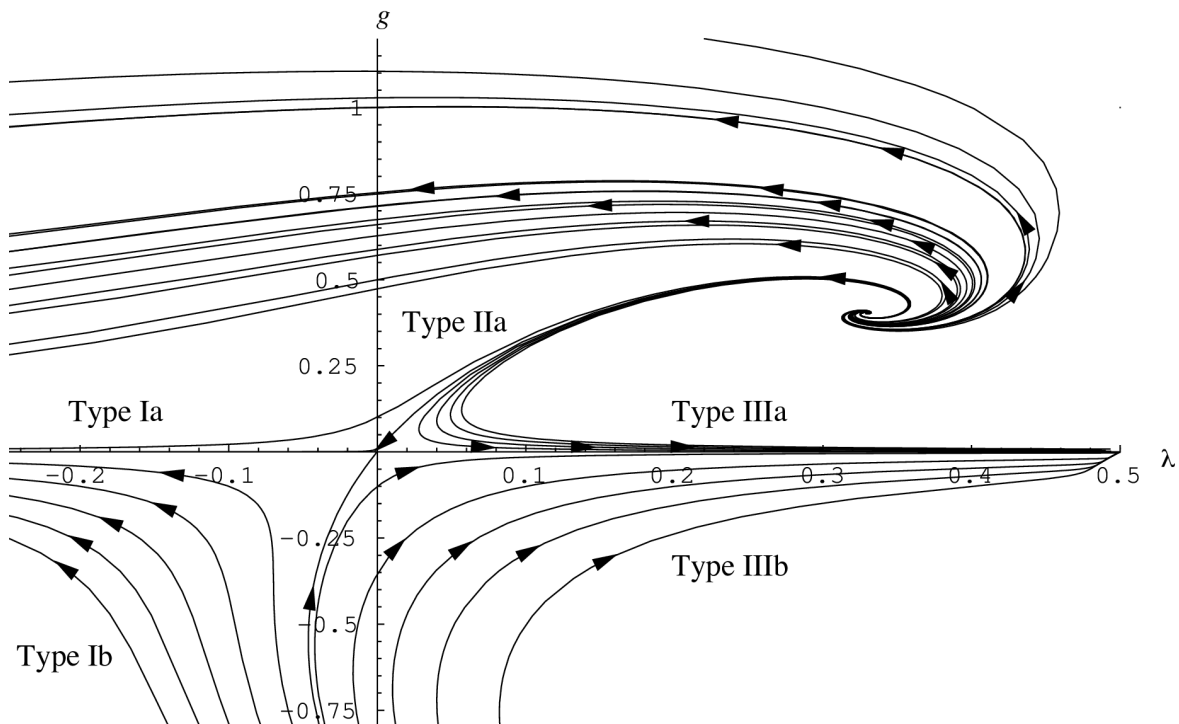
FIGURE 3.3. Part of coupling constant space of the Einstein–Hilbert truncation with its RG flow. The arrows point in the direction of decreasing values of k. The flow pattern is dominated by a non-Gaussian fixed point in the first quadrant and a trivial one at the origin. (First obtained in [97]).

3.5.2. *The trajectories simplified*

The classification of the RG trajectories implied by the ansatz (3.45) on the g-λ–plane of the dimensionless Newton's constant g and cosmological constant λ is well known and has been classified in [97]. As we discussed, they can be divided into three main classes, i.e., trajectories of Type Ia, Type IIa, and Type IIIa, respectively (see Figure 3.3).

They can be divided into two regimes:

(1) Fixed point regime. All these trajectories possess a non-Gaussian fixed point (g_*, λ_*) when $k \to \infty$. In particular the dimensionless cosmological constant behaves as $\lambda(k) = \Lambda(k)/k^2 \to \lambda_*$ in the asymptotic region (UV region). Hence

$$\Lambda(k) = \lambda_* \, k^2 \qquad (k \gtrsim \hat{k}) \qquad (3.56)$$

is a sufficiently good approximation to the exact trajectory in this regime. The approximation regime extends from "$k = \infty$" down to a scale of the order of the Planck mass m_{Pl}, typically denoted as $\hat{k}$. We define the Planck mass $m_{\mathrm{Pl}} \equiv G_0^{-1/2} = G(k=0)^{-1/2}$ in the conventional way by the running Newton's constant at $k = 0$.

(2) Semiclassical regime. Below a short transition regime near $\hat{k}$, all trajectories of the above three types enter a semiclassical regime within which the behavior of $\Lambda(k)$ can be approximate again. Qualitatively, the following simple formula provides a reliable approximation (see (3.55)):

$$\Lambda(k) = \Lambda_0 + \varpi \, G_0 \, k^4 \, . \tag{3.57}$$

The three types of trajectories are classified following the different signs of Λ_0. We have $\Lambda_0 < 0$, $\Lambda_0 = 0$, and $\Lambda_0 > 0$ for trajectories of Type Ia, IIa, and IIIa, respectively (see Table 3.1).

If $\Lambda_0 \neq 0$ it is convenient to introduce the two length scales

$$\ell \equiv \left(\frac{\varpi \, G_0}{|\Lambda_0|} \right)^{1/4} \, , \qquad L \equiv \left(\frac{\lambda_*}{|\Lambda_0|} \right)^{1/2} \, . \tag{3.58}$$

Hence, in the semiclassical regime,

$$\Lambda(k) = |\Lambda_0| \, \left(\ell^4 \, k^4 \pm 1 \right) \, , \tag{3.59}$$

where the plus sign (minus sign) applies to the Type IIIa (Type Ia). This function is required to be continuous at $k = \hat{k} \gg \ell^{-1}$. As a consequence, the RG data (ϖ, λ_*) and integration constants (Λ_0, G_0) determine the transition to occur at

$$\hat{k} = \left(\frac{\lambda_*}{\varpi G_0} \right)^{1/2} = \left(\frac{\lambda_*}{\varpi} \right)^{1/2} m_{\mathrm{Pl}} \, . \tag{3.60}$$

When $\Lambda_0 \neq 0$ the following "caricature" of the function $\Lambda(k)$ is useful:

$$\Lambda(k) = |\Lambda_0| \cdot \begin{cases} \ell^4 \, k^4 \pm 1 & \text{for} \quad 0 \leq k \lesssim \hat{k} \\ L^2 \, k^2 & \text{for} \quad k \gtrsim \hat{k} \end{cases} \tag{3.61}$$

It should be a reliable approximation, except possibly during a short interval of scales near $\hat{k}$ where the transition between the two regimes takes place. We shall investigate this transition regime separately below.

In the case $\Lambda_0 = 0$, the corresponding approximation reads instead

$$\Lambda(k) = |\Lambda_0| \cdot \begin{cases} \varpi \, m_{\mathrm{Pl}}^{-2} \, k^4 & \text{for} \quad 0 \leq k \lesssim \hat{k} \\ \lambda_* \, k^2 & \text{for} \quad k \gtrsim \hat{k} \end{cases} \tag{3.62}$$

Eq.(3.62) applies to the single trajectory of Type IIa, the separatrix [97].

Later on, we are going to employ those trajectories of the Einstein–Hilbert truncation which have a positive cosmological constant throughout, the Type IIIa. They are the theoretically most interesting, and at the same time phenomenologically most relevant ones. The most important property of the Type IIIa trajectories becomes manifest when we switch to the dimensionless cosmological constant $\lambda(k) = \Lambda(k)/k^2$. Then, in
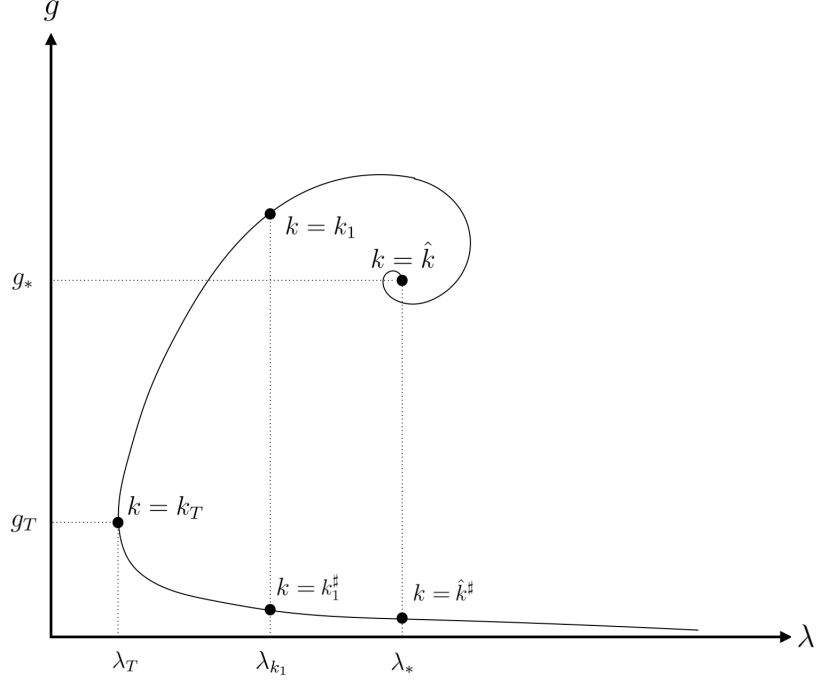
FIGURE 3.4. A typical RG trajectory of Type IIIa on the g-λ theory space. The duality transformation $k \mapsto k_T^2/k$ is seen to map the scale k_1 onto its dual $k_1^\sharp$, at which λ assumes the same value.

the semiclassical regime,

$$\lambda(k) = \frac{1}{2} \lambda_T \left[\left(\frac{k_T}{k} \right)^2 + \left(\frac{k}{k_T} \right)^2 \right] \tag{3.63}$$

Here we introduced the two abbreviations

$$k_T \equiv \ell^{-1} \equiv \left(\frac{\Lambda_0}{\varpi\, G_0} \right)^{1/4}, \tag{3.64}$$

$$\lambda_T \equiv \lambda(k_T) = \left(4\,\varpi\,\Lambda_0\,G_0 \right)^{1/2}. \tag{3.65}$$

Evidently the function $\lambda(k)$ of eq.(3.63) possesses a minimum. It assumes its smallest value, λ_T, at the scale $k = k_T$, i.e., when the trajectory on the g-λ plane passes the turning point (g_T, λ_T), see Figure 3.4.

We mostly employ the simple, but analytically tractable caricature of the function $\lambda(k)$ in which the semiclassical and the fixed point regimes are simply patched together [221].:

$$\lambda(k) = \begin{cases} \frac{1}{2} \lambda_T \left[\left(\frac{k_T}{k} \right)^2 + \left(\frac{k}{k_T} \right)^2 \right] & \text{for} \quad 0 \leq k \leq \hat{k} \\ \lambda_* & \text{for} \quad \hat{k} < k < \infty. \end{cases} \tag{3.66}$$

Eq.(3.66) correctly captures all features of a Type IIIa trajectory that are of conceptual relevance in the present context. It neglects however the small spirals around the non-Gaussian fixed point which can be seen in Figure 3.4. They play no essential role here.

Remark. Here a remark about the truncation is in order. Coming back to the running cosmological constant within the Einstein–Hilbert truncation, it is easy to generalize eq.(3.61) in a form which makes the required property manifest. In the semiclassical regime, say, with the normalization scale introduced in Subsection 3.2.1 $\mu \in [0, \hat{k}]$ and the running of $G(k) \approx G_{\text{ren}}$ neglected, we have in the present notation:

$$\Lambda^{(\Lambda_{\text{ren}}, \mu)}(k) \;=\; \Lambda_{\text{ren}} \;+\; \varpi \, G_{\text{ren}}(k^4 - \mu^4) \,. \tag{3.67}$$

In (3.67) the implicit μ-dependence assigned to Λ_{ren} by the Callan–Symanzik equation cancels precisely the explicit one, $\mu \frac{\mathrm{d}}{\mathrm{d}\mu}\Lambda^{(\Lambda_{\text{ren}}, \mu)}(k) = 0$, while the FRGE tells us that $k \frac{\mathrm{d}}{\mathrm{d}k}\Lambda^{(\Lambda_{\text{ren}}, \mu)}(k) = 4\varpi G_{\text{ren}}k^4$ at fixed renormalized parameters.

In the rest of the paper we shall continue to employ the choices $\mu = 0$ and $\Lambda_{\text{ren}} \equiv \Lambda_0$ adopted in the previous Subsection.

3.6. Self-consistent backgrounds

As we discussed above, the crucial feature of the GEAA approach is that it complies with the pivotal requirement of Background Independence by providing the $h_{\mu\nu}$-dynamics simultaneously on all backgrounds possible. The correlation functions $\langle \hat{h}_{\mu\nu}(x_1) \, \hat{h}_{\rho\sigma}(x_2) \cdots \rangle_{\bar{g}}$ are then obtained by differentiating repeatedly Γ_k, with respect to $h_{\mu\nu}$, and they are functionals of $\bar{g}_{\mu\nu}$.

The expectation value of the full metric operator $\hat{g}_{\mu\nu} \equiv \bar{g}_{\mu\nu} + \hat{h}_{\mu\nu}$ in the quantum theory of the fluctuations in the $\bar{g}_{\mu\nu}$-background is given by the one-point function $\langle \hat{h}_{\mu\nu}(x) \rangle_{\bar{g}}$:

$$\langle \hat{g}_{\mu\nu} \rangle_{\bar{g}} \equiv \bar{g}_{\mu\nu} + \langle \hat{h}_{\mu\nu} \rangle_{\bar{g}} \,. \tag{3.68}$$

In general this expectation value differs from the externally prescribed metric $\bar{g}_{\mu\nu}$. However, there exist particular backgrounds, so-called *self-consistent geometries* with metrics $(\bar{g}(k)^{\text{sc}})_{\mu\nu}$, on which the one-point function of $\hat{h}_{\mu\nu}$ vanishes. Hence, even when the quantum fluctuations are switched on, the prescribed self-consistent background remains unaffected:

$$\langle \hat{h}_{\mu\nu} \rangle_{\bar{g}} = 0 \iff \langle \hat{g}_{\mu\nu} \rangle_{\bar{g}} = \bar{g}_{\mu\nu} \quad \text{for} \quad \bar{g} = \bar{g}(k)^{\text{sc}} \,. \tag{3.69}$$

Self-consistent background metrics are calculated by solving the following *tadpole condition*[6] which is properly an effective Einstein equation:

$$\frac{\delta}{\delta h_{\mu\nu}(x)} \Gamma_k\left[h; \bar{g}\right]\bigg|_{h=0, \; \bar{g}=\bar{g}(k)^{\mathrm{sc}}} \;=\; 0 \,. \tag{3.70}$$

Seemingly, generic solutions $\left(\bar{g}(k)^{\mathrm{sc}}\right)_{\mu\nu}$ will depend on the RG scale, k. Assuming a smooth k-dependence, it is natural to interpret the map $k \mapsto \left(\bar{g}(k)^{\mathrm{sc}}\right)_{\mu\nu}$ as a parametrized curve in the space of all metrics, and the *generalized RG trajectory* $k \mapsto \left(\Gamma_k, \; \left(\bar{g}(k)^{\mathrm{sc}}\right)_{\mu\nu}\right)$ as a curve in its product with theory space.

At this point a remark concerning the advocated principle of Background Independence (see Section 1.3) is in order. The principle is implemented in an indirect way: Rather than working with objects that are *literally independent of the background metric*, the actions Γ_k and all the expectation values do have a non-trivial dependence on $\bar{g}_{\mu\nu}$. However, $\bar{g}_{\mu\nu}$ is kept *completely arbitrary*: at no stage of the calculation it is identified with any concrete metric "by hand". On the contrary, it is the dynamics of the gravitational and matter fluctuations which determines the expectation value of the metric: this is what is encoded in the tadpole condition (3.70), it selects a specific $\bar{g}_k^{\mathrm{sc}}$ from the space of all background metrics $\{\bar{g}_{\mu\nu}\}$, such that the $\hat{h}_{\mu\nu}$ fluctuations are "as content as possible" about the background metric offered to them. The fluctuations build up a zero expectation value $\langle\hat{h}_{\mu\nu}\rangle_{\bar{g}}$ that does not further correct the metric found by the effective Einstein equation, $\langle\hat{g}_{\mu\nu}\rangle_{\bar{g}} = \bar{g}_{\mu\nu} \equiv \left(\bar{g}_k^{\mathrm{sc}}\right)_{\mu\nu}$. It is in this sense that the framework of the gravitational effective average action complies with the principle of Background Independence.

3.6.1. *Running Einstein spaces*

Let us introduce a technically particular convenient class of running self-consistent metrics whose k-dependence resides entirely in their conformal factor:

$$g_{\mu\nu}^k = f(k)\, g_{\mu\nu}^{k=0} \,. \tag{3.71}$$

We assume that we are dealing with pure Quantum Gravity (or matter contributions are negligible), and that the Einstein–Hilbert truncation is employed: the effective field

---

[6]One may wonder what the analogous equations for the ghosts and anti-ghosts are: effectively these are solved by assigning vanishing expectation values to them [95]. If one further considers matter coupled gravity, the tadpole condition of the metric is coupled to the respective equations from the matter sector. De facto, eq.(3.70) as it stands applies only under those circumstances where the matter expectation values do not influence the geometry significantly.

equations are $G_{\mu\nu}[g^k_{\alpha\beta}] = -\Lambda(k)g^k_{\mu\nu}$, or equivalently, with $R_\mu{}^\nu[g^k_{\alpha\beta}] = (g^k)^{\nu\rho}R_{\mu\rho}[g^k]$,

$$R_\mu{}^\nu[g^k_{\alpha\beta}] = \frac{2}{d-2}\,\Lambda(k)\,\delta_\mu{}^\nu\,. \tag{3.72}$$

In this setting, the input from the RG equations is the k-dependence of the running cosmological constant, $\Lambda(k)$. The latter can be of either sign, and it also might vanish at isolated scales (see Section 3.5). In full generality, it will be convenient to express it in the form

$$\Lambda(k) = \sigma\,|\Lambda(k)|$$

with the piecewise constant sign function $\sigma = \pm 1$, and to introduce the Hubble parameter

$$H(k) = \left[\frac{2|\Lambda(k)|}{(d-1)(d-2)}\right]^{1/2}. \tag{3.73}$$

The absolute value of the cosmological constant is therefore

$$|\Lambda(k)| = \frac{1}{2}(d-1)(d-2)\,H(k)^2. \tag{3.74}$$

It is known that for every fixed value of k, the solutions to the effective field equation

$$R_\mu{}^\nu[g^k_{\alpha\beta}] = \sigma(d-1)\,H(k)^2\,\delta_\mu{}^\nu \tag{3.75}$$

are arbitrary Einstein manifolds [222] with scalar curvature

$$R[g^k_{\alpha\beta}] = \sigma\,d(d-1)\,H(k)^2. \tag{3.76}$$

Among them, in Euclidean signature, there are the distinguished ones which possess a maximum number of Killing vectors, namely the spheres $\mathbb{S}^d$, pseudo-spheres $\mathbb{H}^d$, and the flat space $\mathbb{R}^d$ (see Appendix E). They exist for $\sigma = +1$ and $\sigma = -1$ when $H(k) \neq 0$, and for $H(k) = 0$, respectively.

The motivation for the d-dependent factors in the definition (3.73) is as follows. Comparing (3.76) with the curvature scalar of maximally symmetric spaces reveals that, when $g^k_{\mu\nu}$ is maximally symmetric, $1/H(k)$ is the radius of curvature of the related sphere or pseudo-sphere. Actually $H(k)$ can be identified with the conventional Hubble parameter. As a result, for maximally symmetric spacetimes the Riemann tensor is normalized as follows:

$$R_{\mu\nu\rho\sigma}[g^k_{\alpha\beta}] = \sigma\,H(k)^2\,[g_{\mu\rho}g_{\nu\sigma} - g_{\mu\sigma}g_{\nu\rho}]\,. \tag{3.77}$$

In what follows, we stress out that that even if we employ the quantity $H(k)$ defined by (3.73) as a convenient way of rewriting the cosmological constant, we are *not* restricting our analysis to maximal symmetry.

Coming back to the problem of finding solutions to (3.72), let us fix some convenient reference scale k_{R} at which

$$\Lambda(k_{\mathrm{R}}) \equiv \Lambda_{\mathrm{R}} \equiv \frac{1}{2}\sigma \, (d-1)(d-2) \, H_{\mathrm{R}}^2 \tag{3.78}$$

and let us pick an arbitrary solution $g_{\mu\nu}^{\mathrm{R}}(x^\rho)$ of the classical vacuum Einstein equation involving this particular value of the cosmological constant:

$$R_\mu{}^\nu[g_{\alpha\beta}^{\mathrm{R}}] = \sigma(d-1) \, H_{\mathrm{R}}^2 \, \delta_\mu{}^\nu \tag{3.79}$$

It then follows that the "running metric" given by

$$g_{\mu\nu}^k(x^\rho) = Y(k)^{-1} \, g_{\mu\nu}^{\mathrm{R}}(x^\rho) \, , \tag{3.80}$$

with $g_{\mu\nu}^k|_{k=k_{\mathrm{R}}} = g_{\mu\nu}^{\mathrm{R}}$, and

$$Y(k) \equiv \frac{|\Lambda(k)|}{|\Lambda_{\mathrm{R}}|} \equiv \frac{H(k)^2}{H_{\mathrm{R}}^2} \tag{3.81}$$

solves the effective field equation (3.72) on all scales k that are sufficiently close to k_{R}. This is to say that Λ must not have any zero between k and k_{R} so that $\sigma = \mathrm{sign}(\Lambda(k)) = \mathrm{sign}(\Lambda_{\mathrm{R}})$ is a constant function. Equation (3.80) is easily proved by noting that the Ricci tensor, with mixed indices, behaves as

$$R_\mu{}^\nu[c^{-2}g_{\alpha\beta}] = c^2 R_\mu{}^\nu[g_{\alpha\beta}] \tag{3.82}$$

under global Weyl transformations with an arbitrary real c.

3.7. Lorentzian spacetimes

It would be extremely interesting to confront the results from the RG flow analysis with real Nature. One of the intriguing questions is whether the fixed point has any implications for the actual Universe, in cosmology for example.

The signature of spacetime represents the principal obstacle preventing a straightforward realistic physical interpretation of the picture emerging from Asymptotic Safety. While the existing analyses all deal with effective spacetimes of Euclidean signature, we need their Lorentzian counterparts in order to determine their potential relevance to the real world.

3.7.1. *Signature change: bare vs. effective level*

Switching from Euclidean to Lorentzian signature, two distinct challenges have to be faced:

(A) Obtain RG trajectories $k \mapsto \Gamma_k$ on a theory space which is constituted of functionals that are constructed on Lorentzian metrics.

(B) Derive, analyze, and interpret the flows of hyperbolic (rather than elliptic) kinetic operators, typically of the d'Alembertian (appearing in the Hessian of the effective action for instance), in the background of the running self-consistent metrics implied by (A).

The difficulties related to (A) and (B) are related to quite different levels of the theory that is important to distinguish: Challenge (A) arise because of the Lorentzian signature of the *bare* metrics. These technical problems are encountered also in "simple" matter field theories. Challenge (B) instead is characteristic of Quantum Gravity, because the novel aspects are due to the Lorentzian character of *effective* (expectation value) metrics.

3.7.2. *Timelike vs. spacelike fluctuation modes*

Regarding the first sector of questions, (A), the following preliminary remarks are in order. To date, most of the FRG studies in the literature employ Euclidean background spacetimes. However, there is a reason for preferring the Euclidean signature in the FRG context: The momentum-square of the fluctuations to be integrated out is *positive semi-definite* and the *order* in which different fluctuation modes are integrated out along the RG trajectory is canonically established: high $(momentum)^2$ first, low $(momentum)^2$ later.[7]

In Lorentzian and curved spacetimes, already on a rigid Minkowski space, no distinguished ordering of the modes with a standard canonical status is given: Momentum-squares can have either sign now, so distinguishing spacelike from timelike fluctuation modes, and already this distinction leads to a variety of different, equally plausible orderings. A first example would be to first integrate out all timelike modes and thereafter all spacelike ones, or the other way around. A more democratic one would alternate them, timelike-spacelike-timelike-spacelike $\cdots$, and clearly many more schemes are conceivable.

Most importantly, not all such schemes are equivalent when it comes to considering nonperturbative continuum limits or when Γ_k is utilized as the action functional underlying an effective field theory.

---

[7]Recently it has been highlighted, that searching for new universality classes in Euclidean Quantum Gravity one should also consider different unconventional mode ordering schemes, which do not rely on the physical momentum [223, 224].

It has also been proposed to relate a hypothetical Lorentzian flow equation and/or its solutions to their Euclidean analogs by some sort of analytic continuation, like a Wick rotation [178, 179, 225]. Such a relationship would strongly constrain the "correct" integration scheme. However, we shall not follow this route here, since in Quantum Gravity the standard form of the Wick rotation is not available (nonetheless for an interested reader we suggest refs.[181, 182, 226]).

Yet another avenue is a purely spatial coarse graining achieved through a spatial cutoff function. This would leave time dependencies untouched, see ref. [183] for recent progress in a gravitational context. For a different, but likewise state-sensitive approach, see ref.[184].

3.7.3. *Path integral vs. FRGE*

For a mixed sequence of timelike and spacelike modes it may not be straightforward to characterize the desired ordering by simple bounds (technically speaking, "cutoffs") on the momenta of the modes, and to find a pseudo differential operator that would implement it in a flow equation. Hence, rather than solving a flow equation, which still has to be constructed, it is best at this stage to think of the piecemeal integrating out of modes that underlies Γ_k, as a procedure of performing the regularized *path integral* step by step.[8]

The path integral formulation has a main advantage: after expanding the integration variable, $\hat{h}_{\mu\nu}(x)$, in the desired basis of field space, $\hat{h}_{\mu\nu} = \sum_{n,m} a_{nm} (\chi_{nm})_{\mu\nu}$, the actual integration can be performed over the coefficients a_{nm}, and this gives direct access to the individual basis modes χ_{nm}.

3.7.4. *RG Lorentzian trajectories employed*

Here, we are not aiming at the construction of a fully general Lorentzian flow equation as this exists in Euclidean spacetime. However, the present investigation does not depend on the explicit form of such an equation. Chapter 7 is devoted to the second complex of problems, part (B). Thereby we shall work within a truncation of theory space, the Einstein–Hilbert truncation [95, 97, 114], which is known to yield identical trajectories in the Euclidean and the Lorentzian setting. As we explained in detail in

---

[8]There are a number of ongoing works on domains of "allowable" complex metrics for a path integral of gravity [181, 227–230] and on applications of Picard–Lefschetz theory to it [231].

Subsection 3.5.2, an approximation to its RG trajectories is perfectly sufficient for our purposes.

Their Lorentzian interpretation corresponds to a totally symmetric ordering scheme for the integrating out of timelike and spacelike modes, respectively. There is one single parameter $k > 0$ which defines two independent cutoffs. At the scale k, the modes which are already integrated out are those with $|\mathcal{F}_n| \geq k^2$, where $\mathcal{F}_n$ is the eigenvalue with respect to the d'Alembertian $-\Box_g$. Hence,

$$
\begin{aligned}
\text{spacelike modes integrated out:} & \quad \mathcal{F}_n \; \geq \; + k^2 \,, \\
\text{timelike modes integrated out:} & \quad \mathcal{F}_n \; \leq \; - k^2 \,.
\end{aligned}
\tag{3.83}
$$

The use of these trajectories is also motivated by recent work that established the Asymptotic Safety of Quantum Einstein Gravity on foliated spacetime manifolds [115, 116, 232–235]. Also, the framework is broad enough for a comparison with Monte-Carlo data from Causal Dynamical Triangulations [236–239], an approach in which Lorentzian geometries play a critical role, see [100, 240–244].

CHAPTER 4

Recent developments of the FRG

Executive summary. Built on the functional renormalization group equation for gravity, we follow the derivation of another flow equation that governs the evolution of renormalized composite operators. This evolution becomes encoded into that of the composite operators' anomalous dimensions. Their values in the UV fixed-point regime can be interpreted as quantum corrections to the classical scaling dimensions of the composite operators. As a recent technical development, we introduce the essential scheme. It has been shown that one can restrict the flow to the running of the couplings appearing in expressions for physical observables, so-called essential couplings. This freedom can then be exploited to simplify and optimize the calculation of physical quantities of interest.

What is new? The main results of this chapter are taken from the literature. The discussion around the role of the source has been extracted from a publication of the author.

Based on: Partially based on reference [RF7].

Plan of this Chapter. In this chapter, we will introduce recent developments in the FRG framework, which constitute important building blocks in the program, in order to construct observables and evaluate their scaling.

To make contact with quantum-gravitational observables, it is required to study the renormalization behavior of so-called geometric or relational operators which constitute an important class of *composite operators*. Inspired by the Effective Average Action derivation, C. Pagani [195] initiated the program of the renormalization in the FRG framework by adding a cutoff term to the generator functional for the connected Green functions of the composite operator. In Section 4.1 we review the derivation of the flow equation for the composite operators.

Pursuing the goal of the Asymptotic Safety program and generalizing it to the construction of observables, one should get rid of possible redundancies contained in theory space. In fact, not all couplings appearing in the given basis will also enter into the observables. In Section 4.2 we explore further details and consequences of this fact, what appeared under the name of the *Essential Renormalization Group*.

4.1. Composite operators

The existence of a NGFP controlling the high-energy behavior of gravity (or any other completion of the gravitational force laws at microscopic scales) raises the intriguing question how to characterize the properties of spacetime in the quantum regime. A possible characterization could then be based on the anomalous scaling dimensions of geometric operators comprising for instance, the volumes of spacetime, volumes of surfaces embedded into spacetime, the geodesic length, or correlation functions of fields separated by a fixed geodesic distance.

The key strength of the FRG formalism is that it can be extended to compute the scaling of composite operators which are not part of the EAA. This approach was pioneered by C. Pagani [195] and developed further in [192, 245, 246].

Parts of this chapter have been extracted and rearranged from the author's publication [RF7].

4.1.1. *Flow of composite operators*

We will generalize the inclusion of composite operators into the FRG framework constructed in Chapter 3. The main result of this subsection will be the composite operator FRGE which, together with the GEAA, describes the renormalization of composite operators. In particular, the *anomalous dimension matrix* of the composite operators can be computed.

(1) Technically, we will define as *composite operator*, any operator O, function of the fields and their derivatives. For example, we could consider the field to some power n, i.e., $O(x) = \phi^n(x)$. In the functional integral formulation of standard QFT one can treat composite operators $\hat{\mathcal{O}}(x) = \mathcal{O}[\hat{\phi}](x)$ coupling them to external sources by adding to the microscopic action a term

$$\int \mathrm{d}^d x \, \hat{\mathcal{O}}(x)\varepsilon(x)\,, \tag{4.1}$$

where $\varepsilon(x)$ denotes the source at the point x. In this way one obtains insertions of composite operators in correlation functions by taking suitable functional derivatives of the path integral with respect to the source [195, 246]. For example the expectation value of the composite operator reads

$$\langle \hat{\mathcal{O}}(x) \rangle = -\frac{\delta}{\delta \varepsilon(x)} \int \mathcal{D}\hat{\phi} \, \exp\left\{ -S[\hat{\phi}] - \int \mathrm{d}^d x \, \hat{\mathcal{O}}(x)\varepsilon(x) \right\} \Bigg|_{\varepsilon=0}. \tag{4.2}$$

Then, analogously to Section 3.4, we define the generating functional $W[J, \varepsilon]$ for the connected Green's functions of the fields and the connected correlation functions of the composite operators by

$$e^{W[J,\varepsilon]} \equiv \int \mathcal{D}\hat{\phi} \, \exp\left\{-S[\hat{\phi}] - \int \mathrm{d}^d x \, \hat{\mathcal{O}}(x)\varepsilon(x) + \int \mathrm{d}^d x J(x)\hat{\phi}(x)\right\}. \tag{4.3}$$

The associated effective action is obtained via a Legendre transform with respect to J at fixed ε to obtain a functional $\Gamma[\phi, \varepsilon]$ where ϕ is the expectation value of the field $\hat{\phi}$ in the presence of the source J. The expectation of the composite operator is then given by expanding the effective action around $\varepsilon = 0$

$$\Gamma[\phi, \varepsilon] = \Gamma[\phi] + \int \mathrm{d}^d x \, \varepsilon(x)\langle\hat{\mathcal{O}}(x)\rangle + O(\varepsilon^2), \tag{4.4}$$

(2) As it has been performed in Section 3.4, the effective action $\Gamma[\phi, \varepsilon]$ can also be modified to allow for a regulator $\mathcal{R}_k$ which suppresses infra-red fluctuations of the fields ϕ around their mean values. In particular, $\Gamma_k[\phi, \varepsilon]$ can be defined by its functional integro-differential representation (compare with (3.6)):

$$\begin{aligned} e^{-\Gamma_k[\phi,\varepsilon]} = & \int \mathcal{D}\hat{\phi} \, \exp\left\{-S[\hat{\phi}] - \int \mathrm{d}^d x \, \hat{\mathcal{O}}(x)\varepsilon(x) \right. \\ & \left. + \int \mathrm{d}^d x \sqrt{\bar{g}}(\hat{\phi} - \phi)\frac{\delta}{\delta\phi}\Gamma_k[\phi, \varepsilon] - \frac{1}{2}\int \mathrm{d}^d x \sqrt{\bar{g}}(\hat{\phi} - \phi)\mathcal{R}_k[\bar{g}](\hat{\phi} - \phi)\right\} \end{aligned} \tag{4.5}$$

The k- and ϕ-dependent expectation value is given by of $\mathcal{O}_k(x) \equiv \langle\hat{\mathcal{O}}(x)\rangle$ is again given by expanding $\Gamma_k[\phi, \varepsilon]$ to first order in ε

$$\Gamma_k[\phi, \varepsilon] = \Gamma_k[\phi] + \int \mathrm{d}^d x \, \varepsilon(x) \, \mathcal{O}_k(x) + O(\varepsilon^2). \tag{4.6}$$

The FRGE (3.7) for $\Gamma_k[\phi, \varepsilon]$ is given by the usual equation [89, 208]:

$$k\partial_k \Gamma_k[\phi, \varepsilon] = \frac{1}{2}\mathrm{Tr}\left[\left(\Gamma_k^{(2,0)}[\phi, \varepsilon] + \mathcal{R}_k\right)^{-1} k\partial_k \mathcal{R}_k\right]. \tag{4.7}$$

Now comparing order by order in ε, the flow equation for composite operators is given by [195, 247], to lowest order,

$$\int \mathrm{d}^d x \, \varepsilon \, k\partial_k \mathcal{O}_k = -\frac{1}{2}\mathrm{Tr}\left[\left(\Gamma_k^{(2)} + \mathcal{R}_k\right)^{-1}\left(\int \mathrm{d}^d x \, \varepsilon \mathcal{O}_k^{(2)}\right)\left(\Gamma_k^{(2)} + \mathcal{R}_k\right)^{-1} k\partial_k \mathcal{R}_k\right], \tag{4.8}$$

where $\mathcal{O}_k^{(2)}$ is the Hessian of the composite operator.

(3) The flow equation for the composite operator $\mathcal{O}_k$ must be supplied by an initial condition at $k = \Lambda$. Since, in the limit $k \to \infty$ we have that

$$\lim_{k\to\infty} \mathcal{O}_k = \mathcal{O}|_{\hat{\phi}\to\phi}, \tag{4.9}$$

setting the initial condition for $\Lambda \to \infty$ specifies which composite operator $\hat{\mathcal{O}}$ we are taking the expectation value of. Then by following the flow to $k = 0$ we obtain the expectation value

$$\mathcal{O}_0 = \langle \hat{\mathcal{O}} \rangle . \tag{4.10}$$

In this manner *solving the flow equation for the composite operator gives us a concrete method to compute expectation values of observables.*

(4) To concretely solve the equation (4.8), some approximation must be implemented. In particular, one may expand the composite operator $\mathcal{O}_k$ in a basis of k-independent operators $\{\mathcal{O}_i(x)\}$

$$\mathcal{O}_k(x) = \sum_i a^i(k)\mathcal{O}_i(x) , \tag{4.11}$$

so that their k-dependence can be parametrized as

$$k\partial_k a_j = \sum_i a^i \gamma_{ij} , \tag{4.12}$$

It has been shown in [246] that the scaling operators of the theory have dimensions, with quantum corrections included, given by the eigenvalues of the *stability matrix*

$$S_{ij} = d_i \delta_{ij} + \gamma_{ij} . \tag{4.13}$$

where S_{ij} is a function of the couplings included in the effective action Γ_k. The *anomalous dimension matrix* γ_{ij} can be directly found, inserting the expansion (4.11) in the flow equation (4.8) and expanding the trace. To lowest order in ε

$$\sum_j \gamma_{ij} \int \mathrm{d}^d x \, \varepsilon(x) \mathcal{O}_j(x) =$$
$$- \frac{1}{2} \mathrm{Tr} \left[\left(\Gamma_k^{(2)} + \mathcal{R}_k \right)^{-1} \left(\mathrm{d}^d x \, \varepsilon(x) \, \mathcal{O}_i^{(2)}(x) \right) \left(\Gamma_k^{(2)} + \mathcal{R}_k \right)^{-1} \partial_t \mathcal{R}_k \right] . \tag{4.14}$$

For the sake of comparison with other results in the literature, it is useful to work out the relation between scaling operators defined by means of explicit introduction of the sources and those found by linearizing the RG flow around the fixed point.

4.1.2. *Interpretation of the anomalous dimension matrix*

We had already defined the anomalous dimension in Chapter 3. In general, given a set of RG equations, we define the *stability matrix* as

$$S_{ij} \equiv \frac{\partial}{\partial a^j} \beta_i = d_i \delta_{ij} + \gamma_{ij} . \tag{4.15}$$

One can argue that the negative eigenvalues of $\gamma_{ij}|_{u=u_*}$ at the fixed point are the anomalous scaling dimensions that encode the quantum corrections to the classical scaling

dimensions of the couplings [195]. If we interpret $\{O_1[g,\bar{g}](x),\cdots,O_n[g;\bar{g}](x)\}$ as the basis of a first truncation for the effective action, we can identify the stability matrix B_{ij} defined in (3.15) with the beta function matrix S_{ij} [246].

4.1.3. (Non-)constant source

Let us reconsider the role of the source $\varepsilon(x)$ in calculating γ_{ij}. In particular, suppose we choose to make the source a constant $\varepsilon(x) = \varepsilon$. Then, we can factor out ε from the integral and it appears therefore as a source for the observable integrated over spacetime

$$\int \mathrm{d}^d x \, \varepsilon \, \mathcal{O}_k(x) = \varepsilon \sum_i a^i(k) \int \mathrm{d}^d x \, \mathcal{O}_i(x) \tag{4.16}$$

Hence, if the integrated basis operators $\int \mathrm{d}^d x \, \mathcal{O}_i(x)$ are linearly dependent then we are not able to determine all components of γ_{ij}. Essentially this means that, in the absence of boundaries, the flow of all the operators which are total derivatives is lost by restricting the source to be constant.

Let us therefore employ a basis where all linearly independent *boundary operators* of the form $\mathcal{O}_i = \partial_\mu \mathcal{O}_i^\mu$ form a subset of the total basis, the latter being is completed by adding a set of *bulk operators* which are linearly independent of all boundary operators. Then, if i is a boundary index and j a bulk index, then $\gamma_{ij} = 0$.

To see this, note that

$$\int \mathrm{d}^d x \, \varepsilon(x)(\partial_\mu \mathcal{O}_i^\mu)^{(2)} = -\int \mathrm{d}^d x \, (\partial_\mu \varepsilon(x)) \, \mathcal{O}_i^{\mu\,(2)}, \tag{4.17}$$

and thus if $\mathcal{O}_i(x) = \partial_\mu \mathcal{O}_i^\mu$ is inserted into the LHS (4.14), then RHS must be given by $-\sum_{j \in \text{boundary indices}} \gamma_{ij} \int \mathrm{d}^d x \partial_\mu \varepsilon(x) \mathcal{O}_j^\mu(x)$. A consequence of this is that by taking the source to be constant, we project out all the boundary operators. In this way, we are still able to compute the flow of the bulk terms in a consistent manner.

On the other hand, allowing the source to be non-constant, we are then able to compute the flow of the boundary operators in addition.

4.2. ESSENTIAL SCHEME

Seeking for observables carrying physical information in Quantum Gravity we will now review a recent development in the FRG framework: the *essential renormalization group scheme*. It entails a substantial a simplification of the necessary computations, since

it disentangles unphysical information (encoded in the inessential couplings) and the physical content (encoded in the essential couplings).

The *essential renormalization group scheme* was developed in 2021 by A. Baldazzi, R. Ben Alì Zinati and K. Falls [175, 199]. We will follow their derivation of the covariant flow equation and solve it in the so-called *minimal essential scheme*.

In this section we review the essential RG approach using the case of a single scalar field [199] to avoid pure technicalities and then we present the generalization for gravity developed in [175].

4.2.1. *Frame covariant QFT*

We have discussed in the approach of Chapter 3, which we will now denote as the *standard approach*, the EAA obtains a dependence on the RG scale k from only one source: a momentum-dependent IR cutoff which implements the coarse graining procedure. In the essential scheme we introduce a second source of k-dependence, which results from performing scale-dependent field reparameterization along the flow. The latter are k-dependent diffeomorphisms $\phi \mapsto \hat{\varphi}_k[\phi]$ of configuration space, i.e., the space we integrate over in the functional integral.

In order to analyze the field dependencies, in this subsection, we will state the principle of *frame covariance* in QFT. In particular the notion of *frame* is central.

(1) Frames and frame transformations. In classical field theory the dynamics is encoded in an action $S[\phi(x)]$, which can be considered as a scalar function on the configuration space $\mathcal{M}$. This manifold is viewed as the manifold where the points are field configurations $\phi : \mathbb{R}^d \to \mathbb{R}$. The dynamical field variable $\phi(x)$ represents then a preferred coordinate system for which the action takes a particular form. The variable $\phi(x)$ is then typically defined as the "field", if it assumes a straightforward physical significance, that is, if it can be associated to an easily accessible observable experimentally. From a geometrical point of view, the identification of a field is equivalent to defining a particular local set of "frames" on $\mathcal{M}$.

The variation of S wrt. $\phi(x)$ provides the equations of motion for the field variable ϕ. However, it could be the case that the equations of motion are relatively difficult to solve when written in terms of the original ϕ. Possibly they can be simplified by re-expressing the action in terms of different variables $\varphi[\phi]$: Provided the map $\varphi[\phi]$ is invertible, i.e., assuming that the inverse map $\phi[\chi]$ exists, this amounts to choosing a different frame. Since the invertibility ensures that the Jacobian between the two frames is non-singular, the solutions to the two equations of motion are then in a one-to-one correspondence.

Formally, actions in two different frames will transform as scalars on $\mathcal{M}$, where a change of frame is understood as a *diffeomorphism* from $\mathcal{M}$ to itself. Under an infinitesimal frame transformation $\phi \to \xi[\phi]$, the action transforms as

$$S[\phi] \;\to\; S[\phi] + \int \mathrm{d}^d x \, \xi[\phi](x) \frac{\delta}{\delta\phi(x)} S[\phi] \, . \tag{4.18}$$

Accordingly, classical field theory can be formulated in a language covariant under such transformation: This allows one to easily pick different convenient frames suitable to calculate observables.

This freedom is analogous to the freedom to pick a particular gauge condition in GR, which corresponds to picking a set of local frames on spacetime.

In the following we are going to generalize the notion of general frame transformations with the aim of developing a frame covariant formulation of Quantum Field Theory.

(3) Frame covariant effective action. Starting with a field frame $\hat{\phi}$, in QFT the expectation value of an observable

$$\langle \hat{\mathcal{O}} \rangle = \int \mathcal{D}\hat{\phi}\, \mathcal{O}[\hat{\phi}] \, e^{-S[\hat{\phi}]} \tag{4.19}$$

represents a functional of the fields $\hat{\phi}$. In a similar fashion, in order to compute correlation functions, in Section 3.4 we coupled the field $\hat{\phi}$ to a source J, which serves as a mathematical tool. Note that, in general, there is the possibility to couple the source to different powers of the field $\hat{\phi}$. Effectively, at this stage we are interested in this generalization, where the source J is coupled to a composite operator $\hat{\varphi} = \hat{\varphi}[\hat{\phi}]$ such that we generate the correlation functions of $\hat{\varphi}$ rather than those of $\hat{\phi}$. In addition to this, we demand that $\hat{\varphi}$ to define a diffeomorphism in order to guarantee that these correlation functions contain the same physical information.

(i) Frame covariance. For the rest of the thesis, we will define as the *frame covariant* (or reparameterization, or field-redefinition covariant) a theory where physical quantities are independent of the choice of frame. Consequently, in this formalism all physical couplings, possibly including a coupling to an external field, should be part of the action. The source represents merely a device to compute correlation functions such that, after differentiating the generating functional, we are setting the source to zero.

(ii) How to achieve frame covariance. As we discussed in Section 3.4, we can construct the generating functional $W[J]$ by transformations and the addition of further sources. In addition to the standard derivation, here we can also consider a bare theory where $S[\hat{\phi}]$ is replaced by $S[\hat{\phi}] - \int \mathrm{d}^d x J(x) \hat{\varphi}[\hat{\phi}](x)$ resulting in a physical dependence on the choice of frame. In practice, source-dependent expectation values can be computed

as

$$\langle \hat{\mathcal{O}} \rangle = e^{-W[J]} \, \hat{\mathcal{O}} \left[\hat{\phi}[\hat{\varphi}] \frac{\delta}{\delta J} \right] e^{W[J]} \,, \tag{4.20}$$

where $\hat{\phi}[\hat{\varphi}]$ is the inverse diffeomorphism of $\hat{\varphi}[\hat{\phi}]$. Now, we adopt the principle of frame covariance, which demands a frame covariant formalism where physical quantities are independent of the choice of frame. After differentiating $W[J]$, without loss of generality we can take $J = 0$. Therefore, physical quantities are expressed by the frame covariant expression

$$\langle \hat{\mathcal{O}} \rangle = e^{-W[J]} \, \hat{\mathcal{O}} \left[\frac{\delta}{\delta J} \right] e^{W[J]} \Bigg|_{J=0} \,. \tag{4.21}$$

Working with a frame covariant setup has the advantage that the choice of a specific frame reduces the complexity of computations for given physical quantities. For many quantities the specific choice of the frame may simply be $\hat{\varphi} = \hat{\phi}$; this is the case for the correlation functions of the physical field $\hat{\phi}$. However, in the case of universal quantities near the continuous phase transition, or quantities which are computed at vanishing external field, the choice of frame is highly non-intuitive. Nevertheless, it is important to emphasize at this stage that *in principle we can compute any observable in any frame. Then in practice we can exploit the frame where computations become most manageable.*

(iii) Change of integration variables. Together with the freedom of fixing a frame by choosing a particular $\hat{\varphi}[\hat{\phi}]$ which couples to the source, we have as well the freedom to make a change of integration variables. Correspondingly, the expectation value of an observable can be rewritten as:

$$\langle \hat{\mathcal{O}} \rangle = \int \mathcal{D}\hat{\varphi} \, \hat{\mathcal{O}}[\hat{\varphi}] \, e^{-S[\hat{\varphi}]} \,. \tag{4.22}$$

Analogously, for the functional integral of the generating functional $W[J]$, considering the simple composite operator $\hat{\varphi}[\hat{\phi}]$, also called *parameterized field*, we can integrate over $\hat{\varphi}$

$$e^{W[J]} = \int \mathcal{D}\hat{\varphi} \exp \left(-S[\hat{\varphi}] + \int \mathrm{d}^d x J(x) \hat{\varphi}[\hat{\phi}](x) \right) \,. \tag{4.23}$$

Then, the effective action $\Gamma_{\hat{\varphi}}[\varphi]$ is obtained by the Legendre transform

$$e^{-\Gamma_{\hat{\varphi}}[\varphi]} = \int \mathcal{D}\hat{\varphi} \exp \left(-S[\hat{\varphi}] + \int \mathrm{d}^d x J(x) \hat{\varphi}[\hat{\phi}](x) - \int \mathrm{d}^d x J(x) \varphi(x) \right) \,, \tag{4.24}$$

where $\varphi = \langle \hat{\varphi}[\hat{\phi}] \rangle$. Equivalently, in terms of a integro-differential equation

$$e^{-\Gamma_{\hat{\varphi}}[\varphi]} = \int \mathcal{D}\hat{\varphi} \exp \left(-S[\hat{\varphi}] + \int \mathrm{d}^d x (\hat{\varphi} - \varphi) \frac{\delta}{\delta \varphi} \Gamma_{\hat{\varphi}}[\varphi] \right) \,. \tag{4.25}$$

In particular, there exist a particular class of generating functionals that generalize the effective action in the presence of an additional source $K(x_1, x_2)$ for two-point functions:

$$
e^{-\Gamma_{\hat{\varphi}}[\varphi, K]} = \int \mathcal{D}\hat{\varphi} \exp\left(-S[\hat{\varphi}] + \int \mathrm{d}^d x (\hat{\varphi} - \varphi) \frac{\delta}{\delta\varphi} \Gamma_{\hat{\varphi}}[\varphi, K] \right.
$$
$$
\left. -\frac{1}{2} \int \mathrm{d}^d x (\hat{\varphi} - \varphi) K (\hat{\varphi} - \varphi) \right) . \tag{4.26}
$$

This source K will be identified with the cutoff function $\mathcal{R}_k$, giving rise to a *frame covariant flow equation*.

4.2.2. *Frame covariant flow equation*

(1) Essential vs. inessential. In general, during the renormalization process all operators compatible with the symmetries of the theory are generated but not all of them are associated to *essential couplings*, i.e., couplings that appears in physical quantities. Some of the couplings are *inessential* meaning that they can be removed by field redefinitions.

We will define as *inessential couplings* those couplings that when changing their values is equivalent to the change induced by a local frame transformation. By contrast, we define *essential couplings* to be those which enter physical observables as in (4.22).

(2) Frame covariant EAA. Locally in theory space, we can work in a coordinate system $\{g_i\} = \{\lambda_a, \zeta_\alpha\}$, where we denote λ_a the essential couplings and ζ_α the inessential ones. By their very definition, changing the values of the inessential couplings $\zeta \to \zeta + \delta\zeta$ is equivalent to a local frame transformation:

$$
\hat{\varphi}[\hat{\phi}] \to \hat{\varphi}[\hat{\phi}] - \hat{\Phi}[\hat{\phi}] \zeta \delta\zeta + O(\delta\zeta^2) . \tag{4.27}
$$

Then, the generating functional and the effective actions transform respectively as[1]

$$
W[J] \to W[J] - \int \mathrm{d}^d x J(x) \langle \hat{\Phi}[\hat{\phi}] \zeta \delta\zeta \rangle_J + O(\delta\zeta^2) \tag{4.28}
$$

$$
\Gamma[\varphi] \to \Gamma[\varphi] + \int \mathrm{d}^d x \langle \hat{\Phi}[\hat{\phi}](x) \zeta \delta\zeta \rangle_\varphi \frac{\delta}{\delta\varphi} \Gamma[\varphi] + O(\delta\zeta^2) \tag{4.29}
$$

$$
\Gamma[\varphi, K] \to \Gamma[\varphi, K] + \int \mathrm{d}^d x \langle \hat{\Phi}[\hat{\phi}](x) \zeta \delta\zeta \rangle_{\varphi, K} \frac{\delta}{\delta\varphi(x)} \Gamma[\varphi, K]
$$
$$
- \mathrm{Tr}\left[(\Gamma^{(2)}[\varphi, K] + K)^{-1} \frac{\delta}{\delta\varphi} \langle \hat{\Phi}[\hat{\phi}](x) \zeta \delta\zeta \rangle_{\varphi, K} K \right] + O(\delta\zeta^2) . \tag{4.30}
$$

---

[1]Starting from this point, in order to simplify the notation, we will drop the subscript $\hat{\varphi}$ in the EAA $\Gamma_{\hat{\varphi}}[\varphi]$.

In (4.30) the form of the term with the trace comes from the definition of the two-point function

$$\left(\Gamma^{(2)}[\varphi, K] + K\right)^{-1}(x_1, x_2) \equiv \langle(\hat{\varphi}(x_1) - \varphi(x_1))\,(\hat{\varphi}(x_2) - \varphi(x_2))\rangle_{\varphi, K} \ . \qquad (4.31)$$

We note that (4.30) has the same form of the classical frame transformation (4.18). Significantly, then, the derivative of the effective action $\Gamma[\varphi]$ with respect to an inessential coupling is proportional to the equations of motion. For some functional $\Phi[\varphi]$ it reads:

$$\zeta\frac{\partial}{\partial\zeta}\Gamma[\varphi] = \int \mathrm{d}^d x\,\Phi[\varphi]\frac{\delta}{\delta\varphi}\Gamma[\varphi]\ , \qquad (4.32)$$

i.e., on-shell

$$\frac{\partial\Gamma}{\partial\zeta} = 0\ . \qquad (4.33)$$

This is the origin of the statement that one can may take advantage of the equations of motion while calculating running of essential couplings [96].

Moreover, a change in the values for the inessential couplings keeping the essential couplings fixed can be associated to a frame transformation. Specific values of the inessential couplings fully characterize the frame choice. From this observations the analogy between frame covariance and gauge symmetry in GR is then manifest: *gauge transformations are analogous to the frame transformations while gauge-fixing conditions are analogous to conditions that specify the inessential couplings.*

As for the $\Gamma[\varphi, K]$,

$$\zeta\frac{\partial}{\partial\zeta}\Gamma[\varphi, K] = \int \mathrm{d}^d x\Phi[\varphi, K]\frac{\delta}{\delta\varphi}\Gamma[\varphi, K] - \mathrm{Tr}\int\left[\left(\Gamma^{(2)}[\varphi, K] + K\right)^{-1}\frac{\delta}{\delta\varphi}\Phi[\varphi, K]K\right]\ , \tag{4.34}$$

this transformation includes an additional second term. The first term vanishes on the equation of motion. We define the operator on the RHS of (4.30) as the redundant operator conjugate to the inessential coupling ζ (see Section 3.2 for the definition of redundant operators). We conclude that: *every inessential coupling is conjugate to a redundant operator which is determined by some (quasi-)local field $\Phi(x)$ which characterizes the frame transformation.*

Note that a derivative with respect to an inessential coupling can be understood as an "averaged" derivative. While $\Gamma[\varphi]$ is in this sense a scalar, the averaged derivative of $\Gamma[\varphi, K]$ is nonlinear due to the presence of K.

(3) Frame covariant flow equation. In dimensionful variables, the frame covariant effective average action is obtained by introducing the cutoff scale k and the cutoff function $\mathcal{R}_k$, which we identify with K:

$$K = \mathcal{R}_k \qquad (4.35)$$

Explicitly, analogously to (4.26), the EAA action $\Gamma_k[\varphi]$ is defined by the functional integro-differential equation

$$e^{-\Gamma_k[\varphi]} \equiv \int \mathcal{D}\hat\varphi \, \exp\left\{ -S[\hat\varphi] + \int \mathrm{d}^d x \left(\hat\varphi_k[\hat\phi] - \varphi \right) \frac{\delta}{\delta\varphi}\Gamma_k[\varphi] \right.$$
$$\left. -\frac{1}{2} \int \mathrm{d}^d x \sqrt{\bar g} \left(\hat\varphi_k[\hat\phi] - \varphi \right) \mathcal{R}_k \left(\hat\varphi_k[\hat\phi] - \varphi \right) \right\} , \tag{4.36}$$

from which it follows that every given operator $\mathcal{O}$ has a φ- and k-dependent expectation value given by

$$\langle \hat{\mathcal{O}} \rangle_{\varphi,k} \equiv e^{\Gamma_k[\varphi]} \int \mathcal{D}\hat\varphi \, \exp\left\{ -S[\hat\varphi] + \int \mathrm{d}^d x (\hat\varphi_k[\hat\phi] - \varphi) \frac{\delta}{\delta\varphi}\Gamma_k[\varphi] \right.$$
$$\left. -\frac{1}{2} \int \mathrm{d}^d x \sqrt{\bar g} (\hat\varphi_k[\hat\phi] - \varphi)\mathcal{R}_k(\hat\varphi_k[\hat\phi] - \varphi) \right\} \hat{\mathcal{O}}[\hat\phi] . \tag{4.37}$$

The generalized flow equation satisfied by $\Gamma_k[\varphi]$ in (4.36) is given by

$$\left(k\partial_k + \int \mathrm{d}^d x \, \Phi_k[\varphi]\frac{\delta}{\delta\varphi} \right) \Gamma_k[\varphi] = \frac{1}{2}\mathrm{Tr}\left[\frac{\left(k\partial_k + 2\int \mathrm{d}^d x \, \frac{\delta}{\delta\varphi}\Phi_k[\varphi] \right)\mathcal{R}_k}{\Gamma_k^{(2)}[\varphi] + \mathcal{R}_k} \right] . \tag{4.38}$$

Herein

$$\Phi_k[\varphi] := \langle k\partial_k\hat\varphi_k[\phi] \rangle \tag{4.39}$$

is the RG kernel which takes into account the k-dependent field reparameterizations. Crucial here is the utility of $\hat\varphi_k[\phi]$ that allows us to choose to reparameterize the field to fix the values of inessential couplings. We note that the flow equation (4.38) reduces to the standard flow for the EAA (3.7) when $\Phi_k = 0$. The additional terms arise due to the k-dependence of $\hat\varphi_k$, which assume the form of an infinitesimal frame transformation.

Now the central question is shifted to the search of a criterium to determine $\Phi_k[\varphi]$. In fact we can arrive at a closed flow equation for $\Gamma_k[\varphi]$ in terms of a yet-to-be determined $\Phi_k[\varphi]$ in some explicit manner. Crucially, by inverse logic $\Phi_k[\varphi]$ can be determined by $\Gamma_k[\varphi]$ itself. This is the approach pursued in earlier work [248, 249] in order to describe bound states through flowing bosonization and hadronization in QCD [250, 251]. The alternative, which we shall pursue, is instead to specify those renormalization conditions that constrain the form of $\Gamma_k[\varphi]$ by fixing the values of the inessential couplings and solve the flow equation for the essential couplings. In this way we can also solve for the parameters appearing in $\Phi_k[\varphi]$ in order to determine the form of the frame transformation.

Remark. The RG transformation can be interpreted itself as a frame transformation, where the RG scale k is the associate inessential coupling. This can be easily seen by deriving a dimensionless version of the flow equation (4.38) [199].

One advantage of the flow equations (4.38) is that the regulator is disentangled from the RG kernel, meaning that the trace will be regularized for any Φ_k provided $\mathcal{R}_k$ decreases fast enough in the large momentum limit, as usually demanded. Therefore, in the EAA formulation we have two different independent RG scheme ingredients to tune in order to analyze a particular physical system.

4.2.3. Standard scheme

As an example, in this section, we focus on the simple case where one eliminates only a single inessential coupling, namely the wave function renormalization Z_k. The removal of Z_k then introduces the anomalous dimension of the field,

$$\eta_k = -k\partial_k \log(Z_k) \,. \tag{4.40}$$

This choice is what is usually called the *standard renormalization scheme*. Now, we set in our new framework

$$\Phi_k[\varphi] = -\frac{1}{2}\eta_k\varphi \qquad \Longleftrightarrow \qquad \hat{\varphi}_k = Z_k^{1/2}\hat{\varphi} \,, \tag{4.41}$$

where we impose $Z_0 = 1$ as boundary condition. The EAA reads:

$$
\begin{aligned}
e^{-\Gamma_k[\varphi]} = \int \mathcal{D}\hat{\varphi} \exp\Bigg(&-S[\hat{\varphi}] + \int \mathrm{d}^d x (Z_k^{-1/2}\hat{\varphi} - Z_k^{-1/2}\varphi)\frac{\delta}{\delta\varphi}\Gamma_k[\phi] \\
&-\frac{1}{2}\int \mathrm{d}^d x \sqrt{\bar{g}}(Z_k^{-1/2}\hat{\varphi} - Z_k^{-1/2}\varphi)Z_k\mathcal{R}_k(Z_k^{-1/2}\hat{\varphi} - Z_k^{-1/2}\varphi)\Bigg\} \,.
\end{aligned}
\tag{4.42}
$$

Hence the corresponding flow equation becomes

$$\left(k\partial_k - \frac{1}{2}\int \mathrm{d}^d x \, \eta_k\varphi\frac{\delta}{\delta\varphi}\right)\Gamma_k[\varphi] = \frac{1}{2}\,\mathrm{Tr}\left[\frac{k\partial_k\mathcal{R}_k - \eta_k\mathcal{R}_k}{\Gamma_k^{(2)}[\varphi] + \mathcal{R}_k}\right] \,. \tag{4.43}$$

It is now manifestly independent of Z_k and is equal to (4.38) with Φ_k given by (4.41). The terms proportional to η_k have the form of a redundant coupling, and this simply is the manifestation of the fact that the wave function renormalization was inessential.

(1) Renormalization conditions. The flow equation (4.43) was obtained without specifying the inessential coupling Z_k. This means that we have the freedom to impose a renormalization condition that constrains the form of $\Gamma_k[\varphi]$ by fixing the value of one coupling to some fixed value. Finally we can solve the flow equation under the chosen renormalization, determining η_k as a function of the remaining couplings.

A typical choice is to expand the Γ_k in fields and in derivatives, then identify Z_k with the coefficient of the term $\int \mathrm{d}^d x \, \partial\varphi\partial\varphi$, and choose it to be $1/2$. However this choice is not the only one possible. For instance, expanding $\Gamma_k[\varphi]$ in derivatives, introducing

two functions of the field $V_k(\varphi)$ and $z_k(\varphi)$, one can write

$$\Gamma_k[\varphi] = \int d^d x \left(V_k(\varphi) + \frac{1}{2} z_k(\varphi) \partial_\mu \varphi \partial^\mu \varphi \right) + O(\partial^4) \, . \qquad (4.44)$$

The *essential scheme* we are going to present generalizes the renormalization condition

$$z_k \Big(\varphi(x) = \bar{\varphi} \Big) = 1 \qquad (4.45)$$

for a given x-independent value of the field, $\bar{\varphi}$.

(2) Gaussian fixed point. It is important to remark that at the Gaussian fixed point the EAA equals

$$\Gamma_{\text{GFP}} \equiv \frac{1}{2} \int d^d x \, \partial_\mu \varphi \partial^\mu \varphi \, , \qquad (4.46)$$

which is quadratic in φ. *Thus any of the renormalization conditions* (4.45), *for any value of $\bar{\varphi}$, will fix the same inessential coupling at the Gaussian fixed point.* Alternatively, one can also fix inessential couplings at a different free fixed point by imposing an alternative renormalization condition to eliminate Z_k. This makes it clear that the renormalization condition (4.45) is closely related to the kinematics of the Gaussian fixed.

Note that here we are discussing only a single inessential coupling. In general there is an infinite number of inessential couplings and by imposing renormalization conditions we wish to eliminate all of them. We shall then investigate whether there is a systematic procedure. Next section, is devoted to the *minimal essential scheme*, the scheme where this operation is practically performed.

Furthermore, the task of distinguishing the scaling operators (related to the essential couplings) from redundant operators (related to inessential couplings) at the Gaussian fixed point is made simpler by the following observation. The redundant operators at the GFP have the general structure (compare with (4.34)):

$$\int d^d x \, \Phi_\alpha[\varphi](x) \partial^2 \varphi - \text{Tr} \left[(\partial^2 + \mathcal{R}_k)^{-1} \frac{\delta}{\delta \varphi} \Phi_\alpha[\varphi](x) \right] \, . \qquad (4.47)$$

If $\{e_a[\varphi]\}$ is a set of operators which are linearly independent of $\Phi_\alpha[\varphi] \partial^2 \varphi$, they will also be linearly independent of the second term in (4.47). Hence, in order not to include redundant operators, one should eliminate all operators of the form $\Phi \partial^2 \phi$.[2]

---

[2]If Φ is a homogeneous function of the field of degree n, then the first term is a homogeneous function of degree $n + 1$, while the second term is a homogeneous function of degree $n - 1$.

4.2.4. *Minimal essential scheme*

In order to solve the flow equation (4.38), we allow Φ_k to depend on a set of γ *functions* $\{\gamma_\alpha\}$. In particular, one gamma function for each renormalization condition has to be introduced. Together with the beta functions for the remaining running couplings, the gamma functions turn out to be functions of the remaining couplings. For example, we saw that usually (in the *standard scheme*) one fixes $\Phi_k = -\frac{1}{2}\eta_k\varphi$, applying a single renormalization condition.

Now instead, let us choose for example $\Phi_k = \gamma_1(k)\varphi + \gamma_2(k)\varphi^3$, imposing two renormalization conditions. This choice fixes the values of two inessential couplings then.

Let us parameterize Φ_k in the general form

$$\Phi_k[\varphi](x) = \sum_\alpha \gamma_\alpha(t)\Psi_\alpha[\varphi](x) \ . \tag{4.48}$$

In essential schemes we include all possible local operators in the set $\{\Psi_\alpha[\varphi]\}$. Applying a renormalization conditions for all $\Psi_\alpha[\varphi]$ then fixes the values of all inessential couplings. For this purpose, we wish to find a practical set of renormalization conditions that generalize the one applied in the standard scheme.

Following the line of reasoning of the previous section, in the *minimal essential scheme* one fixes the values of the inessential couplings at the Gaussian fixed point. Then, we can write the EAA such that it depends only on the essential couplings λ_a:

$$\Gamma_k[\varphi] = \Gamma_{\mathrm{GFP}}[\varphi] + \sum_a \lambda_a(k)e_a[\varphi] \tag{4.49}$$

where $\{e_a[\varphi]\}$ are a set of operators which are linearly independent of the redundant operators associated to the inessential couplings.

Without loss of generality we can assume that the couplings behave as $\lambda_a(k) = e^{-\theta_G k}\lambda_a(0) + \cdots$ in the vicinity of the Gaussian fixed point. In this case $\{e_a[\varphi]\}$ are the scaling operators at the Gaussian fixed point, θ_G the corresponding Gaussian critical exponents and the essential couplings $\lambda_a(k)$ are the scaling fields.

Remark. Having set the renormalization conditions at the Gaussian fixed point, we know that the couplings λ_a will be the essential couplings in the vicinity of the Gaussian fixed point.

Away from the Gaussian fixed point, the form of the redundant operators will change, since the RG scheme can exclude regions of the theory space. Therefore, adopting the minimal essential scheme puts a restriction on which theory we can have access to. However, it is intuitively clear that this restriction has a physical meaning since the theories in question are those that share the kinematics of the Gaussian fixed point. In

fact, a remarkable consequence of the minimal essential scheme is that the propagator evaluated at any constant value of the parameterized field $\varphi[\phi](x) = \bar{\varphi}$ will be of the form

$$(p^2 + V_k^{(2)} + \mathcal{R}_k(p^2))^{-1} \tag{4.50}$$

where $V_k^{(2)}$ is the second derivative of the potential. Let us point out that this does not imply that the propagator for the physical field φ is of this form, but only that the propagator can be brought into this form by a frame transformation.

(1) Generic fixed points. In the vicinity of fixed points one obtains scaling exponents which are universal, i.e., independent of the renormalization conditions that distinguish different schemes. However, there are also critical exponents associated with redundant operators they are all scheme dependent. We will show the different features of essential schemes with those of the standard scheme in these respects.

Rewriting the flow equation (4.38) in dimensionless variables yields

$$\left(k\partial_k + \int d^d x\, \psi_k[\tilde{\varphi}]\frac{\delta}{\delta\tilde{\varphi}}\right) \Gamma_k[\tilde{\varphi}] = \mathrm{Tr}\left[\frac{\int d^d x\, \frac{\delta}{\delta\tilde{\varphi}}\psi_k[\tilde{\varphi}]R^{(0)}}{\Gamma_k^{(2)}[\tilde{\varphi}] + R^{(0)}}\right], \tag{4.51}$$

where $\tilde{\varphi}$ denotes the dimensionless field and ψ_k the dimensionless RG kernel. Furthermore $R^{(0)}$ is understood as a function of the dimensionless Laplacian. Fixed points of the RG flow are uncovered by searching for k-independent solutions of this equation. Here the fixed point action Γ_* and the RG kernel at the fixed point, ψ_*, obey

$$\int d^d x\, \psi_*[\tilde{\varphi}]\frac{\delta}{\delta\tilde{\varphi}}\Gamma_*[\tilde{\varphi}] = \mathrm{Tr}\left[\frac{\int d^d x\, \frac{\delta}{\delta\tilde{\varphi}}\psi_*[\tilde{\varphi}]R^{(0)}}{\Gamma_*^{(2)}[\tilde{\varphi}] + R^{(0)}}\right]. \tag{4.52}$$

The critical exponents associated with the fixed point are then found by perturbing the fixed point solution (Γ_*, ψ_*). The critical exponents θ are obtained by looking for eigenperturbations of the form

$$\delta\Gamma_k \propto e^{-k\theta}\mathcal{O}[\tilde{\varphi}], \tag{4.53}$$

where the eigenvectors $\mathcal{O}[\tilde{\varphi}]$ is k-independent. We note that the form of $\mathcal{O}$ depends on the frame and hence on the renormalization scheme. This operator can be redundant, and therefore multiplied by an inessential coupling, or scaling, if it is linearly independent from the redundant ones. If the redundant operator is is of the form (4.34), then the associated critical exponent θ is entirely scheme dependent and carries no physical information.

In the standard scheme, one removes only a single inessential coupling and thus one will have an infinite number of redundant eigenperturbations which must be disregarded. In essential schemes instead, *all inessential couplings are removed and thus we automatically disregard all redundant eigenperturbations.*

(2) Derivative expansion. In [199] the authors derived the flow equation in the minimal essential scheme at up to order ∂^8 in the derivative expansion. In the minimal essential scheme, the renormalization condition is generalized such that $z_k(\varphi) = 1$ for all values of the field and all scales k. Thus, it would be like going from fixing a single coupling in the standard scheme, to fixing a whole function of the field in the essential one.

To close the flow equations under this renormalization condition, the authors set the RG kernel to $\Phi_k[\varphi](x) = F_k(\varphi(x))$, where $F_k(\varphi(x))$ is a function of the fields, without derivatives, constrained such that the flow equation under the renormalization condition can be solved. The first application was to the 3D Ising model in the vicinity of the Wilson-Fisher fixed point.

Remarkable is the simplification of the equation due to the reduced number of physical running coupling to analyze. For instance, at order ∂^6 in the derivative expansion, the number of operators in Γ_k reduces from 13 in the standard scheme to 4 in the essential scheme. This reduction comes with an increasing number of renormalization schemes functions $F_k^i(\varphi(x))$ to be determined (13-4 = 9 $F_k^i(\varphi(x))$ at the order ∂^6).

Summary. At a given order ∂^s, the procedure of minimal essential scheme can be summarized as follows:

(1) Apart from the canonical kinetic term with coefficient $1/2$, eliminate all operators of the form $\Phi_k \partial^2 \varphi$ from the ansatz of Γ_k (because we are expanding around a Gaussian fixed point);

(2) Insert all the possible terms up to order ∂^{s-2} into the RG kernel Φ_k;

(3) Use equation (4.38) to find a set of beta functions for the essential operators which remain in the EAA, plus a set of equations which determine the functions appearing in the RG kernel Φ_k.

The final number of equations which one must solve at each order of the derivative expansion is the same as in the standard scheme. However, in the minimal essential scheme we obtain beta functions only for the essential couplings. Moreover, since the ansatz for EAA becomes simpler in the minimal essential scheme, the complexity in the calculation is reduced. In particular, the simple form of the propagator (4.50) evaluated at a constant field configuration is guaranteed.

A. Baldazzi and K. Falls [175] applied the essential renormalization group scheme also to gravity. Solving the flow equation for the EAA within an essential scheme allows us to discuss the criteria of asymptotic safety as formulated by Weinberg [96].

4.2.5. *Essentially safe gravity*

(1) Weinberg's formulation of Asymptotic Safety. Weinberg's criteria necessitate that we have a UV-complete QFT when there is no UV cutoff, which is achieved if the theory lies on an RG trajectory that originates from a UV fixed point. However, as has been emphasized recently by J. Donoghue [185], Weinberg's formulation is more precise since it is concentrated on the absence of unphysical UV divergences in physical quantities. In particular, the scaling behavior of inessential couplings is entirely scheme dependent and they must not be included in the set of relevant couplings.

In particular, attempts to find a suitable fixed point have required fixed points for all gravitational couplings, included in a given approximation, instead of incorporating field reparameterizations into the RG equations and checking which of the couplings are inessential. In [175] the authors remedied this oversight by incorporating field reparameterizations in the gravitational flow equations which allow us to eliminate the inessential couplings from the flow equations. Crucially, *it is only the essential couplings that need to attain a UV fixed point.* In fact, inessential couplings are simply not present in physical observables and, therefore, their behavior is not restricted a priori.

To understand the connection, note that if we supply an initial condition for the flow at a scale $k = \mu$, the flow equation supplies a function

$$\lambda_a^{\text{phys}} = \lambda_a^{\text{phys}}(\lambda_b(\mu), \mu) \qquad (4.54)$$

We can write every observable which depends on energy scales E and the physical couplings λ_a^{phys} as a function

$$\mathcal{O} = \mathcal{O}(E, \lambda_a(\mu), \mu) \qquad (4.55)$$

By dimensional analysis, the dimensionless observables will read

$$\mathcal{O} = \mu^D \tilde{\mathcal{O}}(E/\mu, \tilde{\lambda}_a(\mu)) , \qquad (4.56)$$

where $\tilde{\lambda}(\mu) = \mu^{-d_a}\lambda_a(\mu)$ are the dimensionless couplings. It is clear that its limit $\lim \mu \to \infty$ only exists if $\lim_{\mu \to \infty} \tilde{\lambda}_a(\mu)$ exists. This is exactly the requirement for Asymptotic Safety: all the essential couplings $\tilde{\lambda}(\mu)$ remain finite at $\mu \to \infty$, meaning that they reach an UV fixed point $\lim_{\mu \to \infty} \tilde{\lambda}_a(\mu) = \lambda_a^*$.

(2) Universality class: QEG. For a scalar field there are Gaussian fixed points associated to kinetic operators $(-\partial^2)^{s/2}$ for every even integer s in the derivative expansion. As such, there is a minimal essential scheme associated to each Gaussian fixed point, that is physically distinct since they are associated with different degrees of freedom. Within a given minimal essential scheme, the flow is then constrained to the physical

theory space associated to those degrees of freedom. In other words, the minimal essential scheme restricts the RG flow to a universality class that contains the corresponding Gaussian fixed point.

(2a) For Quantum Gravity, we will consider the universality class of QEG meaning that it is associated to the quantization of the physical degrees of freedom that are carried by the metric. More specifically, in this chapter by the Gaussian fixed point in the context of gravity we refer to the one associated to the linearized Einstein-Hilbert action. In particular, this specifies also the actual number of physical degrees of freedom. In this sense, a quantization of higher derivative gravity can be carried out by quantizing the metric assuming diffeomorphism invariance, but it is a quantization of more degrees of freedom than Einstein's theory. This different interpretation about the physical degrees of freedom and the physical essential couplings will bring our investigation of asymptotic safety closer to the original formulation.

(2b) For metric Quantum Gravity the EAA is denoted $\Gamma_k[h, \xi, \bar{\xi}; \bar{g}]$. The diffeomorphism invariant action has the derivative expansion at second order

$$\Gamma_k[g] = \int \mathrm{d}^d x \sqrt{g} \left(\frac{\Lambda(k)}{8\pi} - \frac{R}{16\pi G(k)} + a(k)R^2 + b(k)R_{\mu\nu}R^{\mu\nu} + c(k)E \right) , \qquad (4.57)$$

with $E = R_{\mu\nu\rho\sigma}R^{\mu\nu\rho\sigma} - 4R_{\mu\nu}R^{\mu\nu} + R^2$ the Euler density, which in $d = 4$ represents a topological invariant.

For gravity the RG kernel now has component for each field $\Phi_k = \{\Phi^g_{k,\mu\nu}, \Phi^{\xi\mu}_k, \Phi^{\bar{\xi}}_{k,\mu}\}$. In the background field approximation, we choose $\Phi^{\xi\mu}_k = 0 = \Phi^{\bar{\xi}}_{k,\mu}$, while we choose the RG kernel for the metric to be given by

$$\Phi^g_{k,\mu\nu}[g] = \gamma_g g_{\mu\nu} + \gamma_R R g_{\mu\nu} + \gamma_{Ricci} R_{\mu\nu} + O(\partial^4) , \qquad (4.58)$$

where the gamma functions which, along with the beta functions, will be determined as functions of the couplings that appear in (4.57). Each gamma function allows us to impose a renormalization condition which fixes the flow of one inessential coupling. Thus, retaining three gamma functions allows us to impose three renormalization conditions which are constraints on the form of Γ_k that we impose along the flow.

(2c) Following Subsection 4.2.4, we now choose the minimal essential renormalization scheme:

(1) As with the derivative expansion for a scalar field, if we work at order ∂^s in the derivative expansion, we include all terms of order ∂^{s-2} in the RG kernel.

(2) The minimal essential scheme for Quantum Gravity, puts to zero any term that vanishes when the vacuum Einstein equations

$$R_{\mu\nu} = 0 \qquad (4.59)$$

apply apart from the Einstein–Hilbert term itself. The reasoning is that the fixed point where $g = \lambda = 0$ is the analog of the GFP for a scalar field theory. This means that we can set to zero $a(k)$ and $b(k)$ for Einstein gravity.

(3) We expand the eq.(4.38) to order ∂^4 to obtain five flow equations from the independent tensor structures present in (4.57) using off-diagonal heat kernel techniques [252]. Having set $a(k)$ and $b(k)$ to zero, we can solve the equations for γ_R and γ_{Ricci}. Which renormalization condition we should apply to freeze the inessential coupling associated to γ_g has still to be determined. That must consist of some combination of $G(k)$ and $\Lambda(k)$.

This freedom to apply one RG condition afforded by the presence of γ_g, makes evident that there is a inessential coupling which needs to be fixed. In particular, since we will consider trajectories inside the subspace of theory space which contains the GFP, we will take into account the values of $g = \lambda = 0$ at the GFP. Therefore, to determine which dimensionless coupling we should fix, we analyze the GFP to understand which particular combination of g and λ is inessential. However, we should understand this limit as the approach to a free theory on an arbitrary background spacetime where Γ_k reduces to the linearized Einstein–Hilbert action. If we decompose the metric

$$\hat{g}_{\mu\nu} = \bar{g}_{\mu\nu} + \kappa(k)\hat{h}_{\mu\nu} , \qquad (4.60)$$

and we differentiate wrt. the RG scale k, we obtain

$$k\partial_k \hat{g}_{\mu\nu} = \frac{1}{2}\eta_N \kappa_k \hat{h}_{\mu\nu} + \kappa(k)k\partial_k \hat{h}_{\mu\nu} + O(\kappa(k)) \qquad (4.61)$$

The GFP corresponds to the theory where $\kappa(k) = 0$. The expectation value of $k\partial_k \hat{h}_{\mu\nu}$ is then given by

$$\Phi^h_{k,\mu\nu} = \langle k\partial_k \hat{h}_{\mu\nu}(k)\rangle = \frac{1}{\kappa(k)}\Phi^g_{k,\mu\nu} - \frac{1}{2}\eta_N h_{\mu\nu} \qquad (4.62)$$

and inserting (4.58) we obtain

$$\Phi^h_{k,\mu\nu} = \frac{\gamma_g}{\kappa(k)}\bar{g}_{\mu\nu} - \frac{1}{2}\eta_h h_{\mu\nu} , \qquad \text{where} \qquad \eta_h := \eta_N - 2\gamma_g \qquad (4.63)$$

is the anomalous dimension of the graviton field. Imposing that $\Phi^h_{k,\mu\nu}$ is finite when $\kappa_k = 0$ (i.e., when $G(k) = 0$) requires that $\gamma_g = 0$ a the GFP.

Inserting this ansatz in the flow equation, in [175] it was found that also $\eta_h = \eta_N = 0$ at the Gaussian fixed point. The authors noted that at the GFP, the dimensionless vacuum energy is constant and its value depends from the cutoff function:

$$\rho_{\mathrm{GFP}} = \frac{\lambda}{g}\bigg|_{\mathrm{GFP}} = \frac{1}{8\pi}\int \mathrm{d}z \frac{k\partial_k \mathcal{R}_k(z)}{z + \mathcal{R}_k(z)} . \qquad (4.64)$$

We conclude that the GFP is characterized uniquely by $g = \eta_N = \gamma_g = 0$ and a scheme-dependent value for the dimensionless vacuum energy ρ_{GFP}.

Remarks:

(1) Note that a higher derivative Gaussian fixed point, more analogous to the fourth order fixed point. At this fixed point the degrees of freedom are those of Stelle's higher derivative gravity [65] rather than Einstein gravity. Furthermore, since the equations of motion for higher derivative gravity do not imply (4.59) the couplings $a(k)$ and $b(k)$ are essential at the higher derivative Gaussian fixed point.

(2) Concerning the vacuum energy, let us note that we could also choose a more general cutoff scheme allowing for different cut-off functions for the ghosts and gravitons in such a manner that ρ_{GFP} would vanish. At the exact level no physics should depend on the choice of cutoff so the value of ρ_{GFP} should be of no significance. We can conclude that *the vacuum energy is inessential.*[3]

(3) We note that it may seem we could satisfy the flow with $\Lambda(k)/G(k) = k^4 \rho_{\mathrm{GFP}} + \rho_0$ allowing for a non-zero cosmological constant, since ρ_0 is a constant of integration that will not be furnished by the solutions of the flow equations. However, only with $\rho_0 = 0$ do we have a fixed point.

A remarkable consequence of the vacuum energy being inessential is that we may simply choose that the vanishing of the vacuum energy is achieved by a renormalization condition. Thus, at least in pure gravity, *there is no fine tuning problem related to the cosmological constant once we apply this condition.* However, this condition dictates the vanishing of the cosmological constant and by imposing it we are restricting which theories we can have access to. *This suggests that there is a universality class of Quantum Gravity where the cosmological constant is zero.* This universality class possesses the IR GFP where G_0 is a constant and $\rho_0 = 0$. Although there may be other universality classes where the cosmological constant is non-zero.

Importantly, any change in the coupling constants corresponding to a frame transformation furnishes a physically equivalent theory. Hence, there are directions in theory space along which all physical quantities remain unchanged. For instance, if we flow along an inessential direction, we might describe a different action with $\rho_0 \neq 0$.

(3) Reuter fixed point and minimal essential scheme. To test the aforementioned hypothesis, the minimal essential scheme can be carried out at each order in the

---

[3]See [253] for a recent analysis of curvature square operators, understood as composites operators, determining the spectrum of scaling operators at the scale-invariant fixed point.

derivative expansion.

$$\Gamma_k[g] = \int \mathrm{d}^d x \sqrt{g} \left(\frac{\rho_{\mathrm{GFP}} k^4}{8\pi} - \frac{R}{16\pi G(k)} + c(k)E \right) , \qquad (4.65)$$

At order ∂^4 the minimal essential flow is characterized by five dimensionless functions of g: $\gamma_g(g)$, $\beta_g(g)$, $\gamma_R(g)$, $\gamma_{\mathrm{Ricci}}(g)$ and $\beta_c(g)$. Expanding them in g, the authors derived the nonperturbative beta function of $g(k)$: there exists an UV fixed point which can be identified with the Reuter fixed point.

Summarizing, in [175], performing the FRG analysis for EH gravity including all diffeomorphism-invariant four derivative terms in the flow equation, in the essential scheme further evidence in favor of the existence of the UV fixed point was provided. Furthermore Newton's constant turns out to be the only relevant essential coupling at the Reuter fixed point. Although this conclusion could change by including higher-order terms, this seems unlikely since all higher-order terms are canonically irrelevant and, thus, the quantum correction to their scaling dimensions would have to be large. Additionally, the stability of the fixed point going from order ∂^2 to order ∂^4 indicates that the approximations do not miss another relevant coupling.

CHAPTER 5

Discussion and Summary of Part I

In order to describe quantum theories, in this Part we followed the route of the generating functional approach to QFT. Generating functionals are universal applicable technical objects: they are used to describe the Standard Model (SM) of particle physics and at the same time they are suitable to discuss statistical and quantum field theories on different scales. However, their abstract and general structure is at the same time the source of its severest problems which bother physicists since many decades. To practically manipulate and address direct computation with the purpose of extracting physical predictions, a regularization procedure is required. In order to install such a regularization, instead of direct computations addressing the full integration, one systematically restricts its evaluation by approximating the underlying measures in an appropriate way. The hope is that this procedure may lead to predictions beyond the involved scales, by extrapolating the obtained results. Technically, these techniques were mostly implemented in the context of perturbation theory.

Perturbation theory has furnished very fruitful insights into a wide range of interactions up to the TeV scale. However, gravitational interactions are still excluded. In fact, while for the SM interactions the described approximation methods seem to be appropriate on certain scales, there are severe conceptual issues in studying a quantum version of General Relativity. The point of view adopted in this thesis is not that the present results suggest gravity to be not renormalizable, but rather that we have to go beyond the standard, perturbative, techniques and enter the realm of nonperturbative effects to judge the UV behavior of gravity.

A deeper understanding of the necessity of the renormalization procedure, and conditions for the existence of fundamental field theories was needed, therefore.

(1) A very successful guiding principle was discovered by the path integral approach that in certain cases promotes a classical theory to its quantum counterpart and thus translates physics on macroscopic scales to a microscopic level. However, the technical difficulties have shown that, in order to take account of the scale dependence of Nature, different methods are necessary that are particularly designed to give rise to a mathematical realization of the scale-evolution of physical laws.

In this Part we presented a brief introduction into a very promising, intrinsically nonperturbative method: the Functional Renormalization Group. Its first implementation was related to the block spin transformations of Kadanoff and its generalization pioneered by Wilson [86, 87]. Exact RG techniques were developed basing on the idea of evaluating the path integral not all at once, but in a piecewise manner. Starting from this idea an RG flow of action functionals can be defined, that describes the same system at different momentum scales. In the following it was understood that the general condition for a theory to be considered fundamental is satisfied whenever its RG flow approaches a fixed point in the high momentum UV limit.

We focus in this thesis on regularized functional integrals, described indirectly by the Effective Average Action [85, 208]. The EAA turns out to satisfy an Exact RG equation in the form of a Functional Renormalization Group Equation. For the block spin transformation and the Wilsonian RG approach, the idea is to iteratively evaluate a preexisting UV theory by absorbing the microscopic effects up to a scale k in an effective, averaged theory and continue this procedure in a subsequent manner down to the infrared. We will see that within the Asymptotic Safety Program [49, 50] introducing the Effective Average Action and computing its RG evolution using the FRGE can even lead to a prediction of the fundamental UV theory, related to the bare action.

In this **Part I** we introduced the main idea of the exact Renormalization Group, reviewed a concrete example of a Functional Renormalization Group Equation, and described a relation between this highly non-trivial differential equation for the EAA and the path integral procedure based on the generating functional. Thereafter we addressed the notion of *renormalizability* in the context of the Exact RG.

(2) The corresponding nonperturbative definition of renormalizability also applies to all perturbatively renormalizable, fundamental theories, like Yang–Mills theory or QCD, as these approach the GFP in the UV limit, which corresponds to an asymptotically free, non-interacting theory. This insight provided raised the question whether perturbatively non-renormalizable theories could turn out to be nonperturbatively renormalizable. In this case the RG flow approaches a NGFP, that corresponds to an interacting theory, which may occur outside the realm of perturbation theory.

(3) These considerations also apply to metric gravity, that might as well be defined as a QFT only nonperturbatively. Weinberg conjectured in 1979 [96] that a non-Gaussian fixed point might also exist for gravity in four dimensions. Theories whose continuum limit is defined at such a NGFP he called *asymptotically safe*. Unfortunately, at that time no computational tool was known that would have allowed for a thorough investigation of this conjecture. It took until the '90s that such an appropriate tool was found: the FRGE for the EAA which was first derived for scalar [208] and Yang–Mills theory [90, 209, 210, 254] and later on generalized such that it could be applied to gravity [95].

This FRGE rendered the investigation of the flow of metric gravity possible in arbitrary dimensions of spacetime.

(4) The equation for the running effective action functional can typically not be solved in full generality but allows for nonperturbative approximations by choosing an ansatz for the form of the action functional, a so-called truncation. Later this route was taken in numerous studies of different approximations have been carried out, all of which indicate the existence of a NGFP for metric gravity in $d = 4$ spacetime dimensions (see for an overview [49, 50, 67]). Also the inclusion of matter fields, that causes first divergences in the perturbative approach, has been explored in detail [107].

(5) In this thesis we focus on *Quantum Einstein Gravity*, the asympototically safe Quantum Field Theory that takes the metric as the dynamical field variable, whose symmetry is given by diffeomorphism invariance, and which is Background Independent. Note that we did not require that the bare theory is given by the Einstein–Hilbert action necessary; rather it is an *output* that follows from the fixed point condition. Nevertheless the simplest truncation of QEG, the Einstein–Hilbert truncation, had been found in 1996 M. Reuter [95] in order to prove, in this truncation, the existence of an ultraviolet fixed point, the first approximation to the so-called Reuter fixed point.

(6) The Asymptotic Safety Program is a well-established approach to Quantum Gravity which is based on a *nonperturbative* generalization of *renormalizability* with the fundamental requirement of *Background Independence* within theories of Quantum Gravity.

Within this program, we insisted on two essential requirements a consistent theory of Quantum Gravity must meet by all means: It must be renormalizable and it must be Background Independent as the spacetime geometry should be an outcome of the theory rather than a prescribed input. Traditionally the first of these conditions seemed to be ruled out quantum GR, being non-renormalizable from the perturbative point of view.

In the Asymptotic Safety program, however, a more general, nonperturbative notion of renormalizability is proposed, on the basis of which quantum gravity could be defined within the framework of conventional QFT. The key ingredient to this approach is given by the interacting renormalization group fixed point governing the high energy behavior in such a way that the infinite cutoff limit is well defined.

As for the Background Independence, the presence of a rigid reference metric which never gets changed and thus conxstitutes an "absolute element" in the RG formalism would destroy its Background Independence. In the EAA approach to Quantum Einstein Gravity, no background metric is fixed "by hand" and hence it does comply with the principle of Background Independence. In the present context we realize Background Independence by quantizing the fluctuations of the metric in all possible background

spacetimes at a time. Concretely, we presented a special class of backgrounds, which "know" about the true "on-shell" metrics of spacetime, the *self-consistent background metrics*.

Novel in **Part I**, is the use of self-consistent backgrounds with Lorentzian signature. The signature of spacetime represents one of the main obstacles for Asymptotic Safety to furnish a direct image of the world. This is why the main existing analyses deal with effective spacetimes of Euclidean signature, their Lorentzian counterparts is needed, however, if one wants to determine their real physical implications.

Critically, the RG tools (the FRG as well) have no precise prescription about how to integrate out non semi-definite momentum eigenmodes and hence how to derive the flow integrating out spacelike or timelike eigenmodes. In this thesis, inspired by the path integral approach, we adopt a strategy to integrate out in a symmetric way both timelike and spacelike modes. Following this procedure, we derive the running Lorentzian self-consistent backgrounds.

(7) In the second half of **Part I** we presented two recent developments in the FRG framework to Quantum Gravity, and we reported their main results, to the extent they will be relevant to our own work later on:

(7a) Composite operator formalism. The longstanding problem of constructing meaningful observables in Quantum Gravity is still open even in the Asymptotic Safety scenario. However, studies of the renormalization behavior of composite operators have been performed. This allows us to resort to such operators when it comes to constructing full-fledged observables. Typically such observables are non-local operators, so realistically it is impossible to include then into a truncation of the FRGE. Hence the investigation of composite operators in the FRG formalism is further motivated due to the need to renormalize operators that one usually cannot include as a basis element into the EAA truncation.

The new composite operator flow equation had been applied to illustrate the renormalization and in particular the scaling behavior of composite operators. In this thesis, we shall come back to this composite operator formalism in Chapter 13, where we will apply this formalism in order to compute the scaling dimensions of relational observables.

(7a) Essential Renormalization Group. The RG provides a framework to iteratively perform a change of variables with the purpose of describing physics at different length scales. This, in practice, translates into a flow in a space spanned by the couplings which parameterize all possible interactions between the physical degrees of freedom. However, the theory space is divided into equivalence classes. As a consequence, we do not have to compute the flow of all coupling constants, but instead, we only need

to compute the flow of the essential couplings, which are those eventually appearing in expressions for physical observables. The other coupling constants, known as the inessential couplings, can take quite arbitrary values since changing them amounts to moving within an equivalence class

It follows, therefore, that an inessential coupling is any coupling for which a change in its value can be reabsorbed by a change of field variables.

The prototypical example of an inessential coupling is the one related to a simple linear rescaling or renormalization of the dynamical variables, namely, in a field-theoretic language, the wave function renormalization. However, there is an infinite number of other inessential couplings related to more general, nonlinear changes of variables. Hence, one is free to specify the values of all inessential couplings instead of computing their flow.

In order to optimize computations, we presented a concrete scheme, the *minimal essential scheme*. Essential schemes can be defined more generally as those for which we only compute the running of the essential couplings, having specified renormalization conditions that determine the values of the inessential couplings as functions of the former.

This leads to a precise definition of an *inessential coupling* and its *conjugate redundant operator*, whose identification is crucial to the concrete implementation of essential schemes.

In order to make contact with the previous versions of the exact RG, we reduce our general equations to the standard scheme where only a single inessential coupling, namely the wave function renormalization, is specified.

Wegner proved [200] that a fixed point of the RG, critical exponents associated with redundant operators are entirely scheme dependent. We discussed the corresponding fixed point equations and how the corresponding critical exponents can be obtained, contrasting the differences between the standard and (minimal) essential schemes.

Finally we reviewed how the *minimal essential scheme* devised in [175, 199] can be employed to remove all inessential couplings in the higher derivative scalar theory and in pure gravity. We saw this can be carried out order by order in the derivative expansion, where only terms with up to s derivatives of the fields are included in the Effective Action. At each order s the minimal essential scheme is implemented by identifying the inessential couplings at a Gaussian fixed point of the theory and fixing their values, such that one obtains beta functions for the essential couplings only. For QEG we wrote down a systematic derivative expansion of the diffeomorphism-invariant part of the RG. In particular, expanding the EAA to fourth order in derivatives, we analyzed the GFP

properties: in particular, from this analysis, we calculated that the vacuum energy is inessential.

Finally, studying the RG flow of QEG in the minimal essential scheme at orders two and four of the derivative expansion, confirmation of the existence of the Reuter fixed point is provided.

However, from the known flow diagram of the cosmological constant and Newton's constant stemming from the Einstein–Hilbert action (see Figure 3.3), there are RG trajectories which do not end at the Gaussian fixed point (where $\Lambda_0 = 0$). Trajectories of the Type IIIa and Ia possess instead in the IR a cosmological constant $\Lambda_0 > 0$ and $\Lambda_0 < 0$, respectively. Finally, we speculated how this fact could entails two different physical consequences:

- Either the different trajectories compatible with $\Lambda_0 \neq 0$ are stemming from effective actions which are parameterized by different field variables with different numbers of degrees of freedom and possibly contain also non-local terms (this would be equivalent to flowing along an inessential direction of the QEG universality class; a flow along an essential coupling, aka a field transformation leading to a different metric, would lead to the same theory with Λ_0).
- The distinction between essential and inessential couplings cannot be performed in a gravitational context. This could represent another manifestation of the very special nature of gravity and its Background Independence.
  To investigate more in this direction it would be important to study the flow of essential couplings in a bimetric truncation.

We shall come back to the essential RG in Chapter 13 where we adopt this scheme to the analysis of the renormalization of relational observables in asymptotically safe gravity.

Part II

Fluctuation modes on dS space: geometrized RG evolution, spectral flows, and scattering amplitudes

CHAPTER 6

Introduction and Survey of Part II

In **Part I** we introduced the Asymptotic Safety scenario in a continuum-based approach, where the ultraviolet completion of Quantum Gravity is realized via a non-trivial fixed point of the renormalization group flow. We now present several novel lines of research, which explore the implications of nonperturbative renormalizability, Background Independence and scattering amplitudes for the geometrical aspects of quantum dynamics in de Sitter spacetime. This **Part II** is based on the author's work published in [RF1], [RF2], [RF3], [RF4] and [RF5].

Cosmological observations suggest that we are living in a Universe with an accelerating expansion. Evidence for this is provided by observations of distant galaxies [255, 256] and the Cosmic Microwave Background [257]. In General Relativity, this is modeled by a de Sitter Universe: the unique constantly curved solution to Einstein's equation with a positive cosmological constant. To understand the interplay between its geometrical and quantum dynamical aspects is one of the main challenges for Quantum Gravity: Firstly, because it represents the natural arena to address quantum field theoretical questions in curved spacetime; secondly, because there are a number of theoretical issues which seem to be special to de Sitter spacetime.

The novel investigations described in the following exploit several different techniques. We make use of the RG trajectories for dynamical gravity, in particular those supplied by the established apparatus of the functional renormalization group for Quantum Einstein Gravity. At first, we initiate a systematic search for natural geometric structures which can help to efficiently structure the RG data, understand their physical interpretation, and consider concrete applications (**Project (II.A)**). In particular, we examine the geometrization of the resulting family of solutions of self-gravitating quantum system living in a 4D scale-dependent de Sitter spacetime.

Furthermore, we explore the scale-dependent effective geometry of the de Sitter solution by using a new ingredient: the modified spectral flow (**Project (II.B)**). This tool is particularly useful to encode the information about the nonperturbative backreaction of the dynamically gravitating quantum fluctuations on the mean field geometry.

While non-renormalizability of gravity becomes relevant at short distances, defining quantum observables that include long-distance curvature effects has not been without

problems either. In this direction, in the third line of research, we set up a new formalism to consistently construct scattering amplitudes in curved spacetime (**Project (II.C)**).

Let us be more explicit about these projects and discuss them in turn.

Project (II.A): Geometrization of renormalization group histories: a novel AdS/CFT correspondence

We saw already that the gravitational Effective Average Action (GEAA) is a versatile framework of Quantum Field Theory for the Background Independent and generally covariant quantization of gravity and matter fields coupled to it [95] (see Chapter 3). The concepts involved in, and practical tools provided by this approach are fully nonperturbative and do not assume a pre-existing spacetime. Being rooted in the functional renormalization group, the GEAA describes gravitational systems in terms of a one-parameter family of effective field theories. They describe the properties of a dynamically generated spacetime, and the dynamics of gravitational and matter fluctuations therein on different resolution scales.

While the bare field representing gravity at the microscopic level is not restricted to be a metric tensor [117, 258–261], the expectation values encoded in the GEAA functionals include a scale-dependent spacetime metric [195, 246]. Its dependence on the coarse graining scale gives rise to a fractal-like picture of the quantum gravity spacetimes at the mean field level [262]. Thereby the emergence of a classic world from the quantum regime hinges on whether or not the RG evolution comes to a halt eventually [49].

As described in Section 3.6, separately for each RG scale $k \in \mathbb{R}^+$, the respective GEAA functional Γ_k implies a quantum corrected variant of Einstein's equation (self-consistency equation); its solutions are the resolution dependent metrics $g_{\mu\nu}^k$. They are different for different scales usually, but establish (pseudo-) Riemannian structures on one and the same smooth manifold, $\mathcal{M}_d$.

(1) Geometrization. If we regard the primary RG trajectory on the theory space under consideration, $\mathcal{T}$, as a map $\mathbb{R}^+ \to \mathcal{T}$, $k \mapsto \Gamma_k$, then the "running" solution to the scale-dependent Einstein equations can be seen as an associated map from $\mathbb{R}^+$ into the space of metrics on $\mathcal{M}_d$. Thereby the association $k \mapsto g_{\mu\nu}^k$ describes the family of (pseudo-) Riemannian structures $\left(\mathcal{M}_d, g_{\mu\nu}^k\right)$ which quantum spacetime displays for different values of the RG parameter. Heuristically, we may think of $g_{\mu\nu}^k$ as the effective metric which is detected in experiments that involve a typical momentum scale of the order of k.

This represents a longstanding conjecture that beyond the RG flow further natural geometric objects might be "living" on the manifold $\mathcal{T}$. For example, after the advent of Zamolodchikov's c-theorem [263, 264], related investigations in more than 2 dimensions focused on searching for a scalar "c-function" and a metric on $\mathcal{T}$ by means of which the RG flow could be promoted to a *gradient flow*. Even though this program was not fully successful in the generality originally hoped for, it ultimately led to important developments such as the proof of the a-theorem [265].

The conjectured *AdS/CFT correspondence* "geometrizes" RG flows by a different approach which identifies the scale variable of the RG equations with a specific coordinate on a higher-dimensional (bulk) spacetime [45, 229, 266, 267]. In this way the 'RG scale' (and its related 'RG time" $t \equiv \log k$) acquires a status similar to the ordinary spacetime coordinates.

Along a different line of research, the fundamental idea of *dimensionally extending spacetime by scale variables* has been developed in considerable generality in the work of L. Nottale [268]. In his approach the RG time is on a par with the usual spacetime coordinates, both conceptually and geometrically.

The present investigation is devoted to a different notion of geometrized RG flows. While it does have certain traits in common with the various theoretical settings mentioned above, it is more conservative, however, in that its starting point does not involve any unproven assumptions. This starting point consists of nothing but the standard RG trajectories supplied by a functional renormalization group equation (FRGE). We propose to exploit those RG-derived data, and only those, to initiate a systematic search for *natural geometric structures* which can help in efficiently structuring those data and/or facilitate their physical interpretation or application.[1]

(2) GEAA-based geometrization. Here we deal with the nonperturbative functional RG flows of Quantum Einstein Gravity which we reviewed in Chapter 3. We assume that it is described by an effective action functional $\Gamma_k[g_{\mu\nu}]$ which depends both on a 4D spacetime metric $g_{\mu\nu}$, and on some kind of RG scale, $k \in \mathbb{R}^+$, implemented as an infrared cutoff, for example. Furthermore, we suppose that we managed to solve the corresponding FRGE for (partial) trajectories in theory space, i.e., maps $k \mapsto \Gamma_k[g_{\mu\nu}]$ whereby the curve parameter k does not necessarily cover all scales $k \in \mathbb{R}^+$.

For every given value of k, the running effective action Γ_k implies an effective field equation for the expectation value of the metric, typically a generalization of Einstein's equation. Solutions to those effective Einstein equations inherit a k-dependence from $\Gamma_k[\cdot]$, and we shall denote them $g_{\mu\nu}^k(x^\rho)$ in the following. More precisely, in this paper we are going to analyze a situation where the solutions at differing scales are selected

---

[1]A first analysis along these lines can be found in [269] where contact was made with the Randall–Sundrum model.
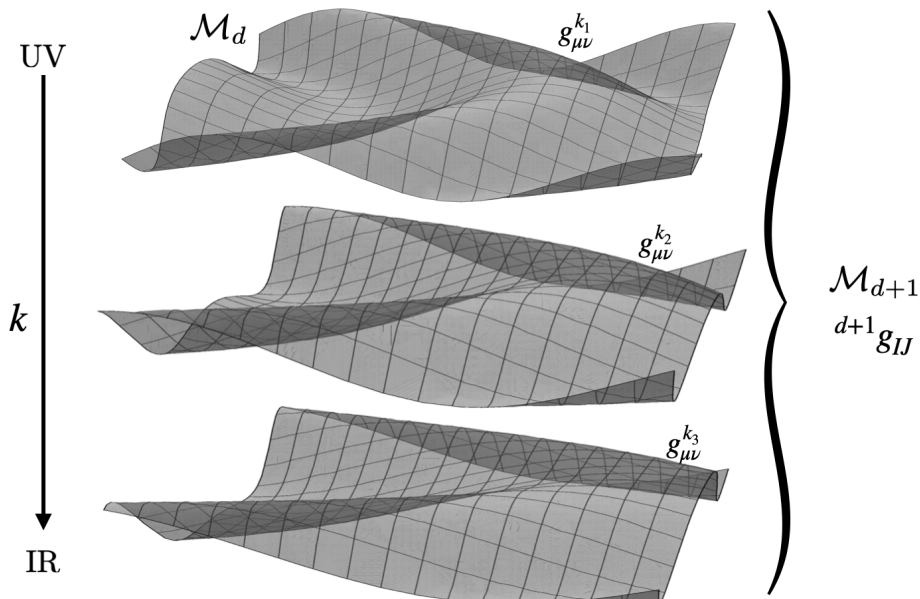
FIGURE 6.1. Geometrization of the RG evolution: For $d = 4$, the leaves of the foliation of $\mathcal{M}_5$ describe the 4-dimensional spacetime at different values of the RG scale k.

such that $g_{\mu\nu}^k$ depends on k smoothly. Therefore, we may regard the map $k \mapsto g_{\mu\nu}^k(x^\rho)$ as a smooth trajectory in the space of all metrics that are compatible with a given differentiable manifold, $\mathcal{M}_4$. Thus, technically speaking, the output of the functional RG - and effective Einstein equations amounts to a family of Riemannian structures on one and the same spacetime manifold:

$$\left\{ (\mathcal{M}_4,\, g_{\mu\nu}^k) \mid k \in \mathbb{R}^+ \right\}. \tag{6.1}$$

This represents a new way of analyzing the family of metrics $g_{\mu\nu}^k$ that furnish the same, given 4-dimensional manifold $\mathcal{M}_4$. The idea is to interpret the 4D spacetimes $\left(\mathcal{M}_4,\, g_{\mu\nu}^k \right)$, $k \in \mathbb{R}^+$, as different slices through a single 5-dimensional (pseudo-) Riemannian manifold:

$$\left(\mathcal{M}_5,\, {}^{(5)}g_{IJ} \right). \tag{6.2}$$

Thereby the $g_{\mu\nu}^k$'s are related to the 5D metric ${}^{(5)}g_{IJ}$ by an *isometric embedding* of the 4D slices into $\mathcal{M}_5$. Stated the other way around, $\left(\mathcal{M}_5,\, {}^{(5)}g_{IJ} \right)$ is a single *foliated manifold*, the leaves of whose foliation describe the spacetime at different values of the RG parameter (see Figure 6.1). If k has the interpretation of an (inverse) coarse graining scale on $\mathcal{M}_4$, then $\mathcal{M}_5$ naturally comes close to a "scale-space-time" manifold [268]. In addition to the usual event coordinates x^μ, its points involve a certain value of the scale or coarse graining parameter: (k, x^μ).

Actually $\mathcal{M}_5$, equipped with some metric $^{(5)}g_{IJ}$ can encode more information than is contained in the underlying family $\left(\mathcal{M}_4, g_{\mu\nu}^k\right)$. This is most obvious if we use local coordinates which are adapted to the foliation by the surfaces of equal scale. The scale parameter (or an appropriate function thereof) plays the role of a 5th coordinate then, and the basic trajectory of 4D metrics $g_{\mu\nu}^k(x^\rho) \equiv g_{\mu\nu}(k, x^\rho)$ is reinterpreted as 10 out of the 15 independent components which $^{(5)}g_{IJ}(k, x^\rho)$ possesses.

Our main interest is in its additional components, $^{(5)}g_{\mu k}(k, x^\rho)$ and $^{(5)}g_{kk}(k, x^\rho)$, respectively. The question we are going to address is whether those functions can be determined in a mathematically or physically interesting way such that a single 5D geometry not only encapsulates or "visualizes" a trajectory of 4D geometries, but also enriches it by additional information. Schematically,

$$\boxed{\text{trajectory of 4D geometries}} \; + \; \boxed{?} \; = \; \boxed{\text{unique 5D geometry}}$$

Loosely speaking, what we are proposing here is a bottom-up approach which starts out from the safe harbor of a well understood and fully general RG framework and only in a second step tries to assess whether, and under what conditions there exist natural options for geometrizing the RG flows.

This approach must be contrasted with top-down approaches like the one based upon the AdS/CFT conjecture, for instance. They would rather begin by postulating the geometrization and ask about its relation to standard RG flows at the second stage only (see Table 6.1).

Top-down approach	Bottom-up approach
Postulate a geometry	Start from the well understood and fully general RG framework
Ask about its relation to standard RG flows	Look for conditions for a natural geometrization

TABLE 6.1. The top-down and bottom-up approached contrasted.

In this thesis, Chapter 7 will be devoted to a detailed exposition of **Project (II.A)**.

Project (II.B): Spectral geometry of de Sitter space

This second research line (Chapter 8) is devoted to the role played by the principle of Background Independence in Quantum Gravity. Concretely we explore its implications for the microstructure of de Sitter spacetime and its effective quantum geometry.

We partly follow ideas from spectral flow methods applied to kinetic operators. This technique turned out to be a powerful tool for uncovering properties of "quantum spacetimes" which, in a generalized sense, are of a geometric nature.

(1) IR vs. UV. In treatises on QFT and its manifold applications, hardly any terminology is as ubiquitous as the pair of opposites "ultraviolet" and "infrared". And yet, almost never a precise explanation, let alone a mathematical definition of these notions is provided. This is particularly noteworthy given the wealth of connotations these terms have. Often these connotations are intended in order to cut a long argument short, but sometimes they are not, and this can cause a considerable amount of confusion.

For a long time the Quantum Field Theory parlance of UV and IR has never been examined critically. Clearly the reason is that in simple (non-gauge or weakly coupled) theories that live on an invariable Minkowski spacetime, there is little room for misinterpretations. Here, UV (IR) is traditionally considered synonymous to high momentum (low momentum), and thanks to the relationship $\vec{p} = \hbar\,\vec{k}$ this generalized meaning is still quite close to the original one in optics, i.e., high (low) wave number $|\vec{k}|$ or equivalently small (large) wavelength $\lambda = 2\pi/|\vec{k}|$. If one speaks of periods in time rather than space one similarly associates the UV (IR) with a regime of high (low) frequencies. Obviously,this jargon is particularly befitting to special relativistic theories that contain particles (photons) with a massless dispersion relation $\omega = c\,|\vec{k}|$.

A slightly less trivial extension of the meaning attached to UV (IR) consists in generalizing the correspondence UV (IR) ⇔ *small (large) wavelength* from the wavelengths of photons to arbitrary length scales. Then the UV-IR jargon often is meant to refer to a general dichotomy of "tiny things" vs. "big things", i.e., UV (IR) ⇔ *small (large) length scales.*

In renormalization group theory yet another, in principle logically independent usage of the UV-IR pair is common. RG trajectories on theory space come with a natural orientation. It is defined by the direction of successively integrating out further fluctuation modes, for instance by the iteration of block spin transformations. This natural direction is said to be "the direction from the UV to the IR", the reason being that, usually, block spin transformations integrate out short wavelength fluctuations first, and those with larger wavelengths only later. This then motivates the terminology UV (IR) ⇔ *beginning (end) of RG trajectories.*

As we shall see later in this thesis, the latter correspondence, when used together with the other ones, can become the source of severe misconceptions, in particular in the realm of Quantum Gravity.

At a more technical level, the various connotations of UV (IR) are meaningful, and mutually consistent, if the physical situation under consideration is essentially determined by the d'Alembert operator of Minkowski space,[2] $\Box_\eta \equiv \eta^{\mu\nu}\partial_\mu\partial_\nu$. Its eigenfunctions are plane waves which comply with the assumed proportionalities ($\vec{p} = \hbar \, \vec{k}$, $\omega = c \, |\vec{k}|$), and moreover, the uncertainty principle of classical Fourier analysis establishes the desired reciprocity *small (large) lengths $\Leftrightarrow$ high (low) momenta* in full generality.

On the other side, the meaning of the labels UV and IR tends to become increasingly dubious the stronger the phenomena considered deviate from the physics of (quasi-)free fields or plane waves. A hardly avoidable first step in this direction occurs whenever local gauge invariances play a role, so that the relevant kinetic operator is now a co-variantized d'Alembertian, $\Box_A = \eta^{\mu\nu}D_\mu D_\nu +$ "more", involving a certain covariant derivative $D_\mu = \partial_\mu + iA_\mu$. Then, canonical and kinetic momenta must be distinguished, and importantly, the spectrum of $\Box_A$ and the properties of its eigenfunctions may differ substantially from those of the free d'Alembertian.

Similar remarks apply to theories coupled to gravity where the covariantization is with respect to spacetime diffeomorphisms.

In the worst case, strong Yang–Mills or gravitational fields may ruin the essential justifications of the UV-IR folklore, the correspondence between short lengths and high momenta in particular. In extreme cases this can give rise to expressions as rich in connotations as "the infrared of QCD", or "the ultraviolet of Quantum Gravity". Very often, rather than describing regimes of well defined physical quantities, they are just meant to express the very horrors in the respective branches of physics, strong nonperturbative effects in the first, and lack of fundamental knowledge in the second case.

In Quantum Field Theories coupled to dynamical gravity, the UV-IR terminology is bound to become problematic almost by definition. When the spacetime metric is variable, there are now two equally plausible candidates for what one may call "the ultraviolet". Namely, first, the term again could describe a regime of high momenta of some type. But second, it also might stand for a physical situation in which no momentum assumes any particular value, but rather the dynamically determined metric coefficients $g_{\mu\nu}$ happen to turn out very small so as to render all proper lengths extremely tiny. It goes without saying that these two notions of "UV-ness" are entirely different.

In fact, in Chapter 8 of this thesis we shall explore asymptotically safe Quantum Einstein Gravity [49, 50, 95, 96] and find that, in a precise sense, the pertinent "ultraviolet of Quantum Gravity" does indeed satisfy the expectations of one of the two candidates for "UV-ness", *but not of the other.*

---

[2]Or the Laplacian on flat Euclidean space.

Finally, we strictly adhere to the following rule: *The denomination UV (IR) is used exclusively to indicate the limiting regime $k \to \infty$ ($k \to 0$) of an RG trajectory, whereby the parameter value $k = \infty$ ($k = 0$) corresponds to no (all) modes being integrated out.*

This is an unambiguous definition as it does not rely on any properties of the mode functions (short or long wavelength, etc.). In fact, we shall try to be as unbiased as possible with respect to the (un-) importance of particular distance or momentum scales in the effective field theories defined by $\Gamma_{k \to \infty}$ in the UV, and $\Gamma_{k \to 0}$ in the IR case.

(2) Effective field theory. In the GEAA context, the above "UV-IR confusion" hints at a severe problem with a nontrivial physics contents since the parameter k gives us the scale at which the GEAA could possibly define an effective field theory. In fact, the action functional $\Gamma_k [h_{\mu\nu}; \bar{g}_{\mu\nu}]$ introduced in (3.5) defines an effective field theory that governs the dynamics of $h_{\mu\nu}$ on a background spacetime furnished with the metric $\bar{g}_{\mu\nu}$. This is to say that if an experiment or observation involves only a single characteristic momentum scale of the order of k, then a tree-level evaluation of Γ_k can suffice to describe it reliably. Typically this is the case when the experimental setting gives rise to a physics-generated cutoff mechanism, at some scale k_{phys}, which then acts as the true cutoff and renders the integrating-out of further field modes superfluous once k is lowered below k_{phys}. By this decoupling mechanics [49] the action Γ_k becomes approximately k-independent in the IR, i.e., for $k \lesssim k_{\text{phys}}$. Hence the standard effective action $\Gamma = \Gamma_{k=0}$ agrees basically with $\Gamma_k \big|_{k=k_{\text{phys}}}$ then. In this case the functional integral is essentially determined by those field configurations which, according to the relative weights given by ΔS_k, are characterized by the scale k_{phys}. In physical situations which involve more than one relevant scale the analysis is more involved usually and one is forced to go beyond the tree level evaluation of Γ_k.[3]

(3) Spacetime properties from a spectral flow. In order to prevent this sort of problems arising from an incomplete implementation of Background Independence, in this thesis we chose to adopt spectral methods in order to investigate the properties of quantum spacetime in a Background Independent fashion.

First we review how spectral data of Laplace-type operators can furnish information about the quantum spacetime within the GEAA framework (in Euclidean signature [270–

---

[3]The limitation one encounters if one wants to stay within the class of single-scale problems can be illustrated by an example from the cosmology of the real Universe: A group of physicists perform in their terrestrial laboratory experiments that probe a region of spacetime of Planckian size which can be assumed independent of the rest of the Universe. Furthermore, a group of astronomers explore the very young, still "small" Universe at the age of about one Planck time. Then, within a single-scale and tree-level approximation, the findings of both groups are expected to be described optimally by the very same effective field theory, namely $\Gamma_{k=m_{\text{Pl}}}$ which reflects the presence of the UV fixed point. In neither case the descriptions will be perfect, and one may want to improve upon the single-scale, tree level approximation. Only at this second stage differences will occur between the respective descriptions of the two physical situations.
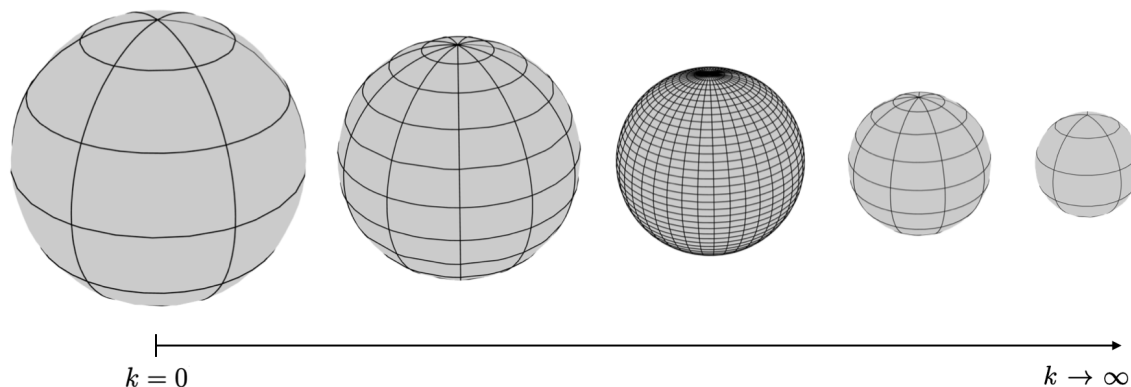
FIGURE 6.2. Thinning out of degrees of freedom in the UV: The size of the various spheres indicates the self-consistent radius $L^{\text{sc}}(k)$ at increasing values of k, and the coordinate grids shown visualize the (first increasing, then decreasing) angular resolving power of the spherical harmonics.

272]. The authors elaborate in particular on the distinction between the standard ("off-shell") eigenvalue problem on a rigid background geometry, and the "on-shell" spectral problems typical of Background Independent Quantum Gravity. They introduced and applied a number of tools for extracting physics information from the EAA which arises only after going on-shell, or by choosing the background self-consistently and setting the fluctuations to zero. They focused on the eigenvalue equation of the background Laplacian which, when still off-shell, organizes the coarse graining and "integrating out" of field modes that underlies the functional RG.

Letting the background become self-consistent, the most surprising result was found: the eigenvalue equation turns into a complicated nonlinear relationship between the quantum number characteristic of a mode's "fineness" and the RG parameter k. This relation is particularly striking: After a particular value, increasing k no longer leads to a finer resolution of the modes, but rather the opposite, brings one back to coarser ones. This phenomenon is associated to the RG trajectories drawn in Chapter 3 and is schematically sketched in Figure 6.2.

In general there exist particular backgrounds, so-called self-consistent geometries, that are dynamically preferred (see Section 3.6). Concretely, it has been found that the ultraviolet regime of Quantum Einstein Gravity has far fewer effective degrees of freedom than (incorrectly) predicted by a background dependent analysis. The "ultraviolet regime of Quantum Gravity", defined unambiguously as the $k \to \infty$ limit on an asymptotically safe RG trajectory, is not at all the realm of probes or "microscopes" with an unlimited resolving power. In the limit $k \to \infty$ in fact, not every point on the manifold can be distinguished with an infinite precision. Instead, its this regime can be

classified as "IR-like". This phenomenon can be attributed to the gravitational backreaction on the quantum system, which breaks the traditional large k, large momentum, high-resolution association.

The origin of this phenomenon is related to the spacetime properties from the spectral flow. In [271, 272] it was proposed to analyze the physics contents of generalized trajectories obtained in [97] (see Section 3.5) by means of *spectral flow techniques* similar to those used in index theory, for example [273]. In fact, the action functional $\Gamma_k[h_{\mu\nu}; \bar{g}_{\mu\nu}]$ defines an effective field theory that governs the dynamics of the metric fluctuations $h_{\mu\nu}$ on a background spacetime furnished with the metric $\bar{g}_{\mu\nu}$. We plan to analyze the physical contents of such generalized trajectories by means of spectral flow techniques. These involve constructing the associated Laplacian operator and consider its eigenvalue problem. The central idea is to perform this analysis for all points of the generalized RG trajectory; if we manage to solve this family of differential equations, we have an entire trajectory of spectra at our disposal.

Given a metric $\bar{g}_{\mu\nu}$ we can construct the associated Laplacian operator $\Box_{\bar{g}} = \bar{g}^{\mu\nu} D_\mu D_\nu$ and consider its eigenvalue problem.

$$\boxed{\text{Running action}} \Rightarrow \boxed{\text{Running metric}} \Rightarrow \boxed{\text{Running spectrum}}$$

Switching to Lorentzian signature, one of the new aspects to be investigated, we introduce various spectral problems related to the d'Alembertian in curved spacetime that we shall encounter; In this way, we can analyze the Lorentzian analog of the Euclidean phenomenon sketched in Figure 6.2.

In particular, we carry out the same analysis on de Sitter space. We study the d'Alembertian on 4-dimensional de Sitter space and determine the spectrum and the eigenfunctions. We give a detailed account of the eigenfunction's resolving power. Subsequently we exploit the RG trajectories of the Einstein–Hilbert truncation that have a positive cosmological constant throughout. We obtain the spectral flow along these trajectories in a fully explicit form. We solve the scale-dependent self-consistent condition for all k in de Sitter spacetimes with an appropriate running Hubble parameter $H = H(k)$. We analyze the Lorentzian analog of the gravitational backreaction phenomenon. In the Euclidean setting, the boundedness of the modes implies a fundamental limitation on the distinguishability of points in spacetime. In the Lorentzian setting instead, we find no analogous restriction for the resolvability of points on the 3D spatial manifold related to the foliation. However, rather than at very small distances, quantum phenomena will make their appearance in the regime of macroscopic proper distances.

Project (III.C): Scattering amplitudes in de Sitter spacetime

The third research line (Chapter 9) deals with the fully covariant construction of scattering amplitudes in de Sitter spacetime.

(1) Scattering amplitudes and Newtonian potential. While when studying short-distance properties of gravity infinities arise, defining quantum observables which include long-distance curvature effects is also non trivial. In this direction, a consistent construction of scattering amplitudes in curved spacetime may provide a first hint on how to make progress in setting up a theory of Quantum Gravity.

Scattering amplitudes in flat spacetime have been applied to understand diverse aspects of gravity. A classic result is the construction of the Newtonian potential from the scattering amplitude in the tree-level Born approximation. The potential is then obtained by taking the Fourier transform in momentum space. Treating gravity as an effective field theory, loop diagrams will give rise to two types of contributions to the gravitational potential: classical corrections due to the post-Newtonian expansion of GR, and purely quantum corrections.

Treating gravity as an effective field theory, loop diagrams will give rise to two types of contributions to the gravitational potential: classical corrections due to the post-Newtonian expansion of GR, and purely quantum corrections. The implementation of extracting quantum corrections from the scattering amplitude of two gravitationally interacting massive particles has been explored in e.g. [42, 274–276].

An alternative way to compute quantum corrections to the Newtonian potential is presented in [277–280]. When sources are moving slowly with respect to the speed of light and the gravitational field is weak, then the metric tensor can be expanded and expressed in terms of the so-called Bardeen variables. Computing the quantum-corrected equations of motion then allows to compute both post-Newtonian and quantum corrections to the gravitational potential.

(2) What is special about de Sitter. The computation of scattering amplitudes in de Sitter spacetime has a long history [281–285]. There are a number of theoretical issues which seem to be special to de Sitter spacetime, like the choice of the vacuum (and the coordinate system), the technical problems related to the analytic continuation, the ill-defined notion of momentum space, the absence of positive-definite energy-like conserved quantities and asymptotic states.

First attempts to construct such an amplitude gave divergent results [284]. This was attributed to the large-distance behavior of the graviton propagator [285–287]. Later work showed that the divergence was a gauge artefact [281, 283, 288–292]. Different

quantization prescriptions [293–296] and invariance requirements [297, 298] were imposed, in order to obtain a finite form for the graviton propagator. In these works, the graviton propagator was obtained by projecting the two-point function into a complete basis for symmetric rank-2 tensor fields on the (Euclidean) four-sphere [299] and then performing an analytic continuation.

There are a number of theoretical issues which seem to be special to dS spacetime (see e.g. [300–313]). The choice of the vacuum (and of the coordinate system) can furnish distinct results for the propagator [314–317]. Moreover, in the analytical continuation of the propagator, different choices of the orientation of the branch cut can be made, producing different Lorentzian Green's functions. Finally, in dS spacetime there exists a separate notion of spatial and temporal Fourier transformations, leading to subtleties in the representation in momentum space [318, 319].

Closely related to the dS universe is the AdS spacetime. Here, the AdS/CFT correspondence allows one to compute correlators in the boundary CFT [320, 321]. This was originally formulated for Euclidean signature [322–324]. In such a background, working in Euclidean signature usually does not lead to any restrictions since the results obtained in Euclidean AdS/CFT can be analytically continued to Minkowski space [325–329].

The struggle in the construction of observables related to scattering amplitudes also comprises the effort of computing the S-matrix in a dS background [330–334]. The relation between the early and late time descriptions of particle states contains a great amount of dynamical information about the interacting theory. However, in dS spacetime even one-particle states can decay and all particles are unstable [335–338]: there are no viable asymptotic states. This is related to the fact that there are no positive-definite energy-like conserved quantities. Furthermore, any observer will interact with a complete set of ingoing and outgoing states. Therefore, the S-matrix is not experimentally accessible to a single observer. Nonetheless, as we will demonstrate in this paper, it is perfectly possible to generalize Feynman diagrams to curved spacetime. We will adopt the assumption that the resulting object can still be interpreted as transition probabilities for scattering processes in dS spacetime.

In our research work, we put forward a novel technique to compute scattering amplitudes in de Sitter background. We assume that the resulting object can still be interpreted as transition probabilities for scattering processes in de Sitter spacetime. We present the amplitude of gravity-mediated scattering of two massive scalars in de Sitter spacetime (see Figure 6.3). In this investigation we use two new features. Firstly, we represent Feynman diagrams by differential operators, generalizing the Minkowskian notion of momentum: the curvature of spacetime is provided by the noncommutativity of the differential operators. Secondly, we employ an expansion around infinite scalar
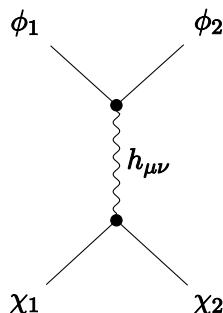
FIGURE 6.3. Feynman diagram of the scattering process considered $\phi\chi \to \phi\chi$ mediated by a graviton $h_{\mu\nu}$. Time flows from the left to the right.

masses, we use this amplitude to compute the de Sitter spacetime generalization of the Newtonian potential.

(3) Quadratic Gravity. Of particular interest in this context are modified theories of gravity, such as Quadratic Gravity (QuadG). First, QuadG successfully provides the dynamics of primordial graviton fluctuations [339, 340]. Its predictions for inflationary power spectra and spectral indices are in excellent agreement with observational data [341, 342], and lead to constraints on the gravitational couplings [27, 343–346]. QuadG is also attractive from a theoretical perspective. As was shown by Stelle [65, 66] it is perturbatively renormalizable in flat spacetime, in contrast to Einstein–Hilbert gravity. However, this does not come for free. The addition of four-derivative terms in the action implies that the resulting Hamiltonian is unbounded from below. Classically, this leads to the Ostrogradsky instability [347]. At the quantum level, it is signaled by the appearance of a massive spin-2 ghost [282, 348, 349].

Accordingly, we will extend our formalism to include non-minimal interactions. More specifically, we consider the tree-level scattering of two scalar fields in QuadG, given by R^2- and C^2-terms in the action, in addition to the Einstein-Hilbert action with cosmological constant. Apart from a kinetic term and mass term, the action for the scalar fields is given by an $R\phi\phi$ interaction.

(4) Modified Newtonian Dynamics. Replacing the classical Newtonian potential by a more general potential falls into the class of Modified Newtonian Dynamics [350–353]. This has been used to successfully account for the observed properties of rotation curves of galaxies [354–356]. Therefore, it is seen as an alternative to the DM hypothesis. In our setting, we will test whether the modifications to the Newtonian potential due to QuadG in de Sitter spacetime give rise to a DM-like Modified Newtonian Dynamics (MOND) scenario.

Plan of Part II

In the following table we schematize how this part is structured:

Part II	**Project (II.A)**	Chapter 7	Geometrization of RG histories AdS/CFT
	Project (II.B)	Chapter 8	Spectral geometry of de Sitter space
	Project (II.C)	Chapter 9	Scattering amplitudes in de Sitter spacetime

TABLE 6.2. Plan of **Part II**.

Finally, an overall Discussion and Summary of this Part can be found in Chapter 10.

CHAPTER 7

Geometrization of renormalization group histories: AdS/CFT

Executive summary. We discuss the geometrization of entire evolution histories by means of a single, $(d+1)$-dimensional manifold furnished with a fixed (pseudo-) Riemannian structure. We propose a universal form of the higher-dimensional metric and discuss its properties. In Euclidean signature, under precise conditions, it turns out that this metric is always Ricci flat and admits a homothetic Killing vector field; if the evolving spacetimes are maximally symmetric, their $(d+1)$-dimensional representative has a vanishing Riemann tensor even. The monotonicity requirement for the running of the cosmological constant, which we test in the case of asymptotic safety, is crucial to obtain non-degenerate geometrizations.

Further, we admit Lorentzian signature and $(d+1)$-dimensional Einstein spaces, focusing on maximally symmetric metrics. Embedding the resulting family of 4D de Sitter solutions with a running Hubble parameter, it turns out that there are only two possible 5D spacetimes: the anti-de Sitter manifold AdS$_5$ and the de Sitter manifold dS$_5$. Employing the cross-over trajectory connecting the non-Gaussian to the Gaussian RG fixed point, we show that if the scale invariance of the QEG fixed points extends to full conformal invariance, the 5D picture of the resulting geometric and field theoretic structure displays a novel kind of "AdS/CFT correspondence". While strongly reminiscent of the usual string theory-based AdS/CFT correspondence, also clear differences are found.

What is new? All results of this chapter represent novel research results.

Based on: References [RF1] and [RF2].

Plan of this Chapter. We set up a convenient framework, based upon a generalization of the Arnowitt–Deser–Misner (ADM) construction, for the embedding of a given family $g_{\mu\nu}^k$ in a higher-dimensional geometry. Then, we then provide a simple, yet fully explicit and sufficiently general class of such families $g_{\mu\nu}^k$. They correspond to running Einstein metrics, and all subsequent demonstrations refer to this class of solutions. A priori our goal of searching of "interesting" 5D geometries is an extremely broad one; to be able to make practical progress we therefore narrow its scope to a particular class of ADM metrics, which we introduce and discuss. Then, we show that, under precise conditions, the running 4D Einstein spaces can always be embedded in a 5D geometry which admits a *homothetic Killing vector field* and is *Ricci flat*; should the Einstein

107

spaces be maximally symmetric, it is even strictly, i.e., Riemann flat. The important point about these options for a geometrization of RG flows is that they neither follow from pure geometry alone, nor are they "for free" what concerns the properties of the RG trajectory. Rather, they are a global geometric manifestation of a specific general feature of the RG trajectory. In the present example, this *sine qua non* is that the running cosmological constant $\Lambda(k)$ is a strictly increasing function of the scale. Finally, we show that for the asymptotically safe trajectories of QEG this is indeed the case.

In Section 7.4 we are going to investigate the possibility of embedding scale histories of d-dimensional effective metrics $g_{\mu\nu}^k$ in a unique $(d+1)$-dimensional manifold. In fact, most discussions in this paper are valid for arbitrary dimensionalities d. Working within the same class of higher-dimensional metrics $^{(d+1)}g_{IJ}$, we now investigate the particularly relevant case where $^{(d+1)}g_{IJ}$ is Einstein, and both $g_{\mu\nu}^k$ and $^{(d+1)}g_{IJ}$ are Lorentzian. We impose maximum symmetry on $g_{\mu\nu}^k$, and find that under this condition $^{(d+1)}g_{IJ}$ can be chosen maximally symmetric, too. This leaves us with two potential candidates for an embedding spacetime, namely $\mathcal{M}_{d+1} = \text{AdS}_{d+1}$ and $\mathcal{M}_{d+1} = \text{dS}_{d+1}$, respectively. Moreover, we prove that both options are viable actually, i.e., that there exists an admissible coordinate transformation that relates the RG parameter k to the coordinate which labels the leaves of the foliation displayed by $^{(d+1)}g_{IJ}$. In this step, essential use will be made of the monotone k-dependence of the running cosmological constant. Then, we analyze the global properties of the embeddings obtained, and we show that the picture of a certain "(A)dS/CFT correspondence" emerges from the RG flow of QEG, thanks to its Asymptotic Safety.

In Section 7.10 we compare this non-standard correspondence to the usual one based upon string theory, highlighting their similarities and main differences.

Appendix E contains the details regarding the possible geometrization and embedding procedure for maximally symmetric spacetimes.

This chapter is composed by a rearrangement of the author's publications [RF1], [RF2].

7.1. FROM TRAJECTORIES OF METRICS TO HIGHER DIMENSIONS

We start by describing a geometrization procedure of renormalization group trajectories of $d = 4$ Quantum Einstein Gravity. The first part of this section is generically valid in any d and $d + 1$ dimensions, later on, along the procedure, we will specify to $d = 4$ trajectories embedded in $d = 5$. Furthermore, here the indices $I, J, K, \cdots$ assume values in $\{0, 1, 2, \cdots, d\}$, while Greek indices run from 1 to d only.

We will start by exploiting the resulting solutions of FRG framework, whose specifics do not matter here, in order to derive a scale-dependent effective field equation. Let us assume further that the generalized effective Einstein's equation can be solved, obtaining families of metrics $g_{\mu\nu}^k$ labeled by the RG scale k.

In [357, 358] the set $\{g_{\mu\nu}^k\}_{k\geq 0}$ was associated to a *family of different Riemannian structures*. These structures furnish one and the same d-dimensional manifold $\mathcal{M}_d$. Accordingly, we can regard the mapping $k \mapsto (\mathcal{M}_d, g_{\mu\nu}^k)$ for $k \in \mathbb{R}^+$ as a trajectory in the space of d-dimensional (Euclidean) spacetimes.

Their associated line elements can be expressed in local coordinates

$$\mathrm{d}s_d^2 = g_{\mu\nu}^k(x^\rho)\mathrm{d}x^\mu\mathrm{d}x^\nu, \qquad \mu, \nu, \cdots = 1, 2, \cdots, d. \tag{7.1}$$

The main novelty of this approach is to interpret the RG parameter k, or after a convenient reparametrization $\tau = \tau(k)$, as an additional *coordinate*. This additional coordinate, together with x^μ, coordinatizes a $(d+1)$-dimensional manifold $\mathcal{M}_{d+1}$. This corresponds to an isometric k-dependent embedding of the original manifold $\mathcal{M}_d$ in $\mathcal{M}_{d+1}$. Hence, through the k-dependence, $\mathcal{M}_{d+1}$ results already equipped with a natural foliation.

Along these lines, a new picture is emerging: The entire RG trajectory of ordinary spacetimes is described by *a single* higher-dimensional Riemannian manifold, $\left(\mathcal{M}_{d+1}, {}^{(d+1)}g_{IJ}\right)$. Its corresponding line element reads

$$\mathrm{d}s_{d+1}^2 = {}^{(d+1)}g_{IJ}(y^K)\mathrm{d}y^I\mathrm{d}y^J \tag{7.2}$$

Here, $y^I \equiv (y^0, y^\mu)$ are generic local coordinates on $\mathcal{M}_{d+1}$ and the indices $I, J, K, \cdots$ assume values in $\{0, 1, 2, \cdots, d\}$.

7.1.1. *ADM formalism*

Since $\mathcal{M}_{d+1}$ is emerging with a natural foliation it will be convenient to exploit the construction of the ADM formalism [49].

Assume we are given with an arbitrary manifold $\left(\mathcal{M}_{d+1}, {}^{(d+1)}g_{IJ}\right)$ and we introduce a scalar "RG time function" $y \mapsto \tau(y)$ which maps a specific scale to each of its points, such that the level sets of this function are $\Sigma_\tau \equiv \{y \in \mathcal{M}_{d+1} | \tau(y) = \tau\}$. We can interpret them as a stack of standard, d-dimensional spacetimes with associated different resolution scale $\tau \equiv \tau(k)$.

We can construct the gradient $n_I \equiv N\partial_I\tau$ as a vector n^I which is everywhere normal to the slices Σ_τ. We normalize it in such a way that

$$^{(d+1)}g_{IJ}\, n^I n^J = \varepsilon \,, \tag{7.3}$$

where the sign $\varepsilon = \pm 1$ is determined whether the normal vector is space- or time-like. At this stage, we allow $^{(d+1)}g_{IJ}$ to be a metric of any signature, but $g^k_{\mu\nu}$ is assumed to have Euclidean signature. Later on, we shall establish criteria which determine whether the RG time τ really turns into a time coordinate ($\varepsilon = -1$) and describes a Lorentzian metric on $\mathcal{M}_{d+1}$, or whether it amounts to a further spatial dimension ($\varepsilon = +1$).

We perform a transformation of the coordinates $y^I = y^I(x^J)$ to foliation-adapted ones $x^I \equiv (x^0, x^\mu) \equiv (\tau, x^\mu)$, in order that τ labels different "RG time slices" and the x^μs are coordinates on a given Σ_τ. That is to say, by defining a vector field t^I such that $t^I\partial_I\tau = 1$, requiring that the coordinates x^μ are constant along the integral curves of t^I we relate the coordinate systems on neighbouring slices.

At any point of $\mathcal{M}_{d+1}$ the tangent space can be decomposed into a subspace spanned by vectors tangent to Σ_τ and its complement. The corresponding basis vectors are given by derivatives of the functions $y^I = y^I(x^J) = y^I(\tau, x^\mu)$

$$e_\mu{}^I = \frac{\partial}{\partial x^\mu}y^I(\tau, x^\alpha), \qquad t^I = \frac{\partial}{\partial\tau}y^I(\tau, x^\alpha) \,. \tag{7.4}$$

These vectors describe the embedding of Σ_τ into $\mathcal{M}_{d+1}$. Accordingly, the e_μ's are orthogonal to n:

$$^{(d+1)}g_{IJ}\, n^I e_\mu{}^J = 0 \,. \tag{7.5}$$

Furthermore, the embedding induces the following metric from the ambient metric $^{(d+1)}g_{IJ}$ on the slices Σ_τ:

$$^{(d)}g_{IJ} = e_\mu{}^I e_\nu{}^J\, ^{(d+1)}g_{IJ} \,. \tag{7.6}$$

Since, in general the vector t^I has nonvanishing components in the directions of both n^I and $e_\mu{}^I$, it can be expanded in terms of the lapse function $N(\tau, x^\mu)$ and the shift vector $N^\mu(\tau, x^\mu)$:

$$t^I = Nn^I + N^\mu e_\mu{}^I \tag{7.7}$$

The relation between the two coordinate systems is given by the definitions (7.4). Using (7.7):

$$dy^I = t^I d\tau + e_\mu{}^I dx^\mu = Nn^I d\tau + e_\mu{}^I(dx^\mu + N^\mu d\tau) \,, \tag{7.8}$$

and inserting (7.8) into $ds^2_{d+1} = {}^{(d+1)}g_{IJ}dy^I dy^J$ the line element in terms of the ADM variables $\{N, N^\mu, {}^{(d)}g_{\mu\nu}\}$ is obtained:

$$ds^2_{d+1} = \varepsilon N(x^I)^2 d\tau^2 + {}^{(d)}g_{\mu\nu}(x^I)\Big[dx^\mu + N^\mu(x^I)d\tau\Big]\Big[dx^\nu + N^\nu(x^I)d\tau\Big] \,. \tag{7.9}$$

7.1.2. *Contact with RG*

The connection with the RG approach is established by identifying in (7.9) the metric $^{(d)}g_{\mu\nu}$ with the output of the FRGE computation:

$$^{(d)}g_{\mu\nu}(\tau, x^\rho) = g_{\mu\nu}^k(x^\rho)\Big|_{k=k(\tau)} . \tag{7.10}$$

Here $k(\tau)$ amounts to be an optional and physically irrelevant redefinition of the original scale parameter in terms of a convenient RG time τ. A typical example is $\tau = \ln(k/\kappa)$, or even simpler, $\tau = k/\kappa$.[1]

In the following we will assume that both $g_{\mu\nu}^k(x^\rho)$ and $k(\tau)$ are known, established functions, given from the RG. Thus, what is still lacking in order to fully specify the higher-dimensional line element (7.9) are the lapse and shift functions N and N^μ, respectively, as well as the sign ε. These quantities do *not* follow from the flow equations and are properties of the metric on $\mathcal{M}_{d+1}$. We will look for general reasons or principles, above those inherent in the RG framework, that determine those missing ingredients in a meaningful and physically relevant way.

Remark. It is important here to emphasize that the possibility of performing coordinate transformations has been exhausted already in solving the k-dependent effective field equations. This means that we cannot change N and N^μ in an arbitrary way. From the RG side, the ADM framework in $d+1$ dimensions establish concrete functions $g_{\mu\nu}^k(x^\rho)$, referring to a specific set of coordinates. We do not allow those functions to be changed by a $\mathscr{D}\mathit{iff}(\mathcal{M}_{d+1})$ transformation, we allow the functions N and N^μ of any form in the gauge picked by $g_{\mu\nu}^k$. As a consequence, we first must find a certain triple $\{N, N^\mu, \varepsilon\}$ which completes the specification of ds_{d+1}^2, before to be free to perform general coordinate transformations.

7.1.3. *Focusing on the lapse function*

Our aim is to explore the theoretical possibilities of fixing the missing ingredients of the higher-dimensional metric, $\{N, N^\mu, \varepsilon\}$, in a way that is physically or mathematically relevant.

In a first approach it can help to narrow down the setting in order to make the problem technically more clear-cut, and the physics interpretation more transparent.

---

[1] We adopt the conventions of dimensionless coordinates (see Section A.1), while all metric coefficients have mass dimension -2. Since the scale $[k] = +1$, then also the constant κ must have $[\kappa] = +1$.

(1) For this reason we will focus in the following on a vanishing shift vector and on lapse functions that depend only on τ: $N^\mu(x^I) = 0$, $N(x^I) = N(\tau)$. As a consequence eq.(7.9) boils down to

$$ds^2_{d+1} = \varepsilon\, N(\tau)^2\, d\tau^2 + {}^{(d)}g_{\mu\nu}(\tau, x^\rho)dx^\mu dx^\nu \ . \tag{7.11}$$

This simplified form of the ADM metric is still sufficiently rich, but yet simple enough to allow for our purposes, in order to make contact with RG data.

(2) Regarding the RG input, we now insert the explicit trajectory of Einstein metrics described in Section 3.5:

$$ds^2_{d+1} = \varepsilon\, N(\tau)^2\, d\tau^2 + Y(k(\tau))^{-1}\ g^{(0)}_{\mu\nu}(x^\rho)dx^\mu dx^\nu \ . \tag{7.12}$$

If there exist a yet to be discovered general principle, with information which goes beyond the input data provided by the RG equations, that impart a specific metric on $\mathcal{M}_{d+1}$, this information must reside in the lapse function $N(\tau)$.

Again, it is important to remember that the $g^R_{\mu\nu}$ is externally prescribed and we do not want to change it by coordinate transformations. Hence, the particular functional form $\tau \mapsto N(\tau)$ refers to an already *fully gauge fixed metric*, the corresponding gauge being selected in the process of solving the effective field equations.

(3) With this parameterization at hand we now face the following question: What is a single Riemannian or pseudo-Riemannian manifold $\left(\mathcal{M}_{d+1}, {}^{(d+1)}g_{IJ}\right)$ capable of doing for us that would not already be possible using the original stack of unrelated manifolds $\left\{ (\mathcal{M}_d, g^k_{\mu\nu}) \,|k \in \mathbb{R}^+\right\}$?

For instance, this parameterization can ascribe proper lengths to curves in $\mathcal{M}_{d+1}$ which are not confined to a single slice of the foliation. Such curves explore not only different points of spacetime, but also different scales. In other words, this integral allows us to answer questions like: "What is the distance between an object at high-scale and an object at low-scale corresponding to one and the same spacetime event (x^μ)?"

As an example let us consider a curve $\mathcal{C}(P_1, P_2)$ connecting two points $P_{1,2} \in \mathcal{M}_{d+1}$. In the coordinate system of (7.12), they are assumed to possess the same x^μ-, but different τ-coordinates, namely τ_1 and τ_2, respectively. Furthermore, we assume that $x^\mu = $ const is constant along $\mathcal{C}(P_1, P_2)$, so that the curve projects onto a single point of $\mathcal{M}_d$. Then, if $\varepsilon = +1$ say, the metric in eq.(7.12) tells us that this curve has the proper length

$$\Delta s_{d+1} \equiv \int_{\mathcal{C}_{(P_1, P_2)}} \sqrt{ds^2_{d+1}} \ = \ \int_{\tau_1}^{\tau_2} d\tau N(\tau) \ . \tag{7.13}$$

Furthermore, this parameterization is of particular interest in cosmology. One could for instance ascribe Δs_{d+1} to have a physical meaning, by relating it to the results of certain measurements. A well known model for achieving this on ordinary spacetimes equips $\mathcal{M}_d$ with a set of scalar fields ϕ^μ whose observable values represent x^μ then (see the Chapter 13 on observables [77]). In this case one must invoke an additional field (in cosmology one might think of a local temperature field, for instance) which allows to determine the scale $k(\tau)$.

In fact, as already mentioned, there is freedom in the choice of the function $k(\tau)$. For instance, the proper time Δs_{d+1} in (7.13) is independent of this choice. Assume that two such functions belong to the same foliation, i.e., $k(\tau) = k = \bar{k}(\bar{\tau})$, and the respective RG times are related by the coordinate transformation $\tau = \tau(\bar{\tau})$. This coordinate transformation latter belongs to the foliation-preserving subgroup of $\mathscr{D}\!iff(\mathcal{M}_{d+1})$, and it acts on the lapse function according to [49]

$$\bar{N}(\bar{\tau}) = N(\tau)\left(\frac{\mathrm{d}\tau}{\mathrm{d}\bar{\tau}}\right). \tag{7.14}$$

As a result, $\bar{N}(\bar{\tau})\mathrm{d}\bar{\tau} = N(\tau)\mathrm{d}\tau$, and (7.13) is invariant.

7.2. DISTINGUISHED HIGHER-DIMENSIONAL GEOMETRIES

The crucial geometrization question is what kind of physical or mathematical principle determining the higher-dimensional metric. Furthermore, we ask what are the universal geometric features of the manifold $\left(\mathcal{M}_{d+1},\, {}^{(d+1)}g_{IJ}\right)$ which result from the given principles. Using the prescribed coordinate system of eq.(7.12), and the information coming from the RG trajectory, what is left to be determined by this principle are $N(\tau)$ and ε.

We start by postulating that the RG trajectories under consideration possess the following monotonicity property:

(**P**) The cosmological constant $\Lambda(k)$ is a strictly increasing function of k.   (7.15)

Assuming (**P**), we can show that it is always possible to complete the specification of the $(d+1)$-dimensional (pseudo-) Riemannian geometry in such a way that it enjoys universal features[2]:

(**G**) The higher-dimensional metric ${}^{(d+1)}g_{IJ}$ is *Ricci flat*: ${}^{(d+1)}R_{IJ} = 0$.   (7.16)

---

[2]This property is universal in the sense that it pertains to arbitrary k-dependent Einstein metrics $g^k_{\mu\nu}(x^\rho)$.

If we further assume that the d-dimensional Einstein metrics $g^k_{\mu\nu}(x^\rho)$ happen to be *maximally symmetric* (see Appendix E), then **(G)** can be replaced by the stronger statement:

(G') The higher-dimensional metric $^{(d+1)}g_{IJ}$ is *Riemann flat*: $^{(d+1)}R^I{}_{JKL} = 0$. (7.17)

(P) is necessary such that **(G)** and **(G')** are made possible. De facto, this principle allows to postulate a highly distinguished and universal form of $^{(d+1)}g_{IJ}$. In the end we will investigate whether the postulated property **(P)** is actually realized in Asymptotic Safety.

7.2.1. *The Hubble length as a coordinate*

We consider k-intervals with different signs of $\Lambda(k)$ separately, as they occur along the Type Ia trajectories. Let us start by considering $\Lambda(k) > 0$. Then **(P)** implies that $Y(k)$ and $H(k)$ are monotonically increasing with the scale, while the Hubble length

$$L_H(k) \equiv \frac{1}{H(k)} = \left[\frac{(d-1)(d-2)}{2|\Lambda(k)|}\right]^{1/2} \tag{7.18}$$

is a decreasing function of k. If instead $\Lambda(k) < 0$, the postulate **(P)** requires $Y(k)$ and $H(k)$ to decrease, and $L_H(k)$ to increase with k. In either case the postulated strict monotonicity implies the invertibility of the function $L_H(k)$, meaning the relationship between k and L_H is one-to-one. As a consequence, we may regard the map $k \mapsto L_H(k)$ as a concrete example of an RG time $\tau = \tau(k)$. While up to this stage, the τ-k relationship has been kept arbitrary free, at this point we make a specific choice for this coordinate, appealing to the RG trajectory itself.

For clarity we denote this special RG time coordinate related to the Hubble length by ξ. The corresponding coordinate transformation $k = k(\xi)$ is determined by the implicit condition

$$\xi \equiv L_H\big(k(\xi)\big). \tag{7.19}$$

Its inverse is known and reads

$$\xi(k) = \left[\frac{(d-1)(d-2)}{2|\Lambda(k)|}\right]^{1/2} \tag{7.20}$$

In the expression of ds^2_{d+1} in terms of ξ appears the conformal factor

$$Y(k(\xi))^{-1} = H_0^2 \; H(k(\xi))^{-2} = H_0^2 \; L_H(k(\xi))^2 = H_0^2 \, \xi^2 \; . \tag{7.21}$$

As a consequence, in the new system of coordinates the dependence on the RG time turns out to be very simple, since the second term on the RHS of eq.(7.12) is just proportional to ξ^2.

After having set up the convenient coordinates[3] $x^I \equiv (x^0, x^\mu) \equiv (\xi, x^\mu)$, the principle that should determine the $(d+1)$-dimensional geometry must be realized through a unique function $\xi \mapsto N(\xi)$, which will allow to completely specify the line element $ds_{d+1}^2 \equiv {}^{(d+1)}g_{IJ}(x^K)dx^I dx^J$ in eq.(7.12).

In order to prove that the postulate **(P)** indeed allows us to achieve **(G)** or **(G')**, respectively, we establish a simple rule: the coordinates realizing the "proper RG time gauge" are required to coincide with those which employ the Hubble length as the scale coordinate. This means:

> **(R)** *In the (ξ, x^μ) system, the lapse function must assume the simplest*
>
> form possible, namely $N(\xi) = 1$. $\hspace{5cm}$ (7.22)

The rule **(R)** completes ${}^{(d+1)}g_{IJ}$ and enforces that the higher-dimensional metric is explicitly given by

$$ds_{d+1}^2 = \varepsilon \, (d\xi)^2 + \xi^2 \; H_0^2 \; g_{\mu\nu}^{(0)}(x^\rho)dx^\mu dx^\nu \, . \tag{7.23}$$

The line element is now completely determined except for the sign ε.

It is important to stress out that the property **(P)** is a key property for making the rule **(R)** valid. The requirement of strict monotonicity of $\Lambda(k)$ allow to replace k with $\xi \propto |\Lambda(k)|^{-1/2}$ in its role as a coordinate.[4]

Note that the metric (7.23) is remarkably *universal*: There is no explicit dependence on the function $\Lambda(k)$. In the (ξ, x^μ) coordinate system, the proposed metric "remembers" $\Lambda(k)$ only through the implicit requirement (made through **(P)** that $\xi \leftrightarrow |\Lambda(k)|^{-1/2}$ must be one-to-one. In this system, the information about the actual RG evolution enters only in the "time function" $k = k(x^I) \equiv k(\xi, x^\mu)$: This describes how the slices $\Sigma_\tau \equiv \Sigma_\xi$ are embedded into $\mathcal{M}_{d+1}$. Through the rule **(R)** we enforced that the time function has no dependence on x^μ, and boils down to $k = k(\xi)$. It is this function that, by imposing $\xi = L_H(k(\xi))$, has been adjusted in (8.25). Since the inverse function $\xi = \xi(k)$ is given by (7.20), we recover the time function belonging to the line element (7.23) by solving $\xi \propto |\Lambda(k)|^{-1/2}$ for $k = k(\xi)$.

Finally, Eq.(7.23) is our proposal for the single higher-dimensional metric which "geometrizes" the entire RG history of the original metrics.[5] In the following subsections we are going to discuss which equivalent forms can be derived from our specific proposal, clarifying the motivations for our choice.

---

[3]Conventionally we chosed dimensionless coordinates, however, the special RG time ξ and its "conformal" analogue η are the only exceptions to our conventions. While $[x^\mu] = 0$, ξ and η have the dimension of a *length*: $[\xi] = [\eta] = -1$.

[4]For a similar discussion of coordinate transformations on the g-λ theory space see ref.[121].

[5]It is interesting to note that the metric (7.23) appears to be a distinguished one also in the 5D "space-time-matter theory" à la Wesson in [359–361].

7.2.2. *Equivalent forms of the postulated metric*

Choosing a particularly simple, but still physically relevant lapse function, namely $N = 1$, we derived a special system of coordinates (ξ, x^μ). After having set up the metric $^{(d+1)}g_{IJ}$ we may transform it to any convenient other coordinate system $\bar{x}^I \equiv (\bar{x}^0, \bar{x}^\mu)$, provided it only involve foliation preserving transformations. Here we mention two simple applications.

(1) The conformal RG time. In practical computations it is often convenient to transfer the scale dependence from the conformal factor of $g_{\mu\nu}^{(0)}$ to the overall conformal factor of $^{(d+1)}g_{IJ}$. This is achieved by the transformation trading $\xi \in \mathbb{R}^+$ for $\eta \in \mathbb{R}$ via $\xi = H_0^{-1}e^{H_0\eta}$, or vice versa,

$$\eta = H_{\mathrm{R}}^{-1} \ln(H_{\mathrm{R}}\xi) = L_H^{\mathrm{R}} \ln\big(\xi/L_H^{\mathrm{R}}\big) , \qquad (7.24)$$

with $L_H^{\mathrm{R}} \equiv H_{\mathrm{R}}^{-1} \equiv L_H(k_{\mathrm{R}})$. Note that this transformation is x^μ-independent. The new coordinate η is positive (negative) if the length ξ is of super- (sub-) Hubble size, according to the metric at the reference scale k_{R}. In the $(x^0 \equiv \eta, x^\mu)$ system the line element (7.23) assumes the desired form:

$$\mathrm{d}s_{d+1}^2 = e^{2H_{\mathrm{R}}\eta} \left[\varepsilon \,(\mathrm{d}\eta)^2 + g_{\mu\nu}^{\mathrm{R}}(x^\rho)\mathrm{d}x^\mu\mathrm{d}x^\nu\right] . \qquad (7.25)$$

In its original form in (7.23) the variable ξ remembers the cosmological time in a Friedmann–Lemaître–Robertson–Walker (FLRW) metric. Then the new variable η would have the interpretation of the corresponding conformal RG time.

(2) The IR cutoff as a coordinate. Both in the (ξ, x^μ) and the (η, x^μ) system of coordinates the metric does not contain the expression for $\Lambda(k)$, even if the time functions $k = k(\xi)$ and $k = k(\eta)$ know about it. We can reverse the situation and introduce directly the cutoff k (or the dimensionless $L_H^{\mathrm{R}} k$) as the new coordinate, making the time function trivial. The change of coordinates $\xi \to k$ defined by (7.20) brings the metric (7.23) to the form

$$\mathrm{d}s_{d+1}^2 = \left|\frac{\Lambda_{\mathrm{R}}}{\Lambda(k)}\right| \left\{\varepsilon \left(\frac{1}{2}\partial_k \ln|\Lambda(k)|\right)^2 \left(L_H^{\mathrm{R}} \,\mathrm{d}k\right)^2 + g_{\mu\nu}^{\mathrm{R}}(x^\rho)\mathrm{d}x^\mu\mathrm{d}x^\nu\right\} , \qquad (7.26)$$

which depends manifestly $\Lambda(k)$.

It immediately stands out that in this form of the metric (7.26), a degeneracy appears when $\partial_k\Lambda(k) = 0$, hinting at the importance of principle (P) again. We emphasize furthermore that the proposed metric ascribes at the same x^μ to high- and low-scale objects nonzero distances only if $\partial_k\Lambda(k) \neq 0$, i.e., only when there is a non-trivial RG running: The effective spacetimes acquire fractal properties [100, 240].

7.2.3. *Self-similarity*

The $(d+1)$-dimensional geometry described by equation (7.23), or equivalently by (7.25), has a particular feature: it admits a homothetic Killing vector field $X \equiv X^I \partial_I$. With $\mathscr{L}_X$ denoting the Lie derivative along X, this vector field satisfies the defining equation

$$\mathscr{L}_X \, {}^{(d+1)}g_{IJ} = 2 \, C \, {}^{(d+1)}g_{IJ} \tag{7.27}$$

for $C = H_R$. Note how (7.27) differs from the condition for a generic conformal Killing vector field because C is a constant rather than an arbitrary function on $\mathcal{M}_{d+1}$ as it would have been sufficient for a Killing vector [362, 363].

In this particular metric the homothetic vector field is explicitly given by

$$X = \frac{\partial}{\partial \eta} = H_R \, \xi \frac{\partial}{\partial \xi} \, . \tag{7.28}$$

It is easily checked therefore that it generates x^μ- independent rescalings of the metric. The existence of such a vector field is the distinctive feature of self-similarity in the General Relativity [364]. This manifestation is coordinate independent and is proper of the underlying foliation with self-similar leaves.

7.2.4. *Ricci flatness*

Finally, we turn to the curvature of the postulated higher-dimensional geometry. In order to better appreciate its rather unique character, we generalize the form of the conformal time metric (7.25) . We consider a general overall conformal factor $\Omega^2(\eta)$ and hence the following slightly more general class of metrics:

$$ {}^{(d+1)}g_{IJ}(x^K)\mathrm{d}x^I\mathrm{d}x^J = \Omega^2(\eta)\Big[\varepsilon(\mathrm{d}\eta)^2 + g_{\mu\nu}^R(x^\rho)\mathrm{d}x^\mu\mathrm{d}x^\nu\Big] \, . \tag{7.29}$$

Here we employ the same coordinates $x^K \equiv (x^0 = \eta, x^\mu)$ as in eq.(7.25).

Working out the Ricci tensor of (7.29) one finds (see Section A.1 for the conventions):

$$ {}^{(d+1)}R^0{}_0 = -\varepsilon \, d \, \Omega^{-2}\left[\frac{\ddot{\Omega}}{\Omega} - \left(\frac{\dot{\Omega}}{\Omega}\right)^2\right] \tag{7.30a}$$

$$ {}^{(d+1)}R^0{}_\mu = 0, \qquad {}^{(d+1)}R^\mu{}_0 = 0 \tag{7.30b}$$

$$ {}^{(d+1)}R^\mu{}_\nu = \Omega^{-2}\left\{R^\mu{}_\nu - \varepsilon \, \delta^\mu{}_\nu\left[\frac{\ddot{\Omega}}{\Omega} + (d-2)\left(\frac{\dot{\Omega}}{\Omega}\right)^2\right]\right\} \tag{7.30c}$$

Here $R^\mu{}_\nu$ denotes the Ricci tensor of $g^R_{\mu\nu}(x^\rho)$, and the dot indicates derivative with respect to η.

Now let us ask under what circumstances (7.29) is Ricci flat:

$$^{(d+1)}R^I{}_J = 0 \ . \tag{7.31}$$

The component (7.30a), to be zero, i.e., demanding $^{(d+1)}R^0{}_0 = 0$, implies a necessary and sufficient condition on the conformal factor, which in particular has to satisfy the following differential equation $\Omega\,\ddot\Omega = (\dot\Omega)^2$. This most general solution for $\Omega(\eta)$ is given by

$$\Omega(\eta) = e^{B(\eta - \eta_R)} \ , \tag{7.32}$$

where B and η_R represent arbitrary real constants. On the other hand, the third group of components in (7.30c), the demanded condition $^{(d+1)}R^\mu{}_\nu = 0$ is found to be equivalent to

$$R^\mu{}_\nu - \varepsilon(d-1)\,B^2\,\delta^\mu{}_\nu = 0 \ . \tag{7.33}$$

Up to this point, $g^R_{\mu\nu}(x^\rho)$ has not been specified and so also its related Ricci tensor $R^\mu{}_\nu$. When we now exploit the requirement that $g^R_{\mu\nu}(x^\rho)$ actually should describe an Einstein space complying with eq.(3.79), the condition (7.33) reduces to the simple equation $\sigma H^2_R - \varepsilon B^2 = 0$, having as unique solution $\varepsilon = \sigma$ and $B = H_R$.

Finally the conclusion is that for every d-dimensional metric with $g^R_{\mu\nu}$ describing an Einstein space, there exist a *Ricci flat* higher-dimensional metric of the form (7.29).This is what is postulated in (G). In addition to this, the higher-dimensional metric is unique and is obtained by plugging

$$\varepsilon = \sigma \qquad \text{and} \qquad \Omega(\eta) = e^{H_R(\eta - \eta_R)} \tag{7.34}$$

into the family of line elements (7.29):

$$ds^2_{d+1} = e^{2H_R(\eta - \eta_R)} \left[\sigma\,(d\eta)^2 + g^R_{\mu\nu}(x^\rho)dx^\mu dx^\nu \right] \ . \tag{7.35}$$

At this stage we can set $\eta_R = 0$ go back to the metric (7.25) which we set out to investigate. However, we gained an additional piece of information: originally we had admitted an arbitrary sign $\varepsilon = \pm 1$, now instead we see that Ricci flatness can be achieved only if we allow the sign of the cosmological constant $\sigma = \Lambda_R/|\Lambda_R|$ to determine the signature of $^{(d+1)}g_{IJ}$. If the cosmological constant is positive (negative) the scale parameter becomes a spacelike (timelike) coordinate.

7.2.5. *Strict flatness*

Let us go one step further, look at the postulate **(G')**, asking under what conditions metrics of the form (7.29) are not only Ricci flat but even strictly, i.e., Riemann flat:

$$^{(d+1)}R^I{}_{JKL} = 0. \tag{7.36}$$

Modulo the usual symmetries, the Riemann tensor of (7.29) has only the following nonzero components:

$$^{(d+1)}R^{0\mu}{}_{0\nu} = \varepsilon\,\Omega^{-2}\left[\left(\frac{\dot\Omega}{\Omega}\right)^2 - \frac{\ddot\Omega}{\Omega}\right]\delta^\mu{}_\nu \tag{7.37a}$$

$$^{(d+1)}R^{\mu\nu}{}_{\rho\sigma} = \Omega^{-2}\left\{R^{\mu\nu}{}_{\rho\sigma} - \varepsilon\left(\frac{\dot\Omega}{\Omega}\right)^2\left[\delta^\mu{}_\rho\delta^\nu{}_\sigma - \delta^\mu{}_\sigma\delta^\nu{}_\rho\right]\right\} \tag{7.37b}$$

Here $R^{\mu\nu}{}_{\rho\sigma}$ is the Riemann tensor that belongs to $g^{\mathrm{R}}_{\mu\nu}(x^\rho)$.

Demanding that $^{(d+1)}R^{0\mu}{}_{0\nu} = 0$, eq.(7.37a) reproduces the requirement $\Omega\,\ddot\Omega = (\dot\Omega)^2$ and (7.32) as its general solution, as in the Ricci flat case. Inserting this solution into the mixed components (7.37b), the vanishing of the second set of components, $^{(d+1)}R^{\mu\nu}{}_{\rho\sigma} = 0$, implies the following condition on the curvature tensor of $g^{\mathrm{R}}_{\mu\nu}(x^\rho)$:

$$R^{\mu\nu}{}_{\rho\sigma} = \varepsilon B^2\left[\delta^\mu{}_\rho\delta^\nu{}_\sigma - \delta^\mu{}_\sigma\delta^\nu{}_\rho\right] \tag{7.38}$$

The tensor structure on the RHS of (7.38) is the hallmark of a maximally symmetric manifold, see eq.(3.77). We conclude therefore that if, *first*, $\Omega(\eta)$ and ε are fixed according to (7.34), and *second*, the running Einstein metric at $k = k_{\mathrm{R}}$, i.e., $g^{\mathrm{R}}_{\mu\nu}$, corresponds to a maximally symmetric d-dimensional space, then the metric (7.29) is strictly flat.

This completes our demonstration that, under this symmetry constraint, the geometric feature **(G)** of the higher-dimensional manifold can be tightened to **(G')**.

It is quite remarkable that the inclusion of the scale variable has "flattened" the curved spacetime. In the case at hand, the metric (7.23) becomes

$$ds^2_{d+1} = (\mathrm{d}\xi)^2 + \xi^2\,\mathrm{d}\Omega^2_d \qquad (\Lambda_{\mathrm{R}} > 0) \tag{7.39}$$

$$ds^2_{d+1} = -(\mathrm{d}\xi)^2 + \xi^2\,\mathrm{d}H^2_d \qquad (\Lambda_{\mathrm{R}} < 0) \tag{7.40}$$

where $\mathrm{d}\Omega^2_d$ and $\mathrm{d}H^2_d$ are the line elements for, $\mathbb{S}^d$ and $\mathbb{H}^d$ with unit length scale, respectively. Both of these higher-dimensional metrics are well known to be flat: Eq.(7.39) describes $(d+1)$-dimensional spherically sliced Euclidean space. Here ξ plays the role of the radial variable, $\mathcal{M}_{d+1} \equiv \mathbb{R}^{d+1}$ being foliated by d-spheres of radius ξ. Here the RG time has become a spacelike coordinate.

Similarly the metric (7.40) describes Minkowski space $M^{1,d}$. The RG time has become a genuine time coordinate in this case. Here Minkowski space is foliated by hyperbolic d-spaces whose radius of curvature is given by ξ. For $d = 3$, eq.(7.40) is nothing but the metric of Milne's universe.

7.3. ASYMPTOTIC SAFETY

In the previous section we saw that the "principle" or "property" **(P)** is a necessary condition for being able to define $^{(d+1)}g_{IJ}$ as a (Ricci) flat metric in the higher-dimensional space. In this section we are going to test the actual monotonicity of $\Lambda(k)$ within the concrete setting of pure quantum gravity in $d = 4$ dimensions.

We employ the prototypical Einstein–Hilbert truncation of the Effective Average Action, the one traditionally used to demonstrate Asymptotic Safety [95, 97, 114]. The truncation is based upon the ansatz (3.45). The resulting RG equations for the running couplings $G(k)$ and $\Lambda(k)$ were obtained in [95] and solved numerically in [97] (see Section 3.5). In the following we are particularly interested in the properties of the function $\Lambda(k)$ along typical RG trajectories.

7.3.1. *Mode counting functions*

Analyses and considerations about 5D representations of the histories of 4D geometries have already led to scrutinize the monotonicity properties of $\Lambda(k)$. In fact, in ref. [146], even if for different reasons, the monotonicity of the dimensionless product $G(k)\,\Lambda(k)$, has been explored already, for different reason though. In this context a c-function-like quantity $\mathscr{C}(k)$ has been proposed in 4D quantum gravity. This function, when evaluated exactly, should be monotonically decreasing along RG trajectories, and be stationary at fixed points. In simple truncations $\mathscr{C}(k)$ turns out to be proportional to the product $\left[G(k)\,\Lambda(k)\right]^{-1}$. In spirit close to Zamolodchikov's c-function, $\mathscr{C}(k)$ can be interpreted to count the number of the fluctuation modes already integrated out: this would explain its monotonicity when evaluated exactly. As for approximate calculations, it was found however that the above Einstein–Hilbert truncation is *not* precise enough to render $\mathscr{C}(k)$ monotonic, while it does turn out monotone if we use more general truncations [147] of the bi-metric type [103, 365, 366].

Consequently we expect that $\Lambda(k)$ might have similar or better mode counting properties. Ultimately, in the most naive picture every bosonic fluctuation mode which

is not suppressed by the cutoff gives a positive zero-point energy contribution to the cosmological constant and therefore the fluctuations should add to $\Lambda(k)$.

Regarding the monotonicity, we observe that, whenever (3.61) and (3.62) are applicable, the *dimensionful* cosmological constant $\Lambda(k)$ is indeed a strictly monotonic function of k, and all trajectories of the Types Ia, IIa, and IIIa do satisfy the property **(P)**.

7.3.2. *The signature*

A second important piece of information concerning $\Lambda(k)$ is that it is a function with piecewise constant sign $\sigma(k) \equiv \Lambda(k)/|\Lambda(k)|$. Eqs.(3.61) and (3.62) yield

$$\text{for Type Ia:} \qquad \varepsilon(k) = \begin{cases} -1 & \text{for} \quad 0 \leq k < \ell^{-1} \\ +1 & \text{for} \quad k > \ell^{-1} \end{cases} \tag{7.41}$$

$$\text{for Type IIa:} \qquad \varepsilon(k) = +1 \qquad \text{for all} \quad k \geq 0 \tag{7.42}$$

$$\text{for Type IIIa:} \qquad \varepsilon(k) = +1 \qquad \text{for all} \quad k \geq 0 \tag{7.43}$$

Thus we conclude that everywhere along RG trajectories of the Types IIa and IIIa the RG "time" amounts to a *spatial coordinate* actually. Starting out from a Euclidean spacetime $\mathcal{M}_4$ with signature $(+ + + +)$, the proposed geometrization of the RG flow leads us unavoidably to a manifold $\mathcal{M}_5$ having $(+ + + + +)$. For trajectories of the Type Ia the situation is more interesting. They possess an intermediate scale $k = \ell^{-1}$ at which the cosmological constant vanishes, $\Lambda(\ell^{-1}) = 0$ and changes sign. When k passes this given scale, the solutions to the effective field equations undergo a *change of topology*. Coming from higher to lower scales k, the scalar curvature changes from $R[g_{\alpha\beta}^k] > 0$, via $R[g_{\alpha\beta}^{1/\ell}] = 0$, to $R[g_{\alpha\beta}^k] < 0$. In the maximally symmetric case, for example, this topology change corresponds to a sequence of spaces $\mathbb{S}^4 \to \mathbb{R}^4 \to \mathbb{H}^4$.

We have to emphasize that currently Asymptotic Safety cannot yet describe topology change processes dynamically at this stage of the development of the theory, neither in physical time nor in RG time. For this reason one may follow a conservative approach here and consider the two branches of the Ia trajectories as two unrelated (but incomplete) trajectories, the first having $\Lambda(k) > 0$ and the second $\Lambda(k) < 0$, respectively. We will study them separately: The upper branch $(k > \ell^{-1})$ of a Type Ia trajectory augments the Euclidean $\mathcal{M}_4$ to a Euclidean $\mathcal{M}_5$ with signature $(+ + + + +)$, while its lower branch $(k < \ell^{-1})$ geometrizes to a Lorentzian 5D manifold with $(- + + + +)$, effectively adding a time coordinate. It is a very compelling conjecture that an RG

trajectory of this kind could explain a mechanism of *chronogenesis*, namely a time in an a priori purely Euclidean system is emerging.

7.3.3. *The coordinate change*

The dimensionless function $Y(k)$ can be written as

$$Y(k) = \frac{|\Lambda(k)|}{|\Lambda_{\rm R}|} = \frac{H(k)^2}{H_{\rm R}^2} = \left(\frac{L_H^{\rm R}}{L_H(k)}\right)^2 \tag{7.44}$$

with $\Lambda_{\rm R} = 3H_{\rm R}^2$ in $d = 4$, and $L_H^{\rm R} \equiv 1/H_{\rm R}$. Hence eq.(3.61) yields the following "running Hubble length" $L_H(k) = L_H^{\rm R} Y(k)^{-1/2}$. By taking the limit $k \to 0$ we can take the reference value to be the $k \to 0$ limit: hence, along the trajectories of Type IIIa (plus sign) and of Type Ia (minus sign), respectively:

$$L_H(k) = L_H^0 \cdot \begin{cases} \dfrac{1}{\sqrt{|\ell^4\, k^4 \pm 1|}} & \text{for} \quad 0 \le k \lesssim \hat{k} \\ \dfrac{1}{L\, k} & \text{for} \quad k \gtrsim \hat{k} \end{cases} \tag{7.45}$$

This function is sketched in Figure 7.1.

For the Type IIIa trajectories, the Hubble length $L_H(k)$ is found to be a strictly decreasing function of the scale for all $k \in (0, \infty)$. Therefore, it is one-to-one, and so $\xi = L_H(k)$ is a well-defined change of coordinates on the interval $(0, \infty)$. The same is true for the Type IIa case, i.e., in the limiting case $\Lambda_0 \searrow 0$. Type Ia trajectories on the other hand has to be decomposed into two branches with $k \in (0, \ell^{-1})$ and $k \in (\ell^{-1}, \infty)$, respectively, and treated separately. Then, on each branch, setting $\xi = L_H(k)$ is an allowed change of coordinates: on the upper (lower) branch the RG time ξ becomes a strictly decreasing (increasing) function of k.

7.3.4. *The transition region*

Finally let us deal more carefully with the monotonicity requirement in the transition region near $\hat{k} = O(m_{\rm Pl})$. For a first orientation the RG flow linearized about the fixed point (g_*, λ_*) can be used. The linearization is governed by a pair of complex conjugate critical exponents $\theta_{1,2} = \theta' \pm i\theta''$, with $\theta', \theta'' \in \mathbb{R}^+$, which give rise to the spiral shaped trajectories $k \mapsto (g(k), \lambda(k))$ encircling the fixed point. The latter is typically located in the first quadrant of the g-λ−plane for pure gravitational systems: $g_* > 0$, $\lambda_* > 0$. In the linear regime the condition $\partial_k \Lambda(k) > 0$, or equivalently $k\partial_k \lambda(k) + 2\lambda(k) > 0$,
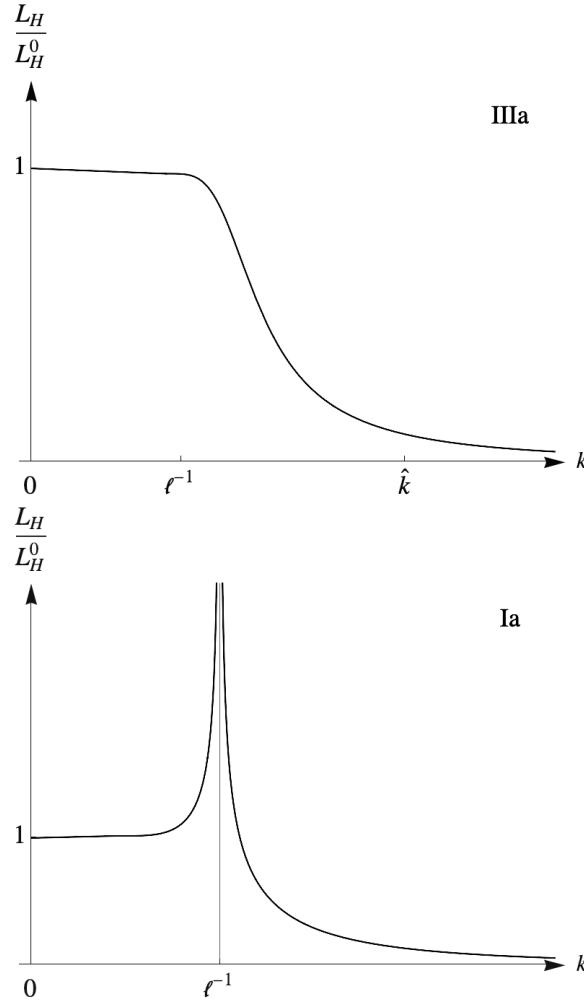
FIGURE 7.1. The scale-dependent Hubble length along trajectories of Type IIIa (left) and Type Ia (right), respectively.

assumes the form

$$\lambda_* + \zeta \left(\frac{k_0}{k}\right)^{\theta'} \cos\left(\theta'' \ln(k/k_0) + \alpha\right) > 0 \tag{7.46}$$

Here α and ζ are dimensionless parameters which depend on the constants of integration, or, in other words, on the trajectory under consideration, as well as on the eigenvectors of the stability matrix.[6] For k sufficiently large eq.(7.46) shows that the monotonicity condition is always satisfied since the potentially negative cosine is multiplied by a too small coefficient in comparison with the positive value of λ_*. However, once the scale is low enough for $\zeta(k_0/k)^{\theta'}$ to be of order unity, there exist parameters α, ζ for which (7.46) could be violated. On the other hand, it is also true that at those low scales the linear approximation is not any longer necessarily reliable. If by then the trajectory is already in the semiclassical regime, the trajectory is well described by

---

[6]See eq.(5.30) of ref.[114] for a discussion about this point.

the "caricature" trajectory (see Subsection 3.5.2) and monotonicity is guaranteed; but if not, violations may occur.

Detailed numerical analysis demonstrate on reality that in the transition region there are no such violations of monotonicity: One finds that on all scales $\partial_k \Lambda(k) > 0$ for all three types of trajectories. In Figure 7.2 we represent the numerical result for $\Lambda(k)$ and compare the outcome with the product $G(k)\,\Lambda(k)$ and the anomalous dimension of Newton's constant, $\eta_N(k) = k\dfrac{\partial}{\partial k}\ln G(k)$, along the same exemplary Type IIIa trajectory (since the plot focuses on the transition region it would look basically the same for the other types). It is really remarkable to notice that, even in the transition regime, $\Lambda(k)$ is indeed perfectly monotonic. This is not the case for $G(k)\,\Lambda(k)$ and $\eta_N(k)$, in the transition regime they display significant oscillations.

This completes the demonstration that the asymptotically safe trajectories of QEG in 4 dimensions do indeed satisfy the general property **(P)** and, applying the rule **(R)**, they are eligible for a geometrization.

Here we conclude the first part dealing with the geometrization of RG trajectories in Euclidean signature. In the following, we are going to extend these investigations in two directions: First, we allow the higher-dimensional manifold $\mathcal{M}_5$ to be an arbitrary *Einstein space*, and second, we admit the possibility that the spacetimes to be embedded, $\left(\mathcal{M}_4, g^k_{\mu\nu}\right)$, have a *Lorentzian signature*. As a first example we will consider a stack of de Sitter spaces dS_4 with a k-dependent Hubble parameter.

7.4. Embedding in Einstein manifolds

To place the metric of the embedding manifold $\left(\mathcal{M}_{d+1},\, {}^{(d+1)}g_{IJ}\right)$ in a broader context, we start from $(d+1)$-dimensional line elements of the same form as in (8.20), namely:

$$
{}^{(d+1)}g_{IJ}(x^K)\,\mathrm{d}x^I\,\mathrm{d}x^J = \Omega^2(\gamma)\left[\varepsilon\,(\mathrm{d}\gamma)^2 + g^{\mathrm{R}}_{\mu\nu}(x^\rho)\,\mathrm{d}x^\mu\,\mathrm{d}x^\nu\right]. \tag{7.47}
$$

The sign factor $\varepsilon = \pm 1$ allows the scale variable γ to be introduced either as a time or a space coordinate. For now, this choice is unrelated to the signature of the d-dimensional "reference metric", $g^{\mathrm{R}}_{\mu\nu}(x^\rho)$. In fact, this signature is left upon at this point, and $g^{\mathrm{R}}_{\mu\nu}(x^\rho)$ can be a Lorentzian or a Euclidean metric.

In either case, the components of the Ricci tensor ${}^{(d+1)}R^I{}_J$ of the above metric ${}^{(d+1)}g_{IJ}$ have been computed in (7.30a), (7.30b) and (7.30c).
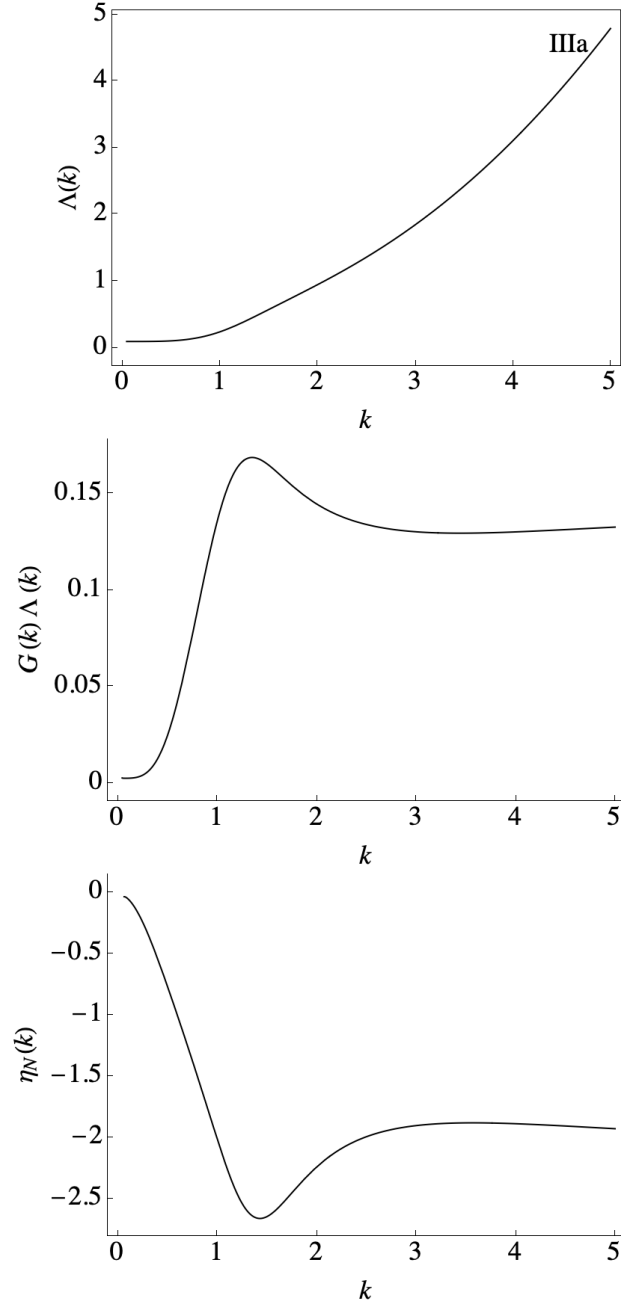
FIGURE 7.2. Numerical results for $\Lambda(k)$, the product $G(k)\,\Lambda(k)$, and the anomalous dimension $\eta_N(k)$ along a typical Type IIIa trajectory.

7.4.1. *The reference metric*

Concerning the family of metrics $\left\{g_{\mu\nu}^k(x^\rho)\,|\,k\in\mathbb{R}^+\right\}$ delivered by the GEAA, we assume that they are related to a trajectory of Type IIIa or IIa of the Einstein–Hilbert truncation (we won't consider Type Ia trajectories at this stage). The GEAA entails the classical-looking effective field equation $G_{\mu\nu}[g_{\alpha\beta}^k] = -\Lambda(k)g_{\mu\nu}^k$, whose solutions $g_{\mu\nu}^k$

are d-dimensional Einstein metrics. Since $g^k_{\mu\nu}$ is related to $g^R_{\mu\nu}$ by the x^ρ-independent conformal factor Ω^2, we can make the following assumptions about the k-independent reference metric:

(i) *The d-dimensional reference metric $g^R_{\mu\nu}(x^\rho)$ is Einstein*, meaning that the Ricci tensor has the form:

$$R^\mu{}_\nu \left[g^R_{\alpha\beta} \right] = \frac{2}{(d-2)} \Lambda_R \, \delta^\mu{}_\nu \qquad (7.48)$$

(ii) *The corresponding cosmological constant is strictly positive*:

$$\Lambda_R > 0 \, . \qquad (7.49)$$

Often it will be convenient in the following to trade Λ_R for the Hubble parameter

$$H_R \equiv \sqrt{\frac{2\,\Lambda_R}{(d-1)(d-2)}} \, , \qquad (7.50)$$

In therms of the Hubble parameter the cosmological constant is $\Lambda_R \equiv \frac{1}{2}(d-1)(d-2)H_R^2$, and the Ricci tensor and scalar

$$R^\mu{}_\nu \left[g^R_{\alpha\beta} \right] = (d-1)\, H_R^2 \, \delta^\mu{}_\nu \, , \qquad (7.51)$$

$$R \left[g^R_{\alpha\beta} \right] = R^\mu{}_\mu \left[g^R_{\alpha\beta} \right] = d\,(d-1)\, H_R^2 \, . \qquad (7.52)$$

For the special case of the de Sitter solution, the parameter H_R happens to coincide with its Hubble constant. However, for the time being we consider fully generic Einstein metrics $g^R_{\mu\nu}$.

7.4.2. *The Einstein condition*

Let us now impose the condition that the embedding metric in $d+1$ dimensions, eq.(7.12), too, is an Einstein metric. This means that the Ricci tensor is proportional to a delta function:

$$^{(d+1)}R^I{}_J = C \, \delta^I{}_J \, . \qquad (7.53)$$

Here C is essentially the higher-dimensional cosmological constant: $C = \left(\frac{2}{d-1} \right)\, ^{(d+1)}\Lambda$. The Einstein condition leads to the following constraints on ε and $\Omega(\gamma)$:

$$\varepsilon\, d\, \dot{\Omega}^2 - \varepsilon\, d\, \Omega\, \ddot{\Omega} = C\, \Omega^4 \, , \qquad (7.54a)$$

$$(d-1)\, H_R^2\, \Omega^2 - \varepsilon\,(d-2)\, \dot{\Omega}^2 - \varepsilon\, \Omega\, \ddot{\Omega} = C\, \Omega^4 \, . \qquad (7.54b)$$

To proceed, it is advantageous to replace these differential equations by their sum and difference, respectively, and to express them in terms of the function

$$\omega(\gamma) \equiv 1/\Omega(\gamma) \, . \qquad (7.55)$$

We obtain, respectively,

$$(d+1)\,\dot{\omega}\,\ddot{\omega} - 2\,d\,\dot{\omega}^2 + \varepsilon\,(d-1)\,H_R^2\,\omega^2 \;=\; 2\,\varepsilon\,C\,, \tag{7.56a}$$

$$\ddot{\omega} - \varepsilon\,H_R^2\,\omega \;=\; 0\,. \tag{7.56b}$$

The second equation above is easily solved. Depending on whether γ is a space or a time coordinate, we obtain, with integration constants α_1 and α_2:

$$\varepsilon = +1: \qquad \omega(\gamma) = \alpha_1\,\sinh(H_R\,\gamma) + \alpha_2\,\cosh(H_R\,\gamma)\,, \tag{7.57}$$

$$\varepsilon = -1: \qquad \omega(\gamma) = \alpha_1\,\sin(H_R\,\gamma) + \alpha_2\,\cos(H_R\,\gamma)\,. \tag{7.58}$$

For practical calculations it is often better not to use the explicit solutions but simply to exploit that (7.56b) admits the first integral

$$\dot{\omega}^2 - \varepsilon\,H_R^2\,\omega^2 = \mathrm{const} \equiv E\,. \tag{7.59}$$

If desired, one can express the γ-independent "energy" E in terms of the integration constants α_1 and α_2 according to

$$E = \left(\alpha_1^2 - \varepsilon\,\alpha_2^2\right) H_R^2\,. \tag{7.60}$$

Therefore, turning to the first differential equation (7.56a) now, we are entitled to make the following substitutions there:

$$\dot{\omega}^2 = E + \varepsilon\,H_R^2\,\omega^2 \qquad \text{and} \qquad \omega\,\ddot{\omega} = \varepsilon\,H_R^2\,\omega^2\,. \tag{7.61}$$

As a result, the dependence on $\omega(\gamma)$ drops out completely from (7.56a). What remains is a condition that relates C to the constants of integration:

$$C \;=\; -\varepsilon\,d\,E \tag{7.62}$$

$$=\; d\left(-\varepsilon\,\alpha_1^2 + \alpha_2^2\right) H_R^2 \tag{7.63}$$

In terms of the conventionally normalized cosmological constant in $(d+1)$ dimensions, $^{(d+1)}\Lambda$, this value of C amounts to

$$^{(d+1)}\Lambda \;=\; \frac{1}{2}\,(d-1)\,C \tag{7.64}$$

$$=\; \frac{1}{2}\,d\,(d-1)\left[-\varepsilon\,\alpha_1^2 + \alpha_2^2\right] H_R^2\,. \tag{7.65}$$

Obviously, $^{(d+1)}\Lambda$ can have either sign, depending on the relative magnitude of α_1 and α_2, and on the factor ε.

The case of a vanishing $^{(d+1)}\Lambda = 0$ is included here as well, and it leads us back to the Ricci flat metrics considered in Subsection 7.2.5. By eq.(7.65), this case is seen to require that $\varepsilon = +1$ and $\alpha_1 = \pm\alpha_2$. Hence, from (7.57), we obtain $\omega(\gamma) \propto \exp\left(\pm H_R\gamma\right)$,

and choosing the upper sign this yields the metric given in (7.35) for the presently assumed positive sign of Λ_{R}, $\sigma = +1$.

However, while the discussion in the previous sections assumed *Euclidean* metrics $g^k_{\mu\nu}$, we now see that under the same conditions it is possible to embed also *Lorentzian* spacetimes $\left(\mathcal{M}_d, g^k_{\mu\nu}\right)$ in a Ricci flat $\mathcal{M}_{d+1}$.

The point to be noted here is that the above investigation of differential equations is of a local nature and hence yields criteria for the existence of *local* embeddings only. But, importantly, in trying to extend a local embedding to a *global* one, the signature of $\left(\mathcal{M}_d, g^k_{\mu\nu}\right)$ is of crucial importance.

In this sense, the spacetimes $\mathcal{M}_{d+1}$ found above merely have the status of *candidates* for a global embedding.

Before turning to specific solutions, let us look at the Riemannian tensor $^{(d+1)}R^{IJ}{}_{KL}$ of the higher-dimensional metrics $^{(d+1)}g_{IJ}$ based upon an arbitrary d-dimensional Einstein metric $g^{\mathrm{R}}_{\mu\nu}$. For metrics of the type (7.12), its only nonzero components, up to the usual symmetries, are

$$^{(d+1)}R^{0\mu}{}_{0\nu} = C \, d^{-1} \, \delta^\mu_\nu \, , \tag{7.66a}$$

$$^{(d+1)}R^{\mu\nu}{}_{\rho\sigma} = C \, d^{-1} \left[\delta^\mu_\rho \, \delta^\nu_\sigma - \delta^\mu_\sigma \, \delta^\nu_\rho \right] + \left\{ R^{\mu\nu}{}_{\rho\sigma} - H^2_{\mathrm{R}} \left[\delta^\mu_\rho \, \delta^\nu_\sigma - \delta^\mu_\sigma \, \delta^\nu_\rho \right] \right\} \omega(\gamma)^2 \, . \tag{7.66b}$$

Here $R^{\mu\nu}{}_{\rho\sigma}$ is the Riemann tensor of the d-dimensional metric $g^{\mathrm{R}}_{\mu\nu}(x^\rho)$. While we assume the latter to be Einstein, all other properties of $g^{\mathrm{R}}_{\mu\nu}(x^\rho)$, in particular its Riemann tensor, are still completely unconstrained. In particular no assumptions about possible symmetries of $\left(\mathcal{M}_d, g^{\mathrm{R}}_{\mu\nu}\right)$ have been made.

7.4.3. *Maximum symmetry*

If $\left(\mathcal{M}_d, g^{\mathrm{R}}_{\mu\nu}\right)$ happens to be maximally symmetric, its curvature tensor satisfies

$$R^{\mu\nu}{}_{\rho\sigma} = H^2_{\mathrm{R}} \left[\delta^\mu_\rho \, \delta^\nu_\sigma - \delta^\mu_\sigma \, \delta^\nu_\rho \right] \, , \tag{7.67}$$

and as a result, the components (7.66b) simplify correspondingly. In this case it is not difficult to see that, in higher-dimensional language, the equations (7.66a) and (7.66b) with (7.67) read:

$$^{(d+1)}R^{IJ}{}_{KL} = C \, d^{-1} \left[\delta^I_K \, \delta^J_L - \delta^I_L \, \delta^J_K \right] \, . \tag{7.68}$$

This leads us to the following conclusion:

For every choice of $\{\varepsilon, \alpha_1, \alpha_2\}$ and of the d-dimensional Einstein metric $g^{\mathrm{R}}_{\mu\nu}$, the $(d+1)$-dimensional metric $^{(d+1)}g_{IJ}(\gamma, x^\mu)$ defined by eq.(7.12) is maximally symmetric

if, and only if, $g_{\mu\nu}^{\mathrm{R}}(x^\rho)$ is maximally symmetric. In this case, $g_{\mu\nu}^{\mathrm{R}}$ has $\frac{1}{2}d(d+1)$ Killing vectors, while $^{(d+1)}g_{IJ}$ has $\frac{1}{2}(d+1)(d+2)$.

Recall also that in the present paper we have fixed the sign of the cosmological constant from the outset: $\sigma \equiv \Lambda(k)/|\Lambda(k)| = +1$. Hence, in the maximally symmetric case, we are bound to consider families of spheres or de Sitter spacetimes, $\mathcal{M}_d = \mathbb{S}^d$ or $\mathcal{M}_d = \mathrm{dS}_d$, respectively, depending on whether the to-be-embedded manifolds are Euclidean or Lorentzian.

Furthermore, let us emphasize that this alternative, $\mathcal{M}_d$ being Euclidean or Lorentzian, did not get linked to the sign ε in the course of the above calculations, neither by requiring $^{(d+1)}g_{IJ}$ to be Einstein, nor by demanding maximum symmetry.

7.5. THE CANDIDATES: AdS_{d+1} AND dS_{d+1}

Let us return to the question raised in Section 6: Which principles and criteria can constrain or, in the ideal case, determine uniquely a manifold $\mathcal{M}_{d+1}$ that geometrizes a given trajectory, now in of Lorentzian spacetimes $\left(\mathcal{M}_d, g_{\mu\nu}^k\right)$?

(1) Symmetry. A natural principle of this kind, which we shall adopt here, is the following: The higher-dimensional $\mathcal{M}_{d+1}$ should display the maximum amount of symmetry that is consistent with the symmetry properties of the lower-dimensional metrics $g_{\mu\nu}^k$.

This principle unfolds its power in full if $\mathcal{M}_{d+1}$ can be required to be maximally symmetric. But, as we know, this will be possible only for generalized RG trajectories where already the original $\mathcal{M}_d$'s possess a corresponding symmetry.

Since it is our goal to find examples in which $\left(\mathcal{M}_{d+1}, {}^{(d+1)}g_{IJ}\right)$ is constrained as strongly as possible, we henceforth insist on maximally symmetric embedding manifolds $\mathcal{M}_{d+1}$.

To make sure that the latter can actually arise, we assume that, on all scales, $\left(\mathcal{M}_d, g_{\mu\nu}^k\right)$ is a maximally symmetric, and Lorentzian Einstein space with a positive cosmological constant. Hence from now on $\left(\mathcal{M}_d, g_{\mu\nu}^k\right)$ amounts to de Sitter spacetimes dS_d with a running Hubble parameter $H = H(k)$.

The k-dependent effective field equation tells us that $g_{\mu\nu}^k \propto 1/\Lambda(k)$, and so we may write the running de Sitter metrics as follows:

$$g_{\mu\nu}^k = Y(k)^{-1}\, g_{\mu\nu}^{\mathrm{R}} \qquad \text{where} \qquad Y(k) \equiv \frac{\Lambda(k)}{\Lambda_{\mathrm{R}}} . \tag{7.69}$$

This identifies the reference metric $g_{\mu\nu}^{\mathrm{R}}$ used above with the running metric $g_{\mu\nu}^{k}$ evaluated at some arbitrary $k \equiv k_{\mathrm{R}} > 0$.

AdS$_{d+1}$ and dS$_{d+1}$ arise. At this point, the basic problem has boiled down to a question that we addressed already in the previous section, namely: Given a stack of de Sitter spaces $\left(\mathcal{M}_d = \mathrm{dS}_d,\, Y(k)^{-1} g_{\mu\nu}^{\mathrm{R}}\right)$, i.e., a family of spacetimes whose members are all *Lorentzian* and *maximally symmetric*, in which manifolds $\left(\mathcal{M}_{d+1},\, {}^{(d+1)}g_{IJ}\right)$ can they be embedded if we demand that the higher-dimensional scale-space-time, too, is Lorentzian and maximally symmetric?

The demand of being Lorentzian fixes the signature of $\mathcal{M}_{d+1}$ in the form $(-+++\cdots)$, thus avoiding the (exotic and potentially problematic) situation with two times, $(--++\cdots)$. Hence the only time direction of $\mathcal{M}_{d+1}$ is the one inherited from $\mathcal{M}_d$, and so *the scale coordinate is determined to be a spatial one*.

As a consequence, we must set $\varepsilon = +1$ in our above catalog of possible local embeddings.

The remaining freedom lies in the choice of the integration constants (α_1, α_2) then. It leaves us with only two principally different cases, namely $(\alpha_1, \alpha_2) = (1, 0)$ and $(\alpha_1, \alpha_2) = (0, 1)$, respectively. According to (7.65), the resulting cosmological constant of $\mathcal{M}_{d+1}$ is negative in the first, and positive in the second case:

$$
{}^{(\mathbf{d+1})}\Lambda_{(1,0)} = -\frac{1}{2}\, d\,(d-1)\, H_{\mathrm{R}}^2 = -\left(\frac{d}{d-2}\right) \Lambda_{\mathrm{R}}\,, \tag{7.70}
$$

$$
{}^{(\mathbf{d+1})}\Lambda_{(0,1)} = +\frac{1}{2}\, d\,(d-1)\, H_{\mathrm{R}}^2 = +\left(\frac{d}{d-2}\right) \Lambda_{\mathrm{R}}\,. \tag{7.71}
$$

Thus, insisting that $\mathcal{M}_{d+1}$ is maximally symmetric narrows down the possibilities to just two cases, namely $\mathcal{M}_{d+1}$ *is either the anti-de Sitter spacetime* AdS$_{d+1}$, *or the de Sitter spacetime* dS$_{d+1}$ (see Table E.3 and Table E.4 in Appendix E).

7.5.1. Scale coordinates γ vs. ξ

Our conclusions are easily checked explicitly on the basis of the conformal factors given by (7.57):

$$
\Omega_{(1,0)}(\gamma) = 1/\sinh(H_{\mathrm{R}}\,\gamma)\,, \tag{7.72}
$$

$$
\Omega_{(0,1)}(\gamma) = 1/\cosh(H_{\mathrm{R}}\,\gamma)\,. \tag{7.73}
$$

(1a) In the $(\mathbf{1}, \mathbf{0})$ **case** the line element (7.12) assumes the following form:

$$
{}^{(d+1)}g_{IJ}^{\mathrm{AdS}}(x^K)\, \mathrm{d}x^I\, \mathrm{d}x^J = \frac{1}{\sinh^2(H_{\mathrm{R}}\,\gamma)} \left[(\mathrm{d}\gamma)^2 + \mathrm{d}\Sigma_d^2 \right], \qquad \gamma \in (-\infty, 0)\,. \tag{7.74}
$$

Here we introduced the special notation

$$d\Sigma_d^2 \equiv g_{\mu\nu}^{\mathrm{R}}(x^\rho)\ dx^\mu\, dx^\nu \tag{7.75}$$

for the metric of the d-dimensional de Sitter space dS_d with the Hubble parameter H_{R}. By the coordinate transformation $\gamma \leftrightarrow \xi$ with

$$\xi(\cdot):\ (-\infty,\, 0)\ \to\ (0,\, \infty),\qquad \gamma \mapsto \xi(\gamma) = -H_{\mathrm{R}}^{-1}\ \ln\, \tanh\left(-\frac{1}{2}\, H_{\mathrm{R}}\, \gamma\right) \tag{7.76}$$

the metric (7.74) can be brought to the alternative form

$$^{(d+1)}g_{IJ}^{\mathrm{AdS}}(x^K)\, dx^I\, dx^J = (d\xi)^2\ + \sinh^2(H_{\mathrm{R}}\, \xi)\ d\Sigma_d^2,\qquad \xi \in (0,\, \infty) \tag{7.77}$$

The line element (7.77) is known to describe a patch of the AdS_{d+1} manifold by slicing it with d-dimensional de Sitter spaces.[7]

(1b) In the $(\mathbf{0}, \mathbf{1})$ **case** we are similarly led to

$$^{(d+1)}g_{IJ}^{\mathrm{dS}}(x^K)\, dx^I\, dx^J = \frac{1}{\cosh^2(H_{\mathrm{R}}\, \gamma)}\left[(d\gamma)^2\ +\ d\Sigma_d^2\right],\qquad \gamma \in (-\infty,\, \infty) \tag{7.78}$$

which, by means of a different coordinate transformation,

$$\xi(\cdot):\ (-\infty,\, \infty)\ \to\ (0,\, \pi\, H_{\mathrm{R}}^{-1}),\qquad \gamma \mapsto \xi(\gamma) = 2H_{\mathrm{R}}^{-1}\, \arctan\left(e^{H_{\mathrm{R}}\gamma}\right), \tag{7.79}$$

can be brought to the form

$$^{(d+1)}g_{IJ}^{\mathrm{dS}}(x^K)\, dx^I\, dx^J = (d\xi)^2\ + \sin^2(H_{\mathrm{R}}\, \xi)\ d\Sigma_d^2,\qquad H_{\mathrm{R}}\, \xi \in (0,\, \pi) \tag{7.80}$$

Eq.(7.80) is nothing but the well known metric of dS-sliced de Sitter space [369].

Note that in the above both γ and ξ have the dimension of a length, $[\gamma] = [\xi] = -1$, being the only exceptions to our convention that coordinates should be dimensionless.

(2) (A)dS$_{d+1}$ cases combined. It is convenient to combine the two relevant metrics, (7.77) and (7.80), respectively, in the following fashion:

$$^{(d+1)}g_{IJ}^{\mathrm{AdS/dS}}(x^K)\, dx^I\, dx^J = (d\xi)^2\ + F(H_{\mathrm{R}}\, \xi)^2\ d\Sigma_d^2. \tag{7.81}$$

Herein, the function F is given by

$$F(x) = \begin{cases} \sinh(x) & \text{for } \mathrm{AdS}_{d+1} \\ \sin(x) & \text{for } \mathrm{dS}_{d+1} \end{cases}, \tag{7.82}$$

and, as before, $d\Sigma_d^2$ stands for a dS_d metric with the Hubble parameter H_{R}.

---

[7]This AdS metric is used comparatively rarely; exceptions include [367, 368].

7.5.2. *Global coordinates on dS_d*

So far the system of coordinates within the $\xi = const$ surfaces has been left unspecified. When explicit coordinates are needed, we shall choose them in a way such that $x^\mu \equiv (t, \sigma^i)$, with spatial coordinates σ^i and the time coordinate t, covers the maximal extension of de Sitter space. In such global coordinates the dS_d metric reads [369]:

$$d\Sigma_d^2 = \frac{1}{H_R^2} \left[- dt^2 + \cosh^2(t) \; d\Omega_{d-1}^2 \right] . \tag{7.83}$$

Here $d\Omega_{d-1}^2$ denotes the line element of a unit $(d-1)$-sphere coordinatized by the σ^i's.

7.5.3. *Dimensionless scale coordinate $\bar{\xi} = H_R \xi$*

Adopting the line element $d\Sigma_d^2$ from eq.(7.83), the combined metrics (7.81) assume the form

$$^{(d+1)}g_{IJ}^{\text{AdS/dS}}(x^K) \, dx^I \, dx^J \;=\; H_R^{-2} \; ds_{d+1}^2 \Big|_{\bar{\xi}=H_R \xi} \tag{7.84}$$

where ds_{d+1}^2 denotes the dimensionless line element

$$ds_{d+1}^2 = (d\bar{\xi})^2 + F(\bar{\xi})^2 \left[- dt^2 + \cosh^2(t) \; d\Omega_{d-1}^2 \right] . \tag{7.85}$$

It depends on dimensionless coordinates only. They include

$$\bar{\xi} \equiv H_R \, \xi \tag{7.86}$$

which labels the leaves of the foliation. This dimensionless scale coordinate amounts to the original one, ξ, when expressed in units of the Hubble length $L_H^R \equiv H_R^{-1}$ in the reference spacetime.

7.6. RELATING FOLIATION AND RG SCALE

The spacetime $\left(\mathcal{M}_{d+1}, \, ^{(d+1)}g_{IJ} \right)$ is foliated by leaves with $\xi = const$ which we would like to interpret as surfaces of equal RG scale k. By eq.(7.81), our two candidates $\mathcal{M}_{d+1} = \text{AdS}_{d+1}$ and $\mathcal{M}_{d+1} = \text{dS}_{d+1}$ induce certain metrics on those d-dimensional leaves. We insist that these metrics coincide exactly with those delivered by the renormalization group:

$$^{(d+1)}g_{IJ}^{\text{AdS/dS}} \, dx^I \, dx^J \Big|_{d\xi=0} \;=\; F(H_R \xi)^2 \; d\Sigma_d^2 \;\overset{!}{=}\; Y(k)^{-1} \; d\Sigma_d^2 \tag{7.87}$$

This condition leads us to the following fundamental requirement for the viability of the suggested embeddings:

$$F\left(H_{\mathrm{R}}\,\xi\right) \;=\; Y(k)^{-1/2}\,, \qquad k \in \mathbb{R}^+ \tag{7.88}$$

The all-decisive question is whether eq.(7.88) gives rise to an acceptable relationship between ξ and k, namely an admissible coordinate transformation $\xi = \xi(k) \leftrightarrow k = k(\xi)$.

Note that by virtue of

$$Y(k) = \frac{\Lambda(k)}{\Lambda_{\mathrm{R}}} = \frac{H(k)^2}{H_{\mathrm{R}}^2} \qquad \text{and} \qquad Y(k)^{-1/2} = \frac{H_{\mathrm{R}}}{H(k)} = \frac{L_H(k)}{L_H^{\mathrm{R}}} \tag{7.89}$$

the requirement (7.88), when expressed in terms of the respective Hubble lengths $L_H(k) = 1/H(k)$ and $L_H^{\mathrm{R}} = 1/H_{\mathrm{R}}$, writes

$$\hat{F}(\xi) = L_H(k) \qquad \text{where} \qquad \hat{F}(\xi) \equiv L_{\mathrm{R}}\, F\left(\frac{\xi}{L_H^{\mathrm{R}}}\right). \tag{7.90}$$

It can be observed that this condition is a "deformation" of the one occurring in the Ricci flat case studied in Section 7.2. There, the simpler condition $\xi = L_H(k)$ had appeared instead of (7.90). However, as one might expect, at small arguments $\hat{F}$ approaches $\hat{F}(\xi) = \xi + O\!\left((\xi/L_H^{\mathrm{R}})^3\right)$ for the "deformed" functions of (7.82), $\hat{F}(\xi) = L_{\mathrm{R}}\sin(\mathrm{h})\!\left(\xi/L_{\mathrm{R}}\right)$.

In the sequel we investigate the properties of the relationship (7.88) for the most interesting case of $d = 4$, i.e., the embedding of 4-dimensional scale-dependent spacetimes into a 5-dimensional manifold $\mathcal{M}_5$.

In the rest of this paper, in discussions of a general nature that do not depend on the input from the RG flow, we shall continue to leave the dimensionality d arbitrary, however.

7.6.1. Information from the RG

To decide about the viability of an embedding, essential use must be made of the properties of the function $Y(k)^{-1/2} \equiv \sqrt{\Lambda_{\mathrm{R}}/\Lambda(k)}$. The latter is determined by the RG trajectories of the Einstein–Hilbert truncation, concretely those of Type IIIa if $\Lambda_0 > 0$, and of Type IIa for $\Lambda_0 = 0$, respectively. Their investigation by both analytical and numerical means has revealed the following properties that are going to be relevant [95, 97] [RF1]:

(a) Case $\Lambda_0 > 0$: The function $Y(\cdot)^{-1/2} : \mathbb{R}^+ \to \mathbb{R}^+,\ k \mapsto Y(k)^{-1/2}$ is a smooth, strictly decreasing function which maps the k-interval $(0, \infty)$ invertibly on the interval $(0, y^{-1})$.
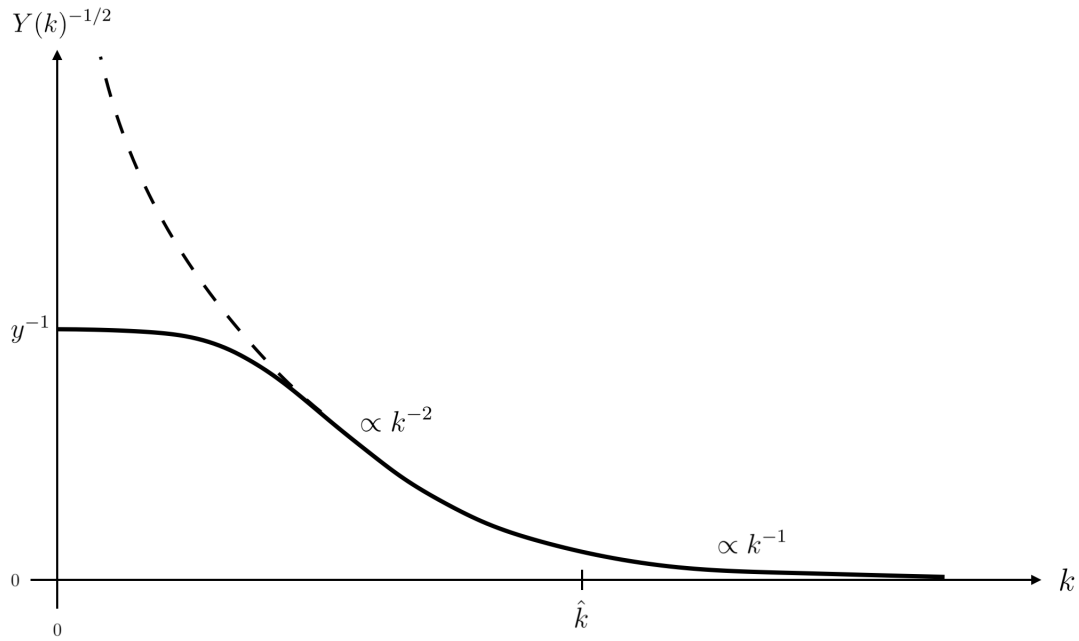
FIGURE 7.3. The schematic behavior of the function $Y(k)^{-1/2}$ for $\Lambda_0 > 0$ (solid line) and $\Lambda_0 = 0$ (dashed line).

Here we introduced the parameter $y^2 \equiv Y(0) = \Lambda_0/\Lambda_R > 0$, or equivalently, $y = H(0)/H_R = L_H^R/L_H(0)$, employing the standard definitions $L_H(k) \equiv 1/H(k)$ and $L_H^R \equiv 1/H_R$.

(b) Case $\Lambda_0 = 0$: The function $Y(\cdot)^{-1/2} : \mathbb{R}^+ \to \mathbb{R}^+$, $k \mapsto Y(k)^{-1/2}$ is a smooth, strictly decreasing function which maps the k-interval $(0, \infty)$ invertibly on the interval $(0, \infty)$.

In either case, the domain and the codomain of $Y(\cdot)^{-1/2}$ are always $\mathbb{R}^+$. The two cases differ however with respect to the actual image of $\mathbb{R}^+$ under $Y(\cdot)^{-1/2}$: If $\Lambda_0 > 0$, the image consists of the interval $(0, y^{-1})$ only, while it comprises all of $\mathbb{R}^+$ for $\Lambda_0 = 0$. This is related to the fact that $Y(k)^{-1/2}$ approaches a finite limit $\lim_{k \to 0} Y(k)^{-1/2} = y^{-1}$ when $\Lambda_0 > 0$, but it diverges to $+\infty$ if we let $k \to 0$ for $\Lambda_0 = 0$.

In Figure 7.3 we schematically depict the behavior of $Y(k)^{-1/2} \equiv Z(k)$ in the two cases. The relevant characteristics of this function are also well described by the analytic approximation (3.61).

It is obvious from Figure 7.3 that, for $\Lambda_0 > 0$, $Z(k) = Y(k)^{-1/2}$ possesses a monotone inverse function $Z^{-1} : (0, y^{-1}) \to \mathbb{R}^+$, and that the image of $(0, y^{-1})$ under Z^{-1} is the full $\mathbb{R}^+$, i.e., the complete half-line of scales k. If instead $\Lambda_0 = 0$, the inverse is a certain function $Z^{-1} : \mathbb{R}^+ \to \mathbb{R}^+$, but again, Z^{-1} is monotone and has an image that covers the entire $\mathbb{R}^+$ of k-values.

7.6.2. *The k-ξ transformation: the AdS_5 candidate*

As a step towards establishing the viability of the $AdS_{d+1} \equiv AdS_5$ embedding, let us now try to satisfy the requirement

$$\sinh\left(H_{\mathrm{R}}\,\xi\right) \;=\; Y(k)^{-1/2} \;\equiv\; Z(k) \tag{7.91}$$

by some monotone function $\xi = \xi(k)$, or $k = k(\xi)$, respectively.

(1) Existence. Solving the relation (7.91) for ξ yields a function which is well defined for all $k \in \mathbb{R}^+$, and assumes values in $\mathbb{R}^+$:

$$\xi(\cdot) : \mathbb{R}^+ \to \mathbb{R}^+, \qquad k \to \xi(k) \;=\; H_{\mathrm{R}}^{-1}\,\mathrm{arsinh}\left(Y(k)^{-1/2}\right). \tag{7.92}$$

The key observation in the previous subsection, namely that $Y(\cdot)^{-1/2}$ has an everywhere negative derivative, for both $\Lambda_0 = 0$ and $\Lambda_0 > 0$, implies that the function (7.92) is strictly decreasing, too: $\frac{d}{dk}\xi(k) < 0$ for all $k > 0$. This is precisely as it must be if the k-ξ relationship is to qualify as an orientation reversing[8] diffeomorphism.

As for the inverse map $\xi \mapsto k(\xi)$, we solve (7.91) for k this time:

$$k(\xi) \;=\; Z^{-1}\left(\sinh\left(H_{\mathrm{R}}\,\xi\right)\right). \tag{7.93}$$

The monotonicity of $Z^{-1}(\cdot)$ and $\sinh(\cdot)$ implies that, as expected, $\frac{d}{d\xi}k(\xi) < 0$ everywhere. From the properties of Z^{-1} we furthermore infer the domain of the function defined by the expression (7.93):

$$k(\cdot) : \left(0, \xi_{\max}(y)\right) \to \mathbb{R}^+, \qquad \xi \mapsto k(\xi) \qquad \text{for} \quad \Lambda_0 > 0 \tag{7.94}$$

$$k(\cdot) : \mathbb{R}^+ \to \mathbb{R}^+, \qquad \xi \mapsto k(\xi) \qquad \text{for} \quad \Lambda_0 = 0 \tag{7.95}$$

Here we introduced the y-dependent interval boundary

$$\xi_{\max}(y) \;\equiv\; H_{\mathrm{R}}^{-1}\,\mathrm{arsinh}\left(y^{-1}\right). \tag{7.96}$$

Since the image of $k(\cdot)$ equals $\mathbb{R}^+$ in both cases, we can conclude that it is sufficient to draw ξ-values from the interval $(0, \xi_{\max})$ in the first, and from $\mathbb{R}^+$ in the second case, in order to parameterize all scales $k \in \mathbb{R}^+ \equiv (0, \infty)$ in a smooth and invertible manner.

This proves the existence of an admissible transformation $\xi \leftrightarrow k$ which possesses the desired properties of a one-dimensional diffeomorphism. It entails the viability of an embedding into the 5-dimensional anti-de Sitter space AdS_5, and this is what we wanted to establish.

---

[8]The orientation reversing character of the coordinate transformation $k \to \xi$ is a trivial consequence of ξ being a *length*, while k is a *momentum*.

(2) Asymptotic form. Within the approximation of eq.(3.61), we can write down the coordinate transformation relating ξ and k in closed form. In the asymptotic scaling regime near the UV fixed point, $k \gtrsim \hat{k}$, we obtain for the Type IIIa and IIa trajectories alike:

$$\xi(k) \approx H_{\mathrm{R}}^{-1} \operatorname{arsinh}\left(\frac{1}{L\,k}\right) \approx \frac{1}{H_{\mathrm{R}}\,L\,k} \tag{7.97}$$

Using the definitions of H_{R} and L in $d = 4$, this relation becomes

$$\xi(k) \approx \left(\frac{\lambda_*}{3}\right)^{1/2} \frac{1}{k} . \tag{7.98}$$

It expresses a perfect inverse proportionality between the RG parameter k and the value of the (dimensionful) coordinate ξ.

In the semiclassical regime $0 < k \lesssim \hat{k}$, the properties of the corresponding transformation

$$\xi(k) \approx H_{\mathrm{R}}^{-1} \operatorname{arsinh}\left(\left[y^2 + (\ell\,k)^4\right]^{-1/2}\right) \tag{7.99}$$

depend on the type of the RG trajectory in a significant way.

For Type IIIa trajectories, $y^2 \equiv \Lambda_0/\Lambda_{\mathrm{R}}$ is non-zero, and the ξ coordinate corresponding to the limit $k \searrow 0$ is *finite*:

$$\xi(k = 0) \approx H_{\mathrm{R}}^{-1} \operatorname{arsinh}\left(y^{-1}\right) . \tag{7.100}$$

For the Type IIa trajectory, on the other hand, $y = 0$ implies the following behavior of ξ at low RG scales $k \ll \ell^{-1}$:

$$\xi(k) \approx H_{\mathrm{R}}^{-1} \operatorname{arsinh}\left(\frac{1}{\ell^2\,k^2}\right) \approx H_{\mathrm{R}}^{-1} \ln\left(\frac{2}{\ell^2\,k^2}\right) . \tag{7.101}$$

Hence $\xi(k)$ approaches $+\infty$ when k decreases towards zero.

7.6.3. *The k-ξ transformation: the dS_5 candidate*

Let us return to the fundamental requirement (7.88) with a generic function $F(\cdot)$ appearing on its LHS. Since, first, $Y(k)^{-1/2}$ was found to be monotone, and second, $k = k(\xi)$ was demanded to be monotone, it follows that the requirement (7.88) can be satisfied only if $F(H_{\mathrm{R}}\xi)$ on its LHS has a monotone dependence on ξ.

Above, in the AdS case, this has indeed been the case, thanks to the monotonicity of the sinh-function in eq.(7.91).

For the second candidate, the de Sitter space dS_{d+1}, the requirement reads

$$\sin(H_{\mathrm{R}}\,\xi) = Y(k)^{-1/2} \equiv Z(k) , \tag{7.102}$$

and here the situation is different, for two reasons:

(a) The line element (7.80) is non-degenerate only for $H_R\xi \in (0,\pi)$. Therefore, right from the outset we must restrict the range of the ξ coordinate to the interval $\xi \in (0,\pi)\, H_R^{-1}$.

(b) On this latter interval, the LHS of (7.102), $\sin(H_R\xi)$, is *not* a monotone function of ξ. As a way out, we restrict ξ even further, namely to only half of the original range:

$$\xi \in \left(0, \frac{\pi}{2}\right) H_R^{-1} \, . \tag{7.103}$$

For coordinate values in the interval (7.103), the metric (7.80) is well defined, and at the same time the LHS of (7.102) is monotone with respect to ξ. Hence we can hope to find a diffeomorphism relating ξ to k.

A discussion analogous to the one above shows that there is indeed such a coordinate transformation, albeit only for certain values of y.

(1) Existence for $y > 1$. Clearly, when it exists ($y > 1$), the transformation has the form

$$\xi(k) = H_R^{-1} \arcsin\left(Z(k)\right) \quad \Longleftrightarrow \quad k(\xi) = Z^{-1}\left(\sin(H_R\xi)\right) \tag{7.104}$$

and every RG scale $k \in \mathbb{R}^+$ gets related in a 1-1 way to a unique $\xi \in \left(0, \xi_{\max}(y)\right)$ whereby

$$\xi_{\max}(y) = H_R^{-1} \arcsin\left(y^{-1}\right) \, . \tag{7.105}$$

For the expressions in (7.104) to make sense, the argument of the arcsin-function must satisfy $Z(k) \equiv Y(k)^{-1/2} \in (0,1)$ for all $k \in \mathbb{R}^+$. A quick glance at Figure 7.3 reveals that this is the case if, and only if $y > 1$. Recalling the definition of the parameter y,

$$y \equiv Y(0)^{1/2} = \left(\Lambda_0/\Lambda_R\right)^{1/2} = H(0)/H_R = L_H^R/L_H(0) \, , \tag{7.106}$$

we see that $y > 1$ imposes a constraint on the value of the Hubble length at the trajectory's endpoint, $L_H(0) \equiv \lim_{k\to 0} L_H(k)$, in relation to the Hubble radius of the reference metric:

$$y > 1 \quad \Longleftrightarrow \quad L_H^R > L_H(0) \quad \Longleftrightarrow \quad \Lambda_0 > \Lambda_R \, . \tag{7.107}$$

If the constraint (7.107) is satisfied, (7.104) does indeed define a diffeomorphic map $\xi(\cdot) : \mathbb{R}^+ \to \left(0, \xi_{\max}\right)$, $k \mapsto \xi(k)$, as it is necessary for the embedding in dS_5 to exist. In the opposite case, $y < 1$, no such map exists.[9]

---

[9]This is obvious from the relation (7.102) already: Its RHS, $Y(k)^{-1/2}$, assumes values between zero and $y^{-1} > 1$, while the magnitude of the LHS, $\sin(H_R\xi)$, never exceeds unity.

(2) Asymptotic form. For the k-ξ relationship at asymptotically large and small RG parameters, the analytic approximation (3.61) yields, respectively,

$$\xi(k) \approx \left(\frac{L_H^R}{L}\right)\frac{1}{k} \qquad\qquad (L\,k \to \infty)\,, \qquad (7.108)$$

$$\xi(k) \approx \xi_{\max}(y) - \frac{L_H^R \ell^4}{2y^2\sqrt{y^2-1}}\,k^4 \qquad\qquad (\ell\,k \to 0)\,. \qquad (7.109)$$

The y-dependence in the prefactor of the k^4 term in (7.109) makes it quite clear that $y = 1$ amounts to a threshold that cannot be crossed. We shall come back to it towards the end of the next section.

In this section we saw that ξ, the coordinate that labels the leaves of the foliation, and k, the RG scale, are indeed related by an admissible coordinate transformation. The next question we must address is how much of the total (A)dS$_{d+1}$ manifold is actually covered by the embedded spacetimes $\left\{\left(\mathcal{M}_d, g_{\mu\nu}^k\right),\, k \in \mathbb{R}^+\right\}$ from the renormalization group. We consider the cases $\mathcal{M}_{d+1} = \text{AdS}_{d+1}$ and $\mathcal{M}_{d+1} = \text{dS}_{d+1}$ in turn.

7.7. Global structure and AdS connection

7.7.1. *The AdS embedding*

We start by discussing the geometrization of the RG flow by means of $\mathcal{M}_{d+1} = \text{AdS}_{d+1}$. According to eq.(7.85), the dS-sliced AdS metric reads, in dimensionless form:[10]

$$ds_{d+1}^2 = (d\xi)^2 + \sinh^2(\xi)\left[-dt^2 + \cosh^2(t)\,d\Omega_{d-1}^2\right] \qquad (7.110)$$

If we leave the relation of ξ to k aside for a moment, the maximal range of the coordinate values at which (7.110) can be applied is given by

$$t \in \left(-\infty, +\infty\right) \qquad \text{and} \qquad \xi \in \left(0, \infty\right)\,. \qquad (7.111)$$

(1) Relationship ξ-k disregarded. At first instance we will disregard the relationship ξ-k. To find out how (7.110) is connected to the global AdS spacetime, and also in order to derive the corresponding Penrose diagram, let us perform the coordinate transformation $(\xi, t) \to (r, \tau)$ given by

$$r = \sinh(\xi)\,\cosh(t)\,,$$
$$\tan(\tau) = \tanh(\xi)\,\sinh(t)\,. \qquad (7.112)$$

---

[10]For simplicity, we omit the overbar from $\bar\xi$ in this subsection, i.e., now ξ is understood to be measured in units of the reference Hubble length H_R^{-1}.
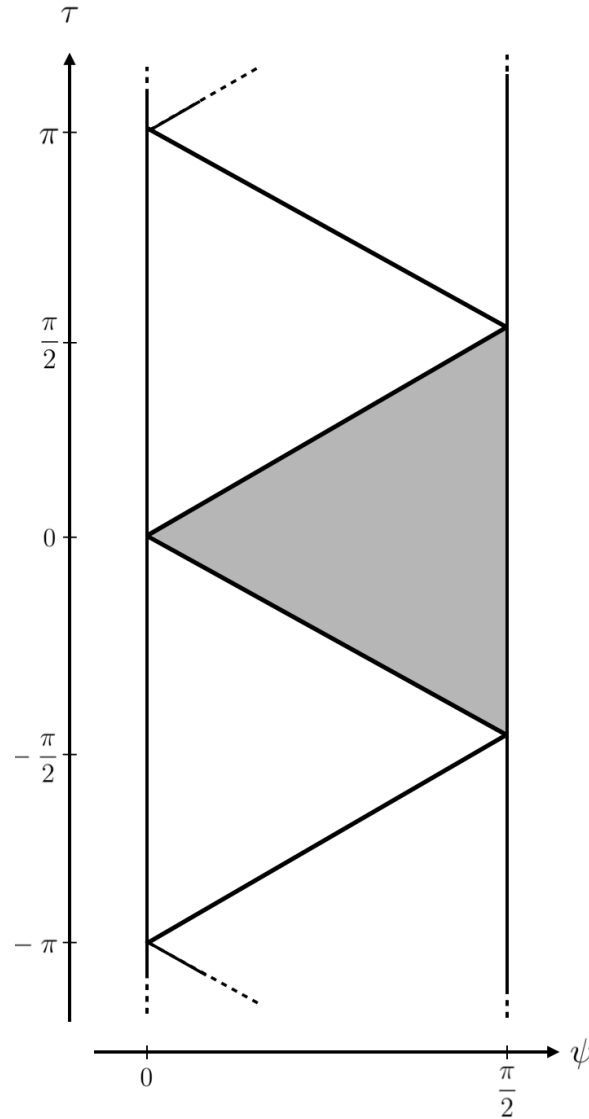
FIGURE 7.4. The Penrose diagram of (the universal cover of) the AdS_{d+1} spacetime. The shaded triangle corresponds to the part where the metric (7.110) applies when its maximum coordinate range (7.111) is exploited.

This transformation turns the line element (7.110) into

$$ds^2_{d+1} = -\left(1 + r^2\right) \, d\tau^2 \, + \, \frac{dr^2}{1 + r^2} \, + \, r^2 \, d\Omega^2_{d-1} \tag{7.113}$$

which is the well known AdS_{d+1} metric in *global coordinates*, and for a unit Hubble parameter. The latter metric can be applied for the coordinate ranges

$$\tau \in \left(-\infty, +\infty\right) \quad \text{and} \quad r \in \left(0, \infty\right), \tag{7.114}$$

which actually correspond to the universal cover of the AdS_{d+1} spacetime. The causal
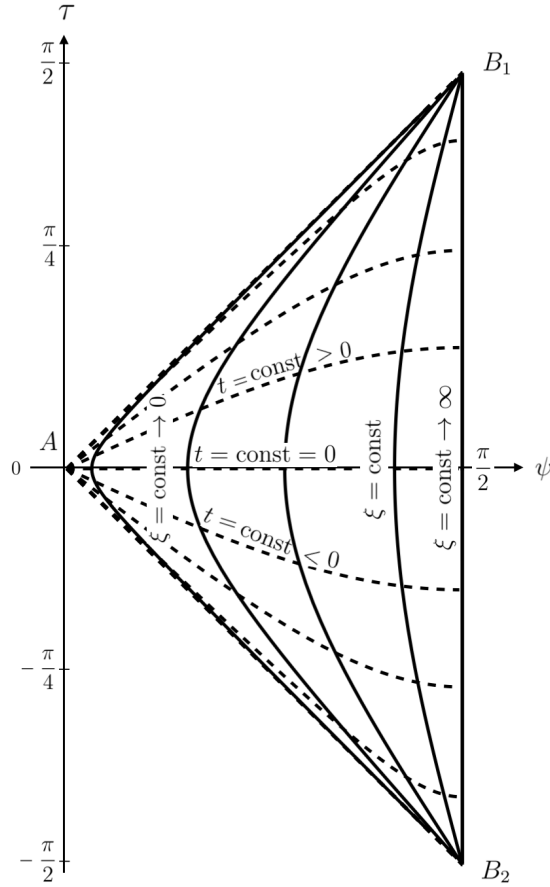
FIGURE 7.5. The shaded triangle of the AdS_{d+1} Penrose diagram in Figure 7.4 is redrawn. On the τ-ψ plane, various coordinate lines are shown on which $\xi = const$ (solid lines) or $t = const$ (dashed lines). In the limits $\xi = const \to \infty$, and $\xi = const \to 0$, the surfaces of constant scale are seen to approach the line segment $B_1 B_2$, and the null cone $B_1 A B_2$, respectively.

structure of the global manifold becomes manifest after an additional coordinate transformation $r \to \psi$:

$$\tan(\psi) = r. \tag{7.115}$$

It converts (7.113) to the manifestly conformally flat metric

$$\mathrm{d}s_{d+1}^2 = \frac{1}{\cos^2(\psi)} \left[-\mathrm{d}\tau^2 + \mathrm{d}\psi^2 + \sin^2(\psi) \, \mathrm{d}\Omega_{d-1}^2 \right]. \tag{7.116}$$

This metric is applicable for $\tau \in (-\infty, \infty)$, $\psi \in \left(0, \frac{\pi}{2}\right)$.

In Figure 7.4 we sketch the Penrose diagram obtained from (7.116) after multiplication by $\cos^2(\psi)$. In this diagram, every point on the τ-ψ plane corresponds to a sphere S^{d-1} with radius $\sin^2(\psi)$.

It can be checked that the original metric (7.110) with coordinate ranges (7.111) covers only a part of the entire manifold. In Figure 7.4 the corresponding patch is indicated by the shaded triangle.

Furthermore, in Figure 7.5, various coordinate lines having constant t- or ξ-values are shown within this triangular region. Every line with $\xi = const$ represents one of the d-dimensional spacetimes $\left.\left(\mathrm{dS}_d,\, g_{\mu\nu}^k\right)\right|_{k=k(\xi)}$ which were supplied by the renormalization group.

(2a) Relationship ξ-k imposed: Type IIIa. In Section 7.6 we concluded that, if $\Lambda_0 \neq 0$, the scale coordinate $\xi = \xi(k) \in (0, \xi_{\max})$ does not exhaust the full range of theoretically possible values, $\xi \in (0, \infty)$:

$$\left\{ (\mathrm{dS}_d,\, g_{\mu\nu}^k),\, k \in \mathbb{R}^+ \right\} \;=\; \left\{ (\mathrm{dS}_d,\, g_{\mu\nu}^{k(\xi)}),\, \xi \in \left(0,\, \xi_{\max}(y)\right) \right\}. \qquad (7.117)$$

As a consequence, the entirety of all spacetimes that occur along a complete Type IIIa trajectory require for their embedding only a part of the triangular region in the τ-ψ plane. It is given by the shaded area of the Penrose diagram in Figure 7.6. This area is coordinatized by $\xi \in (0, \xi_{\max}(y))$, $t \in (-\infty, \infty)$.

(2b) Relationship ξ-k imposed: Type IIa. If $\Lambda_0 = 0$ on the other hand, i.e., for the Type IIa trajectory, the complete shaded triangle of Figure 7.4, but not more than that, is needed in order to embed the entire stack of spacetimes $\left\{ \left(\mathrm{dS}_d,\, g_{\mu\nu}^k\right),\, k \in \mathbb{R}^+ \right\}$. See Figure 7.7 for an illustration of this case.

7.8. THE POSSIBILITY OF A NON-STANDARD ADS/CFT

We started out from a stack of de Sitter spacetimes which emerged as solutions to the scale-dependent effective field equations derived from Type IIIa and IIa trajectories of running actions, $k \mapsto \Gamma_k$, $k \in \mathbb{R}^+$. We tried to interpret them as the leaves of a $(d+1)$-dimensional manifold that carries a natural foliation induced by the RG scale. We demanded that its metric $^{(d+1)}g_{IJ}$ should, (i), be Einstein and Lorentzian, (ii), have vanishing shift vector and x^μ-independent lapse when presented in "scale-ADM" form, and (iii), possesses as many Killing vectors as it is compatible with the other requirements and the symmetries of the input metrics $g_{\mu\nu}^k$.

We have then shown that, besides the dS candidate to be discussed below, an embedding into AdS_d is the only option. Moreover, at least for $d = 4$, the properties of the RG flow are indeed such that the viability of the program can be demonstrated, i.e.,
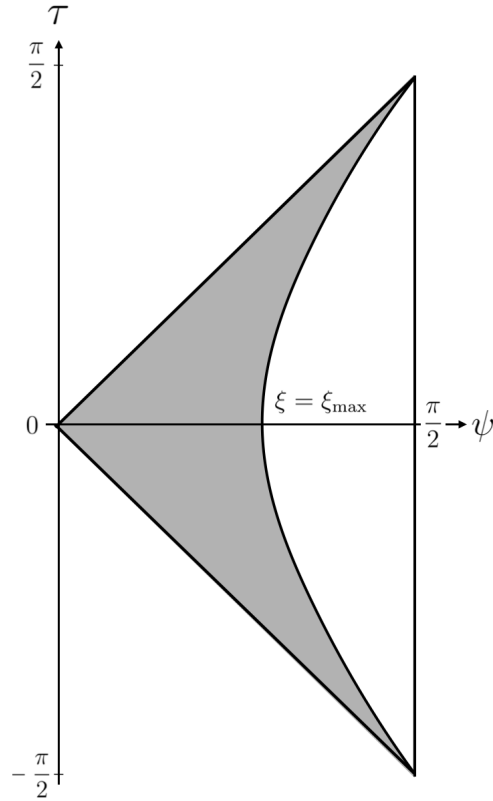
FIGURE 7.6. The shaded area in this diagram indicates the part of the AdS$_5$ Penrose diagram in Figure 7.4 andFigure 7.5 that is needed in order to embed all 4D spacetimes occurring along an RG trajectory of Type IIIa. The area is bounded by the $\xi = const$ line with $\xi = \xi_{\mathrm{max}}(y)$ given in eq.(7.96).

there exists a scalar function $k = k(x^I)$ on the embedding manifold which describes the foliation by leaves of constant scale in a (in principle) coordinate independent manner.

We demonstrated that embedding the set of all spacetimes (7.117) does not exhaust the entire AdS$_5$ manifold. The part of the latter which actually comes into play is represented pictorially in the causal diagrams of Figure 7.6 and Figure 7.7. They apply to 4D cosmological constants $\Lambda_0 > 0$ and $\Lambda_0 = 0$, respectively.

As for the interpretation, let us begin with the case $\Lambda_0 = 0$, i.e., the Type IIa trajectory. It is special in that it terminates in the GFP, and that $\lim_{k \to 0} \Lambda(k) = 0$.[11] As a result, at the endpoint of the IIa trajectory the solution of the field equation changes from dS$_4$ to Minkowski space.

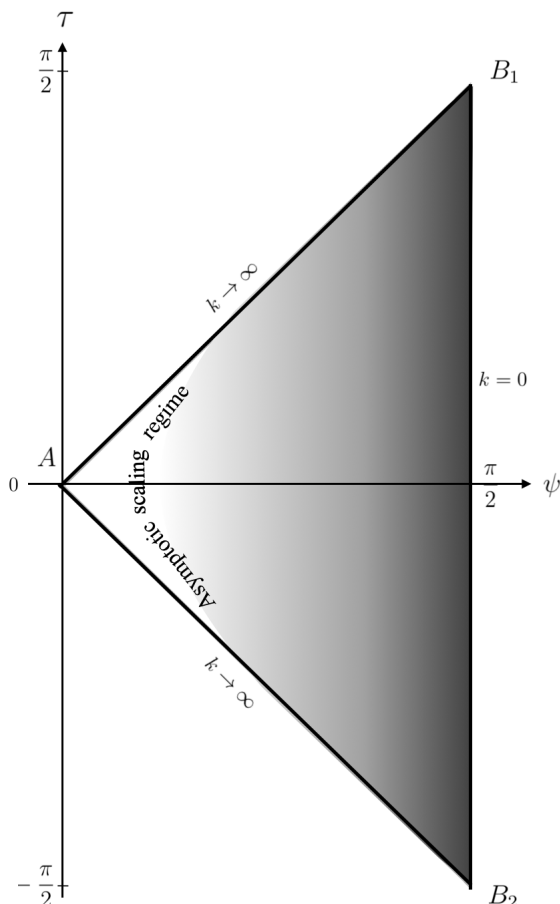[11]For recent work that independently hints at a special status of the Type IIa trajectory see [224, 370, 371].

FIGURE 7.7. Penrose diagram illustrating the portion of the AdS_5 manifold that is necessary to embed all dS_4 spacetimes along the Type IIa trajectory. The gray shading indicates the local value of k. Dark (light) regions correspond to low (high) values of the RG parameter k.

7.8.1. Geometry

In Figure 7.7, the triangle represents the part of AdS_5 covered by the embedding, and its causal properties in a global fashion. We denote this part as $\mathrm{AdS}_5^{\mathrm{emb}}$ in the following. We also recall that all points of the diagram are actually representatives of 3-dimensional spatial spheres. In Figure 7.7, the τ-ψ projection of the boundary of $\mathrm{AdS}_5^{\mathrm{emb}}$ is seen to comprise 3 components: the lightlike ones AB_1 and AB_2, and a timelike one, B_1B_2, residing at spatial infinity. While the line segments AB_1 and AB_2 consist of inner points of the full AdS_5 manifold[12], the segment B_1B_2 is a boundary of both $\mathrm{AdS}_5^{\mathrm{emb}}$ and the total AdS_5.

---

[12]except for the points A, B_1, and B_2.

7.8.2. *Quantum field theory à la GEAA*

Now let us switch from geometry to quantum field theory, formulated in GEAA language. For this purpose we decorated the Penrose diagram in Figure 7.7 with information concerning the local value of $k(x^I)$ by means of a variable gray shading. It highlights the following properties of the foliation carried by $\mathrm{AdS}_5^{\mathrm{emb}}$:

(i) In the UV limit $k \to \infty \Leftrightarrow \xi \to 0$, the leaves of constant scale which describe 4D spacetime at a given resolution, get squeezed into the null cone B_1AB_2: the smaller is ξ, the more the lines with $\xi = const$ approach the diagonals $AB_{1,2}$ in the τ-ψ plane, see Figure 7.5. As a result, those particular (spacelike!) leaves whose internal dynamics is ruled by the GEAA in the *"bare" limit*, $\Gamma_{k\to\infty} \sim S$, are situated infinitely close to the null cone B_1AB_2, the lightlike boundary of $\mathrm{AdS}_5^{\mathrm{emb}}$.

(ii) Conversely, in the *physical limit* $k \to 0$, i.e., when the IR cutoff is removed, the 4D dynamics is governed by the ordinary effective action $\lim_{k\to 0}\Gamma_k = \Gamma$. This is the relevant action for the effective theory on the leaves in the limit $\xi \to \infty$ when dS_4 approaches Minkowski space. In Figure 7.7, those leaves are represented by almost straight, essentially vertical lines connecting B_1 and B_2. They get infinitely close to the (perfectly straight) vertical line B_1B_2 at $\psi = \pi/2$, the timelike boundary of $\mathrm{AdS}_5^{\mathrm{emb}}$ at spatial infinity.

7.8.3. *The novel AdS/CFT correspondence*

Thus, taking the above remarks together we are led to the picture of a 5-dimensional geometry with certain QFT's attached to it in a specific way. It is strikingly similar to the AdS/CFT correspondence proposed in the literature [45, 229, 266]. In the string theory-related correspondence, too, a theory involving gravity, namely full-fledged string theory or a low energy approximation thereof, lives on the bulk of AdS_5 and is "holographically" related to a CFT on the boundary, whereby the isometry group of the 5D manifold, $SO(4,2)$, acts as the conformal group on the 4D boundary [372–376].

The analogies to the picture based upon the functional renormalization group are obvious. In particular the task of defining a theory of quantum gravity beyond the confines of perturbation theory is taken over by Asymptotic Safety now, replacing string theory.

The analogy is particularly striking if the field theory that is defined by the asymptotically safe Type IIa trajectory $\left\{\Gamma_k^{\mathrm{IIa}},\ k \in \mathbb{R}^+\right\}$ is *conformal*, i.e., if $\lim_{k\to 0}\Gamma_k \equiv \Gamma$ defines the action of a 4-dimensional CFT. As we mentioned in the Introduction, for

the time being this is unproven in $d = 4$, but has already been established in two dimensions, where also the unitarity of the CFT was shown [377].

In this regard it is also important to note that recently it has been demonstrated that 4D quantum gravity based upon the action $\int d^4x \sqrt{g}\, R$, linearized about Minkowski space, is indeed conformal, rather than merely scale invariant at the IR fixed point [378]. The pertinent CFT, having no stress tensor, and no relevant or marginal scalar operators, is of a non-standard type which is defined at the level of the correlation functions. This result is consistent with our expectation that the endpoint of the Type IIa trajectory is indeed a CFT.[13]

7.8.4. *Meaning of holography in the GEAA approach*

Within the framework of the gravitational Effective Average Action there exists a natural and perfectly general notion of *holography*. It is exemplified by the above AdS/CFT picture, but its scope is much broader.

Loosely speaking, the corresponding "holographic principle" conjectures, purely at a 4D level, that all actions Γ_k at $k > 0$, including the bare one, $S \sim \Gamma_{k\to\infty}$, can be reconstructed from the standard effective action $\Gamma_{k=0} = \Gamma$.

This is equivalent to saying that the functional RG equation defines a meaningful initial value problem also when the direction of the k-evolution is changed from "downward" to "upward", and the initial condition $\Gamma_{k=0} \overset{!}{=} \Gamma$ is imposed in the IR rather than UV.

A solution to this "inverse quantization problem" extends the dynamics from the "holographic screen", aka, the foliation's leave at $k = 0$, into the "bulk" comprised of the leaves with $k > 0$.

In general, it may be problematic to give a mathematical meaning to such a functional variant of a boundary value problem. Along asymptotically safe RG trajectories, followed in the reversed direction, this should be possible though. A first proof of principle has appeared in refs.[94, 215, 379] already.

---

[13]Note however that while the limit $k \to 0$ renders Minkowski space a solution of the effective field equation, as such it does not *linearize* the equation: Near the GFP, the dimensionless Newton constant scales like $g(k) \approx G_0 k^2$ with a nonzero renormalized Newton constant $G_0 \neq 0$ in general.

7.8.5. *Nonzero IR cosmological constant*

In the Type IIIa case, having $\Lambda_0 \neq 0$, the situation is different in that dS_4 continues to be a solution of the effective Einstein equation even when k is *strictly* zero. Contrary to the IIa case discussed above, the limit $k \to 0$ involves no change from the de Sitter solution to Minkowski space at $k = 0$ at the final point of the trajectory.

Comparing Figure 7.6 and Figure 7.7 shows that a non-zero value $\Lambda_0 \neq 0$ prevents the boundary of AdS_5^{emb} to get close to the timelike boundary of the full AdS_5. It always remains crescent-shaped when $\Lambda_0 \neq 0$, and this spoils the analogy to the AdS/CFT picture.

7.9. GLOBAL STRUCTURE AND DS CONNECTION

7.9.1. *The dS embedding*

A geometrization of the RG flow by means of our second candidate, $\mathcal{M}_{d+1} = dS_{d+1}$, would rely upon the (dimensionless) de Sitter metric

$$ds_{d+1}^2 = (d\xi)^2 + \sin^2(\xi) \left[-dt^2 + \cosh^2(t) \ d\Omega_{d-1}^2 \right] . \qquad (7.118)$$

As before, let us begin by investigating the spacetime furnished with (7.118) for the full range of coordinate values for which the metric is non-degenerate:

$$\xi \in (0, \pi) \qquad \text{and} \qquad t \in (-\infty, +\infty) . \qquad (7.119)$$

So, for a moment, we ignore the constraints due to the matching of ξ with k.

(1) Relationship ξ-k disregarded. To begin with, disregarding the ξ-k relationship, we trade ξ and t for new coordinates, ψ and τ, by means of a transformation

$$
\begin{aligned}
(0, \pi) \times \mathbb{R} \quad &\to \quad (0, \pi) \times \left(-\frac{\pi}{2}, +\frac{\pi}{2} \right) , \\
(\xi, t) \quad &\mapsto \quad \left(\psi(\xi, t), \tau(\xi, t) \right) ,
\end{aligned}
\qquad (7.120)
$$

which is defined by the following functions:[14]

$$\psi(\xi, t) = \arccos \left(\frac{\cos(\xi)}{\sqrt{1 + \sin^2(\xi) \sinh^2(t)}} \right) , \qquad (7.121a)$$

$$\tau(\xi, t) = \arctan \left(\sin(\xi) \ \sinh(t) \right) . \qquad (7.121b)$$

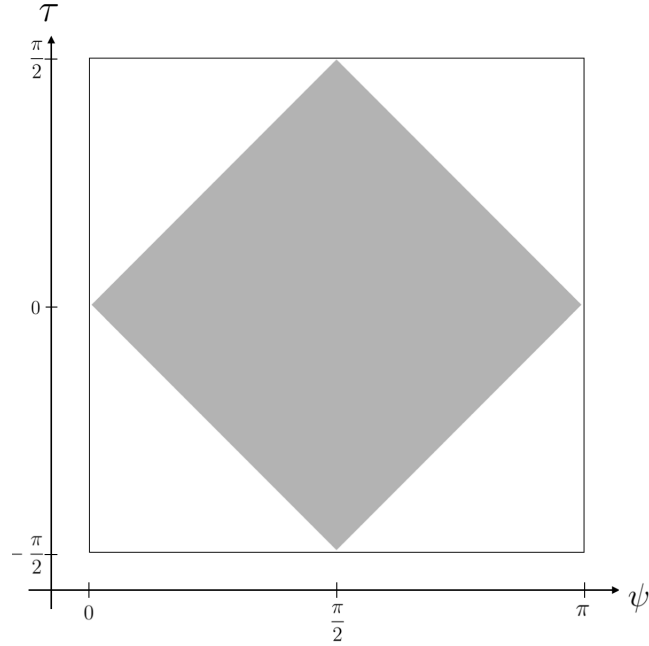[14] All inverse trigonometric functions are understood to be principal values.

FIGURE 7.8. The Penrose diagram of dS_{d+1} on the τ-ψ plane. Every point corresponds to a sphere $\mathbb{S}^{d-1}$ of radius $\sin^2(\psi)$. The shaded square indicates the part of the de Sitter manifold which is covered by the ξ-t coordinate system.

This transformation recasts the metric (7.118) in the manifest conformally flat form

$$
ds_{d+1}^2 = \frac{1}{\cos^2(\tau)} \left[-d\tau^2 + d\psi^2 + \sin^2(\psi)\, d\Omega_{d-1}^2 \right]. \tag{7.122}
$$

Further useful properties of this coordinate transformation include

$$
\begin{aligned}
\xi \in \left(0, \frac{\pi}{2}\right) &\implies \psi \in \left(0, \frac{\pi}{2}\right), \\
\xi \in \left(\frac{\pi}{2}, \pi\right) &\implies \psi \in \left(\frac{\pi}{2}, \pi\right),
\end{aligned} \tag{7.123}
$$

as well as $\mathrm{sign}\big(\tau(\xi, t)\big) = \mathrm{sign}(t)$, and

$$
\tau(\xi, t = 0) = 0, \qquad \psi(\xi, t = 0) = \xi \qquad , \quad \forall\, \xi \in (0, \pi), \tag{7.124}
$$

$$
\psi\left(\xi = \tfrac{\pi}{2}, t = 0\right) = \tfrac{\pi}{2} \quad , \quad \forall\, t \in \mathbb{R}. \tag{7.125}
$$

If one allows ψ and τ to freely and independently draw values from the intervals $\psi \in (0, \pi)$ and $\tau \in \left(-\frac{\pi}{2}, +\frac{\pi}{2}\right)$, respectively, (7.122) amounts to the familiar de Sitter metric in global coordinates, from which the Penrose diagram can be deduced in the usual way [369]. However, the actual image of the above coordinate transformation is smaller than the codomain written in (7.120). Thus, the original ξ, t coordinates do not cover the de Sitter manifold fully.
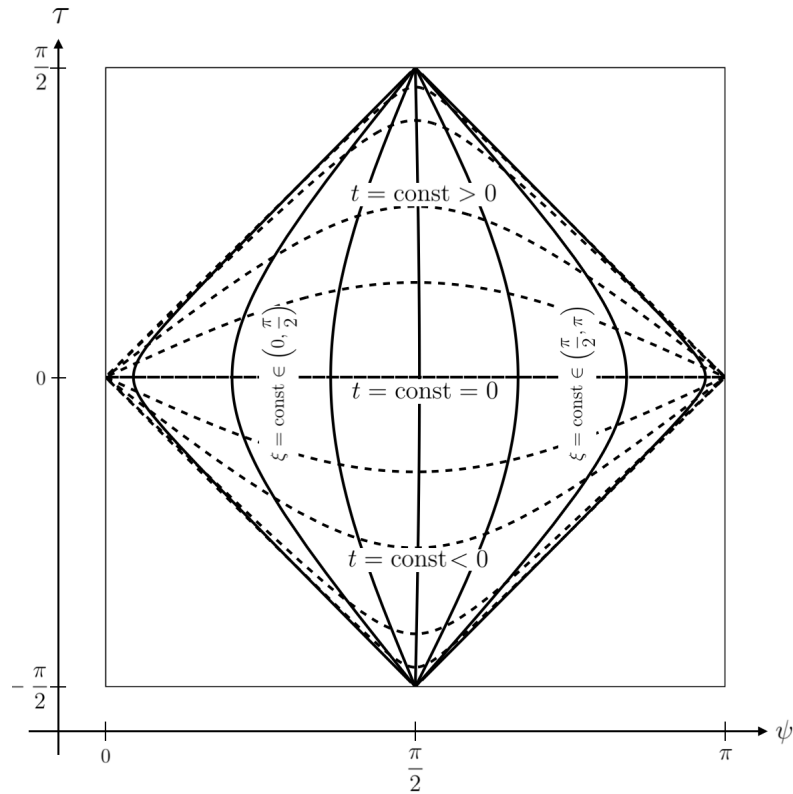
FIGURE 7.9. The part of the dS_{d+1} Penrose diagram that is covered by ξ-t coordinate systems. Coordinate lines with $\xi = const$ (solid lines) and $t = const$ (dashed lines) are shown.

In Figure 7.8 we draw the Penrose diagram of dS_{d+1} on the ψ-τ plane, and we indicate which part of spacetime is actually covered by the ξ, t coordinate system. It corresponds to the shaded square.

Furthermore, Figure 7.9 focuses on this particular portion of spacetime and additionally shows the net of coordinate lines with $\xi = const$ and $t = const$, respectively.

(2) Imposing the ξ-k relationship. Now we impose the ξ-k relationship. In Subsection 7.6.3 we concluded that the dS_5 embedding is viable for $y > 1$ only, in which case the coordinate ξ assumes values in the interval $\big(0, \xi_{\mathrm{max}}(y)\big)$. Using (7.106) in (7.105), we can express the upper boundary of this interval as

$$\xi_{\mathrm{max}}(y) \;=\; L_H^{\mathrm{R}} \, \arcsin\big(y^{-1}\big) \;=\; L_H^{\mathrm{R}} \, \arcsin\left(\frac{L_H(0)}{L_H^{\mathrm{R}}}\right) \tag{7.126}$$

Regarding its dependence on y, the values assumed by $\xi_{\mathrm{max}}(y)$ range from $\xi_{\mathrm{max}} = 0$ in the limit $y \to \infty$, to

$$\lim_{y \searrow 1} \xi_{\mathrm{max}}(y) \;=\; \left(\frac{\pi}{2}\right) L_H^{\mathrm{R}} \,, \tag{7.127}$$

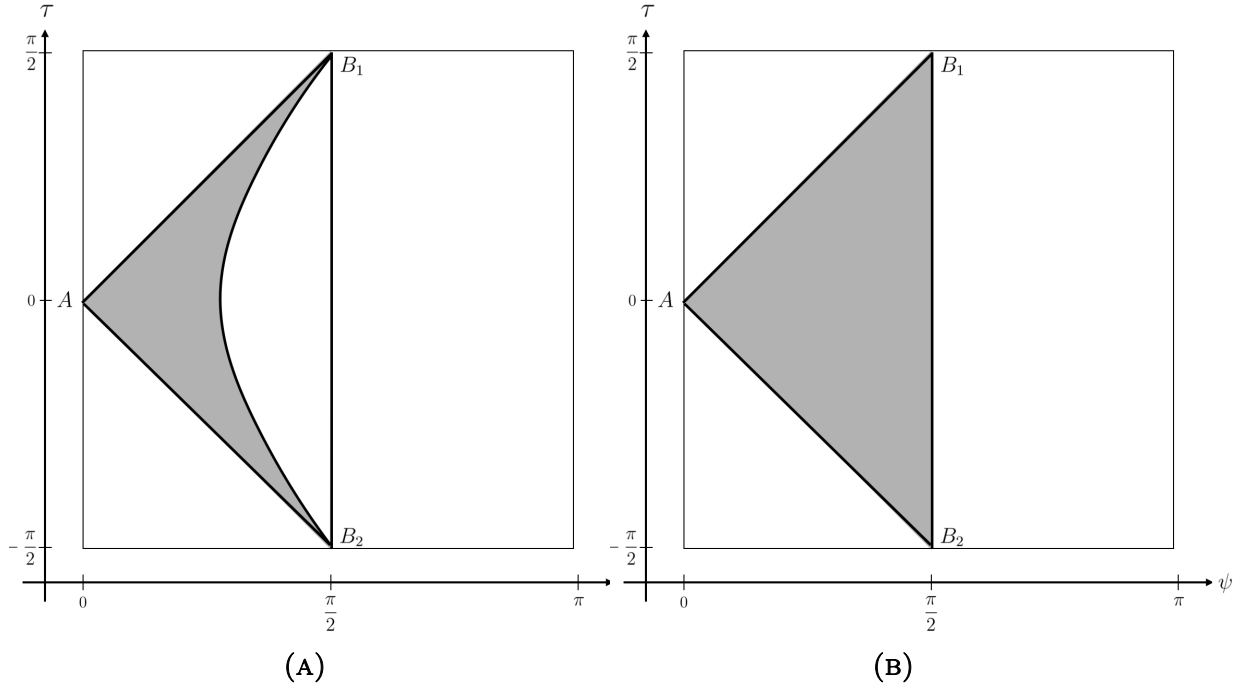when the threshold at $y = 1$ is approached.

FIGURE 7.10. The shaded area indicates the part of the de Sitter manifold which is needed in order to fully geometrize a Type IIIa trajectory with, respectively $\Lambda_0 > \Lambda_R$ (left diagram) and $\Lambda_0 = \Lambda_R$ (right diagram).

Also in the case of the de Sitter candidate dS_5, the embedding of all dS_4-spacetimes along a complete Type IIIa trajectory covers only a part of the 5-dimensional manifold. Henceforth denoting it by dS_5^{emb}, let us now determine this part of the de Sitter manifold.

In Subsection 7.6.3 we saw already that, for monotonicity reasons, we must restrict the range of ξ, namely from the original interval $(0, \pi)$ to $\left(0, \frac{\pi}{2}\right)$, in units of $L_H^R \equiv H_R^{-1}$. Using the properties (7.124) and (7.125), this restriction is seen to imply a corresponding restriction for the newly introduced ψ coordinate, namely $\psi \in \left(0, \frac{\pi}{2}\right)$.

In geometrical terms this means that, in the Penrose diagram of Figure 7.8, only that subset of the shaded square is available for the geometrization which lies to the left of the vertical line at $\psi = \frac{\pi}{2}$, $\tau \in \left(-\frac{\pi}{2}, \frac{\pi}{2}\right)$. Thus the dS_5^{emb} part of dS_5, embedding all 4D spacetimes, must fit into a triangular region with corners at $(\tau, \psi) = (0, 0)$, $\left(\frac{\pi}{2}, \frac{\pi}{2}\right)$, and $\left(\frac{\pi}{2}, -\frac{\pi}{2}\right)$, respectively.

Furthermore, taking advantage of Figure 7.9 in order to translate the condition $\xi < \xi_{\max}$ to the τ-ψ coordinate system, it becomes clear that only a subdomain of the above triangle is actually required for the embedding. In the Penrose diagram of Figure 7.10a, the subdomain is represented by the shaded crescent-shaped area. This diagram refers to a y-value strictly larger than unity, implying a $\bar{\xi}_{\max}$ value strictly smaller than $\frac{\pi}{2}$. On the τ-ψ plane, this latter value is responsible for the curved boundary of the subdomain.
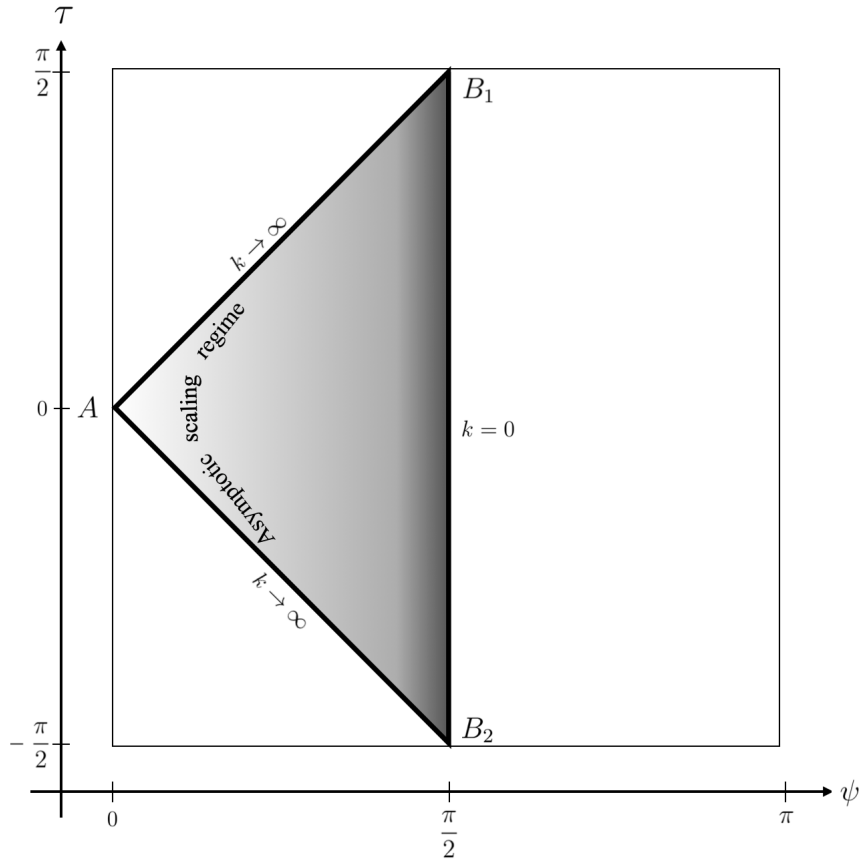
FIGURE 7.11. Penrose diagram highlighting the triangular portion of the dS_5 manifold that embeds all dS_4 spacetimes along the Type IIa trajectories in the limit $y = (\Lambda_0/\Lambda_R)^{1/2} \searrow 1$. The gray shading indicates the local value of the RG scale $k(x^I)$.

On the other hand, if we perform the limit $y \searrow 1$, then $\bar{\xi}_{\max} \nearrow \frac{\pi}{2}$, and as a consequence the curved boundary of the crescent approaches a vertical line at $\psi = \frac{\pi}{2}$. In this limit, the full triangular region is needed for the embedding. This case is depicted in Figure 7.10b.

7.9.2. The $\Lambda_0 = 0$ problem

Note that despite a superficial similarity of the triangular regions in, respectively, Figure 7.10b and its anti-de Sitter analog for $\Lambda_0 = 0$, the running cosmological constant on the boundary line $B_1 B_2$ does not vanish for the de Sitter embedding. It rather equals the cosmological constant of the reference spacetime, $\Lambda(k)\big|_{k=0} \equiv \Lambda_R > 0$, so that $g_{\mu\nu}^{k=0} = g_{\mu\nu}^R$ has nonzero curvature. The consequence is that, strictly speaking, the embedding fails for the Type IIa trajectory: The limit $\Lambda_0 \to 0$ cannot be taken *while Λ_R is held fixed.*

However, since Λ_R can be given a value as small as we like, the embedding can at least approximate the geometrization of the complete Type IIa trajectory at any desired level of accuracy.

7.9.3. *Interpretation and dS/CFT connection*

The status of the dS_5-candidate is less obvious than it has been for its anti-de Sitter counterpart. This concerns in particular its role in a possible dS/CFT correspondence.

First of all, there is the following crucial difference. As illustrated in Figure 7.11, the boundary components of dS_5^{emb} include a 4D timelike component with RG parameter $k = 0$, as did those of AdS_5^{emb}. Now, while in the anti-de Sitter case this component was a boundary of both AdS_5^{emb} and the complete AdS_5 manifold, this is not so in the de Sitter case: The Penrose diagram of Figure 7.11 represents the component in question by the (open) line segment $B_1 B_2$, and obviously it entirely consists of *inner* points of dS_5 only.

As a consequence, there seems to be no natural way of linking the fully quantized asymptotically safe theory, governed by $\Gamma_{k \to 0}$, to the boundary at spatial infinity of de Sitter space proper.

This fact motivates invoking the early and late time boundaries of dS_5 instead. Indeed, in Figure 7.11, the two horizontal lines represent the spacelike past and future infinity of dS_5, respectively. The triangle representing dS_5^{emb} touches them in the points B_1 and B_2, which amount to 3-spheres actually.

The remarkable situation in the 3D spaces at B_1 and B_2 is appreciated best in Figure 7.9, where the t- and ξ-coordinate lines are shown on the τ-ψ plane. On the one hand, the $\mathbb{S}^3$'s at B_1 and B_2 are seen to correspond to the early and late time limits $t \to \pm\infty$. But on the other hand, also *all* the $\xi = const$ lines accumulate at B_1 and B_2, i.e., the leaves of constant scale. This includes even the limiting leave of the foliation, $\xi = const \to 0$, which is ruled by the NGFP action $\Gamma_{k \to \infty}$.

From the effective field theory perspective, it is quite remarkable that the actions Γ_k with $k = k(\xi)$ and $t \to \pm\infty$, $\xi \in \left(0, \frac{\pi}{2}\right)$ all seem to "meet" at B_1 and B_2. It is natural to interpret this situation by saying that all effective actions Γ_k, $k \in \mathbb{R}^+$, are equally relevant there, and that therefore the geometry and matter fluctuations of all scales must be equally important. Clearly this is nothing but the standard characterization of a critical phenomenon at some RG fixed point.

Thus, if we hypothesize again that the QEG fixed points are conformal, the overall conclusion is that the $\mathbb{S}^3$ spaces at $t \to \pm\infty$ indeed carry a 3D conformal field theory related to the GEAA in its early/late time regime.

Remarkably, this type of a "dS/CFT correspondence" which emerges here as a special solution to the QEG flow and field equations has essentially the same general structure as the one proposed in the literature on the basis of entirely different arguments [380].

7.10. THE STANDARD AdS/CFT CORRESPONDENCE: A COMPARISON

Above we saw that the result of the proposed geometrization procedure has a number of features in common with the usual AdS/accft correspondence based upon string theory. Nevertheless, there are also marked differences between the string theory- and the GEAA-based picture, respectively. In this subsection we are going to compare the two approaches in some detail, highlighting their similarities and dissimilarities. We focus on the anti-de Sitter case here; for the dS/CFT correspondence the situation is analogous in most regards.

7.10.1. *More than pure kinematics*

It is a well-known fact, predating the AdS/CFT correspondence, that the conformal group of a CFT in d-dimensions is realized by isometries of a $(d+1)$-dimensional hyperbolic space. Therefore any construction that starts out from a CFT, adds an extra dimension, and furnishes the higher-dimensional spacetime with (standard) gravity while preserving the symmetries, is bound to find an anti-de Sitter space [381].

It is important to emphasize that the GEAA approach goes beyond this simple kinematic realization of the symmetries present, for the following reasons:

(i) Our main result, the fact that the RG trajectory considered geometrizes by means of an AdS_5 space, was obtained without any assumption about whether or not the scale invariance at the NGFP and the GFP extends to full conformal symmetry. It does not rely on the boundary theory being a CFT, and is equally true in the (unlikely) case that the NGFP, or the GFP, or both are not conformal. Hence the geometrization which we found reveals first of all a general AdS/QFT relationship which may or may not be a AdS/CFT one, depending on the properties of the GFP.

(ii) Conversely, our construction does depend on critical properties of its input from the FRG. The latter encodes information about the theory's *dynamical* properties. In particular, the choice of a Type IIa trajectory, and the monotonicity of its running $\Lambda(k)$ were indispensable in order to obtain AdS_5.

(iii) Unlike the standard AdS/CFT correspondence, our approach to the geometrization of RG flows does *not* yield **5D** Einstein–Hilbert gravity on AdS$_5$. Rather, every 4-dimensional leave of the AdS$_5$ foliation carries its own copy of **4D** Einstein–Hilbert gravity, with parameter values $G(k)$ and $\Lambda(k)$ depending on the leave.

By contrast, in the usual AdS/CFT correspondence, applying the holographic RG to the energy momentum tensor perturbation in a flat boundary $O(N)$ model (without gravity!) is known to give rise to a *propagating graviton in the bulk* - something that is not found here. Within the geometrization construction the **5D** Einstein equation does not play any particular role. The basic field equations rather consist of an infinite stack of **4D** Einstein equations labeled by k.

As a consequence, instead of one **5D** graviton, we deal with an infinite family of **4D** gravitons, which do not get coupled by the *field equations*. Rather, it is the *FRG flow equation* that connects the leaves of the foliation and their respective gravitons at different scales k and $k + dk$. Since our entire geometrization is based upon *one single* solution to the FRG equation, namely the selected RG trajectory chosen as the input, the relation between neighboring leaves appears to be "non-dynamical" from the point of view of the field equations.

(iv) In this context we also mention that from the GEAA viewpoint of the present paper the astonishing "miracle" behind the standard AdS/CFT correspondence is that, *under very special conditions*, the universally applicable but enormously complicated FRG equation can be replaced with something much simpler, namely the **5D** Einstein equation.[15] One of the motivations for the present work is the hope that ultimately one might be able to actually *derive* what these specific conditions are, and thus understand better why the usual AdS/CFT correspondence works for some gravity-matter systems but not for others.

7.10.2. *Duality*

A key property of the standard AdS/CFT correspondence is that it constitutes a duality, in the sense that the boundary values of the gravity etc. fields that live in the bulk act as sources of the boundary operators. The duality provides a map between two dynamical theories that are described by two actions that look very different and involve different degrees of freedom. One of them includes dynamical gravity, the other does not. The map leads to a one-to-one relationship between gravity fields and operators of a flat space QFT on the boundary [382].

---

[15]Clearly in most other connections one hardly would call Einstein's equation "simple". And yet it is true that the FRGE is a by far more complex mathematical object: It is a *functional* equation, it is highly *non-local*, and it is an *integro-differential* equation.

Within the GEAA-based geometrization approach, no duality of this sort has emerged so far, at least not within the specific example worked out in the present paper.

The situation may change however once in the future more complex RG trajectories are considered which include a nontrivial matter part added to the running gravitational action. At least in principle, something comparable to a duality in the sense above is given a chance then to arise dynamically, provided one employs the generalized FRG approach, already well developed for flat space, which allows for a continuous change of the dynamical variables during the RG evolution. A typical example of this kind is in QCD the transition from quarks and gluons to hadrons [248, 383].

Whether or not this extended framework is employed, there always remains a main difference between standard AdS/CFT and the GEAA geometrization approach: In the former case the boundary theory is a pure matter theory on flat space, while in the latter it includes dynamical gravity, *quantum* gravity even.

In fact, the present approach deals with dynamical, quantized gravity in the boundary, and this goes beyond what is done in the usual AdS/CFT correspondence. For technical simplicity the scale-dependent actions considered here are even *only* for gravity, containing no matter fields for the time being (see below).

7.10.3. *Holographic RG*

The idea of combining the AdS/CFT setting with the RG, interpreting the additional dimension as the RG scale, is an old one [373, 384, 385]. In the usual AdS/CFT correspondence, one considers an UV-CFT "living" on the boundary and one perturbs this fixed point field theory by relevant operators, thus generating an RG flow towards the IR.

In the GEAA geometrization approach the situation is different. In the first step we derived an "AdS/QFT correspondence" which involves

(i) a UV-QFT given by the NGFP, i.e., the fixed point related to the nonperturbative renormalizability;

(ii) an IR-QFT which is defined by the GFP and lives on the boundary.

Then we argued that both the UV-QFT and the IR-QFT are likely to be CFT's, but this has not been proven yet. Clearly the similarity with the traditional string theory related setting is strongest if at least the IR-QFT is conformal; it would then define the "CFT" appearing in the designation "AdS/CFT".

By contrast, our UV-QFT as given by the NGFP has no counterpart in the traditional AdS/CFT correspondence. The existence of the NGFP is the very hallmark of Asymptotic Safety which, rather than string theory, provides the UV completion in the present case.

7.10.4. *Internal space*

Besides the UV completion, string theory plays yet another role in the usual AdS/CFT scenario: In addition to AdS_5, the string theory construction in 10 dimensions supplies an additional internal space, for example S^5 in the simplest case. The internal space fixes further symmetries beyond conformal symmetry and thus determines the field content of the theory involved.

On the GEAA side, a similar role is played by the choice of the *theory space* the functional RG equation is operating upon. For different such choices, the pertinent functionals $\Gamma_k [g_{\mu\nu}, \textit{matter fields}, \cdots]$ depend on different sets of matter fields, and therefore entail RG flows that are to be computed from different functional RG equations. Hence, the component form of the functional RG trajectories, $k \mapsto (G(k), \Lambda(k), \cdots, u^1(k), u^2(k), \cdots)$, will include additional running couplings and masses, $u^i(k)$. They reflect the invariants that can be built from the specific set of matter fields chosen.

In the present paper we analyzed the geometrization in the simplest case only, namely for pure gravity, since its RG flow is fairly well understood by now [49]. However, it will be interesting to explore also possible geometrizations of matter-coupled gravity in future work. The above $AdS_5 \times S^5$ example, for instance, determines the boundary CFT to be $N = 4$ Super-Yang-Mills theory. It is highly intriguing that this theory may emerge from the GEAA approach as a $k \to 0$ limit. For the time being this system is still beyond our computational possibilities, but steady progresses are made in this direction [186].

CHAPTER 8

Spectral flows in Asymptotic Safety

Executive summary. Within the functional renormalization group approach to Background Independent Quantum Gravity, we explore the scale-dependent effective geometry of the de Sitter solution dS$_4$. The investigation employs a novel approach whose essential ingredient is a modified spectral flow of the metric dependent d'Alembertian, or of similar hyperbolic kinetic operators. The corresponding one-parameter family of spectra and eigenfunctions encodes information about the nonperturbative backreaction of the dynamically gravitating vacuum fluctuations on the mean field geometry of the quantum spacetime. Used as a diagnostic tool, the power of the spectral flow method resides in its ability to identify the scale-dependent subsets of field modes that supply the degrees of freedom which participate in the effective field theory description of the respective scale. A central result is that the ultraviolet of Quantum Einstein Gravity comprises far fewer effective degrees of freedom than predicted (incorrectly) by background dependent reasoning. Exploring the quantum spacetime's spatial geometry carried by physical fields, we find that 3-dimensional space disintegrates into a collection of coherent patches which individually can, but in their entirety cannot be described by one of the effective average actions occurring along the renormalization group trajectory. A natural concept of an entropy is introduced in order to quantify this fragmentation effect. Tentatively applied to the real Universe, surprising analogies to properties of the observed cosmic microwave background are uncovered. Furthermore, a set of distinguished field modes is found which, in principle, has the ability to transport information about the asymptotic fixed point regime from the ultraviolet, across almost the entire "scale history", to cosmological distances in the observed Universe.

What is new? All results of this chapter represent novel research results.

Based on: Reference [RF3].

Plan of this Chapter. Firstly, we introduce the various spectral problems related to the d'Alembertian in curved spacetime that we shall encounter; we elaborate in particular on the distinction between the standard ("off-shell") eigenvalue problem on a rigid background geometry, and the "on-shell" spectral problems typical of Background Independent quantum gravity. Then we focus on the d'Alembertian on 4-dimensional de Sitter space, dS$_4$. Keeping its only free parameter, the Hubble constant H, fixed at this stage, we determine the spectrum and the eigenfunctions, and in particular we give

a detailed account of the eigenfunction's resolving power (fineness). Furthermore, we introduce the special type of (Lorentzian as well as Euclidean) RG trajectories we are going to employ later on, namely those of the Einstein-Hilbert truncation which have a positive cosmological constant throughout, the Type IIIa. Then we obtain the spectral flow along trajectories of this kind in fully explicit form, whereby the scale-dependent tadpole conditions, for all k, are solved by de Sitter spacetimes with an appropriate running Hubble parameter $H = H(k)$.

On the basis of the spectra and eigenfunctions thus obtained, we determine the cutoff modes by finding their scale-dependent principal quantum number. We discuss them further in Section 8.6 where we analyze the Lorentzian analog of the phenomenon sketched in Figure 6.2.

Moreover, we compute the proper wavelength of the cutoff modes at the time when they leave the harmonic regime. It constitutes an important second length scale alongside the Hubble distance, $L_H(k)$.

In Section 8.8 we advocate for the idea of physics-based geometry, and explore which kinds of geometric patterns can be "drawn" on 3D space by the dynamical fields which are governed by Γ_k.

Using a different approach, this question further investigated. There, we also demonstrate that for quantum spacetimes like the one under consideration there exits a remarkable similarity between the usual cosmological histories with respect to ordinary time, and "scale histories" with respect to RG time. In Section 8.10 we briefly describe a surprising analogy between the features of the quantum spacetime that has emerged, and the thermal gas of the CMBR photons in the present Universe.

Parts of this this chapter have been taken and rearranged from the author's publication [RF3].

8.1. SPACETIME PROPERTIES FROM A SPECTRAL FLOW

Henceforward, we will assume that we solved the RG flow equation and have a certain trajectory $k \to \Gamma_k$ in our hands. Furthermore, using this running action as an input, we can solve the tadpole equation (3.70) and find a family of running (self-consistent metrics) g_k^{sc}. At every point of the generalized RG trajectory, we can use this metric to construct the associated Laplacian $\Box_{g_k^{\mathrm{sc}}}$ (see Section 3.6). For every given value of k the corresponding Laplacian gives rise to an eigenvalue equation. Finally, this eigenvalue problem can be solved for the spectrum, furnishing a running spectrum. In [271, 272] it was proposed to analyze the physics contents of generalized trajectories obtained

in [97] (see Section 3.5) by means of *spectral flow techniques* similar to those used in index theory, for example [273]. Given a (Euclidean, to start with) metric $\bar{g}_{\mu\nu}$ we can construct the associated Laplacian operator $\Box_{\bar{g}} = \bar{g}^{\mu\nu}\nabla_\mu\nabla_\nu$ and consider its eigenvalue problem. The idea is to do this at all points of the generalized RG trajectory, that is, to find and to analyze the solutions of the equation

$$-\Box_{\bar{g}_k^{sc}}\,\chi_{nm}(x;k) \;=\; \mathcal{F}_n(k)\,\chi_{nm}(x;k) \tag{8.1}$$

at all $k \in [0,\infty)$. If we manage to solve this family of differential equations, we have an entire trajectory of spectra at our disposal, i.e., a *spectral flow* $k \mapsto \{\mathcal{F}_n(k)\}$, as well as the associated eigenbases $\{\chi_{nm}(x;k)\}$.

In refs.[271, 272] it has been shown how this spectral flow can be employed in order to gain information about the physics and the spacetime geometry of the Quantum Gravity system under consideration. One of the questions that has been investigated in this manner is under what conditions Γ_k can define a useful effective field theory. More precisely, if we assume that the physical situation, or process under consideration can be described by a classical (tree level) evaluation of such an action functional, what then is the optimum value of k to choose?

A first hint is known to come from the properties of the so-called *Cutoff mode (COM)* [270, 271]. By definition, they are those eigenfunctions $\chi_{nm}(x;k)$ whose eigenvalue $\mathcal{F}_n(k)$, at every scale k, equals precisely k^2. Their principal quantum number $n_{\mathrm{COM}}(k)$, i.e, the one which determines the eigenvalue, is found by solving the implicit equation

$$\mathcal{F}_n(k)|_{n=n_{\mathrm{COM}}(k)} \;=\; k^2\,. \tag{8.2}$$

For typical choices of $\mathcal{R}_k$, the cutoff modes are located precisely at the threshold between "already integrated out at RG scale k", and "not yet integrated out". Thus we may expect that the x-dependence of the mode functions $\chi_{nm}(x;k)|_{n=n_{\mathrm{COM}}(k)}$ contains information about the circumstances under which Γ_k has a chance of providing a satisfactory effective field theory.

8.1.1. *Limitations on the distinguishability of spacetime points*

In ref.[271], the spectral flow of an analytically tractable class of Euclidean solutions to the effective Einstein equations has been scrutinized in detail, namely self-consistent spheres $\mathbb{S}^4(L)$. Their radius $L \equiv L^{sc}(k)$ follows from the tadpole condition, hence it "knows" about the underlying RG trajectory, while the rest of the metric $(\bar{g}_k^{sc})_{\mu\nu}$ is fixed by symmetry.
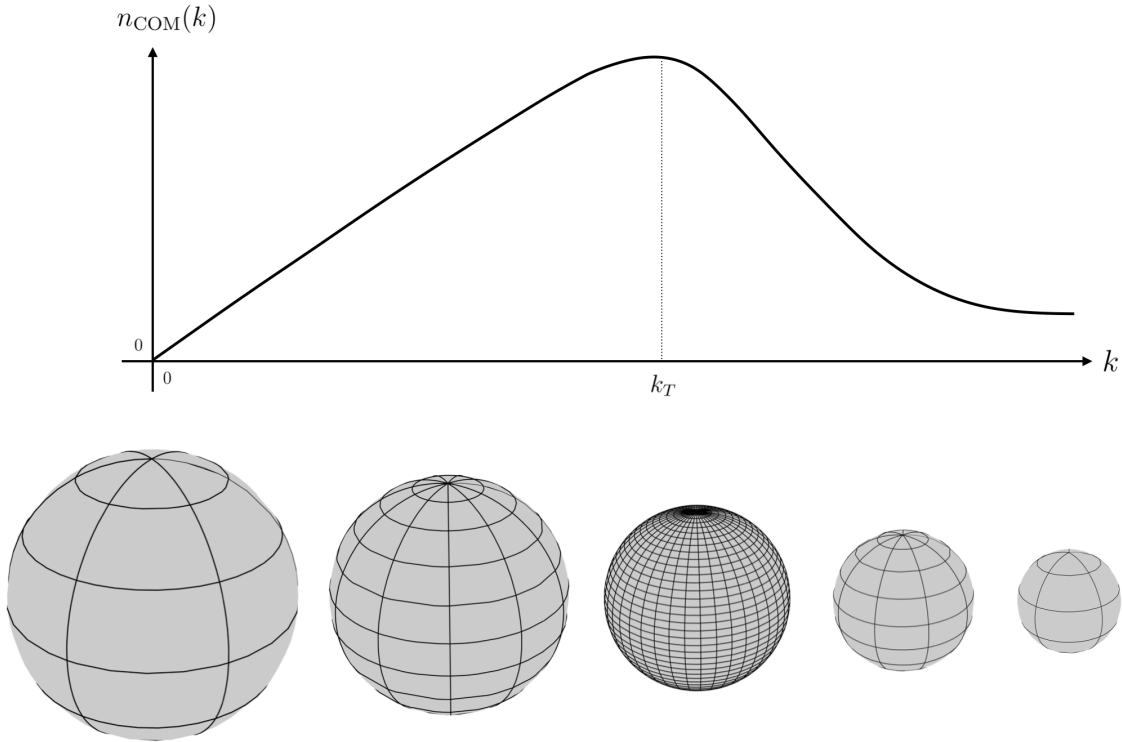
FIGURE 8.1. The principal quantum number of the cutoff modes, n_{COM}, in dependence on the RG scale k. The size of the various spheres indicates the self-consistent radius $L^{\mathrm{sc}}(k)$ at increasing values of k, and the coordinate grids shown visualize the (first increasing, then decreasing) angular resolving power of the spherical harmonics with $n = n_{\mathrm{COM}}(k)$.

On $\mathbb{S}^4(L)$, the eigenvalues of the tensor Laplacian $-\square$ are labeled by an angular momentum-like quantum number, a positive integer n. When $n \gg 1$ they are approximately given by $\mathcal{F}_n(L) \approx n^2/L^2$, and within this approximation, they are the same for tensor harmonics of any rank. As a result, the n-quantum number of the corresponding cutoff modes is given by

$$n_{\mathrm{COM}}(k) \approx k\, L^{\mathrm{sc}}(k)\,. \tag{8.3}$$

Figure 8.1 shows a schematic plot of this function as obtained from a typical RG trajectory (of Type IIIa) in asymptotically safe Quantum Einstein Gravity [95, 97, 99, 102, 114].

The behavior of $n_{\mathrm{COM}}(k)$ is quite remarkable and perhaps irritating at first sight. For a proper interpretation, it is best to start off near the trajectory's endpoint, $k = 0$. There, in the classical regime, $n_{\mathrm{COM}}(k)$ increases with k, implying that the cutoff modes are $\mathbb{S}^4$-harmonics of increasing angular momentum which, therefore, possess a continuously improving resolving power of order $2\pi/n_{\mathrm{COM}}(k)$. The interpretation of this part of the trajectory ($0 \le k < k_T$, see Figure 3.4) is the one we are familiar with from non-dynamical flat space: A higher scale k implies a "probe" or "microscope"

(i.e., cutoff modes) with higher momenta, smaller wavelengths, and therefore a better angular resolving power with respect to angular distances on the sphere.

In Figure 8.1 this general trend is visualized by the increasingly fine meshes of the coordinate nets on the various spheres. The circles shown can be thought of as nodal lines of the tensor harmonics with $n = n_{\mathrm{COM}}(k)$.

At a critical RG scale, k_T, the behavior changes, however. Once scales $k > k_T$ are reached, the angular momentum of the relevant spherical harmonics, $n_{\mathrm{COM}}(k)$, has become a decreasing function of k. This entails a decreasing number of maxima, minima, nodes etc. displayed by the harmonics, and therefore an increasingly poor angular resolution.

In fact, in the limit $k \to \infty$, i.e., in the extreme UV according to our nomenclature, we are in the regime which is governed by the non-Gaussian fixed point, and there the resolving power of the cutoff modes is almost as poor as in the extreme IR, $k \to 0$. Thanks to Asymptotic Safety, $n_{\mathrm{COM}}(k)$ approaches a finite limit $\lim_{k \to \infty} n_{\mathrm{COM}}(k) \equiv n^*_{\mathrm{COM}}$ at the fixed point. As explained in [271], this indicates that the field modes (spherical harmonics) which constitute the degrees of freedom governed by the effective field theory $\Gamma_{k \to \infty}$, possess an angular momentum quantum number $n \approx n^*_{\mathrm{COM}}$, and this number is bounded above. As a result, they are unable to distinguish points in spacetime which have an angular separation smaller than about $2\pi/n^*_{\mathrm{COM}}$.

This fundamental fuzzyness of spacetime is an instance of the "UV-IR confusion" we tried to warn the reader of at the beginning of this Introduction: The "ultraviolet of Quantum Gravity", defined unambiguously as the $k \to \infty$ regime on an asymptotically safe RG trajectory, is not at all the realm of probes or "microscopes" with an unlimited resolving power. Quite the reverse, its properties in this respect would rather be classified "IR-like" by the traditional jargon.

8.1.2. *Gravitational backreaction*

There exists a general mechanism which can destroy the traditional association *large k ⇔ large momenta ⇔ high resolution* very easily, namely the dynamical backreaction of the spacetime's geometry on the quantum system which it accommodates. In the example at hand this backreaction is indeed responsible for the unusual $k \to \infty$ behavior: For growing $k > k_T$, the self-consistent radius $L^{\mathrm{sc}}(k)$ shrinks faster than $\propto k^{-1}$, with the result that $n_{\mathrm{COM}}(k) = k\, L^{\mathrm{sc}}(k)$ never reaches the unlimited resolving power of $n_{\mathrm{COM}} = \infty$, the traditionally expected hallmark of "the ultraviolet".

In the following we are going to address the question whether the fuzzyness of the self-consistent spheres, their impossibility to distinguish spacetime points that are too close. In order to assess potential implications to the real world, we need a Lorentzian generalization (see Section 3.7 for a discussion of the Lorentzian counterpart).

8.2. FROM OFF-SHELL TO ON-SHELL SPECTRA

In this section we prepare the stage for the eigenvalue problems we are going to consider later in this article. In particular we emphasize the difference between those based upon rigid unchanging background geometries, and the more complex ones relying on dynamically generated self-consistent background metrics.

8.2.1. *Off-shell spectra*

(1) Rigid spectral problems. Let us assume we are given an arbitrary Lorentzian manifold furnished with an invariable metric $\bar{g}_{\mu\nu}$. We construct the associated covariant d'Alembertian $\Box_{\bar{g}} = \bar{g}^{\mu\nu}\bar{\nabla}_\mu\bar{\nabla}_\nu$ and set up its eigenvalue equation:

$$-\Box_{\bar{g}}\,\chi_{nm}[\bar{g}](x) \;=\; \mathcal{F}_n[\bar{g}]\;\chi_{nm}[\bar{g}](x) \tag{8.4}$$

Both the eigenfunctions χ_{nm} and the eigenvalues $\mathcal{F}_n$ are considered functionals of the externally provided metric $\bar{g}_{\mu\nu}$. They are enumerated by continuous or discrete (multi-) indices n and m, whereby the "principal quantum number" n determines the eigenvalue, while m is a degeneracy index.

For a reason that will become clear below, we shall refer to $\{\mathcal{F}_n[\bar{g}]\}$ as the *off-shell (rigid) spectrum* of the d'Alembertian related to the metric $\bar{g}_{\mu\nu}$.

(2) Organizing the eigenfunctions, first stage. At this stage, we can start organizing the eigenfunctions.

Taking account of the indefiniteness of $\Box_{\bar{g}}$, we consider the set of its eigenfunctions, denoted $\Upsilon[\bar{g}] \equiv \{\chi_{nm}[\bar{g}]\}$, and decompose it according to $\Upsilon = \Upsilon^+ \cup \Upsilon^0 \cup \Upsilon^-$, thereby introducing the subsets

$$\begin{aligned}
\Upsilon^+[\bar{g}] &\equiv \{\chi_{nm}[\bar{g}] \mid \mathcal{F}_n[\bar{g}] > 0\}\,, \\
\Upsilon^0[\bar{g}] &\equiv \{\chi_{nm}[\bar{g}] \mid \mathcal{F}_n[\bar{g}] = 0\}\,, \\
\Upsilon^-[\bar{g}] &\equiv \{\chi_{nm}[\bar{g}] \mid \mathcal{F}_n[\bar{g}] < 0\}\,.
\end{aligned} \tag{8.5}$$

Using the "mostly plus" metric convention, these subsets comprise the eigenfunctions which we refer to as spacelike, null, and timelike, respectively.

(3) Organizing the eigenfunctions, second stage. Now let us assume that in addition to the metric we are given a positive constant $k > 0$ with the dimension of a mass. This allows us to further classify the eigenfunctions according to whether the modulus of their eigenvalue is smaller, larger or equal to k^2, i.e., $|\mathcal{F}_n| < k^2$, $|\mathcal{F}_n| > k^2$, or $|\mathcal{F}_n| = k^2$. This distinction implies a refined decomposition of the space- and timelike sectors:

$$\Upsilon^{\pm}[\bar{g}](k) = \Upsilon_>^{\pm}[\bar{g}](k) \cup \Upsilon_=^{\pm}[\bar{g}](k) \cup \Upsilon_<^{\pm}[\bar{g}](k) . \tag{8.6}$$

Explicitly, the subsets are given by, in the spacelike case,

$$\begin{aligned}
\Upsilon_>^+[\bar{g}](k) &\equiv \left\{ \chi_{nm}[\bar{g}] \mid \mathcal{F}_n[\bar{g}] \in (k^2, \infty) \right\}, \\
\Upsilon_=^+[\bar{g}](k) &\equiv \left\{ \chi_{nm}[\bar{g}] \mid \mathcal{F}_n[\bar{g}] = +\, k^2 \right\}, \\
\Upsilon_<^+[\bar{g}](k) &\equiv \left\{ \chi_{nm}[\bar{g}] \mid \mathcal{F}_n[\bar{g}] \in (0, k^2) \right\},
\end{aligned} \tag{8.7}$$

and similarly for the timelike eigenfunctions:

$$\begin{aligned}
\Upsilon_>^-[\bar{g}](k) &\equiv \left\{ \chi_{nm}[\bar{g}] \mid \mathcal{F}_n[\bar{g}] \in (-\infty, -k^2) \right\}, \\
\Upsilon_=^-[\bar{g}](k) &\equiv \left\{ \chi_{nm}[\bar{g}] \mid \mathcal{F}_n[\bar{g}] = -\, k^2 \right\}, \\
\Upsilon_<^-[\bar{g}](k) &\equiv \left\{ \chi_{nm}[\bar{g}] \mid \mathcal{F}_n[\bar{g}] \in (-k^2, 0) \right\}.
\end{aligned} \tag{8.8}$$

This particular refinement of the decomposition should be considered merely an example; it is motivated by the symmetric cutoff scheme (3.83).

(4) Interpretation. To see the relevance of the above $\bar{g}$-dependent eigenvalue problem, recall that in the *Euclidean* setting a generic effective average action $\Gamma_k[\phi; \bar{g}]$, governing a set of dynamical fields $\phi \equiv \langle \hat{\phi} \rangle$, derives from a path integral of the kind (3.1).

The bilinear mode suppression term ΔS_k in eq.(3.2) involves a $\bar{g}$-dependent pseudo-differential operator which is usually a function of the corresponding Laplacian, $\mathcal{R}_k[\bar{g}] \equiv R_k(-\Box_{\bar{g}})$. The profile of the function $R_k(\cdot)$ is such that, after expanding ϕ in a basis of $-\Box_{\bar{g}}$ eigenfunctions, $\phi = \sum_{nm} a_{nm} \chi_{nm}$, the modes with eigenvalues $\lesssim k^2$ are given a "mass term" $\propto k^2 |a_{nm}|^2$, which counteracts its being "integrated out". Conversely, modes with eigenvalues $\gtrsim k^2$ remain unaffected and are integrated out as usual.

In the computation of $\Gamma_k[\phi; \bar{g}]$, at a fixed set of arguments, within the Euclidean framework, those eigenmodes of the Laplacian that satisfy

$$-\Box_{\bar{g}} \, \chi_{\text{eucl}} = k^2 \, \chi_{\text{eucl}} \tag{8.9}$$

are particularly interesting: They are situated precisely at the threshold between being, and not being integrated out. Their importance resides in the fact that the resolution

properties of those χ's (typical distances of extrema, etc.) determine at which scale, and under what conditions, the action $\Gamma_k[\phi; \bar{g}]$ defines a reliable effective field theory, see [49] for further details.

Returning to the Lorentzian setting, the eigenmodes of the d'Alembertian in $\Upsilon^{\pm}_{\underline{=}}[\bar{g}](k)$, having $\mathcal{F}_n = \pm k^2$, should be regarded as the analogs of the χ_{eucl}'s in (8.9), coming with the additional feature of a spacelike-timelike discrimination.

More generally, we note that the metric $\bar{g}_{\mu\nu}$ appearing in the "off-shell" eigenvalue problem (8.4) should be thought of as *the second argument of* $\Gamma_k[\phi; \bar{g}]$. Therefore, loosely speaking, this eigenvalue problem refers to the off-shell world under the path integral, and this is in fact what motivates its name. The solutions $\chi_{nm}[\bar{g}](x)$ to eq.(8.4) constitute the natural basis of field space to expand the integration variables $\hat{\phi}$ in, when it comes to computing the functional $\hat{\phi} \mapsto \Gamma_k[\phi; \bar{g}]$ in the Lorentzian context.

8.2.2. *Rigid and flat: Minkowski space*

Before continuing, let us have a brief look at the most familiar example of a Lorentzian manifold, namely Minkowski space with $\bar{g}_{\mu\nu} = \eta_{\mu\nu}$. In cartesian coordinates, we denote $x^{\mu} \equiv (t, \vec{x})$ and $p^{\mu} \equiv (\omega, \vec{p})$, with $|\vec{p}| \equiv p$. The wave operator reads then

$$- \Box_{\eta} = -\eta^{\mu\nu} \partial_{\mu} \partial_{\nu} = \partial_0^2 - \nabla^2 \ . \tag{8.10}$$

Its eigenfunctions are plane waves $\chi = e^{i p_{\mu} x^{\mu}} = e^{i(-\omega t + \vec{p} \cdot \vec{x})}$ characterized by a 4-vector $p^{\mu} = (\omega, \vec{p})$, the eigenvalues being $\mathcal{F} = p_{\mu} p^{\mu} = -\omega^2 + \vec{p}^2$. Clearly an eigenfunction is spacelike, timelike, or null, respectively, if the vector p^{μ} is so.

To be in accord with the (n, m) enumeration employed above we label the χ's directly by their eigenvalue $\mathcal{F} \,\hat{=}\, n$, alongside with a degeneracy index m whose character depends on the case considered. Decomposing $\Upsilon[\eta]$, we have at the first stage:

$$\Upsilon^{+}[\eta] \equiv \left\{ \chi_{\mathcal{F}, \omega, \vec{m}}(x) = \exp\left(i \left[-\omega t + \vec{m} \cdot \vec{x} \sqrt{\omega^2 + \mathcal{F}} \right] \right) \Big| \mathcal{F} > 0, \, \omega \in \mathbb{R}, \, \vec{m} \in \mathbb{S}^2 \right\},$$

$$\Upsilon^{0}[\eta] \equiv \left\{ \chi_{0, \vec{p}}(x) = \exp\left(i \left[-|\vec{p}| t + \vec{p} \cdot \vec{x} \right] \right) \Big| \vec{p} \in \mathbb{R}^3 \right\}, \tag{8.11}$$

$$\Upsilon^{+}[\eta] \equiv \left\{ \chi_{\mathcal{F}, \vec{p}}(x) = \exp\left(i \left[-\sqrt{\vec{p}^2 + |\mathcal{F}|} \, t + \vec{p} \cdot \vec{x} \right] \right) \Big| \mathcal{F} < 0, \, \vec{p} \in \mathbb{R}^3 \right\}.$$

As for the spacelike modes, $\vec{m}$ denotes a unit 3-vector, $\vec{m} \cdot \vec{m} = 1$.[1]

Picking a number $k > 0$, the refined classification of the Minkowski eigenfunctions is also easily worked out. Instead of presenting formulas we sketch the results in Figure 8.2 which shows a quadrant of the ω-p plane.

---

[1]Note also that in our conventions an ordinary, i.e., non-tachyonic free Klein–Gordon field of mass M satisfies $(-\Box + M^2)\chi = 0$, thus corresponding to a timelike eigenfunction with a negative $\mathcal{F} = -M^2$.
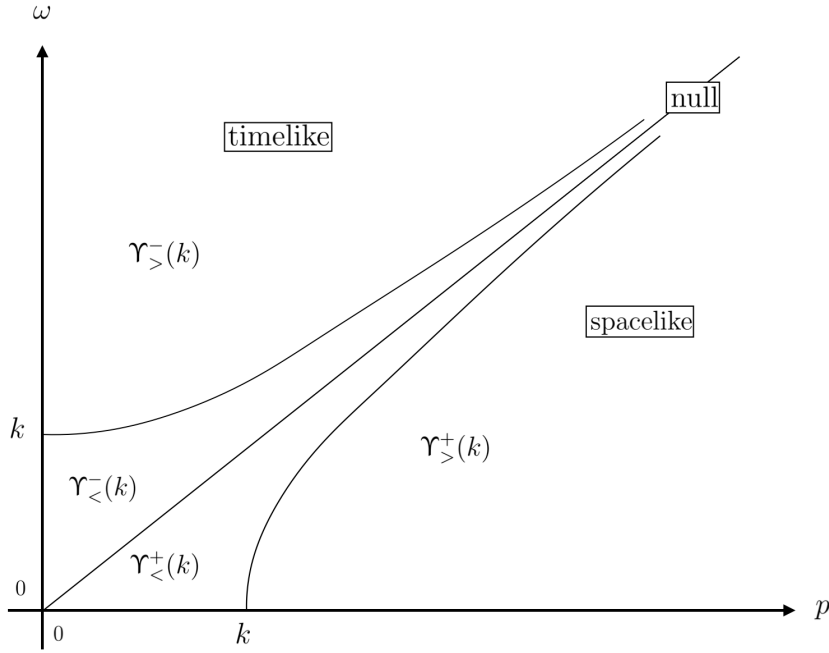
FIGURE 8.2. Refined classification of the plane wave eigenfunctions on a part of ω-p space. The two hyperbolas are given by $\omega = \sqrt{p^2 \mp k^2}$.

8.2.3. *On-shell spectra*

The spectra $\{\mathcal{F}_n[\bar{g}]\}$ discussed above and their eigenfunctions are referred to as "off-shell" since they are based upon an arbitrary externally prescribed metric $\bar{g}_{\mu\nu}$. Generically, this metric is different from the true metric that would be selected by the internal dynamics of the quantum gravitational system. The state in which the system settles down after turning on the quantum effects is partially described by a particular *self-consistent* background metric (see Section 3.6). It has the defining property that, in this state, the operator $\hat{g}_{\mu\nu} - \bar{g}_{\mu\nu} \equiv \hat{h}_{\mu\nu}$ has zero expectation value: $\langle \hat{h}_{\mu\nu} \rangle_{\bar{g}} = 0$.

As we reviewed in Chapter 3 already, this tadpole condition plays the role of a quantum-corrected generalization of Einstein's equation. It governs the dynamics of the expectation value $g_{\mu\nu} = \langle \hat{g}_{\mu\nu} \rangle$. In the framework of the effective average action it assumes the concrete form of the k-dependent equation (3.70). Typically it admits many solutions $(\bar{g}_k^{\text{sc}})_{\mu\nu}$ at every k. We are free to select any of them, the only constraint we impose is that the resulting map $k \mapsto \bar{g}_k^{\text{sc}}$ is a smooth curve in the space of metrics. Picking one such curve of solutions is analogous to selecting an RG trajectory on theory space in the first place. We combine the two into a generalized RG trajectory on the product space, $k \mapsto (\Gamma_k, \bar{g}_k^{\text{sc}})$.

(1) The running spectral problem. Henceforth we assume that we selected a certain generalized RG trajectory $k \mapsto (\Gamma_k, \bar{g}_k^{\text{sc}})$ which we keep fixed in the sequel. We define

the related running covariant d'Alembertian

$$\Box_k \equiv \Box_{\bar{g}}\big|_{\bar{g}=\bar{g}_k^{\mathrm{sc}}} \, , \tag{8.12}$$

and set up the associated one-parameter family of eigenvalue equations that are labeled by the curve parameter k:

$$-\Box_k \ \chi_{nm}(x;k) = \mathcal{F}_n(k) \ \chi_{nm}(x;k) \tag{8.13}$$

We refer to $\{\mathcal{F}_n(k)\}$ and $\{\chi_{nm}(\cdot \ ; \ k)\} \equiv \Upsilon[\bar{g}_k^{\mathrm{sc}}]$ as *on-shell spectra and eigenfunctions*, respectively. Since the generalized RG trajectory is never varied, they are simply functions of k, rather than functionals of $\bar{g}_{\mu\nu}$.

Let us now classify the eigenfunctions:

(2) Classifying eigenfunctions, first stage. For every fixed value of the curve parameter k, we now decompose $\Upsilon[\bar{g}_k^{\mathrm{sc}}] = \Upsilon^+(k) \cup \Upsilon^0(k) \cup \Upsilon^-(k)$ with the following k-dependent sets of spacelike, null, and timelike modes:

$$\begin{aligned}
\Upsilon^+(k) &\equiv \{\chi_{nm}(\cdot \ ; \ k) \ | \ \mathcal{F}_n(k) > 0\} \, , \\
\Upsilon^0(k) &\equiv \{\chi_{nm}(\cdot \ ; \ k) \ | \ \mathcal{F}_n(k) = 0\} \, , \\
\Upsilon^-(k) &\equiv \{\chi_{nm}(\cdot \ ; \ k) \ | \ \mathcal{F}_n(k) < 0\} \, .
\end{aligned} \tag{8.14}$$

(3) Classifying eigenfunctions, second stage. Now let us refine the classification by distinguishing eigenmodes for which $|\mathcal{F}_n(k)|$ is, respectively, smaller, larger, or equal to a given positive constant, κ^2, say: $|\mathcal{F}_n(k)| < \kappa^2$, $|\mathcal{F}_n(k)| > \kappa^2$, or $|\mathcal{F}_n(k)| = \kappa^2$.

In principle the number κ is completely unrelated conceptually to the curve parameter k. However, as it will turn out, the most relevant and interesting information is obtained by choosing $\kappa = k$. With this identification, the scale k acquires a double meaning: it is both a curve parameter along the generalized RG trajectory, and it is the divide between the $(<)$-type and $(>)$-type eigenfunctions. In fact, choosing $\kappa = k$ here, we now introduce, for the spacelike eigenfunctions,

$$\begin{aligned}
\Upsilon_>^+(k) &\equiv \{\chi_{nm}(\cdot \ ; \ k) \ | \ \mathcal{F}_n(k) \in (k^2, \infty)\} \, , \\
\Upsilon_{\mathrm{COM}}^+(k) &\equiv \{\chi_{nm}(\cdot \ ; \ k) \ | \ \mathcal{F}_n(k) = + k^2\} \, , \\
\Upsilon_<^+(k) &\equiv \{\chi_{nm}(\cdot \ ; \ k) \ | \ \mathcal{F}_n(k) \in (0, k^2)\} \, ,
\end{aligned} \tag{8.15}$$

and similarly for the timelike modes:

$$\begin{aligned}
\Upsilon_>^-(k) &\equiv \{\chi_{nm}(\cdot \ ; \ k) \ | \ \mathcal{F}_n(k) \in (-\infty, -k^2)\} \, , \\
\Upsilon_{\mathrm{COM}}^-(k) &\equiv \{\chi_{nm}(\cdot \ ; \ k) \ | \ \mathcal{F}_n(k) = - k^2\} \, , \\
\Upsilon_<^-(k) &\equiv \{\chi_{nm}(\cdot \ ; \ k) \ | \ \mathcal{F}_n(k) \in (-k^2, 0)\} \, .
\end{aligned} \tag{8.16}$$

Thus, we are led to the following decomposition of the Υ^+ and Υ^- sectors, respectively:

$$\Upsilon^\pm(k) \;=\; \Upsilon^\pm_>(k) \;\cup\; \Upsilon^\pm_{\mathrm{COM}}(k) \;\cup\; \Upsilon^\pm_<(k)\,. \qquad (8.17)$$

8.2.4. *The COMs*

The on-shell counterpart of the $(=)$-type eigenfunctions is commonly referred to as the *cutoff modes* [270, 271]. Explicitly, they are solutions to the differential equation

$$-\,\Box_{\bar g}\big|_{\bar g = \bar g^{\mathrm{sc}}_k} \;\; \chi_{\mathrm{COM}} \;=\; \pm\, k^2\; \chi_{\mathrm{COM}}\,. \qquad (8.18)$$

At a fixed scale, $k = k_1$, say, this equation can be looked at in two different ways: First, as the "running" or "on-shell" spectral problem at the point $k = k_1$ on the RG trajectory, and second, as the off-shell problem underlying the computation of the functional $\Gamma_{k_1}[\hat\phi; \bar g]$ at a particular value of the second argument, namely $\bar g = \bar g^{\mathrm{sc}}_{k_1}$. Thus we see that the elements in $\Upsilon^\pm_{\equiv}\big[\bar g^{\mathrm{sc}}_{k_1}\big](k_1)$ and $\Upsilon^\pm_{\mathrm{COM}}(k_1)$, respectively, are actually the same function.

This explains the importance of the cutoff modes: On the one side, they can be obtained from an *effective* action, Γ_{k_1}, while on the other side, in the expansion of the *bare* metric fluctuation $\hat h_{\mu\nu}$ they are precisely those modes that get integrated out at the point k_1 of the trajectory, *if the fluctuations propagate on a background which is self-consistent at k_1*.

Therefore, the cutoff modes are a valuable link between the bare off-shell world under the path integral, and the effective level of the on-shell expectation values.

8.3. Spectrum and eigenfunctions on rigid dS$_4$

This section is devoted to another prerequisite of our investigation, namely the spectral problem of the scalar d'Alembertian on a rigid de Sitter space. Its Hubble parameter is considered a fixed constant here; the scale dependence of H will be introduced at a later stage only.

8.3.1. *De Sitter spacetime*

Throughout this paper we focus on the *expanding Poincaré patch* of the 4D de Sitter manifold (see conventions in Appendix E). When expressed in terms of the (dimensionful) cosmological time t, its metric reads

$$ds^2 = -dt^2 + a(t)^2 \, d\vec{x}^2 \quad \text{with} \quad a(t) = a_0 \, e^{Ht} \, , \tag{8.19}$$

while it turns into

$$ds^2 = b(\eta)^2 \left[-dt^2 + d\vec{x}^2 \right] = \frac{-dt^2 + d\vec{x}^2}{H^2 \, \eta^2} \tag{8.20}$$

with the scale factor

$$b(\eta) = -\frac{1}{H\eta} = \frac{1}{H \, |\eta|} \tag{8.21}$$

when the (dimensionless) conformal time

$$\eta = -\frac{1}{a_0 \, H} e^{-Ht} \ \in \ (-\infty, 0) \tag{8.22}$$

is introduced.

Given a certain comoving, or coordinate length Δx on de Sitter space, we denote the associated proper length by

$$L_{\Delta x}(\eta) \equiv b(\eta) \, \Delta x \, . \tag{8.23}$$

When $\Delta x = 2\pi/|\vec{p}| \equiv \Delta x_p$ is in particular the coordinate wavelength of a wave function $e^{i\vec{p}\cdot\vec{x}}$ with comoving 3-momentum $\vec{p}$, we write the associated proper wavelength as

$$L_p(\eta) \equiv b(\eta) \, \Delta x_p \equiv (H \, |\eta|)^{-1} \frac{2\pi}{|\vec{p}|} \equiv \frac{2\pi}{|\vec{p}_{\text{phys}}|} \, , \tag{8.24}$$

with $\vec{p}_{\text{phys}}$ the proper or "physical" counterpart of the coordinate momentum $\vec{p}$.

Proper distances are conveniently expressed in units of the Hubble distance,

$$L_H \equiv H^{-1} \, . \tag{8.25}$$

Dividing (8.24) by (8.25) the Hubble parameter drops out and we obtain the ratio

$$\frac{L_p(\eta)}{L_H} = \frac{2\pi}{|\eta| \, p} \, . \tag{8.26}$$

This is a very useful relation. Often also occurring in the form

$$\eta^2 \, p^2 = \left(2\pi \frac{L_H}{L_p(\eta)} \right)^2 \, , \tag{8.27}$$

it will play a prominent role later on when H becomes scale dependent.

Note that even though $L_p(\eta)$ and L_H are *proper* quantities, eq.(8.26) fully determines their ratio in terms of *coordinate* time and *coordinate* momentum. Conceptually

speaking, the latter two quantities come into being already at the level of spacetime's smooth (and not only pseudo-Riemannian) structure. They have no logical relation to a metric which one may, or may not put on the spacetime manifold. In the example at hand where we furnish it with a de Sitter metric of a specific Hubble parameter H, the value of H cannot have any bearing therefore on η, p, and hence $L_p(\eta)/L_H$.

This simple, yet powerful fact allows us to characterize sub- and super-Hubble size spatial structures, say wavelengths $L_p < L_H$ and $L_H > L_p$, respectively, by:

$$\begin{aligned}
\text{sub-Hubble size proper wavelength:} & \quad |\eta|\, p > 2\pi \\
\text{super-Hubble size proper wavelength:} & \quad |\eta|\, p < 2\pi
\end{aligned} \tag{8.28}$$

This requires *no explicit reference to the value of the Hubble parameter.*

8.3.2. *Mode functions and their eigenvalues*

Writing the metric as in eq.(8.20), the eigenvalue equation on dS_4,

$$- \Box_{\mathrm{dS}_4}\, \chi_{\nu,\vec{p}}(\eta, \vec{x}) = \mathcal{F}_\nu\, \chi_{\nu,\vec{p}}(\eta, \vec{x}) \tag{8.29}$$

is satisfied by mode functions of the form

$$\chi_{\nu,\vec{p}}(\eta, \vec{x}) = -\eta\, v_{\nu,p}(\eta)\, e^{i\vec{p}\cdot\vec{x}}\,, \tag{8.30}$$

provided $v_{\nu,p}$, where $p \equiv |\vec{p}|$, is a solution to the differential equation

$$v_{\nu,p}''(\eta) + \left[p^2 - \left(2 + \frac{\mathcal{F}_\nu}{H^2} \right) \frac{1}{\eta^2} \right] v_{\nu,p}(\eta) = 0\,. \tag{8.31}$$

Primes denote derivatives with respect to η here. The principal quantum number, traditionally denoted ν in this case, enumerates the eigenfunctions together with the 3-vector $\vec{p} \in \mathbb{R}^3$; the latter plays the role of a degeneracy index here. If we set

$$\frac{\mathcal{F}_\nu}{H^2} + 2 \equiv \nu^2 - \frac{1}{4}\,, \tag{8.32}$$

whence

$$\nu \equiv \sqrt{\frac{9}{4} + \frac{\mathcal{F}_\nu}{H^2}}\,, \tag{8.33}$$

the eigenvalues are indeed determined by the first quantum number of $\chi_{\nu,\vec{p}}$ alone:

$$\mathcal{F}_\nu = \left(\nu^2 - \frac{9}{4} \right) H^2 \tag{8.34}$$

In this manner also the similarity of the differential (8.31) with Bessel's equation becomes manifest:

$$v_{\nu,p}''(\eta) + \left[p^2 - \frac{\nu^2 - 1/4}{\eta^2} \right] v_{\nu,p}(\eta) = 0\,. \tag{8.35}$$

The general solution to (8.35) reads

$$v_{\nu,p}(\eta) = (p\,|\eta|)^{1/2} \left[A_p\,J_\nu\,(p\,|\eta|) + B_p\,Y_\nu\,(p\,|\eta|) \right].$$

(8.36)

Here J_ν and Y_ν denote the Bessel functions of the first and the second kind, respectively [386], while A_p and B_p are arbitrary constants.

In standard quantum field theory on de Sitter space the quantity ν is a constant which is fixed once and for all by the particle mass, $\nu = \sqrt{\frac{9}{4} - \frac{m^2}{H^2}}$. In the spectral problem at hand, ν is a variable however, a continuous quantum number in one-to-one correspondence with the eigenvalues. For us it is important therefore to scan the properties of $v_{\nu,p}$ for all ν that are compatible with real eigenvalues of either sign, $-\infty < \mathcal{F}_\nu < +\infty$.

Eq.(8.32) shows that ν is either *real*, namely when $\mathcal{F}_\nu \geq -9/4\,H^2$, or it is *purely imaginary*, for $\mathcal{F}_\nu < -9/4\,H^2$. The transition occurs at $\nu = 3/2 \Leftrightarrow \mathcal{F}_\nu = 0$.

When ν is imaginary, we set $\nu = -i\bar{\nu}$ with $\bar{\nu}$ real, and we replace (8.36) with[2]

$$v_{\nu,p}(\eta) = (p\,|\eta|)^{1/2} \left[A_p\,\tilde{J}_{\bar{\nu}}\,(p|\eta|) + B_p\,\tilde{Y}_{\bar{\nu}}\,(p|\eta|) \right]$$

(8.37)

Here $\tilde{J}$ and $\tilde{Y}$ denote the Bessel functions of imaginary order as defined in [386]:

$$\tilde{J}_\nu(x) = \operatorname{sech}\left(\frac{1}{2}\pi\nu\right) \operatorname{Re}\left(J_{i\nu}(x)\right)$$

(8.38)

$$\tilde{Y}_\nu(x) = \operatorname{sech}\left(\frac{1}{2}\pi\nu\right) \operatorname{Re}\left(Y_{i\nu}(x)\right)$$

(8.39)

These definitions apply for all $\nu \in \mathbb{R}$ and $x \in (0, \infty)$.

Table 8.1 summarizes the various cases of timelike ($\mathcal{F} < 0$), null ($\mathcal{F} = 0$), and spacelike ($\mathcal{F} > 0$) eigenfunctions, displaying in particular the respective domains of the quantum numbers and eigenvalues.

Type	Eigenvalue	$\mathcal{F}_\nu/\mathrm{H}^2 + 2$	Index
spacelike: $\mathcal{F} > 0$	$\mathcal{F}_\nu \in (0, \infty)\,H^2$	$\nu^2 - \frac{1}{4} \in (2, \infty)$	$\nu \in \left(\frac{3}{2}, \infty\right)$
null: $\mathcal{F} = 0$	$\mathcal{F}_\nu = 0$	$\nu^2 - \frac{1}{4} = 2$	$\nu = \frac{3}{2}$
timelike: $\mathcal{F} < 0$	$\mathcal{F}_\nu \in \left(-\frac{9}{4}, 0\right)\,H^2$	$\nu^2 - \frac{1}{4} \in \left(-\frac{1}{4}, 2\right)$	$\nu \in \left(0, \frac{3}{2}\right)$
	$\mathcal{F}_\nu \in \left(-\infty, -\frac{9}{4}\right)\,H^2$	$\nu^2 - \frac{1}{4} \in \left(-\infty, -\frac{1}{4}\right)$	$i\,\nu \equiv \bar{\nu} \in (0, \infty)$

TABLE 8.1. The types of eigenvalues of $-\square$ on de Sitter space.

---

[2]The constants A_p, B_p in (8.37) and similar equations below are not the same as those in (8.36).

8.3.3. *The "dispersion relation"*

Sometimes it is helpful to write (8.31) in the style[3]

$$v''(\eta) + \omega^2(\eta)\, v(\eta) = 0 \tag{8.40}$$

with a time dependent "frequency" given by

$$\omega^2(\eta) = \vec{p}^2 - \left(2 + \frac{\mathcal{F}}{H^2}\right)\frac{1}{\eta^2}\,, \tag{8.41}$$

or, when (8.32) is used,

$$\omega^2(\eta) = \frac{1}{\eta^2}\left[\eta^2\vec{p}^2 - \left(\nu^2 - \frac{1}{4}\right)\right] \equiv \omega^2_{\nu,\vec{p}}(\eta)\,. \tag{8.42}$$

It is instructive to solve (8.41) for the eigenvalue and to express η in terms of the scale factor $b(\eta)$. One obtains

$$\mathcal{F} = \frac{-\omega(\eta)^2 + \vec{p}^2}{b(\eta)^2} - 2H^2 \tag{8.43}$$

This is nothing but the de Sitter analog of $\mathcal{F} = -\omega^2 + \vec{p}^2$ valid on Minkowski space. Besides the time dependence of ω, there are two main differences: First, 3-momentum and frequency are red-shifted by a factor of $b(\eta)$, and second, the eigenvalue is shifted by an amount $-2H^2$.

8.3.4. *Limiting forms of the eigenfunctions*

The functions $v(\eta)$ show a simple limiting behavior if either the first or the second term in the square brackets of eq.(8.42) dominates $\omega^2(\eta)$. We discuss the two cases in turn.

(1) The harmonic regime. Dealing with eigenfunctions $\chi_{\nu,\vec{p}}$ whose quantum numbers ν and $p = |\vec{p}|$ are such that

$$\eta^2\, p^2 \gg \left|\nu^2 - \frac{1}{4}\right| = \left|\frac{\mathcal{F}_\nu}{H^2} + 2\right| \tag{8.44}$$

during a certain η-interval, we can approximate $\omega^2(\eta) \approx p^2$. The resulting simplified equation $v''(\eta) + p^2 v(\eta) = 0$ has the obvious general solution, with A and B constants,

$$v(\eta) = A\,\cos\left(p\,|\eta|\right) + B\,\sin\left(p\,|\eta|\right)\,. \tag{8.45}$$

We refer to the regime where (8.45) applies as the *harmonic regime*.

---

[3]Where dispensable we suppress the indices ν and p.

The solution (8.45) follows also by inserting the well known $x \to \infty$, ν fixed, limiting forms of the Bessel functions [386] into eq.(8.36):

$$J_\nu(x) \approx \sqrt{\frac{2}{\pi x}} \cos\left(x - \nu\frac{\pi}{2} - \frac{\pi}{4}\right) , \quad Y_\nu(x) \approx \sqrt{\frac{2}{\pi x}} \sin\left(x - \nu\frac{\pi}{2} - \frac{\pi}{4}\right) . \quad (8.46)$$

These formulae cover the case of real ν's. For ν imaginary, the corresponding ones for $\tilde{J}_{\bar\nu}$ and $\tilde{Y}_{\bar\nu}$ are

$$\tilde{J}_{\bar\nu}(x) \approx \sqrt{\frac{2}{\pi x}} \cos\left(x - \frac{\pi}{2}\right) , \quad \tilde{Y}_{\bar\nu}(x) \approx \sqrt{\frac{2}{\pi x}} \sin\left(x - \frac{\pi}{2}\right) , \quad (8.47)$$

thus yielding the same asymptotics [386].

(2) The power and log-oscillatory regimes. In the opposite range of (ν, p)-quantum numbers where

$$\eta^2 p^2 \ll \left|\nu^2 - \frac{1}{4}\right| = \left|\frac{\mathcal{F}_\nu}{H^2} + 2\right| \quad (8.48)$$

we may approximate $\omega^2(\eta) \approx -(\nu^2 - 1/4)/\eta^2$. The solutions of the resulting differential equation $v'' - (\nu^2 - \frac{1}{4})\eta^{-2}v = 0$ involve powers of η that are controlled by ν:

$$v(\eta) = C_+ |\eta|^{1/2+\nu} + C_- |\eta|^{1/2-\nu} . \quad (8.49)$$

For ν real, they have a power and and inverse power dependence on $|\eta|$, while they display a logarithmic oscillatory (or "log-periodic") behavior when $\bar\nu \equiv i\nu$ is real instead:

$$v(\eta) = |\nu|^{1/2} \left[A \cos\left(\bar\nu \ln(|\eta|)\right) + B \sin\left(\bar\nu \ln(|\eta|)\right)\right] . \quad (8.50)$$

We refer to the corresponding regimes as the *power* and the *log-oscillatory regimes*, respectively.

The same behavior of the eigenfunctions obtains also from the $x \to 0$, $\nu \in \mathbb{R}$ fixed, limiting forms of the Bessel functions,

$$J_\nu(x) \approx \frac{1}{\Gamma(\nu+1)}\left(\frac{1}{2}x\right)^\nu , \quad Y_\nu(x) \approx -\left(\frac{\Gamma(\nu)}{\pi}\right)\left(\frac{1}{2}x\right)^{-\nu} . \quad (8.51)$$

and their slightly more complicated counterparts for $\tilde{J}_{\bar\nu}$ and $\tilde{Y}_{\bar\nu}$:

$$\tilde{J}_{\bar\nu}(x) \propto \cos\left(\bar\nu \ln\left(\frac{1}{2}x\right) - \gamma_{\bar\nu}\right) , \quad \bar\nu \geq 0, \quad (8.52)$$

$$\tilde{Y}_{\bar\nu}(x) \propto \sin\left(\bar\nu \ln\left(\frac{1}{2}x\right) - \gamma_{\bar\nu}\right), \quad \bar\nu > 0 , \quad (8.53)$$

$$\tilde{Y}_0(x) \approx \frac{2}{\pi}\left[\ln\left(\frac{1}{2}x\right) + \gamma\right] . \quad (8.54)$$

For the x-independent prefactors in (8.52) and (8.53) and the definition of the phase angle $\gamma_{\bar\nu}$ we must refer to [386].
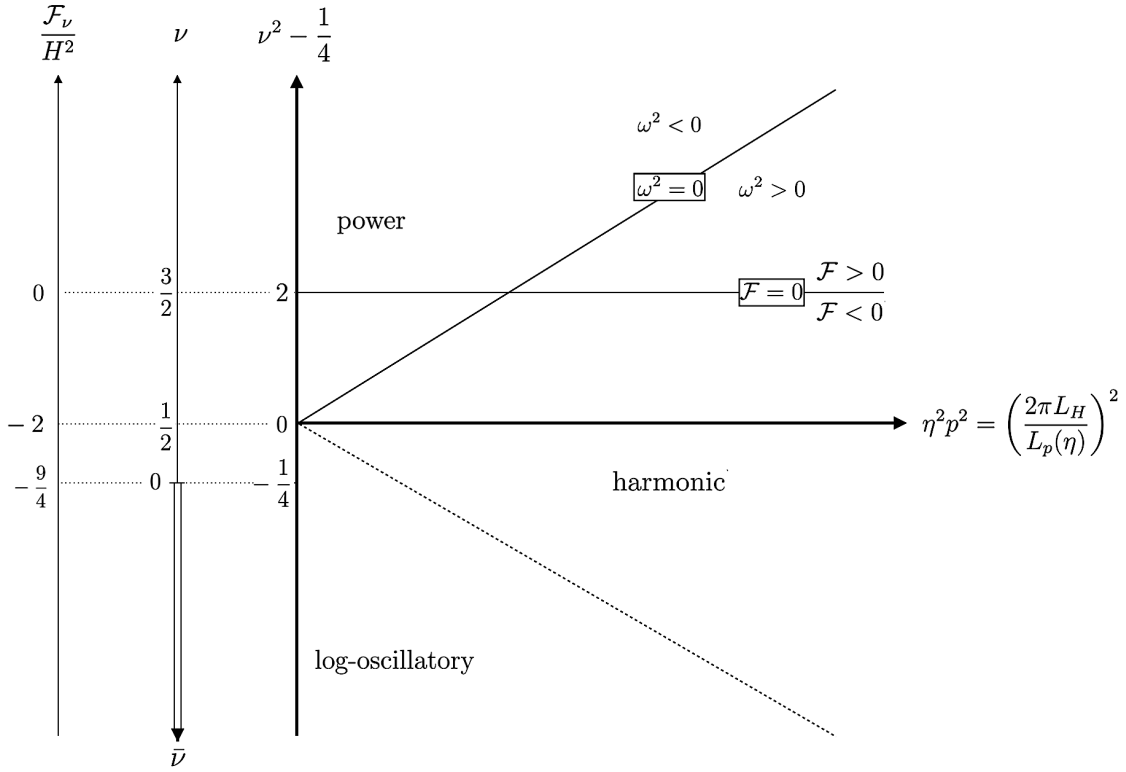
FIGURE 8.3. The ν-p plane of the eigenfunctions $\chi_{\nu,\vec{p}}$. The vertical axis corresponds to the spectrum of the d'Alembertian. It is labeled in three different ways, each convenient in its own right. The horizontal axis represents the square of the degeneracy index $\vec{p}$ (multiplied by η^2). The two diagonals separate the power-, harmonic-, and logarithmic oscillation regimes, respectively. The horizontal line at $\nu = 3/2$ separates spacelike from timelike modes.

(3) Regime boundaries. For a rough orientation, we may assume that the regimes of (ν, p) space within which either the first or the second contribution to $\omega^2(\eta)$ dominates are sharply separated by the curve along which $\eta^2 \, p^2 = \left|\nu^2 - \frac{1}{4}\right| = \left|\frac{\mathcal{F}_\nu}{H^2} + 2\right|$. Since $\nu^2 - \frac{1}{4}$ can be both positive and negative, two cases must be distinguished.

Case $\nu^2 - 1/4 > 0$: The curve is a straight line of positive slope, namely the solid diagonal in the diagram of Figure 8.3: $\nu^2 = \frac{1}{4} + \eta^2 p^2$. The frequency vanishes everywhere on this line, $\omega(\eta)^2 \equiv 0$. The power (harmonic) regime sets in above (below) the line.

Case $\nu^2 - 1/4 < 0$: A straight line with negative slope obtains, $\nu^2 = \frac{1}{4} - \eta^2 \, p^2$, the dashed diagonal in Figure 8.3. On this line, $\eta^2 \, p^2$ and $\nu^2 - 1/4$ are equal in magnitude, but their signs differ, resulting in a nonzero $\omega(\eta)^2 = 2 \, \eta^2 \, p^2$. Above (below) the line the harmonic (log-oscillatory) regime extends.

8.3.5. *The ν-p plane*

The diagram in Figure 8.3, and similar ones that will follow are useful tools for visualization purposes. We refer to them as a representation of the "ν-p plane" even though the Cartesian axes drawn carry linear scales not for ν and p directly, but rather simple functions thereof. Plotting $\nu^2 - \frac{1}{4}$ versus $\eta^2 p^2$ has not only the practical advantage of rendering the regime boundaries straight lines, it also allows us to interpret the diagram in several different ways, and each one of them is useful in its own right:

(i) We can look at the diagram for a fixed time, $\eta = 1$, for example. Then every point of the ν-p plane is seen to represent a particular eigenfunction $\chi_{\nu,\vec{p}}$, modulo the direction of $\vec{p}$ (since $p = |\vec{p}|$). Hence, loosely speaking, the ν-p plane is the space of all eigenmodes for a given $\vec{p}$-direction.

(ii) We may shift the perspective and interpret the diagram for a fixed comoving momentum, $p = p_1$, say, so that the horizontal axis has the character of a time axis now. The coordinate (wave-)length $2\pi/p_1$ is then seen to be represented by a point which moves horizontally from right to left when conformal time progresses from $\eta = -\infty$ towards $\eta = 0$.

(iii) The interpretation of this motion comes from yet another property of the diagram. Thanks to eq.(8.27), i.e., $\eta^2 \, p^2 = \left(2\pi \frac{L_H}{L_p(\eta)} \right)^2$, the scale on the diagram's horizontal axis is also a measure of the proper length L_p in Hubble units. As a consequence, the above horizontal motion of the point corresponding to the fixed comoving momentum p_1 describes precisely how the associated physical wavelength $L_{p_1}(\eta)$ increases with time.

In the sequel we shall find it helpful to freely switch back and forth between these interpretations.

8.3.6. *Crossing the regime boundaries*

Let us consider the subspace of all those eigenfunctions

$$\chi_{\nu,\vec{p}}(\eta, \vec{x}) = |\eta| \; v_{\nu,p}(\eta) \, e^{i\vec{p}\cdot\vec{x}} \tag{8.55}$$

which possess a prescribed eigenvalue $\mathcal{F}_\nu$, i.e., a given principal quantum number ν. Their degeneracy index $\vec{p} \in \mathbb{R}^3$ is left arbitrary instead. Its magnitude $p = |\vec{p}|$ can vary between $p = 0$ and $p = \infty$, respectively.

In Figure 8.3 the collection of those eigenfunctions is represented by a horizontal line at the corresponding value of ν. For instance, if $\nu = 3/2 \Leftrightarrow \mathcal{F}_\nu = 0$, this line happens

to coincide with the demarcation line drawn in the Figure to separate the domains of positive and negative eigenvalues, respectively.

(1) Let us assume that $\nu > 1/2$ first. Then, moving from left to right in the Figure, every $\nu = $ const line starts out in the power regime for sufficiently small p, at a certain point intersects the transition line, and then enters the harmonic regime for large p. It depends on η whether a given p is "sufficiently small" for the power-, or already large enough for the harmonic regime. Clearly the association of a given eigenfunction with one of the regimes is a time dependent one.

By eq.(8.27), a $\nu = $ const line crosses the transition line at the time when $L_p(\eta)$, the spatial proper wavelength of $\chi_{\nu,\vec{p}}$, assumes the value

$$L_\nu^{\text{trans}} \;=\; \frac{2\pi\, L_H}{\left[\nu^2 - \frac{1}{4}\right]^{1/2}} \;=\; \frac{2\pi\, L_H}{\left[\frac{\mathcal{F}_\nu}{H^2} + 2\right]^{1/2}} \tag{8.56}$$

This equation shows that if ν is a number of order unity, and only then, the wavelength at the transition is of the order of the Hubble length. Stated differently, the eigenmode then changes its behavior just when it "crosses the horizon".

In general this is not true, however. Eigenfunctions pertaining to large eigenvalues $\mathcal{F}_\nu \gg H^2$, i.e., $\nu \gg 1$, possess a proper wavelength at the transition which is *much shorter* than the Hubble radius:

$$L_\nu^{\text{trans}} \approx \frac{2\pi\, L_H}{\nu} \tag{8.57}$$

They cross over to the new regime "deeply inside the horizon". This effect is illustrated in Figure 8.4.

Here we encounter a characteristic difference between the general spectral investigation on the one hand, and a textbook-style quantization of a (massless, say) scalar field on the other. The latter requires only the eigenfunctions with $\nu = 3/2$, i.e., $\mathcal{F} = 0$, when it comes to, say, expanding the Heisenberg field operator in terms of creation and annihilation operators. In the present context we are instead particularly interested in very large quantum numbers $\nu \gg 1$.

As a consequence, the setting is more involved, but at the same time much richer from the physics point of view. The Hubble and the transition lengths, L_H and L_H/ν, constitute two vastly different scales typically, and the interplay of those two scales will be a recurring theme in the sequel.

One of the novel features one encounters at large eigenvalues is that the crossover between the regimes develops into an increasingly pronounced, drastic change of the eigenfunctions' behavior. While the crossover is fairly smooth for the familiar $\nu = 3/2$ modes, it has an increasingly sudden and abrupt appearance when $\nu \to \infty$.
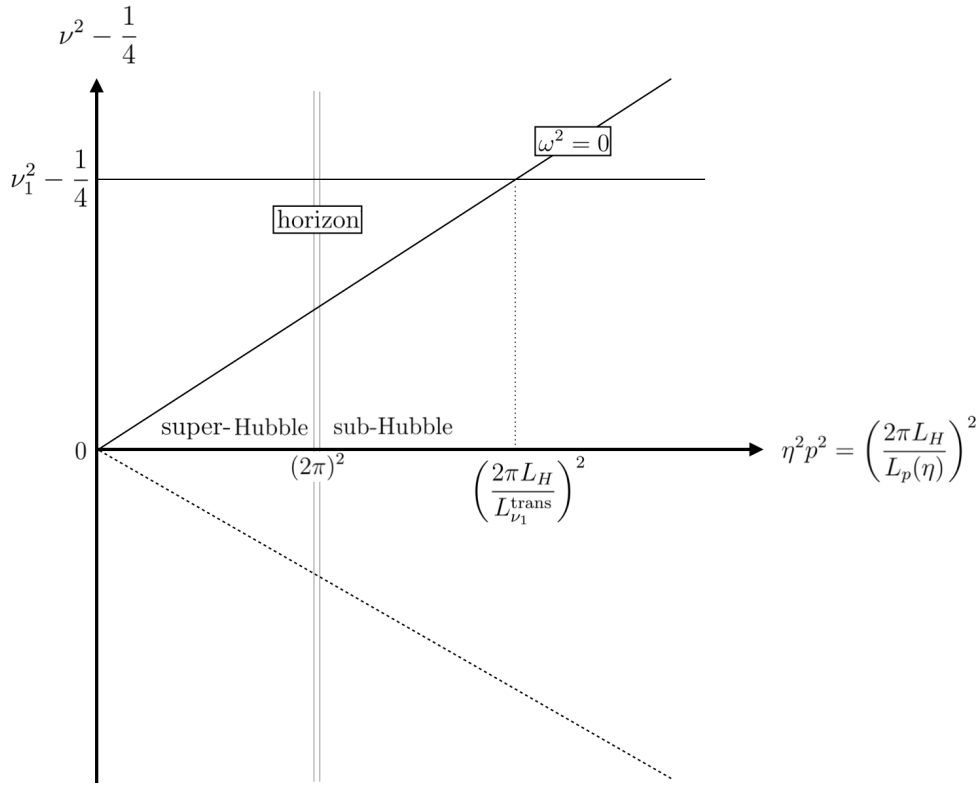
FIGURE 8.4. The ν-p plane of eigenfunctions as in Figure 8.3. The vertical line at $|\eta|\, p = 2\pi$ delineates the boundary between sub- and super-Hubble size proper wavelengths, respectively. The modes with $\nu = \nu_1$ are seen to cross over from the harmonic to the power regime well within the Hubble horizon.

We illustrate this phenomenon for a mode function of the $B = 0$ type. For (ν, p) fixed, eqs.(8.36) and (8.55) yield for them:

$$\chi_{\nu,\vec{p}}(\eta, \vec{x}) \propto e^{i\vec{p}\cdot\vec{x}}\; y^{3/2}\; J_\nu(y)\; \Big|_{y\equiv p|\eta|=2\pi L_H/L_p(\eta)}. \tag{8.58}$$

For $\nu \gg 1$, the qualitative properties of these modes are entirely determined by the Bessel functions J_ν. The latter switch between their limiting forms (8.46) and (8.51), respectively, when the argument is of the order of the index, $y \approx \nu$.

Figure 8.5 shows the graph of J_ν for $\nu = 100$. Obviously $J_{100}(y)$ assumes rather tiny values, and it varies only little in the power regime $0 \le y \lesssim 100$. Near $y \approx 100$ a clear "phase transition" can be seen which marks the onset of the harmonic oscillations.

Thus we observe that the temporal resolving power of $\chi_{\nu,\vec{p}}$ in the harmonic regime $(y \gtrsim \nu)$ is as perfect as it possibly could be, comparable to a sine or cosine, but it deteriorates tremendously in the power regime, $y \lesssim \nu$.
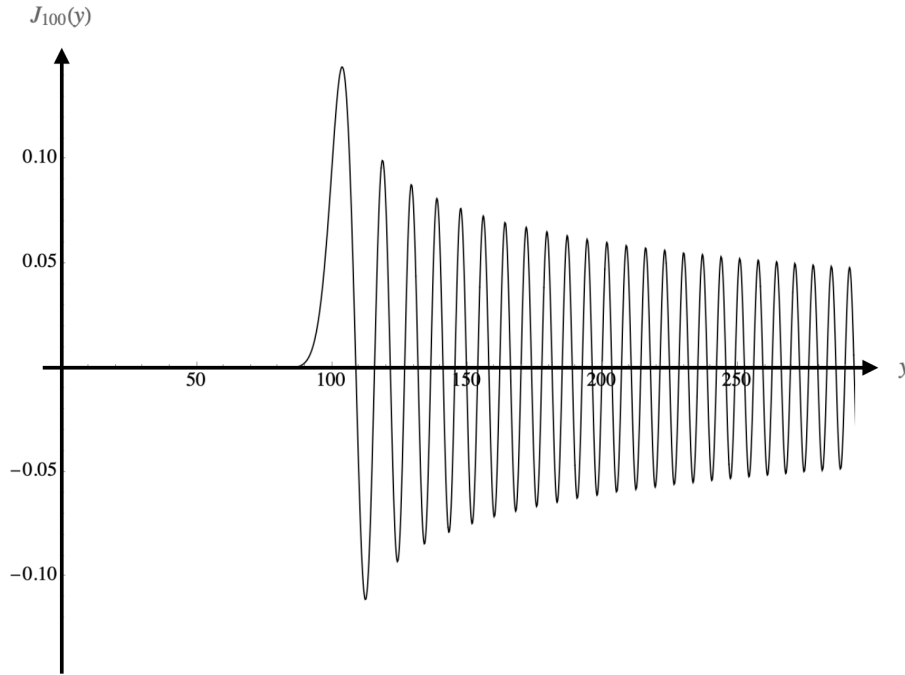
FIGURE 8.5. The Bessel function $J_{100}(y)$. It displays a transition from the power- to the harmonic regime near $y = 100$.

In the above example the proper wavelength of the function $\chi_{\nu,\vec{p}}$ at the transition is 100 times smaller than the Hubble radius, and its eigenvalue is about $\mathcal{F}_\nu \approx 10^4 H^2$. Needless to say that for modes with even larger eigenvalues the disparity between the Hubble- and the transition scale grows unboundedly.

(2) In the second case $\nu^2 - \frac{1}{4} < 0$, similar remarks apply to the divide between the log-oscillatory and the harmonic regimes, the dashed diagonal in Figure 8.3. It is intersected by all $\nu = \text{const}$ lines having real $\nu \in \left(0, \frac{1}{2}\right)$, or imaginary ν with $\bar{\nu} > 0$.

Eigenfunctions with large negative eigenvalues $\mathcal{F}_\nu \ll -\frac{9}{4}H^2$ show a characteristic transition between harmonic and logarithmic oscillation at a proper wavelength

$$L_{\bar{\nu}}^{\text{trans}} \approx \frac{L_H}{\bar{\nu}} \,. \tag{8.59}$$

The pertinent eigenfunctions of the $B = 0$ type are similar to (8.58), with $J_\nu(y)$ replaced by the Bessel functions $\tilde{J}_{\bar{\nu}}(y)$ though, which determine the essential features. In Figure 8.6 we plot the example of $\tilde{J}_{\bar{\nu}}(y)$ with $\bar{\nu} = 20$. Over the entire range of $y \equiv 2\pi \frac{L_H}{L_p}$ there are no strong changes in the amplitude of the oscillations. Their frequency, however, is constant (proportional to $\log(y)$) for y above (below) the transition point $y \approx \bar{\nu}$.
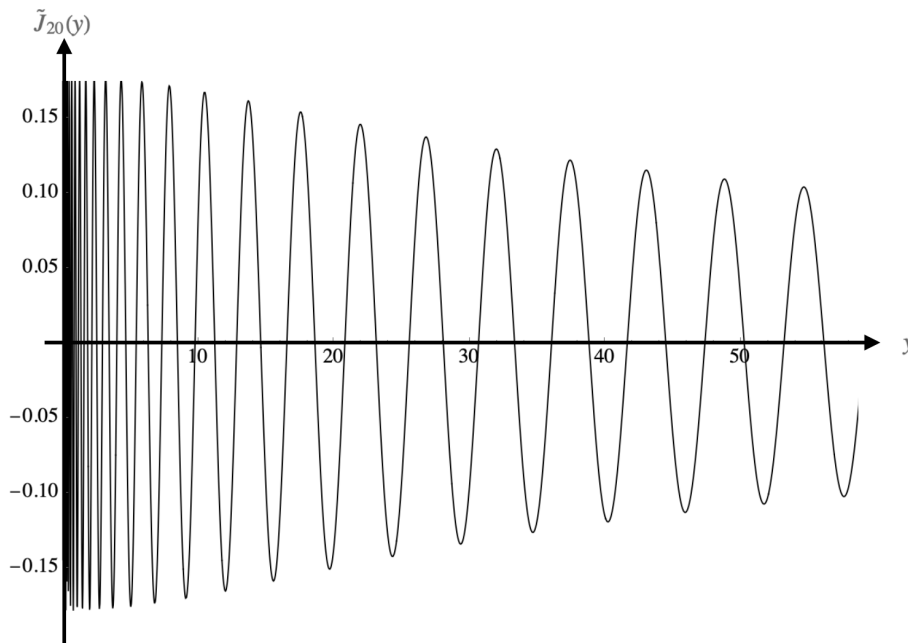
FIGURE 8.6. The Bessel function of imaginary order $\tilde{J}_{20}(y)$. Lowering y, it displays a transition from harmonic to logarithmic oscillations near $y = 20$.

8.4. THE RG TRAJECTORIES, AND A DUALITY TRANSFORMATION

In the sequel we study the concrete spectral flows arising from the GEAA in the Einstein–Hilbert truncation [95]. It is based upon the ansatz and the associated trajectories described in Section 3.5.

8.4.1. *Lorentzian signature*

An explicit inspection of the derivation of β_g and β_λ from the FRGE in ref.[95] reveals that, within the Einstein-Hilbert truncation, the flow equation and the calculation of β_g and β_λ are meaningful both in the Euclidean and Lorentzian case, and that the resulting beta functions agree for the two signatures.

In fact, this holds true more generally within all truncations whose projection on the corresponding truncated theory space is based upon the asymptotic short time expansion of the traced heat kernel $\text{Tr}\left[e^{-K\tau}\right]$ or the Schrödinger kernel, $\text{Tr}\left[e^{-iK\tau}\right]$. Here, typically, $K \equiv -\Box_g + \textit{curvature terms}$, or generalizations thereof. The functional trace of the FRGE has a representation in terms of a proper time integral involving the Schrödinger kernel. Contrary to its heat kernel based counterpart, is not restricted to

positive operators K, and therefore also applies to the Lorentzian signature case, see [95] and [182] for more detailed discussions.[4]

Concerning the relative ordering of timelike and spacelike modes in these RG equations, it can also be observed that the corresponding cutoff scheme is a "maximally democratic" one. That is, the effective action $\Gamma_k[h; \bar{g}]$ has all $\Box_{\bar{g}}$-eigenmodes with $|\mathcal{F}_n[\bar{g}]| > k^2$ and either sign of $\mathcal{F}_n$ integrated out, but no others.[5] This is the property anticipated in (3.83).

Despite the formal character of these arguments, the Einstein-Hilbert trajectories are well motivated examples for a first "proof of principle" of the new spectral methods. Indeed, only rather limited information about the trajectory enters the analysis. The function $G(k)$ is entirely irrelevant, for example, and regarding $\Lambda(k)$ a very schematic and robust "caricature" of the actual scale dependence suffices (see Subsection 3.5.2). Moreover, most aspects of our results do not even depend on the asymptotic safe completion of Quantum Einstein Gravity.

8.4.2. *High-low scale duality*

The dimensionless cosmological constant in eq.(3.63) is invariant under an intriguing duality transformation that relates small and large RG scales [270]. Within its domain of validity, the semiclassical cosmological constant (3.63) assumes every given value $\lambda > \lambda_T$ precisely *twice*. In fact, we have $\lambda(k) = \lambda(k^\sharp)$ for any k and its dual partner scale

$$k^\sharp = \frac{k_T^2}{k} \, . \tag{8.60}$$

If k is smaller than k_T, the associated $k^\sharp$ is larger, and vice versa.

Let us mention that also the scale $\hat{k}$ which marks the end of the semiclassical regime towards the UV, has an IR partner, $\hat{k}^\sharp$. It satisfies

$$\lambda(\hat{k}^\sharp) = \lambda(\hat{k}) = \lambda_* \, , \tag{8.61}$$

---

[4]Note also that the applicability of Schrödinger kernel-based propertime representations to computations in Lorentzian signature is well established since the early days of Quantum Electrodynamics already. In ref.[387], Schwinger introduced the idea of proper time regularization *on Minkowski space*, and building on that, proper time RG equations have been successfully employed for several decades both in perturbative and nonperturbative applications, see ref.[388] for examples.

[5]An easy way to see this is to recall from [122] that within the Einstein-Hilbert truncation the FRGE with a generic higher derivative cutoff operator $\mathcal{R}_k[\bar{g}]$ is very well approximated by a proper time RG equation. This includes the simplest type of proper time flow equations, which have the structure $k\partial_k \Gamma_k = \frac{1}{2} \mathrm{Tr} \exp\left(-i\,\Gamma_k^{(2)}/k^2\right)$ in the Lorentzian setting. Since in the case at hand $\Gamma_k^{(2)}$ equals essentially $-\Box_{\bar{g}}$, this structure implies that a mode with eigenvalue $\mathcal{F}_n$ makes a contribution to the trace proportional to $\exp\left(-i\,\mathcal{F}_n/k^2\right)$. Hence the cutoff affects modes with $\mathcal{F}_n < -k^2$ and $\mathcal{F}_n > +k^2$, respectively, in a symmetric fashion. (See ref. [388] for explicit calculations in this framework.)

and is explicitly given by

$$\hat{k}^\sharp = \left(\frac{\Lambda_0}{\lambda_*}\right)^{1/2} \equiv \left(\frac{3}{\lambda_*}\right)^{1/2} H_0 \ . \tag{8.62}$$

In (8.62) we introduced already the mass parameter

$$H_0 \equiv \left(\frac{\Lambda_0}{3}\right)^{1/2} \ . \tag{8.63}$$

For the de Sitter solution, it will acquire the interpretation of the Hubble constant.

By (8.60), the three scales $\hat{k}^\sharp$, k_T, and $\hat{k}$ are interrelated by

$$\frac{k_T}{\hat{k}^\sharp} = \frac{\hat{k}}{k_T} \quad \Longleftrightarrow \quad \frac{k_T}{H_0} = \left(\frac{3}{\varpi}\right)^{1/2} \frac{m_{\text{Pl}}}{k_T} \ . \tag{8.64}$$

Hence, on a logarithmic scale, $\hat{k}^\sharp$ is as far away from k_T as is $\hat{k}$, in the opposite direction though. Their (inverse) ratio can be expressed as

$$\frac{k_T}{\hat{k}^\sharp} = \frac{\hat{k}}{k_T} = \left(\frac{\lambda_*^2}{\varpi \, \Lambda_0 \, G_0}\right)^{1/4} \tag{8.65}$$

when (3.60) and (3.64) are used.

We mentioned already that the two sets of data, the RG predictions $\{\varpi, \lambda_*\}$ and the integration constants $\{\Lambda_0, G_0\}$, respectively, have a different logical status.

(i) The dimensionless numbers ϖ and λ_* are an explicitly computable output of the RG differential equations. They depend on the coarse graining scheme and the field contents of the matter system, if any [49, 50]. For pure Quantum Gravity, and with all plausible matter system admitting Type IIIa solutions, they are known to be of order unity,

$$\varpi = O(1), \qquad \lambda_* = O(1) \ . \tag{8.66}$$

By (3.60) and (8.62) this fact entails that $\hat{k}$ and $\hat{k}^\sharp$ coincide essentially with the Planck and the Hubble scale, respectively:

$$\hat{k} = O(m_{\text{Pl}}), \qquad \hat{k}^\sharp = O(H_0) \ . \tag{8.67}$$

(ii) The dimensionful quantities Λ_0 and G_0 are constants of integration which appear only in the *solutions* to the RG equation. Their value selects one specific RG trajectory from the set of all solutions to the RG equations. They can be chosen freely.

A special class of choices which is of particular interest both theoretically and phenomenologically is characterized by values of Λ_0 and G_0 whose product is extremely tiny:

$$G_0 \, \Lambda_0 \ll 1 \ . \tag{8.68}$$

Under this condition, eq.(8.65) yields a pronounced *double hierarchy* for the triple of mass scales $\left(\hat{k}^{\sharp}, k_T, \hat{k}\right)$, and likewise for $(H_0, k_T, m_{\text{Pl}})$:

$$\hat{k}^{\sharp} = O(H_0) \ll k_T \ll \hat{k} = O(m_{\text{Pl}}) \,. \tag{8.69}$$

See Figure 3.4 for an illustration of this hierarchy.

It is also amusing to note that the values of G_0 and Λ_0 measured in real Nature yield roughly $G_0 \Lambda_0 \approx 10^{-120}$, such that

$$\frac{k_T}{\hat{k}^{\sharp}} = \frac{\hat{k}}{k_T} \approx 10^{30} \tag{8.70}$$

and $k_T \approx 10^{-30} m_{\text{Pl}} \approx 10^{30} H_0$, see also refs. [221, 389, 390].

8.5. The spectral flow

In the following we consider the two dimensional theory space of the Einstein–Hilbert truncation, coordinatized by dimensionless pairs (g, λ), and select a certain RG trajectory on it, i.e., a solution $k \mapsto (g(k), \lambda(k))$ of the dimensionless RG differential equations [95]. This solution implies a corresponding trajectory of the dimensionful couplings, $k \mapsto (G(k), \Lambda(k)) \equiv (g(k)/k^2, \lambda(k)k^2)$, and a trajectory of Lorentzian action functionals, $k \mapsto \Gamma_k$, given by (3.45). In the following spectral flow analysis we keep the trajectory fixed once and for all. We assume that it is of the Type IIIa and also, but merely for the sake of a transparent presentation, that it features a clearcut double hierarchy (8.69).

Following the scheme in Section 8.1:

(1) Running Einstein equation. Let us now embark on a journey through theory space, thereby always walking along the Type IIIa trajectory we are provided with. At each point of our route we encounter a new action functional then. We derive its associated effective field equation, find its solutions, and select one of them. Within the Einstein-Hilbert truncation this equation happens to have the structure of the classical Einstein equation, but with scale-dependent coupling constants:

$$G_{\mu\nu}\left[g_{\alpha\beta}^k\right] + \Lambda(k)\, g_{\mu\nu}^k = 0 \, + \, \cdots \tag{8.71}$$

Here the dots symbolize terms that might come from the matter sector.

We restrict the analysis to pure Quantum Gravity, or matter-coupled gravity in a vacuum dominated regime. Within the latter, stress tensor contributions from the matter sector are negligible relative to the cosmological constant term in the Einstein equation (8.71), whence its RHS equals zero effectively.

(2) Scale-dependent dS$_4$ solutions. Clearly eq.(8.71) in vacuo and with a fixed k admits many solutions, well known from classical General Relativity. Here we select on all scales the unique maximally symmetric one with $\Lambda(k) > 0$, i.e., de Sitter spacetime. More precisely, as before, we consider the expanding Poincaré patch of dS$_4$. Using the (η, x^i) coordinates again, its metric writes

$$g_{\mu\nu}^k \, \mathrm{d}x^\mu \, \mathrm{d}x^\nu = \frac{-\,\mathrm{d}\eta^2 + \mathrm{d}\vec{x}^2}{\eta^2 \, H(k)^2} \tag{8.72}$$

It has the interpretation of an effective, or mean-field metric of spacetime at scale k. Its Hubble parameter is determined by the point in theory space we just stay at:

$$H(k) = \sqrt{\frac{\Lambda(k)}{3}} \tag{8.73}$$

We are now equipped with a generalized trajectory $k \mapsto \left(g(k), \ \lambda(k), \ g_{\mu\nu}^k \right)$ which, besides the running couplings, comprises a specific solution to the k-dependent field equations, namely dS$_4$ with $H = H(k)$.

The Hubble parameter $H(k)$ defines a corresponding k-dependent Hubble length:

$$L_H(k) \equiv \frac{1}{H(k)} \ . \tag{8.74}$$

Furthermore, since we employ the same system of coordinates at all k, a fixed (i.e., k-independent) comoving length Δx gives rise to a whole "trajectory of proper lengths", $k \mapsto L_{\Delta x}(\eta, k)$. By (8.23) with (8.21), it entangles a scale with a time dependence:

$$L_{\Delta x}(\eta, k) = \frac{\Delta x}{|\eta| \, H(k)} \ . \tag{8.75}$$

For example, a mode with a position dependence proportional to $e^{i\vec{p}\cdot\vec{x}}$ has the proper (aka, physical) wavelength

$$L_p(\eta, k) = \frac{2\pi}{p \, |\eta| \, H(k)} \ . \tag{8.76}$$

A nontrivial k-dependence of such proper quantities is the very hallmark of an *effectively fractal-like* spacetime [100, 240, 270].

(3) Scale-dependent spectrum. Given the metrics (8.72), we construct the associated d'Alembert operators all along the trajectory:

$$\Box_k \equiv \Box_g \Big|_{g_{\mu\nu} = g_{\mu\nu}^k} \ . \tag{8.77}$$

Since $H(k)$ enters $g_{\mu\nu}^k$ only by a x^μ-independent conformal factor, $\Box \equiv g^{\mu\nu} \mathrm{D}_\mu \mathrm{D}_\nu$ depends on the Hubble parameter by a multiplicative constant only:

$$\Box_k = \left(\frac{H(k)}{H(k_0)} \right)^2 \Box_{k_0} \ . \tag{8.78}$$

The next step is to solve the spectral problem of $\Box_k$ for all k. Because of (8.78), the solutions to its eigenvalue equation at any scale $k \geq 0$,

$$-\Box_k \; \chi_{\nu,\vec{p}}(x;k) = \mathcal{F}_\nu(k) \; \chi_{\nu,\vec{p}}(x;k) \; , \tag{8.79}$$

can be expressed in terms of those at an arbitrary normalization scale k_0, as follows:

$$\mathcal{F}_\nu(k) = \left(\frac{H(k)}{H(k_0)}\right)^2 \mathcal{F}_\nu(k_0) \; , \tag{8.80}$$

$$\chi_{\nu,\vec{p}}(x;k) = \chi_{\nu,\vec{p}}(x;k_0) \; . \tag{8.81}$$

Taking advantage of (8.34) we see therefore that the spectra of $\Box_k$, for all k, are given by

$$\mathcal{F}_\nu(k) = \left(\nu^2 - \frac{9}{4}\right) H(k)^2 = \left(\nu^2 - \frac{9}{4}\right) \frac{\Lambda(k)}{3} \tag{8.82}$$

This is the sought-for running spectrum. A map like $k \mapsto \mathrm{spec}\,(-\Box_k) = \{\mathcal{F}_\nu(k)\}$ is commonly referred to as a *spectral flow* [273].

While the result (8.82) involves no approximation beyond the Einstein-Hilbert truncation, the simplified caricature trajectory (3.61) makes it fully explicit

$$\mathcal{F}_\nu(k) = H_0^2 \left(\nu^2 - \frac{9}{4}\right) \times \begin{cases} [1 + \ell^4 \, k^4]^{-1} & \text{for} & 0 \leq k \leq \hat{k} \\ (L \, k)^{-2} & \text{for} & \hat{k} \leq k < \infty \end{cases} \tag{8.83}$$

When working with this trajectory we choose $k_0 = 0$ and identify $\Lambda(0) \equiv \Lambda_0$, $H(0) \equiv H_0$.

According to eq.(8.83) the eigenvalue $\mathcal{F}_\nu(k)$, for every fixed quantum number ν, increases monotonically with the scale $k \in [0, \infty)$. Obviously, this particular spectral flow displays *no level crossing*.

(4) The cutoff modes. Knowing the spectral flow, let us determine the cutoff modes of all spectra along the trajectory. We denote their k-dependent principal quantum numbers by $\nu_{\mathrm{COM}}^+(k)$ and $\nu_{\mathrm{COM}}^-(k)$, respectively, in the sectors with $\mathcal{F}_\nu(k) > 0$ and $\mathcal{F}_\nu(k) < 0$. The defining property of the COMs, eq.(8.18), yields an implicit equation which determines the quantum numbers:

$$\mathcal{F}_\nu(k)|_{\nu=\nu_{\mathrm{COM}}^\pm(k)} = \pm k^2 \; . \tag{8.84}$$

From the spectra (8.82) we obtain the following condition for $\nu_{\mathrm{COM}}^\pm(k)$:

$$\nu_{\mathrm{COM}}^\pm(k)^2 - \frac{9}{4} = \pm\frac{3k^2}{\Lambda(k)} \tag{8.85}$$

Noting that the ratio $\Lambda(k)/k^2 \equiv \lambda(k)$ is nothing but the usual dimensionless cosmological constant, we see that the quantum numbers of the cutoff modes are given by

$$\nu_{\mathrm{COM}}^\pm(k)^2 = \frac{9}{4} \pm \frac{3}{\lambda(k)} \tag{8.86}$$

The equation (8.86) is the main result of this section. On the branch of positive eigenvalues (spacelike modes) it is to be used with the upper, i.e., plus sign, while the lower sign applies to the $\mathcal{F} < 0$-part of the spectrum (timelike modes).

8.6. EVOLVING SETS OF CUTOFF MODES

By definition, the cutoff modes are those eigenmodes of the running d'Alembertian $-\Box_k$ whose eigenvalues equal to k^2 or $-k^2$, respectively. In the previous section we obtained their ν-quantum numbers. Taking also the degeneracy into account, we can write

$$\Upsilon^\pm_{\text{COM}}(k) = \left\{ \chi_{\nu,\vec{p}} \; \middle| \; \nu = \nu^\pm_{\text{COM}}(k), \; \vec{p} \in \mathbb{R}^3 \right\}. \tag{8.87}$$

The real or purely imaginary functions $\nu^\pm_{\text{COM}}(k)$ are given by (8.86) or, equivalently,

$$\nu^\pm_{\text{COM}}(k)^2 - \frac{1}{4} = 2 \pm \frac{3}{\lambda(k)}. \tag{8.88}$$

In particular when dealing with diagrams like that in Figure 8.3, the equation (8.88) is the natural one to use.

Note that the square root

$$\nu^\pm_{\text{COM}}(k) = \sqrt{\frac{9}{4} \pm \frac{3}{\lambda(k)}} \tag{8.89}$$

is always real in the spacelike case of $\nu^+_{\text{COM}}(k)$, whereas in the timelike case, $\nu^-_{\text{COM}}(k)$ is real for scales such that $\lambda(k) > \frac{4}{3}$, but purely imaginary when $\lambda(k) < \frac{4}{3}$.

8.6.1. *Explicit result*

Obviously the running COM quantum numbers $\nu^\pm_{\text{COM}}(k)$ are related to the input of our analysis, the RG trajectory $k \mapsto (g(k), \lambda(k))$, in a quite direct way, and so it is straightforward to obtain the precise functions $\nu^\pm_{\text{COM}}(k)$ by solving the RG equations numerically. Here we take advantage of the simplified caricature trajectory instead. With $\lambda(k)$ approximated as in (3.66), eq.(8.88) assumes the explicit form

$$\nu^\pm_{\text{COM}}(k)^2 - \frac{1}{4} = 2 \pm 3 \times \begin{cases} \left(\dfrac{2}{\lambda_T} \right) \dfrac{k_T^2 \, k^2}{k_T^4 + k^4} & \text{for} \quad 0 \leq k \leq \hat{k} \\[2ex] \lambda_*^{-1} & \text{for} \quad \hat{k} < k < \infty \end{cases} \tag{8.90}$$

The functions (8.90) are plotted in Figure 8.7. We observe that, say, $\nu^+_{\text{COM}}(k)$ is essentially constant at very low scales $k \ll k_T$, but then increases $\propto k^2$ until it reaches a maximum at $k = k_T$. Thereafter it decreases $\propto 1/k^4$ up to the scale $k = \hat{k}$ where it
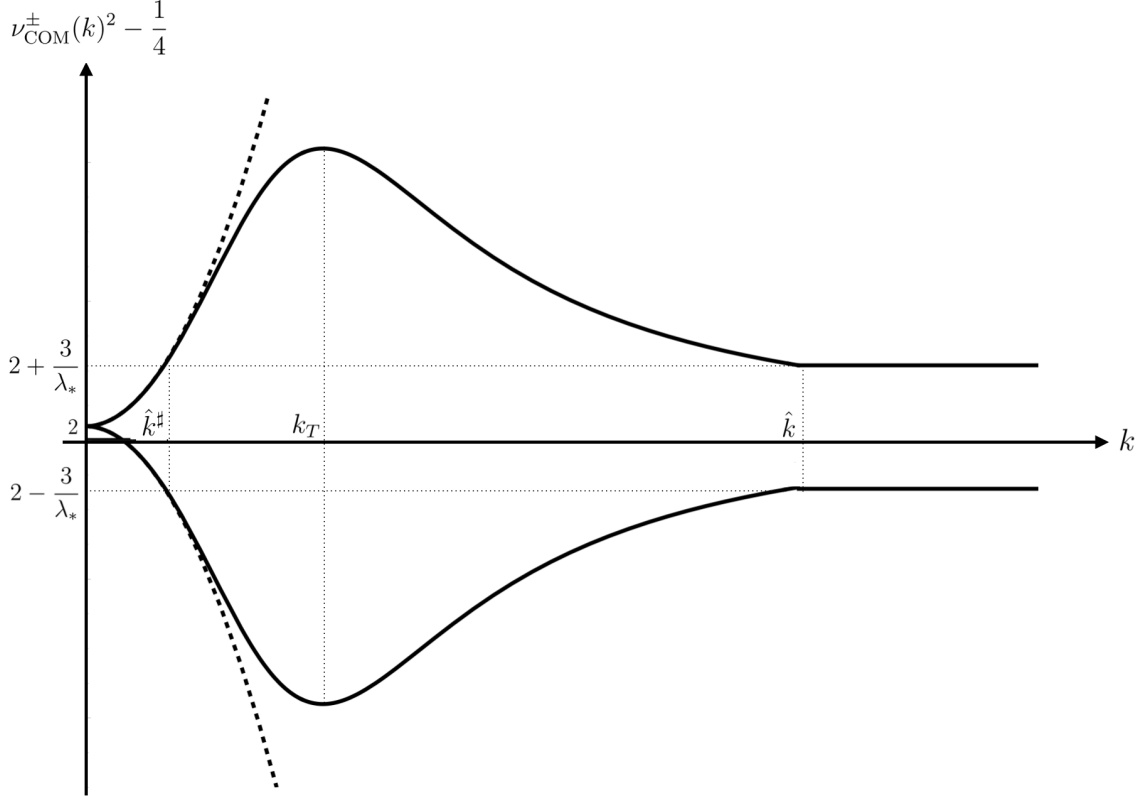
FIGURE 8.7. The functions $\nu_{\text{COM}}^+(k)^2 - \frac{1}{4}$ (upper graph) and $\nu_{\text{COM}}^-(k)^2 - \frac{1}{4}$ (lower graph), respectively. The dashed lines are their classical analogs for a scale independent geometry.

reaches the end of the semiclassical regime. Beyond this point, in the fixed point regime, λ and hence $\nu_{\text{COM}}^\pm$ are constant, assuming finite, nonzero fixed point values there:

$$\nu_*^\pm \equiv \lim_{k \to \infty} \nu_{\text{COM}}^\pm(k) = \sqrt{\frac{9}{4} \pm \frac{3}{\lambda_*}} \tag{8.91}$$

Note that the graph of $\nu_{\text{COM}}^-(k)^2$ it is obtained from $\nu_{\text{COM}}^+(k)^2$ by a reflection at the horizontal axis, plus a constant shift.

The shape of (8.90) has some important features:

(1) UV-IR duality In Figure 8.7 we also indicate the scale $\hat{k}^\sharp$ at which λ and, as a consequence, $\nu_{\text{COM}}^\pm$ assume their respective fixed point values for a second time:

$$\nu_{\text{COM}}^\pm(\hat{k}^\sharp) = \nu_*^\pm \quad \text{at} \quad \hat{k}^\sharp = \left(\frac{3}{\lambda_*}\right)^{1/2} H_0 \tag{8.92}$$

We recall that $\hat{k}^\sharp = (3/\lambda_*)^{1/2} H_0$ is the IR dual of the UV scale $\hat{k} = (\lambda_*/\varpi)^{1/2} m_{\text{Pl}}$.

(2) Double hierarchy. We choose the integration constants Λ_0 and G_0 such that $\Lambda_0 G_0 \ll 1$. As we discussed in connection with (8.62) already, this leads to a clear

separation of the three relevant scales $\left(\hat{k}^{\sharp} \ll k_T \ll \hat{k} \right)$, *making $\hat{k}^{\sharp}$ an extremely low mass scale situated far in the IR.* By (3.65) this choice also implies a very small value of

$$\lambda_T \equiv \lambda(k_T) \ll 1 \qquad (\Lambda_0 \, G_0 \ll 1) \qquad (8.93)$$

at the trajectory's turning point.

(3) Upper bound on ν^+_{COM}. Both in the spacelike and the timelike case the extremum of the function (8.90) occurs at $k = k_T$, i.e., at the turning point of the RG trajectory where $\lambda(k)$ has its minimum. At this scale,

$$\nu^{\pm}_{\text{COM}}(k_T)^2 = \frac{9}{4} \pm \frac{3}{\lambda_T}. \qquad (8.94)$$

Therefore, specializing for the parameter regime (8.93) and using (3.65), we obtain the following maximum value of ν^+_{COM}:

$$\nu^+_{\text{COM, max}} = \nu^+_{\text{COM}}(k_T) \approx \left(\frac{3}{\lambda_T} \right)^{1/2} = \left(\frac{9}{4 \, \varpi \, \Lambda_0 \, G_0} \right)^{1/4} \qquad (8.95)$$

Furthermore, $\nu^-_{\text{COM}}(k_T) = i \, \nu^+_{\text{COM, max}}$.

Thus we arrive at the conclusion that *along the entire RG trajectory, there do not occur any spacelike cutoff modes having principal quantum numbers larger than $\nu^+_{\text{COM, max}}$.*

While $\nu^+_{\text{COM, max}} \gg 1$ is large[6] when $\Lambda_0 G_0 \ll 1$, finding a finite upper bound

$$\nu^+_{\text{COM}}(k) \le \nu^+_{\text{COM, max}} < \infty \qquad \text{for all} \qquad k \in [0, \infty) \qquad (8.96)$$

is strikingly different from all expectations based upon standard background dependent field theory. We shall discuss the origin of this Quantum Gravity effect in a moment.

(4) Timelike case. As for the timelike cutoff modes, the situation is similar. Since $\left| \nu^-_{\text{COM}}(k_T) \right| \approx \left| \nu^+_{\text{COM}}(k_T) \right|$ when $\lambda_T \ll 1$, there is an analogous bound on this modulus: $\left| \nu^-_{\text{COM}}(k) \right| \lesssim (3/\lambda_T)^{1/2}$. Note that in the parameter range we are mostly interested in, $\lambda_T \ll 1$, the quantum number ν^-_{COM} is always purely imaginary.

(5) The subsets $\Upsilon^{\pm}_{\gtrless}(k)$. According to Section 8.2, the eigenfunctions in $\Upsilon^{\pm}_{\gtrless}(k)$ and $\Upsilon^{\pm}_{\lessgtr}(k)$ are those that possess principal quantum numbers ν such that $|\mathcal{F}_\nu(k)| > k^2$ and $|\mathcal{F}_\nu(k)| < k^2$, respectively. As the COMs sit just in-between these two cases, and since we know their quantum numbers, $\nu^{\pm}_{\text{COM}}(k)$, the sets $\Upsilon^{\pm}_{\gtrless}(k)$ are fully determined now. In Figure 8.8a we represent them graphically on the ν-p plane.

---

[6]For instance, the example of $\Lambda_0 G_0 \approx 10^{-120}$ leads to $\nu^+_{\text{COM, max}} \approx 10^{30}$.
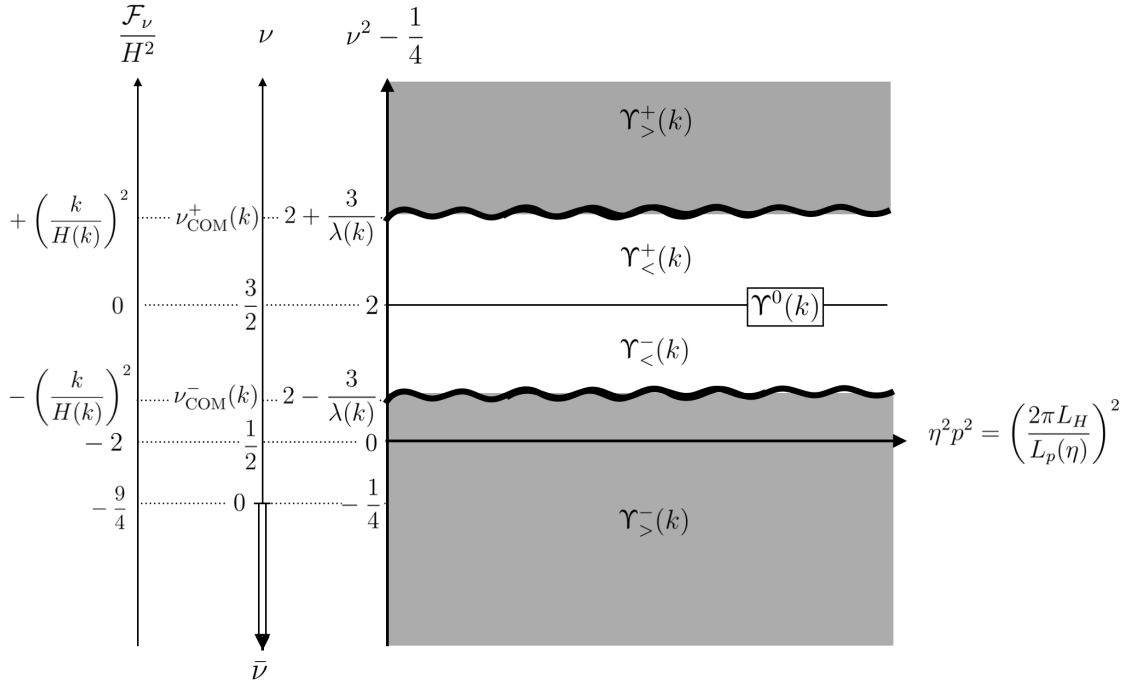
(A) The subspaces $\Upsilon^0(k)$ and $\Upsilon^{\pm}_{\gtrless}(k)$, respectively. In the example shown, the quantum number $\nu^-_{\text{COM}}(k)$ is real.
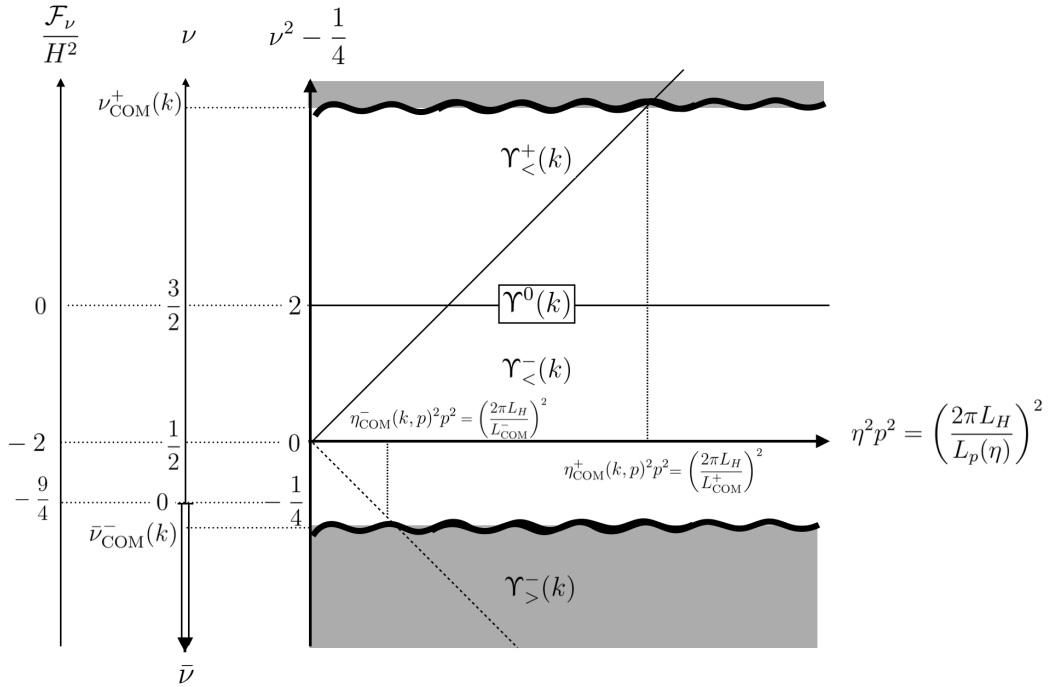
(B) Determination of the transition times $\eta^{\pm}_{\text{COM}}(k,p)$. In the example shown, the quantum number $\nu^-_{\text{COM}}(k)$ is purely imaginary.

FIGURE 8.8. The space of eigenfunctions represented as in Figure 8.3. For a specific scale k, the refined subsets of space- and timelike UV modes $\Upsilon^{\pm}_{\gtrless}(k)$ are shown. The lightlike Υ^0 modes correspond to the $\nu = 3/2$ line. In the second diagram, spacelike (timelike) cutoff modes, indicated by the upper (lower) wiggly line, transit from the harmonic to the power (log-oscillating) regime at the conformal time η^+_{COM} (η^-_{COM}).

8.6.2. *Classical vs. Quantum Gravity*

To illuminate the physical significance of the bound (8.96) it is instructive to contrast $\nu_{\text{COM}}^+(k)$ with its classical counterpart. To this end we turn off the quantum effects for a moment and repeat the above discussion for the "classical RG trajectory"

$$\lambda_{\text{class}}(k) = \frac{\Lambda_0}{k^2} \quad \Longleftrightarrow \quad \Lambda_{\text{class}}(k) = \Lambda_0 = \text{const}. \tag{8.97}$$

It describes a scale independent dimensionful cosmological constant. The effective spacetime is a classical manifold then, showing no fractal features, and the entire spectral flow refers to one and the same operator, namely the d'Alembertian for dS_4 with k-independent Hubble parameter $\sqrt{\Lambda_0/3}$.

Using (8.97) in (8.88) the classical trajectory is seen to imply

$$\left[\nu_{\text{COM}}^\pm(k)^2 - \frac{1}{4}\right]_{\text{class}} = 2 \pm 3\frac{k^2}{\Lambda_0} \equiv 2 \pm \frac{k^2}{H_0^2} \tag{8.98}$$

As it should be, this equation agrees with the classical relationship between $\mathcal{F}$ and ν, i.e., $\mathcal{F}_\nu = \left(\nu^2 - \frac{9}{4}\right) H_0^2$, if one parametrizes the eigenvalues as $\mathcal{F}_\nu = \pm k^2$.

In Figure 8.7 the two functions (8.98) are represented by the dashed curves. In the spacelike case, say, the quantum number $\nu_{\text{COM, class}}^+(k)$ is monotonically increasing and approaches a linear k dependence at large scales:

$$\nu_{\text{COM, class}}^+(k) \approx \frac{k}{H_0} \qquad (k \gg H_0). \tag{8.99}$$

Obviously (8.99), relevant on a rigid spacetime manifold, is markedly different from the result for dynamical gravity displayed in Figure 8.7.

8.6.3. *Physical interpretation*

According to eq.(8.82), there are two different mechanisms by means of which we can increase a (positive, say) eigenvalue $\mathcal{F}_\nu$: First, by increasing the index ν which controls the "fineness" of the eigenfunctions, and second, by increasing the Hubble parameter $H(k)$ so as to shrink the entire spacetime.

In classical gravity, where the metric is fixed, only the first option is available: The COM-condition $\mathcal{F}_\nu = k^2$ must be satisfied by increasing the ν-index $\propto k^2$ at fixed H_0, and this is what eq.(8.99) expresses.

In Background Independent Quantum Gravity on the other hand, the more complex k-dependence of $\nu_{\text{COM}}(k)$ is the result of an interplay between both of these mechanisms. Thereby the first (second) mechanism is the dominant one when $k < k_T$ ($k > k_T$). The

regime $k > k_T$ is exceedingly non-classical in that a *higher* eigenvalue comes with an eigenfunction of *lower* fineness, i.e., fewer zeros or nodal lines.

This apparent paradox is explained by the rapid shrinking of spacetime caused by the enormous growth of $H(k)$ for $k \to \infty$. This shrinking scales up all eigenvalues so strongly that $\mathcal{F}_\nu = k^2$ can only be solved by a function $\nu \equiv \nu_{\text{COM}}^{\pm}(k)$ which decreases when $k \to \infty$.

This basic mechanism is very similar to what occurs in Euclidean gravity [271, 272] and was reviewed in connection with Figure 8.1 in Subsection 8.1.1.

8.6.4. *The AS modes*

The following remark concerns specifically the asymptotic safe completion of Quantum Gravity. As it is obvious in Figure 8.7, the comparatively small set of modes $\chi_{\nu,\vec{p}}$ with $\nu^2 - \frac{1}{4}$ in the interval $\left[2 - \frac{3}{\lambda_*}, 2 + \frac{3}{\lambda_*}\right]$ enjoys a special status: At all scales $k \geq \hat{k}^\sharp$, and this includes of course the fixed point regime $k \geq \hat{k}$, these modes constantly belong to $\Upsilon_{\lessgtr}^{\pm}(k)$ or $\Upsilon_{\text{COM}}^{+}(k)$, if they are spacelike, and to $\Upsilon_{\lessgtr}^{-}(k)$ or $\Upsilon_{\text{COM}}^{-}(k)$, if they are timelike. At no scale $k \geq \hat{k}^\sharp$ they would show up in $\Upsilon_{>}^{+}(k)$ and $\Upsilon_{>}^{-}(k)$, respectively. We refer to those distinguished eigenfunctions as the Asymptotic Safety modes or, for brevity, *Asymptotic Safety (AS) modes*.

Being a bit vague, one could say that the AS modes participate as degrees of freedom in all effective field theories given by Γ_k, with k ranging from the extreme IR, $k = \hat{k}^\sharp$, up to the asymptotic scaling regime and the fixed point ultimately; they never get "integrated out" all along these scales.

In a way, the AS modes are the only available "eyewitnesses" to the unusual physics in the fixed point regime.

As an example, let us consider the modes $\chi_{\nu,\vec{p}}$ with $\nu = \left(\frac{9}{4} + \frac{3}{\lambda_*}\right)^{1/2} \equiv \nu_*^{+}$. In the asymptotic scaling regime $k > \hat{k}$, precisely these eigenfunctions play the role of the spacelike cutoff modes.

For an order of magnitude estimate, we can take $\lambda_* = 0.1$ as a typical value, yielding $\nu_*^{+} \approx 5.7$. As this value is not overly large, the ν-quantum numbers of the AS modes are still of order unity, typically, and so their η-dependence is correspondingly slow.[7]

---

[7]It is also interesting that, for the same value $\lambda_* = 0.1$, the IR scale $\hat{k}^\sharp$, when converted to a distance, amounts to about the 18% of the Hubble radius $L_H^0 = 1/H_0$, i.e., $\left(\hat{k}^\sharp\right)^{-1} \approx 0.183 \, L_H^0$.

8.7. The characteristic COM proper length scale

Let us study the spacelike $(k, \vec{p})$-cutoff modes in more detail now, i.e., the eigenfunctions $\chi_{\nu, \vec{p}}(x)$ with $\nu = \nu_{\text{COM}}^+(k)$ for some fixed scale $k \in \mathbb{R}^+$ and wave vector $\vec{p} \in \mathbb{R}^3$. In order to do so, we will introduce some scale-dependent quantities:

(1) Transition time. For any choice of k and $\vec{p}$ there always exists a time, $\eta_{\text{COM}}^+(k, p)$, at which this mode transits from the harmonic into the power regime, see Figure 8.8b. Since, in this diagram, the regime boundary ($\omega^2 = 0$ line) is at 45 degrees, we read off that at the moment of the transition the equality $\nu^2 - \frac{1}{4} = \eta^2 \, p^2$ must hold. It implies the transition time

$$\eta_{\text{COM}}^+(k, p) = -\frac{1}{p} \sqrt{\nu_{\text{COM}}^+(k)^2 - \frac{1}{4}} = -\frac{1}{p} \sqrt{2 + \frac{3}{\lambda(k)}} \qquad (8.100)$$

where also (8.94) has been used in the second equality.

(2) Proper wavelength. The $(k, \vec{p})$-cutoff mode possess the time independent coordinate wavelength

$$\Delta x_p = \frac{2\pi}{p} \equiv \frac{2\pi}{|\vec{p}|} \, . \qquad (8.101)$$

It is most natural to employ the running metric at the scale chosen for the COM, i.e., $g_{\mu\nu}^k$, in order to associate a *proper* wavelength to the mode. It reads

$$L_p(\eta, k) \equiv b_k(\eta) \, \Delta x_p = 2\pi \, \frac{b_k(\eta)}{p} = \frac{2\pi}{|\eta| \, p \, H(k)} \, , \qquad (8.102)$$

and it is both time- and scale- dependent.

(3) Transition wavelength. A scale of special physical interest is the proper wavelength of the $(\nu, \vec{p})$ cutoff mode at the moment when it transits from the harmonic to the power regime. We denote it by

$$L_{\text{COM}}^+(k) \equiv L_p\Big(\eta_{\text{COM}}^+(k, p), k\Big) \qquad (8.103)$$

and obtain from (8.102) with (8.100):

$$L_{\text{COM}}^+(k) = \frac{2\pi}{k} \sqrt{\frac{3}{3 + 2\,\lambda(k)}} \qquad (8.104)$$

This result can also be expressed as

$$L_{\text{COM}}^+(k) = \frac{2\pi}{H(k)} \sqrt{\frac{\lambda(k)}{3 + 2\,\lambda(k)}} \qquad (8.105)$$

Hence we find that the dimensionless ratio of the COM's transition wavelength and the running Hubble radius at the same scale, $L_H(k) \equiv 1/H(k)$, is given by

$$\frac{L_{\mathrm{COM}}^+(k)}{L_H(k)} = 2\pi \sqrt{\frac{\lambda(k)}{3 + 2\,\lambda(k)}} \qquad (8.106)$$

(4) Interpretation. The relation (8.106) can also be read off directly from Figure 8.8b by intersecting the (diagonal) $\omega^2 = 0$ line with the (wiggly) COM line, and projecting the point of intersection down on to the horizontal axis, thus confirming that

$$\left(\frac{2\pi\,L_H(k)}{L_{\mathrm{COM}}^+(k)}\right)^2 = 2 + \frac{3}{\lambda(k)} \ . \qquad (8.107)$$

This construction illustrates the precise physical interpretation of the COM length scale: $L_{\mathrm{COM}}^+(k)$ is the largest possible *proper* wavelength a cutoff mode can posses while in the oscillatory regime.

Importantly, while $L_{\mathrm{COM}}^+(k)$ depends on k, it is independent of η. Hence, $L_{\mathrm{COM}}^+(k)$ *is a time independent proper distance characteristic of the spacetime at scale k.*

Let us analyze the different regimes:

(5a) UV and IR limits. At the terminal points of the RG trajectory, the relation (8.106) asymptotes to

$$\lim_{k\to\infty} \frac{L_{\mathrm{COM}}^+(k)}{L_H(k)} = 2\pi \sqrt{\frac{\lambda_*}{3 + 2\lambda_*}}, \qquad \lim_{k\to 0} \frac{L_{\mathrm{COM}}^+(k)}{L_H(k)} = 2\pi \ . \qquad (8.108)$$

In both the UV and the IR limit the COM scale agrees with the Hubble length basically.

(5b) Near the turning point. At intermediate points of the RG trajectory, L_{COM}/L_H is extremely tiny on most scales, as it becomes obvious when (8.106) is expressed in terms of the COM quantum number (8.94):

$$\frac{L_{\mathrm{COM}}^+(k)}{L_H(k)} = \frac{2\pi}{\sqrt{\nu_{\mathrm{COM}}^+(k)^2 - \frac{1}{4}}} \approx \frac{2\pi}{\nu_{\mathrm{COM}}^+(k)} \qquad (8.109)$$

The second, approximate equality in (8.109) applies at intermediate scales where $\nu_{\mathrm{COM}}^+(k)$ is large. In fact, the ratio assumes its maximum at the turning point scale:

$$\left(\frac{L_{\mathrm{COM}}^+(k)}{L_H(k)}\right)_{\mathrm{max}} \approx \frac{2\pi}{\nu_{\mathrm{COM}}^+(k_T)} \approx 2\pi \left(\frac{\lambda_T}{3}\right)^{1/2} = 2\pi \left[\frac{4}{9}\,\varpi\,G_0\,\Lambda_0\right]^{1/4} \ . \qquad (8.110)$$

Here we also used (8.95). Thus, the smaller is $\Lambda_0 G_0$, the larger the disparity between the Hubble and the COM scale can become maximally.

(6) Timelike case, higher spin operators. As it is obvious from Figure 8.8b, we can define a proper length analogous to L_{COM}^+ also for timelike cutoff modes. While L_{COM}^+ and L_{COM}^- are different in principle, they become essentially identical in the regime

which we consider usually, namely when $\left|\nu_{\text{COM}}^{\pm}(k)\right| \gg 1$:

$$L_{\text{COM}}^{-}(k) \approx L_{\text{COM}}^{+}(k) \ . \tag{8.111}$$

See also Figure 8.9, which refers to this case.

In the regimes of either large real or purely imaginary quantum numbers with $|\nu| \gg 1$, the above discussions carry over unmodified in yet another direction, namely to more general kinetic operators of the form $-\Box + (curvature\ terms)$. On the dS$_4$ background the curvature terms evaluate to a constant number times the identity operator, hence they cause only a simple constant shift of the eigenvalues: $\mathcal{F}_\nu \to \mathcal{F}_\nu + C$. As a result, the effect of the curvature terms becomes negligible when $|\mathcal{F}_\nu| \gg |C|$, i.e., $|\nu| \gg 1$, so that we are back then to the pure d'Alembertian.

This remark concerns not only the kinetic operator of the metric fluctuations $h_{\mu\nu}$, but also that of gauge fields, fermions, and conformally coupled scalars, for instance. Hence, the range of validity of our results extends well beyond minimally coupled scalar test fields.

(7) Classical vs. Quantum Gravity. We also mention that the classical analog of the ratio (8.106) is given by

$$\left. \frac{L_{\text{COM}}^{+}(k)}{L_H(k)} \right|_{\text{class}} = \frac{2\pi}{\sqrt{2 + \frac{3\,k^2}{\Lambda_0}}} \tag{8.112}$$

Hence the classical variant of $\frac{L_{\text{COM}}^{+}(k)}{L_H(k)}$ is seen to *vanish* in the limit $k \to \infty$, in sharp contradistinction to the Quantum Gravity case, where the gravitational backreaction and Asymptotic Safety bestows us with a well defined nonzero ratio, (8.108).

8.8. Spatial geometry, effective field theory, and COMs

We are still on our journey through theory space along a certain Type IIIa trajectory. At each point visited we have solved the effective field equations related to the action $\Gamma_k[h_{\mu\nu}, A, \cdots ; \bar{g}_{\mu\nu}]$ which we encountered there. Next we ask about the geometrical features that could possibly be displayed by the "on-shell" mean field configurations thus obtained, notably by the metric $g_{\mu\nu} \equiv \langle \hat{g}_{\mu\nu} \rangle$, or by the vacuum expectation value of some optional matter field, $A(x)$.

8.8.1. *Geometry by means of physical fields*

In principle, we would like to find exactly those geometrical features which, intuitively speaking, have a size that is comparable to the length scale at which Γ_k defines a "good effective field theory". Clearly it is not possible to make the latter notion fully precise in a general way. Therefore we follow a closely related, yet simpler and more clearcut strategy [270].

Namely, we consider the set of all cutoff modes at a given scale, $\Upsilon^+_{\mathrm{COM}}(k) \cup \Upsilon^-_{\mathrm{COM}}(k)$, form arbitrary linear combinations of those functions, and investigate the geometric properties of the field configurations that are accessible in this manner.

The overall outcome constitutes what can be regarded as an *effective quantum geometry at scale k*, with some justification.

8.8.2. *Resolving structures on a time slice*

We emphasize that while the special eigenfunctions $\chi_{\nu,\vec{p}}(\eta, \vec{x})$ collected in

$$\Upsilon^\pm_{\mathrm{COM}}(k) = \left\{ \chi_{\nu,\vec{p}} \ \middle| \ \nu = \nu^\pm_{\mathrm{COM}}(k), \ \vec{p} \in \mathbb{R}^3 \right\}, \tag{8.113}$$

have a definite ν-quantum number to enforce the eigenvalue $\mathcal{F}_\nu = \pm k^2$, their degeneracy index $\vec{p}$ is an arbitrary coordinate 3-momentum of any direction and magnitude. Since all eigenmodes have a $\vec{x}$-dependence $\chi_{\nu,\vec{p}}(\eta, \vec{x}) \propto e^{i\vec{p}\cdot\vec{x}}$, it follows therefore that by superimposing basis functions, from $\Upsilon^+_{\mathrm{COM}}(k)$ or $\Upsilon^-_{\mathrm{COM}}(k)$ alone, it is possible to manufacture field configurations with any desired $\vec{x}$-dependence at some fixed time η:

$$A(\eta, \vec{x}) = \int_{\mathbb{R}^3} \mathrm{d}^3p \ \alpha(\vec{p}) \ \chi_{\nu^\pm_{\mathrm{COM}},\vec{p}}(\eta, \vec{x}) \ . \tag{8.114}$$

These field configurations satisfy

$$- \Box_k \ A(\eta, \vec{x}) = \pm k^2 \ A(\eta, \vec{x}) \tag{8.115}$$

for any choice of the coefficients $\alpha(\vec{p})$. And in fact, it is perfectly possible to choose $\alpha(\vec{p})$ in such a way that $A(\eta, \vec{x})$ has nontrivial structure on arbitrarily small distance scales in $\vec{x}$-space. In other words: *For every fixed time η and scale k, field configurations spanned by $\Upsilon^\pm_{\mathrm{COM}}(k)$ possess an unlimited resolving power for spatial structures on the respective 3D time slice of the* dS$_4$ *manifold*.

This Lorentzian result should be contrasted with the analogous one in Euclidean gravity which was reviewed in the Introduction and illustrated in Figure 8.1: There, we did actually encounter a limited resolution, not in space, however, but in 4D spacetime.

(1) Spatial geometry vs. time dependence. The above seemingly unlimited resolving power comes at a price, however. Namely, insisting on the eigenfunctions property (8.115), we have no way of controlling the η-dependence of the COM-superposition (8.114) if we use up all our freedom of choosing $\alpha(\vec{p})$ by optimizing the spatial resolution. The time dependence of $A(\eta, \vec{x})$, with $\alpha(\vec{p})$ designed so as to describe a given *purely spatial* geometry, might however be physically unacceptable, say undetectable because the detector setup is "too slow" to follow it, or because of other experiment-related constraints.

To avoid such unwanted η-dependencies it may be necessary to impose further conditions on the space of admissible basis modes.

Let us try to put this issue into a broader context. **(2) Hypotheses underlying field-based geometry.** It is important to emphasize that the (as to yet, hypothetical) geometry which we try to uncover is carried by *physical fields*. It follows therefore that this kind of geometry cannot be a property of the "quantum spacetime" alone, but rather must depend also to some extent on the experimental setup that is used in order to observe or probe it.

At this point, we are not embarking on a detailed physical description of this setup and of the "detectors" or "microscopes" it employs. To proceed, we instead formulate certain plausible but still very general *model assumptions* about the experimental setting, and we explore their implications. Every set of such assumptions, or "axioms" will then define a clearcut *model of a field-based geometry*.

Typical model assumptions include, for instance, a specification of the time dependence which detectable mean fields like $A(\eta, \vec{x})$ are allowed to display. The importance of this specification stems from the fact that we want to learn about the structure of *space* here, and not of *spacetime*. Clearly this is impossible if, say, the η-dependence is too fast for the detector to follow it so that it averages over a stack of time slices.

We stress that by no means we are constraining the mean field configurations which are occurring. We are neither modifying the RG trajectory, nor the running solutions to the effective field equations. The restrictions concern only the "test" or "spectator" systems corresponding to a physically realistic measurement or observation. Nevertheless, every physics-based geometry will depend on them to some degree.

8.8.3. *The models A and B*

In the sequel we explore the implications of two prototype models. We specify them by means of the following k-dependent conditions on the COMs which can be registered by
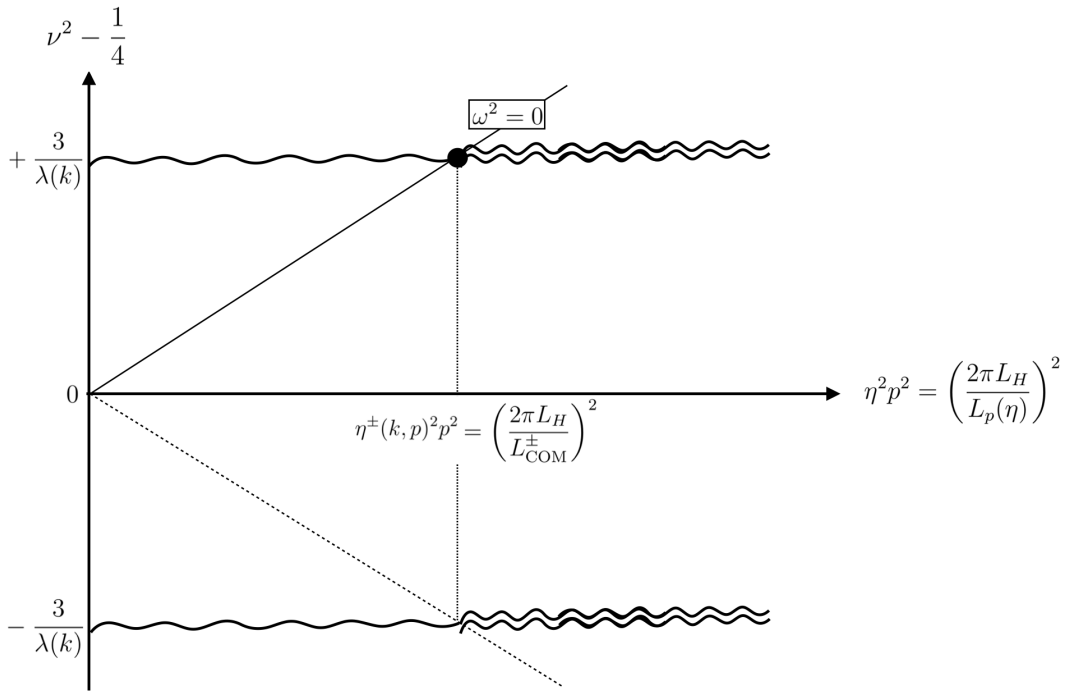
FIGURE 8.9. The cutoff modes, and the respective subsets of the COMs which are detected according to Models A and B. The black dot indicates the detected modes of Model A, the wavy double lines those of Model B. The diagram assumes that $\lambda(k) \ll 1$, in which case $L_{\text{COM}}^-(k) \approx L_{\text{COM}}^+(k)$.

the respective detectors:

> **Model A**: For every fixed k, only η-*independent* cutoff modes and combinations thereof are registered.

All observed structures of field configurations $A(\eta, \vec{x}) \equiv A(\vec{x})$ are strictly time independent then.[8]

This model comes closest to the ideal of reducing the wealth of physical patterns and processes to precisely the eternal geometric properties one would ascribe to 3D space as such.

> **Model B**: For every fixed k, only cutoff modes in the *harmonic regime* and combinations thereof are registered.

For $k^2 = 0$ ($k^2 = -m^2$), the COMs selected in Model B are a generalization of the familiar sub-horizon modes on classical de Sitter spacetime. They are solutions to the

---

[8]The precise assumption is that $v_{\nu,p} = \text{const}$, allowing for the prefactor $\propto \eta$ in eq.(8.30).

massless (massive) Klein-Gordon equation, and yet are almost unaffected by curvature effects.

Model B is motivated by the strong qualitative changes the eigenmodes undergo when crossing the regime boundaries. See Figure 8.5 for example, where the resolving power of the respective mode is seen to deteriorate dramatically outside the harmonic regime.

In Figure 8.9, the COMs that are detectable according to these two models are represented on the ν-p plane.

8.8.4. *Implications of the detector models A and B*

Detection through Models A or B have different physical implications:

Model A. A necessary condition for the time independence of a certain $v_{\nu,p}$ is that the corresponding frequency $\omega_{\nu,p}^2$ vanishes. Specializing for cutoff modes, the eqs.(8.42) and (8.86) tell us that

$$\omega^2_{\nu^\pm_{\text{COM}}(k),p}(\eta) = \frac{1}{\eta^2} \left[\eta^2 p^2 - \left(2 \pm \frac{3}{\lambda(k)} \right) \right] . \qquad (8.116)$$

Focusing on the $\lambda(k) \ll 1$ regime again, eq. (8.116) makes it manifest that $\omega^2 = 0$ can be achieved for spacelike COMs only. For them, eq. (8.116) reads, in "proper" terms,

$$\omega^2_{\nu^+_{\text{COM}}(k),p}(\eta) = \left(\frac{2\pi}{\eta} \right)^2 \left(\frac{L_H}{L^+_{\text{COM}}} \right)^2 \left[\left(\frac{L^+_{\text{COM}}}{L_p} \right)^2 - 1 \right] . \qquad (8.117)$$

Hence we conclude that according to Model A the experiment is sensitive to precisely those modes $\chi_{\nu^\pm_{\text{COM}},\vec{p}}(\eta,\vec{x})$ which possess the proper wavelength $L_p = L^+_{\text{COM}}(k)$ at the time of the measurement.

Note that the condition which defines the subset of detectable modes,

$$L_p = L^+_{\text{COM}}(k) \qquad \text{(Model A)} \qquad (8.118)$$

is actually a time independent one if expressed in physical, i.e., proper quantities. It is only in coordinate (comoving) language that it appears η-dependent. In fact, with (8.100), the comoving wave number p is seen to require a time dependence such that

$$p = \frac{1}{|\eta|} \left(2 + \frac{3}{\lambda(k)} \right)^{1/2} \qquad \Longleftrightarrow \qquad \eta^+_{\text{COM}}(k,p) = \eta . \qquad (8.119)$$

Having now fixed both their ν-quantum number and, by (8.119), the magnitude of $\vec{p}$, the left-over modes, $\chi_{\nu^\pm_{\text{COM}},\vec{p}=p\vec{n}}$, possess only two remaining free parameters, angles θ and ϕ, say, which specify the direction of $\vec{p}$ by a unit vector $\vec{p}/p = \vec{n}(\theta,\phi)$.

Hence the detectable modes are just sufficient to represent, by superposition, an arbitrary function *on the unit two-sphere* S^2. The S^2 has a natural interpretation as the *celestial sphere* of an observer located at some fixed $\vec{x}$, and perceiving certain distributions $A(\theta, \phi)$ inscripted in the sky.

Model B. For the second model the situation is similar except that the condition $\omega^2 = 0$ is replaced by the weaker requirement $\omega^2 > 0$, and that timelike COMs are admitted as well. Since we assume $\lambda(k) \ll 1$, there is no essential difference between L_{COM}^+ and L_{COM}^- though. Instead of the strict equality (8.118), we now have the upper bound

$$L_p \leq L_{COM}^+(k) \approx L_{COM}^-(k) \qquad \text{(Model B)} \qquad (8.120)$$

for the proper wavelengths L_p of the detected modes.

On the ν-p plane, the subset of COMs eligible for Model A is found by intersecting the horizontal $\nu = \nu_{COM}^+$ line with the upper diagonal on which $\omega^2 = 0$, see Figure 8.9. In this diagram, the corresponding modes are symbolized by the black dot, thus confirming the condition for their detectability: $L_p = L_{COM}^+(k)$.

In the case of Model B, we intersect both the ν_{COM}^+- and the ν_{COM}^--line with the two diagonals at $\pm 45°$, i.e., the regime boundaries. The relevant subset, indicated by the wavy double lines in the Figure, is given by all COMs to the right of the intersection point then. Hence the detectable modes are seen to be those satisfying $L_p \leq L_{COM}^+(k) \approx L_{COM}^-(k)$.

8.8.5. *Maximum size of patterns describable by effective field theory*

We interpret $L_{COM}^+(k)$ as the physical length scale at which Γ_k, for the same value of k, provides the best description possible in terms of an effective field theory. According to both detector models considered, the proper wavelengths L_p of the modes that carry the quantum geometry satisfy $L_p \leq L_{COM}^+(k)$.

Next let us construct superpositions like (8.114) of such modes only, and let us investigate the $\vec{x}$-dependence of the functions $A(\eta, \vec{x})$ that can be fabricated in this manner. We consider in particular a situation in which the distribution of the field amplitude $A(\eta, \vec{x})$ over the time slice features a distinguished proper length scale, which we denote by L.

Now, since the proper wavelengths L_p of all partial waves contributing to $A(\eta, \vec{x})$ are bounded above by $L_{COM}^+(k)$, it follows that also typical features displayed by $A(\eta, \vec{x})$

cannot be too much larger than $L^+_{\mathrm{COM}}(k)$. This implies that *the $\vec{x}$-dependence of physically detected field configurations $A(\eta, \vec{x})$ cannot display geometric structures with proper sizes L that are (much) larger than $L^+_{COM}(k)$:*

$$L \;\le\; L^+_{\mathrm{COM}}(k) \approx L^-_{\mathrm{COM}}(k) \qquad \text{(Models A and B)} \qquad (8.121)$$

This upper bound is one of our main results. It expresses a limitation of the cutoff mode's resolving power under realistic experimental conditions. However, contrary to the Euclidean example reviewed in the Introduction, here the COMs are "blind" towards too large, rather than too small structures.

Let us furthermore recall that, by (8.106), $L^+_{\mathrm{COM}}(k)$ is a much shorter length scale than the Hubble radius if $\lambda(k) \ll 1$, which holds true on virtually all scales. This implies that our upper bound on the proper size of observed patterns, L, is much more stringent than a conceivable (causality-related) bound given by the Hubble scale:

$$L \le L^{\pm}_{\mathrm{COM}}(k) \ll L_H(k) \qquad \text{(Models A and B)} \qquad (8.122)$$

Concerning the physical interpretation of the running Hubble radius $L_H(k)$, the following remark is in order.

8.8.6. *Causality and k-dependent Hubble radius*

In the classical theory, the sphere with Hubble radius $L^0_H \equiv H^{-1}_0$ is known to represent an event horizon of de Sitter space. Note however that the classical concept of horizons relies upon a notion of causality whose physical underpinning are the laws of light propagation, and that in an effective theory it cannot be taken for granted that those are the same still [258].

Nevertheless, being a massless particle, the on-shell photon with zero virtuality is unaffected by the virtuality cutoff at $k > 0$ which we consider here. As a consequence, we can establish the same notion of causality on each one of the k-dependent dS$_4$ spacetimes (8.72). Thereby the Hubble length $L_H(k) \equiv H(k)^{-1}$ acquires the interpretation of a horizon distance in the effective theory for the scale k, too.

Summarizing, if we define the "quantum geometry of 3D space" to encompass all spatial structures that are detected by time independent, or by harmonically oscillating physical fields, then the proper size L of those observed geometric patterns which are describable by a certain effective theory Γ_k is bounded above by $L^+_{\mathrm{COM}}(k)$. Typically the latter length scale is significantly shorter than the radius of the de Sitter horizon for the same RG parameter k.
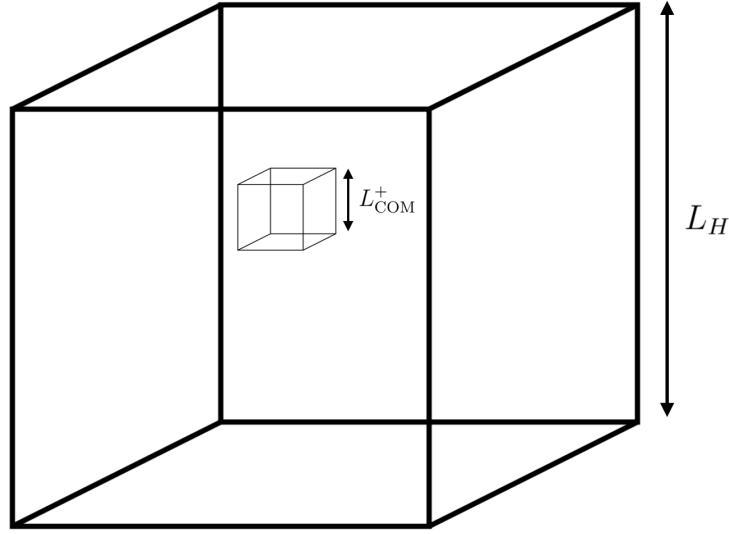
FIGURE 8.10. Filling a Hubble volume with L^+_{COM}-size cubes. Every such cube contains a single evaluation point $\vec{x}_j$ of the function $A(\vec{x})$, see Subsection 8.8.7.

8.8.7. *Coherence length of Γ_k-describable detected structures*

The consequences of the above bound on the spatial proper lengths of the detected structures, describable by Γ_k, can be visualized in several ways. The following one prepares at the same time also the stage for a discussion of entropy-related aspects later on.

(1) Counting boxes. Let us fix an arbitrary time slice of de Sitter space at scale k, and let us furthermore consider a set of little cubic boxes in this 3D space whose physical, proper edge length is equal to $L^+_{\text{COM}}(k)$. Then, loosely speaking, all objects detected by the model detectors A or B would fit into such a box.

Now let us ask how many of those "COM boxes" in turn would fit into one Hubble volume, or more precisely, into a cube with physical edge length $L_H = H(k)^{-1}$, see Figure 8.10. According to eqs.(8.106) and (8.109), the number of COM boxes within a Hubble cube, $N_{\text{b}}(k) = \big(L_H(k)/L^+_{\text{COM}}(k)\big)^3$, is given by

$$N_{\text{b}}(k) = \frac{1}{(2\pi)^3} \left[\nu^+_{\text{COM}}(k)^2 - \frac{1}{4} \right]^{3/2} = \frac{1}{(2\pi)^3} \left[2 + \frac{3}{\lambda(k)} \right]^{3/2} \qquad (8.123)$$

The number N_{b} is of order unity for both $k \to 0$ and $k \to \infty$, while it assumes its maximum value $N_{\text{b}}^{\text{max}} \gg 1$ at the turning point $k = k_T$. With (8.110) we obtain

explicitly

$$N_{\text{b}}^{\text{max}} = N_{\text{b}}(k_T) \approx \left(\frac{\nu_{\text{COM}}^+(k)}{2\pi} \right)^3 \approx \frac{1}{(2\pi)^3} \left[\frac{4}{9}\, \varpi\, G_0\, \Lambda_0 \right]^{-3/4} \qquad (8.124)$$

Using the figures provided by real Nature for an illustration, $G_0\Lambda_0 \approx 10^{-120}$, we find that N_{b} can become as large as approximately

$$N_{\text{b}}^{\text{max}} \approx 10^{90}\,, \qquad (8.125)$$

which corresponds to the quantum number $\nu_{\text{COM}}^+(k_T) \approx 10^{30}$. Up to factors of order unity, the hierarchy between the Hubble and the COM scale comprises 30 orders of magnitude at the maximum:

$$L_{\text{COM}}(k_T) \approx 10^{-30}\, L_H(k_T) \approx 10^{-30}\, H_0^{-1}\,. \qquad (8.126)$$

For H_0 the Hubble parameter of the real Universe, this COM scale is in the range of millimeters.

We come back to the number N_{b} in Section 8.9 where we put it in a proper perspective.

(2) Fragmentation of space and a coherence length. For clarity, let us adopt the most "canonical" definition of a spatial geometry now, i.e., the strict time independence requested by Model A.

Then, for every given RG parameter k, the Γ_k-describable experiments ("detectors", "microscopes", ...) see only objects of size $L = L_{\text{COM}}^+(k)$ sharply. If the running of Γ_k, and hence $L_{\text{COM}}^+(k)$, happens to be slow, also objects with a typical proper size L slightly above, or slightly below $L_{\text{COM}}^+(k)$ might still yield a fairly sharp picture. However, generically, the image of spatial structures with size L will be strongly blurred if either $L \ll L_{\text{COM}}^+(k)$ or $L \gg L_{\text{COM}}^+(k)$.

In this precise sense, *the running proper length $L_{\text{COM}}^+(k)$ has the interpretation of a coherence length.* This coherence length is characteristic of the effective spatial geometry which pertains to a specific RG parameter value k.

It goes without saying that the existence of this distinguished length scale per se does not imply that the (vacuum) spacetimes obtained from Γ_k necessarily would show any regular or even periodic structure (like the above "cubulation", for example).

Nevertheless, our findings suggest a certain *fragmentation of the 3-dimensional space.* It should have the appearance of a patchwork consisting of many small patches with a size of about L_{COM}^+, or smaller. While physics and geometry within a patch is well described by one of the effective field theories $\{\Gamma_k\}_{k\geq 0}$, this is not the case for the entire patchwork.

In fact, the present spectral flow analysis leads to the following prediction for the vacuum dominated epochs of cosmology:

Since no effective theory describes coherent patches with $L \gtrsim L_{\mathrm{COM}}^{+}(k)$, and since the COM scale is bounded above, $L_{\mathrm{COM}}^{+}(k) \lesssim (2\pi/\nu_{\mathrm{COM}}^{+}(k_T))L_H(k)$ by (8.110), patterns actually observed in the Universe should display a maximum size which is significantly smaller than the Hubble radius, the scale ordinarily considered the ultimate bound.

8.9. The scale history of quantum de Sitter space

In this section we change our vantage point and describe quantum de Sitter space from an evolutionary perspective in which the RG parameter k plays a role which is almost on a par with the conformal time η. Among other insights, this "scale history" will lead to a better understanding of the spatial fragmentation encountered above.

While until now the focus was on distances smaller than the coherence length, $L < L_{\mathrm{COM}}^{+}$, our interest now lies in the regime $L_{\mathrm{COM}}^{+} < L < L_H$, that is, in the entire "patchwork" rather than the individual patches.

8.9.1. *Dimensionless logarithmic variables*

To display the scale structure of quantum de Sitter space with its entangled η and k dependencies in a transparent way, the use of dimensionless logarithmic variables is helpful. We introduce in particular:

(1) The logarithmic RG time:

$$\tau(k) \equiv -\ln\left(\frac{k}{k_T}\right) \tag{8.127}$$

Its normalization is such that τ is negative (positive) for all scales above (below) the turning point $k = k_T$. Along a RG trajectory with natural orientation, the decreasing dimensionful $k = +\infty \cdots, k_T, \cdots 0$ corresponds to an increasing $\tau = -\infty \cdots, 0, \cdots +\infty$ then.[9]

(2) The logarithmic Hubble length:

$$\mathscr{L}_H(\tau) \equiv \ln\left(\frac{L_H(k)}{L_H^0}\right) = -\ln\left(\frac{H(k)}{H_0}\right) = -\frac{1}{2}\ln\left(\frac{\Lambda(k)}{\Lambda_0}\right) \tag{8.128}$$

---

[9]The definition (8.127) differs by a sign from the convention used in [221].

The normalization is relative to $L_H^0 \equiv H_0^{-1}$. Exploiting that $\Lambda(k_T) = 2\Lambda_0$ by (3.61), we obtain for the logarithmic Hubble length in terms of $\lambda(\tau) \equiv \lambda(k(\tau))$:

$$\mathscr{L}_H(\tau) = \tau - \frac{1}{2} \ln\left(2\frac{\lambda(\tau)}{\lambda_T} \right) \tag{8.129}$$

Since the running Hubble parameter now can be written as

$$H(k) = H_0 \, e^{-\mathscr{L}_H(\tau)} \, , \tag{8.130}$$

it is often convenient to express the scale factor $b_k(\eta) = (|\eta| \, H(k))^{-1}$ in the form

$$b_{k(\tau)}(\eta) = b_0(\eta) \, e^{\mathscr{L}_H(\tau)} \tag{8.131}$$

where $b_0(\eta) = (|\eta| \, H_0)^{-1}$ denotes the scale factor at $k = 0$, and $k(\tau) = k_T e^{-\tau}$.

(3) The logarithmic proper length related to a coordinate distance Δx with associated proper distance $L_{\Delta x}(k, \eta) = b_k(\eta) \, \Delta x$:

$$\mathscr{L}_{\Delta x}(\tau, \eta) \equiv \ln\left(\frac{L_{\Delta x}(k, \eta)}{L_H^0} \right) . \tag{8.132}$$

Taking advantage of (8.131), eq.(8.132) can be cast in the form

$$\mathscr{L}_{\Delta x}(\tau, \eta) = \mathscr{L}_H(\tau) - \ln\left(|\eta| \right) + \ln(\Delta x) \tag{8.133}$$

In the case of comoving wavelengths $\Delta x = \Delta x_p \equiv 2\pi/|\vec{p}|$ we also use the notation

$$\mathscr{L}_p(\tau, \eta) \equiv \mathscr{L}_{\Delta x_p}(\tau, \eta) = \mathscr{L}_H(\tau) + \ln\left(\frac{2\pi}{p|\eta|} \right) . \tag{8.134}$$

The benefit of the logarithmic representation (8.133) is that it nicely disentangles the three factors which determine a proper length, namely the scale-dependent size of the Universe as a whole, $\mathscr{L}_H(\tau)$, the moment of time, η, and most importantly, certain data characteristic of the actual physical system under consideration, which is Δx here.

In various discussions it will be convenient to combine the latter two contributions to $\mathscr{L}_{\Delta x}$ into a new quantity, ξ, letting

$$\mathscr{L}_{\Delta x}(\tau, \eta) = \mathscr{L}_H(\tau) + \xi, \qquad \text{with} \qquad \xi \equiv \ln\left(\frac{\Delta x}{|\eta|} \right) . \tag{8.135}$$

Since $\frac{\Delta x}{|\eta|} = H_0 \, L_{\Delta x}(\eta, k = 0)$, we see that

$$\xi \equiv \ln\left(\frac{L_{\Delta x}(\eta, k = 0)}{L_H^0} \right) = \mathscr{L}_{\Delta x}(\tau = \infty, \eta) \tag{8.136}$$

is a logarithmic measure for the IR proper length, i.e., the one ascribed to Δx by the $k = 0$ metric.

(4) The logarithmic transition lengths,

$$\mathscr{L}^{\pm}_{\mathrm{COM}}(\tau) \equiv \ln\left(\frac{L^{\pm}_{\mathrm{COM}}(k)}{L^0_H}\right) , \tag{8.137}$$

where $L^{\pm}_{\mathrm{COM}}(k)$ is the proper wavelength of the cutoff modes by the time they leave the harmonic regime.

8.9.2. *Results (piecewise linear approximation)*

(1) Cosmological constant. The dimensionless cosmological constant $\lambda(\tau) \equiv \lambda(k(\tau))$, simplified as in (3.66), reads in dependence on the logarithmic RG time:

$$\lambda(\tau) = \begin{cases} \lambda_* = \lambda_T \cosh(2\hat{\tau}) & \text{for} & \tau \in (-\infty, \hat{\tau}) & (8.138) \\ \lambda_T \cosh(2\tau) & \text{for} & \tau \in (\hat{\tau}, +\infty) & (8.139) \end{cases}$$

Here $\hat{\tau} = \tau(\hat{k})$ denotes the "moment" of RG time at which the trajectory passes from the UV fixed point regime to the semiclassical regime. Explicitly, from (3.60) with (3.64),

$$\hat{\tau} = -\frac{1}{4}\ln\left(\frac{\lambda_*^2}{\varpi}\right) + \frac{1}{4}\ln(G_0\Lambda_0) . \tag{8.140}$$

Since we assume $G_0\Lambda_0 \ll 1$ and $\lambda_*, \varpi = O(1)$, the first term on the RHS of (8.140) is negligible usually.[10] Hence, $\hat{\tau}$ is always negative, and $|\hat{\tau}| = -\hat{\tau} \gg 1$ when $G_0\Lambda_0$ is tiny. Recall also that the function $\lambda(k)$ given in (3.66) is continuous at $k = k_T$. Therefore the same is true for $\lambda(\tau)$ at $\tau = \hat{\tau}$, and this explains the second equality of (8.138).

The semiclassical part of $\lambda(k)$ is invariant under the *duality transformation* $k \mapsto k^{\sharp} = k_T^2/k$. In terms of the RG time τ, the latter assumes the form of a reflection symmetry $\tau \mapsto \tau^{\sharp} = -\tau$, since

$$\tau(k^{\sharp}) = -\tau(k) . \tag{8.141}$$

Being an even function of τ, the cosmological constant in (8.139) is invariant clearly.

The IR scale $\hat{k}^{\sharp}$, at which $\lambda(k)$ equals λ_* again, corresponds to the very "late" RG time

$$\hat{\tau}^{\sharp} \equiv \tau(\hat{k}^{\sharp}) = -\tau(\hat{k}) \equiv -\hat{\tau} \gg 1 . \tag{8.142}$$

It is the negative of the "early" time at which the trajectory departed from the fixed point.

---

[10]The example $G_0\Lambda_0 = 10^{-120}$ yields $\hat{\tau} = -30\ln(10) \approx -69$.
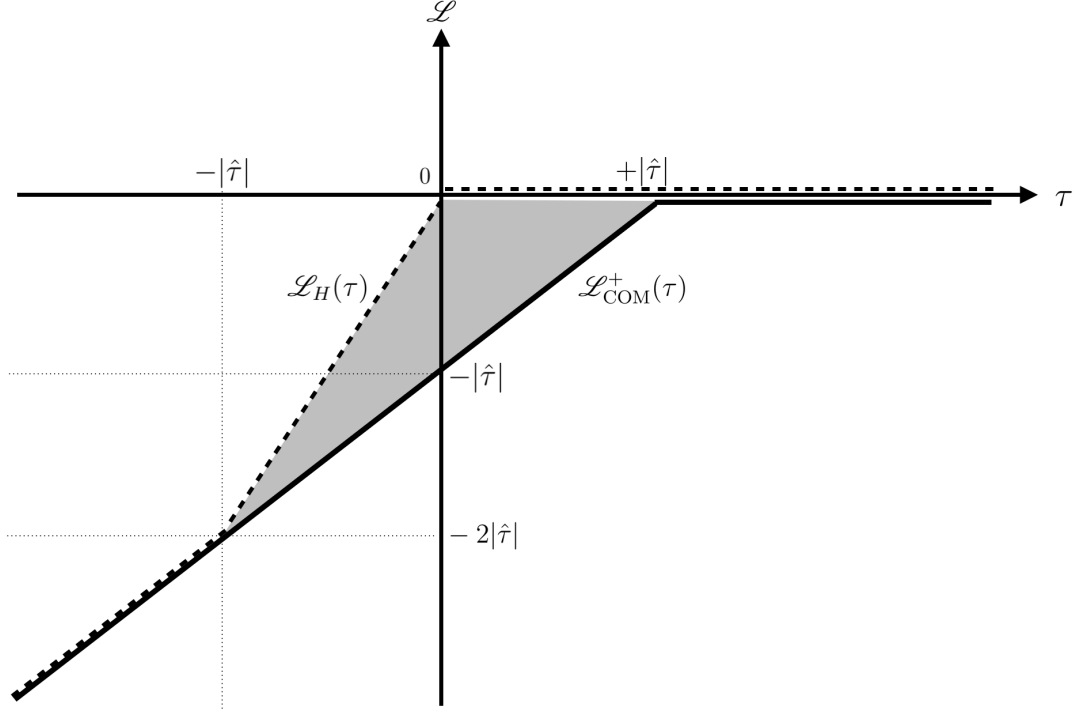
FIGURE 8.11. Schematic scale history of the Hubble length (dashed line) and the COM proper transition wavelength for spacelike modes (solid line) at fixed conformal time. The shaded triangle contains sub-Hubble & super-COM proper length scales.

(2) Hubble scale. For the Hubble radius we obtain from the caricature trajectory:

$$\mathscr{L}_H(\tau) = \begin{cases} \tau - \dfrac{1}{2}\ln\left(2\cosh(2\hat{\tau})\right) \approx \hat{\tau} + \tau & \text{for} \quad \tau \in (-\infty, \hat{\tau}) & (8.143) \\[2mm] \tau - \dfrac{1}{2}\ln\left(2\cosh(2\tau)\right) & \text{for} \quad \tau \in (\hat{\tau}, +\infty) & (8.144) \end{cases}$$

The second equality of (8.143) is valid if $|\hat{\tau}| \gg 1$, which we assume satisfied in the following. Leaving relatively short transition periods aside, the following three "scale epochs" can be distinguished in the course of the τ-evolution:

$$-\infty < \tau < -|\hat{\tau}|: \quad \mathscr{L}_H(\tau) \approx \hat{\tau} + \tau \qquad (8.145)$$

$$-|\hat{\tau}| < \tau \lesssim 0: \quad \mathscr{L}_H(\tau) \approx 2\tau \qquad (8.146)$$

$$\tau \gtrsim 0: \quad \mathscr{L}_H(\tau) \approx 0 \qquad (8.147)$$

In Figure 8.11 the behavior of $\mathscr{L}_H(\tau)$ is sketched in this piecewise linear approximation.

(3) COM scale. For the simplified RG trajectory, eq.(8.137) yields in the spacelike case

$$\mathscr{L}^+_{\text{COM}}(\tau) = \tau - \frac{1}{2}\ln\left(1 + \frac{2}{3}\lambda(\tau)\right) + \hat{\tau} + \ln\left(2\pi\sqrt{\frac{\lambda_*}{3}}\right) \qquad (8.148)$$

with $\lambda(\tau)$ given by (8.138), (8.139). To see the main features of (8.148), we continue to neglect constants of order unity relative to $\hat{\tau}$, and to employ the piecewise linear approximation. The resulting graph of the function $\mathscr{L}^+_{\text{COM}}(\tau)$ is depicted schematically in Figure 8.11. Its characteristic behavior in the various scale epochs is as follows:

$$-\infty < \tau \lesssim +|\hat{\tau}|: \qquad \mathscr{L}^+_{\text{COM}}(\tau) \approx \hat{\tau} + \tau \qquad (8.149)$$

$$\tau \gtrsim +|\hat{\tau}|: \qquad \mathscr{L}^+_{\text{COM}}(\tau) \approx 0 \qquad (8.150)$$

In particular, at the turning point scale, $\mathscr{L}^+_{\text{COM}}(0) \approx \hat{\tau} \equiv -|\hat{\tau}|$.

To obtain a particularly clear qualitative picture, and to avoid a clutter of inessential constants in the formulas, we are going to mostly utilize the piecewise linear approximations (8.145)-(8.147) and (8.149), (8.150) from now on, rather than the exact relations.

(4) Sub-Hubble & super-COM distances. Spatial proper lengths $\mathscr{L}_{\Delta x}(\tau, \eta)$ above the COM transition scale, yet below the Hubble radius at the respective scale, $\mathscr{L}_H(\tau)$, are of special interest. We refer to them as "sub-Hubble & super-COM" lengths. In Figure 8.11, they constitute a triangle-shaped region on the $\mathscr{L}$-τ plane.

8.9.3. *Leaving and re-entering the harmonic regime*

In 3D space, let us consider an arbitrary comoving (i.e., coordinate) distance Δx. Its precise physical role, if any, is irrelevant for now. The essential point is only that the associated proper length $\mathscr{L}_{\Delta x}(\tau, \eta) = \mathscr{L}_H(\tau) + \xi(\Delta x, \eta)$ depends on both the ordinary conformal time η and the RG time τ.

Note that by eq.(8.135) the auxiliary quantity $\xi \equiv \ln(\Delta x/|\eta|)$ is independent of the RG time. As a result, the τ-dependence of $\mathscr{L}_{\Delta x}$ parallels exactly that of $\mathscr{L}_H$, as the two functions differ by an additive constant only.

(1) Let us consider several distances $\Delta x', \Delta x'', \cdots$ at one and the same arbitrary, but fixed ordinary time, $\eta = \eta_1$, say. Hence we can faithfully represent them by means of their respective ξ-values, $\xi' = \ln(\Delta x'/|\eta_1|), \xi'' = \ln(\Delta x''/|\eta_1|), \cdots$. The τ-evolution of the related proper lengths $\mathscr{L}_{\Delta x'}, \mathscr{L}_{\Delta x''}, \cdots$ is fully determined by that of the Hubble parameter then. As shown in Figure 8.12, the graphs of all functions $\tau \mapsto \mathscr{L}_{\Delta x', \Delta x'', \dots}(\tau, \eta_1)$ run everywhere parallel to $\mathscr{L}_H$, with differing offsets $\xi', \xi'', \cdots$ though.

(2) Figure 8.12 also illustrates that qualitatively different scale histories $\tau \mapsto \mathscr{L}_{\Delta x}(\tau, \eta_1)$ can occur, depending on the size (ξ-value) of the structure under consideration:

(i) Very large structures, like the one with $\xi = \xi'$ in the Figure, are super-Hubble sized at all RG times, $\mathscr{L}_{\Delta x'}(\tau) > \mathscr{L}_H(\tau), \forall \tau \in (-\infty, +\infty)$.
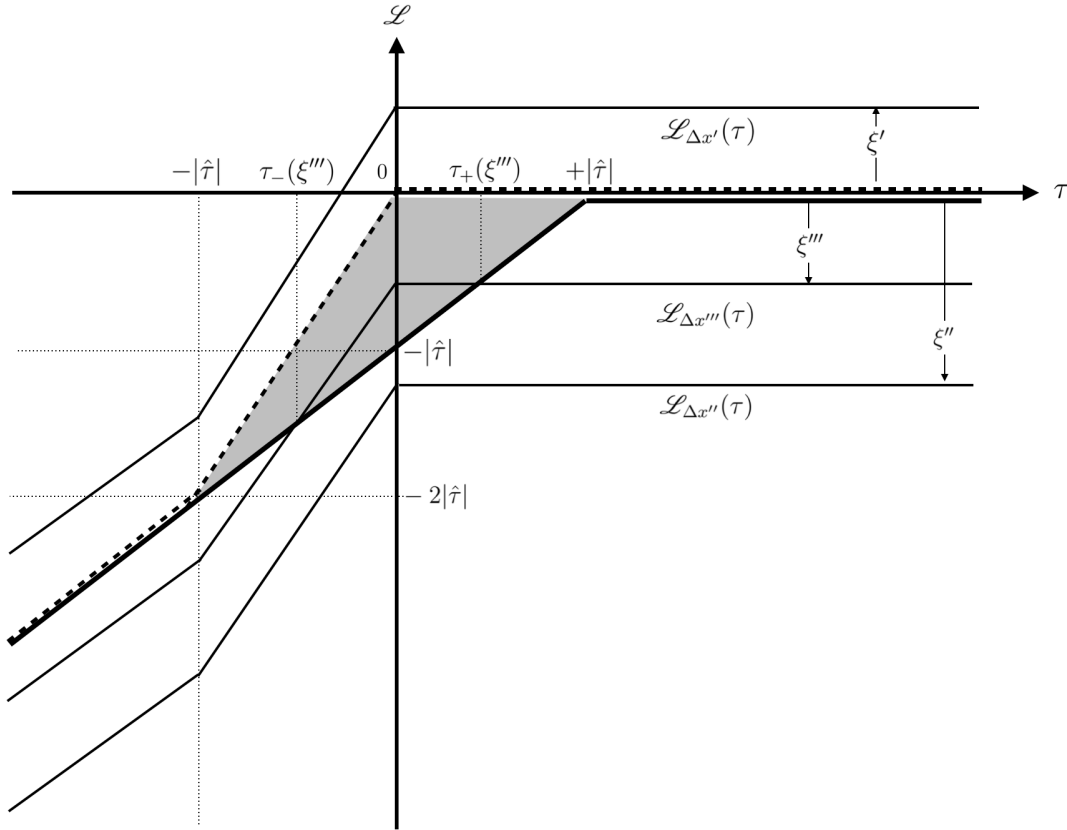
FIGURE 8.12. Scale history analogous to Figure 8.11. The proper length scales $\mathscr{L}_{\Delta x}(\tau)$ of various geometric structures are depicted in addition; they evolve parallel to $\mathscr{L}_H(\tau)$, having different offsets ξ though. The structure with comoving size $\Delta x'''$ is seen to go super-COM between $\tau_-(\xi''')$ and $\tau_+(\xi''')$, respectively. It always remains of sub-Hubble size, however.

(ii) Very small structures, such as the one having $\xi = \xi''$ in Figure 8.12, are sub-COM sized at any RG time, meaning that $\mathscr{L}_{\Delta x''}(\tau) < \mathscr{L}_{\mathrm{COM}}^+(\tau)$, $\forall \tau \in (-\infty, +\infty)$.

(iii) Structures of intermediate magnitude ξ''' can be sub-Hubble on all scales, and simultaneously sub-COM sized on all scales *except* for a finite interval of RG times during which they go "super-COM":

$$\mathscr{L}_{\mathrm{COM}}^+(\tau) < \mathscr{L}_{\Delta x'''}(\tau) < \mathscr{L}_H(\tau), \qquad \forall \tau \in \left[\tau_-(\xi'''), \tau_+(\xi''')\right] \subset \left[-|\hat{\tau}|, +|\hat{\tau}|\right] \quad (8.151)$$

In Figure 8.12, the proper lengths of all such structures pass through the shaded triangle pertaining to the sub-Hubble & super-COM length scales. At the times $\tau_-(\xi''')$ and $\tau_+(\xi''')$ the structures, respectively, exit and re-enter the range of the sub-COM scales, i.e., the harmonic regime.

(3) Exit and re-entry times $\tau_\pm(\xi''')$. Let us compute the RG times τ_- and τ_+, respectively, at which a certain geometric structure of the third type leaves and re-enters the harmonic regime. We can characterize the structure by, equivalently, its coordinate

length $\Delta x'''$, the proper length $\mathscr{L}_{\Delta x'''}(\tau, \eta)$, or its ξ-parameter $\xi''' = \ln\left(\Delta x'''/|\eta|\right)$, the ordinary time η being held fixed.

The exit/entry RG time is determined by the requirement $\mathscr{L}_{\Delta x}\left(\tau_\pm(\xi'''), \eta\right) = \mathscr{L}^+_{\mathrm{COM}}\left(\tau_\pm(\xi''')\right)$. Upon using (8.135) it reads

$$\mathscr{L}^+_{\mathrm{COM}}\left(\tau_\pm(\xi''')\right) - \mathscr{L}_H\left(\tau_\pm(\xi''')\right) = \xi''' \ . \tag{8.152}$$

Note that the sought-for RG times $\tau_\pm$ depend on Δx and the usual time η only via the combination $\Delta x/|\eta| \equiv e^\xi$. The condition (8.152) could easily be solved exactly after inserting eq.(8.144), as well as eq.(8.148) with (8.139). For our purposes the piecewise linear approximations (assuming $|\hat\tau| \gg 1$) are sufficient though, yielding for $\xi''' \in (-|\hat\tau|, 0)$:

$$\tau_-(\xi''') \approx -|\hat\tau| - \xi''' \quad \in \ (-|\hat\tau|, 0) \tag{8.153}$$

$$\tau_+(\xi''') \approx +|\hat\tau| + \xi''' \quad \in \ (0, +|\hat\tau|) \tag{8.154}$$

There are no solutions to the exit/entry condition if $\xi''' < -|\hat\tau|$ or $\xi''' > +|\hat\tau|$.

(4) Histories sub-Hubble & super-COM at RG time τ_1. Now we change the perspective and, rather than ξ, freeze the RG time, at $\tau = \tau_1 \in \left[-|\hat\tau|, |\hat\tau|\right]$, say. In this case the question is: Which scale histories $\tau \mapsto \mathscr{L}_{\Delta x}(\tau, \eta) \equiv \mathscr{L}_H + \xi$, when evaluated at $\tau = \tau_1$, yield a proper length in the sub-Hubble & super-COM regime? Concretely, what are the ξ-values that characterize such histories?

The answer is easily read off from Figure 8.12: At the RG time $\tau = \tau_1$, precisely those scale histories of proper lengths are in the sub-Hubble & super-COM range which possess a parameter value $\xi \equiv \xi^{\mathrm{subH}}_{\mathrm{superC}}$ in the interval

$$\xi^{\mathrm{subH}}_{\mathrm{superC}} \in [\xi_{\min}(\tau_1), 0] \quad \text{where} \quad \xi_{\min}(\tau_1) \equiv -|\hat\tau| + |\tau_1| \tag{8.155}$$

In particular, $\xi_{\min}(-|\hat\tau|) = 0 = \xi_{\min}(|\hat\tau|)$, and $\xi_{\min}(0) = -|\hat\tau|$, as it should be.

8.9.4. *Space probed by sub-Hubble & super-COM waves*

In the previous subsection, Δx was a generic distance or length without a particular physical interpretation. Now we are more specific and interpret $\Delta x \equiv 2\pi/|\vec{p}|$ as the spatial coordinate period of the function $e^{i\vec{p}\cdot\vec{x}}$. Thereby we regard the latter as a member of the 3D momentum eigenbasis

$$\mathscr{B} \equiv \left\{ e^{i\vec{p}\cdot\vec{x}}, \ \vec{p} \in \mathbb{R}^3 \right\} \ . \tag{8.156}$$

Importantly, we shall now consider those plane waves in their own right, that is, unrelated to any $\Box$-eigenfunctions or COMs. This allows us in particular to admit proper wavelengths larger than L^+_{COM}.

Taking advantage of the basis $\mathscr{B}$ we can expand any functions over a fixed time slice:

$$A(\vec{x}) = \int_{\mathbb{R}^3} d^3p \; a(\vec{p}) \, e^{i\vec{p}\cdot\vec{x}} \; . \qquad (8.157)$$

By eq.(8.135), every basis element $e^{i\vec{p}\cdot\vec{x}}$ comes with an associated ξ-value. It parametrizes the comoving and physical period lengths, and the comoving wave number by, respectively,

$$\Delta x = \frac{2\pi}{|\vec{p}|} = |\eta| \, e^{\xi}, \qquad \mathscr{L}_{\Delta x}(\tau,\eta) = \mathscr{L}_H(\tau) + \xi \, , \qquad p = \frac{2\pi}{|\eta|} \, e^{-\xi} \, . \qquad (8.158)$$

It should be kept in mind that henceforth the ordinary time is considered frozen at some arbitrary given value η.

(1) Sets of 3D plane waves. In a self-explaining notation, it is natural to decompose the 3D plane wave basis $\mathscr{B}$ as follows:

$$\mathscr{B} = \mathscr{B}_{\text{subC}}(\tau) \; \cup \; \mathscr{B}_{\text{superC}}^{\text{subH}}(\tau) \; \cup \; \mathscr{B}^{\text{superH}}(\tau) \qquad (8.159)$$

In this order, the three subsets comprise exponentials having proper wavelengths in the ranges $\mathscr{L}_{\Delta x} < \mathscr{L}_{\text{COM}}^{+}$, $\mathscr{L}_{\text{COM}}^{+} \leq \mathscr{L}_{\Delta x} \leq \mathscr{L}_H$, and $\mathscr{L}_{\Delta x} > \mathscr{L}_H$, respectively.

The decomposition (8.159) depends on the RG time τ (and on η). Figure 8.12 shows that $\mathscr{B}_{\text{superC}}^{\text{subH}}(\tau)$ is non-empty for $\tau \in \left[-|\hat{\tau}|, |\hat{\tau}| \right]$ only.

On such scales, the plane waves in the subsets $\mathscr{B}_{\text{subC}}(\tau)$, $\mathscr{B}_{\text{superC}}^{\text{subH}}(\tau)$, and $\mathscr{B}^{\text{superH}}(\tau)$, in this order, are characterized by the following ξ-intervals:

$$\xi \in \left(-\infty, \, \xi_{\min}(\tau) \right), \quad \xi \in \left[\xi_{\min}(\tau), \, 0 \right], \quad \text{and} \quad \xi \in \left(0, \, +\infty \right) . \qquad (8.160)$$

Here $\xi_{\min}(\tau) \equiv -|\hat{\tau}| + |\tau|$, see eq.(8.155).

The equivalent intervals for the coordinate wave numbers $p = |\vec{p}|$ of the exponentials in the respective sets are, again in the same order,

$$p \in \left(\frac{2\pi}{|\eta|} e^{|\hat{\tau}|-|\tau|}, \, +\infty \right), \quad p \in \frac{2\pi}{|\eta|}\left[1, \, e^{|\hat{\tau}|-|\tau|} \right], \quad \text{and} \quad p \in \left(0, \, \frac{2\pi}{|\eta|} \right) . \qquad (8.161)$$

In writing down (8.160) and (8.161) we relied again on the piecewise linear approximation.

In Figure 8.12, the basis elements in $\mathscr{B}_{\text{superC}}^{\text{subH}}(\tau)$ are precisely those that have physical wavelengths $\mathscr{L}_{\Delta x}(\tau,\eta)$ which are inside the shaded triangle at the respective RG time τ.[11]

(2) The span of sub-Hubble & super-COM plane waves. The class of functions $A(\vec{x})$ which can be expanded in terms of basis elements *from $\mathscr{B}_{\text{subC}}(\tau)$ alone*

---

[11]We omit the primes on Δx from now on.

were discussed already in the context of $\Box$-eigenmodes in the harmonic regime and the A/B-models.

Next we are going to explore the spatial properties of quantum de Sitter space on *physical distance scales between the COM and the Hubble scale.*

It is therefore natural to ask about the properties of those functions which can be constructed by superposing plane waves *from $\mathscr{B}_{\mathrm{superC}}^{\mathrm{subH}}(\tau)$ alone.* At the RG time τ, they are given by the Fourier integrals

$$A(\vec{x}) = \int_{|\vec{p}| \in [p_1,\, p_2]} \mathrm{d}^3 p \; a(\vec{p}) \, e^{i\vec{p}\cdot\vec{x}} , \tag{8.162}$$

$$[p_1, p_2] \equiv \frac{2\pi}{|\eta|} \left[1 , \, e^{|\hat{\tau}| - |\tau|} \right] , \tag{8.163}$$

whose τ-dependent range of contributing momenta projects on *plane waves of the sub-Hubble & super-COM brand.*

Inspired by the methodology of non-commutative geometry [61, 391], we expect that the space of functions defined by (8.162), (8.163) reflects properties of the "quantum manifold" the functions are defined upon, in this case quantum de Sitter space[12] on length scales between L_{COM}^+ and L_H. As we saw in the previous section, this regime is a terra incognita for the effective field theory.

(3) The information content of $A(x)$. It will prove instructive to ask how much information can be "stored" in functions of the form (8.162), or what amounts to the same, how much information is needed in order to uniquely specify a function A within the class (8.162).

We would like to quantify the information contents by the number $\mathcal{N}$ of points $\vec{x}_j, j = 1, \cdots, \mathcal{N}$, at which a given $A(\vec{x})$ must be evaluated in order to identify the function unambiguously. If $\mathcal{N}$ such evaluations are needed, the entire information carried by the function A is encoded in the array of complex numbers $\left(A\left(\vec{x}_j\right), j = 1, \cdots, \mathcal{N} \right) \in \mathbb{C}^{\mathcal{N}}$.

Equivalently, it should be possible to identify a unique function A from the class (8.162) if we are given the same number of Fourier coefficients, $\left(a(\vec{p}_j), j = 1, \cdots, \mathcal{N} \right)$, so that we can replace the $\vec{p}$-integral in (8.162) by a discrete Fourier sum over momenta with $|\vec{p}_j| \in [p_1, p_2]$.

To make this counting and reconstruction well defined we discretize the $\vec{p}$-spectrum by defining $A(\vec{x})$ over a compact domain, namely a huge 3-dimensional ball B^3 within

---

[12]Recall that in our approach the "quantum" property of spacetime resides in its scale dependence, not in modified geometric properties of the underlying smooth manifold at fixed τ.

the η-slice. Assuming a large radius, very many discrete momenta will lie in the interval (8.163).

Then, by standard statistical mechanics, the sought-for number $\mathcal{N}$ of independent (distinguishable) functions $A(\vec{x})$ is obtained by integrating the measure

$$\frac{1}{(2\pi)^3} \prod_{k=1}^{3} \mathrm{d}p_k \wedge \mathrm{d}x^k \tag{8.164}$$

over the respective volumes in coordinate and momentum space. In an expanding universe one must be careful though not to confuse comoving and physical quantities: The measure (8.164) applies if, *either*, p_k and x^k are both comoving (aka, coordinate) quantities, *or*, p_k and x^k are both physical (aka, proper) quantities.

8.9.5. $\mathcal{N}(\tau)$: *derivation*

At this point we decide to evaluate $\mathcal{N}$ by integrating over comoving variables[13] at fixed η and τ, whence

$$\mathcal{N} = \left(\frac{1}{2\pi}\right)^3 \int_{|\vec{p}|\in[p_1,\,p_2]} \mathrm{d}^3 p \int_{\text{coord-Vol}[B^3]} \mathrm{d}^3 x\ . \tag{8.165}$$

Concretely, we are going to consider a ball B^3 in position space whose *proper* radius is given by the Hubble length, $L^{\text{prop}} = L_H(k)$, implying the proper volume

$$\text{proper-Vol}[B^3] = \left(\frac{4\pi}{3}\right) \left(\frac{1}{H(k)}\right)^3 \tag{8.166}$$

Its *coordinate* radius and volume, on the other hand, are $L^{\text{coord}} = L_H(k)/b_k(\eta) = |\eta|$, since $b_k(\eta)^{-1} = |\eta|H(k)$, and

$$\text{coord-Vol}[B^3] = \left(\frac{4\pi}{3}\right) |\eta|^3\ . \tag{8.167}$$

Note that while the proper Hubble volume is scale- but not time-dependent, the coordinate Hubble volume is time-, but not scale-dependent.

Thus eq. (8.165) turns into

$$\begin{aligned} \mathcal{N} &= \left(\frac{1}{2\pi}\right)^3 \times 4\pi \int_{p_1}^{p_2} \mathrm{d}p\, p^2 \times \left(\frac{4\pi}{3}\right) |\eta|^3 \\ &= \left(\frac{4\pi}{3}\right)^2 \left(\frac{|\eta|}{2\pi}\right)^3 \left[p_2^3 - p_1^3\right] \end{aligned} \tag{8.168}$$

---

[13]It can be verified that consistently employing *proper* integration variables leads to the same result. See also ref. [392, 393] for a similar calculation on de Sitter space, as well as a discussion of its subtleties.

Obviously, $\mathcal{N}$ is time dependent for generic wave numbers p_1 and p_2. But if we now insert the interval boundaries in question, (8.163), the conformal time is seen to drop out completely, yielding for all $\tau \in \left[-|\hat{\tau}|, +|\hat{\tau}|\right]$,

$$\mathcal{N}(\tau) = \left(\frac{4\pi}{3}\right)^2 \left(e^{3|\hat{\tau}|}e^{-3|\tau|} - 1\right) \tag{8.169}$$

This is our final result for the number of independent 3D plane waves having physical wavelengths in the sub-Hubble & super-COM regime. Remarkably enough, this number is completely independent of the ordinary time η.

(1) $\mathcal{N}(\tau)$: upper bound. While time independent, the number $\mathcal{N}$ does depend on the RG time. The behavior of $\mathcal{N} = \mathcal{N}(\tau)$ is consistent with Figure 8.12: $\mathcal{N}(\tau)$ vanishes for $\tau \leq -|\hat{\tau}|$, it increases between $\tau = -|\hat{\tau}|$ and $\tau = 0$, reaches its maximum at $\tau = 0$ then, thereupon decreases for τ between $\tau = 0$ and $\tau = +|\hat{\tau}|$, and finally vanishes again for all $\tau \geq +|\tau|$.

Importantly, the number $\mathcal{N}(\tau)$ is bounded above. Assuming, as always, that $|\hat{\tau}| \gg 1$, the upper bound, its maximum value $\mathcal{N}_{\mathrm{max}} = \mathcal{N}(0)$, is given by

$$\mathcal{N}_{\mathrm{max}} = \left(\frac{4\pi}{3}\right)^2 e^{-3\hat{\tau}} = \left(\frac{4\pi}{3}\right)^2 \left(\frac{\hat{k}}{k_T}\right)^3 \tag{8.170}$$

Note that $\mathcal{N}(\tau)$ is largest at the RG time when the trajectory runs through its turning point, $\tau = 0$. Making use of (8.140) we can express (8.170) more explicitly as[14]

$$\mathcal{N}_{\mathrm{max}} = \left(\frac{4\pi}{3}\right)^2 \left(G_0 \, \Lambda_0\right)^{-3/4} \tag{8.171}$$

It is interesting to observe that the value of $\mathcal{N}_{\mathrm{max}}$ is controlled by the dimensionless product $G_0\Lambda_0$ only, and that the latter appears with a characteristic exponent $(-3/4)$. Comparable counts on the basis of Euclidean 4-spheres would yield the exponent (-1) instead [270, 271].

(2) $\mathcal{N}(\tau)$ vs. $N_{\mathrm{b}}(k)$. Comparing (8.171) to (8.149), we observe that $\mathcal{N}_{\mathrm{max}}$ agrees basically with the maximally possible number of COM boxes in a Hubble volume, $N_{\mathrm{b}}^{\mathrm{max}}$, which we computed in Subsection 8.8.7 along different lines. Up to factors of order unity,

$$\mathcal{N}_{\mathrm{max}} \approx N_{\mathrm{b}}^{\mathrm{max}} \approx [G_0 \, \Lambda_0]^{-3/4} . \tag{8.172}$$

For the example of $G_0\Lambda_0 = 10^{-120}$, say, $\mathcal{N}_{\mathrm{max}} \approx N_{\mathrm{b}}^{\mathrm{max}} \approx 10^{90}$.

---

[14]Note that strictly speaking (8.140) would yield $e^{-\hat{\tau}} \equiv \hat{k}/k_T = \left[\varpi \, G_0\Lambda_0/\lambda_*^2\right]^{-1/4}$. However, consistency requires to approximate $e^{-\hat{\tau}} \approx [G_0\Lambda_0]^{-1/4}$ here, since in the derivation of (8.170) we always neglected the factors of order unity multiplying $G_0\Lambda_0 \ll 1$.

Furthermore it is easily checked that, within the approximations, the number of boxes equals the number of independent functions on *all* scales even: $N_b(k(\tau)) = \mathcal{N}(\tau)$.

8.9.6. *Interpretation and summary*

Next, we analyze and interpret the results obtained in the previous subsection. At the same time, we put them in the broader context of our earlier findings, which we also briefly summarize here.

(1) Granularity of space. We set out to study functions expandable in the sub-basis $\mathscr{B}^{\text{subH}}_{\text{superC}}(\tau)$ in order to learn about the properties of quantum de Sitter space between the COM and the Hubble scale. Such properties are *not* described by any single Γ_k-based effective theory.

(i) At every fixed RG time τ, we found that the span of $\mathscr{B}^{\text{subH}}_{\text{superC}}(\tau)$ comprises $\mathcal{N}(\tau) \leq \mathcal{N}_{\max} < \infty$ independent functions A. Hence a certain $A \in \text{Span } \mathscr{B}^{\text{subH}}_{\text{superC}}(\tau)$ is fully characterized by the values which it assumes at $\mathcal{N}(\tau)$ evaluation points $\{\vec{x}_j\}$. As a consequence, the information carried by a field $A \in \text{Span } \mathscr{B}^{\text{subH}}_{\text{superC}}(\tau)$, at the scale τ, amounts to a vector of complex numbers $\left(A(\vec{x}_1), A(\vec{x}_2), \cdots, A(\vec{x}_{\mathcal{N}(\tau)})\right) \in \mathbb{C}^{\mathcal{N}(\tau)}$, with $\mathcal{N}(\tau)$ given in eq.(8.169).

(ii) Spatial geometric structures of de Sitter space involving length scales between L^+_{COM} and L_H, should they exist, must be described by functions $A \in \text{Span } \mathscr{B}^{\text{subH}}_{\text{superC}}(\tau)$. As a result, *the state space related to possible sub-Hubble & super-COM structures is contained in* $\mathbb{C}^{\mathcal{N}(\tau)}$.

This suggests to interpret the function $\tau \mapsto \mathcal{N}(\tau)$ as a scale-dependent, yet time independent measure of the largest possible structural complexity or geometric fineness quantum de Sitter space can display at the respective scale. In fact, it is natural to regard $\mathcal{N}$ as (the negative of) a certain kind of entropy.

(iii) In Subsection 8.8.7, along a different line of reasoning, we used arguments from effective field theory and two natural detector models to demonstrate that on quantum de Sitter space coherent geometric structures, features that are describable by Γ_k for some k, can exist only if their typical proper size does not exceed $L^+_{\text{COM}}(k)$.

We were led to the picture that *the 3D time slices of quantum de Sitter space are split up in L^+_{COM}-sized coherent domains ("boxes")*. While physics within a given domain is describable by some Γ_k, this is not possible for the patchwork of many coherent domains, such as all those that make up a Hubble volume.

For the time being we have no information about a distinguished shape of the coherent domains, if any. For visualization purposes we assumed them to be little cubic boxes.

We found that $N_b(k)$ of them can be placed within one Hubble-size cube, the number $N_b(k)$ being given by eq.(8.123). (It goes without saying though that the shapes of the domains and the Hubble volume are irrelevant here; we consider the regime $N_b \gg 1$ and neglect pre-exponential $O(1)$ factors such as those that would distinguish cubes from spheres, say.)

(iv) The results obtained in the present section corroborate the picture in **(iii)** of a fragmented 3D time slice which splits up in many L_{COM}^+-size, coherent fragments. These results rely directly on the resolving power of plane waves in the sub-Hubble & super-COM regime, while earlier on the latter regime had only been approached from the sub-COM side.

In particular it turned out that the number of independent plane waves $\mathcal{N}(\tau)$, obtained in (8.169) of the present section, coincides with the number of coherent fragments contained in a Hubble volume, $N_b(k)$, found in Subsection 8.8.7. This counting confirms that the boxes of the first approach, and the special class of plane waves employed in the second, actually hint at one and the same phenomenon: The time slices of quantum de Sitter space have a fragmented, granular structure, the grains being constituted by small coherent domains, meaning that within each of them physics and spacetime geometry are well described by one of the effective field theories $\{\Gamma_k\}_{k \geq 0}$.

(2) Interpretation of the entropy uncovered. Given the equivalence of the two approaches, it is natural to relate the boxes of the first approach, in a one-to-one manner, to the evaluation points $\{\vec{x}_j | \ j = 1, \cdots, \mathcal{N}(\tau)\}$ that we can choose freely in the second. The values of some function $A \in \text{Span } \mathcal{B}_{\text{superC}}^{\text{subH}}(\tau)$ at those points are sufficient to reconstruct it, and to find $A(\vec{x})$ for all $\vec{x} \in \mathbb{R}^3$, i.e., everywhere on the time slice.

By this choice, every coherent domain contains one, and only one, point $\vec{x}_j$. In the visualization of Figure 8.10, for example, we can think of $\vec{x}_j$ as the center of the small cube with edge length $L_{COM}^+(k)$. This illustrates the following fact which is generally true:

Functions $A \in \text{Span } \mathcal{B}_{\text{superC}}^{\text{subH}}(\tau)$ assign on average one complex number to every coherent domain, and this is just the largest amount of information that can be encoded in a function of this class.

(i) Since all plane waves in $\mathcal{B}_{\text{superC}}^{\text{subH}}(\tau)$ possess proper wavelengths above L_{COM}^+, it is clear that the information or entropy they carry can have nothing to do with the *internal* structure of the coherent domains. It rather relates to the patchwork of domains making up a Hubble volume *as a whole*.

(ii) The numbers $\mathcal{N}(\tau)$ and N_b quantify a novel "inter-domain entropy", as opposed to the (familiar) "intra-domain entropy". The inter-domain entropy is perfectly finite; both at very early and late RG times ($|\tau| > |\hat{\tau}|$) it vanishes identically even.

Since a typical patch has many internal states, its description requires more than a single complex number. Therefore, the intra-domain entropy of one patch is usually much bigger than the average inter-domain entropy per patch, which is of order unity. The relative smallness of the inter-domain entropy suggests that *there should exist no extended coherent structures on length scales between L_{COM}^{+} and L_H.*

(3) A cautionary remark. It should not be forgotten that the spectral flow analysis presented here made essential use of the assumed *vacuum domination* of the cosmological evolution. Above all else it is valid for pure gravity. In the case of matter coupled gravity, it applies only under the condition that the matter term $8\pi G(k)\langle T_{\mu\nu}\rangle_k$ which, in principle, is present in the effective Einstein equation (8.71), is negligibly small in comparison to the $\Lambda(k)$ term.

In everyday life this condition is violated usually. There the relevant gravitational fields are almost entirely due to scale independent, and large, matter energies and stresses. Therefore, the above fragmentation phenomena cannot be observed in this environment.

8.10. THE CMBR PHOTONS: MORE THAN AN ANALOGY?

One may wonder whether the picture of quantum spacetime that we have drawn so far, while still rudimentary, can be matched already against the cosmology of the real Universe. In this regard the following point deserves being mentioned perhaps.

(1) If we model the present accelerating phase of the Universe by a de Sitter spacetime, the observed cosmological constant yields the order of magnitude estimate $G_0\Lambda_0 \approx 10^{-120}$ for this all-decisive integration constant. If we furthermore assume, as always, that the output of the RG equations, $\varpi, \lambda_*, \cdots$, are numbers of order unity, then we are led to consider a Type IIIa trajectory with a turning point located at $g_T \approx \lambda_T \approx 10^{-60}$, and visited at the RG time $k_T \approx 10^{-30} m_{\text{PL}} \approx (10\ \mu\text{m})^{-1}$.

At this scale, the COM quantum number, as well as the number of sub-Hubble & super-COM plane waves, assume they respective maxima:

$$\nu_{\text{COM}}(k_T) \approx 10^{30}, \qquad \mathcal{N}_{\text{max}} \approx 10^{90} \tag{8.173}$$

Furthermore, eq.(8.109) predicts a proper COM coherence length at the turning point which is in the range of micro-meters:

$$L_{\text{COM}}^{+}(k_T) \approx \left(10^{30} H_0\right)^{-1} \approx \left(10^{-30} m_{\text{Pl}}\right)^{-1} \approx 10\ \mu\text{m} \tag{8.174}$$

Now, the emerging picture of about 10^{90} milli- or micro-meter size coherent fragments which are fitted into one Hubble volume is strikingly reminiscent of the CMBR which

pervades the observed (late, Λ-dominated) Universe. This thermal photon gas has a black body spectrum at a temperature $T_{\text{CMBR}} \approx 2.73$ K whose spectral radiance in wavelength peaks at about $\lambda_{\text{peak}} \approx 1.06$ mm. Given our liberal approximations, this length agrees basically with the smallest occurring COM scale, eq.(8.174).

(2) To illuminate the deeper analogy, will recall that for thermal photons both the total number density N/V, and the entropy density $\mathcal{S}/V$, are proportional to T^3. Their ratio is the universal constant $\mathcal{S}(T,V)/N(T,V) = 2\pi^4 k_B/45\zeta(3)$. It assigns to each photon a temperature independent entropy of about 3.6 k_B on average, or equivalently an information of $3.6/\ln(2) \approx 5.2$ bits.

The energy density of the CMBR photons, like that of all other forms of matter is irrelevant for the cosmic expansion at late times. It is essentially Λ-driven, and this matches precisely the assumption underlying the spectral analysis.

As for the entropy of the present Universe, the photons *are* relevant, however. Within a Hubble volume, the total entropy equals roughly

$$\mathcal{S} \approx 10^{90} \ k_B \ , \tag{8.175}$$

and this entropy stems almost entirely from the CMBR photons.

It is striking that (within the approximations) the thermodynamic entropy (8.175), in units of k_B, agrees precisely with the inter-domain entropy $\mathcal{N}_{\text{max}} = N_b(k_T)$ which we obtain. Fundamentally, the latter has a statistical mechanics character, being the result of counting plane waves and boxes, and having the interpretation of the entropy due to the fragmented structure of space.[15]

(3) The analogy between the CMBR and the fragmented $\vec{x}$-space of a de Sitter universe goes even further. Considering a thermal photon gas, the standard formulas for N/V and Wien's displacement law can easily be combined in order to eliminate the temperature, and to express the total number of photons in the following suggestive fashion:

$$N(T,V) = \frac{V}{[1.27 \ \lambda_{\text{peak}}(T)]^3} \ . \tag{8.176}$$

This relation shows that, on the average, each photon can claim a small volume of order λ_{peak}^3 for itself. If visualized as a cube, its edge length at $T = 2.73$ K equals $1.27 \ \lambda_{\text{peak}} \approx 1.35$ mm.

Clearly this size reminds us again of the milli- or micro-meter length scale set by $L_{\text{COM}}^+(k_T)$. And even more than that, the way of dividing up the total volume into coherent subsystems, each one carrying a rather small, universal share of the total

---

[15]Note that for an order of magnitude estimate it makes no difference whether we evaluate $\mathcal{N}$ and N_b at $k = 0$ or at $k = k_T$. After all, Λ_0 and $\Lambda(k_T) = 2\Lambda_0$ are very close on the logarithmic scale.

entropy or information (5.2 bits here), is strongly reminiscent of the spectral flow based picture of quantum de Sitter space which we have drawn above.

This analogy seems to motivate a scenario in which the CMBR traces out coherent grains of space. It remains to be seen whether the similarity is purely coincidental or there is a deeper reason for it. We hope to come back to this question elsewhere.

CHAPTER 9

Scattering amplitudes in de Sitter spacetime

Executive summary. We present a covariant framework to compute scattering amplitudes and potentials in a dS background. In this setting, we compute the potential of a graviton-mediated scattering process involving two very massive scalars. Although the obtained scattering potential reproduces the Newtonian potential at short distances, on Hubble-size length scales it is affected by the constant curvature: effectively, it yields a repulsive force at sub-Hubble distances. This can be attributed to the expansion of the dS universe. Beyond the dS horizon, the potential vanishes identically. Hence, the scattering amplitude unveils the geometric properties of dS spacetime in a novel and nontrivial way.

Further we generalize the formalism to non-minimally coupled scalar fields in quadratic gravity in a de Sitter background. We study this scattering amplitude in the adiabatic limit, and construct the Newtonian potential. At short distances, the flat-spacetime Yukawa potential is reproduced, while the curvature gives rise to corrections to the potential at large distances. Beyond the Hubble radius, the potential vanishes identically, in agreement with the causal structure of de Sitter spacetime. For sub-Hubble distances, we investigate whether the modifications to the potential reproduce Modified Newtonian Dynamics.

What is new? All results of this chapter represent novel research results.

Based on: References [RF4], [RF5].

Plan of this Chapter. Firstly, we show by means of a Gedankenexperiment which is the experimental applicability of our investigation. We then start with a warmup computation, reviewing the derivation of the Yukawa potential from the scattering amplitude in the Born approximation.

Thereafter, we present the new computation of the scattering amplitude of a tree-level graviton-mediated scalar-to-scalar scattering process in a de Sitter background in both classical GR and QuadG. We describe how to compute the Feynman diagram in a curved background geometry. The tree-level scattering amplitude associated to the diagram in Figure 6.3 is obtained by contracting the graviton-scalar-scalar 3-point vertices with the graviton propagator.

In Section 9.4, we compute the adiabatic expansion of the scattering amplitude. We study the properties of the amplitude in this limit. For simplicity, we will limit ourselves to the case $d = 4$ only. By performing a Fourier transform, we can compute the scattering potential in the adiabatic limit. Furthermore, we consider its phenomenological properties. To this end, we will regard the potential as the source of a Newtonian force. This allows to straightforwardly interpret the potential in terms of potential energies, and the scaling of the force with distance. The main result of this section is the scattering potential presented in Section 9.5. We discuss its short- and long-distance properties by considering full QuadG. We expect to recover the Newtonian potential (including the Yukawa contributions due to higher curvature terms) for small radii and curvature modifications at large distances.

In order to reproduce a DM-like scenario in the spirit of the Modified Newtonian Dynamics, we mimic the additional mass density by modifying the potential such that one obtains an additional attractive force. We consider whether such a modification can arise from the obtained potential by an appropriate choice of higher derivative coupling constants. We distinguish four different regimes: pure GR, R^2-, C^2-gravity and QuadG.

The essentials of dS spacetime, introducing conventions, coordinates and curvature relations can be found in Appendix E. Details regarding the computation of the propagator in curved spacetime, commutation relations in constantly-curved spacetime and technical steps in order to evaluate the scattering amplitude in the adiabatic expansion are relegated to Appendix F.

The sections of this chapter have been extracted from the author's publications [RF4], [RF5].

9.1. Gedankenexperiment: Collision of Bunch–Davies waves

In this section, we will briefly discuss the interpretation of scattering amplitudes from the experimental or observational point of view. Scattering amplitudes represent a technical tool developed with the purpose to connect QFT and collider experiments. However, we previously mentioned, that due to the lack of a description of an S-matrix in QFT in curved spacetime, the generalization to possible collision experiments in general spacetimes has not been performed yet.

Thanks to our new findings related to the construction of a scattering amplitude in de Sitter spacetime in a fully covariant way, we can mimic the connection to experiments generally used in Minkowski spacetime. In this way we circumvent the lack of S-matrix elements in dS. For the sake of simplicity, here we will restrict the discussion

to GR interactions, considering in the gravitational action only the Einstein–Hilbert term (neglecting higher curvature interactions).

(1) In order to furnish an explicit "expression" for the scattering process encoded in $\mathcal{A}$, we can perform an adiabatic expansion of the fields in conformal coordinates.

(1a) Adiabaticity. In a cosmological context adiabaticity assumes that the curvature of spacetime is much smaller than the scales associated to the processes taking place in it, in this case the scattering process. Assuming that the mass of the particles involved is larger than the inverse Hubble length, is then a sufficient condition for adiabaticity.

(1b) Conformal coordinates. At the same time the conformally flat (aka spatially flat) metric is

$$\mathrm{d}s^2 = \frac{1}{(H\eta)^2}\left(-\,\mathrm{d}\eta^2 + \mathrm{d}\vec{x}^2\right)\ . \tag{9.1}$$

This covering is also called the expanding Poincaré patch. The expanding Poincaré patch has a peculiarity in its geometry. The spatial part of their metric has the conformal factor $1/(H\eta)^2$. Due to its presence, every wave experiences strong blue shift towards the past infinity patch.

(1c) Bunch–Davies waves. The Bunch–Davies waves are the wave functions solving to the wave equation in the expanding Poincaré patch. The Bunch–Davies vacuum instead is such a state that has no positive energy excitations at the past infinity of the expanding Poincaré patch. In fact near the boundary we can define what we mean by particle and what we mean by positive energy, because every momentum experiences infinite blue shift towards the past of the patch. Here, high energy harmonics are not sensitive to the comparatively small curvature of the background space and behave as if they are in flat space.

(1d) Accessible position space. Due to the spatial homogeneity of the conformally flat patch and also of the initial states that we consider, it will be natural to perform the Fourier transformation along the $\vec{x}$ directions. The explicit computation of the scattering amplitude will allow us to pass from momentum space to position space and to construct the scattering potential.

(2) The resulting picture is the following: two emitters emit heavy-mass Bunch–Davies waves, which scatter, giving rise to two outgoing waves. These outgoing waves can be in turn expanded in terms of Bunch–Davies waves, performing a heavy-mass expansion (see Figure 9.1).

(3) As discussed in the Introduction, the Newtonian potential passes experimental gravitational tests at small separations. Hence, for small separations between the emitters, we expect the resulting potential to agree with the Newtonian result. In fact, in
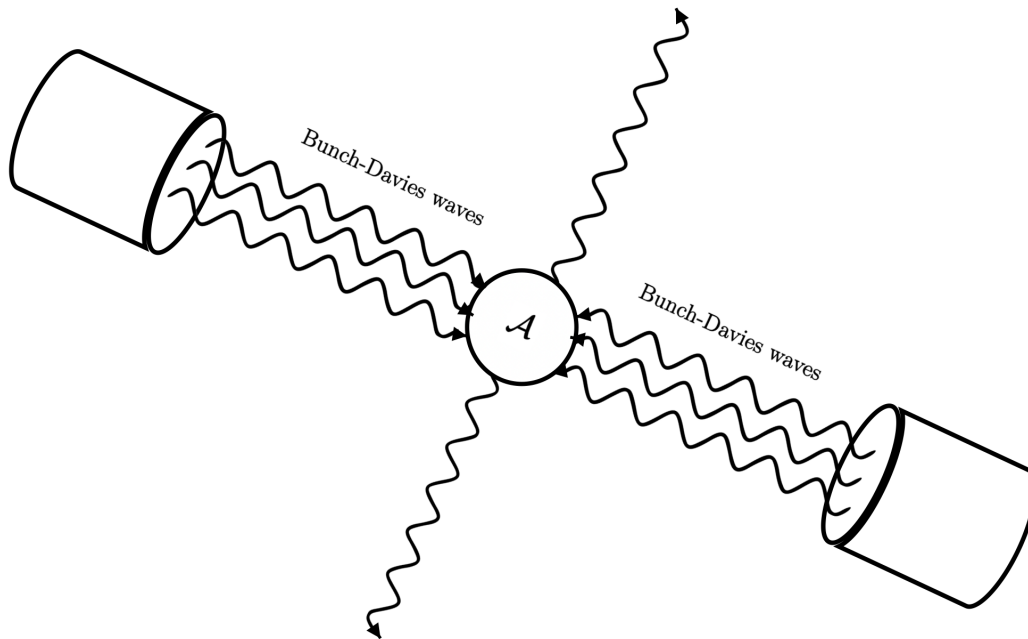
FIGURE 9.1. Gedankenexperiment: two emitters emit Bunch–Davies waves and they scatter. The scattering process is encoded in the scattering amplitude functional $\mathcal{A}$. The process gives wise to outgoing waves, which can be expanded themselves in Bunch–Davies waves.

this regime the expansion of the Bunch–Davies wave function reproduces the free wave function on Minkowski space.

More interestingly, we question whether the potential presents some modifications for larger separations due to the curvature of the background spacetime. In particular, these modifications could give rise to modification in the Newtonian force, possibly fitting the unexplained rotation profiles of galaxy curves.

Finally, de Sitter spacetime is known for its causal structure: particles separated by distances larger than the Hubble distance don't interact, being causally disconnected. Therefore, if the emitters are separated by distances larger than the Hubble radius, the potential should vanish, meaning that nothing can be observed. This would represent the substantial experimental manifestation of the de Sitter horizon.
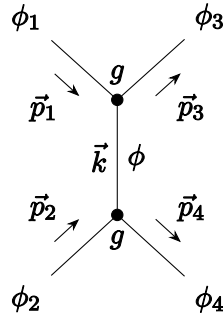
FIGURE 9.2. Tree-level scalar-to-scalar ϕ^3-scattering amplitude for the process $\phi_1\chi_2 \to \phi_3\chi_4$ (t-channel). Time flows from the left to the right.

9.2. WARMUP: THE YUKAWA POTENTIAL

Before constructing the scattering amplitude of a graviton mediated scalar-to-scalar process, we will set the stage and follow the standard derivation of the the Yukawa potential for a massive ϕ^3-scalar theory scalar-to-scalar scattering process in flat spacetime.

The Yukawa potential can be derived as the lowest order amplitude of the interaction of a pair of scalars. The Yukawa interaction couples them to another exchanged scalar field with the interaction term $g\,\phi^3$. The action of the three scalars then reads

$$S = \int \mathrm{d}^d x \, \left(\frac{1}{2}\partial_\mu\phi\partial^\mu\phi - \frac{m^2}{2}\phi^2 + g\,\phi^3 \right) \tag{9.2}$$

The scattering amplitude for two scalars, one with initial momentum p_1 and the other with momentum p_2, exchanging a scalar with momentum k (see Figure 9.2), is constructed applying the Feynman rules:

(1) For each vertex associate a factor of g with the amplitude; since this diagram has two vertices, the total amplitude will have a factor of g^2;

(2) The Feynman rule for a particle exchange is to use the propagator; the propagator for a scalar with mass m is $-\frac{4\pi}{k^2+m^2}$;

(3) Thus, we see that the Feynman amplitude for this interaction is nothing more than

$$V(k) = -g^2 \frac{4\pi}{k^2 + m^2} \overset{m\gg|\vec{k}|}{=} -g^2 \frac{4\pi}{|\vec{k}|^2 + m^2} \tag{9.3}$$

where in the last equality we have applied the so-called *Born approximation* and assumed that the mass is much greater than the exchanged 3-momentum.

This is seen to be the Fourier transform of the Yukawa potential. By examining its Fourier transform:

$$V(r) = \frac{g^2}{(2\pi)^3} \int e^{i\vec{k}\cdot\vec{r}} \frac{4\pi}{|\vec{k}|^2 + m^2} \, \mathrm{d}^3\vec{k} = -g^2 \frac{e^{-m\,r}}{r} \tag{9.4}$$

The potential is monotonically increasing in r and it is negative, implying that the force is attractive.

9.2.1. *Gravitational potential around flat spacetime*

In the following subsection we will extend this computation also to gravitational interactions [42] and sketch the derivation of the Newtonian potential, and to the Quadratic Gravity action. Here, both cases are treated in flat spacetime, the generalization to curved spacetime represents one of the objectives of this Project.

(1a) Newtonian potential. In [42] sketched how the Newtonian $1/r$-potential could be derived by performing the Born approximation to the following scattering process: they considered a two-to-two-scalars graviton mediated scattering amplitude. Due to the masslessness of the exchanged graviton, this resulted in a $1/r$ interaction potential.

(1b) Yukawa terms from Quadratic Gravity. Analogously, by studying the propagating modes corresponding to Quadratic Gravity around flat spacetime, the same sort of Yukawa terms should arise [394, 395]. Consider the four-derivative action (in the metric $\hat{g}_{\mu\nu}$) in 4 dimensions

$$S[\hat{g}] = \frac{1}{16\pi G} \int \mathrm{d}^d x \sqrt{-\hat{g}} \left(-2\Lambda + \hat{R} + \frac{\alpha_R}{6} \hat{R}^2 - \frac{\alpha_C}{2} \hat{C}_{\mu\nu\rho\sigma} \hat{C}^{\mu\nu\rho\sigma} \right). \tag{9.5}$$

By expanding this action around Minkowski space $\hat{g}_{\mu\nu} = \eta_{\mu\nu} + h_{\mu\nu}$ and choosing the de Donder gauge fixing, the action takes the form

$$S_{\mathrm{Mink}}[\hat{g}] = \frac{1}{16\pi G} \int \mathrm{d}^d x \sqrt{-\hat{g}} \left(-2\Lambda + \frac{1}{2} \left(h_{\mu\nu}^{\mathrm{TT}} \Box h^{TT,\mu\nu} + \partial_\mu \phi \partial^\mu \phi \right) \right. \tag{9.6}$$

$$\left. + \frac{1}{3\alpha_R} (\Box\phi)^2 - \frac{4}{3\alpha_C} \Box h_{\mu\nu}^{TT} \Box h^{TT,\mu\nu} \right).$$

where we used the decomposition of the field in terms of the transverse-traceless mode h^{TT} and the scalar trace mode $\phi = h_\mu^\mu$. From this action S_0 we can recognize in the scalar-mode propagator a massive contribution with $m^2 = \frac{1}{\alpha_R}$. As for the spin-2 part, there is an additional mass pole at $m^2 = \frac{1}{\alpha_C}$.

The related potential can be obtained by performing the Fourier transform. We obtain

$$V_{\mathrm{Mink}}(r) \propto G \left(-\frac{1}{r} - \frac{1}{3}\frac{1}{r}e^{-r/\sqrt{\alpha_R}} + \frac{4}{3}\frac{1}{r}e^{-r/\sqrt{\alpha_C}} \right) \tag{9.7}$$
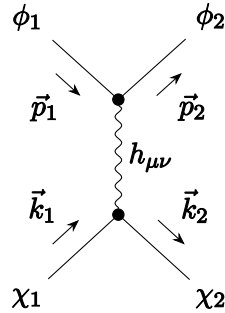
FIGURE 9.3. Tree-level graviton mediated scattering amplitude for the process $\phi_1 \chi_1 \to \phi_2 \chi_2$ (t-channel). Time flows from the left to the right.

The first term represents the Newtonian contribution, while the other two terms are the Yukawa potentials arising due to the presence of quadratic interactions.

Remark. It is important to emphasize, that the two additional Yukawa contributions appear with two opposite signs. The α_C term has a positive sign, meaning that it competes with the Newtonian contribution and is repulsive. Demanding that the potential should reproduce the Newtonian behavior at short distances will impose constraints on the value of α_C.

9.3. THE SCATTERING AMPLITUDE FUNCTIONAL

Having set the stage, we will now turn to the computation of a scattering amplitude. We will consider the graviton-mediated scattering of two particle species ϕ and χ. In flat spacetime, at tree level this amplitude is described by a single t-channel Feynman diagram, depicted in Figure 9.3. In this section, we generalize this Feynman diagram to dS spacetime by promoting propagators and vertices to noncommuting differential operators. Taking into account curvature contributions leads to the main result of this section, given in equations (9.26).

9.3.1. *Action*

Before we describe how to compute the scattering amplitude in dS spacetime, let us for concreteness first introduce the action. We will take an action that is a functional of the (dynamical) spacetime metric $\hat{g}$ and two scalar fields ϕ and χ. Furthermore, we employ the background field method, depending on the background metric $\bar{g}$.

(1) The action is then of the following form:

$$S = S_{\text{grav}}[\hat{g}] + S_{\text{gf}}[\hat{g}; \bar{g}] + S_{\text{sc}}[\phi, \hat{g}] + S_{\text{sc}}[\chi, \hat{g}]. \qquad (9.8)$$

Let us now explicitly formulate each contribution to the action. For the gravitational interaction S_{grav}, we take the four-derivative action

$$S_{\text{grav}}[\hat{g}] = \frac{1}{16\pi G} \int \mathrm{d}^d x \sqrt{-\hat{g}} \left(-2\Lambda + \hat{R} + \alpha_R \frac{d-2}{4(d-1)} \hat{R}^2 \right.$$
$$\left. - \alpha_C \frac{d-2}{4(d-3)} \hat{C}_{\mu\nu\rho\sigma} \hat{C}^{\mu\nu\rho\sigma} + \frac{1}{2(d-3)(d-4)} \alpha_E E_4 \right). \qquad (9.9)$$

Here, we have denoted by a hat those quantities that are defined with respect to the dynamical metric $\hat{g}$. For the time being, no specification of the sign of the cosmological constant Λ is required.

In (9.9), E_4 is the Euler density in four dimensions:

$$E_4 = \hat{R}^2 - 4\hat{R}_{\mu\nu}\hat{R}^{\mu\nu} + \hat{R}_{\alpha\beta\gamma\delta}\hat{R}^{\alpha\beta\gamma\delta}. \qquad (9.10)$$

For $d = 4$, the integral over E_4 is a topological invariant. Thus, for this dimension we set α_E to zero, since it will not contribute to any dynamical quantity. In a similar fashion, the C^2 and R^2 are non-dynamical for $d \leq 3$ and $d \leq 2$ dimensions, respectively. We therefore set the α_C and α_R couplings to zero in these dimensions, too. We have discussed how in flat spacetime, the α_R and α_C couplings induce massive spin-0 and spin-2 poles in the graviton propagator. We have chosen the normalization in such a way that in flat spacetime, α_R denotes the inverse mass of the spin-0 pole, while α_C denotes the inverse mass of the spin-2 pole [65].

(2) Next, we specify in (9.8) a de Donder type gauge-fixing action, necessary to obtain a well-defined graviton propagator:

$$S_{\text{gf}}[\hat{g}; \bar{g}] = -\frac{1}{16\pi G} \frac{1}{2\alpha_{\text{gf}}} \int \mathrm{d}^d x \sqrt{-\bar{g}} \, \bar{g}^{\mu\nu} \mathcal{F}_\mu[\hat{g}, \bar{g}] \mathcal{F}_\nu[\hat{g}, \bar{g}], \qquad (9.11)$$

where the gauge fixing operator is defined as

$$\mathcal{F}_\mu[\hat{g}, \bar{g}] = \delta_\mu^\beta \bar{g}^{\rho\sigma} \bar{\nabla}_\rho \hat{g}_{\sigma\beta} - \beta_{\text{gf}} \bar{g}^{\alpha\beta} \bar{\nabla}_\mu \hat{g}_{\alpha\beta}. \qquad (9.12)$$

Here the gauge fixing parameters α_{gf} and β_{gf} generalize the de Donder gauge, and allow to track gauge dependence explicitly. The Faddeev–Popov ghosts will not contribute to the scattering amplitude, for the reason that they do not couple to the scalar fields. The specific form of their action is therefore not needed for our purposes.

(3) Finally, the matter sector is given by non-minimally coupled massive scalar fields ϕ and χ, whose action takes the form

$$S_{\text{sc}}[\phi, \hat{g}] = -\frac{1}{2} \int \mathrm{d}^d x \sqrt{-\hat{g}} \, \phi \left(-\hat{\Box} + m_\phi^2 + \alpha_\phi \hat{R} \right) \phi. \qquad (9.13)$$

Here we have expressed the covariant d'Alembertian by $\hat{\Box} = \hat{g}^{\mu\nu}\hat{\nabla}_\mu\hat{\nabla}_\nu$.

9.3.2. *Vertices and propagators*

We will now describe how to compute the Feynman diagram from Figure 9.3 in the presence of a curved background metric $\bar{g}$ using the *operator method*.

(1) Propagators. The tree-level scattering amplitude associated to the diagram in Figure 9.3 is obtained by contracting the graviton-scalar-scalar 3-point vertices with the graviton propagator. These are computed by taking functional derivatives of the action S with respect to the fields, and projecting onto a solution to the equation of motion. For the scalar fields, the equation of motion is given by the (non-minimal) Klein–Gordon equation:

$$\hat{\Box}\phi = (m_\phi^2 + \alpha_\phi\hat{R})\phi\,, \qquad\qquad \hat{\Box}\chi = (m_\chi^2 + \alpha_\chi\hat{R})\chi\,. \qquad (9.14)$$

We observe that $\phi = \chi = 0$ is a solution to the equation of motion. The equation of motion for the metric is that of QuadG. We will look for dS solutions, which means that the constant Ricci scalar is the only nonzero curvature tensor. The Ricci scalar R is then given by the quadratic equation

$$R = \frac{2d}{d-2}\Lambda - \frac{d-4}{4(d-1)}\alpha_R R^2\,. \qquad (9.15)$$

We write

$$\hat{g}_{\mu\nu} = \bar{g}_{\mu\nu} + h_{\mu\nu}\,, \qquad (9.16)$$

where $\bar{g}_{\mu\nu}$ is a dS metric whose Ricci scalar $\bar{R}$ satisfies (9.15). Functional derivatives with respect to $\hat{g}$ are then conveniently computed by expanding around $\bar{g}_{\mu\nu}$.

(2) Vertices. By taking one functional derivative with respect to the metric and two with respect to the scalar fields, we obtain the three-point vertices. Subsequently, we set all fields to their background values. Thus, we define

$$\mathcal{T}^{(h\phi\phi)} = \frac{\delta^3 S}{\delta h \delta\phi\delta\phi}\bigg|_{\substack{\hat{g}=\bar{g}\\\phi=\chi=0}}, \qquad\qquad \mathcal{T}^{(h\chi\chi)} = \frac{\delta^3 S}{\delta h \delta\chi\delta\chi}\bigg|_{\substack{\hat{g}=\bar{g}\\\phi=\chi=0}}. \qquad (9.17)$$

The graviton propagator is given by the inverse of the two-point function:

$$\mathcal{G}^{(hh)} = \left[\frac{\delta^2 S}{\delta h \delta h}\right]^{-1}\Bigg|_{\substack{\hat{g}=\bar{g}\\\phi=\chi=0}}. \qquad (9.18)$$

Note that in order to make the inversion well-defined, it was necessary to include the gauge fixing action S_{gf} in (9.8).

We note that the three-point vertices are formally linear operators acting on a graviton fluctuation and two scalar fluctuations, whereas the graviton propagator is a linear operator acting on two graviton fluctuations.

9.3.3. *Computation of the propagator*

Here we will give a brief description of how to compute the graviton propagator.

(1) By general covariance, the propagator can be written as a linear combination of functions of $\Box$ and R, multiplied by an appropriate tensor structure mapping a symmetric rank-two tensor to a symmetric rank-two tensor. Since we are working in dS spacetime, we can choose a specific ordering of propagator functions and tensor structures. We choose to sort all propagator functions to the right, *i.e.*, we write

$$\mathcal{G}^{(hh)} = \sum_i \mathfrak{T}_i \mathcal{G}_i(\Box, R). \qquad (9.19)$$

Here, $\mathfrak{T}_i$ are six tensor structures that span a basis of operators on rank-two tensors,

$$[\mathfrak{T}_i]_{\mu\nu}{}^{\rho\sigma} \in \left\{ \delta^\rho_{(\mu}\delta^\sigma_{\nu)}, g_{\mu\nu}g^{\rho\sigma}, g_{\mu\nu}\nabla^{(\rho}\nabla^{\sigma)}, \nabla_{(\mu}\nabla_{\nu)}g^{\rho\sigma}, \nabla_{(\mu}\delta^{(\rho}_{\nu)}\nabla^{\sigma)}, \nabla_{(\mu}\nabla_{\nu)}\nabla^{(\rho}\nabla^{\sigma)} \right\}, \quad (9.20)$$

and the functions $\mathcal{G}_i$ are the propagator functions that are to be computed.

(2) We compute the propagator functions by demanding that

$$\left[\frac{\delta^2 S}{\delta h \delta h}\right]_{\mu\nu}{}^{\rho\sigma} \left[\mathcal{G}^{(hh)}\right]_{\rho\sigma}{}^{\alpha\beta} = \left[\mathbb{1}\right]_{\mu\nu}{}^{\alpha\beta} = \delta^\alpha_{(\mu}\delta^\beta_{\nu)}. \qquad (9.21)$$

(3) We compute this in practice by acting with this equation onto a symmetric fluctuation $h_{\alpha\beta}$. Next, we sort all occurrences of $\Box$ to the right, so that they act first on $h_{\mu\nu}$. In this way, together with the functions $\mathcal{G}_i$ they form differential operators with the appropriate index structure of an operator mapping symmetric two-tensors to symmetric two-tensors. Finally, we symmetrize all derivatives so that we map the result onto the basis (9.20). The propagator functions can then be read off; since their expressions are rather lengthy, we will not display them here, and refer to the Section F.2 for additional details.

9.3.4. *Computation of the amplitude functional*

It remains to compute the amplitude functional by contracting the propagator with the three-point operators.

(1) We bring the amplitude to a standard form by sorting the contracted derivatives. In order to commute the contracted derivatives with the propagator functions, we employ

the commutation techniques described in Section F.1. These techniques were developed in the context of affine gravity in [396]. Using integration by parts, we can manipulate on which scalar field each derivative acts. Finally, we can simplify the amplitude significantly by using the equation of motion (9.14) for the scalar fields.

The tree-level scattering amplitude associated to the diagram in Figure 9.3 is now obtained by contracting the three-point vertices with the graviton propagator. Rather than treating the amplitude as a multilinear operator acting on fields, it is convenient to contract the amplitude with four test fields:

$$
\mathcal{A}[\chi_1, \chi_2, \phi_1, \phi_2] = \int \mathrm{d}^d x \, \sqrt{-\bar{g}} \, \left[\mathcal{T}^{(h\chi\chi)}(\chi_1, \chi_2) \right]^{\mu\nu} \left[\mathcal{G}^{(hh)} \right]_{\mu\nu}{}^{\rho\sigma} \left[\mathcal{T}^{(h\phi\phi)}(\phi_1, \phi_2) \right]_{\rho\sigma}.
$$
(9.22)

Here the $\mathcal{T}^{(h\chi\chi)}(\chi_1, \chi_2)$ denotes the three-point vertex (9.17) acting on two test fields χ_1 and χ_2. The object $\mathcal{A}$ will be referred to as amplitude functional. Since (9.22) only contains objects in the dS background, to simplify the notation, we will omit the bar to denote the background metric and its derived objects.

Remark. At this point, the following remark is in order. In our operator method setup, we will regard the vertices and propagator as noncummuting differential operators, acting on scalar fields and metric fluctuations. This slightly formal point of view is in contrast to two common implementations of computing scattering amplitudes. First, in flat spacetime one has the Fourier transform at one's disposal. This allows to replace any derivatives with momenta reducing the scattering amplitude to a numerical quantity straightaway. In curved spacetime, such a Fourier transform is in general absent, and one has to take into account noncommutative derivatives. Secondly, the operator viewpoint has an advantage over a description in terms of position-space integral kernels. Regarding vertices and propagators as operators greatly simplifies composition and contraction of Feynman diagram elements, as opposed to computing lengthy integrals over dS spacetime.

(2) We computed the amplitude functional (9.22) using the `Mathematica` tensor algebra package `xAct` [397–400]. We used the procedure outlined in Subsection 9.3.3 to construct the graviton propagator and to sort and contract the covariant derivatives.

The amplitude functional (9.22) consists of covariant derivatives acting on the scalar fields, and scalar curvatures. The amplitude can be simplified using the on-shell conditions (9.14), integration by parts and the commutation techniques developed in [396].

(3) These methods can be used to bring the amplitude functional to a standard form. We will require that the amplitude functional is manifestly symmetric in the external fields. Since the vertices contain at most two uncontracted derivatives, we infer that the amplitude can be built using a scalar vertex structure, and a symmetric rank-two tensor vertex structure.

(3a) Scalar vertex. For the scalar vertex, it is convenient to define

$$V[\phi_1, \phi_2] = \left[m_\phi^2 - (d-1) \left(\alpha_\phi - \frac{d-2}{4(d-1)} \right) \Box \right] \phi_1 \phi_2 \,, \tag{9.23}$$

where the d'Alembertian acts on the product $\phi_1 \phi_2$.

(3b) Tensor vertex. For the tensor vertex we choose

$$T_{\mu\nu}[\phi_1, \phi_2] = (\nabla_{(\mu}\phi_1)(\nabla_{\nu)}\phi_2) - \frac{1}{d}g_{\mu\nu}(\nabla_\gamma\phi_1)(\nabla^\gamma\phi_2) - \alpha_\phi \left[\nabla_\mu\nabla_\nu - \frac{1}{d}g_{\mu\nu}\Box \right] \phi_1\phi_2 \,. \tag{9.24}$$

(3c) Rank-r ropagators. Finally, it will be convenient to define the operators

$$\mathcal{G}_r(\Box; \zeta) = \left(-\Box + \big(r(r+d-2) + \zeta\big)H^2 \right)^{-1} \,. \tag{9.25}$$

Here we define the Hubble parameter by $H^2 = \frac{R}{d(d-1)}$, following the conventions from Appendix E. We will refer to the operator $\mathcal{G}_r(\Box; \zeta)$ as propagator. The label r denotes the rank of the tensor it acts upon. We will refer to the dimensionless number ζ as the mass parameter; using slightly sloppy terminology, it parameterizes the graviton mass and can be related to the unitary irreducible representations of the graviton degrees of freedom [401–406].

9.3.5. *Result*

We will now present the resulting amplitude functional. This constitutes the first major result of this paper.

(1) Quadratic Gravity. The amplitude functional (9.22) is given by

$$\mathcal{A} = 16\pi G\, c(\alpha_R, \alpha_E) \left[-\frac{\zeta_C + d}{\zeta_C - \zeta_h} \Big(\mathcal{A}_2(\zeta_h) - \mathcal{A}_2(\zeta_C) \Big) \right.$$
$$+ \frac{1}{d(d-1)} \frac{\zeta_C}{\zeta_C - \zeta_h} \Big(\mathcal{A}_0(\zeta_h) - \mathcal{A}_0(\zeta_C) \Big) \tag{9.26}$$
$$\left. + \frac{1}{(d-1)(d-2)} \Big(\mathcal{A}_0(\zeta_h) - \mathcal{A}_0(\zeta_R) \Big) \right] \,.$$

Here we have defined the partial amplitude functionals

$$\mathcal{A}_0(\zeta) = \int \mathrm{d}^d x\, \sqrt{-g}\, V[\chi_1, \chi_2]\, \mathcal{G}_0(\Box; \zeta)\, V[\phi_1, \phi_2] \,, \tag{9.27}$$

$$\mathcal{A}_2(\zeta) = \int \mathrm{d}^d x\, \sqrt{-g}\, T_{\alpha\beta}[\chi_1, \chi_2]\, \mathcal{G}_2(\Box; \zeta)\, T^{\alpha\beta}[\phi_1, \phi_2] \,, \tag{9.28}$$

the dimensionless mass parameters

$$\zeta_R = \frac{1}{\alpha_R H^2} + \frac{1}{2}d(d-4) + \frac{\alpha_E}{\alpha_R}, \qquad\qquad \zeta_h = -2(d-1),$$

$$\zeta_C = \frac{1}{\alpha_C H^2} - d + \frac{1}{2}d(d-2)\frac{\alpha_R}{\alpha_C} + \frac{\alpha_E}{\alpha_C}. \tag{9.29}$$

and the coefficient

$$c(\alpha_R, \alpha_E) = \frac{1}{1 + \alpha_E H^2}\frac{\zeta_R - \frac{1}{2}d(d-4)}{\zeta_R + d}. \tag{9.30}$$

(2) Einstein-Hilbert gravity. We can present the result for the Einstein-Hilbert gravity case:

$$\mathcal{A} = 16\pi G \left[-\mathcal{A}_2(\zeta_h) + \frac{2}{d(d-2)}\mathcal{A}_0(\zeta_h) \right]. \tag{9.31}$$

Flat limit. Finally, we can perform a sanity check by taking the flat-spacetime limit by setting $R = 0$ and replacing all covariant derivatives by flat-spacetime derivatives. In this case the graviton masses z_i become actual masses which vanish, making the masslessness of the graviton manifest. Furthermore, going to momentum space, and introducing the standard Mandelstam variables, we find in $d = 4$

$$A = \frac{2\pi G}{3}\frac{-\left(s^2 - 4su + u^2 + 2(m_\phi^2 - m_\chi^2)^2\right) + (t - 2m_\phi^2)(t - 2m_\chi^2)}{t}. \tag{9.32}$$

This is in agreement with the standard result [407, 408].

9.3.6. *Discussion*

From the amplitude functional (9.26), the following observations can be made straight-away.

(1) Gauge independent. First, we note that the scattering amplitude does not depend on the gauge parameters α_{gf} and β_{gf}. This shows that the on-shell scattering amplitude is gauge fixing independent, conform the expectation that the scattering amplitude is related to an observable.

(2) Conformal coupling. Second, we note that the scalar vertex $V[\phi_1, \phi_2]$ vanishes for a conformally coupled scalar field $m_\phi = 0$, $\alpha_\phi = \frac{d-2}{4(d-1)}$. This greatly simplifies the scattering amplitude. For this reason, the conformally coupled scalar field has been studied widely [279, 280, 409–411].

(3) Massive propagators. Third, we observe that the amplitude (9.26) depends on three mass parameters ζ_h, ζ_R and ζ_C. In the limit $H \to 0$, these correspond to masses of zero, α_R^{-1} and α_C^{-1}, respectively. Hence, these mass parameters correspond to the massless graviton, and the spin-0 and spin-2 mass poles. At first inspection, the

negative value of ζ_h may seem to yield a tachyonic particle. However, it is important to keep in mind that due to the nonzero curvature the correspondence between the sign of the mass and the causal behavior is not obvious [401, 402].

(4) GR, R^2- and C^2-gravity. Fourth, it is now relatively simple to obtain the amplitudes of GR, R^2-gravity and C^2-gravity from this expression, by taking the following limits:

$$\text{GR:} \qquad \alpha_C \to 0, \alpha_R \to 0\,; \tag{9.33}$$

$$R^2\text{-gravity:} \qquad \alpha_C \to 0\,; \tag{9.34}$$

$$C^2\text{-gravity:} \qquad \alpha_R \to 0\,. \tag{9.35}$$

(5) Flat limit. Furthermore, we obtain the scattering amplitude in Minkowski spacetime by taking the limit

$$\text{Minkowski spacetime:} \qquad H \to 0\,. \tag{9.36}$$

Let us first consider the latter limit. We note that the mass parameters ζ_C and ζ_R go to infinity; we then find the following limits for the coefficients:

$$\lim_{H \to 0} c(\alpha_R, \alpha_E) = \lim_{H \to 0} \frac{\zeta_C + d}{\zeta_C - \zeta_h} = \lim_{H \to 0} \frac{\zeta_C}{\zeta_C - \zeta_h} = 1\,. \tag{9.37}$$

The propagators reduce to

$$\lim_{H \to 0} \mathcal{G}_0(\Box; \zeta_h) = \lim_{H \to 0} \mathcal{G}_2(\Box; \zeta_h) = -\Box^{-1}\,,$$

$$\lim_{H \to 0} \mathcal{G}_0(\Box; \zeta_C) = \lim_{H \to 0} \mathcal{G}_2(\Box; \zeta_C) = \left(-\Box + \alpha_C^{-1}\right)^{-1}\,, \tag{9.38}$$

$$\lim_{H \to 0} \mathcal{G}_0(\Box; \zeta_R) = \left(-\Box + \alpha_R^{-1}\right)^{-1}\,.$$

This is consistent with the amplitude found in [65, 276]. Inspecting the propagators (9.38), we see that the Minkowski spacetime amplitude corresponds to a massless spin-0 and spin-2 particle, corresponding to the graviton, and in addition a massive spin-0 particle of mass α_R^{-1} and a massive spin-2 particle of mass α_C^{-1} [65, 66].

In a similar fashion, we consider R^2- and C^2-gravity. Taking the limit $\alpha_R \to 0$ and $\alpha_C \to 0$, we find that ζ_R and ζ_C are linearly divergent, respectively. Hence, provided that the coefficients of the propagators remain finite, we conclude that the propagators $\mathcal{G}_0(\Box; \zeta_C)$ and $\mathcal{G}_2(\Box; \zeta_C)$ are suppressed in R^2-gravity, corresponding to a decoupling of the spin-2 Stelle particle, while in C^2-gravity the propagator $\mathcal{G}_0(\Box; \zeta_R)$ is suppressed, corresponding of a decoupling of the spin-0 massive particle from the theory. It remains to check that the coefficients of the propagator stay finite; we compute

$$\lim_{\alpha_R \to 0} c(\alpha_R, \alpha_E) = \frac{1}{1 + \alpha_E H^2}\,, \qquad \lim_{\alpha_C \to 0} \frac{\zeta_C + d}{\zeta_C - \zeta_h} = \lim_{\alpha_C \to 0} \frac{\zeta_C}{\zeta_C - \zeta_h} = 1\,. \tag{9.39}$$

This justifies the assertion that the massive particles decouple in R^2- and C^2-gravity.

9.4. SCATTERING AMPLITUDE IN THE ADIABATIC EXPANSION

We will now inspect the amplitude functional in more detail.

Since the amplitude functional is given by abstract differential operators on dS spacetime, it is not easy to draw conclusions about its physical properties. Therefore, we resort to expansion methods to turn (9.26) into a concrete numerical expression. We employ an expansion around the scalar masses $\mu = m/H = \infty$. This is a specific realization of the so-called adiabatic expansion [412–431]. This can be understood from the observation that an expansion around $\mu = \infty$ implies that the evolution of dS spacetime is much slower than the Compton frequency of the scalar fields.

This section is structured as follows. After a brief review of quantization of scalar fields, we will discuss the adiabatic of the scalar mode functions. We will then apply this expansion to the different objects in the amplitude functional. In Subsection 9.4.2, we describe the algorithm used to compute the adiabatic limit of the amplitude functional. The properties of the resulting amplitude are studied in Subsection 9.4.4. Section F.3 is devoted to the numerical techniques to obtain the amplitude in the adiabatic limit.

9.4.1. *Scalar field quantization and the adiabatic expansion*

In this section we compile several facts about the adiabatic expansion in dS. In general, adiabaticity assumes that the curvature of spacetime is much smaller than the scales associated to the processes taking place in it [412–431]. For quantum field theory in curved spacetime, the adiabatic expansion has the advantage that it does not rely on a strict definition of asymptotic states [332]. This is of particular interest in our work.

In the case of scalar particle scattering in dS spacetime, the adiabatic expansion is implemented concretely by performing an expansion in $\mu^{-1} = H/m$, where m is the mass of the scalar field and H the Hubble parameter. Essentially, in this expansion the Compton frequency of the scalar fields is assumed to be much larger than the expansion rate of dS spacetime.

(1) Quantization of scalars in Minkowski. Let us briefly remind ourselves of the quantization of scalar fields in Minkowski spacetime. The one-particle Hilbert space of a scalar field φ with mass m is constructed from solutions to the Klein–Gordon equation,

whose solutions are plane waves parametrized by the spatial momentum $\vec{p}$:

$$\varphi_{\vec{p}} = a_+ \, e_{\vec{p}} + a_- \, \overline{e_{\vec{p}}}, \qquad\qquad e_{\vec{p}}(t, x) = e^{i(-\omega_p t + \vec{p} \cdot \vec{x})}. \qquad (9.40)$$

Here, $a_\pm$ are constants and $\omega_p = \sqrt{p^2 + m^2}$, with $p = \|\vec{p}\|$ the standard Euclidean norm on spatial vectors, and denoted complex conjugation by a bar. The standard Minkowski vacuum is chosen by promoting a_+ to the annihilation operator $\hat{a}$ and a_- to the creation operator $\hat{a}^\dagger$, corresponding to particles with positive energy ω_p.

We point out two peculiar features of the Minkowski vacuum.

(1a) First, the choice of mode functions $e_{\vec{p}}$ is the unique choice of solutions to the flat-spacetime Klein–Gordon equation such that the general solution can be written as the sum of $e_{\vec{p}}$ and its complex conjugate, as in (9.40).

(1b) For the second property, we define the function

$$\tilde{\mathcal{E}}(m) := i \frac{\partial_t \varphi_{\vec{p}}}{\varphi_{\vec{p}}} = \omega_p \frac{a_+ e_{\vec{p}} - a_- \overline{e_{\vec{p}}}}{a_+ e_{\vec{p}} + a_- \overline{e_{\vec{p}}}}. \qquad (9.41)$$

We now note that in general, $\tilde{\mathcal{E}}$ has an essential singularity at $m = \infty$, due to the appearance of ω_p in the complex exponential. The exception to this when $a_+ = 0$ or $a_- = 0$, i.e., in the Minkowski vacuum. In that case, we have

$$\tilde{\mathcal{E}}(m) = \pm \omega_p = \pm \left(m + \frac{p^2}{2m} \right) + \mathcal{O}(m^{-2}), \qquad (9.42)$$

which is just the nonrelativistic expansion of the particle's energy. This analytic behavior allows to consistently take the heavy-mass limit as an expansion around $m = \infty$.

(2) Quantization of scalars in de Sitter space. We will now extend our analysis to de Sitter spacetime. The procedure runs completely analogous to flat-spacetime quantization. For convenience, we will use conformal coordinates. [1] First, we solve the Klein–Gordon equation in dS spacetime. Again, the solutions are labeled by $\vec{p}$, which is now promoted to a comoving momentum. The solution is well-known [316]:

$$\varphi_{\vec{p}} = a_+ h_{\vec{p},\mu} + a_- \overline{h_{\vec{p},\mu}}, \qquad\qquad h_{\vec{p},\mu}(\eta, \vec{x}) = \eta^{\frac{d-1}{2}} H^{(1)}_{i\sqrt{\mu^2 - \left(\frac{d-1}{2}\right)^2}}(-p\eta) e^{i\vec{p}\cdot\vec{x}}. \qquad (9.43)$$

Here we denoted by $H^{(1)}_\nu(z)$ the Hankel function of the first kind [437], and introduced the dimensionless quantity $\mu = m/H$. Note that for $z > 0$ and $\nu \in \mathbb{R}$, the Hankel function of the second kind is given by $H^{(2)}_{i\nu}(z) \propto \overline{H^{(1)}_{i\nu}(z)}$, which motivates the usual expansion in terms of Hankel functions of first and second kind. We now quantize by promoting a_+ to the annihilation operator $\hat{a}$ and a_- to the creation operator $\hat{a}^\dagger$. This

---

[1] Note that different foliations, which correspond to different boundary conditions, lead to different quantization schemes, see for instance [432–436]. Using different coordinate systems, the labeling of the quantum numbers and hence the unitary representation is different: these are related through a non-trivial transformation between the relative complete basis. In fact, the scattering amplitude and the potential are not affected by the choice of the foliation.

prescription leads to the Bunch–Davies vacuum [438]. This is the canonical generalization of the Minkowski vacuum, in the sense that $h_{\vec{p},\mu}$ reduces to a plane wave as $t \to -\infty$ (the Bunch–Davies boundary condition) [315, 316, 438], and in the limit $H \to 0$ [303].

(2a) Bunch–Davies as generalization of the Minkowski vacuum. In this work, we emphasize that the Bunch–Davies vacuum also generalizes the Minkowski vacuum concerning the properties mentioned above: it is the unique choice of mode functions such that the coefficients of $a_\pm$ are each other's complex conjugates, and are the unique choice of modes that admit an expansion around $\mu = \infty$.[2] The first property is obvious; for the second property, we define the function

$$\mathcal{E}(\mu) = \mathrm{i}\frac{\partial_\eta \varphi_{\vec{p}}}{\varphi_{\vec{p}}}\,. \tag{9.44}$$

In order to compute the heavy-mass limit, we need to compute the expansion of $H_{\mathrm{i}\mu}^{(1)}(z)$ for large μ. To this end, we note that the Hankel functions are defined to be solutions to Bessel's equation,

$$z^2 H''(z) + z H'(z) + (z^2 + \mu^2)H(z) = 0\,, \tag{9.45}$$

The expansion is computed by making the ansatz that the derivative of H can be expressed in terms of H itself, *i.e.*,

$$H'(z) = f(z)H(z)\,. \tag{9.46}$$

Inserting this into Bessel's equation (9.45) gives the nonlinear equation

$$z^2 f'(z) + z^2 f(z)^2 + z f(z) + z^2 + \mu^2 = 0\,. \tag{9.47}$$

In analogy with the Minkowski vacuum, we will now look for a solution that has at most a simple pole in μ^{-1}. Thus, we make the following ansatz for f:

$$f(z) = \mu \sum_{n \geq 0} f_n(z)\mu^{-n}\,. \tag{9.48}$$

Plugging this into (9.47) allows to solve the differential equation order by order in μ. The first few equations read

$$\begin{aligned}
0 &= 1 + z^2 f_0^2\,, & 0 &= f_0 + 2z f_0 f_1 + z f_0'\,, \\
0 &= z^2 + z^2 f_1^2 + 2z^2 f_0 f_2 + z^2 f_1'\,, & 0 &= f_2 + 2z f_1 f_2 + 2z f_0 f_3 + z f_2'\,.
\end{aligned} \tag{9.49}$$

Solving these equations gives

$$f_\pm(z) = \pm\frac{\mathrm{i}\mu}{z} \pm \frac{\mathrm{i}z}{2\mu} - \frac{z}{2\mu^2} - \pm\frac{\mathrm{i}z(4 + z^2)}{8\mu^3} + \mathcal{O}(\mu^{-4})\,. \tag{9.50}$$

---

[2]The requirement $m \gg H$ is a special case of the adiabatic approximation [419]. In general, adiabaticity assumes that the curvature of spacetime (here signified by H) is much smaller than the wavelength of the particle (given by the particle's mass). We refer to future work for a detailed discussion of the expansion in large mass in connection to the adiabatic approximation.

We compute this expansion to higher orders. We note that for $z > 0$, the two solutions are each other's complex conjugate. We now have to show that this solution of (9.47) indeed gives an expansion of the Hankel functions. To this end, we expand $H^{(1)}_{i\mu}(z)$ first around $z = 0$, and subsequently around $\mu = \infty$. This gives

$$H^{(1)}_{i\mu}(z) = \frac{i\mu}{z} + \mathcal{O}(z, \mu^{-1}). \tag{9.51}$$

We see that this matches exactly the leading term of f_+; hence, we conclude that f_+ is indeed the expansion of $H^{(1)}_{i\mu}$. Plugging this into the definition of $\mathcal{E}$ in (9.44), we see that also in de Sitter space, $\mathcal{E}$ has a simple pole in m if and only if a_+ or a_- is zero. This motivates the definition of the Bunch–Davies vacuum as the de Sitter spacetime generalization of the Minkowski vacuum.

(2b) Heavy-mass ingoing and outgoing states. We are now in the position to define the ingoing and outgoing states, and their respective heavy-mass limits. We associate an outgoing scalar field with the mode function $h_{\vec{p},\mu}$ and an ingoing scalar field with the mode function $\overline{h_{\vec{p},\mu}}$. Using the expansion (9.50), we can express their derivatives with respect to η in terms of $h_{\vec{p},\mu}$:

$$\partial_\eta h_{\vec{p},\mu} = -i\,\mathcal{E}(\mu)\,h_{\vec{p},\mu} = \left[\frac{i\mu}{\eta} + \frac{d-1}{2\eta} + i\left(\frac{1}{2}p^2\eta^2 - \frac{(d-1)^2}{8\eta} \right)\frac{1}{\mu} + \mathcal{O}(\mu^{-2}) \right] h_{\vec{p},\mu}. \tag{9.52}$$

With this definition at hand, we finally define the wave functions of the scalar fields to be:

$$\phi_1 = \overline{h_{\vec{p}_1,\mu_\phi}}, \qquad \phi_2 = h_{\vec{p}_2,\mu_\phi}, \qquad \chi_1 = \overline{h_{\vec{k}_1,\mu_\chi}}, \qquad \chi_2 = h_{\vec{k}_2,\mu_\chi}, \tag{9.53}$$

where we have defined the dimensionless masses $\mu_\varphi = m_\varphi/H$. This completes our definition of the scalar wave functions.

This formulas lie at the basis of the expansion of, e.g., the action of the graviton propagator $\mathcal{G}(\square)$ on the vertex tensors V and $T_{\mu\nu}$ used in this work.

9.4.2. *Computation of the scattering amplitude*

Let us begin with formalizing the adiabatic expansion. The adiabatic limit is implemented by performing an expansion in the dimensionless parameters

$$\mu_\phi = m_\phi/H, \qquad \mu_\chi = m_\chi/H. \tag{9.54}$$

around infinity. Using the results in Subsection 9.4.1, we are able to expand the solutions to the wave equation in powers of μ_ϕ and μ_χ. We use this evaluate the amplitude functional. We observe that in order to expand (9.26), it suffices to compute the adiabatic limit of $\mathcal{A}_0$ and $\mathcal{A}_2$. Following the argument in F.3, we find that the leading

terms are proportional to $\mu_\phi^2 \mu_\chi^2$. Thus, we define:

$$\mathcal{A}_0 = \int \mathrm{d}^d x \, \sqrt{-g} \, A_0(\mathfrak{q}; \zeta) \, \chi_1 \chi_2 \phi_1 \phi_2 + \mathcal{O}(\mu_\chi, \mu_\phi) \,,$$

$$\mathcal{A}_2 = \int \mathrm{d}^d x \, \sqrt{-g} \, A_2(\mathfrak{q}; \zeta) \, \chi_1 \chi_2 \phi_1 \phi_2 + \mathcal{O}(\mu_\chi, \mu_\phi) \,. \qquad (9.55)$$

Here the amplitude functionals $\mathcal{A}_i$ are determined by the integration kernels $A_i(\mathfrak{q}; \zeta)$. These are functions of the proper momentum transfer $\vec{\mathfrak{q}} = -\eta \vec{q} = -\eta \, (\vec{p}_1 - \vec{p}_2)$, where $\vec{p}_1$ is the momentum of ϕ_1 and $\vec{p}_2$ is the momentum of ϕ_2. We will refer to A_i as scattering amplitudes.

(1) We now discuss the general strategy to compute A_i. While all expressions in Section 9.3 are valid in any coordinate basis, we will now work explicitly in conformally flat coordinates. This allows to go to momentum space for spatial derivatives.

In these coordinates, we can assert from covariance that the propagator $\mathcal{G}_0(\Box, \zeta)$ acting on the product $\phi_1 \phi_2$ can be parameterized by

$$\mathcal{G}_0(\Box; \zeta) \phi_1 \phi_2 = \left[G_0(\eta; \zeta) + \mathcal{O}(\mu_\phi^{-1}) \right] \phi_1 \phi_2 \,, \qquad (9.56)$$

for some function G_0. The latter is found as follows. Acting with the inverse propagator $\mathcal{G}_0^{-1}(\Box; \zeta) = (-\Box + \zeta H^2)$ should give the identity operator. Distributing the derivatives gives the second-order inhomogeneous differential equation[3]

$$\eta^2 G_0'' + d\eta G_0' + (q^2 \eta^2 + \zeta) G_0 = \frac{1}{H^2} \,, \qquad (9.57)$$

where the primes denote derivatives wrt. η. Following the argument in Section F.3, we require that G_0 is analytic in η for any dimension d. Since the homogeneous solution to (9.57) is in general not analytic in η, G_0 is simply given by the inhomogeneous solution:

$$G_0(\eta; \zeta) = \frac{1}{\zeta H^2} {}_1\tilde{F}_2 \left(1; \frac{d+3}{4}, \frac{\nu(\zeta)}{2}; -\frac{q^2}{4} \right) \,. \qquad (9.58)$$

Here we defined ${}_1\tilde{F}_2 \, (a; b, c; z) = {}_1F_2 \, (a; b - c, b + c; z)$ in terms of a generalized hypergeometric function. In addition, we defined the parameter

$$\nu(\zeta) = \sqrt{\left(\frac{d-1}{2} \right)^2 - \zeta} \,. \qquad (9.59)$$

We thus find

$$A_0(\mathfrak{q}; \zeta) = \frac{\mu_\phi^2 \mu_\chi^2 H^2}{\zeta} {}_1\tilde{F}_2 \left(1; \frac{d+3}{4}, \frac{\nu(\zeta)}{2}; -\frac{q^2}{4} \right) \,. \qquad (9.60)$$

This completes our calculation of A_0. Computing the action of $\Box$ on $\chi_1 \chi_2$ using (9.52), we find that the vertex $V[\chi_1, \chi_2]$ expands to

$$V[\chi_1, \chi_2] = \left[H^2 \mu_\chi^2 + \mathcal{O}(\mu_\chi^0) \right] \chi_1 \chi_2 \,. \qquad (9.61)$$

---

[3]An equation of this type was also derived and solved with similar techniques in [439].

Thus, the terms $\mathcal{A}_0(\zeta)$ will each contribute to leading order μ_χ^2 to the scattering amplitude.

(2) For A_2, we take into account the tensor structure of $T_{\alpha\beta}$. Having studied the adiabatic limit of a single scalar field in Subsection 9.4.1, we now consider the adiabatic expansion of the vertex tensor $T_{\mu\nu}$. For the tensor vertex $T_{\mu\nu}$, we compute the components

$$T_{00}[\chi_1, \chi_2] = \left[\frac{d+1}{d}\frac{1}{\eta^2}\mu_\chi^2 + \mathcal{O}(\mu_\chi^0)\right]\chi_1\chi_2\,,$$

$$T_{0i}[\chi_1, \chi_2] = \left[\frac{1}{2\eta}(k_{1,i} + k_{2,i})\mu_\chi + \mathcal{O}(\mu_\chi^0)\right]\chi_1\chi_2\,, \tag{9.62}$$

$$T_{ij}[\chi_1, \chi_2] = \left[\frac{1}{d\eta^2}\delta_{ij}\mu_\chi^2 + \mathcal{O}(\mu_\chi^0)\right]\chi_1\chi_2\,.$$

where Latin indices denote spatial coordinates. Note that the (00)-component and the (ij)-components are of order μ_χ^2. Therefore, only these will contribute to the leading order in the adiabatic expansion of $\mathcal{A}_2(\zeta)$.

9.4.3. *Expansion of the propagator*

We proceed by showing that the action of the propagator on the scalar fields also has a well-behaved adiabatic expansion. We will show this explicitly for the scalar vertex V; for the tensor vertex $T_{\mu\nu}$, the procedure is completely analogous.

(1) First, we show that $f(-\Box)\phi_1\phi_2$ has an expansion in μ_ϕ^{-1} for any analytic function f. Since f has a Taylor series expansion, it suffices to show that the expansion exists for $(-\Box)^n\phi_1\phi_2$. This is shown by an inductive argument. First, we note that for $n = 0$, we have trivially

$$(-\Box)^n\phi_1\phi_2 = \phi_1\phi_2 \equiv \left[\alpha_0(\eta) + \mathcal{O}(\mu_\phi^{-1})\right]\phi_1\phi_2\,, \tag{9.63}$$

namely for $\alpha_0(\eta) = 1$. We now make the inductive assumption that (9.63) holds for $n \geq 0$. Then acting with one more d'Alembertian gives

$$(-\Box)^{n+1}\phi_1\phi_2 = -\Box\left(\alpha_n(\eta)\phi_1\phi_2\right) = \left[\left(q^2\eta^2\alpha_n + d\eta\alpha_n' + \eta^2\alpha_n''\right)H^2 + \mathcal{O}(\mu_\phi^{-1})\right]\phi_1\phi_2\,. \tag{9.64}$$

Here, the prime denotes a derivative with respect to η. By induction, it follows that $(-\Box)^n\phi_1\phi_2$ is $\mathcal{O}(\mu_\phi^0)\phi_1\phi_2$ for any n. Therefore, for any function f that admits an analytic expansion, $f(-\Box)\phi_1\phi_2$ can be expanded to zeroth order in μ_ϕ^{-1}.

Analogously, one proves that $f(-\Box)T_{\mu\nu}$ has a well-defined expansion, by taking care of the tensor structure of $T_{\mu\nu}$. Here, the leading order is $\mathcal{O}(\mu_\phi^2)$, cf. (9.62).

We note from (9.64) that $(-\Box)^n \phi_1 \phi_2$ also contains n powers of $q^2 \eta^2 = \mathfrak{q}^2$. Thus, we conclude that the expansion of $f(-\Box)\phi_1\phi_2$ is automatically analytic in $\mathfrak{q}$.

In particular, this is true for the propagator. Representing $(-\Box + z)^{-1}$ as a geometric series,

$$(-\Box + z)^{-1} = \frac{1}{z} \sum_{n=0}^{\infty} \left(\frac{\Box}{z}\right)^n, \tag{9.65}$$

we see that for $z \neq 0$ the propagator has an analytic expansion. Thus, we require the adiabatic expansion of the propagator in μ_ϕ^{-1} to be analytic in $\mathfrak{q}$.

As a consequence, the solution to the differential equation (9.57) is fixed.

Remark. Since this is a second-order inhomogeneous differential equation, one would expect the solution to be formed an inhomogeneous solution, accompanied by a two-dimensional homogeneous solution space. However, since the homogeneous solutions are generally not analytic, we will discard these in this thesis.

(2) For A_2, we take into account the tensor structure of $T_{\alpha\beta}$. Due to the two-derivative structure of $T_{\alpha\beta}$, the leading order will be of order μ_ϕ^2 as shown in (9.62). We then make the following ansatz for the propagator acting on $T_{\alpha\beta}$:

$$\begin{aligned}
\mathcal{G}_2(\Box;\zeta)T_{00}[\phi_1,\phi_2] &= \left[G_{00}(\eta)\mu_\phi^2 + \mathcal{O}(\mu_\phi)\right]\phi_1\phi_2\,, \\
\mathcal{G}_2(\Box;\zeta)T_{0i}[\phi_1,\phi_2] &= \left[\left(G_1(\eta)p_{1,i} + G_2(\eta)p_{2,i}\right)\mu_\phi^2 + \mathcal{O}(\mu_\phi)\right]\phi_1\phi_2\,, \\
\mathcal{G}_2(\Box;\zeta)T_{ij}[\phi_1,\phi_2] &= \left[\left(G_{(12)}(\eta)\left(p_{1,i}p_{2,j} + p_{1,j}p_{2,i}\right) + G_\delta(\eta)\delta_{ij}\right.\right. \\
&\qquad \left.\left. + G_{11}(\eta)p_{1,i}p_{1,j} + G_{22}(\eta)p_{2,i}p_{2,j}\right)\mu_\phi^2 + \mathcal{O}(\mu_\phi)\right]\phi_1\phi_2\,.
\end{aligned} \tag{9.66}$$

Acting on these expressions with $\mathcal{G}_2^{-1}(\Box;\zeta) = (-\Box + (\zeta + 2d)H^2)$ gives a set of coupled differential equations. Using the expansion above and the results in Section F.3, we find

$$A_2(\mathfrak{q};\zeta) = \frac{H^4\eta^2}{d}\mu_\phi^2\mu_\chi^2\left[-p_1^2 G_{11}(\eta) - p_2^2 G_{22}(\eta) - 2p_1 \cdot p_2\, G_{(12)}(\eta)\right.$$
$$\left.(d-1)\left(G_{00}(\eta) - G_\delta(\eta)\right)\right]. \tag{9.67}$$

By making linear combinations $g_i(\mathfrak{q}) = \sum_j a_{ij}G_j(\eta)$, the system can be partially decoupled. Since the exact linear combination is rather complicated, we will refrain from reproducing it here. We refer to the Appendix F for details on how to compute this. At this point, it suffices to note that A_2 is given by

$$A_2(\mathfrak{q};\zeta) = \frac{\mu_\phi^2\mu_\chi^2 H^2\mathfrak{q}^2}{2d}\left((d-2)g_1(\mathfrak{q}) + dg_2(\mathfrak{q})\right). \tag{9.68}$$

Here the functions g_1 and g_2 satisfy the differential equations

$$\mathfrak{q}^2 g_1'' + (d+4)\mathfrak{q}g_1' + (\mathfrak{q}^2 + \zeta + 3d + 2)g_1 = \frac{1}{\mathfrak{q}^2} + dg_2\,;$$

$$\mathfrak{q}^2 g_2'' + (d+4)\mathfrak{q}g_2' + (\mathfrak{q}^2 + \zeta + 3d)g_2 = \frac{1}{\mathfrak{q}^2} + (d-2)g_1 + 4i\mathfrak{q}g_3\,; \qquad (9.69)$$

$$\mathfrak{q}^2 g_3'' + (d+4)\mathfrak{q}g_3' + (\mathfrak{q}^2 + \zeta + 3d)g_3 = 4i\mathfrak{q}g_2\,.$$

We solve this system of equations by inserting a power series ansatz [440]:

$$g_i(\mathfrak{q}) = \mathfrak{q}^{\nu_i} \sum_{j\geq 0} b_{ij}\mathfrak{q}^j\,. \qquad (9.70)$$

Requiring that A_2 is analytic in η then implies that $\nu_i \in \mathbb{Z}$, and that the g_i are fixed by the inhomogeneous solution to (9.69). Inserting this ansatz into the differential equations (9.69) allows to resolve ν_i and the coefficients b_{ij}, after which we can resum the power series. The solution can be written as

$$A_2(\mathfrak{q};\zeta) = A_2^{\text{reg}}(\mathfrak{q};\zeta) + A_2^{\text{sing}}(\mathfrak{q};\zeta)\,. \qquad (9.71)$$

Here the term A_2^{reg} is regular for $\zeta = \zeta_h$:

$$A_2^{\text{reg}}(\mathfrak{q};\zeta) = \frac{\mu_\phi^2 \mu_\chi^2 H^2}{\zeta + d} \left[\frac{1}{d-1}{}_1\tilde{F}_2\left(1; \frac{d-1}{4}, \frac{\nu(\zeta)}{2}; -\frac{\mathfrak{q}^2}{4}\right) \right.$$
$$+ \left[\frac{d-3}{\zeta} - \frac{1}{d}\right] {}_1\tilde{F}_2\left(1; \frac{d+3}{4}, \frac{\nu(\zeta)}{2}; -\frac{\mathfrak{q}^2}{4}\right) \qquad (9.72)$$
$$\left. + \frac{2}{\zeta}{}_1\tilde{F}_2\left(2; \frac{d+3}{4}, \frac{\nu(\zeta)}{2}; -\frac{\mathfrak{q}^2}{4}\right) \right]\,.$$

Special care has to be taken into the case $\zeta = \zeta_h$. This is summarized in the function $A_2^{\text{sing}}(\mathfrak{q};\zeta)$, which is given by

$$A_2^{\text{sing}}(\mathfrak{q};\zeta \neq \zeta_h) = \frac{\mu_\phi^2 \mu_\chi^2 H^2}{\zeta + d}\frac{d-2}{d-1}{}_1\tilde{F}_2\left(1; \frac{d-1}{4}, \frac{\nu(\zeta - \zeta_h)}{2}; -\frac{\mathfrak{q}^2}{4}\right) \qquad (9.73)$$

for $\zeta \neq \zeta_h$. For the special value $\zeta = \zeta_h$ we find

$$
\begin{aligned}
A_2^{\text{sing}}(\mathfrak{q}; \zeta = \zeta_h) = {}& -\frac{\mu_\phi^2 \mu_\chi^2 H^2}{2} \left[{}_0F_1\left(\frac{d+1}{2}; -\frac{\mathfrak{q}^2}{4}\right) \right. \\
& - \frac{(d-3)(61 + 252d - 14d^2 - 12d^3 + d^4)}{12(d-1)^2(d+1)(d+5)} {}_0F_1\left(\frac{d-3}{2}; -\frac{\mathfrak{q}^2}{4}\right) \\
& + \frac{(d-3)(-11 - 26d + d^2)(-11 + 2d + d^2)}{12(d-1)^2(d+1)(d+5)} {}_0F_1\left(\frac{d-1}{2}; -\frac{\mathfrak{q}^2}{4}\right) \\
& + \frac{2}{d-1}\left({}_1F_2^{(0;0,1;0)}\left(1; 1, \frac{d-1}{2}; -\frac{\mathfrak{q}^2}{4}\right) \right. \\
& \qquad \left. - {}_1F_2^{(0;0,1;0)}\left(2; 1, \frac{d-1}{2}; -\frac{\mathfrak{q}^2}{4}\right) \right) \\
& - \frac{2}{d-1}\left({}_1F_2^{(0;1,0;0)}\left(1; 1, \frac{d-1}{2}; -\frac{\mathfrak{q}^2}{4}\right) \right. \\
& \qquad \left. \left. - {}_1F_2^{(0;1,0;0)}\left(2; 1, \frac{d-1}{2}; -\frac{\mathfrak{q}^2}{4}\right) \right) \right].
\end{aligned}
$$
(9.74)

This completes the computation of A_0 and A_2. The total amplitude can now be written as

$$
\begin{aligned}
A(\mathfrak{q}) = 16\pi G\, c(\alpha_R, \alpha_E) \Big[{}& -\frac{\zeta_C + d}{\zeta_C - \zeta_h}\Big(A_2(\zeta_h) - A_2(\zeta_C)\Big) \\
& + \frac{1}{d(d-1)}\frac{\zeta_C}{\zeta_C - \zeta_h}\Big(A_0(\zeta_h) - A_0(\zeta_C)\Big) \\
& + \frac{1}{(d-1)(d-2)}\Big(A_0(\zeta_h) - A_0(\zeta_R)\Big) \Big].
\end{aligned}
$$
(9.75)

In (9.75), $A_2(\zeta_h)$ is given by (9.74), $A_2(\zeta_C)$ by (9.73), and $A_0(\zeta)$ by (9.60).

9.4.4. Analysis of the amplitude

In this section, we study the properties of the amplitude computed above. For simplicity, we will limit ourselves to the case $d = 4$ only. We will first list several features of the amplitude and we discuss their interpretation.

(1) Properties of the A_i. In order to get a feeling for the behavior of the A_i, we plot the amplitude A_0 in Figure 9.4 for several values of ζ. In Figure 9.5, the amplitude A_2 is shown.

We distinguish two features of the amplitude. First, we note that since the hypergeometric function ${}_1F_2$ is bounded, the amplitude is bounded too. In particular, it attains
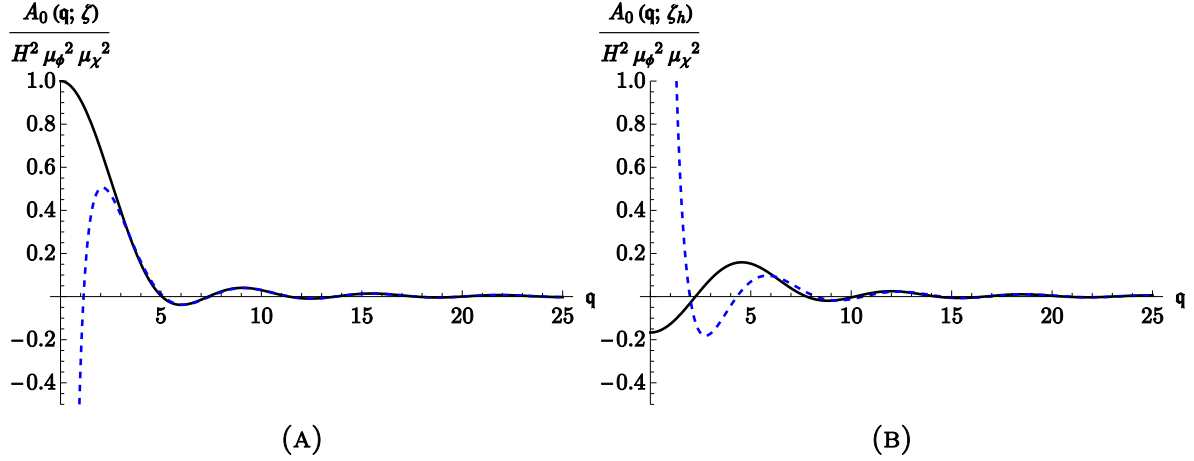
FIGURE 9.4. The amplitude $A_0(\mathfrak{q};\zeta)$ in $d = 4$ for several values of ζ. Left panel: $A_0(\zeta = 1)$. Right panel: $A_0(\zeta = \zeta_h)$. For $\mathfrak{q} = 0$, the amplitude attains the finite value given in (9.76). For large $\mathfrak{q}$, the amplitude behaves as $\sim \mathfrak{q}^{-2}(1 - \alpha\cos(\mathfrak{q}))$, as computed in (9.79). This approximation is depicted by the dashed blue lines.
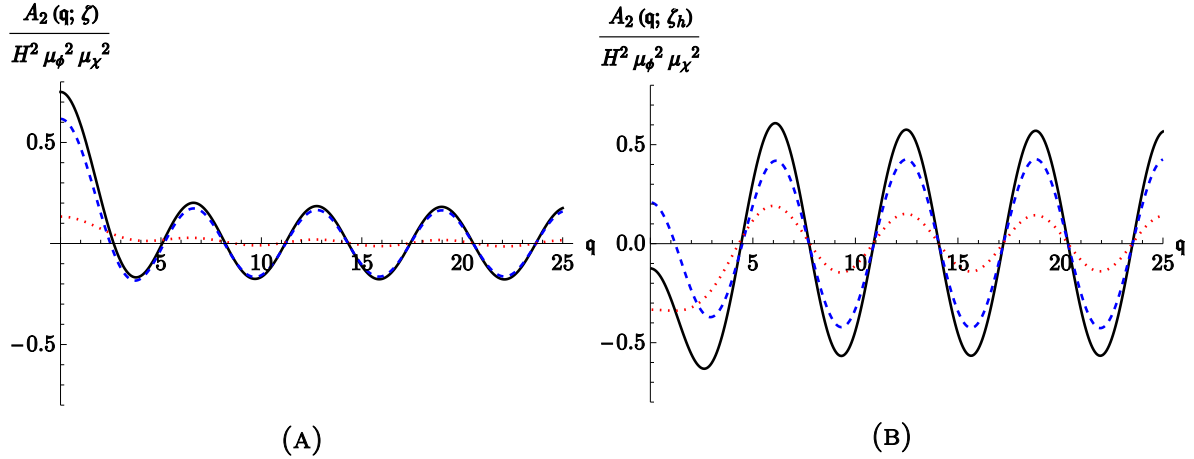

FIGURE 9.5. The amplitude $A_2(\mathfrak{q};\zeta)$ in $d = 4$ for several values of ζ. Left panel: $A_2(\zeta = 1)$. Right panel: $A_2(\zeta = \zeta_h)$. Solid line: the total amplitude A_2. Dashed blue line: A_2^{reg}. Dotted red line: A_2^{sing}. For $\mathfrak{q} = 0$, the amplitude attains the finite values given by (9.77) and (9.78). For large $\mathfrak{q}$, the amplitude behaves as $\sim \cos(\mathfrak{q})$, as computed in (9.80) and (9.81).

a finite value for $\mathfrak{q} \to 0$. For A_0, we find

$$\frac{A_0(\mathfrak{q} = 0;\zeta)}{H^2\mu_\phi^2\mu_\chi^2} = \frac{1}{\zeta}. \tag{9.76}$$

For A_2, we first consider the regular part A_2^{reg}. The limit $\mathfrak{q} \to 0$ reads

$$\frac{A_2^{\mathrm{reg}}(\mathfrak{q} = 0;\zeta)}{H^2\mu_\phi^2\mu_\chi^2} = \frac{2}{3}\frac{1}{\zeta+4} + \frac{3}{4}\frac{1}{\zeta}, \tag{9.77}$$

while for the singular part A_2^{sing}, we compute

$$\frac{A_2^{\text{sing}}(\mathfrak{q}=0;\zeta)}{H^2\mu_\phi^2\mu_\chi^2} = \frac{2}{3}\frac{1}{\zeta+4}\,, \tag{9.78}$$

holding both for $\zeta \neq \zeta_h$ and for $\zeta = \zeta_h$.

The second feature that we study is the behavior at large $\mathfrak{q}$. Expanding around $\mathfrak{q} = \infty$, we obtain for A_0:

$$\frac{A_0(\mathfrak{q};\zeta)}{H^2\mu_\phi^2\mu_\chi^2} \sim \frac{1}{\mathfrak{q}^2} + \frac{4}{\sqrt{\pi}\zeta}\Gamma\left(\frac{7}{4}-\frac{\nu(\zeta)}{2}\right)\Gamma\left(\frac{7}{4}+\frac{\nu(\zeta)}{2}\right)\frac{1}{\mathfrak{q}^2}\cos(\mathfrak{q})\,. \tag{9.79}$$

Expanding A_2^{reg} around large momentum transfer, we find

$$\frac{A_2^{\text{reg}}(\mathfrak{q},\zeta)}{H^2\mu_\phi^2\mu_\chi^2} \sim -\frac{1}{3\sqrt{\pi}}\frac{\Gamma\left(\frac{3}{4}-\frac{\nu(\zeta)}{2}\right)\Gamma\left(\frac{3}{4}+\frac{\nu(\zeta)}{2}\right)}{\zeta+4}\cos(\mathfrak{q})\,. \tag{9.80}$$

The large-$\mathfrak{q}$ expansion of A_2^{sing} reads

$$\frac{A_2^{\text{sing}}(\mathfrak{q};\zeta)}{H^2\mu_\phi^2\mu_\chi^2} \sim \begin{cases} \dfrac{2}{3\sqrt{\pi}}\dfrac{\Gamma\left(\frac{3}{4}-\frac{\nu(\zeta-\zeta_h)}{2}\right)\Gamma\left(\frac{3}{4}+\frac{\nu(\zeta-\zeta_h)}{2}\right)}{\zeta+4}\cos(\mathfrak{q})\,, & \zeta \neq \zeta_h \\[2em] \dfrac{397-360\log(2)}{1080}\cos(\mathfrak{q})\,, & \zeta = \zeta_h \end{cases}\,. \tag{9.81}$$

We therefore find the following behavior: for large $\mathfrak{q}$, the scattering amplitudes are oscillating. Restoring dimensionful quantities, we find that the oscillating terms are suppressed by H^2. Carefully taking the limit $H \to 0$, which we will not further discuss here, allows to recover the flat-spacetime $1/\vec{q}^2$ behavior.

(2) Interpretation of the scattering amplitude. We will now briefly discuss the interpretation of the limits $\mathfrak{q} \to 0$ and $\mathfrak{q} \to \infty$.

Let us first consider the small-momentum limit, which we find to be finite. This behavior is in line with the expectation that $z = \zeta H^2$ acts as a mass, similar to the limit $\vec{q} \to 0$ for a flat-spacetime massive propagator $\propto \frac{1}{\vec{q}^2+z}$. A special case arises when $\zeta = \zeta_h$. Then (9.76), (9.77) and (9.78) are manifestly finite. In flat spacetime, on the other hand, we have a massless propagator, $\frac{1}{\vec{q}^2}$, which is divergent in the limit $\vec{q} \to 0$. We therefore conclude that the background curvature acts as an infrared regulator.

The oscillations in the large-momentum limit are also observed in the context of GR. As discussed there, the oscillations are typical for propagators in dS spacetime [311]. Furthermore, the discrete values where the amplitude vanishes has an interesting interpretation in terms of a probability density. A node at momentum $\mathfrak{q}_0$ then implies that the exchange of a graviton with this momentum is forbidden. These momenta are equidistantly separated with distance $\Delta\mathfrak{q} = 2\pi$. This discrete behavior is reminiscent

of discrete transition probabilities associated to particles in a box. In this context, the Hubble volume then acts as the boundary within which gravitons can propagate.

9.5. SCATTERING POTENTIAL IN THE ADIABATIC EXPANSION

The scattering amplitude $A(\mathfrak{q})$ represents the transition probability of the scattering process $\phi\chi \to \phi\chi$ with momentum transfer $\mathfrak{q}$. Converting to position space, we find the transition amplitude of the same scattering process, where the external states are now localized at well-determined spacetime positions. As a generalization of the Born approximation in flat spacetime, we interpret this object as the scattering potential.

9.5.1. *Computation of the scattering potential*

We obtain the transition amplitude in position space by taking the Fourier transform of (9.75).

(1) Preparing particle ϕ_1 at position $\vec{x}_1$ and particle χ_1 at position $\vec{x}_2$, the transition probability arising from the amplitude A_i is given by

$$V_i(\vec{x}_1, \vec{x}_2) = \frac{1}{2\mu_\phi \mu_\chi} \int \frac{\mathrm{d}^{d-1}\vec{\mathfrak{k}}_1}{(2\pi)^{d-1}} \frac{\mathrm{d}^{d-1}\vec{\mathfrak{p}}_1}{(2\pi)^{d-1}} \mathrm{e}^{\mathrm{i}\vec{\mathfrak{p}}_1 \cdot \vec{x}_1} \mathrm{e}^{\mathrm{i}\vec{\mathfrak{k}}_1 \cdot \vec{x}_2} A_i(\mathfrak{q}; \zeta). \tag{9.82}$$

Here the dimensionless proper momenta $\vec{\mathfrak{p}}_1 = -\eta \vec{p}_1$ and $\vec{\mathfrak{k}}_1$ are integrated over to obtain an invariant expression. In addition, the prefactor of the integral is chosen such that the resulting potential is correctly normalized.

Performing the integral over $\vec{\mathfrak{k}}_1$ and the spherical part of $\vec{\mathfrak{p}}_1$, we find the dimensionless potential:

$$V_i(\vec{x}_1, \vec{x}_2) = \delta^{d-1}(H\vec{x}_2)V_i(\mathfrak{r}), \tag{9.83}$$

$$V_i(\mathfrak{r}) = \frac{1}{2\mu_\phi \mu_\chi} \frac{2^{2-d}\pi^{\frac{1-d}{2}}}{\Gamma\left(\frac{d-1}{2}\right)} \int_0^\infty \mathrm{d}\mathfrak{q}\, \mathfrak{q}^{d-2} {}_0F_1\left(\frac{d-1}{2}; -\frac{\mathfrak{q}^2\mathfrak{r}^2}{4}\right) A_i(\mathfrak{q}). \tag{9.84}$$

Here, $\mathfrak{r} = \|\eta(\vec{x}_1 - \vec{x}_2)\|$ denotes the proper distance between the particles ϕ_1 and χ_1. Central in this computation is the integral

$$\int_0^\infty \mathrm{d}x\, x^{s-1} {}_0F_1(\alpha; -ax) {}_1F_2(n; \beta_1, \beta_2; -bx). \tag{9.85}$$

This has the structure of a Mellin transform, and was studied in [441]. In order to compute the Fourier transform of the functions ${}_1F_2^{(0;i,j;0)}\left(a; b, \frac{d-1}{2}; -\frac{\mathfrak{q}^2}{4}\right)$ in (9.73) and

(9.74), we express the derivatives as the limit of a finite difference. Exchanging the Fourier transform with the limit, the finite difference is of the form (9.85).

(2) The potential is given by a discontinuous function,

$$V_i(\mathfrak{r}) = \begin{cases} V_i^{\mathfrak{r}<1}(\mathfrak{r}) & \mathfrak{r} < 1 \\ 0 & \mathfrak{r} > 1 \end{cases}. \tag{9.86}$$

The potentials $V_i^{\mathfrak{r}<1}$ are conveniently expressed in terms of the following functions, valid for $\mathfrak{r} < 1$ and non-negative integers n and m:

$$\mathcal{V}_{nm}(\mathfrak{r};\zeta) = \frac{2^{2-d}\pi^{\frac{1-d}{2}}}{\Gamma\left(\frac{d-1}{2}\right)} \int_0^\infty d\mathfrak{q}\ \mathfrak{q}^{d-2}{}_0F_1\left(\frac{d-1}{2}; -\frac{\mathfrak{q}^2\mathfrak{r}^2}{4}\right) {}_1\tilde{F}_2\left(n; \frac{d-1}{4}+m, \frac{\nu(\zeta)}{2}; -\frac{\mathfrak{q}^2}{4}\right)$$

$$= \pi^{\frac{1-d}{2}}\frac{\Gamma\left(\frac{d-1}{2}-n\right)}{\Gamma(n)}\frac{\Gamma\left(\frac{d-1}{4}+m-\frac{\nu(\zeta)}{2}\right)\Gamma\left(\frac{d-1}{4}+m+\frac{\nu(\zeta)}{2}\right)}{\Gamma\left(\frac{d-1}{4}+m-n-\frac{\nu(\zeta)}{2}\right)\Gamma\left(\frac{d-1}{4}+m-n+\frac{\nu(\zeta)}{2}\right)}\times$$

$$\mathfrak{r}^{1-d+2n}{}_2\tilde{F}_1\left(\frac{5-d}{4}-m+n, \frac{\nu(\zeta)}{2}; \frac{3-d}{2}+n; \mathfrak{r}^2\right)$$

$$+ \pi^{\frac{1-d}{2}}\frac{\Gamma\left(\frac{1-d}{2}+n\right)}{\Gamma(n)}\frac{\Gamma\left(\frac{d-1}{4}+m-\frac{\nu(\zeta)}{2}\right)\Gamma\left(\frac{d-1}{4}+m+\frac{\nu(\zeta)}{2}\right)}{\Gamma\left(\frac{1-d}{4}+m-\frac{\nu(\zeta)}{2}\right)\Gamma\left(\frac{1-d}{4}+m+\frac{\nu(\zeta)}{2}\right)}\times$$

$$_2\tilde{F}_1\left(\frac{d+3}{4}-m, \frac{\nu(\zeta)}{2}; \frac{d+1}{2}-n; \mathfrak{r}^2\right). \tag{9.87}$$

In this expression, we defined ${}_2\tilde{F}_1(a, b; c; z) = {}_2F_1(a-b, a+b; c; z)$ in terms of a hypergeometric function. Before we start analysing the properties of the potential, let us remark that the appearance of ${}_2F_1$ hypergeometric functions is in accordance with existing computations [300, 442]. This is a signature of the virtual graviton propagator, which written as an integration kernel in position space is proportional to ${}_2F_1$.

It is now straightforward to express the $V_i^{\mathfrak{r}<1}$ in terms of $\mathcal{V}_{nm}$. For V_0, we find

$$V_0^{\mathfrak{r}<1}(\mathfrak{r};\zeta) = \frac{\mu_\phi\mu_\chi}{2\zeta}\mathcal{V}_{1,1}(\mathfrak{r};\zeta). \tag{9.88}$$

Similar to A_2, the potential $V_2^{\mathfrak{r}<1}$ splits into a regular and a singular part:

$$V_2(\mathfrak{r};\zeta) = V_2^{\text{reg}}(\mathfrak{r}) + V_2^{\text{sing}}(\mathfrak{r}). \tag{9.89}$$

The regular part is given by

$$V_2^{\text{reg}}(\mathfrak{r};\zeta) = \frac{\mu_\phi\mu_\chi}{2(\zeta+d)}\left[\frac{1}{d-1}\mathcal{V}_{1,0}(\mathfrak{r};\zeta) + \left[\frac{d-3}{\zeta}-\frac{1}{d}\right]\mathcal{V}_{1,1}(\mathfrak{r},\zeta) + \frac{2}{\zeta}\mathcal{V}_{2,1}(\mathfrak{r};\zeta)\right], \tag{9.90}$$

while the singular part becomes

$$
V_2^{\text{sing}}(\mathfrak{r};\zeta) =
\begin{cases}
\dfrac{\mu_\phi \mu_\chi}{2(\zeta+d)} \dfrac{d-2}{d-1} \mathcal{V}_{1,0}(\mathfrak{r};\zeta-\zeta_h)\,, & \zeta \neq \zeta_h \\[3mm]
-\dfrac{\mu_\phi \mu_\chi}{2}\left[\dfrac{1}{d-1}\mathcal{V}_{1,0}(\mathfrak{r};0) + \dfrac{\pi^{\frac{1-d}{2}}}{2}\Gamma\left(\dfrac{d+1}{2}\right)\right]\,, & \zeta = \zeta_h
\end{cases}
\tag{9.91}
$$

The function $V_2^{\text{sing}}(\mathfrak{r};\zeta=\zeta_h)$ reduces to the rational function

$$
V_2^{\text{sing}}(\mathfrak{r};\zeta=\zeta_h) = \frac{\mu_\phi \mu_\chi}{2}\pi^{\frac{1-d}{2}}\Gamma\left(\frac{d-1}{2}\right)\frac{\mathfrak{r}^{3-d} + \frac{1}{4} - \mathfrak{r}^2 - \frac{1}{4}(d+\mathfrak{r}^2 - d\mathfrak{r}^2)^2}{(d-1)(\mathfrak{r}-1)^2(\mathfrak{r}+1)^2}\,.
\tag{9.92}
$$

The total, dimensionful scattering potential for QuadG can easily be expressed in terms of the V_i. For $\mathfrak{r} < 1$, we have

$$
\begin{aligned}
V^{\mathfrak{r}<1}(\mathfrak{r}) = 16\pi G H^3\, c(\alpha_R, \alpha_E)\Bigg[&-\frac{\zeta_C + d}{\zeta_C - \zeta_h}\Big(V_2(\mathfrak{r};\zeta_h) - V_2(\mathfrak{r};\zeta_C)\Big) \\
&+ \frac{1}{d(d-1)}\frac{\zeta_C}{\zeta_C - \zeta_h}\Big(V_0(\mathfrak{r};\zeta_h) - V_0(\mathfrak{r};\zeta_C)\Big) \\
&+ \frac{1}{(d-1)(d-2)}\Big(V_0(\mathfrak{r};\zeta_h) - V_0(\mathfrak{r};\zeta_R)\Big)\Bigg]\,,
\end{aligned}
\tag{9.93}
$$

while the potential is equal to zero for $\mathfrak{r} > 1$.

9.5.2. *Properties of the potential*

Having computed the potential for QuadG in (9.93), we will now consider its phenomenological properties. To this end, we will regard the potential as the source of a Newtonian force. This allows to straightforwardly interpret the potential in terms of potential energies, and the scaling of the force with distance.

(1) The short-distance regime. We will first consider the regime $\mathfrak{r} \ll 1$. In this region, spacetime can be approximated as locally flat, so that we expect curvature effects to be negligible. Hence, in this limit we should recover the behavior of the potential in Minkowski spacetime. The Yukawa-like potential of QuadG is easily obtained from the Minkowski-spacetime scattering amplitude, and reads

$$
V_{\text{Mink}}(r) = G m_\phi m_\chi \left(-\frac{1}{r} - \frac{1}{3}\frac{1}{r}e^{-r/\sqrt{\alpha_R}} + \frac{4}{3}\frac{1}{r}e^{-r/\sqrt{\alpha_C}}\right)
\tag{9.94}
$$

For dS spacetime, there are four cases to be considered:

(1a) General relativity. In this case, the higher-derivative couplings α_R and α_C are both zero. Upon expanding around $\mathfrak{r} = 0$, we then find

$$V_{\mathrm{GR}}(\mathfrak{r}) \sim -GH^3 \frac{\mu_\phi \mu_\chi}{\mathfrak{r}} \,. \tag{9.95}$$

Hence, we reproduce Newton's law. In the remainder of this paragraph, we will set $d = 4$. We can then plot $V(\mathfrak{r})$, which is given in Figure 9.6. The plot shows several remarkable features. First, we expand around $\mathfrak{r} = 0$. This gives the approximation

$$\frac{V(\mathfrak{r})}{H^3 G \mu_\phi \mu_\chi} \sim V_{\mathrm{app}}(\mathfrak{r}) = -\frac{1}{\mathfrak{r}} + 5 - 4\mathfrak{r} \,. \tag{9.96}$$

This approximation is shown by a dashed blue line in Figure 9.6. As can be seen from the residual plot, this captures the behavior of $V(\mathfrak{r})$ very well. From the (9.96), we see that the leading-order term is exactly the flat-spacetime Newtonian potential. This is in accordance with the observation that at small distances, the background curvature of spacetime can be neglected.

Classically, the Newtonian force is given by the derivative of the potential. This gives

$$F \propto -\frac{V'(\mathfrak{r})}{H^3 G \mu_\phi \mu_\chi} \sim -\frac{1}{\mathfrak{r}^2} + 4 \,. \tag{9.97}$$

Hence, we conclude that the correction to the Newtonian potential gives rise to an approximately constant repulsive force. This is in agreement with the interpretation of the expansion of the universe screening the attractive gravitational force between the two particles. As a matter of fact, we observe that the expanding force dominates at large distances, demonstrated by a maximum of the potential at $\mathfrak{r}_{\mathrm{max}} \approx 0.4998$, where the potential takes the value $V(\mathfrak{r}_{\mathrm{max}}) \approx 1.0420 \, H^3 G \mu_\phi \mu_\chi$. To large extent, this is dominated by the leading-order terms in (9.96), which yields an approximate maximum at $\mathfrak{r} = \frac{1}{2}$ at $V_{\mathrm{app}}(1/2) = 1 \cdot H^3 G \mu_\phi \mu_\chi$.

(1b) R^2-gravity. We continue with R^2-gravity, obtained from the limit (9.34). In this case, the $\mathfrak{r} \to 0$ behavior reads

$$V_{R^2}(\mathfrak{r}) \sim -\frac{4}{3} \frac{\zeta_R}{\zeta_R + 4} G H^3 \frac{\mu_\phi \mu_\chi}{\mathfrak{r}} \,. \tag{9.98}$$

This is in agreement with the short-distance behavior for R^2-gravity in flat spacetime, determined by (9.94).

Remark. At this point, a remark about Newton's constant G is in order. The numerical value of G can be *defined* as the coefficient of the $1/r$ law, which can be obtained e.g. from a Cavendish experiment. For relativistic theories, one then determines numerical prefactors by taking the appropriate Newtonian limit, and comparing coefficients. The prime example of this is the prefactor $8\pi G$ on the right-hand side of the Einstein equation. Therefore, in the case of R^2-gravity, we can renormalize the constant G such

that we obtain exactly the Newtonian potential.[4] Hence, setting

$$\hat{G} = \begin{cases} \frac{4}{3}\frac{\zeta_R}{\zeta_R+4}G\,, & 0 < \zeta_R < \infty \\ \\ G & \text{otherwise} \end{cases}, \qquad (9.99)$$

we conclude that also R^2-gravity yields a Newtonian force law at distances small compared to the Hubble length.

(1c) C^2-gravity. We proceed with C^2-gravity, given by the limit (9.35). Expanding around $\mathfrak{r} = 0$ gives

$$V_{C^2}(\mathfrak{r}) \sim +\frac{1}{3}GH^3\frac{\mu_\phi\mu_\chi}{\mathfrak{r}}\,, \qquad (9.100)$$

which is the same as what we find from (9.94). In contrast to GR and R^2-gravity, we find that C^2-gravity yields a *repulsive* force-law at short distances.

(1d) Quadratic gravity. We finish our discussion of the short-distance regime by considering full QuadG. Here we find that the potential does not possess a pole at $\mathfrak{r} = 0$, similar to what we find by evaluating (9.94) at $r = 0$. The absence of such a short-distance singularity can be seen as the classical analogue of the perturbative renormalizability of QuadG, c.f. [65, 66].

(2) The dS horizon. The second property of the potential that we discuss is the regime $\mathfrak{r} \sim 1$. As we have seen in (9.86), the potential vanishes at distances $\mathfrak{r} > 1$. This is a natural manifestation of dS horizon: since particles that are separated by the horizon are not in causal contact, their scattering potential must be identically zero.

In order to further study the discontinuity, we interpret V as the source of a Newtonian force. We will be interested in the dimensionless quantity

$$\mathfrak{F} = -\frac{V'(\mathfrak{r})}{\hat{G}H^3\mu_\phi\mu_\chi}\,, \qquad (9.101)$$

which can be seen as the Newtonian force expressed in Hubble units.

It is clear that for radii $\mathfrak{r} > 1$, the force $\mathfrak{F}$ is zero. Approaching $\mathfrak{r} = 1$ from below, the discontinuity in $\mathfrak{F}$ can be computed. We find that the discontinuity lies in the interval

$$\lim_{\mathfrak{r}\nearrow 1}\mathfrak{F}_{\zeta\to 0} \leq \lim_{\mathfrak{r}\nearrow 1}\mathfrak{F} \leq \lim_{\mathfrak{r}\nearrow 1}\mathfrak{F}_{\text{GR}}\,, \qquad (9.102)$$

---

[4]Note that the sign of (the derivative of) V is connected to the direction of the corresponding force. Thus, one can only renormalize by a positive number.
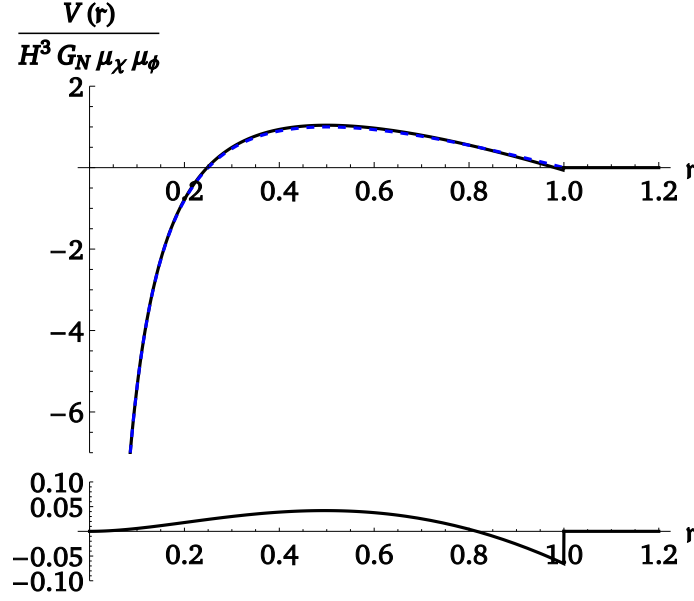
FIGURE 9.6. Plot of the large-mass limit tree-level scattering potential in dS spacetime. Top panel: the potential V is shown by a solid black line. The dashed blue line shows the approximation V_{app} from (9.96). Bottom panel: the residual values $V - V_{\text{app}}$. We observe that the residual values are $\lesssim 0.1$, indicating that the approximation captures the behavior of V well.

where $\mathfrak{F}_{\text{GR}}$ is the force for General Relativity and $\mathfrak{F}_{\zeta \to 0}$ is the force of QuadG in the limit $\zeta_C, \zeta_R \to 0$. These values can be computed exactly:

$$\lim_{\mathfrak{r} \nearrow 1} \mathfrak{F}_{\zeta \to 0} = -\frac{17}{24} - \frac{5\Gamma\left(\frac{3}{4} - \frac{\nu(\zeta_h)}{2}\right) \Gamma\left(\frac{3}{4} + \frac{\nu(\zeta_h)}{2}\right)}{6\sqrt{\pi}} + \frac{4\Gamma\left(\frac{3}{4} - \frac{\nu(-\zeta_h)}{2}\right) \Gamma\left(\frac{3}{4} + \frac{\nu(-\zeta_h)}{2}\right)}{3\sqrt{\pi}}$$

$$\approx 1.647\,;$$

$$\lim_{\mathfrak{r} \nearrow 1} \mathfrak{F}_{\text{GR}} = \frac{5}{6} + \frac{5\Gamma\left(\frac{3}{4} - \frac{\nu(\zeta_h)}{2}\right) \Gamma\left(\frac{3}{4} + \frac{\nu(\zeta_h)}{2}\right)}{3\sqrt{\pi}}$$

$$\approx 3.443\,.$$

(9.103)

We notice that both values are positive. Hence, at the dS horizon, the net gravitational force is repulsive, in contrast to classical Newtonian gravity. We interpret this as an effect of the positive curvature: the expansion of the universe manifests itself as a repulsive effective force.

(3) Modified Newtonian Dynamics from Quadratic Gravity. We now study $\mathfrak{F}$ in the intermediate regime $0 < \mathfrak{r} < 1$. We will pay special attention to the comparison to the classical Newtonian force $\mathfrak{F}_{\text{cl}} = -\mathfrak{r}^{-2}$. Any deviation from this potential can be seen as an instance of Modified Newtonian Dynamics. In recent years, phenomenological
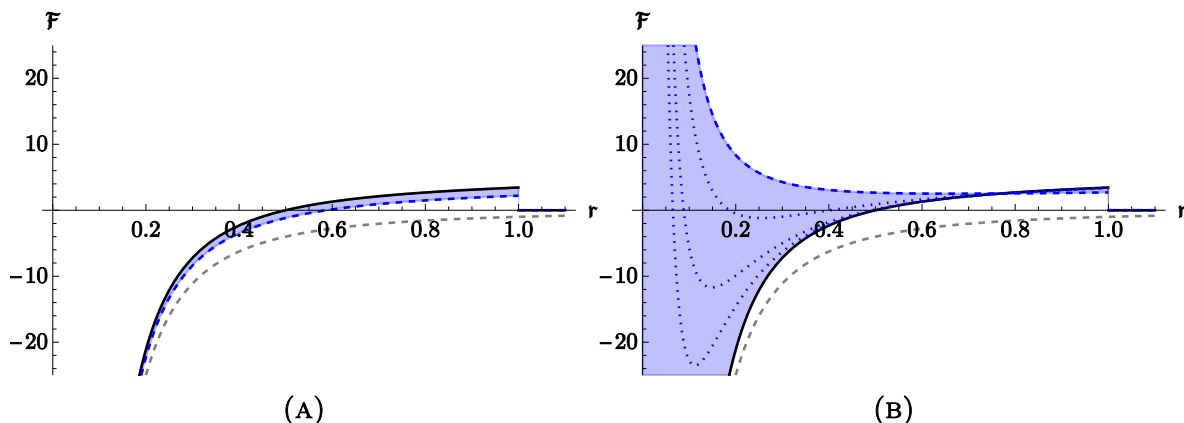
FIGURE 9.7. Dimensionless forces $\mathfrak{F}$ in R^2- and C^2-gravity. In both panels, the black curve denotes $\mathfrak{F}_{GR}$, while the dashed gray curve shows the classical Newtonian force $\mathfrak{F}_{cl} = -\mathfrak{r}^{-2}$ for reference. Left panel: $\mathfrak{F}$ in R^2-gravity. Scanning over ζ_R, the curves $\mathfrak{F}_{\zeta_R}$ fill the shaded blue region, bounded by $\mathfrak{F}_{GR}$ and $\mathfrak{F}_{\zeta_R \to 0}$ (dashed blue curve). Right panel: $\mathfrak{F}$ in C^2-gravity. Scanning over ζ_C fills the shaded blue region, bounded by $\mathfrak{F}_{GR}$ and $\mathfrak{F}_{\zeta_C \to 0}$ (dashed blue curve). For typical finite values of ζ_C, $\mathfrak{F}$ is drawn using dotted blue curves. Both for R^2- and C^2-gravity, the force is strictly larger than $\mathfrak{F}_{cl}$, indicating that a dark matter MOND-like scenario is excluded.

models of MOND have been constructed to explain rotation curves of galaxies, which do not correspond to classical Newtonian gravity [351–354, 443–447]. MOND is therefore an alternative to DM models, which explain the discrepancy of galactic rotation curves by the existence of non-luminous cold matter.

In order to reproduce a DM-like scenario using MOND, one mimics the additional mass density by modifying the potential such that one obtains an additional attractive force. In this section, we will consider whether such a modification can arise from $\mathfrak{F}$ by an appropriate choice of ζ_C and ζ_R. Again, we distinguish four different regimes.

(3a) General Relativity. We begin with GR. The force $\mathfrak{F}_{GR}$ is shown by the black curve in Figure 9.7. Comparing $\mathfrak{F}_{GR}$ to the classical Newtonian force $\mathfrak{F}_{cl} = -\mathfrak{r}^{-2}$ (the dashed gray curve in Figure 9.7), we observe that the two coincide for small $\mathfrak{r}$, as discussed previously. Also the discontinuity is clearly visible. Furthermore, we observe that $\mathfrak{F}_{GR}$ is strictly larger than $\mathfrak{F}_{class}$. Hence, the spacetime curvature causes an additional expanding force, coinciding with the expectation that dS spacetime models an expanding universe.

(3b) R^2-gravity. Turning on the coupling α_R, we find that the addition of an R^2-interaction gives a modification to General Relativity. Letting ζ_R run from 0 to ∞, we find that the curves $\mathfrak{F}$ fill the shaded blue region in the left panel of Figure 9.7. Here the dashed blue line denotes the limiting case $\mathfrak{F}_{\zeta_R \to 0}$. We find that the R^2 modification causes $\mathfrak{F}$

to be lower than $\mathfrak{F}_{\mathrm{GR}}$. Hence, the R^2-interaction effectively causes an attractive force on top of the force due to GR. However, the modification is nowhere strong enough to give rise to DM-like MOND.

(3c) C^2-gravity. In the right panel of Figure 9.7, the force arising from C^2-gravity is shown. Similar to R^2-gravity, varying ζ_C traces out a region bounded by $\mathfrak{F}_{\mathrm{GR}}$ and $\mathfrak{F}_{\zeta_C \to 0}$. In contrast to R^2-gravity, $\mathfrak{F}$ is always positive for sufficiently small $\mathfrak{r}$, due to the $+\mathfrak{r}^{-1}$-like behavior of the potential. In fact, below $\mathfrak{r} \approx 0.770$, $\mathfrak{F}$ is strictly larger than $\mathfrak{F}_{\mathrm{GR}}$. Therefore, in this regime the effect of the C^2-interaction can be interpreted as an additional repulsive force on top of General Relativity. Thus, C^2-gravity cannot be matched to a MOND-potential suitable to explain DM.

(3d) Quadratic Gravity. Finally, we consider full QuadG As we have seen, since the potential of QuadG is finite at $\mathfrak{r} = 0$, there will be no $\mathfrak{r}^{-2}$-like behavior of $\mathfrak{F}$. Instead, we find that $\mathfrak{F} \sim -\frac{3}{2} - \frac{\zeta_C}{2} + \frac{\zeta_R}{8}$ for small $\mathfrak{r}$. Thus, by an appropriate choice of ζ_C and ζ_R, the force $\mathfrak{F}$ can reach any finite value at $\mathfrak{r} = 0$. This includes $\mathfrak{F} = 0$, which can be related to force laws arising from spacetimes with higher regularity [448]. We find that $\mathfrak{F}$ is mostly bounded by $\mathfrak{F}_{\zeta_R \to 0}$ and $\mathfrak{F}_{\zeta_C \to 0}$ (the shaded blue region in Figure 9.8). For $\mathfrak{r} \gtrsim 0.770$, the force is bounded by $\mathfrak{F}_{\mathrm{GR}}$ and $\mathfrak{F}_{\zeta \to 0}$, obtained by taking the limit $\lim_{\zeta_C, \zeta_R \to 0} \mathfrak{F}$. This is shown in detail in the right panel of Figure 9.8.

Thus, we conclude that no choice of ζ_C and ζ_R gives rise to an effective force that is more attractive than the classical Newtonian force. Instead, we find in the entire parameter space a repulsive contribution to the gravitational force. Therefore, dS curvature corrections to QuadG cannot explain galactic rotation curves.
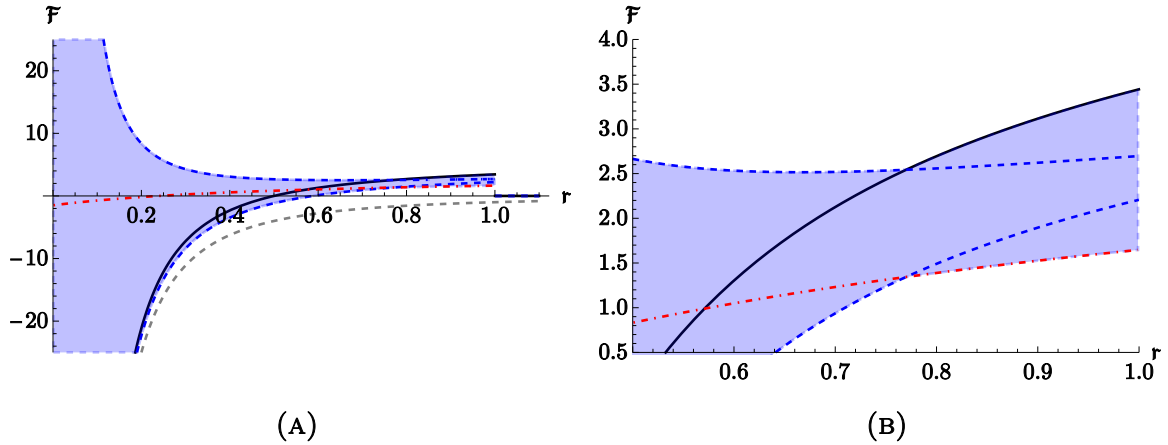
(A)

(B)

FIGURE 9.8. Dimensionless forces $\mathfrak{F}$ in QuadG. The black curve denotes $\mathfrak{F}_{GR}$. The dashed gray curve shows the classical Newtonian force $\mathfrak{F}_{cl} = -\mathfrak{r}^{-2}$. For any point in the shaded blue region, there exist values of ζ_C, ζ_R such that this point is reached by $\mathfrak{F}_{\zeta_C,\zeta_R}$. In particular, for any ζ_C, ζ_R, $\mathfrak{F}$ reaches a finite value at $\mathfrak{r} = 0$. The shaded blue region is bounded by $\mathfrak{F}_{GR}$, $\mathfrak{F}_{\zeta_R \to 0}$, $\mathfrak{F}_{\zeta_C \to 0}$ (dashed blue lines), and $\mathfrak{F}_{\zeta \to 0}$ (dashed-dotted red line). The right panel shows a detail of the left panel, clarifying the boundary of the shaded region near the dS horizon.

CHAPTER 10

Discussion and Summary of Part II

De Sitter spacetime plays a vital role in our current understanding of the Universe at different epochs. In early-time cosmology, de Sitter spacetime provides an accurate description of an inflationary universe, with evidence provided by the CMBR [257]. Also at late cosmic times, observations of distant supernovae suggest an accelerated expansion of the universe, modeled by a de Sitter spacetime [255, 256]. In General Relativity, this universe is uniquely modeled by a constantly curved solution to Einstein's equation with a positive cosmological constant, the de Sitter Universe.

On the other hand, there are still significant open questions regarding dS spacetime. De Sitter spacetime arises in GR as the solution to Einstein's equation including a cosmological constant Λ. Usually attributed to the so-called "dark energy" or an intrinsic "vacuum energy", the origin of the cosmological constant and its small present-day value of 67.66 (km/s)/Mpc = $10^{-122} \ell_P^2$ [449] remain a mystery [450].

This set of problems related to de Sitter spacetime are special of it curved and Lorentzian nature. We speculated that a better understanding of the quantum dynamics in such a geometry can shed light on its yet-to-be-clarified properties.

In order to explore the quantum dynamics of de Sitter geometry, we opened three new research lines in **Part II** of this thesis based on different technical tools. The three project share a first analysis of the mode decomposition of fields in a de Sitter spacetime. In **Project (II.A)** and **Project (II.B)** we employed the fluctuation modes in order to study the RG trajectories in dS: In the first project we investigated the geometrization of RG histories in a 4D de Sitter spacetime; in the second project, we analyzed the Background Independent quantum dynamics of the dS geometry by means of spectral methods. In **Project (II.C)** instead, the fields on dS are involved in a scattering process and we performed the first computation of a covariant scattering amplitude in this spacetime.

Project (II.A)*: Geometrization of RG histories: a novel AdS/CFT correspondence*

The RG equations of QFT are formulated in a mathematical setting, which is rather simple and, in a way, structureless from the geometric point of view. The only ingredients involved are a manifold $\mathcal{T}$, often referred to as the theory space, and a vector field spanned by the beta functions. The data $(\mathcal{T}, \beta)$ suffice to describe what is called the RG flow.

When applied to quantum systems that are able to predict the geometry of the spacetime $\mathcal{M}_d$ they live in, the scale-dependent actions Γ_k provided by the functional renormalization group imply a set of coupled effective field equations that govern the expectation values of the gravitational and matter fields. Their scale-dependent solutions include an effective metric tensor $g_{\mu\nu}^k$. Heuristically, it can be regarded as the description of a coarse-grained, fractal-like spacetime on a variable resolution scale, determined by the value of the RG parameter k.

Separately for each RG scale $k \in \mathbb{R}^+$, the respective GEAA functional Γ_k implies a quantum corrected variant of Einstein's equation; its solutions are the resolution-dependent metrics $g_{\mu\nu}^k$. They are dependent on the scale usually, but establish (pseudo-) Riemannian structures on one and the same smooth manifold $\mathcal{M}_4$.

Typically different generalized RG trajectories (solutions to the combined RG + Einstein equations) will lead to different $(d+1)$-dimensional manifolds. It is therefore an intriguing question which types of such embedding manifolds can actually occur in a given fundamental theory of quantum gravity.

(1) In Chapter 7 we proposed a new way of representing and analyzing the family of metrics $g_{\mu\nu}^k$ that furnish the same, given 4-dimensional manifold $\mathcal{M}_4$. The idea is to interpret the 4D spacetimes $\left(\mathcal{M}_4, g_{\mu\nu}^k\right)$, with $k \in \mathbb{R}^+$, as different slices through a single 5-dimensional (pseudo-) Riemannian manifold $\left(\mathcal{M}_5, {}^{(5)}g_{IJ}\right)$. We then posed the question about the additional 5 components of ${}^{(5)}g_{IJ}$ that are *not* provided by the 4D flow. First we discussed the possibility that there could exist mathematically or physically distinguished ways of fixing these additional components, the idea being that the (then unique) 5D geometry encapsulates not only the entirety of the 4D geometries, but enriches them by additional physics contents.

Within a first, restricted Euclidean setting we were indeed able to identify an additional piece of physics information, namely the property that the running cosmological constant $\Lambda(k)$ is a monotonically increasing function of k, which gets encoded by the very existence of $\left(\mathcal{M}_5, {}^{(5)}g_{IJ}\right)$ of a certain type.

Assuming the monotonicity of $\Lambda(k)$, we showed that 4D *Euclidean* spacetimes can always be embedded in a manifold $\mathcal{M}_5$ that is Ricci flat, or even Riemann flat should the 4D spacetimes be maximally symmetric.

(2) In a second stage, we extended these investigations in two directions. Being particularly interested in the physically relevant case of 4D Lorentzian spacetimes, in the present thesis we examine the most natural generalization beyond flat and Ricci flat $\mathcal{M}_5$s, namely 5D Einstein spaces. We addressed this question within 4D Quantum Einstein Gravity which (almost certainly) is asymptotically safe (see Chapter 3). It owes its nonperturbative renormalizability to a non-Gaussian fixed point. Its RG flow also features a second, Gaussian fixed point. While the fixed point theories are scale invariant, and while their full conformal invariance is likely, it has so far not been demonstrated.

Concretely, we allowed the higher-dimensional manifold $\mathcal{M}_5$ to be an arbitrary *Einstein space*, and second, we admit the possibility that the spacetimes to be embedded, $\left(\mathcal{M}_4,\, g_{\mu\nu}^k\right)$, have a *Lorentzian signature*. A prime example would be a stack of de Sitter spaces dS_4 with a k-dependent Hubble parameter. Then, imposing maximum symmetry on them, we demonstrated that from Asymptotic Safety there arise two solutions for the embedding space, namely certain parts of the AdS_5 and the dS_5 manifold, which we denoted AdS_5^{emb} and dS_5^{emb}, respectively.

The 5-dimensional picture that emerges is particularly striking when combined with the assumption that the QEG fixed points are indeed conformal. Then the foliation furnishing $(A)dS_5^{emb}$ establishes a relationship between quantum theories in the bulk and on the boundary of $(A)dS_5$. This exhibits exactly the same structure as in the well-known AdS/CFT correspondences that have been extensively discussed in the literature.

(3) One of the motivations for the research program was our conjecture that there should be rather a close relationship between Asymptotic Safety on the one side, and the string theory-based AdS/CFT correspondence on the other [45, 229, 266]. Given the scope of the GEAA approach and its applicability to arbitrary systems of fields, it is clear that it also addresses the questions about the CFT on the AdS_5 boundary which the AdS/CFT framework answers by holographic means. Therefore, a presumably harder, but in principle exact GEAA-based calculation should be able to come up with specific answers to the same questions, and clearly it would be extremely interesting to see whether the respective answers agree.

(4) Closely related is the discussion concerning the relationship between the Asymptotic Safety and the AdS/CFT frameworks in general. Hence, we addressed another, more restricted question, namely whether it is possible to "derive" a certain kind of, possibly non-standard version of AdS/CFT correspondence. This involves applying the GEAA approach to a specific system of 4D gravity + matter fields, computing its running

actions Γ_k and background spacetimes $g_{\mu\nu}^k$, by solving the functional RG and effective Einstein equations, and then embedding the 4D metrics into a 5D one.

It is an intriguing possibility that by following these steps of the geometrization program one might be led to a specific solution of the general GEAA flow and field equations which describes a 5D setting with a bulk/surface relationship similar to that of the well-known AdS/CFT conjecture. In Chapter 7 we presented a first indication which indeed points in precisely this direction.

(5) Both the AdS/CFT and the Asymptotic Safety approach rely on a specific UV complete gravity theory in the bulk. While in the standard framework one invokes string theory for this purpose, in our case this role is played by QEG, nonperturbatively renormalized. In particular we found out that the full conformal invariance is established by means of the Type IIa trajectory, i.e., the one that crosses over from the NGFP to the GFP. Its endpoint has a vanishing cosmological constant, and so the corresponding solution to Einstein's equation is (3+1)-dimensional Minkowski space. Hence the effective action which has all fluctuation modes integrated out should amount to a CFT which lives on flat space.

In the anti-de Sitter case, the habitat which the foliation allocates to this CFT is the timelike 4D spatial boundary of AdS$_5$. For the de Sitter embedding, it consists instead of the $\mathbb{S}^3$ spaces (without time) located at the spacelike past and future infinity of dS$_5$. The properties of the emergent bulk/boundary connections have been detailed and discussed in Sections 7.8 and 7.9 already.

Some of the more specific properties of the QEG fixed points still remain to be established. We discussed for instance, that it is an open question whether their scale invariance extends to a full-fledged conformal invariance. In the special case of $d = 2$ spacetime dimensions, however, this question has been already answered in the affirmative. Moreover, a unitary 2D CFT has been identified which governs the fixed point theory [377].

Outlook. In summary, our findings strongly support the idea that, at least in principle it may be possible to discover various forms of "(A)dS/CFT correspondences" as specific solutions to the flow and field equations of matter-coupled QEG. While this may include the known examples[1], the present approach has the potential of identifying new ones also. In practice such an endeavor is beset with a large number of technical difficulties. In particular much more general truncations in theory space must be used which also should be able to discriminate between different matter systems. Nevertheless, this approach may ultimately help in better understanding the *raison d'être* of the known bulk/boundary correspondences.

---

[1]At the level of a field theory approximation to string theory.

Project (II.B): Spectral flows in de Sitter space

In Chapter 8 we considered the prototypical example of a kinetic operator for a quantum field on a Lorentzian manifold, the d'Alembertian. We determined its on-shell spectral flow along the functional RG trajectories of a particularly relevant type, and we showed how to utilize this spectral flow in order to gain physical information about asymptotically safe Quantum Einstein Gravity. As it is demanded for a hyperbolic operator, the respective RG trajectories were chosen to be valid also within a Lorentzian framework of effective average actions.

We displayed the various types of spectral problems that are naturally connected to the d'Alembertian within the gravitational average action approach. We emphasized that there is a crucial difference between the standard, or off-shell, eigenvalue problem of the operator in a fixed geometry, and the one-parameter family of on-shell spectral problems which one encounters in Background Independent Quantum Gravity.

The key physical effect which is captured by their pivotal difference is that in the second case the inhabitants of spacetime are granted the right to self-determine the metric structure of their habitat. It is the backreaction of graviton and matter vacuum fluctuations on the spacetime geometry that is encapsulated in the novel type of spectral flow proposed here.

Project (II.B) provided a first proof of principle showing that the information hidden in the spectral flow can be uncovered systematically, and can provide us with valuable physical insights.

(1) We started the analysis by first studying the eigenvalue problem of the d'Alembertian on an invariable de Sitter background with a scale independent Hubble parameter. After obtaining its spectrum $\{\mathcal{F}_\nu\}$ and the eigenfunctions $\chi_{\nu,\vec{p}}$, we investigated the eigenfunctions' "resolving power", i.e., their structural wealth that decides about the fineness of the patterns which can be drawn on spacetime by superimposing such eigenfunctions.

We saw that, depending on their quantum numbers $(\nu, \vec{p})$ and the conformal time argument η, the eigenfunctions can belong to three different regimes of behavior with correspondingly different resolution properties. In these regimes, they display harmonic oscillations, power law behavior, and log-periodic oscillations, respectively.

The first two cases are generalizations of what in classical cosmology occurs for, respectively, sub- and super Hubble size wave solutions of the massless Klein–Gordon equation. The main difference is that in the present context the attention is not restricted to eigenfunctions with zero eigenvalue, $\mathcal{F}_\nu = 0$. Rather, *all* eigenmodes are relevant, having arbitrary eigenvalues $\mathcal{F}_\nu \in \mathbb{R}$. In particular the extremely large ones,

$\mathcal{F}_\nu \gg H^2$ having $\nu \gg 1$, are essential to determine the maximum resolving power, and for detecting a possible microscopic fuzzyness of the effective quantum spacetimes.

We saw that the harmonic (power law) regime has ideal (very poor) resolution properties, and showed that for principal quantum numbers $\nu \gg 1$, the transition from the harmonic to the power law regime is extremely sharp and sudden. It appears more phase-transition-like than the gradual horizon crossing of the massless modes in standard cosmology (see Fig. 8.5 for an illustration).

(2) Along the (simplified) Type IIIa trajectories, we obtained the spectral flow of the on-shell d'Alembertian in a fully explicit form. We solved the effective Einstein equations at all scales $k \in [0, \infty)$ by a dS$_4$ spacetime with a running Hubble parameter $H = H(k)$.

Then we solved the running eigenvalue problem and, having obtained the spectrum $\{\mathcal{F}_\nu(k), \chi_{\nu,\vec{p}}(x;k)\}_{k\geq 0}$, we determined the corresponding cutoff modes, $\chi_{\nu_{\mathrm{COM}},\vec{p}}(x;k)$. Their resolving power is given by the wave number $\vec{p}$ and the running principal quantum number of the cutoff modes, $\nu_{\mathrm{COM}}(k)$. It determines the range of applicability of the effective field theory defined by Γ_k, for the same value of k.

(3) Having found the quantum number $\nu_{\mathrm{COM}}(k)$ at all scales $k \geq 0$, we saw that as a consequence of the fluctuations' backreaction on the geometry, the function $\nu_{\mathrm{COM}}(k)$ never exceeds its value at the turning point of the RG trajectory: $\nu_{\mathrm{COM}}(k) \leq \nu_{\mathrm{COM}}(k_T)$. Therefore, the fineness and resolving power of the cutoff modes no longer improves when k is increased beyond k_T. Rather, it deteriorates quite considerably when k approaches the Planck scale, until Asymptotic Safety establishes a constant fixed point value $\nu_* \neq 0$ for $k \to \infty$.

While this behavior of $\nu_{\mathrm{COM}}(k)$ is strikingly different from what would happen in standard matter field theories on flat space, it is similar to that of its discrete analog $n_{\mathrm{COM}}(k)$ related to the Euclidean S^4 spacetimes that we reviewed in connection with Figure 8.1.

(4) Nevertheless, in contrast to the Euclidean setting where the boundedness of $n_{\mathrm{COM}}(k)$ implies a fundamental limitation on the distinguishability of points in *spacetime*, the boundedness of $\nu_{\mathrm{COM}}(k)$ in the Lorentzian setting was shown to imply no analogous restriction for the resolvability of points on the 3D *spatial manifold* related to the foliation considered. At first sight this may seem surprising as in some naive sense dS$_4$ is related to S^4 by an analytic continuation. It should be noted, however, that it leads to a non-compact manifold on which the kinetic operator is defined. Moreover, the Euclidean results refer to the distinction of points in 4D spacetime, and a momentum square of the symbolic form $p^2 = p_0^2 + \vec{p}^2$, while the new results pertain to 3D space, embedded in a spacetime on which, likewise symbolic, $p^2 = -p_0^2 + \vec{p}^2$. In the latter

case, thanks to the negative $-p_0^2$ we can make the spatial $\vec{p}^2$ as large as we like without increasing the 4D square p^2, simply by choosing p_0 appropriately.

(5) Regarding the possibility of a nonperturbative, quantum gravity-generated vacuum structure of the three dimensional space, seen as a slice through dS$_4$, the main result of the spectral flow analysis is that, despite the above, such a structure does indeed exist. However, rather than at very small distances, the corresponding quantum phenomena make their appearance *in the regime of macroscopic proper distances*.

(5a) In a nutshell, the basic mechanism can be understood by recalling the familiar textbook discussion of massless Klein–Gordon modes in cosmology which, at some moment, "leave the horizon" or "enter the horizon". In more precise terms, what is referred to here is a transition from the harmonic to the power law regime. For $\Box\chi = 0$ fields, the modes' proper wavelength at the moment of the transition is of the order of the Hubble scale $L_H = 1/H$.

(5b) In Section 8.7 we saw that the equality of the two length scales is a coincidence, in the following sense: If, rather than $\Box\chi = 0$, the scale-dependent on-shell equation $(\Box + \mathcal{F}_\nu)\chi = 0$ for generic eigenfunctions, and the COMs in particular, is considered, then the two scales are extremely different if $\nu \gg 1$. We showed that the cutoff modes' proper wavelength at the transition, $L_{\text{COM}}^+(k)$, is of the order of $L_H(k)/\nu_{\text{COM}}(k)$. As a consequence, the characteristic COM length scale $L_{\text{COM}}^+(k)$ is far smaller than the Hubble radius $L_H(k)$ on almost all scales.

(5c) Thus, the familiar picture of modes "leaving the horizon" gets replaced by a transition which, first, occurs already at a much shorter distance scale $L_{\text{COM}}^+(k) \ll L_H(k)$ that lies "deeply within the horizon", and second, amounts to a much more pronounced change of the modes' behavior. They switch from an η-dependence with perfect temporal resolution properties (harmonic regime) to a behavior with basically no resolving power at all (power regime).

(6) Furthermore, we interpreted the results of the spectral flow analysis from the perspective of a *physics-based spatial geometry*. We argued that any kind of geometric pattern seen in the Universe is ultimately "drawn" on space by physical fields. We therefore asked on which scales such patterns can occur if we require that they are amenable to a description by one of the effective field theories from the collection $\{\Gamma_k\}_{k\geq0}$. In answering this question we made essential use of the resolution properties of the COMs. In brief, it turned out that Γ_k-describable geometric structures displayed by position-dependent expectation values of quantum fields can exist only on length scales smaller than $L_{\text{COM}}^+(k)$. This confers the status of a coherence length to the running COM scale.

(7) In Section 8.9 we investigated the length scales between $L_{\text{COM}}^+(k)$ and $L_H(k)$, which are unaccessible to effective field theory, by a partially independent method, namely

the *direct analysis of the function space* $\text{Span}\,\mathscr{B}^{subH}_{superC}(\tau)$. There, we also introduced "scale histories" and the corresponding evolution diagrams to synoptically represent the structure of the quantum spacetime.

(8) It emerged the overall *picture of 3D space* as a fragmented patchwork of many small, basically unrelated, yet internally coherent patches. Within each patch, physics is describable by one of the actions Γ_k. When observed at scale k, the patches possess a typical proper size of the order $L^+_{\text{COM}}(k)$, whose scale dependence endows space with fractal properties. We refer in particular to Subsection 8.9.6, where we have already presented a detailed interpretation and summary of this picture.

(9) On a more statistical note, we also explored the *information content* that is naturally ascribed to the individual patches, and to the patchwork in its entirety. To quantify the latter, we introduced a special entropy function.

As an application, this led us in Section 8.10 to point out an intriguing analogy between the patchwork structure coming from quantum gravity, and the thermal photon gas of the *Cosmic Microwave Background Radiation* CMBR which inhabits the present Universe. Based upon this analogy and the measured value $G_0\Lambda_0 \approx 10^{-120}$ as our only (!) experimental input, we predicted for the CMBR photons within a Hubble volume an entropy of about $\mathcal{S}_{\text{CMBR}} \approx 10^{90}k_{\text{B}}$. Given the inherent approximations, this number is in perfect agreement with the established value.

Outlook. In future work an obvious generalization of our investigation is towards a nonzero matter stress tensor in the effective field equations, so as to lift the restriction to a vacuum dominated Universe. Furthermore, we saw that there are modes that, due to the presence of the NGFP never get integrated out. It is a highly intriguing possibility, which deserves being studied further, whether these modes carry information about the fixed point regime, and whether they "paint" it on the sky at the cosmological distances where the late Universe is vacuum dominated. Finally, future work will have to analogously scrutinize the role of the timelike modes in more detail, in particular in the context of scattering processes, desirably making contact in this manner with our work on scattering amplitudes in de Sitter space (**Project (II.C)**).

Project (II.C): Scattering amplitudes in de Sitter space

Scattering amplitudes in curved spacetime may provide insight into how to construct a consistent theory of Quantum Gravity. Being at the basis of observables in Quantum Field Theory, a proper understanding of scattering amplitudes in a gravitating background may help to uncover how to incorporate long-distance curvature effects into quantum theory.

(1) In Chapter 9 we presented the amplitude of gravity-mediated scattering of two massive scalars in dS spacetime. In the pure-gravity sector, we included all terms in the action up to four derivatives of the metric, while we also allowed for a non-minimal $R\phi\phi$-coupling between the scalar fields and the Ricci scalar. Our main new finding is that the Newtonian potential receives corrections due to the background curvature. In GR, these corrections should be suppressed by the inverse de Sitter radius, in accord to all observational tests on length scales ranging from table-top to solar system. In QuadG, moreover, we analyzed how the new coupling constants induced additional length scales, leading possibly to corrections to the potential at much smaller lengths. Thus, our computation of the Newtonian potential in QuadG allowed us to put additional constraints on the non-minimal couplings.

Novel in our work are two techniques:

(1a) First, we represented vertices and propagators as differential operators, rather than through integral kernels. We referred to this method as *operator method*. This generalized the Minkowski spacetime concept of momentum. Spacetime curvature was encoded in the noncommutativity of these operators. This came with the additional advantage that the resulting expressions remain fully covariant.

(1b) Secondly, in order to convert the expressions in terms of abstract differential operators into numerical quantities, we employed an expansion around infinite scalar masses. This is achieved by expanding in the dimensionless parameter $\mu = \frac{mc^2}{\hbar H}$, where m is the particle's mass and $H = 68$ km/sec/Mpc is the Hubble constant. We referred to this expansion as *adiabatic limit*.

Taking the limit $H \to 0$, we retrieved the nonrelativistic limit in flat spacetime. It is worth noticing that the expansion around $\mu = \infty$ has a slightly different status than the nonrelativistic limit in flat spacetime. In the latter case, a large-mass expansion is typically achieved by expanding around the dimensionless quantity m/p, or $p \ll m$. This explicitly breaks Lorentz invariance, since one explicitly refers to the frame-dependent spatial momentum. The expansion around $m/H = \infty$, however, is a Lorentz-invariant procedure.

(2) We presented our results in Section 9.3. The amplitude functional is explicitly gauge-independent, and reduces to the well-known flat-spacetime scattering amplitude in the flat limit. Interesting is the appearance of operators of the form $(-\Box + z)^{-1}$, resembling massive propagators. This hints towards a regularization of the graviton propagator in the infrared regime, opposed to the $1/q^2$ divergence in Minkowski spacetime. Furthermore, we found that one of the masses comes with a negative sign: this fact raised questions about the tachyonic nature of the graviton. However, we showed that the nontrivial curvature effects conspire to give a fully regular IR behavior.

For Quadratic Gravity we organized the propagator and vertices in such a way that an effective mass-pole structure for rank-0 and rank-2 vertex tensors could be identified. The poles are modified due to the de Sitter curvature. We observed that in the case of conformally coupled scalars, only the rank-2 vertex contributes.

(3) We extracted the tree-level scattering amplitude and potential from the abstract amplitude functional. Central in this computation was the application of the heavy-mass limit of the scalar fields, allowing us to obtain the distribution of the graviton propagator over the product of two scalar fields.

(3a) From the scattering amplitude, we constructed the following compelling physical picture.

(1) First, we observed that the amplitude has a finite limit as the transferred graviton momentum goes to zero. This is in contrast to the Minkowski-space-time amplitude, which exhibits an IR divergence due to the masslessness of the graviton. We therefore provided evidence for the regularization of the graviton propagator due to corrections from the curved background.

(2) Second, a striking feature of the scattering amplitude is its oscillating behavior as a function of the momentum. We showed that the scattering probability vanishes for discrete values of the graviton momentum, pointing towards discrete transition probabilities. In the cosmological context, this would translate to graviton exchange being bounded by the Hubble volume.

(3) Thirdly, we performed this analysis for any mass parameter of the graviton propagator, necessary to cover Quadratic Gravity. It turned out that the mass parameter associated to the massless graviton in a de Sitter spacetime is special, in the sense that the amplitude for this mass parameter is not continuously connected to the amplitude corresponding to different masses.

(3b) These physical features also appeared in the scattering potential:

(1) For small values of the radius, we reproduced the Newtonian $1/r$ potential.

(2) At larger distances, modifications due to the background curvature induce corrections to the potential, which to leading order can be captured by a constant repulsive force. For distances of approximately half the Hubble radius, this force dominates the attractive Newtonian force, such that particles are repelled. This is in line with the interpretation of the de Sitter Universe as an expanding spacetime.

(3) As the radius approaches the de Sitter horizon, the potential reaches a finite value, before vanishing identically for $r > 1$. Hence, the potential has bounded support while remaining bounded from above.

(4) Finally, the vanishing of the potential at super-Hubble distances is completely in agreement with the causal properties of the de Sitter spacetime, which forbid any causal interaction of particles beyond the horizon.

(5) In case of QuadG, we found for small proper separations r a potential that is in agreement with the flat-spacetime Yukawa potentials. Interpreting the scattering potential as the source of a Newtonian force, we investigated whether the modified potentials in QuadG could give rise to Modified Newtonian Dynamics corresponding to dark-matter-like rotation curves. However, we reported that the de Sitter curvature leads to an effective repulsive force that cannot be matched to a dark-matter-like scenario.

We showed how scattering amplitudes and the non-relativistic Newtonian potential should be modified on a de Sitter spacetime due to (higher) curvature corrections to General Relativity. In particular, this is done by computing the amplitude associated to the amputated diagram with Bunch–Davies boundary conditions. We followed the standard quantum field theoretical procedure, regardless of the unicity of the vacuum. Exactly this point renders non-trivial the interpretation of the amplitude and the potential in the curved case. We plan to further investigate these open questions in future work.

Outlook. Concerning scattering in de Sitter space, a challenge to be taken up in future work is the analysis of the de Sitter horizon. The novel techniques allows to probe the horizon properties of a more general geometry with two masses inside. This may shed light on the outstanding problem of defining a horizon temperature in a Schwarzschild–de Sitter spacetime. In analogy with classical electrodynamics, the discontinuity may be interpreted as a surface energy density situated at the horizon. In a semi-classical interpretation, the discontinuity would allow for tunneling of particles. It would be interesting to study both explanations, and try to make contact with a thermodynamic description of the de Sitter horizon.

Moreover, the first natural extension is to compute higher-order corrections in the heavy-mass expansion in order to include angular and spin-dependence, and to include quantum corrections (loop diagrams). A convenient scheme to capture these is the form factor formalism, which can be extended to curved spacetime. Furthermore, it would be interesting to extract the amplitude and potential for conformally coupled scalar fields. An initial investigation of this system shows that this gives rise to a modification of the differential equations determining the amplitude. Currently it is unknown whether this system of equations can be solved. Finally, this covariant construction of scattering amplitude functionals can be extended to other curved backgrounds that also admit an adiabatic expansion, such as FLRW spacetimes. In particular, it can be applied in slow-roll inflationary spacetimes. A comparison with n-point functions imprinted on

the Cosmic Microwave Background would allow to make contact with astrophysical observations.

Part III

Dynamical diffeomorphisms and scale-dependent relational observables

CHAPTER 11

Introduction and Survey of Part III

As explained in the Introduction, one of the greatest issues for a theory of gravitation is how to generalize the notion of local observables because of the very nature of its underlying symmetries. **Part III**, based on the author's publications [RF6] and [RF7], is mainly devoted to the study of this symmetry, diffeomorphism invariance, and to the construction of relational observables and the evaluation their quantum corrections (**Project (III.A)**). In Chapter 12 we construct models of dynamical diffeomorphisms, discussing the possibility of describing relational observables. In Chapter 13, we open a new line of research computing the renormalization group flow of relational observables in asymptotically safe gravity by using the composite operator formalism (**Project (III.B)**).

(1) Physicists turn reality into numbers. They process these numbers using mathematics, and turn them into predictions about other numbers. The mapping between physical reality and mathematical models is not at all straightforward. It involves a lot of arbitrary choices. When we perform an experiment, we take the readings of our instruments and create one particular parameterization of Nature. There are usually many equivalent parameterizations of the same process and this is one of the sources of redundancy in our description of nature: The Universe does not care about our choice of units or coordinate systems.

This indifference, after we plug the numbers into our models, is reflected in *symmetries* of our models. A change in the parameters of our measuring apparatus must be compensated by a transformation of our model, so that the results of calculations still match the outcome of the experiment.

But there is an even deeper source of symmetries in physics. The model itself may introduce additional *redundancy* in order to simplify the calculations or, sometimes, make them possible. It is often necessary to use parameter spaces that allow the description of non-physical states, states that could never occur in reality.

(2) If you ask physicists what the foundations of physics are, often they will answer: symmetry. Depending on their area of research, they will start talking about various symmetry groups, like $SU(3)$, $U(1)$, $SO(3,1)$, general diffeomorphisms, etc. The foundations of physics are built upon fields and their symmetries. For physicists this is
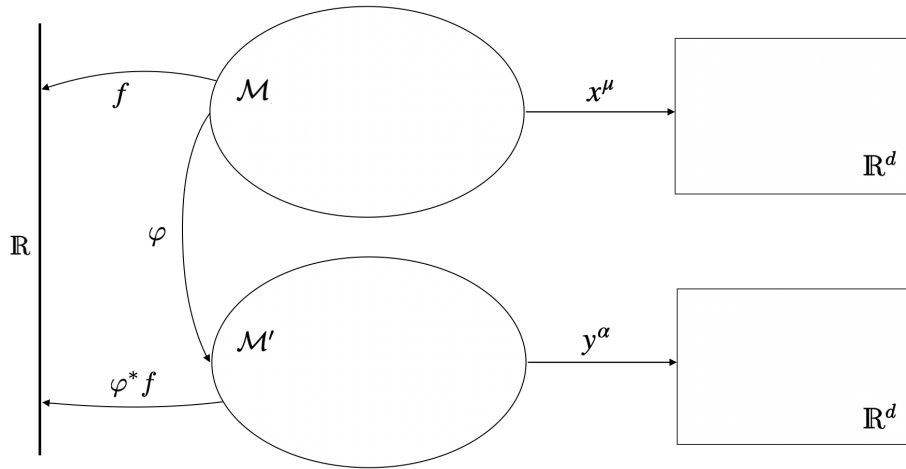
FIGURE 11.1. Maps between two different manifolds and how maps could be composed. We can use of maps to carry along tensor fields from one manifold to another.

such an obvious observation that they assume that the goal of physics is to discover the symmetries of Nature. But are symmetries the property of Nature, or are they the artifact of our tools? This is a difficult question, because the only way we can study Nature is through the language of mathematics. Mathematical models of reality definitely exhibit lots of symmetries, and it is easy to confuse this with the statement that Nature itself is symmetric.

Some crucial terminology

Attempts to understand the significance of diffeomorphism invariance in General Relativity have been obstructed by the confusion surrounding definitions such as *active vs. passive transformations*, *invariance vs. (general) covariance*, as well as *background independence* vs. *Background Independence*. Let us clarify these notions. First of all, a ***diffeomorphism*** φ is a smooth map of manifolds with smooth inverse. Diffeomorphisms can act on tensor fields on a manifold as well by a map called the pullback φ^* (see Figure 11.1). If we consider two manifolds $\mathcal{M}$ and $\mathcal{M}'$ with coordinate systems x^μ and y^α, respectively. We imagine that we have a map (diffeomorphism) $\varphi \colon \mathcal{M} \to \mathcal{M}'$. The name makes sense, since we think of φ^* as "pulling back" a given function f from $\mathcal{M}'$ to $\mathcal{M}$.

(1) Symmetries vs. redundancies. A *symmetry* is a map that transforms physical states or histories of a physical system to other, physically distinguishable states or histories. A symmetry group of a physical system is a group comprised of transformations that leave the system invariant.

Redundancies or synonymously *gauge symmetries* instead map one state or history to a physically indistinguishable state or history. A gauge group of a system is a set of transformations that leave physical states invariant. What this means is that the actual states of the system are equivalence classes of orbits of the gauge group. The reason physicists work with gauge groups in the first place is that the description of the system may simplify after introduction of additional "redundant" parameters that "see" into the equivalence class.

(2) Invariance vs. covariance. A quantity is *invariant* under a transformation if it remains unchanged under it; that is, if F is a functional of the fields ϕ, and we make the transformation $\phi \to \phi'$, then $F[\phi] = F[\phi']$ means that F is invariant under this transformation. Effectively, *invariant quantities transform as scalars*.

Covariance or synonymously *form invariance* states that the form of physical laws does not change under a given transformation.

General covariance is the special case, in which their form is invariant under arbitrary (differentiable) coordinate transformations.

For example, the action of a scalar field ϕ is *invariant* under Lorentz transformations, while the Klein–Gordon equation is Lorentz *covariant* (meaning that if ϕ satisfies the equation of motion, then so will ϕ').

Note that a symmetry is automatically a covariance; while, in general, a covariance does not necessarily correspond to a symmetry.

It becomes clear then, that considering laws which can be derived from a scalar quantity such as the action S, the symmetries of these laws are equivalent to the invariances of this scalar quantity.

(3) Active vs. passive transformation. A *passive transformation* is merely a change of coordinates. In the case of the Lorentz group, which takes x^μ to $x'^\mu = \Lambda^\mu{}_\nu x^\nu$, we define $\phi'(x) = \phi(x') = \phi(\Lambda x)$. In other words, we think of ϕ and ϕ' to be the same field configuration, such that the new function in the original coordinates is the same as the original function in the new coordinates.

Active transformations, even if more abstract, are formally easier to understand. Consider two manifolds $\mathcal{M}$ and $\mathcal{M}'$, respectively equipped with coordinate charts x and x'. Let $\phi : \mathcal{M} \to \mathbb{R}^d$, and $\phi' : \mathcal{M}' \to \mathbb{R}^d$. Now consider a diffeomorphism $\varphi : \mathcal{M} \to \mathcal{M}'$. Then the original field ϕ gets related to the transformed field ϕ' via the pullback, $\phi(x) = (\varphi^* \phi')(x) \equiv (\phi' \circ \varphi)(x)$. In general, $\phi(x)$ and $\phi'(x')$ may map to different points in $\mathbb{R}^d$. But if we demand $\phi'(x') = \phi(x)$, we impose that the new field configuration (on the new manifold) nonetheless maps to the same point in $\mathbb{R}^d$.

In part for this reason, we shall henceforth take the unqualified term "diffeomorphism" to mean an active diffeomorphism, and relegate "passive diffeomorphism" to "coordinate transformation" (see Figure 11.2).

For instance, $\phi'(x) = \phi(x') = \phi(\Lambda x)$ is a passive (Lorentz) transformation, while $\phi'(x') = \phi(x) \implies \phi'(x) = \phi(\Lambda^{-1}x)$ is an active (Lorentz) transformation. The former amounts to a mere coordinate redefinition, while the latter specifies an entirely new field configuration.

(4) The example of GR. When discussing diffeomorphism invariance, general covariance, or background independence in the context of GR, the above distinction is of crucial importance. In particular, the salient feature of *(active) diffeomorphisms* is that they *generate new metrics*, while *(passive) coordinate transformations* merely *re-express the original metric in new terms*.

(5) Background Independence vs. diffeomorphism invariance. When Einstein first introduced GR, he emphasized its Background Independence ("no prior geometry") under the guise of *general covariance*. But as alluded to above, all laws of physics, properly formulated, are generally covariant! Thus to emphasize general covariance as the defining or special feature of GR is both misleading and rather void of content. Misner, Thorne, Wheeler's classic textbook suggests that at the time, mathematics was not sufficiently advanced to properly distinguish Background Independence from coordinate independence, so Einstein's choice of phrasing is only confusing in retrospect [451]:

> Mathematics was not sufficiently refined in 1917 to cleave apart the demands for "no prior geometry" and for a "geometric, coordinate-independent formulation of physics". Einstein described both demands by a single phrase, "general covariance". The "no-prior-geometry" demand actually fathered general relativity, but by doing so anonymously, disguised as "general covariance", it also fathered half a century of confusion.

Rather, the special feature of GR is that it is Background Independent: the metric is a dynamical variable. This is what is meant by "no prior geometry".

However, it is also important to emphasize that diffeomorphism invariance is not the same as Background Independence. In Einstein's equation the metric is a dynamical variable, and thus the background is a solution to the equations rather than something given externally at the outset. Thus diffeomorphism invariance simply means that the manifold on which the theory is formulated is irrelevant (modulo isomorphisms) to the underlying physics (or, to take the passive view, that we can choose any coordinate patch we like). Background Independence is the by far stronger statement that the manifold itself is not fixed a priori. And this is exactly what makes GR special.
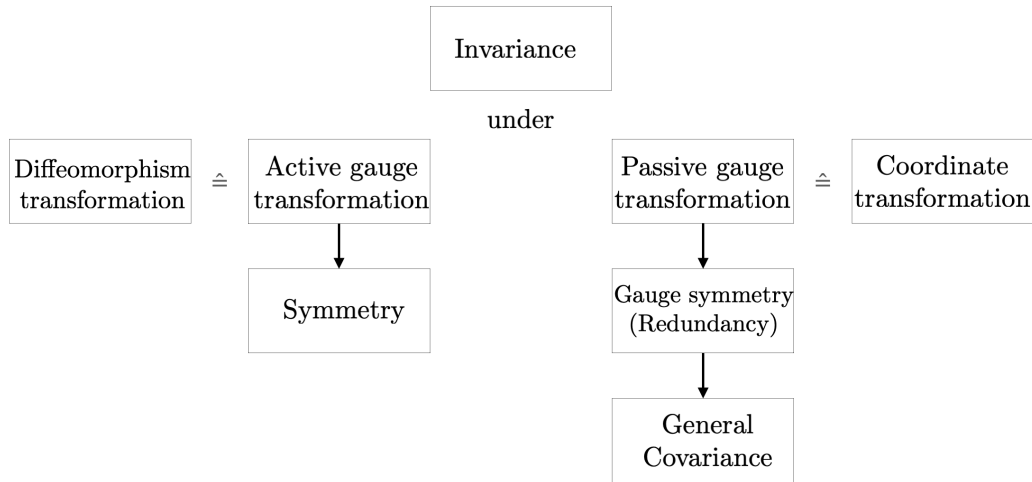
FIGURE 11.2. Diagrammatic representation of the crucial terminology used along **Part III**.

The problem of local observables

It is important to understand what physical principle distinguishes GR from other theories, such as a field theory formulated in a fixed spacetime. This is particularly necessary in order to properly understand how to construct observables in GR. Crucially, *general covariance is not the what distinguishes GR from a theory formulated in a fixed non-dynamical spacetime*. Let's analyze this by means of two different models.

(1) Model 1: Generally covariant but non-predictive.   There are models other than GR which can be formulated in a generally covariant manner even if they have a physically equivalent non-covariant formulation. The claim originates from the observation that we can formulate say a scalar field theory on a flat spacetime in a covariant manner by writing a generally covariant equation of motion for the scalar coupled to a metric tensor and then imposing the constraint equation that the Riemann tensor is zero. However, in such a construction we cannot predict the values of the scalar field in the future even given its values in the past. By general covariance any scalar field history that agrees in the past and is related by a diffeomorphism in the future would be a possible history and thus no unique prediction can be made.

(2) Model 2: Predictive but not generally covariant. To understand this failure we can consider a scalar field model where we pick a particular flat metric tensor and write the equation of motion for the scalar with that metric tensor. This model is not generally covariant and hence it will make predictions about the value of the scalar at a point in spacetime.

This mismatch between the predictive power of the two models can be understood by the fact that the models are *incomplete*: The fact that the second model predicts the value of the field for any value of the coordinates can only be tested if we know what it means for the coordinates to take different values. So if we want to actually measure the field at the point where all the coordinates vanish we must be able to tell where this point is located. This means that there must be some other physical objects which is not parameterized by the scalar field which gives the meaning to the values of the coordinates. Since the second model does not mention these objects, these variables must be *absolute objects* that have a fixed dynamic.

(3) The completion. We now insist on a completion of the second model with absolute objects. We can proceed by incorporating the absolute physical objects of the second model into the generally covariant model by including more variables in the model which parameterize them. The dynamics of the complete theory then dictates that *the variables corresponding to the absolute objects are fixed up to diffeomorphisms.* In particular for any two points there is a diffeomorphism that relates the two sets of values of the absolute variables to each other. Since in this model the metric is also an absolute object we can include its components.

The observables that correspond to the values of the scalar field in the non-generally covariant model can be constructed in the generally covariant model in the following way. In order for a measurement at a point in spacetime $\mathcal{P}$ to be performed *we must be able to distinguish the point $\mathcal{P}$ based on the history of the absolute objects.* This means that for each point $\mathcal{P}$ that is distinguishable there must be a set of scalars. For a field theory the variables are components of various fields which depend on the coordinates. Now, whichever set of variables we are using we can always make a change of variables to use a different set of fields which are functionals of the first set of variables.

(4) Coordinate-free is not enough. Evidently physical systems do not come with a set of coordinates. Coordinates are therefore not a part of physical system but rather a way in which we label points in space and time by a set of numbers within a model. Any observable of the physical system that we can measure can therefore be formulated in a manner that does not refer to coordinates. For example if we ask what is the value of a field at a point in spacetime, in order for the question to be well posed, we must give the location of the point in relation to some physical objects or the behavior of a field.

We discussed how some models are formulated with the help of a fixed coordinate system where the physical objects or fields which give the meaning to the coordinates in this manner are non-dynamical. However, we can incorporate those non-dynamical elements into an equivalent model of the same physical system such that the resulting model is generally covariant. In the resulting generally covariant model we allow in

the set of possible dynamical evolutions all those that are obtained from performing an active diffeomorphism on all elements of the model from any other possible evolution. This is the defining feature of general covariance. All models have such a generally covariant version. These share the property of General Relativity that observables that can be predicted from the theory are invariant under diffeomorphisms.

(5) No absolute objects. What distinguishes General Relativity from other theories is therefore *the lack of absolute elements which can be used to construct a non-dynamical coordinate system.* General covariance is hence not the right physical principle.

Therefore, *it is in fact the lack of certain absolute objects that forbids local observables in GR and not the requirement of diffeomorphism invariance*, which is a property of all physical systems and of all generally covariant models of those systems.

To understand this properly it is essential to understand why and in what sense observables are non-local in General Relativity. Since we can construct local observables in field theory on a fixed spacetime when formulated in a non-covariant manner, we should be able to construct the same local observables in a generally covariant manner. When we consider General Relativity we must then find that the same observable looses its local qualities since the absolute object now becomes dynamical.

(5) Physical consequences. From the previous observations we can draw the following conclusions:

(1) First, one should understand how physical models are modeling actual physical systems.
(2) Consequently, any model needs to be consistent with a set of equations that relate certain variables, or more generally functions of the variables, to elements of the real world.
(3) Only then can we test the model and thus only then can the model be considered as part of Nature.

We typically have differential equations which are obeyed by the variables of the model which determine the possible dynamical evolutions of the system.

(7) Matter is needed. According to GR, as soon as the concept of observables is introduced, the presence of matter fields is required, either to identify spacetime points or to define the spacetime manifold itself. Einstein noted [452]:

> Es ist schon eine harte Zumutung, daß man dem Raum überhaupt physika-
> lische Realität zuschreiben soll, insbesondere dem leeren Raume.

and also:

> Gemäß der allgemeinen Relativitätstheorie dagegen hat der Raum gegenüber
> dem "Raum-Erfüllenden", von den Koordinaten Abhängigen, keine Son-
> derexistenz. Man habe z.B. ein reines Gravitationsfeld durch die g_{ik} (als

Funktionen der Koordinaten) beschrieben durch Lösung der Gravitations-
gleichungen. Wenn man das Gravitationsfeld, d.h. die Funktionen g_{ik}
weggenommen denkt, so bleibt überhaupt nichts übrig, auch kein "topolo-
gischer Raum". Denn die Funktionen g_{ik} beschreiben nicht nur das Feld, son-
dern gleichzeitig auch die topologische und metrische Struktur-Eigenschaften
der Mannigfaltigkeit. Ein solcher Raum ist im Sinne der allgemeinen Rela-
tivitätstheorie nicht etwa ein Raum ohne Feld, sondern ein Spezialfall des
g_{ik}-Feldes, für welchen die g_{ik} (für das verwendete Koordinatensystem, das
an sich keine objektive Bedeutung hat) Werte haben., die nicht von den
Koordinaten abhängen; einen leeren Raum, d.h. einen Raum ohne Feld,
gibt es nicht.

(8) Relational physics. For some models spacetime coordinates may have themselves
a physical meaning such that when we give the values of the coordinates there is some
way to know where that point is in the physical system. Clearly this can only be
done if the values of coordinates are related to physical objects in some fashion. Said
differently, in physics the location of something is always defined *in relation to physical
objects*.

<center>*The hole argument*</center>

In order to fully elaborate on the concepts discussed in the previous section, let us start
reviewing the *hole problem* that Einstein faced in 1914 when contemplating generally
covariant theories.

(1) Coordinate scaffolding. The aim is to introduce coordinates that have an op-
erational meaning. We shall refer to the material system used for such a purpose as
the *coordinate scaffolding* [453], without further specification about its constitution. In
general, an event is characterized by the values of a large number of physical quantities
of the scaffolding, most of which are irrelevant for the purpose of extracting coordi-
nates. The coordinates are thus obtained by generating four real numbers out of these
physical quantities. From this perspective, the coordinates can be viewed formally as
real functions on the set of events. If one now uses these functions to define a chart
on a manifold, the latter is easily interpreted as the set of all events, identified through
convenient physical labels on the scaffolding.

(2) The hole problem. Assume that the gravitational field equations are generally
covariant and consider a solution to these equations in which the gravitational field is
described by the metric g. Assume that there is a hole, a region of the Universe without
matter. Assume further that inside the hole there is a point A where the gravitational
field corresponds to flat space, and a point B where it is not flat. Consider a map
$\varphi : \mathcal{M} \to \mathcal{M}$ s.t. $\varphi(A) = B$. Let $g' = \varphi^* g$ be the pullback of g under φ. The two
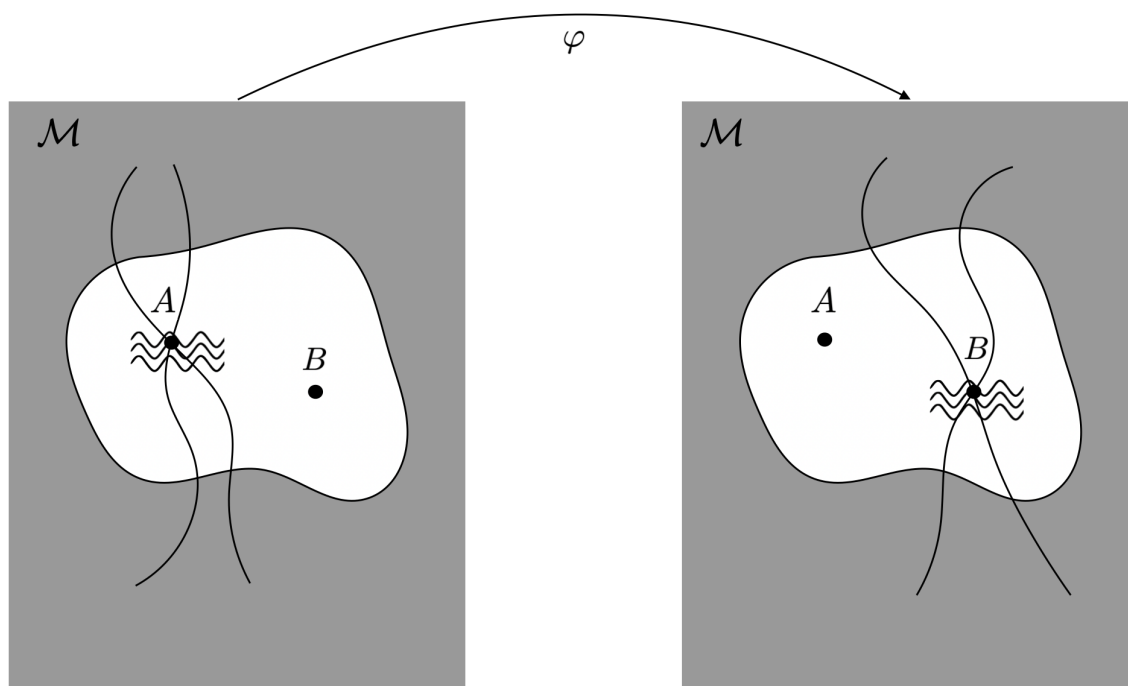metrics g and g' are both solutions of the field equations, but have different properties at

FIGURE 11.3. Hole argument: The diffeomorphism moves the non-flat region as well as the intersection point of the two particles from the point A to the point B.

B. So we are led to conclude that the field equations do not determine the physics at the spacetime point B. This is in contrast with the fact that classical gravitational physics is deterministic. Hence, in a theory whose equations are diffeomorphism invariant the assumption that points of the manifold have operational meaning becomes untenable. Since the Einstein's diffeomorphism-invariant field equations are valid, we conclude that there is no meaning in talking about physical spacetime at a point A. There is no meaning in referring to the point A or the event A, without referring to the coordinate system.

(3) The resolution. We are now presenting a resolution of the problem, namely by introducing matter. Assume that in the Universe there also exist two particles ($i = 1, 2$) and that their wordlines intersect at a point A. Given initial conditions, their worldlines are determined by the gravitational field: they are both geodesics of g. These wordlines are no geodesics of the metric g', hence the described motion of the particles will be different.

However, we can still find the motion of the particles determined by g', because the complete set of equations is generally covariant. We can act with an active diffeomorphism on the gravitational field s.t. the new worldlines are given by $x_i(t)' = \varphi^{-1}(x_i(t))$. They will now intersect in $B = \varphi^{-1}(A)$. The gravitational field is now non-flat at the
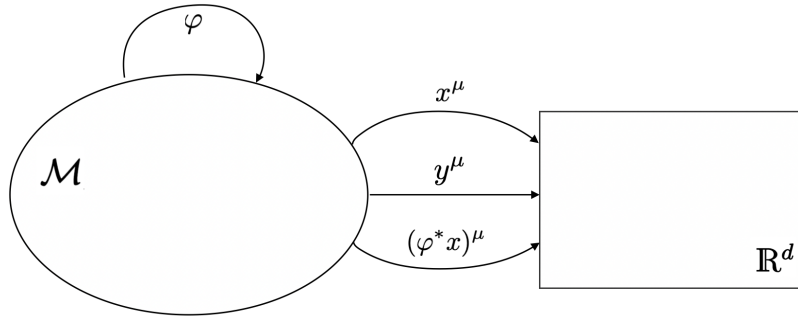
FIGURE 11.4. A change of coordinates can be viewed as an infinitesimal diffeomorphism transformation ϕ: $\mathcal{M} \to \mathcal{M}$, after which the coordinates would just be the pullbacks $(\varphi^*x)_\mu : \mathcal{M} \to \mathbb{R}^d$ ("move the points on the manifold, and then evaluate the coordinates of the new points").

point in which the particles meet.

It turns out that the prediction about the curvature is indeed deterministic, since the curvature R at this point reads:

$$R' = R'(x_i(t)) = R(\varphi(x_i'(t))) = R(\varphi(\varphi^{-1}(x_i(t)))) = R(x_i(t)) = R \qquad (11.1)$$

Einstein called these *spacetime coincidences*: the gravitational theory predicts what happens at locations determined by dynamical elements of the theory itself.

The two sets of geodesics are distinguished by their localization on the manifold $\mathcal{M}$; they are different since they assign different properties to the points. However, if we define localization only with respect to the metric and particles themselves, then we are not able to distinguish between the two solutions physically: the theory is gauge invariant under active diffeomorphisms. A state of the Universe does not correspond to a configuration of fields on $\mathcal{M}$, it corresponds to an equivalence class of field configurations under diffeomorphisms; a diffeomorphism changes localization of the field on $\mathcal{M}$. Therefore, localization on $\mathcal{M}$ is physically irrelevant.

Looking for a more precise analysis of the relationship between the properties of diffeomorphism invariance, Background Independence, and existence of local observables, we opened two new lines of research presented in **Project (III.A)** and **Project (III.B)**, respectively. Let us summarize the two projects in turn.

Project (III.A): Dynamical diffeomorphisms

In this Project we discuss a possible role of diffeomorphisms as dynamical variables. The motivations and inspiration for our modes were essentially two:

(1a) Modeling dark energy. Modeling dark energy is important both for early and late cosmology. A term in the action proportional to the volume of spacetime is the simplest explanation, but it has drawbacks. For this reason a more dynamical origin is often preferred. It turns out that in field theory (and cosmology) a generic non-dissipative medium can be effectively described by the theory of four derivatively coupled scalar fields. These four scalar fields can be interpreted as comoving coordinates of a cosmological medium.

We will link these results to the theory of EFT for fluids or solids, showing how gravitational interactions may be encoded in the interactions of a self-interacting medium. The dynamics follows straightforwardly via standard effective field theory logic once we identify the correct internal symmetries. Such an effective field theory description has first been considered in [454–456].

(1b) No local observables. Another motivation for our study is the absence of local observables in (quantum) gravity. For a field theory in flat spacetime we can consider simply the values of the fields at a point in spacetime, or products thereof, as constituting observables. However, as we discussed extensively, since in gravity the gravitational field is itself dynamical, no absolute objects are present, rendering the localization of observables non-straightforward. One of the greatest issues for a quantum theory of gravitation is how to generalize this notion of local observables [187, 188, 453, 457–466].

However, one can follow the line developed by Dirac in the context of gauge theory, thus treating this aspect of GR similarly to a gauge theory. This then winds up to the conclusion that *observables in (quantum) gravity are quantities which are diffeomorphism invariant, with the diffeomorphism group $\mathscr{D}\!\mathit{iff}$ acting from $\mathcal{M}$ to $\mathcal{M}$.*

Remark. One should note that with respect to physical observations this entails no violation of determinism. An observer can never really observe two different metric fields on one and the same spacetime manifold. She will use a fixed measurement apparatus, using rods and clocks in e.g. a local inertial frame, where special relativity applies locally, and then extend the results to general coordinate frames.

Note also that not even scalars are invariant in general in the above sense, i.e., not even the Ricci scalar is observable. Thus, adopting this point of view implies that the class of admissible observables is usually pretty small.

However, this is in blatant contradiction to the fact that we routinely perform measurements of local fields: for example, one can measure the components of the Riemann tensor near the surface of the earth [467].

(2) "Physical coordinates" and relational observables. A main concept that we shall need in the following is the notion of a *material reference system* or, equivalently,

a *physical coordinate system*. By a material reference system we mean an ensemble of physical bodies, dynamically coupled to gravity, such that these bodies can be used to define the spacetime points in a sense that will be specified. By using this concept, we shall argue that the "local point of view" can be obtained from the "non-local point of view" in the context of a certain approximation.

(2a) Measurements are made possible by the existence of matter. The matter fields can be understood precisely as representing the readings on some physical coordinate scaffolding. By definition, a *physical coordinate frame* constitutes four independent spacetime scalars that are composed of the dynamical fields and their derivatives.

For example, the Ricci scalar R at a point x is not diffeomorphism invariant: under a diffeomorphism ϕ, the scalar is transformed by the pullback

$$R(x) \mapsto \phi * R(x) = R(\phi(x)) . \tag{11.2}$$

As a result, the Ricci scalar is not an observable. However, if X denotes the (spacetime) position of a particle, a diffeomorphism will map $X \mapsto \phi^{-1}(X)$. Thus $R(X)$, the Ricci scalar at the position of the particle, is diffeomorphism invariant, and hence observable [468–470].

(2b) Following this argument, and invoking a bunch of infinitesimally close particles, one can construct a local frame at X, and thus give physical meaning to the components of any tensor at X [468–470]. In a cosmological setting, for example, a dense dust of particles [471, 472], which in the continuum limit becomes a continuous fluid, is commonly used to set up a physical coordinate system, and so give a physical meaning to a continuous tensor field, which can be measured in some region of spacetime.

Further examples of physical frames include curvature scalars formed from the Riemann tensor in pure gravity [468–470, 473], massless scalar fields [474] and scalars derived from cosmological perturbation theory [475, 476]. For a review and recent applications see [477].

(2c) All measurements of tensor or scalar fields, referring to such "physical" coordinate systems, can be thought of as measurements of certain *relational observables*. They have been abundantly discussed in the literature [187, 188, 453, 457–466].

(2d) Given that the matter content in the Universe represents a reference system, or actually a reference medium, with respect to which the points of the target space are defined, the following question arises: What is the dynamics of these fields?

In many applications the "coordinate infrastructure" is sufficiently rarefied that its effect on the geometry can be safely ignored. In general, however, this is not the case and the backreaction of the "coordinate infrastructure" on the geometry must be accounted

for, as for example in cosmology. Even if in the classical limit we could assume that the coordinate fluid is as "diluted" as one wants, but not in the quantum theory.

From these remarks we can draw two general conclusions:

(1) In order to meaningfully talk about local observables in the theory of gravity one has to include a form of matter as a coordinate system, and this matter will always back-react onto the geometry.

(2) At least some of the conceptual issues that arise in (quantum) gravity are in fact the result of this unphysical abstraction, namely neglecting the existence of matter.

These observations represent another motivation for studying models of gravity endowed with physical coordinates.

In the Hamiltonian framework, they involve what is commonly called "deparametrization". The most popular models of this type contain some form of dust [471]. There is a close analogue of this in gauge theories, where gauge-invariant observables can be constructed by suitably dressing local operators [464].

(2e) After these motivations, we remark that treating diffeomorphisms as dynamical variables gives rise to a theory with rather unique features not shared by any other. Ordinary matter propagating in spacetime can be represented either by maps into spacetime, such as the world-lines of point particles or the worldsheets of strings, or maps from spacetime into some other "internal" space, as is the case with all the usual matter fields.

Here instead we are in a peculiar situation where the "matter" field is both a map on spacetime and in spacetime.

Project (III.B): Relational observables in Asymptotic Safety

We discuss that diffeomorphism invariance is usually a concept which goes beyond covariance: it demands that also the content of the equations must be left unchanged by coordinate transformations. In this sense, invariance is achieved imposing that all constants that appear in the equations remain exactly the same. In this context, by constants we mean not only those things that are numerical constants, but also any quantity independent of the state of matter [22, 453]. We will call these constant objects *observables*.

(1) Classical and quantum. By drawing quantum mechanics and gravity together, we may infer that the spacetime structure undergoes quantum fluctuations at small scales. How to detect these fluctuations? In classical physics, spacetime points are

determined by material bodies like particles; but particles themselves are subject to quantum fluctuations. So how can fluctuating particles define a fluctuating spacetime structure down to the Plank scale? The very concept of spacetime points seems to become fuzzy in such a context. The observable quantities in the quantum theory should be the same as in the classical theory, or at least a subset of these. Rather remarkably, the problem of what precisely is observable is far from trivial even in classical General Relativity.

(2) Spacetime points and reference system. Assume that we are given a specific spacetime model $\mathcal{M}$. Although the correspondence between manifold points and values of physical fields is not observable, the correspondence between values of physical fields and values of other physical fields is physically meaningful. This is what we define as *point-coincidences*. This correspondence contains everything one needs to know, as it was already clearly expressed by Einstein [7]:

> Alle unsere zeiträumlichen Konstatierungen laufen stets auf die Bestimmung zeiträumlicher Koinzidenzen hinaus. [...] Die Einführung eines Bezugssystems dient zu nichts anderem als zur leichteren Beschreibung der Gesamtbeit solcher Koinzidenzen.

To define observable quantities, we then need to construct, among all the physical and geometrical fields in our model, four coordinate fields, and express any other quantity in terms of these.

The matter in the Universe, which, in particular, may be so dense that the corresponding points form a continuum, represents a *reference system* with respect to which the points of the target space are defined. Such a system was postulated by DeWitt [15], and recently reconsidered by Rovelli [22].

(3) Events and fields. There are two basic building blocks of modern relativistic cosmology: a manifold of events, and fields defined on it.

Consider our Universe, which relativistic cosmologies attempt to model. Its spacetime is the entirety of all space through all time. The *events* of this spacetime are generalizations of the dimensionless points of ordinary spatial geometry. A geometric point in ordinary spatial geometry is just a particular spot in the space and has no extension. Correspondingly, an event in spacetime is a particular point in a cosmological space at a particular moment of time. To be a 4-dimensional manifold, the set of events must be a little bit more organized. In a real spacetime, we have the idea that each event sits in some local neighborhood of events. This neighborhood sits inside a larger neighborhood of events, and so on. That extra organization comes from the requirement that we can smoothly label the events with four numbers - or at least we can do this for any sufficiently small part of the manifold. These labels form *coordinate systems*.

In specifying that events form a four dimensional manifold, there is still a lot we have not said about the events. We have not specified which events lie in the future and past of which other events, how much time elapses between these events, which events are simultaneous with others so that they can form three dimensional spaces, what spatial distances separates these events and many more related properties.

These additional properties are introduced by specifying the metric field. The minimum information we need is the temporal and spatial distance between each event and all those (loosely speaking) infinitesimally close to it. That information is what the metric field provides. It is a "field" since that information belongs just to one event. We can then piece together temporal and spatial distance along any curve just by summing all the distances between successive infinitesimally close points along the curve.

(4) Relational quantum observables as composite operators. We have discussed in Section 4.1 how within the FRG framework the flow equation for composite operators [195, 245, 247, 478] can be applied to investigate the scaling behavior of couplings in Quantum Gravity. This formalism allows us to compute the expectation of observables by solving a flow equation with running parameter the IR cutoff scale k. The initial condition at the UV cutoff scale $k = \Lambda$ is given by the expression of the observable as a function of the microscopic fields. At the end point of the flow at $k = 0$ the observable has evolved to the expectation value expressed as a function of the mean field. Crucially, in Asymptotic Safety the UV cutoff can be taken to infinity and hence the initial condition is defined in the limit $k \to \infty$ due to the existence of an interacting Reuter fixed point [95, 153, 220, 479]. Thus, this formalism allows the computation of observables in an asymptotically safe theory of Quantum Gravity.

First applications have been performed considering powers of the Ricci scalar integrated over spacetime [480, 481]. However these terms would also naturally appear as terms in the effective action.

On the other hand, the composite operator formalism allows us to compute the flow of terms which are not simply scalar quantities integrated over spacetime. Therefore it provides a formalism to compute quantities that are in principle measurable by a local experiment.

Relational observables are natural candidates for composite operators, which can be studied in Asymptotic Safety.

The research project **(III.B)** of this thesis is devoted to a construction of observables within the Asymptotic Safety program. We are going to set up a general framework for relational observables by introducing a set of four scalar fields[1] $\hat{X}^{\hat{\mu}}(x)$ ($\hat{\mu} = 0, 1, 2, 3$).

---

[1] We denote the fields with a hat when they represent fields living in the "material" (physical) frame.

These fields will represent the physical coordinate system upon which tensorial quantities can be evaluated and "measured". Inspired by the well-established composite operator flow equation, we build a formalism to evaluate the scaling of the relational observables. In addition, we furnish a definition for a relational effective action .

(5) Scaling dimension. Alongside the flowing effective average action, which interpolates between the microscopic fixed point action and the full effective action, our approach will allow access to flowing observables. Through this flow equation, we will compute the scaling dimension of a selection of observables described in the relational action. This set of observables will be chosen in order to self-consistently close the composite operator flow and to keep the truncation under control within a derivative expansion. It will turn out that only tensorial quantities with upper indices satisfy this truncation requirement. In particular, we will select the inverse relational metric $\hat{g}^{\hat{\mu}\hat{\nu}}(\hat{x})$ and the relational scalar curvature $\hat{R}(\hat{x})$, where $\hat{x}^{\hat{\mu}} = \hat{X}^{\hat{\mu}}(x)$. On the other hand, tensorial quantities with lower indices, such as the relational metric, are not generated at any finite order in derivative expansion.

At the Reuter fixed point the corresponding composite operators will have universal scaling exponents. Since they are observables, we expect them not to depend on unphysical elements of the scheme such as the gauge fixing conditions and choice of regulator. Physically these exponents should appear in the scaling behavior of correlation functions of relational observables at small distances less than the Planck length where effects of the fixed point scaling are expected. However, once approximations are made, we expect some dependence on the scheme. As such the computation of these exponents can serve as a way to compare with different approaches to Quantum Gravity and allow us to test the reliability of approximations. The aim of Chapter 13 is to develop the appropriate formalism which allows these investigations.

Plan of Part III

In the following table we schematize how this part is structured:

Part III	Project (III.A)	Chapter 12	Dynamical diffeomorphisms
	Project (III.B)	Chapter 13	Relational observables in AS

TABLE 11.1. Plan of **Part III**.

An overall Discussion and Summary of this Part can be found in Chapter 14.

CHAPTER 12

Dynamical diffeomorphisms

Executive summary. We construct a general effective dynamics for diffeomorphisms of spacetime, in a fixed external metric. Though related to familiar models of scalar fields as coordinates, our models have subtly different properties, both at kinematical and dynamical level. The energy-momentum tensor consists of two independently conserved parts. The background solution is the identity diffeomorphism and the energy-momentum tensor of this solution gives rise to an effective cosmological constant.

What is new? All results of this chapter represent novel research results.

Based on: Reference [RF6].

Plan of this Chapter. We begin by writing a class of actions for diffeomorphisms of a manifold to itself. They differ from the models that have been considered previously because the metrics in the domain and in the target space are one and the same (i.e., $g = h$). We derive the equation of motion (EOM) and show that the energy-momentum tensor (EMT) contains new terms that had not been considered previously, to the best of our knowledge. Interestingly, these new terms are conserved independently of the rest. We show that the equation of motion of the scalar is generically equivalent to the conservation of the EMT, but not always. We discuss the identity solution as a model for dark energy and its stability. Finally we return to the motivations given above and discuss the extent to which the models may provide satisfactory answers.

Appendix G contains a detailed proof of the diffeomorphism invariance of the action, and a demonstration that models where the domain and target space are not identified have different properties from those discussed in the main text. However, they can be related under some additional conditions.

The following sections of this chapter have been taken and rearranged from the author's publication [RF6].

12.1. MOTIVATION: MODELS FOR DARK ENERGY

Modelling dark energy is important both for early and late cosmology. A term in the action proportional to the volume of spacetime is the simplest explanation, but it has

drawbacks. For this reason a more dynamical origin is often preferred. [1] The most popular models are based on the potential of dynamical scalars. There are also many models of scalar fields with derivative interactions.

(1) Dynamics of the coordinates. The models we will discuss in this chapter can be seen as a special subclass of the latter, where the fields are restricted kinematically to be diffeomorphisms of spacetime. The idea of using the dynamics of coordinates or diffeomorphisms to generate an effective cosmological constant goes back at least to [483–485], where it was used to induce spontaneous compactification of certain directions in higher-dimensional theories.

(2) Massive gravity. More recently, it has been used extensively in the literature on massive gravity [486]. A mass term for the graviton breaks diffeomorphism symmetry, but the theory can still be written in a diffeomorphism-invariant way by introducing four "Stückelberg" fields, much in the same way as massive QED can be written in a gauge-invariant way by introducing one real scalar field [487]. In an influential paper, Arkani-Hamed, Georgi and Schwartz [488] have constructed the effective field theory of the four Goldstone bosons that are used to restore diffeomorphism invariance in massive gravity. The theory is formulated in terms of two separate "sites", that can be viewed as two copies of spacetime, each endowed with a separate diffeomorphism invariance, and a field linking the two sites. As with all Goldstone bosons, the Lagrangian of the fluctuation of the linking field is shift-invariant and therefore contains only derivative couplings.

(2a) The problem of the ghost. The major issue with this idea is that one of the four scalars (namely the one associated to the time coordinate) is a ghost.[2] This is because the target space of the scalar fields has a Minkowskian metric. In the original model, the ghost starts propagating at energy scales higher than $(1000\text{km})^{-1}$ [489, 490], leading to strong conflict with observations.

(2b) Possible solutions. This problem can be circumvented in two different ways:

(1) The first goes back to the fully non-linear version of the massive Fierz-Pauli theory, constructed as a bi-metric theory with a specific potential [491–496]. This theory can be made diffeomorphism-invariant by adding suitable scalar fields and is ghost-free. *In vacuo* it is reliable up to energies of order $\sim \text{mm}^{-1}$; above this scale, it becomes invalid due to strong coupling effects. In the presence of sources the situation is much worse.

(2) The second is to construct a ghost-free theory reducing diffeomorphism invariance to foliation-preserving diffeomorphisms [497–500]. This is perhaps not too

---

[1]See [482] for a review of many possible alternatives.
[2]In the models of [483–485], the problem of ghosts did not arise because the compactified dimensions are spacelike.

high a price to be paid, since in the cosmological context a preferred foliation is singled out anyway. [3] The resulting models can be interpreted as describing the dynamics of a medium filling the Universe. We refer the reader to [502–508] for later developments and applications to accelerating cosmological models.

We will show that the models we consider in this thesis share the same issues (and hence the same resolutions) as the theory of massive gravity.

12.2. MODELS FOR DYNAMICAL DIFFEOMORPHISMS

(1) **Nonlinear sigma models.** Technically, the models we shall discuss are very similar to nonlinear sigma models, except that the domain and the target space are the same manifold $\mathcal{M}$. In spite of this identification, we still need to distinguish two types of geometric objects: tensors evaluated at a point x and tensors evaluated at $\varphi(x)$. In order to better keep track of the difference, in component formulas, we shall use letters from the middle greek alphabet for the former and letters from the beginning of the greek alphabet for the latter. The pullback transforms tensors at $\varphi(x)$ to tensors at x, for example given a covariant vector ω (a one-form), its pullback is

$$(\varphi^*\omega)_\mu = \partial_\mu \varphi^\alpha \omega_\alpha(\varphi) \tag{12.1}$$

and

$$(\varphi^*g)_{\mu\nu} = \partial_\mu \varphi^\alpha \partial_\nu \varphi^\beta g_{\alpha\beta}(\varphi) \tag{12.2}$$

is the pullback of the metric. We will always use this notation: a tensor like ω without argument is understood to be evaluated at some point x, whereas $\omega(\varphi)$ has to be understood as a tensor evaluated at $\varphi(x)$.

Remark. In this setting the use of covariant derivatives requires a little explanation. The covariant derivative of tensors at x will be called ∇. It involves only Christoffel symbols with indices μ, ν, ρ etc. Tensors evaluated at $\varphi(x)$ have to be treated as scalars (they are inert under changes of frame at x). Thus for example $\nabla_\nu g_{\mu\nu} = 0$ as usual, but

$$\nabla_\nu g_{\beta\alpha}(\varphi) = \partial_\nu \varphi^\gamma \partial_\gamma g_{\beta\alpha}(\varphi) \ . \tag{12.3}$$

There is also a notion of covariant derivative on tensors at φ. We will write D for this type of covariant derivative. For example

$$D_\mu \omega_\alpha(\varphi) = \partial_\mu \varphi^\gamma D_\gamma \omega_\alpha \ ; \quad D_\gamma \omega_\alpha = \partial_\gamma \omega_\alpha - \Gamma_\gamma{}^\beta{}_\alpha \omega_\beta(\varphi) \ . \tag{12.4}$$

---

[3]We recall that the same symmetry reduction is also present in Hořava-Lifshitz gravity [501], and is sufficient to reconcile ghost freedom with perturbative renormalizability.

Note that in spite of carrying an index, φ^α are not vectors. Their covariant derivative is the same as the ordinary partial derivative. Thus we will use interchangeably the notation $\partial_\mu \varphi^\alpha$ and $\nabla_\mu \varphi^\alpha$, but when the derivative index is raised we always use ∇, so $g^{\rho\mu}\partial_\mu \varphi^\alpha = \nabla^\rho \varphi^\alpha$.

We shall also encounter objects that have indices of both types. For example, $\nabla_\mu \varphi^\alpha$ is a covariant vector at x and a contravariant vector at $\varphi(x)$.[4] In this case we find it convenient to use a covariant derivative ∇ that covariantizes only the index μ, while $\mathcal{D}$ is the full covariant derivative that covariantizes both indices:

$$\nabla_\rho \nabla_\mu \varphi^\alpha \;\;=\;\; \partial_\rho \nabla_\mu \varphi^\alpha - \Gamma_\rho{}^\sigma{}_\mu \nabla_\sigma \varphi^\alpha \; . \tag{12.5}$$

$$\mathcal{D}_\rho \nabla_\mu \varphi^\alpha \;\;=\;\; \nabla_\rho \nabla_\mu \varphi^\alpha + \partial_\rho \varphi^\gamma \Gamma_\gamma{}^\alpha{}_\beta \nabla_\mu \varphi^\beta \; , \tag{12.6}$$

(2) The building block. Let $g_{\mu\nu}$ be a metric on $\mathcal{M}$. The basic dynamical variable φ is a diffeomorphism of $\mathcal{M}$ to itself. The basic building block of the action is the tensor

$$B^\mu{}_\nu = g^{\mu\rho}(\varphi^* g)_{\rho\nu} = g^{\mu\rho}\partial_\rho \varphi^\beta g_{\beta\alpha}(\varphi)\partial_\nu \varphi^\alpha \; . \tag{12.7}$$

In the RHS we have written the factors in a particular order that calls for the use of matrix notation. If we denote $J_\mu{}^\alpha = \partial_\mu \varphi^\alpha$ the Jacobian of φ, we can write (12.7) in the form

$$B = g^{-1}(\varphi^* g) = g^{-1} J g(\varphi) J^T \; . \tag{12.8}$$

This notation is often convenient in calculations.

Let us now construct scalars out of this tensor. Since B is assumed to transform as a mixed tensor, the invariants are traces of products of powers of B. Only four such terms are algebraically independent. An arbitrary scalar can be expressed, generally in a nonlinear way, via four chosen independent scalars. The natural choice of four independent scalars is

$$\tau_k = \mathrm{Tr}(B^k) \; , \qquad k = 1, 2, 3, 4 \; . \tag{12.9}$$

Our action is then

$$S = \int \mathrm{d}^d x \, \sqrt{g}\, \mathcal{L}(\tau_1, \tau_2, \tau_3, \tau_4) \; , \tag{12.10}$$

where $\mathcal{L}$ is the Lagrangian, an arbitrary function of the traces. In the following we will sometimes consider the simplest case

$$\mathcal{L} = -\frac{1}{2}f^2 \tau_1 \; , \tag{12.11}$$

where f is a coupling. In mathematical literature (where g is a Riemannian metric) the stationary points are the *harmonic maps* [509]. Another particularly interesting

---

[4]It is a section of $T^*\mathcal{M} \otimes \varphi^* T\mathcal{M}$. The connection in this bundle is the tensor product of the Levi-Civita connection in $T^*\mathcal{M}$ and the pullback of the Levi-Civita connection in $T\mathcal{M}$.

Lagrangian is the quadratic Lagrangian

$$\mathcal{L} = c \left(\tau_1^2 - \tau_2 \right) . \tag{12.12}$$

We shall discuss some of its properties later on.

(2) Invariances. Let us now discuss the invariances of the theory. As long as φ are the only dynamical fields, and g is a fixed metric, the only symmetries of the action are the isometries of g. Thus, generically, there are no symmetries. Even though we will not discuss dynamical gravity here, we shall consider the invariances of the action when the metric is allowed to transform. This becomes relevant when one couples the fields to a dynamical metric, and will also be important later in the discussion of the energy-momentum tensor and its conservation.

A diffeomorphism ψ acts on tensors on $\mathcal{M}$ in the standard way, in particular the action on covariant tensors is by pullback. For example, the metric g is transformed to $g' = \psi^* g$. The action on φ can be either by left or by right composition. Under right composition

$$\varphi \mapsto \varphi' = \varphi \circ \psi \tag{12.13}$$

we have

$$\varphi^* g \mapsto \varphi'^* g' = \psi^* \varphi^* \psi^* g , \tag{12.14}$$

which is not the correct transformation of a covariant tensor. Thus B does not transform properly as a mixed tensor. Similarly under left composition

$$\varphi \mapsto \varphi' = \psi^{-1} \circ \varphi , \tag{12.15}$$

we find that the pullback of g is invariant:

$$\varphi^* g \mapsto \varphi'^* g' = \varphi^* \psi^{-1*} \psi^* g = \varphi^* g . \tag{12.16}$$

Thus again B does not transform properly. This was to be expected, because right composition (pullback) is the natural transformation for maps *on* spacetime (i.e., maps having spacetime as domain) and left composition is the natural transformation for maps *into* spacetime (i.e., having spacetime as target).

(3a) Diagonal subgroup. Since a diffeomorphism φ is simultaneously a map on and in spacetime, one should act both ways. Indeed, consider now the "diagonal subgroup" acting by conjugation

$$\varphi \mapsto \varphi' = \psi^{-1} \circ \varphi \circ \psi . \tag{12.17}$$

In this case we find that the pullback of the metric transforms as a covariant tensor:

$$\varphi^* g \mapsto \varphi'^* g' = \psi^* \varphi^* \psi^{-1*} \psi^* g = \psi^* \varphi^* g . \tag{12.18}$$

This leads to the correct transformation of B. We have established that the action functional $S[\varphi]$ is invariant under $\mathscr{D}iff(\mathcal{M})$, acting on the metric by pullback and on φ by conjugation.

(3b) Free and transitive: relation to other models. It is important to appreciate the following point: whereas the actions of $\mathscr{D}iff(\mathcal{M})$ on itself by left and right composition are transitive (every $\varphi \in \mathscr{D}iff(\mathcal{M})$ can be mapped to any other φ' by a right- or left-composition) and free (there are no fixed points), the diagonal action is not. In fact, the diagonal action leaves the identity map invariant.

In Appendix G we discuss closely related models where the domain and target spaces are kept separate, and show that the action functional is separately invariant under left- and right-diffeomorphisms. In contrast to those models, neither of these group actions leaves the action functional (12.10) invariant.

Remark. Finally we observe that the identification of the spacetime and target space metrics leads to peculiar properties also from the point of view of dimensional analysis. Since the two metrics appearing in B are functions of x and $\varphi(x)$, respectively, it is most natural to assume that the fields φ^α have the same dimension as the coordinates x^μ.[5]

We will assume this throughout this thesis. Then, the tensor $B^\mu{}_\nu$ is dimensionless, and so are the traces τ_n. The couplings f^2 and c in the Lagrangians (12.11) and (12.12) have mass dimension equal to the spacetime dimension d.[6] In fact, the coefficient of any monomial in the τ_n must have dimension d. Since the Lagrangian $\mathcal{L}$ must have dimension d, we could extract an overall factor f^2 with dimension d and write $\mathcal{L} = f^2 \tilde{\mathcal{L}}$, where $\tilde{\mathcal{L}}$ is a purely numerical function. As usual, one expects that $\tilde{\mathcal{L}}$ does not contain exceedingly large or exceedingly small coefficients. Then, f^2 is the only characteristic scale of the theory and it will be related to the scale of the cosmological constant.

12.2.1. *Equation of motion of φ*

(1) The equation of motion. Let $\varphi(t)$ be a one-parameter family of maps $\mathcal{M} \to \mathcal{M}$. The derivative

$$\left. \frac{d\varphi^\alpha(t)}{dt} \right|_{t=0} = v^\alpha \tag{12.19}$$

---

[5]It is generally the case that when the Lagrangian contains non-polynomial interactions, the fields should be dimensionless. This, together with $[\varphi] = [x]$ leads to dimensionless coordinates, a choice that we find most natural also for other reasons. However, we do not need to commit to this choice here.

[6]Note that in ordinary nonlinear sigma models f^2 would have dimension $d - 2$ and c would have dimension $d - 4$. The difference is due to the identification $h = g$. Also note that one could absorb f^2 in the metric, thereby making it dimensionless.

is a section of the vector bundle $\varphi^* T\mathcal{M}$. The equation of motion is obtained by setting to zero the directional derivative of the action functional (12.10) along an arbitrary vector v:

$$0 = vS = \frac{dS[\varphi(t)]}{dt}\bigg|_{t=0} = \int d^d x \sqrt{g} \sum_n n \frac{\partial \mathcal{L}}{\partial \tau_n} \text{Tr} B^{n-1} \frac{\partial B}{\partial t}\bigg|_{t=0} \tag{12.20}$$

$$= \int d^d x \sqrt{g} \sum_n n \frac{\partial \mathcal{L}}{\partial \tau_n} (B^{n-1})^{\sigma\nu} \left(2\partial_\nu v^\beta g_{\beta\alpha}(\varphi) + \partial_\nu \varphi^\beta v^\gamma \partial_\gamma g_{\beta\alpha}(\varphi)\right) \partial_\sigma \varphi^\alpha \ .$$

We used the fact that $(B^{n-1})^{\sigma\nu}$ is symmetric. In the first term we have to extract the variation v from the derivative. We use that $\partial_\nu v^\beta = \nabla_\nu v^\beta$ and use the standard rules for integration by parts. In this way we find

$$0 = vS = \int d^d x \sqrt{g}\, v^\alpha \left\{ -\nabla_\mu \left[2 \sum_n n \frac{\partial \mathcal{L}}{\partial \tau_n} (B^{n-1})^\mu{}_\rho g^{\rho\tau} \partial_\tau \varphi^\beta g_{\beta\alpha}(\varphi) \right] \right.$$

$$\left. + \sum_n n \frac{\partial \mathcal{L}}{\partial \tau_n} (B^{n-1})^\mu{}_\rho g^{\rho\tau} \partial_\tau \varphi^\beta \partial_\alpha g_{\beta\gamma}(\varphi) \partial_\mu \varphi^\gamma \right\} \tag{12.21}$$

$$= -2 \int d^d x \sqrt{g}\, v^\alpha g_{\alpha\beta}(\varphi) \mathcal{D}_\mu \left[\sum_n n \frac{\partial \mathcal{L}}{\partial \tau_n} (B^{n-1})^{\mu\nu} \partial_\nu \varphi^\beta \right] \ .$$

In the last step, we used (12.3) in the terms where ∇_μ hits $g_{\beta\alpha}(\varphi)$. The resulting terms combine with the second line to produce a Christoffel symbol that enters in the covariant derivative $\mathcal{D}_\mu$. Thus the equation of motion reads

$$\mathcal{D}_\mu \left[\sum_n n \frac{\partial \mathcal{L}}{\partial \tau_n} (B^{n-1})^{\mu\nu} \partial_\nu \varphi^\beta \right] = 0 \ . \tag{12.22}$$

(2) Special cases. One can be more explicit in special cases. For example, in the case of the action (12.11), the only term in the sum has $\frac{\partial \mathcal{L}}{\partial \tau_1} = 1$ and $B^0 = \mathbb{1}$, or $(B^0)^{\mu\nu} = g^{\mu\nu}$. Using the aforementioned rules, and recalling that $\partial_\mu \varphi^\alpha = \nabla_\mu \varphi^\alpha$, this leads to the equation for harmonic maps:

$$\mathcal{D}^\mu \nabla_\mu \varphi^\beta = 0 \ . \tag{12.23}$$

Applying this to the other special case (12.12), the equation of motion becomes

$$\mathcal{D}_\mu [\tau_1 \nabla^\mu \varphi^\beta - B^{\mu\nu} \partial_\nu \varphi^\beta] = 0 \ . \tag{12.24}$$

It will be useful to rewrite (12.23) in another way. Expanding the covariant derivatives one has

$$0 = g^{\mu\nu} \left(\partial_\mu \partial_\nu \varphi^\alpha - \Gamma_\mu{}^\rho{}_\nu \partial_\rho \varphi^\alpha + \partial_\mu \varphi^\beta \Gamma_\beta{}^\alpha{}_\gamma \partial_\nu \varphi^\gamma \right) \ . \tag{12.25}$$

Since φ is a diffeomorphism, from the transformation properties of the connection we can rewrite the first two terms as

$$\partial_\mu J_\nu{}^\alpha - \Gamma_\mu{}^\rho{}_\nu J_\rho{}^\alpha = -J_\mu{}^\beta J_\nu{}^\gamma \Gamma'_\beta{}^\alpha{}_\gamma \tag{12.26}$$

where we defined $J_\mu{}^\alpha = \partial_\mu \varphi^\alpha$, and therefore the equation for harmonic diffeomorphisms amounts to the statement that

$$0 = g'^{\beta\gamma} \left(\Gamma_\beta{}^\alpha{}_\gamma - \Gamma'_\beta{}^\alpha{}_\gamma \right) , \tag{12.27}$$

where $g'^{\beta\gamma} = g^{\mu\nu} \partial_\mu \varphi^\beta \partial_\nu \varphi^\gamma$ and Γ' are the Christoffel symbols of g'. Since the difference of two connections is a tensor, this is a covariant statement.

12.2.2. *Energy-momentum tensor*

(1) Energy-momentum tensor. Next, we vary the action functional with respect to $g_{\mu\nu}(x)$:

$$\delta S = \int \mathrm{d}^d x \sqrt{g} \left\{ \frac{1}{2} g^{\mu\nu} \delta g_{\mu\nu} \mathcal{L} + \sum_n n \frac{\partial \mathcal{L}}{\partial \tau_n} \mathrm{Tr} B^{n-1} \delta B \right\}$$

$$= \int \mathrm{d}^d x \sqrt{g} \left\{ \frac{1}{2} g^{\mu\nu} \delta g_{\mu\nu} \mathcal{L} + \sum_n n \frac{\partial \mathcal{L}}{\partial \tau_n} (B^{n-1})^\sigma{}_\mu \times \right. \tag{12.28}$$

$$\left. \times \left(- g^{\mu\rho} \delta g_{\rho\tau} g^{\tau\lambda} \partial_\lambda \varphi^\gamma g_{\gamma\delta}(\varphi) \partial_\sigma \varphi^\delta + g^{\mu\lambda} \partial_\lambda \varphi^\alpha \delta g_{\alpha\beta}(\varphi) \partial_\sigma \varphi^\beta \right) \right\} .$$

We can obtain the energy-momentum tensor by straightforwardly using the rules of variational calculus and evaluating

$$T^{\mu\nu} = \frac{2}{\sqrt{g}} \frac{\delta S}{\delta g_{\mu\nu}} . \tag{12.29}$$

It is perhaps more instructive to observe that in the last term the variation appears in the combination $\partial_\lambda \varphi^\alpha \partial_\sigma \varphi^\beta \delta g_{\alpha\beta}(\varphi) = (\varphi^* \delta g)_{\mu\nu}(x)$. We exploit the fact that the integral does not change if we replace the integrand by its transform under a diffeomorphism. Let $x'^\alpha = \varphi^\alpha(x)$, and denote by a prime all transformed tensors. Covariant tensors are pulled back by φ^{-1} and contravariant tensors are pushed forward with φ: $A' = \varphi_* A$, $g' = \varphi^{-1*} g$, and $(\varphi^* \delta g)' = \delta g$. Then the last term can be manipulated as follows:

$$\int \mathrm{d}^d x \sqrt{g(x)} \, A^{\mu\nu}(x) (\varphi^* \delta g)_{\mu\nu}(x) = \int \mathrm{d}^d x' \sqrt{g'(x')} \, A'^{\alpha\beta}(x') \delta g_{\alpha\beta}(x') , \tag{12.30}$$

where x' is to be regarded as independent integration variable. Then, from the definition given above, we obtain

$$T^{\mu\nu} = g^{\mu\nu}\mathcal{L} - 2\sum_n n\frac{\partial \mathcal{L}}{\partial \tau_n}(B^{n-1})^{\sigma\mu}\nabla^\nu\varphi^\gamma g_{\gamma\delta}(\varphi)\nabla_\sigma\varphi^\delta + 2\frac{\sqrt{g'}}{\sqrt{g}}\sum_n n\left(\frac{\partial \mathcal{L}}{\partial \tau_n}\right)'(B'^{n-1})^{\mu\nu} \ .$$

(12.31)

(2) Special cases. In particular for the Lagrangian (12.11)

$$T^{\mu\nu} = f^2\left[\nabla^\mu\varphi^\alpha\nabla^\nu\varphi^\beta g_{\alpha\beta}(\varphi) - \frac{1}{2}g^{\mu\nu}g^{\rho\sigma}\nabla_\rho\varphi^\alpha\nabla_\sigma\varphi^\beta g_{\alpha\beta}(\varphi) - \frac{\sqrt{g'}}{\sqrt{g}}g'^{\mu\nu}\right] \ , \qquad (12.32)$$

whereas for (12.12)

$$T^{\mu\nu} = c\,g^{\mu\nu}(\tau_1^2-\tau_2) - 4c(\tau_1 g^{\sigma\mu} - B^{\sigma\mu})\nabla^\nu\varphi^\gamma g_{\gamma\delta}(\varphi)\nabla_\sigma\varphi^\delta + 4\frac{\sqrt{g'}}{\sqrt{g}}c(\tau_1' g'^{\mu\nu} - B'^{\mu\nu}) \ . \quad (12.33)$$

12.2.3. *Diffeomorphism invariance, EOM and EMT conservation*

(1) Infinitesimal diffeomorphism transformation. Let us begin by recalling the general argument relating diffeomorphism invariance to EMT conservation. Given an action $S[\varphi, g]$ for the "matter" fields φ coupled to a metric g, its variation under an infinitesimal diffeomorphism ξ is

$$\delta_\xi S = \int \mathrm{d}^d x \left[\frac{\delta S}{\delta \varphi^\alpha}\delta_\xi\varphi^\alpha + \frac{\delta S}{\delta g_{\mu\nu}}\delta_\xi g_{\mu\nu}\right] \ . \qquad (12.34)$$

We define the equation of motion

$$E^\alpha = \frac{1}{\sqrt{g}}\frac{\delta S}{\delta \varphi^\alpha} \ . \qquad (12.35)$$

An infinitesimal diffeomorphism is defined by

$$\delta_\xi x^\mu = -\xi^\mu(x) \ , \qquad (12.36)$$

where ξ is a vector field. The infinitesimal variation of φ is

$$\delta_\xi\varphi^\alpha(x) = \xi^\lambda\partial_\lambda\varphi^\alpha - \xi^\alpha(\varphi) \ , \qquad (12.37)$$

where the first term comes from the right composition and the second from the left composition. The variation of any tensor T is its Lie derivative $\delta_\xi T = \mathcal{L}_\xi T$. For the metric

$$\delta_\xi g_{\mu\nu} = \xi^\rho\partial_\rho g_{\mu\nu} + g_{\mu\rho}\partial_\nu\xi^\rho + g_{\rho\nu}\partial_\mu\xi^\rho = \nabla_\mu\xi_\nu + \nabla_\nu\xi_\mu \ . \qquad (12.38)$$

Inserting these formulae and (12.29) in (12.34), invariance of the action implies

$$0 = \int \mathrm{d}^4 x\sqrt{g}\left[(\xi^\tau\nabla_\tau\varphi^\alpha - \xi^\alpha(\varphi))E_\alpha - \xi_\mu\nabla_\nu T^{\mu\nu}\right] \ . \qquad (12.39)$$

We find, as expected, that $E_\alpha = 0$ implies EMT conservation.

(2) What is special about dynamical diffeomorphisms. In the case of our theory of diffeomorphisms, there is more to be learned. We observe that for a generic φ, the coefficient of E_α is non-vanishing and therefore, conversely EMT conservation also generically implies the EOM. This makes sense, because both statements amount to four second order differential equations for the fields. However, for the identity map $\varphi^\alpha = x^\alpha$, the coefficient of E_α vanishes and therefore this implication does not hold. This is a consequence of the identity map being a fixed point of the action of the diffeomorphism group.

(3) Conservation of the EMT: left and right EMT. One could further explicitly compute the divergence of the EMT. This calculation is very complicated in general, but we can do it in the case of the Lagrangian (12.11). It turns out to be useful to split the EMT in two parts:

$$T^{\mu\nu} = T^{\mu\nu}_{(R)} + T^{\mu\nu}_{(L)} , \tag{12.40}$$

where the first part arises from the variations with respect to $g_{\mu\nu}$ and consists of the first two terms in (12.32), the second part comes from variation with respect to $g_{\alpha\beta}(\varphi)$ and consists of the third term in (12.32). Interestingly, these two parts are separately conserved. The conservation of $T^{\mu\nu}_{(R)}$ works exactly as for a nonlinear sigma model:

$$\nabla_\mu T^{\mu\nu}_{(R)} = f^2 \nabla^2 \varphi^\alpha \nabla^\nu \varphi^\beta g_{\alpha\beta}(\varphi) + f^2 \left(\nabla^\mu \varphi^\alpha \nabla^\nu \varphi^\beta \nabla_\mu \varphi^\gamma - \frac{1}{2} \nabla^\mu \varphi^\alpha \nabla_\mu \varphi^\beta \nabla^\nu \varphi^\gamma \right) \partial_\gamma g_{\alpha\beta}(\varphi) . \tag{12.41}$$

The two terms in parentheses reconstruct a Christoffel symbol, and the whole expression is then seen to be proportional to the EOM, written in the form (12.25).

For the second part,

$$\begin{aligned}
\nabla_\mu T^{\mu\nu}_{(L)} &= -f^2 \frac{1}{\sqrt{g}} \nabla_\mu(\sqrt{g'} g'^{\mu\nu}) \\
&= -f^2 \frac{1}{\sqrt{g}} \left(\partial_\mu(\sqrt{g'} g'^{\mu\nu}) + \sqrt{g'}\, \Gamma_\mu{}^\nu{}_\rho g'^{\mu\rho} \right) \\
&= -f^2 \frac{\sqrt{g'}}{\sqrt{g}}\, g'^{\mu\rho} \left(\Gamma_\mu{}^\nu{}_\rho - \Gamma'_\mu{}^\nu{}_\rho \right)
\end{aligned} \tag{12.42}$$

which vanishes due to the EOM written in the form (12.27).

While these statements are easy to check in the case of the Lagrangian (12.11), calculating the divergence of the EMT in the general case is very complicated. Still, the preceding statements remain true. One can see this by following in detail the proof of invariance of the action under infinitesimal diffeomorphisms, which is given in Appendix G. One can see there that the terms coming from variations of $g_{\mu\nu}$ (i.e. the divergence of $T^{\mu\nu}_{(R)}$) and those coming from variations of $g_{\alpha\beta}(\varphi)$ (i.e. the divergence of $T^{\mu\nu}_{(L)}$) cancel

separately against terms coming from the variation of φ (i.e. the EOM). More precisely, the differential identity (12.39) can be seen as the sum of two separate identities

$$\int d^4x\sqrt{g}\left[\xi^\tau\nabla_\tau\varphi^\alpha E_\alpha - \xi_\mu\nabla_\nu T^{\mu\nu}_{(R)}\right] = 0 \,, \qquad (12.43)$$

$$\int d^4x\sqrt{g}\left[-\xi^\alpha(\varphi)E_\alpha - \xi_\mu\nabla_\nu T^{\mu\nu}_{(L)}\right] = 0 \,. \qquad (12.44)$$

This is surprising, because the invariance group of the action has four parameters but it seems to imply eight differential identities. This can be explained by looking at the models as special cases of theories with different domain and target space. In these cases, as explained in Appendix G, the invariance group consists separately of left and right diffeomorphisms and therefore implies eight differential identities. The models with identical domain and target space are obtained by choosing a preferred diffeomorphism, and this does not invalidate the identities.

12.3. THE IDENTITY SOLUTION

The identity $\varphi = Id_\mathcal{M}$ is represented, in any local coordinate system, by

$$\varphi^\alpha = x^\alpha \,. \qquad (12.45)$$

In this case the Jacobian reduces to $\partial_\mu\varphi^\alpha = \delta^\alpha_\mu$, $B^{\mu\nu} = g^{\mu\nu}$ and all the traces become constant: $\tau_n = 4$ for $n = 1, 2, 3, 4$. Thus $\mathcal{L}$ and its derivatives are just constants and the EOM (12.22) are satisfied.

(1) Effective cosmological constant. The energy-momentum tensor of the solution becomes proportional to the metric. The last two terms in (12.29) cancel out and

$$T^{\mu\nu} = g^{\mu\nu}\mathcal{L} - 2\sum_n n\frac{\partial\mathcal{L}}{\partial\tau_n}g^{\mu\nu} + 2\sum_n n\left(\frac{\partial\mathcal{L}}{\partial\tau_n}\right)g^{\mu\nu} = g^{\mu\nu}\mathcal{L}(4,4,4,4) \,. \qquad (12.46)$$

We can therefore interpret this energy-momentum tensor as an effective cosmological constant $\Lambda = 8\pi G\,\mathcal{L}(4,4,4,4)$. As already anticipated, if we assume that $\tilde{\mathcal{L}}(4,4,4,4)$ is a number of order one, the effective cosmological constant is $\Lambda \approx 8\pi G f^2$.

(2) Stability of the solution. We will now discuss the stability of the identity solution. This can have two possible meanings: in Euclidean signature one asks whether the action has a minimum at the solution; in Lorentzian signature one asks whether the energy has a minimum. We begin by discussing the simpler problem of Euclidean stability. Since the Euclidean action is also identical to the energy of a static field configuration (in one dimension more) this analysis also says something about the stability of static configurations under static deformations. Full Lorentzian stability will be briefly discussed in Section 12.3.3, where we shall refer to existing results in the literature.

12.3.1. *The second variation*

(1) The Hessian at the identity. Here we compute the Hessian of the action at the identity solution. This is needed to establish whether a Euclidean solution is stable, and is also needed in the study of linearized perturbations. Let $\varphi(t, s)$ be a two-parameter family of maps. We take the double derivatives at $t = s = 0$. We let

$$\left.\frac{d\varphi^\alpha(t, s)}{dt}\right|_{t=s=0} = v^\alpha \,, \qquad \left.\frac{d\varphi^\alpha(t, s)}{ds}\right|_{t=s=0} = w^\alpha \,. \qquad (12.47)$$

The Hessian is defined by

$$H(v, w) = \left.\frac{\partial^2 S[\varphi(t, s)]}{\partial t \partial s}\right|_{t=s=0}$$

$$= -2\frac{\partial}{\partial s}\int d^d x \sqrt{g}\,\frac{\partial\varphi^\alpha}{\partial t}\,g_{\alpha\beta}\left(\mathcal{D}_\mu\sum_n n\frac{\partial\mathcal{L}}{\partial T_n}(B^{n-1})^{\mu\nu}\partial_\nu\varphi^\beta\right)\Bigg|_{t=s=0}. \qquad (12.48)$$

The derivatives with respect to s of the terms $\frac{\partial\varphi^\alpha}{\partial t}$ and $g_{\alpha\beta}$ are proportional to the EOM, and since we are interested in the variation around a solution, we can neglect them. Acting with the s-derivative on all the remaining occurrences of φ, and evaluating at $t = s = 0$, which correspond to $\varphi = Id_\mathcal{M}$, the round bracket becomes

$$\sum_n n\frac{\partial\mathcal{L}}{\partial T_n}\mathcal{D}^\mu\partial_\mu w^\beta + \sum_n n\frac{\partial\mathcal{L}}{\partial T_n}\mathcal{D}_\mu\left(\frac{\partial}{\partial s}(B^{n-1})^{\mu\beta}\Bigg|_{s=0}\right) + \sum_{n,m} n\frac{\partial^2\mathcal{L}}{\partial T_n\partial T_m}D^\beta\left(\frac{\partial T_m}{\partial s}\Bigg|_{s=0}\right)$$

$$+ \sum_n n\frac{\partial\mathcal{L}}{\partial T_n}g^{\mu\delta}\left(\partial_\mu w^\gamma\Gamma_\gamma{}^\beta{}_\delta + w^\epsilon\partial_\epsilon\Gamma_\mu{}^\beta{}_\delta\right)\,. \qquad (12.49)$$

Now consider the general formula

$$\mathcal{D}_\mu D_\nu w^\delta = \nabla_\mu\nabla_\nu w^\delta + \nabla_\mu\nabla_\nu\varphi^\gamma\Gamma_\gamma{}^\delta{}_\beta w^\beta + \partial_\nu\varphi^\gamma\partial_\mu\varphi^\beta\partial_\beta\Gamma_\gamma{}^\delta{}_\epsilon w^\epsilon$$

$$+ \partial_\nu\varphi^\gamma\Gamma_\gamma{}^\delta{}_\beta\partial_\mu w^\beta + \partial_\mu\varphi^\gamma\Gamma_\gamma{}^\delta{}_\epsilon\left(\partial_\nu w^\epsilon + \partial_\nu\varphi^\zeta\Gamma_\zeta{}^\epsilon{}_\beta w^\beta\right) \qquad (12.50)$$

and specialize to the identity map. Comparing this with the preceding formula, and using $\nabla_\mu\nabla_\nu\varphi^\beta = -\Gamma_\mu{}^\beta{}_\nu$, we see that the first and the last term in (12.49) combine to give

$$\sum_n n\frac{\partial\mathcal{L}}{\partial T_n}\left(\mathcal{D}^\mu D_\mu w^\beta + R^\beta{}_\gamma w^\gamma\right)\,. \qquad (12.51)$$

At the identity, we can convert all indices to μ, ν etc and $\mathcal{D}^\mu D_\mu = \nabla^2$. In the remaining two terms we have

$$\frac{\partial}{\partial s}(B^{n-1})^{\mu\nu}\Bigg|_{s=0} = (n-1)\left(\nabla^\mu w^\nu + \nabla^\nu w^\mu\right) \qquad (12.52)$$

and

$$\left.\frac{\partial \tau_m}{\partial s}\right|_{s=0} = 2m\nabla_\mu w^\mu \ . \tag{12.53}$$

Putting everything together, the second variation of the action around the identity is

$$H(v,w) = 2\int \mathrm{d}^d x \sqrt{g}\left[\sum_n n^2 \frac{\partial \mathcal{L}}{\partial \tau_n} v^\mu \left(-\nabla^2 g_{\mu\nu} - R_{\mu\nu}\right) w^\nu \right.$$
$$\left. + \left(\sum_n n(n-1)\frac{\partial \mathcal{L}}{\partial \tau_n} + 2\sum_{m,n} mn\frac{\partial^2 \mathcal{L}}{\partial \tau_n \partial \tau_m}\right)(\nabla_\mu v^\mu)(\nabla_\nu w^\nu)\right] \ . \tag{12.54}$$

(2) Self-adjoint differential operator. We can write $H(v,w) = \langle v, Lw\rangle$, where $\langle\,,\rangle$ is the natural inner product in the space of sections of $\varphi^*T\mathcal{N}$ and L represents the differential operator

$$L = \sum_n n^2 \frac{\partial \mathcal{L}}{\partial \tau_n}\left(-\nabla^2 g_{\mu\nu} - R_{\mu\nu}\right)$$
$$- \left(\sum_n n(n-1)\frac{\partial \mathcal{L}}{\partial \tau_n} + 2\sum_{m,n} mn\frac{\partial^2 \mathcal{L}}{\partial \tau_n \partial \tau_m}\right)\nabla_\mu\nabla_\nu \ . \tag{12.55}$$

Note that the factors involving $\mathcal{L}$ are constants. Using the rules for integrations by parts, one sees that the Hessian is symmetric:

$$H(v,w) = H(w,v) \tag{12.56}$$

which also means that the differential operator L is self-adjoint.

(3) Special cases: harmonic diffeomorphisms and quadratic Lagrangian.
Clearly, stability hinges on the form of the Lagrangian. As a first example consider the action for harmonic diffeomorphisms (12.11). Its Hessian is [510, 511]:

$$H(v,w) = 2\int \mathrm{d}^d x \sqrt{g}\, v^\mu \left(-\nabla^2 g_{\mu\nu} - R_{\mu\nu}\right) w^\nu \ . \tag{12.57}$$

Hence we have to study te spectrum of the Laplace-type operator

$$L_1 = -g_{\mu\nu}D^2 - R_{\mu\nu} \ . \tag{12.58}$$

This spectrum is known for spheres. It consists of transverse and longitudinal fields. The lowest transverse eigenfunctions are the $d(d+1)/2$ Killing vectors, which are zero modes. This is related to the fact that every isometry is harmonic. The lowest longitudinal eigenfunctions are

$$w^i_\nu = \partial_\nu \phi^i \ , \tag{12.59}$$

where ϕ^i are cartesian coordinates of the flat Euclidean space in which the sphere is embedded. These are conformal Killing vectors and have eigenvalue $-\frac{d-2}{d(d-1)}R$ and multiplicity $d+1$. In $d=2$ they are zero modes; this is related to the fact that in $d=2$

conformal isometries are harmonic [512]. All other eigenvalues are positive. Thus, the identity is unstable as a harmonic map of spheres in $d > 2$; in $d = 2$ it is stable and belongs to a six-parameter family of degenerate solutions.

As another example we consider the model (12.12). In this case the Hessian is

$$H(v,w) \;=\; 4\int \mathrm{d}^d x \sqrt{g}\left[(d-2)v^\mu\left(-\nabla^2 g_{\mu\nu} - R_{\mu\nu}\right)w^\nu + (\nabla_\mu v^\mu)(\nabla_\nu w^\nu)\right] \tag{12.60}$$

and, integrating the second term by parts, the associated operator reads

$$L_2 = \left(-\nabla^2 g_{\mu\nu} - R_{\mu\nu}\right) - \frac{1}{d-2}\nabla_\mu \nabla_\nu \; . \tag{12.61}$$

Clearly the spectrum on transverse vectors is the same as that of L_1, but it may differ on longitudinal vectors, and the new contribution is positive, so that the identity may become stable. In fact, the additional non-minimal term, acting on the eigenfunctions (12.59), gives $R/(d-1)(d-2)$, so that the eigenvalue becomes $-\frac{d-4}{d(d-2)}R$. It is negative in all dimensions except four, were it is zero. Also in this case, the zero modes are related to the infinitesimal isometries and conformal isometries.

12.3.2. *Global Euclidean bounds*

The second variation of the action gives information about the local stability of a solution, but there are some cases where absolute bounds on the action can be derived. In this section we assume that $\mathcal{M}$ is compact without boundary. We use the totally antisymmetric tensor $\eta_{\mu_1 \dots \mu_d} = \sqrt{g}\, \varepsilon_{\mu_1 \dots \mu_d}$ where ε is the tensor density with components ± 1. It is the volume form on $\mathcal{M}$, such that $V = \int_{\mathcal{M}} \eta = \int \mathrm{d}^d x \sqrt{g}$ is the volume.

(1) Winding number. The winding number is

$$W = \frac{1}{d!V}\int \mathrm{d}^d x \sqrt{g}\, \eta^{\mu_1 \dots \mu_d} J_{\mu_1}{}^{\alpha_1} \dots J_{\mu_d}{}^{\alpha_d} \eta_{\alpha_1 \dots \alpha_d} \tag{12.62}$$

and is equal to one for orientation-preserving diffeomorphisms.

(2) Harmonic maps in $d = 2$. The action for harmonic maps in two Euclidean dimensions is $S = \frac{1}{2}f^2 \int d^2 x \sqrt{g}\, \tau_1$. We define the double dual $^*J^*$ by $^*J_\mu^{*\alpha} = \eta_\mu{}^\rho J_\rho{}^\gamma \eta_\gamma{}^\alpha$. Integrating the square of $J \pm {}^*J^*$ one obtains the well-known bound $S \geq V f^2 |W|$, [513] and since $|W| = 1$ for diffeomorphisms,

$$S \geq V f^2 \; . \tag{12.63}$$

The absolute minima are the maps for which $J = \pm {}^*J^*$. Indeed, the identity solves this equation.

(3) Quadratic Lagrangian in $d = 4$. There is a parallel example in four Euclidean dimensions. This time we consider the Lagrangian (12.12). Defining the antisymmetric tensor $K_{\mu\nu}{}^{\alpha\beta} = J_{[\mu}{}^{[\alpha} J_{\nu]}{}^{\beta]}$, and the inner product

$$(K, K') = \frac{1}{2} \int \mathrm{d}^4 x \sqrt{g}\, g^{\mu\rho} g^{\nu\sigma} K_{\mu\nu}{}^{\alpha\beta} K'_{\rho\sigma}{}^{\gamma\delta} g_{\alpha\gamma} g_{\beta\delta} \ , \tag{12.64}$$

the action functional associated to (12.12) can be rewritten

$$S = 4c\|K\|^2 \equiv 2c \int \mathrm{d}^4 x \sqrt{g}\, g^{\mu\rho} g^{\nu\sigma} K_{\mu\nu}{}^{\alpha\beta} K_{\rho\sigma}{}^{\gamma\delta} g_{\alpha\gamma} g_{\beta\delta} \ . \tag{12.65}$$

We can define ${}^*K^*$, the double dual of K, by

$$ {}^*K^*_{\mu\nu}{}^{\alpha\beta} = \frac{1}{4} \eta_{\mu\nu}{}^{\rho\sigma} \eta^{\alpha\beta}{}_{\gamma\delta} K_{\rho\sigma}{}^{\gamma\delta} \ . \tag{12.66}$$

Since $\|{}^*K^*\|^2 = \|K\|^2$, we have

$$0 \le \|K \pm {}^*K^*\|^2 = 2\|K\|^2 \pm 2(K, {}^*K^*) = \frac{1}{2c} S \pm 6V W[\varphi] \ , \tag{12.67}$$

where W is the winding number of φ. Since diffeomorphisms have $|W| = 1$, we have the absolute bound

$$S \ge 12\, cV \ . \tag{12.68}$$

The bound is saturated by maps for which H is double-self-dual, and the identity has this property.

For a generic metric, the identity will be an isolated solution. In the presence of isometries and/or conformal isometries, it will be an element of continuous degenerate families of solutions, as we have seen in the end of the preceding section.

12.3.3. *Lorentzian stability*

(1) The timelike ghost. As long as we restrict ourselves to dynamical diffeomorphisms in a fixed external metric, there is no difference, regarding the issues of Lorentzian stability, between the models considered here, where the target space is spacetime itself, and those where the target space is another manifold, as in nonlinear sigma models, or a copy of the same manifold. In all cases, when the target space metric has Minkowski signature $(- + ++)$, the scalar associated to the time coordinate has a kinetic term with opposite sign of those associated to the space coordinates. Assuming that the sign of the Lagrangian is such that the latter have the correct dynamics, the timelike scalar will be a ghost.

(2) The resolutions in massive gravity. As already mentioned, these issues have been discussed extensively in the literature on massive gravity, where two different

strategies have been developed in order to avoid ghost instabilities: the de Rham–Gabadadze–Tolley (dRGT) models [491], that preserve spacetime covariance, and Lorentz-breaking models [497]. Both strategies can be used also for our models.

In the context of dRGT models of massive gravity, it has been observed that certain nonlinear sigma models with Minkowskian target space and special actions built out of $\text{Tr}(\sqrt{B})^n$ will be ghost-free [514]. By expanding $B = 1 + X$ in terms of X, one can write $\text{Tr}(\sqrt{B})^n$ as an infinite series of $\text{Tr}B^n$. Hence, these actions can be viewed as special cases of our action and the same construction can be applied also to our models.

In Lorentz-breaking massive gravity, one gives up Lorentz invariance and preserves only Euclidean symmetry of 3-dimensional space. Dubovsky and Rubakov [497, 498] extended the nonlinear Stückelberg trick to Lorentz-violating massive gravity using the pullback of a 3-dimensional target space metric h_{ab}. Similarly, we can construct ghost-free (but Lorentz-violating) dynamics of the diffeomorphisms of space, rather than spacetime. The target space metric $h(\varphi)$ would be only 3-dimensional in that case. The solution $\varphi = Id_\Sigma$ is again a solution of the EOM and it generates an effective cosmological term in the space directions.

CHAPTER 13

Relational observables in Asymptotic Safety

Executive summary. We introduce an approach to compute the renormalization group flow of relational observables in Quantum Gravity which evolve from their microscopic expressions towards the full quantum expectation value. This is achieved by using the composite operator formalism of the functional renormalization group. These methods can be applied to a large class of relational observables within a derivative expansion for different physical coordinate systems. As a first application we consider four scalar fields coupled to gravity to represent the physical coordinate frame from which relational observables can be constructed. At leading order of the derivative expansion the observables are the inverse relational metric and the relational scalar curvature. We evaluate their scaling dimensions at the fixed point, both in the standard renormalization group scheme and in the essential scheme. This work represents the first steps to describe running observables within Asymptotic Safety; the treatment can be generalized to other observables constructed from different tensors.

What is new? All results of this chapter represent novel research results.

Based on: Reference [RF7].

Plan of this Chapter. We briefly review the ideas leading to the construction of relational observables through a physical coordinate system. We introduce a general formalism to translate the composite operator setting to relational observables and we comment about a natural criterion of choice of observables within a derivative expansion. In Section 13.3 we perform the first application to the flow of two relational observables corresponding to the inverse metric and the scalar curvature. In this example the physical coordinate system is composed of four massless scalar fields. The corresponding observables are those which are found at the leading order in the derivative expansion. In Section 13.4, after having reviewed the matter flow within asymptotically safe gravity, we derive the flow of various physical matter systems (the Standard Model and modifications thereof) allowing for the spacetime metric to be renormalized. Here we consider two schemes, one in which the anomalous dimension of the metric is set to zero, and another one in which we adopt the minimal essential scheme (see Section 4.2), where we fixed the value of the cosmological constant by a renormalization condition.

We then compute the scaling of the chosen observables and calculate their scaling dimensions on the fixed points. In Section 13.5 we present the consistent extension of our application to the next order in the derivative expansion.

In Appendix H we apply this to scalar tensor theories, deriving the flow equations, we compute the Hessian of the observables and we perform the calculations leading to the numerical results for the scaling dimension of the couplings of the observables.

This chapter has been taken from the author's publication [RF7].

13.1. Relational observables in the quantum theory

As discussed extensively in the Introduction to this Part the situation concerning observables for classical GR can be understood *relationally*. The method of relational observables implements the intuitive idea that observables in a background independent theory should encode relations between dynamical quantities. However, for Quantum Gravity the situation of observables is less clear. To a large extent, this is due to the fact that a unique well-established theory of Quantum Gravity does not exist yet. Depending one's point of view concerning the construction of Quantum Gravity the problem of quantum observables takes slightly different forms.

Within the Asymptotic Safety scenario, the UV completion for Quantum Gravity is provided by the UV fixed point: the corresponding observables will have universal scaling exponents at the fixed point. Physically these exponents should appear in the scaling behavior of correlation functions of relational observables at small distances less than the Planck length where effects of the fixed point scaling are expected.

13.2. Physical coordinate frame and relational observables

13.2.1. *Physical coordinate frame*

(1) Physical coordinate frame. In order to construct relational observables we need a *physical coordinate frame* in which to evaluate tensors, or other diffeomorphism-invariant objects, such that when we transform both the tensor and the coordinate system the total transformation leaves the tensor invariant. In other words a physical coordinate frame is a way to label a spacetime point $\mathcal{P}$ not by abstract coordinates x^μ, but by the values which physical quantities take at $\mathcal{P}$. Thus, for example the scalar curvature $R(x)$ is not an observable since the coordinates x do not mean anything physically. However,

if the point $\mathcal{P}$ is specified as the point where a particular physical event happens, then the scalar curvature at $\mathcal{P}$ is an observable. If $\phi^a(x)$ denotes the full set of dynamical fields, which includes the components of the metric tensor $g_{\mu\nu}$ as well as matter fields, we construct a set of four scalars from the dynamical fields and their derivatives

$$\hat{X}^{\hat{\mu}}(x) = \hat{X}^{\hat{\mu}}(\phi(x), \partial\phi(x), \dots), \tag{13.1}$$

which constitute our *physical coordinate frame* with $\hat{\mu} = 0, 1, 2, 3.$[1] As a result a point $\mathcal{P}$ in spacetime is labeled by the values the scalar fields $\hat{X}^{\hat{\mu}}(x)$ take at $\mathcal{P}$.

Since the $\hat{X}$'s are scalars, they transform, under a diffeomorphism of the dynamical fields $\phi \to \phi_\xi$, as $\hat{X}^{\hat{\mu}}(x) \to \hat{X}_\xi^{\hat{\mu}}(x) = \hat{X}^{\hat{\mu}}(\xi(x))$, where here ϕ_ξ is the transformed dynamic field.

In order that (13.1) constitutes a set of coordinates, they must constitute a diffeomorphism from the manifold $\mathcal{M}$ to another manifold $\hat{\mathcal{M}}$ with coordinates $\hat{x}^\mu$ which is the space of all values that the scalar fields $\hat{X}$ can take. Invertibility of the diffeomorphism means that the equation

$$\hat{X}^{\hat{\mu}}(x) = \hat{x}^{\hat{\mu}}, \tag{13.2}$$

can be solved for x. We denote the solution

$$x^\mu = X^\mu(\hat{x}), \tag{13.3}$$

such that $X = \hat{X}^{-1}$ is the inverse of the map $\hat{X}$ (see Figure 13.1). Whether this property holds depends on the configuration ϕ and the choice of scalars $\hat{X}^{\hat{\mu}}$. Thus, a given choice of the scalars $\hat{X}^{\hat{\mu}}$ may define a physical coordinate system for a subset of all possible field configurations ϕ.

(2) Frame fields. Given the set of scalars (13.1) one has a set of four covariant vectors

$$e_\mu^{\hat{\mu}}(x) = \partial_\mu \hat{X}^{\hat{\mu}}(x). \tag{13.4}$$

The *frame fields* $e_{\hat{\mu}}^\mu$ are the inverse of the above $e_\mu^{\hat{\mu}}$ and transform as contravariant vectors on the spacetime such that

$$e_\mu^{\hat{\mu}}(x)e_{\hat{\nu}}^\mu(x) = \delta_{\hat{\nu}}^{\hat{\mu}}, \qquad e_{\hat{\mu}}^\mu(x)e_\nu^{\hat{\mu}}(x) = \delta_\nu^\mu. \tag{13.5}$$

The frame fields $e_{\hat{\mu}}^\mu(x)$ can be obtained by differentiating the maps $X^\mu(\hat{x})$ and evaluating the derivative at $\hat{x} = \hat{X}(x)$. This follows since

$$\delta_\nu^\mu = \partial_\nu x^\mu = e_\nu^{\hat{\mu}}(x)\frac{\partial}{\partial \hat{x}^{\hat{\mu}}}X^\mu(\hat{X}(x)) \tag{13.6}$$

and hence we can write the frame field as

$$e_{\hat{\mu}}^\mu(x) = \frac{\partial}{\partial \hat{x}^{\hat{\mu}}}X^\mu(\hat{X}(x)). \tag{13.7}$$

---

[1]In this chapter we use the hat $\hat{}$ to identify fields living in the physical coordinate system. Note that they will play a similar role to the φ^α's of Chapter 12.

$$\hat{X}^{\hat{\mu}}(x) = \hat{x}^{\hat{\mu}}$$

$$x^{\mu} = X^{\mu}(\hat{x})$$

$\mathcal{M}$

$\hat{\mathcal{M}}$
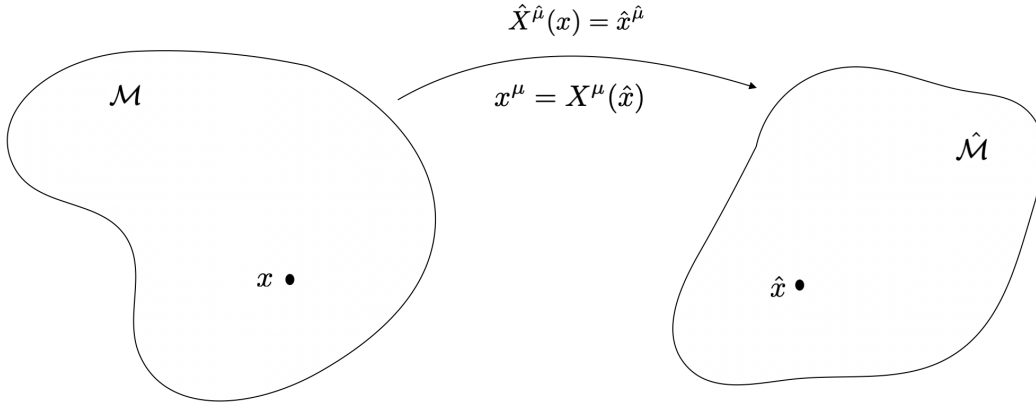
x •

$\hat{x}$ •

FIGURE 13.1. Maps between spacetime $\mathcal{M}$ and physical field frame $\hat{\mathcal{M}}$.

(3) Invariant volume element. Since we assume $e^{\hat{\mu}}_{\mu}$ is invertible it allows us to define an *invariant volume element* on spacetime $\mathrm{d}^4 x\, \tilde{e}$ where

$$\tilde{e} = \det\left(e^{\hat{\mu}}_{\mu}\right). \tag{13.8}$$

This allows us also to write the following identity between Dirac delta functions:

$$\delta(X(\hat{x}), x) = \tilde{e}(x)\, \delta(\hat{x}, \hat{X}(x)). \tag{13.9}$$

It is important to note that $X^{\mu}(\hat{x})$ is itself a functional of the dynamical fields. Let us change the field configuration $\phi \rightarrow \phi'$ and we induce a change in $\hat{X}(x) \rightarrow \hat{X}'(x)$ obtained by replacing ϕ by ϕ' in (13.1). Since the coordinates x are held fixed, we have that $X(\hat{x}) \rightarrow X'(\hat{x})$ such that

$$X'(\hat{X}'(x)) = X(\hat{X}(x)) = x. \tag{13.10}$$

If we consider the case where ϕ' is obtained by a diffeomorphism of ϕ such that $\phi' = \phi_{\xi}$, we have that $\hat{X}'(x) = \hat{X}_{\xi}(x) = \hat{X}(\xi(x))$. We can then infer from (13.10) that $X'(\hat{x}) = X_{\xi}(\hat{x})$ is given by

$$X_{\xi}(\hat{x}) = (\xi^{-1} \circ X)(\hat{x}). \tag{13.11}$$

where ξ^{-1} is the inverse function and $f \circ g$ denotes the composition of two functions.

13.2.2. *Relational observables*

(1) Diffeomorphism invariance. Given a field $\phi^a(x)$, let us denote its transformation under a diffeomorphism $\xi^{\mu}(x)$ by

$$\phi^a_{\xi} = T^a[\phi, \xi], \tag{13.12}$$

which is a functional of both the field ϕ and the diffeomorphism $\xi^\mu(x)$. For example a scalar field ψ transforms to

$$\psi_\xi(x) = \psi(\xi(x)),\tag{13.13}$$

while components of the metric transform as

$$g_{(\xi)\mu\nu}(x) = \partial_\mu \xi^\lambda(x)\partial_\nu \xi^\rho(x)g_{\lambda\rho}(\xi(x)).\tag{13.14}$$

The functionals $T^a[\phi, \xi]$ satisfy the composition identity

$$T^a[\phi_\xi, \xi'] = T^a[\phi, \xi \circ \xi'],\tag{13.15}$$

which follows from the properties that imply diffeomorphisms form a group where the group product is given by $(\xi' \cdot \xi)(x) = \xi(\xi'(x))$.

For example, if we consider a scalar $\psi(x)$, then applying first the diffeomorphism ξ we have $T[\psi, \xi] = \psi_\xi(x) = \psi(\xi(x))$, then applying ξ' we have $T[\psi_\xi, \xi'] = \psi_\xi(\xi'(x)) = \psi(\xi(\xi'(x)))$. Therefore the action of applying first ξ and then ξ' to ψ is the same as applying the composition in the reverse order $\xi \circ \xi'$.

To obtain the gauge-invariant fields, we transform the dynamical fields $\phi^a(x)$ into the physical coordinate frame

$$\hat{\phi}^{\hat{a}}(\hat{x}) = \phi_X^{\hat{a}}(\hat{x})\tag{13.16}$$

such that it now depends on the coordinates $\hat{x}$. The fields $\hat{\phi}^{\hat{a}}(\hat{x})$ are then functionals $\hat{\phi}^{\hat{a}}[\phi]$ of the original fields and constitute a set of local observables at each point $\hat{x}$. As functionals of the fields ϕ we have that

$$\hat{\phi}^{\hat{a}} = T^{\hat{a}}[\phi, X].\tag{13.17}$$

For example, the relational observable corresponding to the spacetime metric is given by the following three equivalent expressions:

$$\begin{aligned}
\hat{g}_{\hat{\mu}\hat{\nu}}(\hat{x}) &= \partial_{\hat{\mu}} X^\mu(\hat{x})\, \partial_{\hat{\nu}} X^\nu(\hat{x})\, g_{\mu\nu}(X(\hat{x})) && (13.18)\\
&= \int \mathrm{d}^4 x\, \delta(x, X(\hat{x}))\, e_{\hat{\mu}}^\mu(x)\, e_{\hat{\nu}}^\nu(x) g_{\mu\nu}(x) && (13.19)\\
&= \int \mathrm{d}^4 x\, \tilde{e}(x)\, \delta(\hat{x}, \hat{X}(x))\, e_{\hat{\mu}}^\mu(x) e_{\hat{\nu}}^\nu(x)\, g_{\mu\nu}(x). && (13.20)
\end{aligned}$$

To see that $\hat{\phi}^{\hat{a}}$ are observables, i.e., that they are diffeomorphism-invariant, we compute

$$\begin{aligned}
\hat{\phi}_\xi^{\hat{a}} &= T^{\hat{a}}[\phi_\xi, X_\xi] && (13.21)\\
&= T^{\hat{a}}[\phi_\xi, \xi^{-1} \circ X] && (13.22)\\
&= T^{\hat{a}}[\phi, X] = \hat{\phi}^{\hat{a}}, && (13.23)
\end{aligned}$$

where to arrive at the second line we used (13.11) and to arrive on the third line we used (13.15).

We can also take any composite operator $O[\phi]$ which transforms as $O[\phi_\xi] = O_\xi[\phi]$ and obtain a diffeomorphism-invariant operator

$$\hat{O}[\phi] = O_X[\phi] = O[\hat{\phi}] \tag{13.24}$$

for any O and any set of physical coordinates. The operators $\hat{O}[\phi]$ constitute relational observables.

(2) A selection of relational observables.

(1) For example, if $A = R(x)$ is the Ricci scalar then

$$\hat{R}(\hat{x}) = R(X(\hat{x}))$$

$$= \int d^d x \, \delta(X(\hat{x}), x) \, R(x) \tag{13.25}$$

$$= \int d^d x \, \tilde{e}(x) \, \delta(\hat{x}, \hat{X}(x)) \, R(x)$$

is the corresponding relational observable which we dub the 'relational Ricci scalar'.

(2) If $O = g^{\mu\nu}(x)$ is the inverse metric, then

$$\hat{g}^{\hat{\mu}\hat{\nu}}(\hat{x}) = e_\mu^{\hat{\mu}}(X(\hat{x})) \, e_\nu^{\hat{\nu}}(X(\hat{x})) \, g^{\mu\nu}(X(\hat{x})) \tag{13.26}$$

is the relational observable corresponding to the inverse metric or the 'relational inverse metric', and

$$\hat{g}^{\hat{\mu}\hat{\nu}}(\hat{x}) = \int d^d x \, \delta(X(\hat{x}), x) \, g^{\mu\nu}(x)$$

$$= \int d^d x \, \tilde{e} \, e_\mu^{\hat{\mu}}(X(\hat{x})) \, e_\nu^{\hat{\nu}}(X(\hat{x})) \, \delta(\hat{x}, \hat{X}(x)) \, g^{\mu\nu}(x) \, . \tag{13.27}$$

Thus, given any diffeomorphism-invariant composite operator $O[\phi]$, the relational observable $\hat{O}[\phi]$ can be dubbed the *relational O*. If the invariant composite operator $O^I(x)$ depends on the coordinates x and some set of indices spacetime I indices, e.g. $I = \mu\nu$, the corresponding relational observable $\hat{O}^{\hat{I}}(\hat{x})$ instead depend on $\hat{x}$ and hatted indices e.g. $\hat{I} = \hat{\mu}\hat{\nu}$. In general, if O^I is a tensor, we can express the corresponding relational observable as

$$\hat{O}^{\hat{I}}(\hat{x}) = \int d^4 x \, \tilde{e}(x) \delta(\hat{x}, \hat{X}(x)) E_I^{\hat{I}}(x) O^I(x) \, , \tag{13.28}$$

where $E_I^{\hat{I}}(x)$ is a product of $e_{\hat{\mu}}^\mu$ and $e_\mu^{\hat{\mu}}$ depending on I, for example $E_I^{\hat{I}}(x) = e_\mu^{\hat{\mu}} e_\nu^{\hat{\nu}}$ when $O^I = g^{\mu\nu}$.

Remarks. A few remarks are now in order:

(1) Given a relational tensor $\hat{O}^{\hat{I}}(\hat{x})$ we can also take derivative of the observable with respect to $\hat{x}$ to get a new relational observable. If D_μ denotes the covariant

derivative compatible with $e_\mu^{\hat\mu 2}$ derivative with and $D^n O^I_{\mu_1\ldots\mu_n} := D_{\mu_1}\ldots D_{\mu_n} O^I$ is the nth derivative of the gauge-invariant composite operator $O[\phi]$, then one can show that

$$\partial_{\hat\mu_1}\ldots\partial_{\hat\mu_n}\hat O^{\hat I} = \widehat{D^n O}^{\hat I}_{\hat\mu_1\ldots\hat\mu_n} \tag{13.29}$$

simply by differentiating (13.28), using that $\partial_{\hat\mu}\delta(\hat x, \hat X(x)) = -e_{\hat\mu}^\mu D_\mu \delta(\hat x, \hat X(x))$ and integrating by parts repeatedly.

(2) Up till now we have assumed that O is a tensor. However, we can consider relational observables which are not related to tensors. For example the Christoffel symbol $\Gamma^\lambda_{\mu\nu}$ transforms inhomogeneously. As a result the relational Christoffel symbol is given by

$$\begin{aligned}
\Gamma^{\hat\rho}_{\hat\mu\hat\nu}(\hat x) &= \int \mathrm d^4 x\, \tilde e\, \delta(\hat x, \hat X)\, e_{\hat\mu}^\mu e_{\hat\nu}^\nu \left(e_\rho^{\hat\rho}\, \Gamma^\rho_{\mu\nu} - \partial_\mu\partial_\nu \hat X^{\hat\rho} \right) \\
&= -\int \mathrm d^4 x\, \tilde e\, \delta(\hat x, \hat X)\, e_{\hat\mu}^\mu e_{\hat\nu}^\nu\, \nabla_\mu\nabla_\nu \hat X^{\hat\rho}\,,
\end{aligned} \tag{13.30}$$

which is diffeomorphism-invariant. However, we observe that this is the relational observable corresponding to the tensor $-\nabla_\mu\nabla_\nu\hat X^{\hat\rho}$.

From these considerations we see that there are many different relational observables that one can construct since there is a immense freedom in both choosing the physical coordinate system and choosing which composite operator $O[\phi]$ to transform into the chosen coordinate system. From this point of view, *there is no lack of observables in Quantum Gravity, but rather perhaps a lack of guiding principles that help finding the observables which are most relevant among the large number of relational observables we can consider.*

13.2.3. *The composite operator formalism applied to relational observables*

To apply the composite operator formalism reviewed in Section 4.1 to relational observables $\hat O^{\hat I}(\hat x)$ and their derivatives, we consider a composite operator $\mathcal O_k(\hat x)$ which can be any function of relational observables at the point $\hat x$. This can be decomposed as

$$\mathcal O_k(\hat x) = \sum_i a_{\hat I_i}(k)\, \hat O_i^{\hat I_i}(\hat x)\,, \tag{13.31}$$

where the index i runs over different relational observables, taking into account that the observables can mix under the RG flow. We note that in general each component of each observable can have a separate coupling $a_{\hat I_i}(k)$.

---

[2] This means that D_μ is the covariant derivative compatible with the metric $e_\mu^{\hat\mu}\delta_{\hat\mu\hat\nu}e_\nu^{\hat\nu}$. Thus the connection for ∇_μ is the Levi-Civita connection for $g_{\mu\nu}$ and the connection for D_μ is the Levi-Civita connection for $e_\mu^{\hat\mu}\delta_{\hat\mu\hat\nu}e_\nu^{\hat\nu}$.

(1) Diffeomorphism-invariant volume element The source term for $\mathcal{O}_k$ can then be written as an integral over $\hat{x}$ as in eq.(13.28)

$$\int \mathrm{d}^4\hat{x}\, \varepsilon(\hat{x})\mathcal{O}_k(\hat{x}) = \sum_i a_{\hat{I}_i}(k) \int \mathrm{d}^4\hat{x}\, \varepsilon(\hat{x})\hat{A}_i^{\hat{I}_i}(\hat{x})\,. \tag{13.32}$$

However, we can also express the source term as an integral over the coordinates x by using

$$\int \mathrm{d}^4\hat{x}\, \varepsilon(\hat{x})\mathcal{O}_k(\hat{x}) = \int \mathrm{d}^4x\, \tilde{e}(x)\, \varepsilon(\hat{X}(x)) \sum_i a_{\hat{I}_i}(k)\, E_{iI_i}^{\hat{I}_i}(x)\, O_i^{I_i}(x)\,. \tag{13.33}$$

Now since $\varepsilon(\hat{x})$ is independent of the dynamical fields, it is clear that variations of the source term with respect to dynamical fields must be proportional to the undifferentiated source $\varepsilon(\hat{x})$. However, in the form (13.33) $\varepsilon(\hat{X}(x))$ depends on the dynamical fields through the physical coordinate system. Thus, in computing the Hessian of the observable with a non-constant source we pick up terms from the variation of $\varepsilon(\hat{X}(x))$ and thus are proportional to the derivative of the source. This is consistent since by using the identity

$$\frac{\partial}{\partial \hat{X}^{\hat{\mu}}(x)}\varepsilon(\hat{X}(x)) = e_{\hat{\mu}}^{\mu}(x)\, \partial_{\mu}\varepsilon(\hat{X}(x))\,, \tag{13.34}$$

and integrating by parts we can always write the variation such that it is proportional to $\varepsilon(\hat{X}(x))$.

According to our considerations in the last section, we can consider constant sources if we concentrate on relational observables which are linearly independent of total derivatives $\hat{O}_i^{\hat{I}_i}(\hat{x}) = \partial_{\hat{\mu}}\hat{O}_i^{\hat{I}_i\hat{\mu}}(\hat{x})$. Indeed, working with integrals over $\hat{x}$ the arguments of the last section go through unchanged. Let us note that when we switch to the form (13.33) we have that

$$\int \mathrm{d}^4\hat{x}\, \varepsilon(\hat{x})\, \partial_{\hat{\mu}}O^{\hat{I}}(\hat{x}) = \int \mathrm{d}^4x\, \tilde{e}(x)\, \varepsilon(\hat{X}(x))\, E_I^{\hat{I}}(x)\, e_{\hat{\mu}}^{\mu}\, D_{\mu}O^I(x)\,, \tag{13.35}$$

where the LHS is a boundary term when $\varepsilon(\hat{X}(x))$ is a constant. So as with any composite operator the computation of scaling dimensions of the subset of observables which are not total derivatives can be calculated at constant source.

(2) Relational Effective Average Action. Taking the source constant, we can define the *relational EAA* by

$$\Gamma_k^{\mathrm{rel}} \equiv \int \mathrm{d}^4x\, \tilde{e}(x)\, \mathcal{L}_k^{\mathrm{rel}}(x) := \int \mathrm{d}^4x\, \tilde{e}(x) \sum_i a_{\hat{I}_i}(k)\, E_{iI_i}^{\hat{I}_i}(x)\, O_i^{I_i}(x)\,, \tag{13.36}$$

where we note that the defining feature that separates terms in Γ_k^{rel} from terms in the standard effective action is that the former is written as an integral over x with the volume element given by $\tilde{e}(x)$ rather than the usual density $\sqrt{g}$. Thus, for constant

source, we can take the total EAA to be given by

$$\Gamma_k[g, \ldots ; \varepsilon] = \Gamma_k[g, \ldots] + \varepsilon \, \Gamma_k^{\mathrm{rel}}[g, \ldots] + O(\varepsilon^2) \,. \tag{13.37}$$

Implicit in the construction of the relational EAA is that $\tilde{e}$ is non-singular. The form (13.36) gives us two different starting points. On the one hand, we can consider a basis of relational observables and give each one a source. On the other hand, we can simply write down some form for $\mathcal{L}_k^{\mathrm{rel}}(x)$ as a basis of scalars and the non-singular nature of $\tilde{e}$ means we can construct these scalars with the vectors $e_{\tilde{\mu}}^{\mu}$ and there derivatives.

For a non-constant source we instead have the more general form

$$\Gamma_k[g, \ldots ; \varepsilon] = \Gamma_k[g, \ldots] + \int \mathrm{d}^4 x \, \tilde{e}(x) \, \varepsilon(\hat{X}(x)) \mathcal{L}_k^{\mathrm{rel}}(x) + O(\varepsilon^2) \,, \tag{13.38}$$

which allows for the calculation of scaling dimensions for relational observables which are total derivatives and hence do not appear in the relational EAA.

13.2.4. *Derivative expansion for the relational EAA*

(1) Flow equation. Applying the composite operator formalism (in particular eq.(4.8)) to the relational EAA to order ε we have that

$$k\partial_k \Gamma_k^{\mathrm{rel}} = -\frac{1}{2} \mathrm{Tr} \left[\left(\Gamma_k^{(2)} + \mathcal{R}_k \right)^{-1} \left(\Gamma_k^{\mathrm{rel}(2)} \right) \left(\Gamma_k^{(2)} + \mathcal{R}_k \right)^{-1} k\partial_k \mathcal{R}_k \right] \tag{13.39}$$

where $\Gamma_k^{\mathrm{rel}(2)}$ is the Hessian of the relational EAA.

(2) Consistent closure. An important question is how to close approximations to eq. (13.39) in a consistent manner. A natural nonperturbative choice is to take $\mathcal{L}_k^{\mathrm{rel}}(x)$ to have a derivative expansion and be approximated by terms with only a finite number of derivatives. However, this only makes sense if $\nabla_\mu \hat{X}^{\tilde{\mu}}$ is polynomial in derivatives since otherwise $\tilde{e}$ would be non-polynomial. This provided, we can pick $\hat{X}^{\tilde{\mu}}$ to involve only a finite number of derivatives, and we can *close our approximation for the relational EAA by picking terms with a up to a finite number of derivatives*. This then gives us a natural basis of relational observables which we project onto when we use the derivative expansion.

(3) Only upper indices. In particular, these observables are formed from tensors O^I with all indices in the upper position, such as $g^{\mu\nu}$, R, $R^{\mu\nu}$ etc., since the corresponding $E_I^{\tilde{I}}$ are products of $\nabla_\mu \hat{X}^{\mu}$ and thus finite order in derivatives. Each order s of the derivative expansion then corresponds to keeping only terms with up to s derivatives in $\mathcal{L}_k^{\mathrm{rel}}(x)$. At each finite order in the derivative expansion, we do not find relational observables corresponding to tensors with lower indices, e.g. $g_{\mu\nu}$, which are non-polynomial in derivatives.

13.3. A FIRST APPLICATION

(1) Dynamical fields. We are now ready to apply the composite operator formalism to the investigation of relational observables in Asymptotic Safety. Here we employ the background field approximation to the action (3.48). Rather than working with pure gravity we take $\bar{\Gamma}_k$ in (3.46) to depend also on matter fields from which we construct the physical coordinate system $\hat{X}^{\hat{\mu}}(x)$ that enters the relational observables. A simple example is the inclusion of a set of four massless scalar fields minimally coupled to gravity (see [120] for gravity coupled to matter in Asymptotic Safety and [174] for a more recent analysis of the fixed point existence)[3]:

$$\bar{\Gamma}_k = \int \mathrm{d}^d x \sqrt{g} \left(-\frac{1}{16\pi G}(R - 2\Lambda) + \frac{1}{2}\delta_{\mathrm{AB}}\, g^{\mu\nu}\, \partial_\mu \varphi^{\mathrm{A}}\, \partial_\nu \varphi^{\mathrm{B}} \right) + \text{Additional matter} , \tag{13.40}$$

where the index $\mathrm{A}, \mathrm{B}, \cdots = 1, 2, 3, 4$ run over the internal space of the scalar fields and δ_{AB} is a flat field space metric.

(2) Four scalars as the physical coordinate system. For the system described by (13.40) there are in principle many choices for the scalars $\hat{X}^{\hat{\mu}}(x)$, here we identify the physical coordinate system with the four scalars $\varphi^A(x)$ such that

$$\hat{X}^{\hat{\mu}}(x) = \varphi^{\hat{\mu}}(x) . \tag{13.41}$$

In this case the physical coordinate system is just composed for fundamental scalars rather than composite fields. After having made the identification (13.41), we simply denote the scalar fields by $\hat{X}^{\hat{\mu}}(x)$ and always use the hatted indices $\hat{\mu}$ such that the field space metric is $\delta_{\hat{\mu}\hat{\nu}}$.

Let us note that the action (13.40) is invariant under shifts $\varphi^A(x) \to \varphi^A(x) + c$ and under a global $O(4)$ symmetry. For simplicity, we consider observables that are invariant under these symmetries also. Since these symmetries are not broken by the regularization, the flow of symmetric composite operators is closed. One can consider observables which break these global symmetries however we do not do so here.

13.3.1. *Inverse relational metric and relational curvature*

We shall use the composite operator formalism to compute the scaling dimensions of relational observables corresponding to the inverse metric and the scalar curvature where the physical coordinates $\hat{X}^{\mu}(x)$ are taken to be a set massless minimally coupled

---

[3]Here the anomalous dimension of the matter fields has been neglected and only one-loop results have been considered. In a more recent paper [107] the running of the anomalous dimension of all the involved matter fields has been taken into account.

scalars. To do so, it suffices to consider the integral of the relational observables over field space. In particular, we take the relational EAA to be linear in the relational inverse metric and the relational curvature integrated over the $\hat{x}$ coordinate

$$\Gamma_k^{\text{rel}} = \int \mathrm{d}^4\hat{x} \left(a_0(k) + a_R(k)\, \hat{R}(\hat{x}) + a_1(k)\, \delta_{\hat{\mu}\hat{\nu}}\, \hat{g}^{\hat{\mu}\hat{\nu}}(\hat{x}) \right) , \tag{13.42}$$

where $\delta_{\hat{\mu}\hat{\nu}}$ is the Kronecker delta which is the same the metric on field space that appears in the EAA. In this case, the sources which couple to the relational inverse metric and the relational curvature are taken to be equal to $\delta_{\hat{\mu}\hat{\nu}}$ and 1 respectively.

We note that the first term in (13.42) represents the volume of the field space which is independent of the dynamical fields. However, we see that $a_0(k)$ has a flow which may depend on the other two couplings $a_1(k)$ and $a_R(k)$ which couple to the relational observables. We can then rewrite Γ_k^{rel} in the form (13.36) where by (13.9) we have

$$\Gamma_k^{\text{rel}} = \int \mathrm{d}^4x\, \tilde{e} \left(a_0(k) + a_R(k)R + a_1(k)\, \delta_{\hat{\mu}\hat{\nu}}\, g^{\mu\nu}\, (\partial_\mu \hat{X}^{\hat{\mu}})(\partial_\nu \hat{X}^{\hat{\nu}}) \right) . \tag{13.43}$$

We note that the corresponding $\mathcal{L}_k^{\text{rel}}(x)$ contains terms with up to two derivatives of the field. Apart from the difference in the volume element the terms in Γ_k^{rel} are the same as Γ_k indicating a consistency in the approximation of both functionals. Moreover, $\mathcal{L}_k^{\text{rel}}(x)$ contains all terms with up to two derivatives compatible with the symmetries of the action Γ_k. Thus, here we are working at order ∂^2 in the derivative expansion.

Let us remark that since the relational action includes the volume element $\tilde{e}$ one has that

$$\int \mathrm{d}^4x\, \tilde{e}\, \delta_{\hat{\mu}\hat{\nu}}\, g^{\mu\nu}(\partial_\mu \hat{X}^{\hat{\mu}})(\partial_\nu \hat{X}^{\hat{\nu}}) \neq -\int \mathrm{d}^4x\, \tilde{e}\delta_{\hat{\mu}\hat{\nu}}\, \hat{X}^{\hat{\mu}}\, \Box \hat{X}^{\hat{\nu}} , \tag{13.44}$$

since integrating by parts leads to terms where the covariant derivatives act on $\tilde{e}$. However, the term on the RHS, which can be expressed as

$$-\int \mathrm{d}^4x\, \tilde{e}\, \delta_{\hat{\mu}\hat{\nu}}\, \hat{X}^{\hat{\mu}}\, \Box \hat{X}^{\hat{\nu}} = \int \mathrm{d}^4\hat{x}\, \delta_{\hat{\mu}\hat{\nu}}\, \hat{x}^{\hat{\mu}}\, \hat{g}^{\hat{\rho}\hat{\lambda}}\, \hat{\Gamma}^{\hat{\nu}}_{\hat{\rho}\hat{\lambda}} , \tag{13.45}$$

is not symmetric under the shift symmetry of the scalar field and so we do not consider it here.

13.3.2. *Flow of the relational observables*

(1) We are now ready to compute the flow of the relational action (13.43) by using (13.39) where the EAA is given by (13.40). We use a cutoff with the same profile function $\mathcal{R}_k$ but now with $-\Box$ as its argument (so-called *type I cutoff*, for more details see [50]) for which the regulated Hessian is

$$\Gamma_k^{(2)} + \mathcal{R}_k = \Gamma_k^{(2)}(-\Box \to P_k) , \tag{13.46}$$

where $P_k = -\Box + \mathcal{R}_k(-\Box^2)$.

The trace in (13.39) is split into two contributions: the trace over the graviton fluctuations and the trace over the scalar fluctuations. Within our approximation, there are no contributions from the ghosts or any additional matter fields. An improved approximation would include terms in (13.43) containing ghosts and additional matter fields since such terms would be generated by the flow equation.

All the intermediate steps which lead to the following expressions can be found in Section H.3 of the Appendix H. Here we use the off-diagonal heat kernel techniques to evaluate the traces.

(2) We also allow for a non-zero anomalous dimension of the metric tensor $g_{\mu\nu}$ and the scalar fields $\hat{X}^{\hat\mu}$. This has two effects on the flow eq.(13.39). On the LHS we replace

$$k\partial_k\Gamma_k^{\text{rel}} \to k\partial_k\Gamma_k^{\text{rel}} - \frac{1}{2}\hat\eta_k \int \mathrm{d}^4x \hat{X}^{\hat\mu}(x)\frac{\delta\Gamma_k^{\text{rel}}}{\delta\hat{X}^{\hat\mu}(x)} + \gamma_g \int \mathrm{d}^4x g_{\mu\nu}(x)\frac{\delta\Gamma_k^{\text{rel}}}{\delta g_{\mu\nu}}(x)\,, \qquad (13.47)$$

where $\hat\eta$ is the anomalous dimension of scalar fields and γ_g accounts for the anomalous dimension of the metric tensor. On the RHS of (13.39) the derivative of the cutoff for the metric fluctuations is replaced by

$$k\partial_k\mathcal{R}_k \to k\partial_k\mathcal{R}_k + 2\gamma_g\mathcal{R}_k\,, \qquad (13.48)$$

while the derivative of the cutoff for the scalar fluctuations is replaced by

$$k\partial_k\mathcal{R}_k \to k\partial_k\mathcal{R}_k - \hat\eta_k\mathcal{R}_k\,. \qquad (13.49)$$

(3) The flow of the coefficients a_0, a_R and a_1 is given by

$$k\partial_k a_0 = -\frac{a_1}{2\pi^2}Q_3\left[\frac{(k\partial_k - \hat\eta_k)\mathcal{R}_k}{P_k^2}\right] - \frac{12a_R\,G}{\pi}Q_3\left[\frac{(k\partial_k - \eta_h)\mathcal{R}_k}{(P_k - 2\Lambda)^2}\right]\,, \qquad (13.50)$$

$$k\partial_k a_R - \gamma_g\,a_R = -\frac{a_1}{24\pi^2}Q_2\left[\frac{(k\partial_k - \hat\eta_k)\mathcal{R}_k}{P_k^2}\right] - \frac{5a_R\,G}{3\pi}Q_2\left[\frac{(k\partial_k - \eta_h)\mathcal{R}_k}{(P_k - 2\Lambda)^2}\right]$$
$$+\frac{12a_R\,G}{\pi}Q_3\left[\frac{(k\partial_k - \eta_h)\mathcal{R}_k}{(P_k - 2\Lambda)^3}\right]\,, \qquad (13.51)$$

$$k\partial_k a_1 - (\gamma_g + \hat\eta_k)\,a_1 = -\frac{4a_1\,G}{\pi}Q_2\left[\frac{(k\partial_k - \eta_h)\mathcal{R}_k}{(P_k - 2\Lambda)^2}\right]$$
$$-\frac{5a_1\,G}{8\pi}Q_3\left[\frac{(k\partial_k - \hat\eta_k)\mathcal{R}_k}{P_k^3}\right] - 6a_R\,G^2Q_3\left[\frac{(k\partial_k - \eta_h)\mathcal{R}_k}{(P_k - 2\Lambda)^3}\right]\,. \qquad (13.52)$$

Here, we used the definition of the Q-functionals (C.11) in Appendix C. Furthermore, η_h denotes the *anomalous dimension of the graviton field*:

$$\eta_h = \eta_N - 2\gamma_g\,, \quad \text{where} \quad \eta_N = \frac{k\partial_k G(k)}{G(k)}\,. \qquad (13.53)$$

The first terms on the RHS of (13.50)-(13.52) originate from the cutoff dependence on $G(k)^{-1}$ and the second terms arise due to the replacement (13.48). The anomalous dimension η_h can be understood as the anomalous dimension of the metric's fluctuations $h_{\mu\nu}$ defined by

$$g_{\mu\nu} = \delta_{\mu\nu} + \sqrt{32\pi G(k)}\, h_{\mu\nu}\,. \tag{13.54}$$

Here $\delta_{\mu\nu}$ is the flat metric and the factor $\sqrt{32\pi G(k)}$ ensures that $h_{\mu\nu}$ has a canonically normalized kinetic term.

Remark. In four dimensions, the scalars have the canonical mass dimension $[\hat{X}] = 1$, the metric has dimension $[g_{\mu\nu} = -2]$, s.t. for the determinant $[\tilde{e}] = 4$, and the inverse relational metric has $[\hat{\delta}_{\hat{\mu}\hat{\nu}} g^{\mu\nu} \partial_\mu \hat{X}^{\hat{\mu}} \partial_\nu \hat{X}^{\hat{\nu}}] = 4$. In 4 dimensions the coefficients have $[a_0] = -4$, $[a_R] = -6$ and $[a_1] = -8$, and are classical irrelevant, therefore.

(4) Going to dimensionless variables[4] and specializing the Q-functionals in (13.51) to the optimized cutoff (see Equation D.27)

$$\mathcal{R}_k(-\Box) = (k^2 + \Box)\theta(k^2 + \Box)\,, \tag{13.55}$$

we can compute the beta functions ($\beta_a = k\partial_k a$):

$$\beta_0 = 4a_0 - \frac{a_1}{6\pi^2} + \frac{a_R g(\eta_\phi - 4)}{\pi(1 - 2\lambda)^2}\,, \tag{13.56}$$

$$\beta_R = a_R \gamma_g + 6a_R - \frac{a_1}{24\pi^2} + \frac{a_R g(10\eta_h \lambda + 4\eta_h - 30\lambda - 21)}{9\pi(2\lambda - 1)^3}\,, \tag{13.57}$$

$$\beta_1 = a_1 \gamma_g + 8a_1 - \frac{a_R g^2(\eta_h - 4)}{2(2\lambda - 1)^3} + \frac{a_1 g(\eta_h - 3)}{6\pi(1 - 2\lambda)^2} - \frac{5a_1 g}{24\pi}\,. \tag{13.58}$$

Here we have set the anomalous dimension to zero $\hat{\eta}_k = 0$.

(4) We can write down the stability matrix (4.13) as $S = \partial\beta_i/\partial a_j$:

$$S = \begin{pmatrix} 4 & \frac{g(\eta_h - 4)}{\pi(1 - 2\lambda)^2} & -\frac{1}{6\pi^2} \\ 0 & 6 + \gamma_g + \frac{g(10\eta_h\lambda + 4\eta_h - 30\lambda - 21)}{9\pi(2\lambda - 1)^3} & -\frac{1}{24\pi^2} \\ 0 & -\frac{g^2(\eta_h - 4)}{2(2\lambda - 1)^3} & 8 + \gamma_g + \frac{g(\eta_h - 3)}{6\pi(1 - 2\lambda)^2} - \frac{5\,g}{24\pi} \end{pmatrix}\,. \tag{13.59}$$

We now can present our main results:

(1) As expected, since the dynamics of the fields will not be affected by the coefficient a_0, the stability matrix always has one critical exponent equal to the canonical dimension of a_0, $\theta_0 = -4$.

(2) The operators instead mix and contribute to the flow of all the other coefficients. Consequently, those other two critical exponents, θ_1 and θ_R, generally

---

[4]Here, we passed to dimensionless variables and we continue denoting as a_i the dimensionless couplings.

do have quantum corrections. These quantum corrections vanish at the Gaussian fixed point, i.e., $g = \gamma_g = \lambda = 0$, where the critical exponents reduce to the canonical dimensions of the corresponding operators, $\theta_R = -6$ and $\theta_1 = -8$.

(3) When the couplings λ and g are of order unity the dependence of the critical exponents θ_1 and θ_R on γ_g is approximately linear. The corrections are as small as 10^{-7} provided we stay sufficiently far from the pole at $\lambda = 1/2$. Thus,

$$\theta_i = \theta_i^{\text{canonical}} + c_{1,i}(\lambda, g) + c_{2,i}(\lambda, g)\, \gamma_g + O(\gamma_g^2)\,. \tag{13.60}$$

Numerically $c_{2,i}(\lambda, g) \simeq -1$. Therefore for every value of g and λ there is a critical value of γ_g for which the quantum correction of the critical exponents vanishes. Increasing γ_g always makes the critical exponents more irrelevant.

In the plots in Figure 13.2 we are showing the critical exponents for θ_R and θ_1 in the whole g-λ-plane. We set $\eta_N = -2$ and $\gamma_g = 0$ for the plots on the left and $\eta_N = -2$ and $\gamma_g = 0.3197$ for the plots on the right. These values correspond to the non-trivial fixed point values in two different renormalization schemes (see Section 13.4).

We noticed that when $\gamma_g = 0$ the quantum corrections are negative, making the exponent more relevant, while when $\gamma_g = 0.3197$ the quantum corrections are positive, making the exponent more irrelevant. Note that along the axis $g = 0$ the quantum corrections vanish if $\gamma_g = 0$ but remain for $\gamma_g = 0.3197$ since the scaling dimension of the metric remains anomalous.

13.4. Asymptotic Safety

13.4.1. *Matter in asymptotically safe gravity: standard and essential scheme*

Here we compute general expression for the scaling dimensions of the relational observables in dependence on the dimensionless Newton's constant g and cosmological constant λ. The exact position of the fixed point depends on which matter fields we include. We consider N_S scalars, N_D fermions, N_V vectors and N_D Dirac fermions minimally coupled to gravity, but not interacting otherwise.

This is the first computation in the essential renormalization group scheme: we will furnish the first numerical values of scaling dimensions of matter coupled to gravity in the minimal essential scheme.

(1) Setup. In order to write down the beta functions, we have to define the cutoff: for a type II cutoff we choose a real function $\mathcal{R}_k\left(S^{(2)}_{\text{matter}}\right)$ where $S^{(2)}_{\text{matter}}$ is the inverse propagator of the matter field (for more details see e.g. [50]).

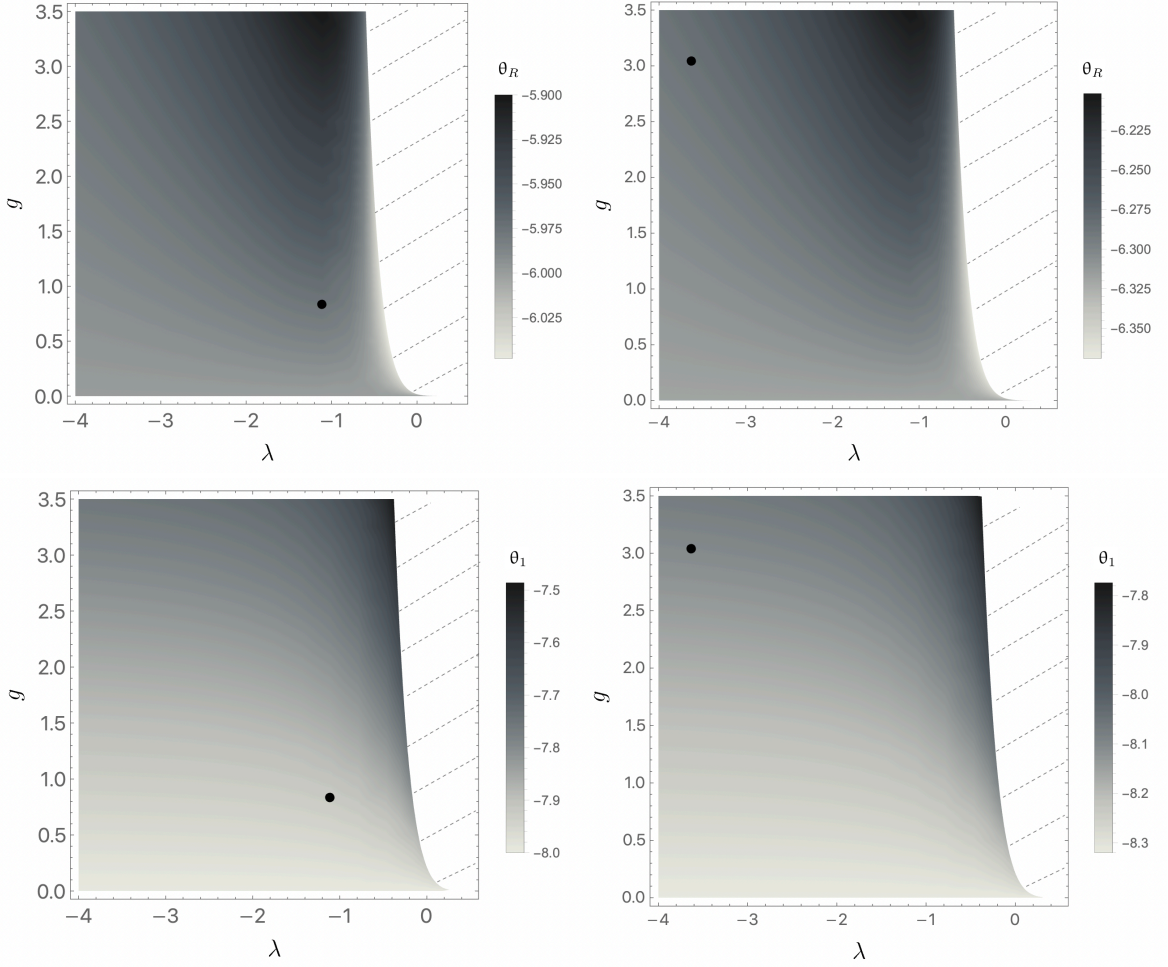FIGURE 13.2. Plot of the critical exponents θ_R (up) and θ_1 (down) of the stability matrix S in the $\lambda - g$ - plane. The plots on the left are for $\eta_N = -2$ and $\gamma_g = 0$; the plots on the right are for $\eta_N = -2$ and $\gamma_g = 0.3197$ (these are the fixed points values which we discuss in Subsection 13.4.2). The dashed region has been excluded from the plot because the critical exponents begin to diverge in this region due to the vicinity of a pole in the propagator. The black points represent the fixed point in the standard scheme with the Standard Model matter content.

In $d = 4$ the beta functions for the dimensionless Newton's coupling g and the dimensionless cosmological constant λ with a type II cutoff for the matter fields become:

$$k\partial_k\lambda = \lambda(-2\gamma_g + \eta_N - 2)$$
$$+ \frac{g}{12\pi}\left(\frac{5(-2\gamma_g + \eta_N - 6)}{2\lambda - 1} + 2\eta_N - 12N_D + 3N_S + 6N_V - 24\right),$$
$$k\partial_k g = g(\gamma_g + 2)$$
$$- \frac{g^2}{6\pi}\left(\frac{5(2\gamma_g - \eta_N + 4)}{4\lambda - 2} + \frac{3(2\gamma_g - \eta_N + 6)}{(1 - 2\lambda)^2} - \frac{3\eta_N}{2} + N_D - N_S + N_V + 14\right).$$
$$(13.61)$$

In the standard renormalization scheme $\gamma_g = 0$. Since we neglect the anomalous dimensions of all the additional matter degrees of freedom ($\hat{\eta}_k = 0$), we do not consider the effect of the anomalous dimension of the scalars $\hat{X}$'s. In this approximation the beta functions have a non-trivial fixed point ($k\partial_k g_* = 0$ and $k\partial_k \lambda_* = 0$). Furthermore, the Newton's constant is experimentally constrained to be positive, this puts a constraint on the matter content which possess a nontrivial fixed point.

(2) Essential scheme: new results. As it is explained in [199] and previously reported in Section 4.2, the essential scheme allows the fields to be reparameterized along the RG flow using the RG kernel. At order ∂^2 the RG kernel of the metric and of the scalars $\hat{X}$ contain both one gamma function, γ_g for the metric and minus one half times the anomalous dimension for the $\hat{X}$s. The anomalous dimension takes into account the normalization of the kinetic term of the $\hat{X}$s, fixing their wave function renormalization constant to one. The γ_g can be used to fixed the vacuum energy $\rho \equiv \lambda/g$ to the value it takes at the GFP $(g, \lambda) = 0$, which is given by

$$\rho \equiv \lambda/g = \frac{2 - 4N_D + N_S + 2N_V}{16\pi}. \tag{13.62}$$

The anomalous dimension γ_g is determined as a function of g by setting $k\partial_k(\lambda/g) = 0$, in addition to (13.61), with the vacuum energy fixed to the value (13.62) for all scales. Indeed, at this order of the derivative expansion, the vacuum energy is the only inessential coupling, see [199], and its flow can be fixed. Therefore, in the standard scheme, where we follow the flow of (g, λ), we get that $\eta_N = k\partial_k G/G \equiv \eta_h$ is equal to -2 at the Reuter fixed point. Using the essential scheme, instead, $\eta_h = \eta_N - 2\gamma_g$, where η_N and γ_g are both functions of g, because of the renormalization condition that fixes the vacuum energy.

(3) Fixed points. For the Standard Model and physically relevant modifications thereof, the fixed points have been computed in the standard and in the essential renormalization scheme (see Table 13.1 and Table 13.2, respectively). For the Standard Model, in order to investigate the cutoff dependence, we considered both a type II and a type I cutoff. Furthermore, we added an extra Scalar Field (SF), that could be a Dark Matter particle or an inflaton [515], for example, and the three neutrinos (3 ν) [516] to the Standard Model matter content.

Let us remark that γ_g is positive for the fixed points displayed in Table 13.1 and Table 13.2, where Standard Model like matter content were considered. This ia in contrast with the case of pure gravity where γ_g is found to be negative at the Reuter fixed point [175].

Matter content	N_S	N_D	N_V	λ_*	g_*	η_h	γ_g
SM (type II)	4	45/2	12	-1.11626	0.834855	-2	0
SM (type I)	4	45/2	12	-3.58874	2.59505	-2	0
SM + SF (type II)	5	45/2	12	-3.79874	2.77608	-2	0
SM + 3 ν (type II)	4	24	12	-4.83385	3.19355	-2	0

TABLE 13.1. Non-Gaussian fixed points in the standard scheme. For every model we define the matter content (number of scalars N_S, number of Dirac fields N_D and number of vectors N_V). At the right part of the table we show the fixed point values of the coupling constants and scaling dimensions in the standard scheme. The graviton anomalous dimension is denoted as η_h here, while γ_g takes into account the contribution of the anomalous dimension of the graviton in the the relational EAA.

Matter content	N_S	N_D	N_V	λ_*	g_*	η_h	γ_g
SM (type II)	4	45/2	12	-3.63186	3.04262	-2.63939	0.319697
SM (type I)	4	45/2	12	-1.11795	0.936571	-2.464896	0.232448
SM + SF (type II)	5	45/2	12	-1.14584	0.959934	-2.470238	0.235119
SM + 3 ν (type II)	4	24	12	-1.07367	0.899477	-2.456218	0.228109

TABLE 13.2. Non-Gaussian fixed points in the essential scheme. For every model we compute the fixed point values of the coupling constants and scaling dimensions in the minimal essential renormalization scheme.

	Standard scheme			Essential scheme		
Matter content	θ_0	θ_R	θ_1	θ_0	θ_R	θ_1
SM (type II)	-4	-5.97643	-7.92358	-4	-6.28653	-8.10472
SM (type I)	-4	-5.97467	-7.8177	-4	-6.20271	-8.14459
SM + SF (type II)	-4	-5.97505	-7.80603	-4	-6.20467	-8.14593
SM + 3 ν (type II)	-4	-5.98015	-7.78084	-4	-6.1996	-8.14236

TABLE 13.3. Critical exponents θ_i of the operators associated to the relational observables. In the central and right part of the table we show the values of the exponents for the standard and the minimal essential scheme, respectively.

13.4.2. *Results*

We can now evaluate the scaling exponents on the NGFP which are displayed in Table 13.3. The scaling exponent of the field space volume term is not affected by any correction and keeps the canonical dimension 4. The other two scaling exponents are affected by quantum corrections: θ_R and θ_1 both become less irrelevant in the standard scheme, while they become more irrelevant in the essential one. This effect is due to the presence of γ_g in the essential scheme, which pushes the scaling exponents in being more irrelevant (see (13.60)). In any case, it is remarkable that the quantum corrections are very small in both schemes.

13.5. HIGHER ORDER OBSERVABLES

In this section, we want to show how the procedure can be generalized to higher order observables. In fact, if we try to go to higher order in the derivative expansion, also terms at fourth order in derivative generated along the flow have to be taken into account.

By plugging the observable (13.43) in the composite operator flow equation, higher order relational observables are generated on RHS of the composite operator flow eq.(13.39). For example we can consider higher powers of the relational metric. For this purpose we consider the *building block matrix*[5] M

$$\mathrm{M}_{\hat{\nu}}^{\hat{\mu}}(x) \;=\; g^{\mu\nu}(x)\,\partial_\mu X^{\hat{\mu}}(x)\,\partial_\nu X^{\hat{\rho}}(x)\,\hat{\delta}_{\hat{\nu}\hat{\rho}} \tag{13.63}$$

is related to the relational inverse metric by

$$\hat{\mathrm{M}}_{\hat{\nu}}^{\hat{\mu}}(\hat{x}) = \mathrm{M}_{\hat{\nu}}^{\hat{\mu}}(X(\hat{x})) = \hat{g}^{\hat{\mu}\hat{\rho}}(\hat{x})\delta_{\hat{\nu}\hat{\rho}}\,. \tag{13.64}$$

For instance, at fourth order we come across terms like $\mathrm{tr}[\mathrm{M}^2]$ and $\mathrm{tr}[\mathrm{M}]^2$. However, at that order we also encounter other terms. Imposing the $O(N)$ and shift symmetry

---

[5]This matrix is reminiscent of the B matrix in Chapter 12.

constraints we have the following terms[6]

$$
\Gamma_k^{\text{rel}} = \int d^d x \tilde{e} \left(a_0 + a_1 \text{tr}[M] + a_R R + a_{1,2}(\text{tr}[M])^2 + a_2 \text{tr}[M^2] \right.
$$

$$
+ a_{\square M} \square(\text{tr} M) + a_{\partial^4 X^4,1} \delta_{\hat{\mu}\hat{\nu}}(\square \hat{X}^{\hat{\mu}})(\square \hat{X}^{\hat{\nu}}) + a_{\partial^4 X^4,2} \delta_{\hat{\mu}\hat{\nu}}(\nabla_\nu \nabla_\mu \hat{X}^{\hat{\mu}})(\nabla^\nu \nabla^\mu \hat{X}^{\hat{\nu}})
$$

$$
+ a_{RM} R \, \text{tr}[M] + a_{Ricci} R^{\mu\nu}(\nabla_\nu X^{\hat{\nu}})(\nabla_\mu X^{\hat{\mu}})\delta_{\hat{\mu}\hat{\nu}}
$$

$$
\left. + a_{R^2} R^2 + a_{Ricci^2} R^{\mu\nu} R_{\mu\nu} + a_{Riemann^2} R^{\mu\nu\alpha\beta} R_{\mu\nu\alpha\beta} + a_{\square R} \square R \right) .
$$

(13.65)

On the first line we have included the lower order terms already present in (13.42) and the two terms which are quadratic in M which therefore involve four powers of the scalar fields $\hat{X}$. On the second line we include all terms with two powers of $\hat{X}$ and four derivatives, of which there are three linearly independent terms. In the last line we have terms which involve scalars which are fourth order in derivatives with no powers of the fields $\hat{X}$.

Now we want to express the terms in the relational action as relational observables integrated over $\hat{x}$. One can introduce the connection

$$
\hat{\Gamma}^{\hat{\rho}}_{\hat{\mu}\hat{\nu}} = -e_{\hat{\mu}}^\mu e_{\hat{\nu}}^\nu \overline{\nabla_\mu \partial_\nu \hat{X}^{\hat{\rho}}} .
$$

(13.66)

The expression of (13.65) in terms of relational observable is given by

$$
\Gamma_k^{\text{rel}} = \int_{\hat{x}} \left(a_0 + a_1 \delta_{\hat{\mu}\hat{\nu}} \hat{g}^{\hat{\mu}\hat{\nu}} + a_R \hat{R} + a_{1,2}(\delta_{\hat{\mu}\hat{\nu}} \hat{g}^{\hat{\mu}\hat{\nu}})^2 + a_2 \delta_{\hat{\mu}\hat{\nu}} \hat{g}^{\hat{\nu}\hat{\rho}} \delta_{\hat{\rho}\hat{\lambda}} \hat{g}^{\hat{\lambda}\hat{\mu}} \right.
$$

$$
- 2 a_{\square M} \hat{\Gamma}^{\hat{\rho}}_{\hat{\rho}\hat{\mu}} \hat{g}^{\hat{\mu}\hat{\lambda}} \hat{\Gamma}^{\hat{\tau}}_{\hat{\lambda}\hat{\sigma}} \hat{g}^{\hat{\sigma}\hat{\kappa}} \delta_{\hat{\kappa}\hat{\tau}} + a_{\partial^4 X^4,1} \delta_{\hat{\mu}\hat{\nu}}(\hat{g}^{\hat{\rho}\hat{\lambda}} \hat{\Gamma}^{\hat{\mu}}_{\hat{\rho}\hat{\lambda}})(\hat{g}^{\hat{\tau}\hat{\sigma}} \hat{\Gamma}^{\hat{\nu}}_{\hat{\tau}\hat{\sigma}}) + a_{\partial^4 X^4,2} \delta_{\hat{\mu}\hat{\nu}} \hat{\Gamma}^{\hat{\mu}}_{\hat{\rho}\hat{\lambda}} \hat{g}^{\hat{\rho}\hat{\tau}} \hat{g}^{\hat{\lambda}\hat{\sigma}} \hat{\Gamma}^{\hat{\nu}}_{\hat{\tau}\hat{\sigma}}
$$

$$
+ a_{RM} \hat{R} \, \delta_{\hat{\mu}\hat{\nu}} \hat{g}^{\hat{\mu}\hat{\nu}} + a_{Ricci} \hat{R}^{\hat{\mu}\hat{\nu}} \delta_{\hat{\mu}\hat{\nu}}
$$

$$
\left. + a_{R^2} \widehat{R^2} + a_{Ricci^2} \widehat{R^{\mu\nu} R_{\mu\nu}} + a_{Riemann^2} \widehat{R^{\mu\nu\alpha\beta} R_{\mu\nu\alpha\beta}} + a_{\square R} \widehat{\square R} \right) .
$$

(13.67)

Note that the canonical dimension of the last two terms of the first line and the terms in the second line is -12, the canonical dimension of the third line is -10 and the canonical dimension of the last line is -8. As we see, the terms in the second line are all expressed as different contractions of two powers of the relational inverse metric and two powers of the relational Christoffel symbol. While for the other terms the transition to relational observables is straight forward, the first term on the second line deserves some explanation. First we note that expanding $\tilde{e}\square(\text{tr} M)$ we have

$$
\tilde{e}\square(\text{tr} M) = \tilde{e} g^{\mu\nu} \square(\partial_\mu \hat{X}^{\hat{\mu}} \partial_\nu \hat{X}^{\hat{\nu}} \hat{\delta}_{\hat{\mu}\hat{\nu}}),
$$

---

[6]It is important to emphasize that some terms which are absent in a $O(N)$ scalar model (see [517] for a complete derivative expansion) in this context cannot be omitted since they do not represent total derivatives. This is due to the different volume element $\tilde{e}$.

which involves three derivatives acting on $\hat{X}$. However, we can instead integrate by parts to obtain

$$\tilde{e}\Box(\mathrm{trM}) + \text{boundary terms} = -\nabla_\mu \tilde{e}\nabla^\mu(\mathrm{trM}) = -2\nabla_\rho \tilde{e}g^{\mu\nu}\nabla^\rho(\partial_\mu \hat{X}^{\hat{\mu}})\partial_\nu \hat{X}^{\hat{\nu}}\hat{\delta}_{\hat{\mu}\hat{\nu}},$$

which now involves only one or two derivatives acting on each $\hat{X}$. In terms of Christoffel symbols

$$\nabla_\mu \tilde{e} = -\tilde{e}e^{\hat{\mu}}_\mu \hat{\Gamma}^{\hat{\rho}}_{\hat{\mu}\hat{\rho}}, \qquad \nabla^\rho \partial_\nu \hat{X}^{\hat{\mu}} = -e^\rho_{\hat{\rho}}e^{\hat{\nu}}_\nu \hat{\Gamma}^{\hat{\mu}}_{\hat{\nu}\hat{\sigma}}\hat{g}^{\hat{\rho}\hat{\sigma}}. \tag{13.68}$$

It is then straightforward to see that this expression can be written in terms of the relational observables as in (13.67).

Remark. One last remark is in order. the scalar term $\tilde{e}\Box R$ appearing in (13.67) could also be expressed as a relational observables linear in $\hat{R}$ and in the connection. In fact, adding boundary terms and integrating by parts

$$\widehat{\tilde{e}\Box R} + \text{boundary terms} \;\;=\;\; -\nabla_\mu \tilde{e}\nabla^\mu \hat{R} = \tilde{e}e^{\hat{\mu}}_\mu \hat{\Gamma}^{\hat{\rho}}_{\hat{\mu}\hat{\rho}}\nabla^\mu \hat{R} \tag{13.69}$$

one obtains the term containing the relational connection and a derivative of the relational Ricci.

CHAPTER 14

Discussion and Summary of Part III

The problem of observables in classical and quantum gravity has generated a lot of discussions in the more recent past [187]. Historically the problem is closely related to some of the consequences of diffeomorphism invariance in GR. The central question is the physical meaning of the points of the event manifold underlying GR.

In contrast to pure mathematics this is a non-trivial point in physics. While in pure differential geometry one simply decrees the existence of, for example, a (pseudo-) Riemannian manifold with a differentiable structure (i.e., an appropriate cover with coordinate patches) plus a (pseudo-) Riemannian metric $g_{\mu\nu}$, the relation to Physics is not a simple one.

This was the main motivation to investigate the inclusion and the analysis of the dynamics of diffeomorphisms in **Project (III.A)** and the incorporation of relational observables within an Asymptotic Safety scenario in **Project (III.B)**.

Project (III.A) Dynamical diffeomorphisms

(1) Diffeomorphism invariance. In textbooks about GR it is frequently stated that all diffeomorphic (spacetime) manifolds $\mathcal{M}$ are physically indistinguishable. This becomes particularly striking in the Einstein hole problem, which is reviewed in Chapter 11.

We argued then that the class of observable quantities have to be drastically reduced in a gravitational theory: observables are only those quantities which are invariant under a diffeomorphism transformation. In fact, with this definition not even scalars, such as the Ricci curvature scalar, are observables.

On the other hand, many authors consider the Ricci scalar at a point to be an observable quantity. This discussion winds up to the question whether GR is a true gauge theory or perhaps only apparently so at a first glance, while on a more fundamental level it is something different.

(2) Physical reference system. The reason for this apparent mismatch stems from the role reference systems are assumed to play in GR. One could argue that the gauge property of general covariance is only of a formal nature. In the hole argument it is for

example argued that it is important to add some particle trajectories which cross each other, thus generating concrete events on $\mathcal{M}$. As these point events transform accordingly under a diffeomorphism, the distance between the corresponding coordinates x, y equals the distance between the transformed points $\phi(x)$, $\phi(y)$, which is therefore an observable. On the other hand, the coordinates x or y are not observables.

Reference systems are needed in order to specify the spacetime points in which the measurements are performed and cannot be considered as independent from the gravitational field. In the classical theory one can always work in an approximation in which the effects and the dynamics of the material reference systems are neglected; in the quantum theory, however, they lead to far reaching consequences. Hence, the main conclusion is that gravitational physics cannot be properly understood unless one takes into account the physical nature and the gravitational interactions of the bodies that form the reference system.

(2) Dynamics of the diffeomorphisms. In Chapter 12 we have constructed a dynamical theory for diffeomorphisms of the spacetime manifold, which is closely related to models of dynamical coordinates. We modeled diffeomorphisms as *maps from spacetime to itself*.

From a geometrical point of view, coordinates are (locally defined) maps of spacetime into a fixed Euclidean space. Thus, our novel analysis of dynamical diffeomorphisms naturally differ from dynamical coordinates because of the identification of spacetime with the target space. Another main motivation given in the Introduction was that in general, coordinates are only defined locally and to cover a manifold with nontrivial topology several coordinate patches are needed. We attempted to overcome this problem by considering generalized models with a target space that is homeomorphic to spacetime itself, rather than flat Euclidean space, constructing a theory of diffeomorphisms from one copy of spacetime into another.

Our model differ from the Nonlinear Sigma Model (NLSM), as we identified the spacetime and target space, and their respective metrics. This lies at the root of all the other differences that we have encountered: along our analysis we found differences both in the kinematics and in the dynamics:

(2a) First we recovered differences in the kinematics. For diffeomorphisms, maps of spacetime into itself, a diffeomorphism transformation must act at both ends, resulting in an action by conjugation, which is neither transitive nor free. Our finding is in contrast with the characteristics of dynamical coordinates, thought of as scalar fields on spacetime. Then diffeomorphisms act on them by right composition. On the other hand, if the coordinates are viewed as a map into spacetime (e.g. as a fluid, analogous to comoving coordinates in cosmology), diffeomorphisms act on them by left composition. In both cases, the action of the group is free and transitive.

(2b) These kinematical differences inevitably give rise to differences in the dynamics: we found that the energy-momentum tensor of diffeomorphisms has an additional term that is not present in the theories of dynamical coordinates, and this term is conserved separately from the rest.

Our analysis of the kinematics and dynamics of diffeomorphisms allowed us to test the physical meaning and application of our class of models:

(1) In the spirit of modeling dark energy, and an effective accelerating solution, we tested that the identity map is always a solution. For our dynamical diffeomorphisms, it is given just by the term that comes from the variation of $\sqrt{g}$ in the action. Our model could then represent a dynamically-generated dark energy model.

(2) As for the observables, the lesson to be drawn from our model is that it is not useful to consider diffeomorphisms of the spacetime manifold to itself in order to construct relational gravitational observables. One has to keep the domain and target space separate. The configuration space of this field must be a copy of the gauge group. This is the case for our models, but more is required: the action of the gauge group on the fields must be free and transitive. To see this, it is enough to consider again the simple example of a reference fluid, already mentioned in the Introduction.

Outlook. We have shown that diffeomorphisms of spacetime to itself cannot define relational observables. However, if there is a field that maps spacetime diffeomorphically (perhaps just locally) on another space, then such a field can be used to set up a physical coordinate system and to define relational coordinates. In future work we plan to specialize to the case when the spacetime is the cosmological FLRW spacetime and the target space is the Standard Model metric. In the Standard Model, the vacuum manifold arises due to a non-vanishing vacuum expectation value of the Higgs field and is homeomorphic to the 3-sphere. On the other hand, the spatial section of the Universe is a 3-sphere (assuming a FLRW-Universe with positive spatial curvature). Moreover, the Standard Model has solitonic states where the Higgs field has nontrivial winding number at fixed time. We plan to consider static and time-dependent solutions of the field equations. In fact, if the Standard Model Higgs field is in such a state, it could be used as a physical coordinate system, whose backreaction is negligible.

Project (III.B) Relational observables in Asymptotic Safety

(1) Relational observables as composite operators. The investigation performed in Chapter 13 represents the first approach to construct observables within an Asymptotic Safety scenario for Quantum Gravity. The technical tool we exploited is the composite operator formalism. Relational observables represent natural candidates for composite operators, which can be studied in Asymptotic Safety. Importantly, as discussed in Chapter 3, at the UV fixed point the composite operators corresponding to physical observables will have universal scaling exponents. Physically these exponents should appear in the scaling behavior of correlation functions of relational observables at small distances less than the Planck length where effects of the fixed point scaling are expected.

(2) Renormalization group scheme. A crucial role in our analysis has been played by the renormalization group scheme. The scheme allows to sort the physical running coupling and to individuate those who enters the value of physical observables. For this reason, it is crucial to simplify the calculations and consider only the flow of couplings contributing to describe the actual physical system: this is the line of reasoning adopted in the essential renormalization scheme.

In the essential scheme (see Section 4.2), changes of variables can be understood geometrically as local frame transformations on configuration space. Field theory can be formulated in a covariant language allowing one the freedom to easily pick different frames to calculate observables. In Section 4.2, it is made manifest that observables are invariant under such frame transformations [199]. The essential scheme allows the fields to be reparameterized along the RG flow. This led to a precise definition of inessential couplings and its conjugate redundant operators, whose identification is crucial to the concrete implementation of GR, which amounts to picking a set of local frames on spacetime.

(3) Relational Effective Average Action. In Chapter 13, in order to construct observables within the Asymptotic Safety framework, we set up a general formalism for relational observables by introducing a set of matter fields. In this context, we performed for the first time an analysis of the RG flow of matter systems coupled to gravity in the minimal essential scheme. In particular, we coupled the gravitational system with the Standard Model matter content and physically relevant modifications thereof. As new intermediate results associated to this analysis we reported the fixed point values of the gravitational couplings (λ_*, g_*) in the standard and in the minimal essential scheme. These can be found in Table 13.2 and can be compared with the values of the fixed points in the standard scheme in [107].

The main new developments and results of our investigation can be summarized as follows:

(1) Inspired by the well-established composite operator flow equation, we set up a formalism to evaluate the scaling of the relational observables. This new framework is fully general and can be applied to any kind of relational observable, constructed from any arbitrary physical field. We furnish a definition for a relational action and derive an equation describing its flow. Therefore, alongside the flowing effective average action, which interpolates between the microscopic action fixed point action and the full effective action, we also have access to flowing observables.

(2) Through this flow equation, we computed the scaling dimension of a selection of observables described in the relational action. This set of observables was chosen in order to self-consistently close the composite operator flow and to keep the truncation under control within a derivative expansion. It turned out that only tensorial quantities with upper indices satisfied this truncation requirement. In particular, we selected the *inverse relational metric* and the *relational scalar curvature*. Tensors with lower indices instead are not generated at any finite order in derivative expansion.

(3) We computed the scaling of the relational volume, the relational inverse metric and the relational Ricci curvature. We noted that the scaling exponent of the field space volume term is not affected by any correction and keeps the canonical dimension 4. The other two scaling exponents are affected by quantum corrections: θ_R and θ_1 both become less irrelevant in the standard scheme, while they become more irrelevant in the essential one (see Table 13.3). This effect is due to the presence of the metric's anomalous dimensions γ_g in the essential scheme, which pushes the scaling exponents to be more irrelevant. In any case, it is remarkable that the quantum corrections are very small in both schemes.

Outlook. The formalism we developed allows us access to universal critical exponents within any asymptotic safe quantum theory of gravity, beyond those that can be found by studying the flow of the effective action. This is important since it provides a new window through which we can compare different approaches to Quantum Gravity. For example the same exponents could be computed in Causal Dynamical Triangulations,[1] Tensor Field Theories and within a perturbative expansion around two dimensions.

It is also important to study the dependence of the critical exponents on the choice of regulator and on the choice of gauge. For simple approximatiosn we might expect these

---

[1] See [71, 518] for curvature profiles, and [519] for a recent analysis including four scalar fields

dependencies to be strong and it will therefore be important to extend the current approximation by including more terms in the effective action beyond the Einstein–Hilbert action. We note however, that the value of critical exponents for the Newton's coupling is stable in the essential scheme, comparing the Einstein–Hilbert approximation and the approximation where all terms with four derivatives are taken into account in the flow equation [175].

We have applied our formalism within a simple approximation and taken the physical system to be a set of four scalar fields. This investigation can be extended in a number of ways. Firstly, we could enlarge the set of observables in a consistent manner by going to higher orders in a derivative expansion. Furthermore, a more general set of observables is accessible both by including terms which break the shift and $O(N)$ symmetry and by including a non-constant source (see Subsection 4.1.3). Finally, alternative coordinate systems can be constructed from other fields which allow access to an array of different relational observables [477].

CHAPTER 15

Summary, Discussion and Outlook

(1) The gravitational Asymptotic Safety program is a conservative approach to Quantum Gravity in the sense that it seeks for a consistent and predictive theory of the gravitational interactions within the framework of QFT by invoking a nonperturbative high-energy completion. Its core assumption is that the gravitational degrees of freedom are encoded in the spacetime metric. Under the program's hypothesis one stipulates that these ingredients give rise to an interacting RG fixed point, called the Reuter fixed point. Phenomenologically, one also requires that the flow emanating from the Reuter fixed point connects to a low-energy regime where the dynamics matches the one of General Relativity to good approximation.

The existence of the Reuter fixed is the central element of the program. Importantly, *it is not an input*. It has been established based on first-principle computations. The Reuter fixed point can manifest itself in (approximate) solutions of the Functional Renormalization Group equation for the Effective Average Action, the Wetterich equation [208]. The adaptation to gravity and first application was performed by M. Reuter in 1996 [95].

The framework of the Gravitational Effective Average Action is well suited for exploring the quest for *nonperturbative renormalizability* in a self-contained manner. In the GEAA framework, we are confronted with a mathematically well-defined, but very complicated, functional differential equation which contains nonperturbative information. In particular, the global properties of its solutions decide about the renormalizability.

Importantly, the approach based on the Gravitational Effective Average Action complies with the principle of *Background Independence*. This principle represents the first and foremost property of classical General Relativity: any pre-exisiting spacetime geometry that could serve as the "habitat" of the dynamical degrees of freedom is absent. It is the geometrical information describing spacetime itself that is rather subject to quantization. Hence the highly "precious" tool of a spacetime metric, indispensable in all developments of standard QFT, is available at best on the level of expectation values only. In the approach to Quantum Gravity based upon the gravitational EAA, Background Independence is built into the formalism by reinterpreting the quantization of a given set of fields without a distinguished background spacetime as equivalent to simultaneously quantizing those fields on all possible backgrounds. This is technically

achieved implementing the background field method. In this sense, a (single) Background Independent quantum field theory has the complexity of an infinite family of background dependent QFTs.

(2) Comparing in detail the consequences of the Asymptotic Scenario with observations and/or different approaches represents one of the main challenges in Quantum Gravity. On the other side, theoretical physicists agree on the fact that the physical behavior of a system has to be probed through observables. Their definition and construction is in general very difficult on curved spacetimes. Already in classical gravity diffeomorphism invariance makes the notion of a spacetime point unphysical, and hence implies that there cannot exist any local observables.

(3) From a technical perspective, the main theme of this thesis followed the objective to open up avenues to unexplored aspects of Quantum Gravity starting from the safe harbor of asympotically safe gravity. Furthermore, developing new methods for extracting its physical contents, we made advancements in the direction of exploring consequences and connections for the quantum theory underlying (asymptotically safe) gravity and of making contact with different approaches to Quantum Gravity.

Concretely, we summarize the projects of this thesis schematically in Table 15.1.

Part I	Review	Chapter 3	RG and Asymptotic Safety
		Chapter 4	Recent developments of the FRG
Part II	**Project (II.A)**	Chapter 7	Geometrization of RG histories AdS/CFT
	Project (II.B)	Chapter 8	Spectral geometry of de Sitter space
	Project (II.C)	Chapter 9	Scattering amplitudes in de Sitter space
Part III	**Project (III.A)**	Chapter 12	Dynamical diffeomorphisms
	Project (III.B)	Chapter 13	Relational observables in AS

TABLE 15.1. Plan of this Thesis.

15.1. PART I OF THIS THESIS

(1) In **Part I**, we focused on the path integral regularization implied by the Effective Average Action. This Part provided a basic introduction to the ideas underlying the gravitational Asymptotic Safety program, after having reviewed the Wetterich equation, and the FRGE for gravity. We illustrated how this tool is used in practical computations by working out the example of the Einstein–Hilbert truncation.

Original in this Part is the construction of self-consistent backgrounds for Lorentzian signature. The existing analyses mostly dealt with effective spacetimes of Euclidean signature. In Lorentzian signature a number of mathematical issues translate in the FRG context in a lacking prescription about how to integrate out momentum eigenmodes of kinetic operators built from Lorentzian metrics. Among the eigenmodes there are spacelike, timelike and null eigenmodes, and it is not a priori clear in which order they should be integrated out.

Inspired by the path integral approach, we chose to integrate timelike and spacelike modes in a symmetric fashion, deriving for the first time running Lorentzian self-consistent backgrounds, in particular Lorentzian Einstein spaces.

(2) The second half of **Part I** was devoted to two recent developments in the FRG framework, with particular focus on our later application to Quantum Gravity: the composite operator formalism and the essential renormalization group scheme. We chose to introduce those frameworks in order to emphasize the necessity to investigate observables to make Quantum Gravity "testable", and discussed possible classes of observables.

(2a) Composite operators and FRG. Observables cannot be directly included in the expansion ansatz of the effective action. In the traditional RG strategy, the renormalized trajectories give the bare coupling constants as functions of the running cutoff. Though one can extract useful information from the trajectories, it remains somehow qualitative because the running parameters of Γ_k are not in general observable quantities.

This is the motivation for considering the inclusion of composite operators:

(i) Firstly, the results are important for the comparison of the different approaches towards Quantum Gravity. In the discrete as well as in the continuum-based approaches, similar analyses of the anomalous dimensions have been performed.

(ii) Secondly, the results presented in Chapter 13 also make an important first step towards the construction of observables within Quantum Gravity. Concretely, the anomalous dimensions presented in **Part III** will inherit some dependence on the gauge-fixing parameters and on the cutoff action. This makes the construction of a full-fledged observable for Quantum Gravity technically more involved. However, it is clear that composite operators will play a crucial role in the construction of a suitable observable for Quantum Gravity.

In **Project (III.B)** we applied for the first time this framework to asymptotically safe gravity-matter systems with the purpose of exploring the scale dependence of relational observables.

(2a) Essential Renormalization Group. Ultimately, the goal of the Asymptotic Safety program is the construction of observables. From this perspective, it turns out

that the theory space spanned by all possible interaction monomials contains redundancies in the sense that not all couplings appearing in this basis will also enter into the observables. In this thesis, we explored a renormalization group scheme which allowed us to take into account the consequences of such redundancies. This is referred to as the *Essential Renormalization Group*. On this basis, we distinguished between *essential* couplings, which enter into the expressions for physical observables, and *inessential* couplings, whose values can be changed without affecting the predictions of the theory.

(i) We showed how a change in an inessential coupling can be absorbed into a reparameterization of the dynamical variables. It turned out that in general operators which are proportional to the equations of motion can be removed by a field redefinition and are thus linked with inessential couplings.

We re-examine the use of the frame covariant flow equation in combination with the minimal essential scheme. Their combination may lead to significant technical simplifications when constructing solutions to the flow equation. In practice, these simplifications could be exploited systematically by parameterizing the field redefinition in k-dependent γ-functions. The freedom gained in this way could then be used to fix the inessential coupling constants to specific values. The scale dependence of the theory was captured by

(1) the β-functions, governing the k-dependence of the essential couplings,
(2) the γ-functions, governing the k-dependence of the inessential ones.

Both sets of equations depend on the essential couplings only, and this simplified the search for RG fixed points significantly.

(ii) Furthermore, we reviewed the nonperturbative renormalizability of gravity taking care to disregard the running of inessential couplings. There are three main consequences of this investigation:

(1) Calculations are much simpler in the minimal essential scheme.
(2) Only Newton's constant is essential and relevant in the considered approximation.
(3) The evidence in favor of the existence of the Reuter fixed point has been strengthened.

Perhaps most profoundly, in the universality class we have investigated, the vacuum energy is inessential both at the GFP and the Reuter fixed point. Hence, no physical meaning can be attributed to its flow.

(iii) To properly address the cosmological constant problem one should understand the situation when matter is coupled to gravity. This has been done for the first time in

Project (III.B). What will remain true even in the presence of matter is that there is an inessential coupling related to a rescaling of the spacetime metric.

The compromise between the inessentiality of the vacuum energy and the appearance of trajectories with different values of the cosmological constant, and hence of the vacuum energy, is still subject of debate. The definition of what which coupling is essential and which is not is not unanimous and still ambiguous, and depends on the given truncation. In fact, different orders of truncation will generate beta functions containing different mixing of the couplings. However, it might be possible to disentangle those dependencies in the beta functions, clarifying which couplings are essential.

In any way, what is univocal is the identification of which operator(s) is (are) redundant, because of the appearance of operators which are proportional to the equations of motion.

A possible way how the disentanglement between essential and inessential couplings in gravity, possibly through the use of observables, represents an ongoing project of the author together with K. Falls.

For the first steps in the computation of critical exponents associated to observables in the minimal essential scheme we refer the reader to **Project (III.B)**.

15.2. PART II OF THIS THESIS

This Part was aimed at studying certain aspects of QFT in de Sitter spacetime, using different techniques and theoretical frameworks. In **Project (II.A)** and **Project (II.B)** we analyzed in two novel ways the results stemming from the functional RG approach to Quantum Gravity and its Asymptotic Safety. In **Project (II.C)** instead, we developed a technique to compute scattering amplitudes directly in de Sitter spacetime. Throughout this Part, we made great use of the mode decomposition of fields in de Sitter spacetime. In fact, the Lorentzian signature and the non-zero curvature of the geometry are encoded in this mode decomposition. The results of this Part represent novel research results based on [RF1], [RF2], [RF3], [RF4] and [RF5].

(1) From a theoretical point of view, the high level of symmetry exhibited by the de Sitter geometry makes it an important and tractable model of spacetime. At the same time, observations suggest that the evolution of our Universe is described by a de Sitter geometry both during the early inflationary phase as well as during the current accelerated phase of expansion. While it is still debatable whether quantum effects should play a serious role in the current phase of the expansion, they probably play

an important role during the early evolution of the Universe. This was part of the motivation to study QFT in the de Sitter background.

(2) Technically speaking, de Sitter spacetime requires us to work in a curved Lorentzian geometry. From the quantum field theoretical perspective, this introduces a number of additional challenges due to the unavailability of several mathematical tools commonly used in a Euclidean (flat) setting. On the other hand, it is exactly these crucial points that encode effects and physical implications typical of de Sitter space. In **Part II** we investigated how precisely the very Lorentzian and curved nature of de Sitter space is giving rise to observable physical features characteristic of Quantum Gravity in such a background.

Project (II.A) deals with the investigation of possible geometrizations of RG trajectories in 4D de Sitter spacetime, **Project (II.B)** is devoted to the study of the spectral properties of quantum de Sitter spacetime and finally in **Project (II.C)** we constructed scattering amplitudes in curved spacetime.

Project (II.A): Geometrization of RG histories and AdS/CFT correspondence

A long-term goal of the Asymptotic Safety program is ultimately trying make contact with "top-down" formalisms like the AdS/CFT approach which also invoke scale-spacetimes, but bear no obvious relation to the Effective Average Action and its functional RG flows. In **Project (II.A)** we addressed this question within 4D Quantum Einstein Gravity. This theory displays a non-Gaussian fixed point by means of which the UV limit can be taken in the asymptotically safe way, guaranteeing nonperturbative renormalizability. Its RG flow also features a second, Gaussian fixed point.

(1) We proposed a new way of representing and analyzing the family of metrics that furnish the same, given 4-dimensional manifold. The idea is to interpret the 4D spacetimes through a single 5-dimensional (pseudo-) Riemannian manifold. Stated the other way around, we question whether there exists a single foliated manifold, the leaves of whose foliation describe the spacetime at different values of the RG parameter.

(2) We assumed that the RG evolution of the 4D metrics is purely multiplicative, and that it is governed by the Einstein–Hilbert truncation of the Effective Average Action. In this setup, we proved that:

(2a) *In Euclidean setting*: it was always possible to complete the specification of the 5D geometry in such a way that it possesses the following distinctive features: First, the metric on $\mathcal{M}_5$ admits a *homothetic Killing vector field* as an intrinsic characterization of its self-similarity, and second, the metric on $\mathcal{M}_5$ is *Ricci flat*. In the special case of maximally symmetric 4D spacetimes it even could be chosen *strictly flat*.

From a more physics oriented point of view we emphasized that in order to be well-defined, i.e., non-degenerate, the proposed metric requires the cosmological constant $\Lambda(k)$ to be a *strictly increasing* function of the cutoff k. In other words, the coefficient $\Lambda(k)$ in the Effective Average Action must have properties similar to a c-function that "counts" the number of fluctuation modes which get integrated out when k is changed. This remarkable feature can be related to the interpretation of the cosmological constant evaluated as a summing up of modes contributing to the vacuum energy.

(2b) *In Lorentzian setting*: Imposing maximum symmetry on the embedding space, we demonstrated that from Asymptotic Safety there arise two solutions for the embedding space, namely certain parts of the AdS_5 and the dS_5 manifold.

We demanded that its $(d + 1)$-dimensional metric should

(1) be Einstein and Lorentzian;

(2) have vanishing shift vector and x^μ-independent lapse when presented in "scale-ADM" form;

(3) possess as many Killing vectors as it is compatible with the other requirements and the symmetries of the input 4D metrics.

As a first result, we demonstrated that embedding the set of all de Sitter spacetimes did not exhaust the entire AdS_5 manifold, depending on which trajectory of the flow diagram we are considering. As for an interpretation in the spirit of an AdS/CFT correspondence, we considered the trajectory that terminates in the Gaussian fixed point, having $\lim_{k\to 0} \Lambda(k) = 0$. At the endpoint of this trajectory, the solution of the field equation changes from dS_4 to Minkowski space. We found that exactly the endpoint $k \to 0$, when the 4D dynamics is governed by the ordinary effective action Γ, corresponds to the timelike boundary of AdS_5 at spatial infinity. Crucially at the timelike boundary, AdS_5 possesses conformal symmetry. Similar to the AdS/CFT correspondence proposed in the literature, especially in the string theory-related correspondence, too, a theory involving gravity lives in the bulk of AdS_5, and is "holographically" related to a CFT on the boundary.

Comparing with the standard AdS/CFT correspondence, our approach to the geometrization of RG flows did not yield 5D Einstein–Hilbert gravity on the bulk. Rather, every 4-dimensional leave of the foliation of the bulk carried its own copy of 4D Einstein–Hilbert gravity, with parameter associated parameter $G(k)$ and $\Lambda(k)$ for each leave. By contrast, in the usual AdS/CFT correspondence, the energy momentum tensor perturbation in a flat boundary $O(N)$ model, which does not include gravity, was giving rise to a propagating graviton in the bulk.

Furthermore, in our approach, no duality between gravity fields and operators of a flat space QFT on the boundary has emerged so far. To test this possibility, further

investigation including higher order truncations and eventually matter systems have still to be performed.

(3) These findings strongly suggested that, at least in principle, it may be possible to recover various forms of "(A)dS/CFT correspondences" as specific solutions to the flow and field equations of matter-coupled QEG. This could be achieved by including higher order truncations in the Effective Average Action. Moreover, the present approach can also be used in order to discover new forms of correspondences.

It is intriguing to speculate that ultimately the envisaged geometrization encodes global information about the underlying flows that is not easily seen at the FRGE level. Hence future work will have to focus on painting a more complete picture by relaxing some, or perhaps all of our assumptions. On the other hand, by discriminating between different matter systems in order to obtain systematic geometrizations, this approach may help in better understanding the meaning of the known bulk/boundary correspondences.

Finally, further investigations to show full conformal invariance of the fixed point theories have to be carried out.

Project (II.B): Spectral flow of de Sitter space

The analysis performed in **Project (II.B)** sheds light on striking consequences of the connection between the RG flow and the spectral properties of the geometry, and the emerging physical picture. The interpretation of the RG flow, generated by introducing a cutoff in the spectrum of the kinetic operator of the scalar field, is strongly modified if the metric itself is subject to a non-negligible induced scale dependence. Disregarding this effect may lead to incorrect physical pictures. This is what happened along different attempts to perform scale identifications or RG improvements.

(1) We showed how the main procedure for extracting physics information from the EAA arises only after going on-shell, or as in our case, by choosing the background self-consistently. Upon considering the scale-dependent d'Alembertian, the eigenvalue equation turned into a complicated nonlinear relationship between the quantum number characteristic of a mode's "fineness" and the RG parameter k. This relation turned out to be particularly counter-intuitive, the reason being the turning point of the dimensionless cosmological constant. Increasing k above the turning point no longer leads to a finer, more structured cutoff mode function, but rather brings one back to coarser ones with a lower "principal quantum number".

(2) We explained and interpreted this phenomenon in terms of the spectral flow along the generalized RG trajectory generated in the Einstein–Hilbert truncation in a de Sitter

spacetime. In particular, we exploited for the first time the mode decomposition of de Sitter spacetime and we discovered that the same picture about the effective resolution cannot be drawn, the reason being that the eigenmodes depended also on the time. On the other hand, the spectral analysis allowed us to uncover some new properties as an effective field theory at the scale k.

Technically speaking, dealing for the first time with a Lorentzian geometry and its associated problem of ordering the eigenmodes, we preferred to think of the piecemeal integrating out of modes as a procedure of performing the basic (regularized) path integral in a stepwise fashion, rather than solving a flow equation. We adapted a fully symmetric ordering scheme for integrating out timelike and spacelike modes. One single parameter k thereby defined two (in principle independent) cutoffs.

(3) The main novel results of **Project (II.B)** can be summarized by the following physical picture that emerged from the investigations:

(3a) We defined the "quantum geometry of 3D space" to encompass all spatial structures that are detected by time independent, or by harmonically oscillating physical fields. We remarkably found that the proper size of those observed geometric patterns which are describable by a certain effective theory resulted to be bounded above by the length related to the cutoff mode. Typically the latter length scale is significantly shorter than the radius of the de Sitter horizon (the length associated to the causal properties of de Sitter) for the same RG parameter k. Consequently, we could conclude that *taking into account the flow of the geometry in Asymptotic Safety puts constraints on the effective macroscopic causal features of spacetime.*

(3b) We were led to the picture that the 3D time slices of quantum de Sitter space are split up in coherent domains or "boxes", whose size is determined by the cutoff mode. While physics within a given domain is describable by some effective action at a scale k, this turns out to not be possible for the patchwork of many coherent domains, such as all those that make up a Hubble volume. This outcome critically puts into question the scale identification, along whose procedure one would just relate at a given scale k the entire effective dynamics.

The picture of the Universe derived in this investigation is constituted of a fragmented 3D time slice which splits up in many coherent boxes. In particular it turned out that the number of independent plane waves coincides with the number of coherent fragments contained in a Hubble volume.

(3c) Along our analysis we introduced for the first time the highly distinguished class of modes, the so-called *asymptotically safe* modes. We interpreted them as witnesses of the cosmological evolution: When the dust of the other modes has settled, they might resurface at cosmological distance scales, being the only relevant modes again. In fact,

they are the only modes excited at the interacting fixed point and as such, they might carry information about the non-Gaussian fixed point. Finally, we speculate how they could carry this information along until the Universe is vacuum dominated again.

(4) In **Project (II.B)** we have assumed that the cosmological evolution was dominated by the vacuum energy. In the case of matter coupled gravity, this assumption applies only under the condition that the matter contribution can be neglected with respect to the cosmological constant. In everyday life this condition is usually violated. There, the relevant gravitational fields are almost entirely due to scale independent, large matter energies.

Up to now we were mainly interested in the spatial geometry and, as a consequence, in the spacelike eigenfunctions of the d'Alembertian. Hence future work will have to analogously scrutinize the role of the timelike modes in more detail, in particular in the context of scattering processes, perhaps making contact in this manner with our construction of scattering amplitudes in de Sitter space (see **Project (II.C)**).

Project (II.C): Scattering amplitudes in de Sitter space

Scattering amplitudes are at the basis of observables in Quantum Field Theory. In **Project (II.C)** we investigated how the curvature of spacetime might affect the long-distance behavior of scattering amplitudes.

(1) We performed the first computation of scattering amplitudes directly in de Sitter space. We circumvented the lack of well-defined momentum space by *working directly with differential operators*, rather than through integral kernels.

Our exposition focused on the gravity-mediated scattering of two distinguishable, massive scalar particles. As a starting point we considered the scalar-gravity action in a constantly curved Lorentzian signature spacetime. By definition the scattering amplitudes was constructed from a tree-level Feynman diagram involving the vertices and propagators obtained from the variation of the action.

In this way, we developed a totally new covariant framework to compute scattering amplitudes and potentials in de Sitter spacetime, including non-minimal interactions. More specifically, we considered the tree-level scattering of two scalar fields in gravity and Quadratic Gravity, given by R^2- and C^2-terms in the action, in addition to the Einstein–Hilbert action with cosmological constant.

(2) We constructed the amplitude functional for this scattering process. We emphasized some interesting features on both the physical and the formal level. These can be summarized in the following points:

(1) The amplitude is fully covariant;

(2) The on-shell amplitude functional is explicitly gauge-independent;

(3) Organizing the propagator and vertices, we can identify an effective mass-pole structure for rank-0 and rank-2 vertex tensors could be identified. Novel in this setting are corrections to the poles due to the de Sitter curvature. We observed that in the case of conformally coupled scalars, only the rank-2 vertex tensor contributes.

(3) In order to extract the explicit expression of the tree-level scattering amplitude, we considered the adiabatic limit of the amplitude functional. This limit was implemented as an expansion in a large mass of the scalar fields compared to the Hubble constant. This expansion was heavily based on the mode decomposition and allowed to use spatial momentum techniques to evaluate the amplitude functional. The amplitude in the adiabatic limit presented two physically interesting properties:

(3a) The amplitude is oscillating as a function of the proper transferred momentum, giving rise to an amplitude vanishing for periodic discrete values. This feature was attributed to the presence of the horizon in a de Sitter spacetime: the particles are bounded to interact within an Hubble volume.

(3b) It is finite for vanishing transferred momentum, similar to the behavior of a mass term in a flat-spacetime massive propagator. This is found to be in contrast to the flat-spacetime case, where a massless graviton propagator gives rise to a divergent amplitude.

(4) We then took the Fourier transform of the amplitude to obtain the scattering potential:

(1) For small proper separations, we found a potential that is in agreement with the flat-spacetime Newtonian potential and Yukawa potentials for pure gravity and quadratic gravity, respectively.

(2) The potential at super-Hubble distances is exactly zero: there is no causal interaction between particles separated by the de Sitter horizon.

(3) At the horizon, there is a coupling-dependent discontinuity in the potential.

Furhermore, we investigated whether the modified potentials in Quadratic Gravity could give rise to Modified Newtonian Dynamics corresponding to dark-matter-like rotation curves. However, we concluded that the de Sitter curvature gives rise to an effective repulsive force that cannot be matched to a dark-matter-like scenario.

(5) At this point, we look ahead to further implications of the adiabatic limit. This approximation differs significantly from the usual derivation of the Newtonian potential in GR, where the "test particle" is assumed to be light, such that the backreaction of the geometry can be neglected. This explained the fact that only to a limited extent,

the scattering potential reproduces the classical GR potential. Instead, taking the scattering amplitude as a tool to reconstruct the backreaction of matter on spacetime, we concluded that the amplitude probes an effective geometry where both a cosmological constant Λ and two heavy (black-hole) masses are present. For such a geometry, no explicit solutions of Einstein's equations are known.

The results found along **Project (II.C)** may also have profound consequences for the properties for the de Sitter horizon. It famously has a temperature [520], comparable to the Bekenstein–Hawking temperature of a black hole [442]. The investigation allowed us to probe the horizon properties of a more general geometry with two masses inside. This may shed light on the outstanding problem of defining a horizon temperature in a Schwarzschild–de Sitter spacetime.

A different line to follow is to connect the novel formalism introduced here to more established methods to compute de Sitter correlators.

On the technical level, this approach can be extended in a number of interesting ways. First, we could go higher order in the adiabatic limit expansion, in order to gain information about the angular dependence of the amplitude. Furthermore, one could also apply the machinery to loop diagrams, in order to compute quantum corrections. Finally, the formalism developed in this work can be extended to other curved backgrounds. Of particular interest in cosmology would be to extend the de Sitter metric to a generic FLRW background.

In conclusion, in this thesis we showed how scattering amplitudes in curved spacetime can give a fascinating outlook on gravitational observables. They provide a set of methods to understand the quantum nature of spacetime and its contents. We believe that the techniques developed in **Project (II.C)** will be an important instrument of this toolbox.

15.3. PART III OF THIS THESIS

Part III is devoted to the analysis of the very special symmetries and properties of gravity and its implications towards the construction of observables. The results of this Part represent novel research results based on [RF6] and [RF7].

(1) In this thesis we discussed how the standard picture of GR suggests an interpretation of the manifold as an independently existing "container" for the histories of fields and particles. Usually, the points are considered as existing independently of geometrical properties and of the fields themselves. Although this point of view may be pleasing

mathematically, we discuss how physically these points in spacetime are in fact distinguished either by local events or non-locally, for example by following the path of a particle from some initial event for a fixed amount of proper time.

Alternatively to this construction, in this thesis we considered spacetime to be a set of intrinsically distinguishable events. Spacetime can be then identified with the total collection of events constructed out of the actual physical and geometrical fields, and its existence (we can observe it!) trivially requires the presence of such fields. Hence, more generally, for the points of the manifold to be in one-to-one correspondence with events there has to be a complete lack of symmetry.

(2) More concretely, we started **Project (III.A)** and **Project (III.B)** from the following observation: If we view spacetime as a manifold then a scalar quantity at a point $\mathcal{P}$ is not an observable, that is, it cannot be determined as a prediction of the theory. An event at a point $\mathcal{P}$ in a manifold moves to other points in the manifold under a diffeomorphism. On the other hand local observables in spacetime certainly do exist (just take a look around to check!).

In the Projects of **Part III** we clearly identified and distinguished which is the property of GR giving rise to such a striking situation. In particular, we focused on the possibility of constructing diffeomorphism-invariant quantities which constitute observables.

Project (III.A): Dynamical diffeomorphisms

In this thesis, we showed how it is possible to turn any field theory into an empirically equivalent and generally invariant theory by reformulating it on a suitable manifold of parameters, which amounts to parametrizing the coordinates themselves.

(1) Usually one constructs a diffeomorphism-invariant theory, considering the coordinates x_μ as four scalar matter fields on some manifold diffeomorphic to $\mathbb{R}^4$ on which one can introduce coordinates ξ^μ. Since the above trick of parametrizing the coordinates can be carried out for any tensorial equation, we conclude that all field theories can be made diffeomorphism-invariant.

The dynamics of the coordinates can be associated to the so-called Nonlinear Sigma Models. Specifically, since physics must be independent of the choice of coordinates on the target space, we force the action to be a functional constructed with tensorial structures on this space. In **Project (III.A)**, inspired by kinematically nonlinear theories, we constructed a nonlinear model describing for the first time the dynamics of diffeomorphisms.

(2) Practically, we considered the peculiar situation where the scalar matter fields are both a map on spacetime and in spacetime. The main novelty of our treatment was that we identified the target space with spacetime. This gave rise to significant differences compared to the dynamics of ordinary matter fields, and also to the dynamics of coordinates, regarded as scalar fields on spacetime:

(2a) At the level of kinematics, we replaced the target space $\mathbb{R}^4$ by spacetime itself. Quite aside from the topological aspect, this subtly changed the invariance group.

(2b) We discovered also dynamical differences. Our new model possesses a new dependence on the metric that affects the definition of the energy-momentum tensor of the scalars, and has further consequences on the relation between the equations of motion and energy-momentum conservation. In particular, the energy-momentum tensor consists of two pieces that are separately conserved.

(3) We emphasized how the new class of models have interesting physical consequences:

(1) The background solution is the identity diffeomorphism and the energy-momentum tensor of this solution gives rise to an effective cosmological constant. This turned out to be highly reminiscent of solutions resulting from cosmological fluid models.

(2) We found that the action of the gauge group on the scalar fields must be free and transitive. Hence, in order to construct diffeomorphism-invariant observables, it is not sufficient to demand that the configuration space of the fields must be a copy of the gauge group. One has to keep the domain and target space separate. Consequently, taking into account the dynamics of diffeomorphism is not useful to construct observables.

Summarizing, the model for dynamical diffeomeorphisms introduced in **Project (III.A)** is not suited to describe relational observables: we cannot use the diffeomorphisms as physical coordinate scaffolding. However, on a more phenomenological point of view, we proved that dynamical diffeomorphisms can be considered a special class of cosmological self-gravitating medium giving rise to an effective accelerated dynamics of the Universe.

Project (III.B): Relational observables in Asymptotic Safety

In **Project (III.B)** we reviewed how in gravitational theories measurements are possible due to the presence of additional matter fields which provide a preferred frame of reference. Indeed, the matter fields can be understood as representing the readings on some physical coordinate scaffolding. All measurements of tensor or scalar fields referring to such physical coordinate systems represent relational observables.

(1) On a conceptual level, we discussed how freedom to construct a physical frame from the involved dynamical matter fields translates in the freedom to construct many different relational observables since there is a immense freedom in both choosing the physical coordinate system and choosing which (composite) operator to transform into the chosen coordinate system. Hence, even if we considered the technical difficulties to construct diffeomorphism-invariant observables in Quantum Gravity, from the point of view of the relational observables we concluded that *there is no lack of observables, but rather perhaps a lack of determining which observables are most relevant.* Concretely, the question was then shifted to the quest of a guiding principle which provides a natural selection of observables for our physical system. In this exploration we claimed that it is the Renormalization Group flow equation which selects "good" classes of observables, by demanding the existence of a self-consistent closure of the flow equations.

(2) Equipped with this ingredients, in **Project (III.B)** we performed the first analysis of the scaling of relational observables within the Asymptotic Safety scenario. Technically, we exploited two main developments established recently within the FRG and reviewed in **Part I**:

(2a) The composite operator formalism represents the natural framework to embed relational observables in an asymptotically safe gravitational scenario. Coupling matter to gravity, we constructed upon the physical matter system a physical coordinate system. In particular, we considered four scalar fields to constitute the four physical coordinates.

(2b) The essential renormalization group [199] disentangles the physical information from the redundancies arising from the freedom to perform reparameterization of the fields. In order to compute the scaling of observables, it is crucial to keep only track of the scaling contributions stemming from physical information.

(3) We defined a relational action and a related equation describing its flow. Therefore, besides the flowing Effective Average Action, we also disposed of information about the the flow of observables constructed upon dynamical matter fields, whose dynamics is described in the EAA. The recipe includes the following steps:

  (1) We chose the field content and their symmetries. Following this choice, we truncate the Effective Average Action, considering the gravitational interactions, the matter interactions and the coupling between matter and gravity. In particular, we considered the Einstein–Hilbert action coupled to a Standard Model - like matter action. Furthermore, using the FRGE we computed their fixed points in the standard and in the minimal essential scheme.

  (2) We identified the physical coordinate system from the matter fields. In particular, as a first application, we chose four scalar fields to represent the four dynamical coordinates.

(3) We constructed the relational observables upon these physical coordinate system. We truncated the expansion following a derivative expansion of the relational EAA: at any finite order of the expansion, we are furnished with a finite number of relational observables. At first order, we were left with three observables: the relational volume term, the relational Ricci term and the relational inverse metric. Furthermore, inserting this ansatz into the flow equation for the relational observables (derived from the composite operator flow equation), we computed the running of the couplings associated to the relational observables.

(4) We evaluated the scaling dimension of the relational observables at the fixed points. This furnished us the main results of this investigation: *We computed the scaling of the relational volume, the relational inverse metric and the relational Ricci curvature.* We noted that the scaling exponent of the field space volume term is not affected by any correction, since this term is purely topological. The other two scaling exponents are affected by quantum corrections: the quantum corrections are very small in both schemes. The scaling exponents become less irrelevant in the standard scheme, while they become more irrelevant in the minimal essential scheme. This effect is due to the presence of the metric's anomalous dimensions in the latter, which pushes the scaling exponents in being more irrelevant.

(4) The formalism introduced in **Project (III.B)** provides a new window through which we can compare different approaches to Quantum Gravity. For instance the same exponents could be computed in other discrete theories of gravity, such as Causal Dynamical Triangulations or Tensor Field Theories.

It is important to extend the current investigation by including more terms in the effective action beyond the Einstein–Hilbert action. Moreover, we have applied our formalism within a simple approximation and taking the physical system to be a set of four scalar fields. There is a wide range of investigation which has to be explored, in order to construct an array of different relational observables. For instance, by going to higher orders in a derivative expansion, one could enlarge the set of observables in a consistent manner. Finally, alternative coordinate systems can be constructed from a different set of fields.

What comes next

While much has been achieved through in the Asymptotic Safety scenario, it has also become clear that remaining key open questions in Quantum Gravity might be addressed by making contact with different approaches, understanding the specific properties of gravity and facing the challenge of constructing observables.

The novel lines of research presented above are in prospect of playing paramount roles in the development of applicable methods. The underlying key open question that we addressed can be parted into three main categories: Firstly, the geometrical and dynamical meaning of the Renormalization Group flow equation in a broader context (such as in connection to old and new AdS/CFT correspondences), secondly, the investigation of nonperturbative Background Independent quantization of gravity, and, thirdly, the construction of observables for Quantum Gravity. Regarding the first it will be imperative to explore also possible geometrizations of matter-coupled gravity. It is highly intriguing that the string theory internal space may emerge from the RG approach in a given limit. Additionally, for a better understanding of the correspondence, it would be instructive to study a possible relationship between gravity fields and operators of a flat space QFT on the boundary. Regarding the second, a first step is to further study the meaning and the cosmological implications of a minimal length in a de Sitter spacetime, longing for a connection with results coming from noncommutative geometry. Regarding the last, it will necessary to construct new observables, such as new scattering amplitudes in curved spacetimes. Of particular interest in cosmology would be to extend the de Sitter metric to a generic FLRW background. In a different direction, a treatment of scattering in a Schwarzschild black-hole background would be relevant to a number of open problems, such as e role of unitarity, and the process of black hole evaporation. Moreover, further investigation has to be devoted to the construction and properties of diffeomorphism-invariant observables, a prime example being relational observables.

Part IV

Appendices

APPENDIX A

Conventions and Notation

In this appendix we list a number of mathematical conventions and notations relevant to this thesis.

A.1. CANONICAL MASS DIMENSIONS

Throughout this thesis, we use natural units in which $\hbar = c = 1$. Canonical mass dimensions can follow the conventions of dimensionless coordinates, i.e., $[x^\mu] = 0$, $[\partial_\mu] = 0$, $[g_{\mu\nu}] = -2$ and $[g^{\mu\nu}] = +2$ etc., or of a dimensionless metric tensor, i.e., $[g_{\mu\nu}] = 0$, $[g^{\mu\nu}] = 0$, $[x^\mu] = -1$, $[\partial_\mu] = +1$.

We model spacetime as an d-dimensional Riemannian manifold $\mathcal{M}$ with associated metric g of Euclidean signature $(+ + \cdots +)$ or Lorentzian mostly-plus signature $(- + \cdots +)$.

We denote as ∇_μ the covariant derivative containing the Levi-Civita connection acting on a spacetime point. The Laplacian is accordingly defined as $\Box = g^{\mu\nu}\nabla_\mu\nabla_\nu$.

Furthermore, we will make of the covariant derivative $D_\mu \equiv \nabla_\mu + A_\mu$, which, in addiction to the Levi-Civita connection implicit in ∇_μ, also includes a Yang–Mills connection A_μ, if present.

A.2. CURVATURE CONVENTIONS

Throughout this thesis we employ the following curvature conventions:

$$R^\sigma{}_{\rho\mu\nu} = \partial_\mu\Gamma^\sigma_{\mu\rho} - \partial_\nu\Gamma^\sigma_{\mu\rho} + \Gamma^\sigma_{\mu\tau}\Gamma^\tau_{\nu\rho} - \Gamma^\sigma_{\nu\tau}\Gamma^\tau_{\mu\rho} \tag{A.1}$$

$$R_{\mu\nu} = R^\sigma{}_{\mu\sigma\nu} \tag{A.2}$$

$$R = g^{\mu\nu}R_{\mu\nu} \,. \tag{A.3}$$

The Riemann tensor satisfies the identities

$$[\nabla_\mu, \nabla_\nu] V^\sigma = R^\sigma{}_{\rho\mu\nu} V^\rho \qquad \text{for vectors} \qquad (A.4)$$

$$[\nabla_\mu, \nabla_\nu] A_\rho = -R^\sigma{}_{\rho\mu\nu} A_\sigma \qquad \text{for 1-forms} \qquad (A.5)$$

$$[\nabla_\mu, \nabla_\nu] H_{\alpha\beta} = -R^\tau{}_{\alpha\mu\nu} H_{\tau\beta} + R^\tau{}_{\beta\mu\nu} H_{\alpha\tau} \qquad \text{for } (0, 2)\text{-tensors} \qquad (A.6)$$

A.3. CONVENTIONS FOR THE SCALAR FIELD IN CURVED SPACETIME

In this section we summarize some important conventions for the representation of operators, such that the position space representation of a scalar field in a classical gravitational field. We model classical spacetime as an d-dimensional Riemannian manifold $\mathcal{M}$ with metric g and we build a framework to handle scalars on a Riemannian manifolds, i.e. the space of square-integrable functions $L^2(\mathcal{M}, g)$.

A.3.1. *Position space representation in curved spacetime*

We define, the delta function is defined by $\delta(x - y) \equiv \prod_{i=1}^{i} \delta(x^i - y^i)$, with $x, y \in \mathbb{R}^d$.

Attached to $(\mathcal{M}, \bar{g})$ is the Hilbert space $L^2(\mathcal{M}, \bar{g})$ of square-integrable functions. Now, we assume that there exist vectors $|x\rangle$ which form a "dirac-normalized" basis (the position basis) for the Hilbert space satisfying

$$\langle y | z \rangle = \frac{\delta(y - z)}{\sqrt{\bar{g}(y)}} = \frac{\delta(y - z)}{\sqrt{\bar{g}(z)}} \qquad (A.7)$$

Next, for each $|\psi\rangle$ in the Hilbert space, we define the position basis wavefunction ψ corresponding to the state $|\psi\rangle$ as

$$\langle x | \psi \rangle \equiv \psi(x) \qquad (A.8)$$

The bra-ket notation is particularly useful in function spaces which have an inner product that allows Hermitian conjugation and identifying a vector with a continuous linear functional, that is a ket with a bra, and vice versa

$$\langle \psi_1 | \psi_2 \rangle = \langle \psi_1 | \mathbb{1} | \psi_2 \rangle = \int d^d x \sqrt{\bar{g}(x)} \langle \psi_1 | x \rangle \langle x | \psi_2 \rangle = \int d^d x \sqrt{\bar{g}(x)} \psi_1^*(x) \psi_2(x) \qquad (A.9)$$

where we used the unit operator as

$$|z\rangle = \mathbb{1} |z\rangle = \int d^d y \sqrt{g(y)} |y\rangle \langle y | z \rangle \equiv \int d^d y |y\rangle \sqrt{g(y)} \langle y | z \rangle \qquad (A.10)$$

(1) Position eigenbasis $\{|x\rangle\}$. Summarizing, in the bra-ket notation, the basis of states in the position representation of the Hilbert space satisfies following two properties.

    (1) Orthogonality:

$$\langle x|y\rangle = \mathbb{1}_{xy} = \frac{\delta(x-y)}{\sqrt{\bar{g}(y)}} \tag{A.11}$$

    (2) Completeness:

$$\int \mathrm{d}^d y\sqrt{\bar{g}(y)}|y\rangle\langle y| = \mathbb{1} \tag{A.12}$$

(2) Generic basis $\{|n\rangle\}$. Again we derive the properties also in a generic basis $\{|n\rangle\}$:

    (1) Orthogonality

$$\langle n|m\rangle = \delta_{nm} \tag{A.13}$$

    (2) Completeness

$$\sum_n |n\rangle\langle n| = \mathbb{1} \tag{A.14}$$

For consistency, we can pass to the position space basis taking the x-y matrix element

$$\sum_n \langle x|n\rangle\langle n|y\rangle = \langle x|\mathbb{1}|y\rangle \tag{A.15}$$

and recovering the orthogonality relation (A.11)

$$\sum_n \phi_n(x)\phi_n^*(y) = \frac{\delta(x-y)}{\sqrt{\bar{g}(y)}} \tag{A.16}$$

(3) Relation $\{|x\rangle\} \iff \{|n\rangle\}$. We define matrix elements of an operator A on $L^2(\mathcal{M},\bar{g})$ by considering the n-m matrix element:

$$\int \mathrm{d}^d y\sqrt{\bar{g}(y)}\langle n|y\rangle\langle y|m\rangle = \langle n|\mathbb{1}|m\rangle \tag{A.17}$$

We can therewith confirm consistency,

$$\int \mathrm{d}^d y\sqrt{\bar{g}(y)}\psi_n^*(y)\psi_m(y) = \delta_{nm} \tag{A.18}$$

(4) Operators. We can also define the matrix elements of the operator A in position space by

$$A_{xy} = \langle x|\,A\,|y\rangle \tag{A.19}$$

The matrix multiplication of A with another operator B is then given by

$$(A\,B)_{xy} \equiv \int \mathrm{d}^d z\sqrt{\bar{g}(z)}A_{xz}B_{zy} \tag{A.20}$$

The operator trace of A is given by

$$\text{Tr}(A) \equiv \int \mathrm{d}^d z \sqrt{\bar{g}(z)} A_{zz} \tag{A.21}$$

These two operations can be also expressed in bra-ket notation as

$$\langle x | A\, B | y \rangle = \int \mathrm{d}^d z \sqrt{\bar{g}(z)} \langle x | A | z \rangle \langle z | B | y \rangle \tag{A.22}$$

$$\text{Tr}(A) = \int \mathrm{d}^d z \sqrt{\bar{g}(z)} \langle z | A | z \rangle \tag{A.23}$$

Exploiting (A.11) can check that

$$(A\, \mathbb{1})_{xy} \equiv \int \mathrm{d}^d z \sqrt{\bar{g}(z)} A_{xz} \mathbb{1}_{zy} = \int \mathrm{d}^d z \sqrt{\bar{g}(z)} A_{xz} \frac{\delta(z-y)}{\sqrt{\bar{g}(z)}} = A_{xy} \tag{A.24}$$

A.3.2. The differential operator associated to A_{xy}

A differential operator $\hat{A}^{\text{diff.op.}}$ associated to the abstract operator A is defined as

$$(A\, f)_x \equiv \int \mathrm{d}^d y \sqrt{\bar{g}(y)} A_{xy}\, f_y := \left(\hat{A}^{\text{diff.op.}}\, f \right)(x) \tag{A.25}$$

for $f \in L^2(\mathcal{M}, g)$.

If we consider for instance the matrix operator

$$A_{xy} = F\left(\bar{\nabla}^y_\mu \right) \frac{\delta(x-y)}{\sqrt{\bar{g}(y)}} \tag{A.26}$$

with $F\left(\bar{\nabla}^y_\mu \right)$ an arbitrary function (no symmetry between $x \leftrightarrow y$ is assumed), then the associated differential operator reads

$$\begin{aligned}
(A\, f)_x \equiv \left(\hat{A}^{\text{diff.op.}}\, f \right)(x) &= \int \mathrm{d}^d y \sqrt{\bar{g}(y)} f(y) F\left(\bar{\nabla}^y_\mu \right) \frac{\delta(x-y)}{\sqrt{\bar{g}(y)}} \\
&= \int \mathrm{d}^d y \frac{\delta(x-y)}{\sqrt{\bar{g}(y)}} F\left(-\bar{\nabla}^y_\mu \right) \sqrt{\bar{g}(y)} f(y) \\
&= \int \mathrm{d}^d y\, \delta(x-y) F\left(-\bar{\nabla}^y_\mu \right) f(y) = F\left(-\bar{\nabla}^x_\mu \right) f(x)
\end{aligned} \tag{A.27}$$

Hence, we can list the following two identities:

$$A_{xy} = F\left(\bar{\nabla}^y_\mu \right) \frac{\delta(x-y)}{\sqrt{\bar{g}(y)}} \cong \hat{A}^{\text{diff.op.}} = F\left(-\bar{\nabla}_\mu \right) \tag{A.28}$$

$$A_{xy} = F\left(-\bar{\Box}^y \right) \frac{\delta(x-y)}{\sqrt{\bar{g}(y)}} \cong \hat{A}^{\text{diff.op.}} = F\left(-\bar{\Box} \right) \tag{A.29}$$

In this section we compute the position space matrix elements of the Hessian-operator.

We start defining the mean field value as the functional derivative of the generating functional W_k wrt. the source $J(x)$

$$\phi(x) = \langle \hat{\phi}(x) \rangle = \frac{1}{\sqrt{g}} \frac{\delta W_k}{\delta J(x)} [J, g, \bar{g}] \ . \tag{A.30}$$

Adding a source term to W_k, we define

$$\tilde{\Gamma}_k \equiv \int d^d x \sqrt{\bar{g}(x)} J(x) \phi(x) - W_k = \Gamma_k + \Delta S_k \ , \tag{A.31}$$

where Γ_k is the Effective Average Action and ΔS_k the smooth cutoff term. The source can then be obtained as

$$\frac{1}{\sqrt{g}} \frac{\delta \tilde{\Gamma}_k}{\delta \phi(x)} [\phi, g, \bar{g}] = J(x) \ . \tag{A.32}$$

Differentiating two times $\tilde{\Gamma}_k$ and W_k wrt. the field and the source, respectively, we obtain the two following identities, defining respectively, the Green function and the Hessian of $\tilde{\Gamma}_k$ x-y-matrix elements:

$$\left(\tilde{\Gamma}_k^{(2)} \right)_{xy} \equiv \left(\Gamma_k^{(2)} \right)_{xy} + (\mathcal{R}_k)_{xy} \equiv \langle x | \tilde{\Gamma}_k^{(2)} | y \rangle$$

$$\equiv \frac{1}{\bar{g}(y)} \frac{\delta J(x)}{\delta \phi(y)} = \frac{1}{\sqrt{\bar{g}(x)} \sqrt{\bar{g}(y)}} \frac{\delta^2 \tilde{\Gamma}_k}{\delta \phi(x) \delta \phi(y)} \ , \tag{A.33}$$

$$G_{xy} \equiv \langle x | G | y \rangle \equiv \frac{1}{\bar{g}(y)} \frac{\delta \phi(x)}{\delta J(y)} = \frac{1}{\sqrt{\bar{g}(x)} \sqrt{\bar{g}(y)}} \frac{\delta^2 W_k}{\delta J(x) \delta J(y)} \ . \tag{A.34}$$

Now, exploiting the chain rule, we can write the delta function as

$$\delta(x - z) = \int dy \frac{\delta \phi(x)}{\delta J(y)} \frac{\delta J(y)}{\delta \phi(z)} \ . \tag{A.35}$$

Or alternatively, combining (A.33) and (A.34), we arrive at

$$\frac{\delta(x-z)}{\sqrt{\bar{g}(z)}} = \int dy \sqrt{\bar{g}(y)} \left(\frac{1}{\sqrt{\bar{g}(y)}} \frac{\delta \phi(x)}{\delta J(y)} \right) \left(\frac{1}{\sqrt{\bar{g}(z)}} \frac{\delta J(y)}{\delta \phi(z)} \right)$$

$$= \int dy \sqrt{\bar{g}(y)} \left(\frac{1}{\sqrt{\bar{g}(x)} \sqrt{\bar{g}(y)}} \frac{\delta^2 W_k}{\delta J(x) \delta J(y)} \right) \left(\frac{1}{\sqrt{\bar{g}(y)} \sqrt{\bar{g}(z)}} \frac{\delta^2 \tilde{\Gamma}_k}{\delta \phi(y) \delta \phi(z)} \right) \tag{A.36}$$

Finally, we can write

$$\frac{\delta(x-z)}{\sqrt{\bar{g}(z)}} = \int dy \sqrt{\bar{g}(y)} G_{xy} \left(\tilde{\Gamma}_k^{(2)} \right)_{yz} \equiv \int dy \sqrt{\bar{g}(y)} \langle x | G | y \rangle \langle \tilde{\Gamma}_k^{(2)} | z \rangle \tag{A.37}$$

and in the bra-ket notation ($A.37$) we obtain the identity

$$\frac{\delta(x-z)}{\sqrt{\bar{g}(z)}} \equiv \langle x|G\,\tilde{\Gamma}_k^{(2)}|z\rangle \Rightarrow G = \left[\tilde{\Gamma}_k^{(2)}\right]^{-1} = \left[\Gamma_k^{(2)} + \mathcal{R}_k\right]^{-1}. \tag{A.38}$$

relating the inverse of the Hessian operator to the Green function.

APPENDIX B

Metric variations

In this appendix we list mathematical conventions and notations relevant to this thesis.

We consider general variations of the metric, $g_{\mu\nu} \rightarrow g_{\mu\nu} + \delta g_{\mu\nu}$, and note the response of various derived geometrical quantities:

$$\delta g^{\mu\nu} = -g^{\mu\alpha}g^{\nu\beta}\delta g_{\alpha\beta} \tag{B.1}$$

$$\delta g = g g^{\mu\nu}\delta g_{\mu\nu} \tag{B.2}$$

$$\delta\sqrt{g} = \frac{1}{2}\sqrt{g}g^{\mu\nu}\delta g_{\mu\nu} \tag{B.3}$$

$$\delta^2\sqrt{g} = \frac{1}{2}\sqrt{g}\left(g^{\mu\nu}g^{\alpha\beta}\delta g_{\mu\nu}\delta g_{\alpha\beta} - g^{\mu\alpha}g^{\nu\beta}\delta g_{\alpha\beta}\delta g_{\mu\nu}\right) \tag{B.4}$$

$$\delta\Gamma^{\sigma}_{\mu\nu} = \frac{1}{2}g^{\sigma\beta}\left(\nabla_{\mu}\delta g_{\nu\beta} + \nabla_{\nu}\delta g_{\mu\beta} - \nabla_{\beta}\delta g_{\mu\nu}\right) \tag{B.5}$$

$$\delta R^{\sigma}{}_{\rho\mu\nu} = \frac{1}{2}\left(-g^{\sigma\beta}R^{\alpha}{}_{\mu\sigma\nu}\delta g_{\alpha\beta} + R^{\alpha}{}_{\nu}\delta g_{\mu\alpha} + \nabla^{\sigma}\nabla_{\mu}\delta g_{\nu\sigma}\right.$$
$$\left. -g^{\sigma\alpha}\nabla_{\nu}\nabla_{\rho}\delta g_{\alpha\mu} + \nabla_{\nu}\nabla^{\lambda}\delta g_{\mu\rho} - \nabla_{\mu}\nabla^{\lambda}\delta g_{\nu\rho}\right) \tag{B.6}$$

$$\delta R_{\mu\nu} = \frac{1}{2}\left(-g^{\sigma\beta}R^{\alpha}{}_{\mu\sigma\nu}\delta g_{\alpha\beta} + R^{\alpha}{}_{\nu}\delta g_{\mu\alpha} + \nabla^{\sigma}\nabla_{\mu}\delta g_{\nu\sigma}\right.$$
$$\left. -g^{\sigma\alpha}\nabla_{\nu}\nabla_{\mu}\delta g_{\sigma\alpha} + \nabla_{\nu}\nabla^{\sigma}\delta g_{\sigma\mu} - \nabla_{\sigma}\nabla^{\sigma}\delta g_{\nu\mu}\right) \tag{B.7}$$

$$\delta R = -R^{\mu\nu}\delta g_{\mu\nu} + \nabla^{\mu}(\nabla^{\nu}\delta g_{\nu\mu} - g^{\nu\alpha}\nabla_{\mu}\delta_{\nu\alpha}) \tag{B.8}$$

$$\delta^2 R = g^{\sigma\alpha}R^{\mu\nu}\delta g_{\mu\alpha}\delta g_{\sigma\nu} - R^{\mu\nu\rho\sigma}\delta g_{\nu\rho}\delta g_{\mu\sigma} + 2g^{\sigma\alpha}\delta g_{\mu\nu}\nabla^{\mu}\nabla^{\nu}\delta g_{\sigma\alpha}$$
$$+2g^{\mu\alpha}g^{\nu\beta}\delta g_{\alpha\beta}\nabla_{\sigma}\nabla^{\sigma}\delta g_{\mu\nu} - 3g^{\mu\alpha}\delta g_{\alpha\nu}\nabla^{\nu}\nabla^{\sigma}\delta g_{\sigma\mu}$$
$$-g^{\nu\alpha}\delta g_{\mu\alpha}\nabla^{\sigma}\nabla^{\mu}\delta g_{\sigma\nu} - 2g^{\mu\alpha}(\nabla^{\nu}g_{\alpha\nu})(\nabla^{\sigma}\delta g_{\sigma\mu})$$
$$-g^{\nu\alpha}(\nabla^{\sigma}g_{\mu\alpha})(\nabla^{\mu}\delta g_{\sigma\nu}) + 2g^{\sigma\alpha}(\nabla^{\mu}g_{\alpha\nu})(\nabla^{\sigma}\delta g_{\sigma\alpha})$$
$$+\frac{3}{2}g^{\mu\alpha}g^{\nu\beta}(\nabla_{\sigma}\delta g_{\mu\nu})(\nabla^{\sigma}\delta g_{\alpha\beta}) - \frac{1}{2}g^{\mu\nu}g^{\alpha\beta}(\nabla_{\sigma}\delta g_{\mu\nu})(\nabla^{\sigma}\delta g_{\alpha\beta}) \tag{B.9}$$

APPENDIX C

Heat kernel expansion

In this Appendix we introduce the heat kernel and present an asymptotic expansion formula for its trace. Traces of the form $\text{Tr}[W(-\Box)]$, where W is a function that decreases sufficiently fast to ensure convergence of the trace, can be evaluated efficientkly by means of heat kernel techniques. These have been extensively employed in the literature.

Let $\mathcal{M}$ be a d-dimensional manifold without boundary and H a second order partial differential operator on $\mathcal{M}$ of the Laplace type, i.e., constructed from covariant derivatives in contracted with the metric, and the internal index structure of the second derivative term is trivial. We can write then H as

$$H = g^{\mu\nu} D_\mu D_\nu + E = D^2 + E \tag{C.1}$$

where E represents an endomorphism, that is, a function on $\mathcal{M}$, acting on internal indices, and $D_\mu \equiv \nabla_\mu + A_\mu$ is a covariant derivative which, in addiction to the Levi-Civita connection implicit in ∇_μ, may also include a Yang–Mills connection A_μ.

The heat kernel $K \equiv K(s; x, y)$ are defined as a solution to the heat equation

$$\frac{\partial K}{\partial s} = HK, \qquad \text{with initial condition } K = (s = 0; x, y) = \frac{1}{\sqrt{g}} \delta(x - y) . \tag{C.2}$$

The formal solution to this equation is

$$K(s; x, y) = e^{sH} \left[\frac{1}{\sqrt{g}} \delta(x - y) \right] . \tag{C.3}$$

Here, we skip the details and focus on the formula for the early time expansion of the diagonal $K(s; x, x)$, a power series in terms of s around the value $s = 0$. This can be found by taking the coincidence limit $y \to x$

$$K(s; x, x) = \left(\frac{1}{4\pi s} \right)^{d/2} \sum_{n=0}^{\infty} s^n \, \text{tr} \, a_n(x) . \tag{C.4}$$

The first three coefficients in eq.(C.4) are

$$a_0(x) = \mathbb{1} \tag{C.5}$$

$$a_1(x) = E + \frac{1}{6}R\,\mathbb{1} \tag{C.6}$$

$$a_2(x) = \frac{1}{180}\left(R_{\mu\nu\rho\sigma}R^{\mu\nu\rho\sigma} + R_{\mu\nu}R^{\mu\nu} + D^2\,R\right)\,\mathbb{1}$$
$$+\frac{1}{2}(E + \frac{1}{6}R\,\mathbb{1})^2 + \frac{1}{12}[D_\mu, D_\nu][D^\mu, D^\nu] + \frac{1}{6}D^2\left(E + \frac{1}{6}R\,\mathbb{1}\right) \tag{C.7}$$

The trace of the heat kernel is of our particular interest since it can be used to compute operator traces. In fact, from eq.(C.4) follows

$$\mathrm{Tr}\left[e^{sH}\right] = \left(\frac{1}{4\pi s}\right)^{d/2}\sum_{n=0}^{\infty} s^n \int \mathrm{d}^d x \sqrt{g}\,\mathrm{tr}\, a_n(x)\,. \tag{C.8}$$

In order to compute traces of the form $\mathrm{Tr}\left[W(-H)\right]$, we assume that $W(-H)$ is given by a Laplace transform

$$W(-H) = \int_0^\infty \mathrm{d}s\, e^{sH}\tilde{W}(s)\,. \tag{C.9}$$

Subsequently, we can insert the early time expansion for $\mathrm{Tr}\left[e^{sH}\right]$ in (C.8) and finally integrate over s separately each term of the expansion

$$\mathrm{Tr}\left[W(-H)\right] = \left(\frac{1}{4\pi}\right)^{d/2}\sum_{n=0}^{\infty} Q_{d/2-n}[W]\int \mathrm{d}^d x\,\sqrt{g}\,\mathrm{tr}\, a_n(x)\,, \tag{C.10}$$

where we introduced the Q-functionals (or generalized Mellin transforms) to be defined as:

$$Q_m[W] = \begin{cases} \dfrac{1}{\Gamma(m)}\displaystyle\int_0^\infty \mathrm{d}z\, z^{m-1}W(z) & \text{for } m > 0 \\ (-1)^{-m}W^{(-m)}(0) & \text{for } m \le 0\,. \end{cases} \tag{C.11}$$

For a vanishing endomorphism E, the heat kernel expansion can be expressed in terms of the Q-functionals as

$$\mathrm{Tr}\left[W(-D^2)\right] = \left(\frac{1}{4\pi}\right)^{d/2}\mathrm{tr}(\mathbb{1})\left\{Q_{d/2}[W]\int \mathrm{d}^d x\sqrt{g} + \frac{1}{6}Q_{d/2-1}[W]\int \mathrm{d}^d x\sqrt{g}R\right\}, \tag{C.12}$$

up to higher order terms in the curvature. If there is a covariant derivative, the first terms in the expansion read

$$\mathrm{Tr}\left[D_\mu W(-H)\right] = \left(\frac{1}{4\pi}\right)^{d/2}Q_{d/2-1}[W]\int \mathrm{d}^d x\sqrt{g}\,\mathrm{tr}\left\{\frac{1}{12}D_\mu R + \frac{1}{2}D_\mu E - \frac{1}{2}D^\mu[D_\nu, D_\mu]\right\}. \tag{C.13}$$

RG equations equations of the Einstein–Hilbert truncation

In this appendix we provide the intermediate steps leading from (3.48) to (3.54) of the main text.

In order to determine the functions $Z_N(k)$ and $\Lambda(k)$ in (3.48) we project the space spanned by the operators $\int \mathrm{d}^d x \sqrt{g}$ and $\int \mathrm{d}^d x \sqrt{g} R$.

The LHS of the flow equation reads:

$$k\partial_k \Gamma_k[g,g] = \frac{1}{16\pi \bar{G}} \int \mathrm{d}^d x \sqrt{g} \left[-R(g)k\partial_k Z_N(k) + 2k\partial_k \left(Z_N(k)\Lambda(k) \right) \right] . \qquad (\mathrm{D.1})$$

On the right hand side of the flow equation can perform a derivative expansion and consider only terms proportional to the monomials $\int \mathrm{d}^d x \sqrt{g}$ and $\int \mathrm{d}^d x \sqrt{g} R$, being able to compare proportional to the same operator and write down the system of differential equations for $Z_N(k)$ and $\Lambda(k)$.

D.1. The Hessian

In order to obtain the second functional derivative of $\Gamma_k[g, \bar{g}]$ appearing under the trace of the flow equation, we need to expand[1]

$$\Gamma_k[\bar{g} + h, \bar{g}] = \Gamma_k[\bar{g}, \bar{g}] + O(h) + \Gamma_k^{\mathrm{quad}}[h; \bar{g}] + O(h^3) ,$$

$$\Gamma_k^{\mathrm{quad}}[h, \bar{g}] = Z_N(k) \frac{1}{32\pi \bar{G}} \int \mathrm{d}^d x \sqrt{\bar{g}} h_{\mu\nu} \left[-K_{\rho\sigma}^{\mu\nu} \bar{\Box} + U_{\rho\sigma}^{\mu\nu} \right] h^{\rho\sigma} . \qquad (\mathrm{D.2})$$

Where the tensors K and U are, respectively:

$$K_{\rho\sigma}^{\mu\nu} = \frac{1}{4} \left[\delta_\rho^\mu \delta_\sigma^\nu + \delta_\sigma^\mu \delta_\rho^\nu - \bar{g}^{\mu\nu} \bar{g}_{\rho\sigma} \right] \qquad (\mathrm{D.3})$$

$$\begin{aligned}
U_{\rho\sigma}^{\mu\nu} =& \frac{1}{4} \left[\delta_\rho^\mu \delta_\sigma^\nu + \delta_\sigma^\mu \delta_\rho^\nu - \bar{g}^{\mu\nu} \bar{g}_{\rho\sigma} \right] (\bar{R} - 2\Lambda(k)) + \frac{1}{2} \left[\bar{g}^{\mu\nu} \bar{R}_{\rho\sigma} + \bar{g}_{\rho\sigma} \bar{R}^{\mu\nu} \right] \\
& - \frac{1}{4} \left[\delta_\rho^\mu \bar{R}^\nu{}_\sigma + \delta_\sigma^\nu \bar{R}^\mu{}_\rho + \delta_\rho^\nu \bar{R}^\mu{}_\sigma + \delta_\sigma^\nu \bar{R}^\mu{}_\rho \right] - \frac{1}{2} \left[\bar{R}^\nu{}_\rho{}^\mu{}_\sigma + \bar{R}^\nu{}_\sigma{}^\mu{}_\rho \right] ,
\end{aligned} \qquad (\mathrm{D.4})$$

where we made use of the variations in Section A.1.

---

[1]From this point on the indices are lowered and raised by means of the background metric $\bar{g}_{\mu\nu}$.

The quadratic form in (D.2) can be diagonalized by decomposing the metric fluctuation $h_{\mu\nu}$ as the sum of a traceless tensor h^{TT} and a trace part $h = g^{\mu\nu}h_{\mu\nu}$ as follows

$$h_{\mu\nu} = h^{\mathrm{TT}} + \frac{1}{d}\bar{g}_{\mu\nu}h \ . \tag{D.5}$$

The quadratic action becomes

$$
\begin{aligned}
\Gamma_k^{\mathrm{quad}}[h;\bar{g}] = Z_N(k)\frac{1}{32\pi\bar{G}}\int \mathrm{d}^d x\sqrt{\bar{g}}\Big\{ & h_{\mu\nu}^{\mathrm{TT}}\left[-\bar{\Box} - 2\Lambda(k) + \bar{R}\right]h^{\mathrm{TT}\mu\nu} \\
& + \left(\frac{d-2}{4d}\right)h\left[-\bar{\Box} - 2\Lambda(k) + \frac{d-4}{d}\bar{R}\right]h \\
& - \bar{R}_{\mu\nu}h^{\mathrm{TT}\nu\rho}h^{\mathrm{TT}\mu}{}_\rho \bar{R}_{\alpha\beta\nu\mu}h^{\mathrm{TT}\beta\nu}h^{\mathrm{TT}\alpha\mu} + \frac{d-4}{d}h\bar{R}_{\mu\nu}h^{\mathrm{TT}\mu\nu}\Big\} \ .
\end{aligned} \tag{D.6}
$$

In the following we will assume that the background $\bar{g}_{\mu\nu}$ is maximally symmetric, i.e., its Riemann and Ricci tensor are proportional to the curvature scalar $\bar{R}$ and have the form (see Appendix E)

$$
\begin{aligned}
\bar{R}_{\mu\nu\rho\sigma} &= \frac{1}{d(d-1)}\left[\bar{g}_{\mu\rho}\bar{g}_{\nu\sigma} - \bar{g}_{\mu\sigma}\bar{g}_{\nu\rho}\right]\bar{R} \\
\bar{R}_{\mu\nu} &= \frac{1}{d}\bar{g}_{\mu\nu}\bar{R} \ .
\end{aligned} \tag{D.7}
$$

Here $\bar{R}$ should not be interpreted as a functional of the metric, but as an externally prescribed parameter. For such spacetimes (D.6) reduces to:

$$
\begin{aligned}
\Gamma_k^{\mathrm{quad}}[h;\bar{g}] = \frac{1}{2}Z_N(k)\frac{1}{32\pi\bar{G}}\int \mathrm{d}^d x\sqrt{\bar{g}}\Big\{ & h_{\mu\nu}^{\mathrm{TT}}\left[-\bar{\Box} - 2\Lambda(k) + C_{\mathrm{T}}\bar{R}\right]h^{\mathrm{TT}\mu\nu} \\
& + \left(\frac{d-2}{2d}\right)h\left[-\bar{\Box} - 2\Lambda(k) + C_{\mathrm{S}}\bar{R}\right]h\Big\}\mathbb{1} \ ,
\end{aligned} \tag{D.8}
$$

where we have introduced the dimensionless constants

$$C_{\mathrm{T}} = \frac{d(d-3)+4}{d(d-1)} \ , \qquad C_{\mathrm{S}} = \frac{d-4}{d} \ . \tag{D.9}$$

At this stage we can specify the form of the cutoff operators $\mathcal{R}_k^{\mathrm{grav}}$ and $\mathcal{R}_k^{\mathrm{gh}}$. In order to combine with the kinetic term of each mode, the cutoff terms can be expressed as

$$\mathcal{R}_k[\bar{g}] = \mathscr{Z}_k k^2 R^{(0)}\left(-\frac{\bar{\Box}}{k^2}\right) \ , \tag{D.10}$$

Inspecting (D.8), we can deduce the following form

$$\left(\mathscr{Z}_k^{\mathrm{grav}}\right)^{\mu\nu\rho\sigma} = \left[(\mathbb{1} - P_h)^{\mu\nu\rho\sigma} - \frac{d-2}{2}P_h^{\mu\nu\rho\sigma}\right]Z_N(k) \ , \tag{D.11}$$

where we used the unity $\mathbb{1}$ on the space of symmetric rank-two tensors and the projector P_h on the trace part of the metric

$$\mathbb{1}_{\mu\nu}{}^{\rho\sigma} = \frac{1}{2}\left(\delta^\rho_\mu \delta^\sigma_\nu + \delta^\rho_\nu \delta^\sigma_\mu\right) , \qquad P_{h,\mu\nu}{}^{\rho\sigma} = \frac{\bar{g}_{\mu\nu}\bar{g}^{\rho\sigma}}{d} . \tag{D.12}$$

For the trace h this normalization is considered, while the traceless tensor has $\mathcal{Z}^{\text{grav}} = Z_N(k)\mathbb{1}$. With this cutoff in the two sectors we obtain the following operators:[2]

$$\left(\frac{1}{32\pi\bar{G}}\Gamma_k^{\text{quad},(2)}[g,g] + \mathcal{R}_k^{\text{grav}}\right)_{h^{\text{TT}}h^{\text{TT}}}$$
$$= Z_N(k)\left[-\Box + k^2 R^{(0)}\left(-\frac{\Box}{k^2}\right) - 2\Lambda(k) + C_{\text{T}}R\right]$$
$$\left(\frac{1}{32\pi\bar{G}}\Gamma_k^{\text{quad},(2)}[g,g] + \mathcal{R}_k^{\text{grav}}\right)_{hh}$$
$$= -\frac{d-2}{2d}Z_N(k)\left[-\Box + k^2 R^{(0)}\left(-\frac{\Box}{k^2}\right) - 2\Lambda(k) + C_{\text{S}}R\right] . \tag{D.13}$$

Finally we need to introduce the Faddeev–Popov operator, This is, with $\bar{g} = g$ being a maximally symmetric spacetime:

$$\mathcal{M}[g,g]^\mu{}_\nu = \delta^\mu_\nu\Box + R^\mu{}_\nu = -\delta^\mu_\nu\left[-\Box + C_{\text{V}}R\right] , \qquad C_{\text{V}} = -\frac{1}{d} . \tag{D.14}$$

Neglecting the renormalization of the ghost action, we can set $\mathcal{Z}_k^{\text{gh}} = 1$ and we obtain

$$-\mathcal{M} + \mathcal{R}_k^{\text{gh}} = -\Box + k^2 R^{(0)}\left(-\frac{\Box}{k^2} + C_{\text{V}}R\right) . \tag{D.15}$$

D.2. Evaluation of the trace

Equipped with the Hessian and the Faddeev–Popov term we can now evaluate the trace on the left hand side of the flow equation in (3.41).

In order to us define the operators:

$$\mathcal{A} \equiv -\Box + k^2 R^{(0)}\left(-\frac{\Box}{k^2}\right) - 2\Lambda(k)$$
$$\mathcal{N} \equiv \frac{1}{2Z_N(k)}k\partial_k\left[Z_N(k)k^2 R^{(0)}\left(-\frac{\Box}{k^2}\right)\right] \tag{D.16}$$
$$= \left[1 - \frac{1}{2}\eta_N(k)\right]k^2 R^{(0)}\left(-\frac{\Box}{k^2}\right) + \Box R^{(0)\prime}\left(-\frac{\Box}{k^2}\right) ,$$

where we introduced the anomalous dimension related to the Newton constants $\eta_N = -k\partial_k Z_N(k)$. The primes denote the derivative with respect to the respective argument.

---

[2]From now on we omit the bar from the metric and the curvature setting $\bar{g} = g$.

Furthermore let's denote

$$\mathcal{A}_0 = \mathcal{A}(\Lambda(k) = 0)$$
$$\mathcal{N}_0 = \mathcal{N}(\eta_N(k) = 0) \,,$$

(D.17)

such that we can write the left hand side of (3.41) as

$$\mathrm{Tr_T}\left[\mathcal{N}(\mathcal{A} + C_\mathrm{T}R)^{-1}\right] + \mathrm{Tr_S}\left[\mathcal{N}(\mathcal{A} + C_\mathrm{S}R)^{-1}\right] - 2\mathrm{Tr_V}\left[\mathcal{N}_0(\mathcal{A}_0 + C_\mathrm{V}R)^{-1}\right] \,.$$

(D.18)

This expression can be further simplified by expanding in R:

$$\mathrm{Tr_T}\left[\mathcal{N}\mathcal{A}^{-1}\right] + \mathrm{Tr_S}\left[\mathcal{N}\mathcal{A}^{-1}\right] - 2\mathrm{Tr_V}\left[\mathcal{N}_0\mathcal{A}_0^{-1}\right]$$
$$-R\left(C_\mathrm{T}\mathrm{Tr_T}\left[\mathcal{N}\mathcal{A}^{-2}\right] + C_\mathrm{S}\mathrm{Tr_S}\left[\mathcal{N}\mathcal{A}^{-2}\right] - 2C_\mathrm{V}\mathrm{Tr_V}\left[\mathcal{N}_0\mathcal{A}_0^{-2}\right]\right) + O(R^2)$$

(D.19)

Finally we evaluate the traces by taking advantage of the heat kernel expansion (C.8).

$$\mathrm{Tr}\left[e^{-is\Box}\right] = \left(\frac{i}{4\pi s}\right)^{d/2}\mathrm{tr}(\mathbb{1})\int \mathrm{d}^dx\sqrt{g}\left\{1 - \frac{1}{6}isR\right\} + O(R^2)$$

(D.20)

where $\mathrm{tr}(\mathbb{1})$ refers to the number of independent field components in each space of fields. We have in particular

$$\mathrm{tr_S}(\mathbb{1}) = 1$$
$$\mathrm{tr_V}(\mathbb{1}) = d$$
$$\mathrm{tr_T}(\mathbb{1}) = \frac{(d-1)(d-2)}{2}$$

(D.21)

In terms of the Q-functional the expansion of the trace is defined in (C.11).

Comparing the coefficients of $\int \sqrt{g}$ we obtain the following equation

$$k\partial_k\left(Z_N(k)\Lambda(k)\right) = \frac{1}{64\pi\bar{G}}\left(\frac{1}{4\pi}\right)^{d/2}\left\{\mathrm{tr_T}(\mathbb{1})Q_{d/2}\left[\mathcal{N}/\mathcal{A}\right]\right.$$
$$\left. + \mathrm{tr_S}(\mathbb{1})Q_{d/2}\left[\mathcal{N}/\mathcal{A}\right] - 2\mathrm{tr_V}(\mathbb{1})Q_{d/2}\left[\mathcal{N}_0/\mathcal{A}_0\right]\right\} \,.$$

(D.22)

Analogously, comparing terms proportional to $\int \mathrm{d}^dx\sqrt{g}R$, we read off the following equation

$$k\partial_k\left(Z_N(k)\right) = \frac{1}{192\pi\bar{G}}\left(\frac{1}{4\pi}\right)^{d/2}\left\{\mathrm{tr_T}(\mathbb{1})\left[Q_{d/2-1}\left[\mathcal{N}/\mathcal{A}\right] - 6C_\mathrm{T}Q_{d/2}\left[\mathcal{N}/\mathcal{A}^2\right]\right]\right.$$
$$+ \mathrm{tr_S}(\mathbb{1})\left[Q_{d/2-1}\left[\mathcal{N}/\mathcal{A}\right] - 6C_\mathrm{S}Q_{d/2}\left[\mathcal{N}/\mathcal{A}^2\right]\right]$$
$$\left. - 2\mathrm{tr_V}(\mathbb{1})\left[Q_{d/2-1}\left[\mathcal{N}_0/\mathcal{A}_0\right] - 6C_\mathrm{V}Q_{d/2}\left[\mathcal{N}_0/\mathcal{A}_0^2\right]\right]\right\} \,.$$

(D.23)

Here we introduce two possible cutoff shape function which is used in this thesis: the *sharp cutoff* and the *optimized cutoff*. We define "threshold functions" and evaluate them for these cutoffs.

The cutoff operator $\mathcal{R}_k$ can be written in terms of the cutoff shape function $R^{(0)}$:

$$\mathcal{R}_k(-\Box) = \mathcal{Z}_k k^2 R^{(0)}(-\Box/k^2) \,. \tag{D.24}$$

where the function $\mathcal{Z}_k$ is usually chosen to be the wave function renormalization. In order to represent an IR cutoff we demand the shape function to satisfy following requirements

$$(i) \qquad R^{(0)}(0) = 1 \tag{D.25}$$

$$(ii) \qquad \lim_{z \to \infty} R^{(0)}(z) = 0 \tag{D.26}$$

Specifically, we consider: the *optimized cutoff*

$$R^{(0)}(z) \equiv (1 - z)\, \theta(1 - z) \tag{D.27}$$

and the *sharp cutoff*

$$R^{(0)}(z) \equiv \hat{R}\, \theta(1 - z), \qquad \text{where} \qquad \hat{R} \to \infty \tag{D.28}$$

where the limit $\hat{R} \to \infty$ is performed after the z-integration. Throughout this thesis it will be convenient to re-express the Q-functionals in terms of the "threshold functions". These are defined as

$$\Phi_n^p(w) \quad := \quad \frac{1}{\Gamma(n)} \int_0^\infty \mathrm{d}z\, z^{n-1} \frac{R^{(0)}(z) - z R^{(0)'}(z)}{(z + R^{(0)}(z) + w)^p} \tag{D.29}$$

$$\tilde{\Phi}_n^p(w) \quad := \quad \frac{1}{n} \int_0^\infty \mathrm{d}z\, z^{n-1} \frac{R^{(0)}(z)}{(z + R^{(0)}(z) + w)^p} \tag{D.30}$$

Using the above mentioned cutoff shape functions, the threshold functions can in fact be analytically evaluated and one obtains for the optimized cutoff

$$\Phi_{n\,\mathrm{opt}}^p(w) \quad = \quad \frac{1}{\Gamma(n+1)} \frac{1}{(1+w)^p} \tag{D.31}$$

$$\tilde{\Phi}_{n\,\mathrm{opt}}^p(w) \quad = \quad \frac{1}{\Gamma(n+2)} \frac{1}{(1+w)^p} \tag{D.32}$$

and for the sharp cutoff

$$\Phi^1_{n\,\text{sc}}(w) = -\frac{1}{\Gamma(n)}\ln(1+w)^p \tag{D.33}$$

$$\Phi^p_n(w)^{\text{sc}} = \frac{1}{\Gamma(n)}\frac{1}{p-1}\frac{1}{(1+w)^{p-1}} \quad \text{for} \quad p > 1 \tag{D.34}$$

$$\tilde{\Phi}^1_{n\,\text{sc}}(w) = \frac{1}{\Gamma(n+1)} \tag{D.35}$$

$$\tilde{\Phi}^p_{n\,\text{sc}}(w) = 0 \quad \text{for} \quad p > 1 \tag{D.36}$$

Exploiting the definitions of the threshold functions, we can rewrite eq.(D.22) and eq.(D.23) as

$$
k\partial_k\left(Z_N(k)\Lambda(k)\right) = \frac{1}{256\pi\bar{G}}\left(\frac{1}{4\pi}\right)^{d/2}k^d\left[2d(d+1)\Phi^1_{d/2}\left(-\frac{2\Lambda(k)}{k^2}\right)\right.
$$
$$
\left. -8d\Phi^1_{d/2}(0) - d(d+1)\eta_N\tilde{\Phi}^1_{d/2}\left(-\frac{2\Lambda(k)}{k^2}\right)\right]
$$

$$
k\partial_k\left(Z_N(k)\right) = \frac{1}{384\pi\bar{G}}\left(\frac{1}{4\pi}\right)^{d/2}k^{d-2}\times
$$
$$
\left[d(d+1)\left(\Phi^1_{d/2-1}\left(-\frac{2\Lambda(k)}{k^2}\right) - \frac{1}{2}\eta_N\tilde{\Phi}^1_{d/2-1}\left(-\frac{2\Lambda(k)}{k^2}\right)\right)\right. \tag{D.37}
$$
$$
\left. -6d(d-1)\left(\Phi^2_{d/2}\left(-\frac{2\Lambda(k)}{k^2}\right) - \frac{1}{2}\eta_N\tilde{\Phi}^2_{d/2}\left(-\frac{2\Lambda(k)}{k^2}\right)\right)\right.
$$
$$
\left. -4d\Phi^1_{d/2-1}(0) - 24\Phi^2_{d/2}(0)\right)\right]
$$

Finally, we can obtain the form of the dimensionless RG equations formulated in terms of the dimensionless running couplings:

Defining the *anomalous dimension* related to the running Newton's constant as:

$$\eta_N(\lambda(k), g(k)) \equiv -k\partial_k\ln Z_N(k) \tag{D.38}$$

Introducing the *dimensionless variables*:

$$g(k) \equiv k^{d-2} = k^{d-2}Z_N(k)^{-1}\bar{G}$$
$$\lambda(k) \equiv k^{-2}\Lambda(k) \tag{D.39}$$

We obtain the flow equations (D.37) in the form

$$k\partial_k g(k) = \left[(d-2) + \eta_N(\lambda(k), g(k))\right]g(k)\,,$$

$$k\partial_k\lambda(k) = -(2 - \eta_N(k))\lambda(k) + \frac{1}{2}g(k)(4\pi)^{1-d/2}\left[2d(d+1)\Phi^1_{d/2}(-2\lambda(k))\right. \tag{D.40}$$
$$\left. -8d\Phi^1_{d/2}(0) - d(d+1)\eta_N(k)\tilde{\Phi}^1_{d/2}(-2\lambda(k))\right]\,.$$

This system depends on the anomalous dimension, which for convenience can be rewritten as

$$k\partial_k \eta_N(k) = \frac{g(k)\, B_1(\lambda(k))}{1 - g(k)\, B_2(\lambda(k))} \, , \tag{D.41}$$

with

$$B_1(\lambda(k)) = 32\pi \left(\frac{1}{4\pi}\right)^{d/2} \left[\frac{d(d+1)}{24}\Phi^1_{d/2-1}(-2\lambda(k)) - \frac{d(d-1)}{4}\Phi^2_{d/2}(-2\lambda(k))\right.$$
$$\left. -\frac{d}{6}\Phi^1_{d/2-1}(0) - \Phi^2_{d/2}(0)\right]$$

$$B_2(\lambda(k)) = 32\pi \left(\frac{1}{4\pi}\right)^{d/2} \left[-\frac{d(d+1)}{48}\tilde{\Phi}^1_{d/2-1}(-2\lambda(k)) + \frac{d(d-1)}{8}\tilde{\Phi}^2_{d/2}(-2\lambda(k))\right]$$
$$\tag{D.42}$$

APPENDIX E

Maximally symmetric spacetimes

E.1. Constant scalar curvature

In this Appendix we discuss some aspects of what are known as maximally symmetric spacetimes. The results reported are useful for the geometrization procedure performed in Chapter 7.

Maximally symmetric spacetime are spaces that admit the maximum number of Killing vectors (which turns out to be $d(d+1)/2$ for a d-dimensional space). We will show how maximal symmetry fixes the curvature tensor: a space is maximally symmetric if and only if its scalar curvature R is constant [521].

Complying with the Cosmological Principle, such spaces, which are simultaneously homogeneous ("the same at every point") and isotropic ("the same in every direction"), provide a description of space in a cosmological spacetime.

In order to understand how to define and characterize maximally symmetric spaces, we need to obtain some more information about how Killing vectors can be classified. A Killing vector field $K_\mu(x)$ is completely and uniquely determined everywhere by the values of $K_\mu(x_0)$ and $\nabla_\mu K_\nu(x_0)$ at a single point x_0. Since, in a d-dimensional space there can be at most d linearly independent vectors $K_\mu(x_0)$ (related to translations) at a point, and at most $d(d-1)/2$ independent anti-symmetric matrices $\nabla_\mu K_\nu(x_0)$ (related to rotations, to the Lie algebra of $SO(d)$), we reach the conclusion that a d-dimensional space can have at most $d(d+1)/2$ independent Killing vectors. A spacetime with this maximal number of Killing vectors is called maximally symmetric. A homogeneous and isotropic space is maximally symmetric.

On the basis of these simple considerations we can already determine the form of the Riemann curvature tensor of a maximally symmetric space. If the metric is supposed to be isotropic at a fixed point x_0, then the curvature tensor at the origin must be invariant under Lorentz rotations. Now we know that the only invariants of the Lorentz group are the metric tensor, the Kronecker-delta, and the Levi-Civita tensor. Furthermore, imposing the symmetries of the Riemann tensor we conclude that it has the structure

$$R_{\mu\nu\rho\sigma} = C(g_{\mu\rho}g_{\nu\sigma} - g_{\mu\sigma}g_{\nu\rho}) .$$ (E.1)

Imposing the Bianchi identity, we are led to require C to be a constant. Then

$$R_{\mu\nu} = C(d-1)g_{\mu\nu} \,, \qquad (E.2)$$

so that a maximally symmetric spacetime is automatically a solution to the vacuum Einstein equations with a cosmological constant.

In terms of the conventionally defined cosmological constant Λ, the Ricci curvature tensor and the Ricci curvature scalar of dS spacetime are given by

$$R_{\mu\nu} = \frac{R}{d}g_{\mu\nu} \,, \qquad\qquad R = \frac{2d}{d-2}\Lambda \,, \qquad (E.3)$$

while the Weyl tensor vanishes.

In Lorentzian signature, the three cases $\Lambda = 0, \Lambda > 0$ and $\Lambda < 0$ correspond to Minkowski M_d, de Sitter dS$_d$, and anti-de Sitter spacetime AdS$_d$, respectively. In the Euclidean setting, we are dealing with the flat $\mathbb{R}^d$, spheres $\mathbb{S}^d$, and hyperbolic spaces $\mathbb{H}^d$ instead.

The d-dimensional dS spacetime is uniquely characterized as the maximally symmetric Lorentzian manifold with constant positive scalar curvature. It is the maximally symmetric solution of the vacuum Einstein equations including a positive cosmological constant Λ.

For a given $\Lambda > 0$, it is convenient to introduce the associated Hubble constant H by:[1]

$$R = d(d-1)H^2 \,, \qquad\qquad H^2 = \frac{2}{(d-1)(d-2)}\Lambda \,. \qquad (E.4)$$

E.2. EMBEDDINGS

A way of explicitly constructing the maximally symmetric spacetimes which makes their symmetries manifest is by invoking an auxiliary $d+1$-dimensional embedding spacetime. The embedding recipe:

(1) Construct the ambient $(d+1)$-dimensional (pseudo-)Riemannian space;
(2) Impose the condition on the points of the $(d+1)$-dimensional (pseudo-)Riemannian space;

---

[1]Recall that in this thesis we use the mostly-plus convention for the metric. For the Riemann tensor, we use the convention $R_{\alpha\beta\gamma}{}^{\delta} = -\partial_\alpha\Gamma^\delta_{\beta\gamma} + \partial_\beta\Gamma^\delta_{\alpha\gamma} + \Gamma^\delta_{\beta\zeta}\Gamma^\zeta_{\alpha\gamma} - \Gamma^\delta_{\alpha\zeta}\Gamma^\zeta_{\beta\gamma}$. The Ricci tensor is given by $R_{\alpha\gamma} = R_{\alpha\beta\gamma}{}^{\beta}$.

(3) Solve this condition. Crucial here is that different parameterizations of the solution can be given, corresponding to different d-dimensional coordinate systems. In fact, any coordinate transformation that keeps the condition in (2) invariant is a representation of the internal symmetries of that given space;

(4) Write the induced line element $\mathrm{d}s_d^2$ in the given coordinate system.

Let us concretely apply this to the maximally symmetric spacetimes in both Euclidean and Lorentzian signature:

(1) Sphere $\mathbb{S}^d$. As an example, we can realize the (unit-radius) sphere $\mathbb{S}^d$ by embedding it into $\mathbb{R}^{d+1}$ equipped with Euclidean line element

$$\mathrm{d}s^2 = \mathrm{d}x_0^2 + \mathrm{d}x_1^2 + \cdots + \mathrm{d}x_d^2 \tag{E.5}$$

The condition to impose is

$$(x_0)^2 + \cdots + (x_d)^2 = +1 \,. \tag{E.6}$$

We note that, as we equip $\mathbb{R}^{d+1}$ with the standard Euclidean metric, which is invariant under translations and rotations $SO(d+1)$ of $\mathbb{R}^{d+1}$, the defining equation above is invariant under the $SO(d+1)$-rotations, and the induced metric on $\mathbb{S}^d$ will therefore be $SO(d+1)$-invariant.

At this stage we show how to satisfy the condition (E.6) in two different ways:

(1) If we choose to eliminate x_0 from (E.6), then

$$\mathrm{d}s_{d+1}^2 = \mathrm{d}x_1^2 + \cdots + \mathrm{d}x_d^2 + \frac{(x_1 \, \mathrm{d}x_0 + \cdots + x_d \, \mathrm{d}x_d)^2}{1 - x_1^2 - \cdots - x_d^2} \tag{E.7}$$

By exploiting the rotational invariance we can write: $x_1 = r \cos \varphi \Omega_{d-1}$, $x_d = r \sin \varphi \Omega_{d-1}$, with $r^2 = x_1^2 + \cdots + x_d^2$, such that $x_1 \, \mathrm{d}x_1 + \cdots + x_d \, \mathrm{d}x_d = r \, \mathrm{d}r$, obtaining:

$$\mathrm{d}s^2 = \mathrm{d}r^2 + r^2 \, \mathrm{d}\Omega_{d-1}^2 + \frac{r^2 \, \mathrm{d}r^2}{1 - r^2} = \frac{\mathrm{d}r^2}{1 - r^2} + r^2 \, \mathrm{d}\Omega_{d-1}^2 \tag{E.8}$$

(2) Another option is to parameterize the coordinates as

$$x_0 = \cos \varphi_1$$
$$x_1 = \sin \varphi_1 \cos \varphi_2$$
$$x_2 = \sin \varphi_1 \sin \varphi_2 \cos \varphi_3$$
$$\vdots \tag{E.9}$$
$$x_{d-1} = \sin \varphi_1 \cdots \sin \varphi_{d-2} \cos \varphi_{d-1}$$
$$x_d = \sin \varphi_1 \cdots \sin \varphi_{d-2} \sin \varphi_{d-1}$$

Inserting this parameterization in (E.5), we obtain:

$$ds^2 = d\theta^2 + \sin^2\theta \, d\Omega_{d-1}^2 \qquad \text{(E.10)}$$

This gives rise to the standard $SO(d+1)$-invariant line element $d\Sigma_d$. We note that the two induced metric are related by a coordinate transformation, i.e., $r = \sin\theta$.

The dimension of the isometry group of $\mathbb{S}^d$ with the above matrix is $(d+1)d/2$. This is the same as the dimension of the Poincaré (or Euclidean) group in d dimensions, and thus the $\mathbb{S}^d$ equipped with this metric is maximally symmetric.

(2) Hyperbolic space $\mathbb{H}_d$. Likewise, we can realize the (unit curvature radius) hyperboloid $\mathbb{H}^d$ by embedding it into a higher-dimensional pseudo-Riemannian manifold. We will now correspondingly choose the embedding space to be $\mathbb{R}^{1,d}$, i.e. the space equipped with the Lorentz-signature metric

$$ds_{d+1}^2 = -(dx_0)^2 + (dx_1)^2 + ... + (dx_d)^2 \, , \qquad \text{(E.11)}$$

via the condition

$$-(x_0)^2 + ... + (x_d)^2 = -1 \qquad \text{(E.12)}$$

Its isometry group is the $(d+1)$-dimensional Poincaré group, which has dimension $(d+1)(d+2)/2$. The equation defining $\mathbb{H}^d$ is left invariant by its $SO(d,1)$ Lorentz-subgroup which has dimension $(d+1)d/2$, and thus the metric induced on $\mathbb{H}^d$ by the Minkowski metric on the embedding space will have isometry-group $SO(d,1)$ and is maximally symmetric. Note that this metric has Euclidean signature because the (-1) on the right-hand side of (E.12) allows one to completely eliminate the timelike direction x_0.

Let's analyze some parameterizations and related coordinate systems:

(1) Let us parameterize

$$
\begin{aligned}
x_0 &= \cosh\varphi_1 \\
x_1 &= \sinh\varphi_1 \cos\varphi_2 \\
x_2 &= \sinh\varphi_1 \sin\varphi_2 \cos\varphi_3 \\
&\vdots \\
x_{d-1} &= \sinh\varphi_1 \cdots \sin\varphi_{d-2} \cos\varphi_{d-1} \\
x_d &= \sinh\varphi_1 \cdots \sin\varphi_{d-2} \sin\varphi_{d-1}
\end{aligned}
\qquad \text{(E.13)}
$$

Inserting this parameterization into the line element (E.11) we obtain:

$$ds^2 = d\theta^2 + \sinh^2\theta \, d\Omega_{d-1}^2 \qquad \text{(E.14)}$$

(2) If we instead choose the parameterization

$$x_0 = \sinh \varphi_1$$
$$x_1 = \cosh \varphi_1 \sinh \varphi_2$$
$$x_2 = \cosh \varphi_1 \cosh \varphi_2 \cos \varphi_3$$
$$\vdots$$
$$x_{d-1} = \cosh \varphi_1 \cdots \cosh \varphi_{d-2} \cos \varphi_{d-1}$$
$$x_d = \cosh \varphi_1 \cdots \cosh \varphi_{d-2} \sin \varphi_{d-1}$$

(E.15)

Inserting this parameterization into the line element (E.11) we obtain:

$$ds^2 = d\rho^2 + \cosh^2 \rho \, d\Omega_{d-1}^2 \tag{E.16}$$

(3) De Sitter dS_d. If we change the sign on the right-hand side of eq.(E.12), the induced metric will still be invariant under $SO(d,1)$, but now the induced metric will be Lorentzian instead of Euclidean and we obtain a realization of a maximally symmetric spacetime, namely de Sitter space

$$- (x_0)^2 + (x_1)^2 + \ldots + (x_d)^2 = +1. \tag{E.17}$$

De Sitter spacetime can be parameterized by various coordinate systems. Of particular importance in cosmology are comoving coordinates, which explicitly show that the universe is spatially homogeneous and isotropic. This property is encoded in the FLRW-like (or exponentially expanding) line element:

$$ds^2 = -dt^2 + e^{2Ht}(dx_1^2 + \cdots + dx_{d-1}^2). \tag{E.18}$$

Introducing conformal time $\eta = -e^{-Ht}/H$, the metric is manifestly conformally flat:

$$ds^2 = \frac{1}{(H\eta)^2}(-d\eta^2 + dx_1^2 - \cdots - dx_{d-1}^2). \tag{E.19}$$

Here, cosmic time t runs from $-\infty$ to $+\infty$, while conformal time η runs from $-\infty$ to 0, corresponding to past and future infinity, respectively.

For a presentation on other possible parametrizations and coordinate systems (see steps (3) and (4) of the recipe), we refer to Table E.3.

(4) Anti-de Sitter AdS_d. By the same token, we can obtain a maximally symmetric Lorentzian signature spacetime from the embedding into a flat ambient space equipped with

$$ds_{d+1}^2 = -(dx_0)^2 - (dx_1)^2 + \ldots + (dx_d)^2 \,, \tag{E.20}$$

by imposing the condition

$$- (x_0)^2 + (x_1)^2 + (x_2)^2 + \ldots + (x_{d-1})^2 - (x_d)^2 = -1 \tag{E.21}$$

Since this equation is $SO(d-1,2)$-invariant, this spacetime will have isometry group $SO(d-1,2)$ induced from the signature $(2, d-1)$ metric on the embedding space $\mathbb{R}^{2,d-1}$. The dimension of $SO(d-1,2)$ is also $d(d-1)-2$, just like that of $SO(d,1)$ or $SO(d+1)$, and this defines the maximally symmetric anti-de Sitter space.

A table with the parametrizations and coordinate systems of the induced AdS, we will refer to Table E.4.

In the following tables we summarize the main properties and embeddings of the maximally symmetric Euclidean and Lorentzian spaces, respectively.

Space	Embedding	Curvature	Isometry	Coset
$\mathbb{R}^d$	$ds_{d+1}^2 = dx_0^2 + dx_1^2 + \dots + dx_d^2$ $x_0^2 + x_1^2 + \dots + x_d^2 = 0$	$R = 0$	$ISO(d)$	$\frac{ISO(d)}{SO(d)}$
$\mathbb{S}^d$	$ds_{d+1}^2 = dx_0^2 + dx_1^2 + \dots + dx_d^2$ $x_0^2 + x_1^2 + \dots + x_d^2 = 1$	$R = d(d-1)$	$SO(d+1)$	$\frac{SO(d+1)}{SO(d)}$
$\mathbb{H}^d$	$ds_{d+1}^2 = dx_0^2 - dx_1^2 + \dots + dx_d^2$ $x_0^2 - x_1^2 + \dots + x_d^2 = -1$	$R = -d(d-1)$	$SO(d+1)$	$\frac{SO(d,1)}{SO(d)}$

TABLE E.1. Explicit embedding, isometry group and representation as a coset for the maximally symmetric geometries in the Euclidean setting with vanishing, positive and negative curvature, respectively.

Space	Embedding	Curvature	Isometry	Coset
M^d	$ds_{d+1}^2 = -dx_0^2 + dx_1^2 + \dots + dx_d^2$ $-x_0^2 + x_1^2 + \dots + x_d^2 = 0$	$R = 0$	$ISO(d-1,1)$	$\frac{ISO(d-1,1)}{SO(d-1,1)}$
dS_d	$ds_{d+1}^2 = -dx_0^2 + dx_1^2 + \dots + dx_d^2$ $-x_0^2 + x_1^2 + \dots + x_d^2 = 1$	$R = d(d-1)$	$SO(d,1)$	$\frac{SO(d,1)}{SO(d-1,1)}$
AdS_d	$ds_{d+1}^2 = -dx_0^2 - dx_1^2 + \dots + dx_d^2$ $-x_0^2 - x_1^2 + \dots + x_d^2 = -1$	$R = -d(d-1)$	$SO(d-1,2)$	$\frac{SO(d-1,2)}{SO(d-2,2)}$

TABLE E.2. Explicit embedding, isometry group and representation as a coset for the maximally symmetric geometries in the Lorentzian setting with vanishing, positive and negative curvature, respectively.

Steps (3) and (4) for de Sitter and anti-de Sitter are summarized in Table E.3 and Table E.4. In these tables we show how to satisfy the conditions for dS and AdS in Table E.2 using different parameterizations.

$-\frac{1}{1+t^2}\mathrm{d}t^2 + t^2\,\mathrm{d}H_d^2$	$t \in (-\infty, +\infty)$	Hyperbolic-slicing
$-\frac{1}{\cos^2\phi}\left(\mathrm{d}\phi^2 + \sin^2\phi\,\mathrm{d}H_d^2\right)$	$\phi \in [-\pi/2, +\pi/2)$	Conformal hyperbolic-slicing
$-\mathrm{d}\rho^2 + \sinh^2\rho\,\mathrm{d}H_d^2$	$\rho \in (-\infty, \infty)$	Hyperbolic-slicing
$-\mathrm{d}t^2 + \cosh^2 t\,\mathrm{d}\Omega_d^2$	$t \in (-\infty, +\infty)$	Spherically-slicing (Global coordinates)
$\frac{1}{\cos^2\tau}\left(-\mathrm{d}\tau^2 + \mathrm{d}\Omega_d^2\right)$	$\tau \in [0, \pi)$	Conformally spherically-slicing
$-(1-r^2)\,\mathrm{d}t^2 + \frac{1}{1-r^2}\mathrm{d}r^2 + r^2\,\mathrm{d}\Omega_{d-1}^2$	$r \in [0,1)$	Static coordinates
$-\mathrm{d}t^2 + e^{2t}\left(\mathrm{d}x^2 + \mathrm{d}y^2 + \cdots + \mathrm{d}z^2\right)$	$t \in (-\infty, +\infty)$	Expanding flat-slicing (Poincaré patch)
$\frac{1}{u^2}\left(-\mathrm{d}u^2 + \mathrm{d}x^2 + \mathrm{d}y^2 + \cdots + \mathrm{d}z^2\right)$	$u \in (-\infty, +\infty)$	Conformally flat-slicing
$\mathrm{d}\xi^2 + \sin^2\xi\,\mathrm{d}\Sigma_d^2$	$\xi \in [0, \pi)$	de Sitter-slicing
$\frac{1}{\cosh^2\gamma}\left(\mathrm{d}\gamma^2 + \mathrm{d}\Sigma_d^2\right)$	$\gamma \in (-\infty, +\infty)$	Conformally de Sitter-slicing

TABLE E.3. Table for de Sitter: possible geometrizations and relation between the original d-dimensional coordinates and the induced $(d+1)$-dimensional coordinates. Note: In the table, $\mathrm{d}\Sigma_d^2$ is the d-dimensional dS space line element in global coordinates: $\mathrm{d}\Sigma_d^2 = -\,\mathrm{d}t^2 + \cosh^2(t)\,\mathrm{d}\Omega_{d-1}^2$. Likewise, $\mathrm{d}H_d^2 = \mathrm{d}t^2 + \sinh^2(t)\,\mathrm{d}\Omega_{d-1}^2$ and $\mathrm{d}\Omega_d^2 = \mathrm{d}t^2 + \sin^2(t)\,\mathrm{d}\Omega_{d-1}^2$ are the d-dimensional hyperbolic and spherical line elements, respectively. Partially inspired by [522].

Metric	Range	Name
$\frac{1}{\cos^2\rho}\left(-\mathrm{d}t^2+\mathrm{d}\rho^2+\sin^2\rho\,\mathrm{d}\Omega_{d-1}^2\right)$	$\rho\in[0,\pi/2)$	Global patch
$-(1+r^2)\mathrm{d}t^2+\frac{1}{1+r^2}\mathrm{d}r^2+r^2\,\mathrm{d}\Omega_{d-1}^2$	$r\in[0,\infty)$	Static patch
$-\cosh^2\rho\,\mathrm{d}t^2+\mathrm{d}\rho^2+\sinh^2\rho\,\mathrm{d}\Omega_{d-1}^2$	$t\in(-\infty,+\infty),\,\rho\in[0,\infty)$	Global static patch
$\frac{1}{w^2}\left(-\mathrm{d}t^2+\mathrm{d}x^2+\mathrm{d}y^2+\cdots+\mathrm{d}z^2+\mathrm{d}w^2\right)$	$w\in(0,+\infty)$	Conformally flat-slicing (Poincaré patch)
$e^{-2u}\left(-\mathrm{d}t^2+\mathrm{d}x^2+\cdots+\mathrm{d}z^2\right)+\mathrm{d}u^2$	$u\in(-\infty,+\infty)$	Flat-slicing
$v^2\left(-\mathrm{d}t^2+\mathrm{d}x^2+\cdots+\mathrm{d}z^2\right)+\frac{1}{v^2}\mathrm{d}u^2$	$v\in(0,\infty)$	Flat-slicing (Poincaré patch)
$-\mathrm{d}t^2+\sin^2 t\,\mathrm{d}H_d^2$	$t\in[0,\pi)$	Hyperbolic-slicing (FLRW open-slicing)
$-\frac{1}{1-u^2}\mathrm{d}u^2+u^2\,\mathrm{d}H_d^2$	$u\in[0,1)$	Hyperbolic-slicing
$\frac{1}{\cosh^2\rho}\left(-\mathrm{d}\rho^2+\sinh^2\rho\,\mathrm{d}H_d^2\right)$	$\rho\in(-\infty,+\infty)$	Conformally hyperbolic-slicing
$\mathrm{d}\xi^2+\sinh^2\xi\,\mathrm{d}\Sigma_d^2$	$\xi\in[0,\infty)$	de Sitter-slicing
$\frac{1}{\sinh^2\gamma}\left(\mathrm{d}\gamma^2+\mathrm{d}\Sigma_d^2\right)$	$\gamma\in(-\infty,0]$	Conformally de Sitter-slicing

TABLE E.4. Table for anti-de Sitter: possible geometrizations and relation between the original d-dimensional coordinates and the induced $(d+1)$-dimensional coordinates. Note: In the table, $\mathrm{d}\Sigma_d^2$ is the d-dimensional dS space line element in global coordinates: $\mathrm{d}\Sigma_d^2 = -\mathrm{d}t^2+\cosh^2(t)\,\mathrm{d}\Omega_{d-1}^2$. Likewise, $\mathrm{d}H_d^2 = \mathrm{d}t^2+\sinh^2(t)\,\mathrm{d}\Omega_{d-1}^2$ and $\mathrm{d}\Omega_d^2 = \mathrm{d}t^2+\sin^2(t)\,\mathrm{d}\Omega_{d-1}^2$ are the d-dimensional hyperbolic and spherical line elements, respectively. Partially inspired by [522].

Propagators in curved background

This appendix is devoted to details and computations leading to the results in Chapter 9. After having derived the commutation relations in a background with constant curvature, we will provide the expressions of the graviton propagator in such a space-time. In the last section, we will report the details about the resolution of differential equations related to the rank-two tensor sector in the adiabatic expansion. All along this appendix, we have made an extensive use of the tensor manipulation package xAct in Mathematica.

F.1. COMMUTATION RELATIONS IN CONSTANTLY-CURVED SPACES

In order to compute the propagator and to bring the amplitude functional to a canonical form, we need to compute the commutator of the operator $f(-\Box)$ with covariant derivatives in a de Sitter background. The following appendix directly follows [396]; here the formalism has been adapted to metric gravity.

(1) We want to obtain a formula of the form

$$f(\Box)\nabla_\alpha \mathbf{X} = \nabla_\alpha f - f(\Box)\mathbf{X} + \dots, \tag{F.1}$$

where f is an arbitrary function and $\mathbf{X}$ is a tensor of rank $(0, n)$,

$$\mathbf{X} = X_{\mu_1 \cdots \mu_n}. \tag{F.2}$$

To derive an equation of the form (F.1), we employ a standard trick: we express the function f as an inverse Laplace transform, so that we can use the Baker–Campbell–Hausdorff formula,

$$f(\Box)\nabla_\alpha \mathbf{X} = \int_0^\infty ds\, \tilde{f}(s)\, e^{-s\Box} \nabla_\alpha \mathbf{X} = \int_0^\infty ds\, \tilde{f}(s) \sum_{\ell \geq 0} \frac{(-s)^\ell}{\ell!} [\Box, \nabla_\alpha]_\ell\, e^{-s\Box}\, \mathbf{X}. \tag{F.3}$$

Here we used the multi-commutator, which is defined recursively by

$$[A, B]_n = [A, [A, B]_{n-1}], \qquad\qquad [A, B]_0 = B. \tag{F.4}$$

In order to compute the multi-commutator, let us first calculate the standard commutator. Assuming that we are working in dS spacetime, we find

$$[\Box, \nabla_\alpha] X_{\mu_1 \cdots \mu_n} = + \frac{R}{d} \nabla_\alpha X_{\mu_1 \cdots \mu_n} - \frac{2}{d-1} \frac{R}{d} \sum_{k=1}^{n} \left[\bar{g}_{\alpha \mu_k} \nabla^\beta X_{\mu_1 \cdots \mu_{k-1} \beta \mu_{k+1} \cdots \mu_n} \right.$$
$$\left. \nabla_{\mu_k} X_{\mu_1 \cdots \mu_{k-1} \alpha \mu_{k+1} \cdots \mu_n} \right] \qquad (F.5)$$
$$\equiv C_{\alpha \mu_1 \cdots \mu_n}{}^{\beta \nu_1 \cdots \nu_n} \nabla_\beta X_{\nu_1 \cdots \nu_n} .$$

We observe that the commutator is a multiplication with a covariantly constant tensor **C**, so that structurally we find

$$[\Box, \nabla]_k \mathbf{X} = \mathbf{C}^k \nabla \mathbf{X} . \qquad (F.6)$$

We can plug this back into the original equation (F.3), so that we are left with

$$f(\Box)\nabla\mathbf{X} = \int_0^\infty ds \, \tilde{f}(s) \, \mathrm{Texp}[-s\mathbf{C}] \, \nabla e^{-s\Box} \mathbf{X} , \qquad (F.7)$$

where Texp is the tensor exponential. This can be defined in terms of its power series.

(2) Since the computation of this exponential for a tensor of arbitrary rank becomes rather complicated, we will illustrate how the procedure works for scalars and vectors. For a scalar, we find

$$[\Box, \nabla_\alpha] X = \frac{R}{d} \nabla_\alpha X , \qquad (F.8)$$

such that for **C**, we obtain

$$C_\alpha{}^\beta = \frac{R}{d} \delta_\alpha{}^\beta . \qquad (F.9)$$

Consequently, inserting this into (F.7), we have

$$f(\Box)\nabla_\alpha X = \nabla_\alpha f\left(\Box + \frac{R}{d}\right) X . \qquad (F.10)$$

The same procedure can be applied for vectors. First, we find for **C**

$$C_{\alpha\mu}{}^{\beta\nu} = \frac{R}{d} \delta_\alpha{}^\beta - \frac{2}{d-1} \frac{R}{d} g_{\alpha\mu} g^{\beta\nu} + \frac{2}{d-1} \frac{R}{d} \delta_\alpha{}^\beta \delta_\mu{}^\nu , \qquad (F.11)$$

which gives for (F.7)

$$f(\Box)\nabla_\alpha X_\mu = \nabla_{(\alpha} f\left(\Box + \frac{d+1}{d-1}\frac{R}{d}\right) X_{\mu)} + \frac{1}{d} g_{\alpha\mu} \nabla^\beta \left[f\left(\Box - \frac{R}{d}\right) - f\left(\Box + \frac{d+1}{d-1}\frac{R}{d}\right) \right] X_\beta$$
$$+ \nabla_{[\alpha} f\left(\Box + \frac{d-3}{d-1}\frac{R}{d}\right) X_{\mu]} . \qquad (F.12)$$

The formula for the rank-two tensor can be found in the same fashion. However, since this is very lengthy, we will not display it here.

In this section, we will provide the explicit expressions for the propagator $\mathcal{G}^{(hh)}$ used in Subsection 9.3.3. The propagator is of the form

$$\mathcal{G}^{(hh)} = \sum_i \mathfrak{T}_i \mathcal{G}_i(\Box, R) \,. \tag{F.13}$$

Here the index $i = 1, \ldots, 6$ runs over the set of tensor structures given in (9.20). We will now present the functions $\mathcal{G}_i(\Box, R)$. For simplicity, we will restrict ourselves to the case $d = 4$. Nontrivial in this computation are the gauge parameters α_{gf} and β_{gf}, which we will keep arbitrary. The functions $\mathcal{G}_i$ are given by

$$
\frac{3}{32\pi G_N}\mathcal{G}_1(\Box, R) = -(\alpha_{\text{gf}} - 1)RG\left(\tfrac{1}{6}\right)^2 - 2\alpha_{\text{gf}}G\left(\tfrac{1}{6}\right) + 2\frac{\alpha_{\text{gf}} - \beta_{\text{gf}}}{\beta_{\text{gf}} - 3}RG\left(\tfrac{2}{3} + \tfrac{1}{\beta_{\text{gf}}-3}\right)^2
$$
$$
+ 2\left(\alpha_{\text{gf}} - 3\right)G\left(\tfrac{2}{3} + \tfrac{1}{\beta_{\text{gf}}-3}\right) \,,
$$

$$
\frac{1}{16\pi G_N}\mathcal{G}_2(\Box, R) = \frac{1}{6}(\alpha_{\text{gf}} - 1)RG\left(\tfrac{1}{6}\right)^2 + \frac{1}{3}(\alpha_{\text{gf}} - 1)G\left(\tfrac{1}{6}\right) - \frac{1}{3}\frac{\alpha_{\text{gf}} - \beta_{\text{gf}}}{\beta_{\text{gf}} - 3}G\left(\tfrac{2}{3} + \tfrac{1}{\beta_{\text{gf}}-3}\right)^2
$$
$$
- \frac{\alpha_{\text{gf}} - 7 - \frac{6}{\beta_{\text{gf}}-3}}{3}G\left(\tfrac{2}{3} + \tfrac{1}{\beta_{\text{gf}}-3}\right) - \frac{2}{\beta_{\text{gf}} - 3}G\left(\tfrac{1}{\beta_{\text{gf}}-3}\right) \,,
$$

$$
\frac{9}{128\pi G_N}\mathcal{G}_3(\Box, R) = (\alpha_{\text{gf}} - 1)G\left(\tfrac{1}{6}\right)^2 - \frac{2\alpha_{\text{gf}} - 15}{R}G\left(\tfrac{1}{6}\right) + 2\frac{\alpha_{\text{gf}} - \beta_{\text{gf}}}{\beta_{\text{gf}} - 3}G\left(\tfrac{2}{3} + \tfrac{1}{\beta_{\text{gf}}-3}\right)^2
$$
$$
+ \frac{(2\alpha_{\text{gf}} - 15)}{R}G\left(\tfrac{2}{3} + \tfrac{1}{\beta_{\text{gf}}-3}\right) \,,
$$

$$
\frac{1}{128\pi G_N}\mathcal{G}_4(\Box, R) = -\frac{2}{9}(\alpha_{\text{gf}} - 1)G\left(\tfrac{1}{6}\right)^2 + \frac{1}{9}\frac{4\alpha_{\text{gf}} - 3}{R}G\left(\tfrac{1}{6}\right)
$$
$$
- \frac{1}{9}\frac{(\alpha_{\text{gf}} - \beta_{\text{gf}})(4\beta_{\text{gf}} - 3)}{(\beta_{\text{gf}} - 3)^2}G\left(\tfrac{2}{3} + \tfrac{1}{\beta_{\text{gf}}-3}\right)^2
$$
$$
- \frac{1}{9}\frac{4\alpha_{\text{gf}} - 3}{R}G\left(\tfrac{2}{3} + \tfrac{1}{\beta_{\text{gf}}-3}\right) + \frac{\alpha_{\text{gf}} - \beta_{\text{gf}}}{(\beta_{\text{gf}} - 3)^2}G\left(\tfrac{1}{\beta_{\text{gf}}-3}\right)^2 \,,
$$

$$
\frac{9}{128\pi G_N}\mathcal{G}_5(\Box, R) = -(\alpha_{\text{gf}} - 1)G\left(\tfrac{1}{6}\right)^2 + 11\frac{\alpha_{\text{gf}} - 3}{R}G\left(\tfrac{1}{6}\right) - 11\frac{\alpha_{\text{gf}} - \beta_{\text{gf}}}{\beta_{\text{gf}} - 3}G\left(\tfrac{2}{3} + \tfrac{1}{\beta_{\text{gf}}-3}\right)^2
$$
$$
- 11\frac{\alpha_{\text{gf}} - 3}{R}G\left(\tfrac{2}{3} + \tfrac{1}{\beta_{\text{gf}}-3}\right) \,,
$$

$$
\frac{1}{256\pi G_N}\mathcal{G}_6(\Box, R) = \frac{\alpha_{\text{gf}} - 1}{R}G\left(\tfrac{1}{6}\right)^2 - 2\frac{\alpha_{\text{gf}} - 3}{R^2}G\left(\tfrac{1}{6}\right) + 2\frac{\alpha_{\text{gf}} - \beta_{\text{gf}}}{\beta_{\text{gf}} - 3}G\left(\tfrac{2}{3} + \tfrac{1}{\beta_{\text{gf}}-3}\right)^2
$$
$$
+ 2\frac{\alpha_{\text{gf}} - 3}{R^2}G\left(\tfrac{2}{3} + \tfrac{1}{\beta_{\text{gf}}-3}\right) \,. \tag{F.14}
$$

Here, we defined the shorthand notation $G_\nu = (-\Box + \nu R)^{-1}$. In the de Donder gauge, $\alpha_{\text{gf}} = 1$, $\beta_{\text{gf}} = \frac{d}{2} - 1$, this reduces to

$$\frac{\mathcal{G}_1(\Box, R)}{16\pi G_N} = -4G\left(\tfrac{1}{6}\right), \qquad \frac{\mathcal{G}_2(\Box, R)}{16\pi G_N} = G\left(-\tfrac{1}{2}\right) + G\left(\tfrac{1}{6}\right), \qquad \mathcal{G}_3 = \mathcal{G}_4 = \mathcal{G}_5 = \mathcal{G}_6 = 0.$$

$$\text{(F.15)}$$

F.3. Differential equations for $(-\Box + z)^{-1}T_{\mu\nu}$

In this appendix, we collect several details regarding the calculation of the propagator in the 2-derivative sector (Subsection 9.4.3).

We begin with a complete list of the differential equations for the propagator functions occurring in the ansatz (9.66). These differential equations read

$$\eta^2 G_{00}'' + (d+4)\eta G_{00}' + \left(q^2\eta^2 + \zeta + 4\right) G_{00} = \frac{1}{H^2\eta^2} - 2(d-1)G_\delta - 4\vec{p}_1 \cdot \vec{p}_2 G_{(12)}$$
$$- 2p_1^2 G_{11} - 2p_2^2 G_{22} + 4i\eta(p_1^2 - \vec{p}_1 \cdot \vec{p}_2)G_1 - 4i\eta(p_2^2 - \vec{p}_1 \cdot \vec{p}_2)G_2;$$

$$\eta^2 G_1'' + (d+4)\eta G_1' + \left(q^2\eta^2 + \zeta + d\right) G_1 = 2i\eta\big(G_{00} - G_\delta$$
$$- (p_1^2 - \vec{p}_1 \cdot \vec{p}_2)G_{11} + (p_2^2 - \vec{p}_1 \cdot \vec{p}_2)G_{(12)}\big);$$

$$\eta^2 G_2'' + (d+4)\eta G_2' + \left(q^2\eta^2 + \zeta + d\right) G_2 = 2i\eta\big(-G_{00} + G_\delta$$
$$- (p_1^2 - \vec{p}_1 \cdot \vec{p}_2)G_{(12)} + (p_2^2 - \vec{p}_1 \cdot \vec{p}_2)G_{22}\big);$$

$$\eta^2 G_{11}'' + (d+4)\eta G_{11}' + \left(q^2\eta^2 + \zeta + 2d\right) G_{11} = -4i\eta G_1;$$

$$\eta^2 G_{22}'' + (d+4)\eta G_{22}' + \left(q^2\eta^2 + \zeta + 2d\right) G_{22} = 4i\eta G_2;$$

$$\eta^2 G_{(12)}'' + (d+4)\eta G_{(12)}' + \left(q^2\eta^2 + \zeta + 2d\right) G_{(12)} = 2i\eta\left(G_1 - G_2\right);$$

$$\eta^2 G_\delta'' + (d+4)\eta G_\delta' + \left(q^2\eta^2 + \zeta + 2d\right) G_\delta = -2G_{00}.$$

$$\text{(F.16)}$$

We now perform linear transformations such that the system of differential equations becomes partially decoupled. Defining $\mathfrak{q} = -q\eta$, we choose coefficients a_{ij} such that

$g_i(\mathfrak{q}) = \sum_j a_{ij} G_j(\eta)$, and the differential equations are cast in the following form:

$$\mathfrak{q}^2 g_1'' + (d+4)\mathfrak{q}g_1' + (\mathfrak{q}^2 + \zeta + d + 2)g_1 = \frac{1}{\mathfrak{q}^2} + dg_2 \,;$$

$$\mathfrak{q}^2 g_2'' + (d+4)\mathfrak{q}g_2' + (\mathfrak{q}^2 + \zeta + d)g_2 = \frac{1}{\mathfrak{q}^2} + (d-2)g_1 + 4i\mathfrak{q}g_3 \,;$$

$$\mathfrak{q}^2 g_3'' + (d+4)\mathfrak{q}g_3' + (\mathfrak{q}^2 + \zeta + d)g_3 = 4i\mathfrak{q}g_2 \,;$$

$$\mathfrak{q}^2 g_4'' + (d+4)\mathfrak{q}g_4' + (\mathfrak{q}^2 + \zeta + 2d)g_4 = -2i\mathfrak{q}g_5 \,; \qquad \text{(F.17)}$$

$$\mathfrak{q}^2 g_5'' + (d+4)\mathfrak{q}g_5' + (\mathfrak{q}^2 + \zeta + d)g_5 = -2i\mathfrak{q}g_4 \,;$$

$$\mathfrak{q}^2 g_6'' + (d+4)\mathfrak{q}g_6' + \left(\mathfrak{q}^2 + \zeta + 2(d+1)\right) g_6 = \frac{1}{\mathfrak{q}^2} \,;$$

$$\mathfrak{q}^2 g_7'' + (d+4)\mathfrak{q}g_7' + (\mathfrak{q}^2 + \zeta + 2d)g_7 = 0 \,.$$

Note that there are now four decoupled systems: $\{g_1, g_2, g_3\}$, $\{g_4, g_5\}$, and the separate equations for g_6 and g_7. For brevity, we will refrain from displaying the coefficients a_{ij} here; these can be computed in `Mathematica`.

F.3.1. *Details regarding solving for $g_{1,2,3}$*

We will now focus on the subsystem of equations in (F.17) for $g_{1,2,3}$, since these contribute to the function G_{00} in the leading-order expansion in μ_χ. This system is solved by inserting the ansatz

$$g_{i,\nu}(\mathfrak{q}) = \mathfrak{q}^\nu \sum_{k \geq 0} a_{i,k} \mathfrak{q}^n \,. \qquad \text{(F.18)}$$

Solving differential equations in this way is also known as the Frobenius method [440, 523–526]. Inserting the ansatz in the differential equations, and collecting powers of $\mathfrak{q}$ allows to read off the following coupled recursion relations for the coefficients $a_{i,k}$:

$$0 = a_{1,k-2} + \left((k+\nu)^2 + (d+3)(k+\nu) + \zeta + d + 2\right) a_{1,k} - da_{2,k} \,;$$

$$0 = a_{2,k-2} + \left((k+\nu)^2 + (d+3)(k+\nu) + \zeta + d\right) a_{2,k} - (d-2)a_{1,k} - 4ia_{3,k-1}; \quad \text{(F.19)}$$

$$0 = a_{3,k-2} + \left((k+\nu)^2 + (d+3)(k+\nu) + \zeta + d\right) a_{3,k} - 4ia_{2,k-1} \,.$$

These equations can be decoupled by substituting one equation into the other. Eventually, this yields three equations that each depend on $a_{i,k}$, $a_{i,k-2}$, $a_{i,k-4}$, $a_{i,k-6}$. We solve these equations using Mathematica's `RSolve` method. The resulting power series can be resummed in terms of generalized hypergeometric functions:

$$g_{i,\nu}(\mathfrak{q}) = \mathfrak{q}^\nu \sum_{j=1,2,3} c_{i,\nu,j} \sum_{\ell=1,2,3} \alpha_{i,j,\ell} {}_1\tilde{F}_2\left(\beta_{i,j,\ell}; \gamma_{i,j,\ell}, \delta_{i,j,\ell}; -\frac{\mathfrak{q}^2}{4}\right) , \qquad \text{(F.20)}$$

where $\beta_{i,j,\ell} \in \{1,2\}$, while $\alpha_{i,j,\ell}$, $\gamma_{i,j,\ell}$ and $\delta_{i,j,\ell}$ depend on ν and ζ. Their values can be found in `Mathematica`. The coefficients $c_{i,\nu,j}$ are free parameters, that remain to be fixed.

The system of three second-order linear differential equations has a six-dimensional solution space. We will consider only the inhomogeneous solution; adding a homogeneous solution will generically lead to non-analyticities. The inhomogeneous solution is given by

$$g_1(\mathfrak{q}) = g_{1,-2}(\mathfrak{q})\,, \qquad g_2(\mathfrak{q}) = g_{2,-2}(\mathfrak{q})\,, \qquad g_3(\mathfrak{q}) = g_{3,-3}(\mathfrak{q}) + g_{3,-1}(\mathfrak{q})\,. \qquad (\text{F.21})$$

At this stage, a remark on the parameter values $\nu \in \{-3, -2\}$, $\zeta = 2$ is in order. The functions (F.20) are singular at these values. This is linked to the massless nature of the graviton. The divergence is removed by carefully choosing part of the parameters $c_{i,\nu,j}$; the other parameters are fixed by inserting the functions (F.21) into the differential equation. For $\zeta \neq 2$, the inhomogeneous solution to the differential equation is given by $g_3 = g_{3,-1}$, while g_1 and g_2 in (F.21) remain unaltered. In this case, all of the coefficients $c_{i,\nu,j}$ can be found by inserting the g_i into the differential equation.

Returning to the case $\zeta = 2$, we have now found the solution to the differential equation. These are given in terms of generalized hypergeometric functions, as well as derivatives thereof with respect to their parameters.

Nonlinearly realized diffeomorphisms

In this section we derive the explicit computations of identities reported in the main text. In the first part of this appendix, we perform a variation of the action under infinitesimal diffeomorphisms and prove the related identities; in the second part, we embed our model of dynamical diffeomorphisms in a broader context, comparing it with the nonlinear sigma models (NLSM).

G.1. Variation under infinitesimal diffeomorphisms

In this subsection we prove the invariance of the action (12.10) under infinitesimal diffeomorphisms.

(1) There are variations of g and variations of φ:

$$
\begin{aligned}
\delta_\xi S = \int \mathrm{d}^d x \sqrt{g} \Bigg\{ &\frac{1}{2} g^{\mu\nu} \delta_\xi g_{\mu\nu} \mathcal{L} - \sum_n n \frac{\partial \mathcal{L}}{\partial \tau_n} (B^{n-1})^{\sigma\mu} \delta_\xi g_{\mu\nu} \nabla^\nu \varphi^\gamma g_{\gamma\delta}(\varphi) \nabla_\sigma \varphi^\delta \\
&+ \sum_n n \frac{\partial \mathcal{L}}{\partial \tau_n} (B^{n-1})^\sigma{}_\mu g^{\mu\lambda} \nabla_\lambda \varphi^\alpha \delta_\xi g_{\alpha\beta}(\varphi) \nabla_\sigma \varphi^\beta \\
&+ \sum_n n \frac{\partial \mathcal{L}}{\partial \tau_n} \Big(2 \nabla_\nu \delta_\xi \varphi^\beta g_{\beta\alpha}(\varphi) \nabla_\sigma \varphi^\alpha (B^{n-1})^\sigma{}_\mu g^{\mu\nu} \\
&+ (B^{n-1})^\sigma{}_\mu g^{\mu\nu} \nabla_\nu \varphi^\beta \delta_\xi \varphi^\alpha \partial_\alpha g_{\beta\gamma}(\varphi) \nabla_\sigma \varphi^\gamma \Big) \Bigg\}
\end{aligned}
\tag{G.1}
$$

$$\delta_\xi S = \int \mathrm{d}^d x \sqrt{g} \left\{ -2\xi_\nu \nabla_\mu \left[\frac{1}{2} g^{\mu\nu} \mathcal{L} - \sum_n n \frac{\partial \mathcal{L}}{\partial T_n} (B^{n-1})^{\sigma\mu} \nabla^\nu \varphi^\gamma g_{\gamma\delta}(\varphi) \nabla_\sigma \varphi^\delta \right] \right.$$

$$+ 2D_\alpha \xi_\beta(\varphi) \sum_n n \frac{\partial \mathcal{L}}{\partial T_n} \nabla_\sigma \varphi^\beta (B^{n-1})^\sigma{}_\mu g^{\mu\lambda} \nabla_\lambda \varphi^\alpha$$

$$+ \xi^\tau \nabla_\tau \varphi^\alpha \left[-\nabla_\mu \left(2 \sum_n n \frac{\partial \mathcal{L}}{\partial T_n} (B^{n-1})^\mu{}_\rho g^{\rho\tau} \nabla_\tau \varphi^\beta g_{\beta\alpha}(\varphi) \right) \right.$$

$$\left. + \sum_n n \frac{\partial \mathcal{L}}{\partial T_n} (B^{n-1})^\mu{}_\rho g^{\rho\tau} \partial_\tau \varphi^\beta \partial_\alpha g_{\beta\gamma}(\varphi) \partial_\mu \varphi^\gamma \right] \tag{G.2}$$

$$- \xi^\alpha(\varphi) \left[-\nabla_\mu \left(2 \sum_n n \frac{\partial \mathcal{L}}{\partial T_n} (B^{n-1})^\mu{}_\rho g^{\rho\tau} \nabla_\tau \varphi^\beta g_{\beta\alpha}(\varphi) \right) \right.$$

$$\left. \left. + \sum_n n \frac{\partial \mathcal{L}}{\partial T_n} (B^{n-1})^\mu{}_\rho g^{\rho\tau} \partial_\tau \varphi^\beta \partial_\alpha g_{\beta\gamma}(\varphi) \partial_\mu \varphi^\gamma \right] \right\} .$$

The first, third and fourth lines are the same as one would have in an ordinary nonlinear sigma model in curved space, where the target space metric is not affected by spacetime diffeomorphisms. By explicitly taking the derivatives of the first line, one finds that they cancel the third and the fourth line.

The second, fifth and sixth lines are novel. They are characterized by the fact that the infinitesimal parameter ξ is evaluated at $\varphi(x)$. The second line can be expanded as follows:

$$2(\partial_\alpha \xi_\beta(\varphi) - \Gamma^\lambda_{\alpha\beta}(\varphi) \xi_\lambda(\varphi)) \sum_n n \frac{\partial \mathcal{L}}{\partial T_n} (B^{n-1})^{\sigma\lambda} \nabla_\lambda \varphi^\alpha \nabla_\sigma \varphi^\beta .$$

As recalled earlier, $\xi_\lambda(\varphi)$ is a scalar under diffeomorphisms, so by the chain rule its covariant derivative is $\partial_\lambda \varphi^\alpha \partial_\alpha \xi_\beta(\varphi) = \nabla_\lambda \xi_\beta(\varphi)$. Therefore the first term can be integrated by parts and we obtain

$$-2\xi_\beta(\varphi) \nabla_\lambda \left(\sum_n n \frac{\partial \mathcal{L}}{\partial T_n} (B^{n-1})^{\sigma\lambda} \nabla_\sigma \varphi^\beta \right) - 2\Gamma^\lambda_{\alpha\beta}(\varphi) \xi_\lambda(\varphi) \sum_n n \frac{\partial \mathcal{L}}{\partial T_n} (B^{n-1})^{\sigma\lambda} \nabla_\lambda \varphi^\alpha \nabla_\sigma \varphi^\beta \tag{G.3}$$

Next, in the fifth line we separate the covariant derivative acting on $g_{\alpha\beta}(\varphi)$ from the rest, and we get

$$2\xi_\beta(\varphi) \nabla_\mu \left(\sum_n n \frac{\partial \mathcal{L}}{\partial T_n} (B^{n-1})^{\mu\tau} \nabla_\tau \varphi^\beta \right) + 2\xi^\alpha(\varphi) \sum_n n \frac{\partial \mathcal{L}}{\partial T_n} (B^{n-1})^{\mu\tau} \nabla_\mu \varphi^\gamma \nabla_\tau \varphi^\beta \partial_\gamma g_{\alpha\beta}(\varphi) \tag{G.4}$$

The first term cancels the first term of (G.3). The second term combines with the sixth line to reconstruct a Christoffel symbol, and the result cancels with the second term in (G.3). In this way also these terms cancel out, and we have proven the invariance of the action.

(2) We can now also see the differential identities that follows from $\mathscr{D}iff(\mathcal{M})$-invariance. To this end, we have to work a little more on the second line of (G.2). Namely, as in the derivation of the EMT, we want to have the infinitesimal parameter ξ evaluated at x rather than $\varphi(x)$. This is dealt with by the method already used in Section 12.2 namely changing coordinates from x to $x' = \varphi(x)$. Then the second line becomes

$$
\int \mathrm{d}^d x \sqrt{g'} \sum_n n \left(\frac{\partial \mathcal{L}}{\partial \tau_n}\right)' (B'^{n-1})^{\alpha\beta} \nabla_\alpha \xi_\beta
$$

$$
= -\int \mathrm{d}^d x \sqrt{g}\, \xi_\beta \nabla_\alpha \left(\frac{\sqrt{g'}}{\sqrt{g}} \sum_n n \left(\frac{\partial \mathcal{L}}{\partial \tau_n}\right)' (B'^{n-1})^{\alpha\beta}\right) .
$$

(G.5)

Note that ∇ is the connection obtained from the metric g, so $\nabla_\rho g_{\mu\nu} = 0$, but $\nabla_\rho g'_{\mu\nu}$ is not zero in general. We recognize that the content of the round bracket is the tensor $T_{(L)}^{\mu\nu}$ consisting of the last term in (12.31), whereas the round bracket in the first line of (G.2), is just the tensor $T_{(R)}^{\mu\nu}$ consisting of the first two terms of (12.31). On the other hand, the expression in square brackets in the third and fourth lines, and in the fifth and sixth lines is nothing but the EOM. Therefore (G.2) is just (12.39) written more explicitly, and where we recognize the separate conservation of $T_{(R)}^{\mu\nu}$ and $T_{(L)}^{\mu\nu}$.

G.2. Models with different domain and target

In this section we discuss models of dynamical diffeomorphisms where, in contrast to the models discussed in the main text, the domain $\mathcal{M}_R$ and the target space $\mathcal{M}_L$ are viewed as different manifolds, and consequently also their metrics are different. Of course since the manifolds are diffeomorphic one can also view them as "the same manifold", but this presupposes a preferred identification, whereas here we will not assume one, at least not to begin with.

The formalism lends itself to two rather different interpretations. In the "field theoretic" interpretation, $\mathcal{M}_R$ is spacetime and $\mathcal{M}_L$ is some internal space, endowed with a fixed metric. In the "brane" interpretation, $\mathcal{M}_R$ is the brane worldsheet and $\mathcal{M}_L$ is spacetime.

G.2.1. *Left and right diffeomorphisms*

We denote $\mathscr{D}iff$ the space of diffeomorphisms of $\mathcal{M}_R$ to $\mathcal{M}_L$. The diffeomorphisms of $\mathcal{M}_R$ and $\mathcal{M}_L$ into themselves will be denoted $\mathscr{D}iff(\mathcal{M}_R)$ and $\mathscr{D}iff(\mathcal{M}_L)$ respectively (see Figure G.1). They act in the usual way on tensors on $\mathcal{M}_R$ and $\mathcal{M}_L$ respectively.
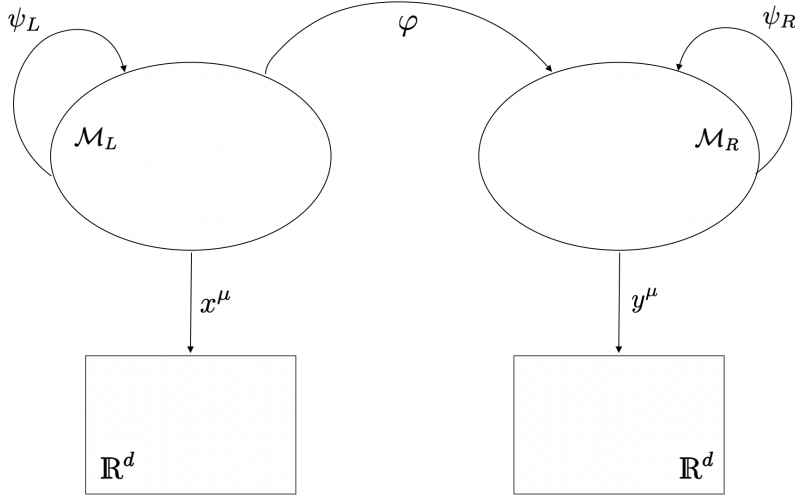
FIGURE G.1. Nonlinear sigma models: the domain $\mathcal{M}_R$ and the target space $\mathcal{M}_L$ are considered different manifolds. The diffeomorphism φ acts from $\mathcal{M}_R$ to $\mathcal{M}_L$, while the diffeomorphisms acting into themselves are denoted as ψ_R and ψ_L, respectively.

The groups $\mathscr{D}iff(\mathcal{M}_R)$ and $\mathscr{D}iff(\mathcal{M}_L)$ act on $\mathscr{D}iff$ by right and left composition

$$\varphi \mapsto \varphi' \;=\; \varphi \circ \psi_R \,,$$
$$\varphi \mapsto \varphi' \;=\; \psi_L^{-1} \circ \varphi \,. \tag{G.6}$$

Each of these actions is free and transitive. In particular, $\mathscr{D}iff(\mathcal{M}_L) \times \mathscr{D}iff(\mathcal{M}_R)$ acts transitively on $\mathscr{D}iff$, so we can transform any $\varphi \in \mathscr{D}iff$ to any other φ'. Now pick some fixed $\bar{\varphi} \in \mathscr{D}iff$. It defines an isomorphism $\iota : \mathscr{D}iff(\mathcal{M}_R) \to \mathscr{D}iff(\mathcal{M}_L)$ by

$$\iota(\psi_R) = \bar{\varphi} \circ \psi_R \circ \bar{\varphi}^{-1} \,. \tag{G.7}$$

The stabilizer of $\bar{\varphi}$ is the "diagonal" subgroup $\Delta\mathscr{D}iff$ consisting of transformations $(\psi_L, \psi_R) \in \mathscr{D}iff(\mathcal{M}_R) \times \mathscr{D}iff(\mathcal{M}_L)$ of the form

$$(\psi_L, \psi_R) = (\iota(\psi), \psi) \,.$$

The diagonal subgroup acts on $\mathscr{D}iff$ as follows: for $f \in \mathscr{D}iff(\mathcal{M}_R)$,

$$f : \varphi \mapsto \iota(f^{-1}) \circ \varphi \circ f = \bar{\varphi} \circ f^{-1} \circ \bar{\varphi}^{-1} \circ \varphi \circ f \tag{G.8}$$

and indeed under such action $\bar{\varphi}$ is invariant

$$f : \bar{\varphi} \mapsto \bar{\varphi} \circ f^{-1} \circ \bar{\varphi}^{-1} \circ \bar{\varphi} \circ f = \bar{\varphi} \,.$$

We have shown that the configuration space $\mathscr{D}iff$ can be regarded as a homogeneous space

$$(\mathscr{D}iff(\mathcal{M}_R) \times \mathscr{D}iff(\mathcal{M}_L))/\Delta\mathscr{D}iff \,. \tag{G.9}$$

All this bears a striking similarity to chiral models of particle physics, but here the groups are infinite dimensional.

G.2.2. *Dynamics*

Let us denote g and h the metrics in $\mathcal{M}_R$ and $\mathcal{M}_L$, respectively. The actions we are interested in have the form

$$S = \int_{\mathcal{M}_R} \mathrm{d}^d x \, \sqrt{g} \, \mathcal{L}(\sigma_1, \sigma_2, \sigma_3, \sigma_4) \,, \tag{G.10}$$

where $\sigma_n = \mathrm{tr} B^n$ and $B^\mu{}_\nu$ is given by (12.7). The usual action for nonlinear sigma models corresponds to $\mathcal{L} = -\frac{1}{2}\sigma_1$ and one may keep this example in mind in the following.

Remark. As long as the metrics g and h are kept fixed, the action has, generically, no symmetries. In the field theoretic interpretation the target space metric h can be interpreted as an infinite set of coupling constants. Symmetries of a theory correspond to transformations that act on the dynamical variables leaving the couplings fixed, so left diffeomorphisms are not symmetries, unless h has some isometries. The proper interpretation of left (target space) diffeomorphisms is as field redefinitions. In the brane interpretation, h represents the spacetime metric and its dynamics, in the quantum theory, comes from the beta functions of the worldsheet quantum field theory. Once again, left (spacetime) diffeomorphisms cannot be interpreted as symmetries. We shall use the word "invariances" for transformations that leave the action invariant, from a mere mathematical viewpoint, and irrespective of their physical interpretation.

With these cautionary remarks in mind, the action is separately invariant under $\mathscr{D}\!iff(\mathcal{M}_R)$ and $\mathscr{D}\!iff(\mathcal{M}_L)$, as we shall now see. Under a right-diffeomorphism the metric g is pulled back but the metric h is invariant. The pullback $\varphi^* h$ transforms like an ordinary tensor on $\mathcal{M}_R$:

$$\varphi'^* h' = (\varphi \circ \psi_R)^* h = \psi_R^* (\varphi^* h) \,.$$

Since the integrand of the action is a scalar density on $\mathcal{M}_R$, the action is $\mathscr{D}\!iff(\mathcal{M}_R)$-invariant.

On the other hand under a left-diffeomorphism h gets pulled back but g is invariant. The pullback $\varphi^* h$ is invariant, because:

$$\varphi'^* h' = (\psi_L^{-1} \circ \varphi)^* (\psi_L^* h) = \varphi^* \circ \psi_L^{-1*} \circ \psi_L^* h = \varphi^* h \,.$$

Since g is also invariant, the action is trivially $\mathscr{D}\!iff(\mathcal{M}_L)$-invariant.

The equation of motion of these models has the form (12.22), except that B is given by $g^{\mu\rho} \partial_\rho \varphi^\beta h_{\beta\alpha}(\varphi) \partial_\nu \varphi^\alpha$ instead of (12.7), i.e., $g_{\alpha\beta}(\varphi)$ is replaced everywhere by $h_{\alpha\beta}(\varphi)$

and the Christoffel symbol appearing in (12.5) is the Christoffel symbol of $h_{\alpha\beta}$ (whereas ∇_μ in (12.6) is still constructed with the Christoffel symbols of $g_{\mu\nu}$). The EMT defined by (12.29) is equal to (12.31), but the last term is absent. It thus agrees with what we called $T^{\mu\nu}_{(R)}$. Separately, we define the tensor

$$T^{\alpha\beta}_{(L)}(y) = \frac{2}{\sqrt{h(y)}} \frac{\delta S}{\delta h_{\alpha\beta}(y)} \ . \tag{G.11}$$

In the next subsections we consider the infinitesimal versions of these transformations and the differential identities that follow from the invariances of the action.

G.2.3. *Consequences of right diffeomorphism invariance*

A right diffeomorphism acts on points of $\mathcal{M}_R$ by $x \mapsto x' = \psi^{-1}(x)$. The infinitesimal version is

$$\delta x^\alpha = -\xi^\alpha(x) \ .$$

The variation of any tensor T on $\mathcal{M}_R$ is its Lie derivative $\delta_\xi T = \mathcal{L}_\xi T$. For the metric

$$\delta_\xi g_{\mu\nu} = \xi^\rho \partial_\rho g_{\mu\nu} + g_{\mu\rho}\partial_\nu \xi^\rho + g_{\rho\nu}\partial_\mu \xi^\rho = \nabla_\mu \xi_\nu + \nabla_\nu \xi_\mu \ .$$

The infinitesimal variation of φ is

$$\delta_\xi \varphi^\rho(x) = \xi^\lambda \partial_\lambda \varphi^\rho \tag{G.12}$$

and $\delta_\xi h_{\alpha\beta} = 0$. Now varying the pullback we have

$$
\begin{aligned}
\delta_\xi(\varphi^* h_{\mu\nu}) &= \delta_\xi(\partial_\mu \varphi^\alpha \partial_\nu \varphi^\beta h_{\alpha\beta}(\varphi)) \\
&= \partial_\mu \delta\varphi^\alpha \partial_\nu \varphi^\beta h_{\alpha\beta}(\varphi) + \partial_\mu \varphi^\alpha \partial_\nu \delta\varphi^\beta h_{\alpha\beta}(\varphi) + \partial_\mu \varphi^\alpha \partial_\nu \varphi^\beta \partial_\gamma h_{\alpha\beta}(\varphi)\delta\varphi^\gamma \ .
\end{aligned}
$$

Inserting the above formulae for the variation and expanding, one arrives after a few steps at

$$\xi^\rho \partial_\rho(\varphi^* h)_{\mu\nu} + (\varphi^* h)_{\mu\rho}\partial_\nu \xi^\rho + (\varphi^* h)_{\rho\nu}\partial_\mu \xi^\rho = \mathcal{L}_\xi(\varphi^* h)_{\mu\nu} \ . \tag{G.13}$$

which just confirms that $\varphi^* h$ transforms as a tensor.

As usual, from the diffeomorphism invariance one can obtain a differential identity. The derivation follows the steps of the previous section, but with some terms now absent. In the end one obtains

$$0 = \int d^4x \sqrt{g} \left[\xi^\tau \partial_\tau \varphi^\alpha E_\alpha - \xi_\mu \nabla_\nu T^{\mu\nu}_{(R)} \right] \ . \tag{G.14}$$

In contrast to (12.39), since $\partial_\tau \varphi^\alpha$ is nondegenerate, the coefficient of the EOM is always nonzero and therefore we find that the EOM and EM conservation are completely equivalent. This is a consequence of the action of the group being free and transitive.

G.2.4. *Consequences of left diffeomorphism invariance*

A left diffeomorphism acts on points of $\mathcal{M}_L$ by $x \mapsto x' = x$ and $\varphi(x) \mapsto \psi^{-1}(\varphi(x))$. The infinitesimal versions are

$$\delta_\xi x^\mu = 0 \,, \quad \delta_\xi \varphi^\alpha(x) = -\xi^\alpha(\varphi(x)) \,.$$

The variation of any tensor T on $\mathcal{M}_L$ is its Lie derivative $\delta_\xi T = \mathcal{L}_\xi T$, and tensors on $\mathcal{M}_R$ are invariant. For the metric in $\mathcal{M}_L$

$$\delta_\xi h_{\alpha\beta} = \xi^\rho \partial_\rho h_{\alpha\beta} + h_{\alpha\rho} \partial_\beta \xi^\rho + h_{\rho\beta} \partial_\alpha \xi^\rho = D_\alpha \xi_\beta + D_\beta \xi_\alpha \,, \tag{G.15}$$

where we used the notation (12.4). Now varying the pullback and using this formula we have

$$
\begin{aligned}
\delta_\xi(\varphi^* h_{\mu\nu}) &= \delta_\xi(\partial_\mu \varphi^\alpha \partial_\nu \varphi^\beta h_{\alpha\beta}(\varphi)) \\
&= \partial_\mu \delta_\xi \varphi^\alpha \partial_\nu \varphi^\beta h_{\alpha\beta}(\varphi) + \partial_\mu \varphi^\alpha \partial_\nu \delta_\xi \varphi^\beta h_{\alpha\beta}(\varphi) \\
&\quad + \partial_\mu \varphi^\alpha \partial_\nu \varphi^\beta \delta_\xi \varphi^\gamma \partial_\gamma h_{\alpha\beta}(\varphi) + \partial_\mu \varphi^\alpha \partial_\nu \varphi^\beta \delta_\xi h_{\alpha\beta}(\varphi) \\
&= 0 \,.
\end{aligned}
\tag{G.16}
$$

As we have already seen at the level of finite transformations, both g and $\varphi^* h$ are invariant, and therefore the invariance of the action is trivial.

Since the metric g is unaffected by these transformations, no consequence can be derived from $\mathscr{D}iff(\mathcal{M}_L)$-invariance concerning the energy-momentum tensor $T^{\mu\nu}_{(R)}$. Nevertheless, we can obtain another differential identity involving the tensor (G.11).

Since in the action the metric h always appears evaluated at $\varphi(x)$, it is convenient to change integration variable from x to $x' = \varphi(x)$, and write

$$S = \int \mathrm{d}^d x' \sqrt{g'(x')} \mathcal{L}'(x') \,.$$

Since $\mathcal{L}$ is a given function of the trace invariants $\mathcal{L}(x) = F(\tau_1(x), \tau_2(x), \tau_3(x), \tau_4(x))$, the transformed Lagrangian $\mathcal{L}'$ will be the same function of the transformed invariants $\mathcal{L}'(x') = F(\tau_1'(x'), \tau_2'(x'), \tau_3'(x'), \tau_4'(x'))$ and since $\tau_n'(x') = \tau_n(x)$, also $\mathcal{L}'(x') = \mathcal{L}(x)$.

For example, for the Lagrangian (12.11), we can write

$$\mathcal{L}'(x') = -\frac{1}{2}(\varphi_* g^{-1})^{\alpha\beta}(x') h_{\alpha\beta}(x')$$

and therefore

$$T^{\alpha\beta}_{(L)}(y) = -f^2 \frac{\sqrt{g'}}{\sqrt{h}} g'^{\alpha\beta}(y) \,,$$

where we write $g'^{\alpha\beta}$ for the push-forward of the inverse metric, $(\varphi_* g^{-1})^{\alpha\beta}(x')$. In general

$$T^{\alpha\beta}_{(L)}(y) = 2\frac{\sqrt{g'}}{\sqrt{h}} \sum_{n=1}^{4} n \left(\frac{\partial \mathcal{L}}{\partial \tau_n}\right)' (B'^{n-1})^{\alpha\beta}(y) \,, \tag{G.17}$$

Using the infinitesimal variation (G.15) and the invariance of the action under left diffeomorphisms, one finds that

$$0 = \delta_\xi S = \int \mathrm{d}^d x' \sqrt{h(x')} \left[-\xi^\alpha(x') E_\alpha(x') + \xi_\beta(x') D_\alpha T^{\alpha\beta}_{(L)}(x') \right] \tag{G.18}$$

and therefore, on shell

$$D_\alpha T^{\alpha\beta}_{(L)} = 0 \,. \tag{G.19}$$

G.2.5. *Relation to the models in the main text*

Even though the manifolds $\mathcal{M}_R$ and $\mathcal{M}_L$ are, by assumption, diffeomorphic, there will in general be no relation between the respective metrics. Consider the special case in which there exists a diffeomorphism $\bar{\varphi}$ such that:

$$\bar{\varphi}^* h = g \,. \tag{G.20}$$

If h and g have isometries, $\bar{\varphi}$ will not be unique. We disregard this case here. We can use $\bar{\varphi}$ to define a preferred identification of $\mathcal{M}_R$ and $\mathcal{M}_L$ and, via equation (G.7), a preferred identification of the respective diffeomorphism groups.

Since $\bar{\varphi}$ is a diffeomorphism, without loss of generality we can choose atlases on $\mathcal{M}_L$ and $\mathcal{M}_R$ to be related by $\bar{\varphi}$. This means that on any chart, if x^α are the coordinates of a point x and y^α are the coordinates of $\bar{\varphi}(x)$, then

$$y^\alpha = x^\alpha \,. \tag{G.21}$$

If we use $\bar{\varphi}$ to identify $\mathcal{M}_R$ and $\mathcal{M}_L$, we have only one manifold $\mathcal{M}$, $\bar{\varphi}$ can be thought of as the identity mapping of $\mathcal{M}$ to itself and the action (G.8) becomes conjugation. Since $\bar{\varphi}$ is now a fixed element of the theory, the original invariance under $\mathscr{D}\!iff(\mathcal{M}_R) \times \mathscr{D}\!iff(\mathcal{M}_L)$ is broken to $\Delta\mathscr{D}\!iff$, acting by conjugation. In this way we recover the models of the main text (see Figure G.2).
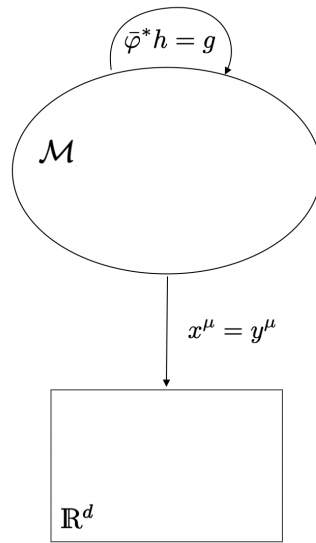
FIGURE G.2. The models in the main text have only one manifold $\mathcal{M}$. Here $\bar{\varphi}$ can be thought of as the identity mapping of $\mathcal{M}$ to itself.

RG equations of the relational observables

H.1. Flow equations of the scalar-tensor theory

In the standard approach the EAA that contains all terms at first order in the derivative expansion for a general scalar-tensor theory[1] in Euclidean signature [527] is

$$\Gamma_k = \int \mathrm{d}^d x \sqrt{g} \left[\frac{\rho_k}{8\pi} - Z_N R + \frac{1}{2} Z_k \delta_{\hat{\mu}\hat{\nu}} \nabla_\mu \hat{X}^{\hat{\mu}} \nabla^\mu \hat{X}^{\hat{\nu}} \right] + \text{gauge fixing} + \text{ghosts}, \quad \text{(H.1)}$$

In view of the application of the essential scheme, here we parameterized $\rho_k = \Lambda(k)/G(k)$ and $Z_N = 1/(16\pi G(k))$. Using the essential scheme we can choose the RG kernel in order to impose the following renormalization conditions along the RG flow

$$\rho_k = \rho_{\mathrm{GFP}} = \frac{8\pi}{d(4\pi)^{d/2}} \int_0^\infty \mathrm{d}z \, z^{\frac{d}{2}-1} \frac{k\partial_k \mathcal{R}_k(z)}{z + \mathcal{R}_k(z)}, \qquad Z_k = 1. \quad \text{(H.2)}$$

The first condition fixes the k-dependent vacuum energy to the value of the vacuum energy in the pure gravity GFP, while the second one is the standard renormalization condition for the wave function renormalization in order to canonically normalize the kinetic term. To achieve this, the RG kernels are

$$\Psi^g_{\mu\nu} = \gamma_g \, g_{\mu\nu}, \qquad\qquad \Psi^{\hat{\mu}} = -\frac{\hat{\eta}_k}{2} \hat{X}^{\hat{\mu}}, \quad \text{(H.3)}$$

and in this way the EAA takes the following form

$$\Gamma_k = \int \mathrm{d}^d x \sqrt{g} \left[\frac{\rho_{\mathrm{GFP}}}{8\pi} - Z_N R + \frac{1}{2} \delta_{\hat{\mu}\hat{\nu}} \nabla_\mu \hat{X}^{\hat{\mu}} \nabla^\mu \hat{X}^{\hat{\nu}} \right] + \text{gauge fixing} + \text{ghosts}. \quad \text{(H.4)}$$

Using the previous RG kernels, on the RHS of (4.38) we get

$$\int \mathrm{d}^d x \left(\frac{\delta \Gamma}{\delta \hat{X}^{\hat{\mu}}} \Psi^{\hat{\mu}}(x) + \frac{\delta \Gamma}{\delta g_{\mu\nu}(x)} \Psi^g(x)_{\mu\nu} \right) =$$
$$= \int \mathrm{d}^d x \sqrt{g} \left\{ d \, Z_N \Lambda \gamma_g + \left[-\frac{\hat{\eta}_k}{2} + \frac{d-2}{4} \gamma_g \right] \delta_{\hat{\mu}\hat{\nu}} \nabla_\mu \hat{X}^{\hat{\mu}} \nabla^\mu \hat{X}^{\hat{\nu}} + \frac{2-d}{2} Z_N \gamma_g R \right\}. \quad \text{(H.5)}$$

In order to evaluate the LHS of (4.38), we use the background field method with linear parameterization

$$g_{\mu\nu} \to g_{\mu\nu} + \frac{1}{\sqrt{Z_N}} h_{\mu\nu}, \qquad\qquad \hat{X}^{\hat{\mu}} \to \hat{X}^{\hat{\mu}} + \delta \hat{X}^{\hat{\mu}}, \quad \text{(H.6)}$$

---

[1] For a recent analysis about scalar-tensor theories in Asymptotic Safety see [174].

where both fluctuations around the background have the same dimensions. Because of the presence of $1/\sqrt{Z_N}$ in front of $h_{\mu\nu}$, the ghost are expanded in following way

$$\Xi^\mu \to Z_N^{-1/4}\xi^\mu\,, \qquad\qquad \bar{\Xi}_\mu \to Z_N^{-1/4}\bar{\xi}_\mu\,, \qquad\qquad \text{(H.7)}$$

and we have

$$\Psi^h_{\mu\nu} = -\frac{1}{2}\left(\eta_N - 2\gamma_g\right)h_{\mu\nu}\,, \qquad\qquad \Psi^{\xi\mu} = -\frac{\eta_N}{4}\xi^\mu\,, \qquad\qquad \Psi^{\bar{\xi}}_\mu = -\frac{\eta_N}{4}\bar{\xi}_\mu\,. \quad \text{(H.8)}$$

Using de Donder gauge, the Hessian evaluated at zero value of the fluctuations reads

$$\frac{1}{\sqrt{g}}\frac{\delta^2\Gamma_k}{\delta h_{\mu\nu}\delta h_{\rho\sigma}} = K^{\mu\nu,\rho\sigma}\left(-\Box - 2\Lambda\right) + U^{\mu\nu\rho\sigma} + \frac{1}{Z_N}S^{\mu\nu\rho\sigma}\,, \qquad\qquad \text{(H.9)}$$

$$\frac{1}{\sqrt{g}}\frac{\delta^2\Gamma_k}{\delta\hat{x}^{\hat{\mu}}\delta\hat{x}^{\hat{\nu}}} = -\delta_{\hat{\mu}\hat{\nu}}\Box\,, \qquad\qquad \text{(H.10)}$$

$$\frac{1}{\sqrt{g}}\frac{\delta^2\Gamma_k}{\delta\hat{x}^{\hat{\mu}}\delta h_{\mu\nu}} = -\frac{1}{\sqrt{Z_N}}K^{\mu\nu,\rho\sigma}\nabla_\rho\hat{X}_{\hat{\mu}}\nabla_\sigma\,, \qquad\qquad \text{(H.11)}$$

$$\frac{1}{\sqrt{g}}\frac{\delta^2\Gamma_k}{\delta h_{\mu\nu}\delta\hat{x}^{\hat{\mu}}} = \frac{1}{\sqrt{Z_N}}K^{\mu\nu,\rho\sigma}\nabla_\rho\hat{X}_{\hat{\mu}}\nabla_\sigma - \frac{1}{2\sqrt{Z_N}}\left(g^{\mu\nu}\Box + 2\nabla^\mu\nabla^\nu\right)\hat{X}_{\hat{\mu}}\,, \qquad \text{(H.12)}$$

where

$$U^{\mu\nu}{}_{\rho\sigma} = K^{\mu\nu}{}_{\rho\sigma}R + \frac{1}{2}g^{\mu\nu}R_{\rho\sigma} + \frac{1}{2}R^{\mu\nu}g_{\rho\sigma} - \delta^{(\mu}_{(\rho}R^{\nu)}_{\sigma)} - R^{(\mu}{}_{(\rho}{}^{\nu)}{}_{\sigma)}\,, \qquad\qquad \text{(H.13)}$$

$$S^{\mu\nu,\rho\sigma} = \delta_{\hat{\mu}\hat{\nu}}\nabla_\alpha\hat{X}^{\hat{\mu}}\nabla_\beta\hat{X}^{\hat{\nu}}\times \qquad\qquad \text{(H.14)}$$

$$\left(-\frac{1}{2}K^{\mu\nu,\rho\sigma}g^{\alpha\beta} + g^{\alpha(\mu}\mathbb{1}^{\nu)\beta\rho\sigma} - \frac{1}{4}g^{\mu\nu}g^{\rho\alpha}g^{\sigma\beta} - \frac{1}{4}g^{\rho\sigma}g^{\mu\alpha}g^{\nu\beta}\right)\,,$$

$$K^{\mu\nu,\rho\sigma} = \frac{1}{4}\left(g^{\mu\rho}g^{\nu\sigma} + g^{\mu\sigma}g^{\nu\rho} - g^{\mu\nu}g^{\rho\sigma}\right)\,, \qquad\qquad \text{(H.15)}$$

$$\left(K^{-1}\right)^{\mu\nu,\rho\sigma} = g^{\mu\rho}g^{\nu\sigma} + g^{\mu\sigma}g^{\nu\rho} - \frac{2}{d-2}g^{\mu\nu}g^{\rho\sigma}\,. \qquad\qquad \text{(H.16)}$$

Since we have mixed terms in the Hessian, we can proceed in different ways that differs by the renormalization scheme procedure.

H.1.1. *First possibility*

We are dealing with a Hessian of the form

$$\frac{1}{\sqrt{g}}\left(\Gamma^{(2)}\right)^{AB} = -\delta^{AB}g^{\mu\nu}\nabla_\mu\nabla_\nu - 2\Gamma^{AB\mu}\nabla_\mu + E^{AB}\,, \qquad\qquad \text{(H.17)}$$

where

$$
\Gamma_\sigma \;=\; \frac{1}{2\sqrt{Z_N}} K^{\mu\nu,\rho\sigma} \nabla_\rho \hat{X}_{\hat\mu}
\begin{pmatrix} 0 & -\mathbb{1} \\ \mathbb{1} & 0 \end{pmatrix} ,
\tag{H.18}
$$

$$
E \;=\;
\begin{pmatrix} -2\Lambda\, K^{\mu\nu,\rho\sigma} + U^{\mu\nu\rho\sigma} + \frac{1}{Z_N} S^{\mu\nu\rho\sigma} & 0 \\ 0 & 0 \end{pmatrix} .
\tag{H.19}
$$

Defining

$$
\mathcal{D}^{AB}{}_\sigma \equiv \delta^{AB}\nabla_\sigma + \Gamma^{AB}{}_\sigma ,
\tag{H.20}
$$

such that this derivative applied to the fluctuations gives

$$
(\mathcal{D}h)_{\alpha\beta,\mu} \equiv \nabla_\mu h_{\alpha\beta} + \Gamma_{\alpha\beta,\hat\mu,\mu}\delta\hat{x}^{\hat\mu} ,
\tag{H.21}
$$

$$
(\mathcal{D}\mathcal{D}h)_{\alpha\beta,\mu\nu} \equiv \nabla_\mu\nabla_\nu h_{\alpha\beta} + \Gamma_{\alpha\beta,\hat\mu,\mu}\Gamma^{\hat\mu,\gamma\delta}{}_\nu h_{\gamma\delta} + \nabla_\mu\left(\Gamma_{\alpha\beta,\hat\mu,\nu}\delta\hat{x}^{\hat\mu}\right) + \Gamma_{\alpha\beta,\hat\mu,\mu}\nabla_\nu\delta\hat{x}^{\hat\mu} ,
\tag{H.22}
$$

$$
(\mathcal{D}\delta\hat{x})^{\hat\mu}{}_\mu \equiv \nabla_\mu\delta\hat{x}^{\hat\mu} + \Gamma^{\hat\mu,\alpha\beta}{}_\mu h_{\alpha\beta} ,
\tag{H.23}
$$

$$
(\mathcal{D}\mathcal{D}\delta\hat{x})^{\hat\mu}{}_{\mu\nu} \equiv \nabla_\mu\nabla_\nu\delta\hat{x}^{\hat\mu} + \Gamma^{\hat\mu}{}_{\alpha\beta,\mu}\Gamma^{\alpha\beta}{}_{\hat\nu,\nu}\delta\hat{x}^{\hat\nu} + \nabla_\mu\left(\Gamma^{\hat\mu,\alpha\beta}{}_\nu h_{\alpha\beta}\right) + \Gamma^{\hat\mu,\alpha\beta}{}_\mu\nabla_\nu h_{\alpha\beta} ,
\tag{H.24}
$$

we can express the previous operator in the form

$$
\mathcal{O}^{AB} \;=\; -g^{\mu\nu}\mathcal{D}^{AC}{}_\mu\mathcal{D}_C{}^B{}_\nu + \tilde{E}^{AB} ,
\tag{H.25}
$$

$$
\tilde{E}^{AB} \;=\; E^{AB} + \nabla_\mu\Gamma^{AB\mu} + \Gamma^{AC\mu}\Gamma_C{}^{B\mu} ,
\tag{H.26}
$$

$$
\Omega^{AB}_{\mu\nu} \;\equiv\; \left[\mathcal{D}^A_{C\mu}, \mathcal{D}^{CB}{}_\nu\right] = \nabla_\mu\Gamma^{AB}{}_\nu - \nabla_\nu\Gamma^{AB}{}_\mu + \Gamma^{AC}{}_\mu\Gamma_C{}^B{}_\nu - \Gamma^{AC}{}_\nu\Gamma_C{}^B{}_\mu .
\tag{H.27}
$$

Note that $\tilde{E}$ and Ω have the following structures

$$
\tilde{E} \;=\;
\begin{pmatrix} -2\Lambda\, K^{\mu\nu,\rho\sigma} + U^{\mu\nu\rho\sigma} + \frac{1}{Z_N} S^{\mu\nu\rho\sigma} + (\Gamma^2_{11})^{\mu\nu\rho\sigma} & \nabla_\alpha\Gamma^{\hat\nu\rho\sigma,\alpha} \\ \nabla_\alpha\Gamma^{\mu\nu\hat\mu,\alpha} & (\Gamma^2_{22})^{\hat\mu\hat\nu} \end{pmatrix}
\tag{H.28}
$$

$$
\Omega_{\alpha\beta} \;=\;
\begin{pmatrix} \Gamma^{\mu\nu\hat\mu}{}_\alpha\Gamma_{\hat\mu}{}^{\rho\sigma}{}_\beta - \Gamma^{\mu\nu\hat\mu}{}_\beta\Gamma_{\hat\mu}{}^{\rho\sigma}{}_\alpha & \nabla_\alpha\Gamma^{\hat\nu\rho\sigma}{}_\beta - \nabla_\beta\Gamma^{\hat\nu\rho\sigma}{}_\alpha \\ \nabla_\alpha\Gamma^{\mu\nu\hat\mu}{}_\beta - \nabla_\beta\Gamma^{\mu\nu\hat\mu}{}_\alpha & \Gamma^{\hat\mu\mu\nu}{}_\alpha\Gamma_{\mu\nu}{}^{\hat\nu}{}_\beta - \Gamma^{\hat\mu\mu\nu}{}_\beta\Gamma_{\mu\nu}{}^{\hat\nu}{}_\alpha \end{pmatrix}
\tag{H.29}
$$

where

$$
(\Gamma^2_{11})^{\mu\nu}{}_{\alpha\beta} \;\equiv\; \Gamma^{AC\mu}\Gamma_{CB}{}^\mu\Big|_{A=\mu\nu,B=\alpha\beta} = -\frac{1}{4Z_N} K^{\mu\nu,\rho\sigma} K_{\alpha\beta}{}^\gamma{}_\sigma \nabla_\rho\hat{X}_{\hat\mu}\nabla_\gamma\hat{X}^{\hat\mu} ,
\tag{H.30}
$$

$$
(\Gamma^2_{22})^{\hat\mu}{}_{\hat\nu} \;\equiv\; \Gamma^{AC\mu}\Gamma_{CB}{}^\mu\Big|_{A=\hat\mu,B=\hat\nu} = -\frac{1}{4Z_N} K^{\mu\nu,\rho\sigma} K_{\mu\nu}{}^\alpha{}_\sigma \nabla_\rho\hat{X}^{\hat\mu}\nabla_\alpha\hat{X}_{\hat\nu} .
\tag{H.31}
$$

It is important to stress out that the mixed terms of $\Omega_{\alpha\beta}$ are total derivatives. We then insert the regulator in such a way that

$$-g^{\mu\nu}\mathcal{D}^{AC}{}_\mu \mathcal{D}_C{}^B{}_\nu \rightarrow P_k{}^{AB} \equiv -g^{\mu\nu}\mathcal{D}^{AC}{}_\mu \mathcal{D}_C{}^B{}_\nu + \mathcal{R}_k{}^{AB}\,.$$

Thus, the propagator has the following form

$$\mathcal{G}_k = \frac{1}{\sqrt{g}}\begin{pmatrix} \mathcal{G}_{gg} & 0 \\ 0 & \mathcal{G}_{XX} \end{pmatrix},\qquad\qquad (\text{H}.32)$$

where

$$(\mathcal{G}_{gg})_{\mu\nu\rho\sigma} = \left(K^{-1}\right)_{\mu\nu\rho\sigma}\frac{1}{P_k - 2\Lambda}$$

$$- \frac{1}{P_k - 2\Lambda}\left[K^{-1}\cdot\left(U + \frac{1}{Z_N}S + \Gamma^2_{11}\right)\cdot K^{-1}\right]_{\mu\nu\rho\sigma}\frac{1}{P_k - 2\Lambda}, \quad (\text{H}.33)$$

$$(\mathcal{G}_{XX})_{\hat{\mu}\hat{\nu}} = \delta_{\hat{\mu}\hat{\nu}}\frac{1}{P_k} - \frac{1}{P_k}\left(\Gamma^2_{22}\right)_{\hat{\mu}\hat{\nu}}\frac{1}{P_k}, \qquad\qquad (\text{H}.34)$$

modulo four derivative terms, coming from squares of the curvature and derivatives of $\hat{X}$. The LHS of (4.38) is composed by three traces, which read the following

$$\mathcal{T}_{hh} = \frac{1}{2}\text{Tr}\left[\frac{1}{P_k - 2\Lambda}\right. \qquad\qquad (\text{H}.35)$$

$$\left. - \frac{K^{-1}}{P_k - 2\Lambda}\left(U + \frac{1}{Z_N}S + \Gamma^2_{11}\right)\frac{1}{P_k - 2\Lambda}\right]K^{-1}\left(k\partial_k - \eta_N + 2\gamma_g\right)\mathcal{R}_k^{hh}\,,$$

$$\mathcal{T}_{xx} = \frac{1}{2}\text{Tr}\left[\frac{1}{P_k} - \frac{1}{P_k}\Gamma^2_{22}\frac{1}{P_k}\right]\left(k\partial_k - \hat{\eta}_k\right)\mathcal{R}_k^{xx}\,, \qquad\qquad (\text{H}.36)$$

$$\mathcal{T}_{\bar{c}c} = -\text{Tr}\left[\frac{1}{P_k} + Ricci\frac{1}{P_k^2}\right]\left(k\partial_k - \frac{\eta_N}{2}\right)\mathcal{R}_k^{\bar{c}c}\,, \qquad\qquad (\text{H}.37)$$

and the regulator is chosen in the following way[2]

$$\left(\mathcal{R}_k^{hh}\right)^{\mu\nu,\alpha\beta} = \sqrt{g}\,K^{\mu\nu,\alpha\beta}\,\mathcal{R}_k\,,\qquad \left(\mathcal{R}_k^{xx}\right)^\nu_\mu = \sqrt{g}\,\hat{\delta}^{\hat{\nu}}_{\hat{\mu}}\mathcal{R}_k\,,\qquad \left(\mathcal{R}_k^{\bar{c}c}\right)^\nu_\mu = \sqrt{g}\,\delta^\nu_\mu\mathcal{R}_k\,.\quad (\text{H}.38)$$

---

[2]Note that the factor $\sqrt{g}$ in the propagator and in the regulator cancels when they are multiplied.

Defining $\eta_N = -k\partial_k \ln Z_N$, the traces for a generic regulator $\mathcal{R}_k$ and generic dimensions are

$$
\begin{aligned}
\mathcal{T}_{hh} &= \frac{1}{2(4\pi)^{d/2}} \int \mathrm{d}^d x \sqrt{g} \left\{ \frac{d(d+1)}{2} Q_{d/2}\left[\frac{(k\partial_k - \eta_N + 2\gamma_g)\mathcal{R}_k}{P_k - 2\Lambda}\right] \right. \\
&\quad + \frac{d(d+1)}{12} R\, Q_{d/2-1}\left[\frac{(k\partial_k - \eta_N + 2\gamma_g)\mathcal{R}_k}{P_k - 2\Lambda}\right] \\
&\quad - \left(\frac{d(d-1)}{2} R - \frac{1}{Z_N}\left(\frac{(d+1)(d-4)}{4} + \frac{d}{16}\right)\nabla_\mu \hat{X}_{\hat{\mu}} \nabla^\mu \hat{X}^{\hat{\mu}}\right) \times \\
&\quad \left. \times\, Q_{d/2}\left[\frac{(k\partial_k - \eta_N + 2\gamma_g)\mathcal{R}_k}{(P_k - 2\Lambda)^2}\right] \right\}, \quad\quad (H.39)
\end{aligned}
$$

$$
\begin{aligned}
\mathcal{T}_{xx} &= \frac{1}{2(4\pi)^{d/2}} \int \mathrm{d}^d x \sqrt{g} \left\{ N_S\, Q_{d/2}\left[\frac{(k\partial_k - \hat{\eta}_k)\mathcal{R}_k}{P_k}\right] + \frac{N_S}{6} R\, Q_{d/2-1}\left[\frac{(k\partial_k - \hat{\eta}_k)\mathcal{R}_k}{P_k}\right]\right. \\
&\quad \left. + \frac{1}{Z_N}\frac{3d-2}{64}\nabla_\mu \hat{X}_{\hat{\mu}} \nabla^\mu \hat{X}^{\hat{\mu}}\, Q_{d/2}\left[\frac{(k\partial_k - \hat{\eta}_k)\mathcal{R}_k}{P_k^2}\right] \right\}, \quad\quad (H.40)
\end{aligned}
$$

$$
\begin{aligned}
\mathcal{T}_{\bar{c}c} &= -\frac{1}{(4\pi)^{d/2}} \int \mathrm{d}^d x \sqrt{g} \left\{ d\, Q_{d/2}\left[\frac{\left(k\partial_k - \frac{\eta_N}{2}\right)\mathcal{R}_k}{P_k}\right] + \frac{d}{6} R\, Q_{d/2-1}\left[\frac{\left(k\partial_k - \frac{\eta_N}{2}\right)\mathcal{R}_k}{P_k}\right]\right. \\
&\quad \left. + R\, Q_{d/2}\left[\frac{\left(k\partial_k - \frac{\eta_N}{2}\right)\mathcal{R}_k}{P_k^2}\right] \right\}. \quad\quad (H.41)
\end{aligned}
$$

Putting everything together, the flow equations are

$$
\begin{aligned}
(2k\partial_k + d\gamma_g) Z_N \Lambda &= \frac{1}{2(4\pi)^{d/2}}\left\{\frac{d(d+1)}{2} Q_{d/2}\left[\frac{(k\partial_k - \eta_N + 2\gamma_g)\mathcal{R}_k}{P_k - 2\Lambda}\right]\right. \\
&\quad \left. + N_S\, Q_{d/2}\left[\frac{(k\partial_k - \hat{\eta}_k)\mathcal{R}_k}{P_k}\right] - 2d\, Q_{d/2}\left[\frac{\left(k\partial_k - \frac{\eta_N}{2}\right)\mathcal{R}_k}{P_k}\right]\right\}, \quad (H.42)
\end{aligned}
$$

$$
\begin{aligned}
-\left(k\partial_k + \frac{d-2}{2}\gamma_g\right) Z_N &= \frac{1}{2(4\pi)^{d/2}}\left\{\frac{d(d+1)}{12} Q_{d/2-1}\left[\frac{(k\partial_k - \eta_N + 2\gamma_g)\mathcal{R}_k}{P_k - 2\Lambda}\right]\right. \\
&\quad - \frac{d(d-1)}{2} Q_{d/2}\left[\frac{(k\partial_k - \eta_N + 2\gamma_g)\mathcal{R}_k}{(P_k - 2\Lambda)^2}\right] + \frac{N_S}{6} Q_{d/2-1}\left[\frac{(k\partial_k - \hat{\eta}_k)\mathcal{R}_k}{P_k}\right] \\
&\quad \left. - \frac{d}{3} Q_{d/2-1}\left[\frac{\left(k\partial_k - \frac{\eta_N}{2}\right)\mathcal{R}_k}{P_k}\right] - 2\, Q_{d/2}\left[\frac{\left(k\partial_k - \frac{\eta_N}{2}\right)\mathcal{R}_k}{P_k^2}\right]\right\}, \quad (H.43)
\end{aligned}
$$

$$
\begin{aligned}
-\frac{\hat{\eta}_k}{2} + \frac{d-2}{4}\gamma_g &= \frac{1}{2(4\pi)^{d/2}}\frac{1}{Z_N}\left\{\left(\frac{(d+1)(d-4)}{4} + \frac{d}{16}\right) \times\right. \\
&\quad \left. Q_{d/2}\left[\frac{(k\partial_k - \eta_N + 2\gamma_g)\mathcal{R}_k}{(P_k - 2\Lambda)^2}\right] + \frac{3d-2}{64} Q_{d/2}\left[\frac{(k\partial_k - \hat{\eta}_k)\mathcal{R}_k}{P_k^2}\right]\right\}. \quad (H.44)
\end{aligned}
$$

H.1.2. *Second possibility*

We insert the regulator in such a way that $-\Box \to P_k \equiv -\Box + \mathcal{R}_k(-\Box)$, i.e., eq.(H.38), and then we calculate the inverse regularized propagator at first order in the curvature and second order in derivative of the scalars. The regularized Hessian takes the form

$$\frac{1}{\sqrt{g}}\left(\Gamma_k^{(2)} + \mathcal{R}_k\right) = \begin{pmatrix} K_{\mu\nu}{}^{\rho\sigma}\left(P_k - 2\Lambda\right) + U_{\mu\nu}{}^{\rho\sigma} + \frac{1}{Z_N}S_{\mu\nu}{}^{\rho\sigma} & -\frac{1}{\sqrt{Z_N}}K_{\mu\nu}{}^{\gamma\delta}\nabla_\gamma\hat{X}_{\hat{\mu}}\nabla_\delta \\ \frac{1}{\sqrt{Z_N}}K^{\rho\sigma\gamma\delta}\nabla_\gamma\hat{X}_{\hat{\mu}}\nabla_\delta & \hat{\delta}_{\hat{\mu}\hat{\nu}}P_k \end{pmatrix}$$
(H.45)

and its inverse is

$$\sqrt{g}\left[\left(\Gamma_k^{(2)} + \mathcal{R}_k\right)^{-1}_{11}\right]_{\rho\sigma}{}^{\alpha\beta} = \frac{1}{P_k - 2\Lambda}\left(K^{-1}\right)_{\rho\sigma}{}^{\alpha\beta}$$

$$- \frac{1}{(P_k - 2\Lambda)^2}\left(K^{-1}\right)_{\rho\sigma}{}^{\gamma\delta}\left(U + \frac{1}{Z_N}S\right)_{\gamma\delta}{}^{\epsilon\eta}\left(K^{-1}\right)_{\epsilon\eta}{}^{\alpha\beta}$$

$$- \frac{1}{Z_N}\frac{1}{P_k\left(P_k - 2\Lambda\right)^2}\left(K^{-1}\right)_{\rho\sigma}{}^{\gamma\delta}K_{\gamma\delta}{}^{\epsilon\eta}\nabla_\epsilon\hat{X}_{\hat{\mu}}K^{\tau\phi\lambda\omega}\nabla_\lambda\hat{X}^{\hat{\mu}}\left(K^{-1}\right)_{\tau\phi}{}^{\alpha\beta}\nabla_\eta\nabla_\omega\,,$$

$$\sqrt{g}\left[\left(\Gamma_k^{(2)} + \mathcal{R}_k\right)^{-1}_{12}\right]_{\rho\sigma\hat{\mu}} = \frac{1}{\sqrt{Z_N}}\frac{1}{P_k\left(P_k - 2\Lambda\right)}K_{\rho\sigma}{}^{\lambda\omega}\nabla_\lambda\hat{X}_{\hat{\mu}}\left(K^{-1}\right)_{\rho\sigma}{}^{\alpha\beta}\nabla_\omega\,,$$

$$\sqrt{g}\left[\left(\Gamma_k^{(2)} + \mathcal{R}_k\right)^{-1}_{21}\right]^{\alpha\beta}{}_{\hat{\mu}} = -\frac{1}{\sqrt{Z_N}}\frac{1}{P_k\left(P_k - 2\Lambda\right)}K^{\rho\sigma\lambda\omega}\nabla_\lambda\hat{X}_{\hat{\mu}}\left(K^{-1}\right)_{\rho\sigma}{}^{\alpha\beta}\nabla_\omega\,,$$

$$\sqrt{g}\left[\left(\Gamma_k^{(2)} + \mathcal{R}_k\right)^{-1}_{22}\right]_{\hat{\mu}\hat{\nu}} = \hat{\delta}_{\hat{\mu}\hat{\nu}}\frac{1}{P_k} - \frac{1}{P_k^2\left(P_k - 2\Lambda\right)}K_{\alpha\beta}{}^{\epsilon\eta}\nabla_\epsilon\hat{X}_{\hat{\mu}}K^{\tau\phi\lambda\omega}\nabla_\lambda\hat{X}_{\hat{\nu}}\left(K^{-1}\right)_{\tau\phi}{}^{\alpha\beta}\nabla_\eta\nabla_\omega\,.$$
(H.46)

Then the traces read

$$\mathcal{T}_{hh} = \frac{1}{2(4\pi)^{d/2}}\int d^d x\sqrt{g}\left\{\frac{d(d+1)}{2}Q_{d/2}\left[\frac{(k\partial_k - \eta_N + 2\gamma_g)\mathcal{R}_k}{P_k - 2\Lambda}\right]\right.$$

$$+ \frac{d(d+1)}{12}R\,Q_{d/2-1}\left[\frac{(k\partial_k - \eta_N + 2\gamma_g)\mathcal{R}_k}{P_k - 2\Lambda}\right]$$

$$- \left(\frac{d(d-1)}{2}R - \frac{1}{Z_N}\frac{(d+1)(d-4)}{4}\nabla_\mu\hat{X}_{\hat{\mu}}\nabla^\mu\hat{X}^{\hat{\mu}}\right)Q_{d/2}\left[\frac{(k\partial_k - \eta_N + 2\gamma_g)\mathcal{R}_k}{(P_k - 2\Lambda)^2}\right]$$

$$\left. + \frac{1}{Z_N}\left(\frac{d+1}{2} - \frac{1}{d-2}\right)\nabla_\mu\hat{X}_{\hat{\mu}}\nabla^\mu\hat{X}^{\hat{\mu}}Q_{d/2+1}\left[\frac{(k\partial_k - \eta_N + 2\gamma_g)\mathcal{R}_k}{P_k\left(P_k - 2\Lambda\right)^2}\right]\right\}\,,$$
(H.47)

$$\mathcal{T}_{xx} = \frac{1}{2(4\pi)^{d/2}}\int d^d x\sqrt{g}\left\{N_S Q_{d/2}\left[\frac{(k\partial_k - \hat{\eta}_k)\mathcal{R}_k}{P_k}\right] + \frac{N_S}{6}R\,Q_{d/2-1}\left[\frac{(k\partial_k - \hat{\eta}_k)\mathcal{R}_k}{P_k}\right]\right.$$

$$\left. + \frac{1}{Z_N}\frac{d}{8}\nabla_\mu\hat{X}_{\hat{\mu}}\nabla^\mu\hat{X}^{\hat{\mu}}\,Q_{d/2+1}\left[\frac{(k\partial_k - \hat{\eta}_k)\mathcal{R}_k}{P_k^2(P_k - 2\Lambda)}\right]\right\}\,,$$
(H.48)

$$
\mathcal{T}_{\bar{c}c} = -\frac{1}{(4\pi)^{d/2}} \int \mathrm{d}^d x \sqrt{g} \left\{ d\, Q_{d/2} \left[\frac{\left(k\partial_k - \frac{\eta_N}{2} \right) \mathcal{R}_k}{P_k} \right] + \frac{d}{6} R\, Q_{d/2-1} \left[\frac{\left(k\partial_k - \frac{\eta_N}{2} \right) \mathcal{R}_k}{P_k} \right] \right.
$$

$$
\left. + R\, Q_{d/2} \left[\frac{\left(k\partial_k - \frac{\eta_N}{2} \right) \mathcal{R}_k}{P_k^2} \right] \right\} . \tag{H.49}
$$

H.2. Hessian of the observable

In this section, we present the details of the calculation of the Hessian of the observable

$$
\Gamma_k^{\mathrm{rel}} = \int \mathrm{d}^d x\, \tilde{e}\, (A_0 + a_R R + a_1 \operatorname{tr}[\mathrm{M}]) . \tag{H.50}
$$

The first and second variations read

$$
\delta\tilde{e} = \tilde{e}\, e_{\hat{\mu}}^{\mu} \partial_\mu \delta \hat{X}^{\hat{\mu}} , \tag{H.51}
$$

$$
\delta^2 \tilde{e} = 2\tilde{e}\, e_{\hat{\mu}}^{[\mu} e_{\hat{\nu}}^{\nu]} \partial_\mu \delta \hat{X}^{\hat{\mu}} \partial_\nu \delta \hat{X}^{\hat{\nu}} , \tag{H.52}
$$

$$
\delta\operatorname{trM} = 2 g^{\mu\nu} \hat{\delta}_{\hat{\mu}\hat{\nu}} \partial_\mu \delta \hat{X}^{\hat{\mu}} \partial_\nu \hat{X}^{\hat{\nu}} + \delta g^{\mu\nu} \hat{\delta}_{\hat{\mu}\hat{\nu}} \partial_\mu \hat{X}^{\hat{\mu}} \partial_\nu \hat{X}^{\hat{\nu}} , \tag{H.53}
$$

$$
\delta^2 \operatorname{trM} = 2 g^{\mu\nu} \hat{\delta}_{\hat{\mu}\hat{\nu}} \partial_\mu \delta \hat{X}^{\hat{\mu}} \partial_\nu \delta \hat{X}^{\hat{\nu}} + 4 \delta g^{\mu\nu} \hat{\delta}_{\hat{\mu}\hat{\nu}} \partial_\mu \delta \hat{X}^{\hat{\mu}} \partial_\nu \hat{X}^{\hat{\nu}} + \delta^2 g^{\mu\nu} \hat{\delta}_{\hat{\mu}\hat{\nu}} \partial_\mu \hat{X}^{\hat{\mu}} \partial_\nu \hat{X}^{\hat{\nu}} . \tag{H.54}
$$

Since it holds

$$
\nabla_\mu \tilde{e} = \tilde{e} e_{\hat{\mu}}^{\alpha} \nabla_\alpha e_\mu^{\hat{\mu}} = -\tilde{e} e_\mu^{\hat{\mu}} \nabla_\alpha e_{\hat{\mu}}^{\alpha} \implies \nabla_\mu \left(\tilde{e}\, e_{\hat{\mu}}^{\mu} \right) = 0 , \tag{H.55}
$$

then

$$
\int \mathrm{d}^d x\, \delta\tilde{e} = \int \mathrm{d}^d x\, \partial_\mu \left(\tilde{e}\, e_{\hat{\mu}}^{\mu} \delta \hat{X}^{\hat{\mu}} \right) . \tag{H.56}
$$

Thus, the variation of the term coupled to A_0 is identically zero: this is a consequence of the fact that this term is a total derivative and so it behaves like a topological term. Moreover, the following identities hold

$$
\delta \int \mathrm{d}^d x\, \tilde{e}\, S = \int \mathrm{d}^d x\, \tilde{e} \left(\delta S - e_{\hat{\mu}}^{\mu} \delta \hat{X}^{\hat{\mu}} \partial_\mu S \right) , \tag{H.57}
$$

$$
\delta^2 \int \mathrm{d}^d x\, \tilde{e}\, S = \int \mathrm{d}^d x\, \tilde{e} \left(\delta^2 S - 2 e_{\hat{\mu}}^{\mu} \delta \hat{X}^{\hat{\mu}} \partial_\mu \delta S + 2 e_{\hat{\mu}}^{[\mu} e_{\hat{\nu}}^{\nu]} \partial_\mu \delta \hat{X}^{\hat{\mu}} \partial_\nu \delta \hat{X}^{\hat{\nu}} S \right) . \tag{H.58}
$$

Using the essential scheme on the LHS we have the following additional contribution[3]

$$
\int \mathrm{d}^d x\, \frac{\delta\Gamma^{\mathrm{rel}}}{\delta g_{\mu\nu}} \Psi_{\mu\nu}^g + \frac{\delta\Gamma^{\mathrm{rel}}}{\delta \hat{X}^{\hat{\mu}}} \Psi_{\hat{\mu}}^x = \int \mathrm{d}^d x\, \tilde{e}\, \{ -\gamma_g a_R R - (\gamma_g + \hat{\eta}_k) a_1 \operatorname{trM} \} . \tag{H.59}
$$

---

[3]Note that using eqs.(H.57) and (H.56) the variation of $\tilde{e}$ gives no contribution.

The Hessian of the term associated to a_1 is

$$\frac{1}{Z_N} g_{\rho\alpha} g_{\sigma\beta} \frac{\delta^2}{\delta g_{\mu\nu} \delta g_{\alpha\beta}} \int d^d x \, \tilde{e} \, \mathrm{trM} = 2\tilde{e} \, \delta^{(\mu}_{(\rho} g^{\nu)\alpha} \delta^\beta_{\sigma)} \hat{\delta}_{\hat{\mu}\hat{\nu}} \partial_\alpha \hat{X}^{\hat{\mu}} \partial_\beta \hat{X}^{\hat{\nu}} \,, \tag{H.60}$$

$$\frac{\delta^2}{\delta \hat{X}^{\hat{\mu}} \delta \hat{X}^{\hat{\nu}}} \int d^d x \, \tilde{e} \, \mathrm{trM} = \tilde{e} \Big\{ -2\hat{\delta}_{\hat{\mu}\hat{\nu}} \Box - 2 g^{\mu\nu} \hat{\delta}_{\hat{\mu}\hat{\nu}} \, e^\alpha_{\hat{\rho}} \nabla_\mu \nabla_\alpha \hat{X}^{\hat{\rho}} \nabla_\nu \tag{H.61}$$

$$-4 g^{\mu\nu} \hat{\delta}_{\hat{\rho}(\hat{\mu}} e^\alpha_{\hat{\nu})} \partial_\mu \hat{X}^{\hat{\rho}} \nabla_\nu \nabla_\alpha - 4 g^{\mu\nu} \hat{\delta}_{\hat{\rho}(\hat{\mu}} e^\alpha_{\hat{\nu})} \nabla_\mu \nabla_\alpha \hat{X}^{\hat{\rho}} \nabla_\nu \Big\} \,,$$

$$\frac{1}{\sqrt{Z_N}} \frac{\delta^2}{\delta \hat{X}^{\hat{\mu}} \delta g_{\mu\nu}} \int d^d x \, \tilde{e} \, \mathrm{trM} = \tilde{e} \mathbb{1}^{\mu\nu\alpha\beta} \Big\{ -2 \, \hat{\delta}_{\hat{\mu}\hat{\nu}} \partial_\alpha \hat{X}^{\hat{\mu}} \nabla_\beta \tag{H.62}$$

$$-\hat{\delta}_{\hat{\nu}\hat{\rho}} e^\rho_{\hat{\mu}} \partial_\alpha \hat{X}^{\hat{\nu}} \partial_\beta \hat{X}^{\hat{\rho}} \nabla_\rho - 2 \hat{\delta}_{\hat{\nu}\hat{\rho}} e^\rho_{\hat{\mu}} \nabla_\alpha \nabla_\rho \hat{X}^{\hat{\nu}} \partial_\beta \hat{X}^{\hat{\rho}} + 2 \hat{\delta}_{\hat{\nu}\hat{\rho}} e^\rho_{\hat{\mu}} \nabla_\alpha \nabla_\rho \hat{X}^{\hat{\nu}} \partial_\beta \hat{X}^{\hat{\rho}} \Big\} \,,$$

$$\frac{1}{\sqrt{Z_N}} \frac{\delta^2}{\delta g_{\mu\nu} \delta \hat{X}^{\hat{\mu}}} \int d^d x \, \tilde{e} \, \mathrm{trM} = \tilde{e} \mathbb{1}^{\mu\nu\alpha\beta} \Big\{ 2 \, \hat{\delta}_{\hat{\mu}\hat{\nu}} \partial_\alpha \hat{X}^{\hat{\mu}} \nabla_\beta + 2 \, \hat{\delta}_{\hat{\mu}\hat{\nu}} \nabla_\alpha \nabla_\beta \hat{X}^{\hat{\nu}} \tag{H.63}$$

$$+ 2 \, \hat{\delta}_{\hat{\mu}\hat{\nu}} e^\rho_{\hat{\rho}} \nabla_\alpha \nabla_\rho \hat{X}^{\hat{\rho}} \partial_\beta \hat{X}^{\hat{\nu}} + \hat{\delta}_{\hat{\nu}\hat{\rho}} e^\rho_{\hat{\mu}} \partial_\alpha \hat{X}^{\hat{\nu}} \partial_\beta \hat{X}^{\hat{\rho}} \nabla_\rho + 2 \hat{\delta}_{\hat{\nu}\hat{\rho}} e^\rho_{\hat{\mu}} \nabla_\alpha \nabla_\rho \hat{X}^{\hat{\nu}} \partial_\beta \hat{X}^{\hat{\rho}} \Big\} \,.$$

The Hessian of the term associated to a_R is

$$\frac{1}{Z_N} g_{\rho\alpha} g_{\sigma\beta} \frac{\delta^2}{\delta g_{\mu\nu} \delta g_{\alpha\beta}} \int d^d x \, \tilde{e} \, R = \tilde{e} \, \Big\{ \frac{1}{2} \left(\mathbb{1}^{\mu\nu}{}_{\rho\sigma} + g^{\mu\nu} g_{\rho\sigma} \right) \Box$$

$$- 2\delta^{(\mu}_{(\rho} g^{\nu)\alpha} \delta^\beta_{\sigma)} \nabla_{(\alpha} \nabla_{\beta)} + \delta^{(\mu}_{(\rho} R^{\nu)}_{\sigma)} + R^{(\mu}{}_{(\rho}{}^{\nu)}{}_{\sigma)} \Big\} \tag{H.64}$$

$$+ \tilde{e} e^\delta_{\hat{\mu}} \left(\nabla^\gamma \nabla_\delta \hat{X}^{\hat{\mu}} \right) \left\{ -\frac{3}{2} \mathbb{1}^{\mu\nu}{}_{\rho\sigma} \nabla_\gamma - \frac{1}{2} g^{\mu\nu} g_{\rho\sigma} \nabla_\gamma \right\}$$

$$+ \tilde{e} e^\delta_{\hat{\mu}} \left\{ 3 \delta^{(\mu}_{(\rho} g^{\nu)\alpha} \delta^\beta_{\sigma)} \left(\nabla_\delta \nabla_{(\alpha} \hat{X}^{\hat{\mu}} \right) \nabla_{\beta)} \right\}$$

$$- \left(\mathbb{1}^{\mu\nu\alpha\beta} g_{\rho\sigma} + \mathbb{1}_{\rho\sigma}{}^{\alpha\beta} g^{\mu\nu} \right) \left(\nabla_\delta \nabla_{(\alpha} \hat{X}^{\hat{\mu}} \right) \nabla_{\beta)} \,,$$

$$\frac{\delta^2}{\delta \hat{X}^{\hat{\mu}} \delta \hat{X}^{\hat{\nu}}} \int d^d x \, \tilde{e} \, R = 0 \,, \tag{H.65}$$

$$\frac{1}{\sqrt{Z_N}} \frac{\delta^2}{\delta \hat{X}^{\hat{\mu}} \delta g_{\mu\nu}} \int d^d x \, \tilde{e} \, R = \tilde{e} \, e^\rho_{\hat{\mu}} \mathbb{1}^{\mu\nu\alpha\beta} \left\{ \nabla_\alpha \nabla_\beta - g_{\alpha\beta} \Box - R_{\alpha\beta} \right\} \nabla_\rho \,, \tag{H.66}$$

$$\frac{1}{\sqrt{Z_N}} \frac{\delta^2}{\delta g_{\mu\nu} \delta \hat{X}^{\hat{\mu}}} \int d^d x \, \tilde{e} \, R = -\tilde{e} \, e^\rho_{\hat{\mu}} \mathbb{1}^{\mu\nu\alpha\beta} \left\{ \nabla_\rho \nabla_\alpha \nabla_\beta - g_{\alpha\beta} \nabla_\rho \Box - R_{\alpha\beta} \nabla_\rho \right\} \,. \tag{H.67}$$

H.3. Calculations of the flow of the observables

In this section we report the calculations outsourced from Subsection 13.3.2. For the action in eq.(H.1), in Subsection H.1.1 we define the new covariant derivative in eq.(H.20) in order to have the propagator in the form given in (H.32). The same must be done also in the Hessian of the observable. Therefore, we change the "free" derivatives acting on the right with the new covariant derivative (H.20).

Using the following identities of the Heat kernel machinery [252] (see Appendix C)

$$H = \frac{1}{(4\pi s)^2}(A_0 + s\,A_1)\,, \tag{H.68}$$

$$H_\mu = \frac{1}{(4\pi s)^2}(\mathcal{D}_\mu A_0 + s\,\mathcal{D}_\mu A_1)\,, \tag{H.69}$$

$$H_{(\mu\nu)}(x,s) = \frac{1}{(4\pi s)^2}\left(-\frac{1}{2s}g_{\mu\nu}A_0 - \frac{1}{2}g_{\mu\nu}A_1 + \mathcal{D}_{(\mu}\mathcal{D}_{\nu)}A_0\right)\,, \tag{H.70}$$

where s represents the proper time and

$$A_0 = 1\,, \qquad \mathcal{D}_\mu A_0 = 0\,, \qquad \mathcal{D}_{(\mu}\mathcal{D}_{\nu)}A_0 = \tfrac{1}{6}R_{\mu\nu}\,, \qquad \ldots \tag{H.71}$$

$$A_1 = \tfrac{1}{6}R\,, \qquad \mathcal{D}_\mu A_1 = -\tfrac{1}{2}\nabla_\mu E + \tfrac{1}{6}\nabla_\nu\Omega^\nu{}_\mu + \tfrac{1}{12}\nabla_\mu R\,, \qquad \ldots \tag{H.72}$$

it is clear that all the terms in the Hessian of the observables with one derivative acting on the right contribute to order ∂^4 since they are proportional to the curvature or to at least one derivative of the scalar fields. The terms with three derivatives contains as well higher order terms.

Analyzing in a schematic way the core of the RHS of eq.(13.39), we have

$$\mathrm{Tr}\left[\mathcal{G}_k \cdot \left(\Gamma_k^{\mathrm{rel}(2)}\right)\cdot \mathcal{G}_k \cdot k\partial_k \mathcal{R}_k\right] =$$

$$= \mathrm{Tr}\left[\frac{1}{g}\begin{pmatrix}\mathcal{G}_{gg} & 0 \\ 0 & \mathcal{G}_{XX}\end{pmatrix}\cdot\begin{pmatrix}\left(\Gamma_k^{\mathrm{rel}(2)}\right)_{gg} & \left(\Gamma_k^{\mathrm{rel}(2)}\right)_{gX} \\ \left(\Gamma_k^{\mathrm{rel}(2)}\right)_{Xg} & \left(\Gamma_k^{\mathrm{rel}(2)}\right)_{XX}\end{pmatrix}\cdot\begin{pmatrix}\mathcal{G}_{gg}\cdot k\partial_k\mathcal{R}_k^{hh} & 0 \\ 0 & \mathcal{G}_{XX}\cdot k\partial_k\mathcal{R}_k^{xx}\end{pmatrix}\right]$$

$$= \mathrm{Tr}\left[\frac{1}{g}\begin{pmatrix}\mathcal{G}_{gg}\cdot\left(\Gamma_k^{\mathrm{rel}(2)}\right)_{gg}\cdot\mathcal{G}_{gg}\cdot k\partial_k\mathcal{R}_k^{hh} & \mathcal{G}_{gg}\cdot\left(\Gamma_k^{\mathrm{rel}(2)}\right)_{gX}\cdot\mathcal{G}_{XX}\cdot k\partial_k\mathcal{R}_k^{xx} \\ \mathcal{G}_{XX}\cdot\left(\Gamma_k^{\mathrm{rel}(2)}\right)_{Xg}\cdot\mathcal{G}_{gg}\cdot k\partial_k\mathcal{R}_k^{hh} & \mathcal{G}_{XX}\cdot\left(\Gamma_k^{\mathrm{rel}(2)}\right)_{XX}\cdot\mathcal{G}_{XX}\cdot k\partial_k\mathcal{R}_k^{xx}\end{pmatrix}\right]$$

$$= \mathrm{Tr}\left[\frac{1}{\sqrt{g}}\mathcal{G}_{gg}\cdot\left(\Gamma_k^{\mathrm{rel}(2)}\right)_{gg}\cdot\mathcal{G}_{gg}\cdot k\partial_k\left(\frac{\mathcal{R}_k^{hh}}{\sqrt{g}}\right)\right]$$

$$+ \mathrm{Tr}\left[\frac{1}{\sqrt{g}}\mathcal{G}_{XX}\cdot\left(\Gamma_k^{\mathrm{rel}(2)}\right)_{XX}\cdot\mathcal{G}_{XX}\cdot k\partial_k\left(\frac{\mathcal{R}_k^{xx}}{\sqrt{g}}\right)\right]\,. \tag{H.73}$$

We can see that defining the covariant derivative (H.20), it is possible to simplify the analysis also for the flow of the observable since we don't need the mixed terms of the Hessian at second order in derivative.

In eq.(H.73) then the propagators must be expanded using eqs.(H.33) and (H.34) keeping only terms at order ∂^2.

Moreover, note that the first factor $1/\sqrt{g}$ simplifies with the factor $\sqrt{g}$ coming from the heat kernel coefficients, while the second factor $1/\sqrt{g}$ under the regulators cancels using the eq.(H.38), which is needed to have the form (H.32) for the propagator. This

implies that in all the integrals we find only the factor $\tilde{e}$ in the measure, like the RHS of (H.50).

At this point, we are ready to calculate the RHS of (13.39) using (H.73).

The contributions on the RHS proportional to a_1 from graviton

$$-\frac{a_1\,G}{2\pi}\left(\int \mathrm{d}^d x\,\tilde{e}\,8\,\mathrm{tr}\,\mathrm{M}\right)Q_2\left[\frac{(k\partial_k - \eta_h)\,\mathcal{R}_k}{(P_k - 2\Lambda)^2}\right].\tag{H.74}$$

The contributions on the RHS proportional to a_1 from scalar

$$-\frac{a_1}{16\pi^2}\left(\int \mathrm{d}^d x\,\tilde{e}\,8\right)Q_3\left[\frac{(k\partial_k - \hat{\eta}_k)\,\mathcal{R}_k}{P_k^2}\right] - \frac{a_1}{16\pi^2}\left(\int \mathrm{d}^d x\,\tilde{e}\,\frac{2}{3}R\right)Q_2\left[\frac{(k\partial_k - \hat{\eta}_k)\,\mathcal{R}_k}{P_k^2}\right]\tag{H.75}$$

$$-\frac{a_1\,G}{\pi}\left(\int \mathrm{d}^d x\,\tilde{e}\,\frac{5}{8}\,\mathrm{tr}\,\mathrm{M}\right)Q_3\left[\frac{(k\partial_k - \hat{\eta}_k)\,\mathcal{R}_k}{P_k^3}\right].$$

The contributions on the RHS proportional to a_R from graviton

$$-\frac{a_R\,G}{\pi}\left(\int \mathrm{d}^d x\,\tilde{e}\,12\right)Q_3\left[\frac{(k\partial_k - \eta_h)\,\mathcal{R}_k}{(P_k - 2\Lambda)^2}\right]\tag{H.76}$$

$$-\frac{a_R\,G}{2\pi}\left(\int \mathrm{d}^d x\,\tilde{e}\,\frac{10}{3}R\right)Q_2\left[\frac{(k\partial_k - \eta_h)\,\mathcal{R}_k}{(P_k - 2\Lambda)^2}\right]\tag{H.77}$$

$$+\frac{a_R\,G}{\pi}\int \mathrm{d}^d x\,\tilde{e}\left(12R - \frac{3}{8}16\pi G\,\mathrm{tr}\,\mathrm{M}\right)Q_3\left[\frac{(k\partial_k - \eta_h)\,\mathcal{R}_k}{(P_k - 2\Lambda)^3}\right].$$

The contributions on the RHS proportional to a_R from the scalars are zero. Therefore, putting all the contributions together

$$k\partial_k A_0 = -\frac{a_1}{2\pi^2}Q_3\left[\frac{(k\partial_k - \hat{\eta}_k)\,\mathcal{R}_k}{P_k^2}\right] - \frac{12a_R\,G}{\pi}Q_3\left[\frac{(k\partial_k - \eta_h)\,\mathcal{R}_k}{(P_k - 2\Lambda)^2}\right],\tag{H.78}$$

$$k\partial_k a_R - \gamma_g\,a_R = -\frac{a_1}{24\pi^2}Q_2\left[\frac{(k\partial_k - \hat{\eta}_k)\,\mathcal{R}_k}{P_k^2}\right] - \frac{5a_R\,G}{3\pi}Q_2\left[\frac{(k\partial_k - \eta_h)\,\mathcal{R}_k}{(P_k - 2\Lambda)^2}\right]$$

$$+\frac{12a_R\,G}{\pi}Q_3\left[\frac{(k\partial_k - \eta_h)\,\mathcal{R}_k}{(P_k - 2\Lambda)^3}\right],\tag{H.79}$$

$$k\partial_k a_1 - (\gamma_g + \hat{\eta}_k)\,a_1 = -\frac{4a_1\,G}{\pi}Q_2\left[\frac{(k\partial_k - \eta_h)\,\mathcal{R}_k}{(P_k - 2\Lambda)^2}\right] - \frac{5a_1\,G}{8\pi}Q_3\left[\frac{(k\partial_k - \hat{\eta}_k)\,\mathcal{R}_k}{P_k^3}\right]$$

$$- 6a_R\,G^2Q_3\left[\frac{(k\partial_k - \eta_h)\,\mathcal{R}_k}{(P_k - 2\Lambda)^3}\right].\tag{H.80}$$

Author's publications

[RF1] R. Ferrero and M. Reuter. "Towards a Geometrization of Renormalization Group Histories in Asymptotic Safety". In: *Universe* 7.5 (2021), p. 125. arXiv: 2103.15709 [hep-th].

[RF2] R. Ferrero and M. Reuter. "On the possibility of a novel (A)dS/CFT relationship emerging in Asymptotic Safety". In: *JHEP* 12 (2022), p. 118.arXiv: 2205.12030 [hep-th].

[RF3] R. Ferrero and M. Reuter. "The spectral geometry of de Sitter space in asymptotic safety". In: *JHEP* 08 (2022), p. 040. arXiv: 2203.08003 [hep-th].

[RF4] R. Ferrero and C. Ripken. "De Sitter scattering amplitudes in the Born approximation". In: *SciPost Phys.* 13 (2022), p. 106. arXiv: 2112.03766 [hep-th].

[RF5] R. Ferrero and C. Ripken. "Quadratic gravity potentials in de Sitter spacetime from Feynman diagrams". In: *JHEP* 08 (2023), p. 199. arXiv: 2212.08052 [hep-th].

[RF6] R. Ferrero and R. Percacci. "Dynamical diffeomorphisms". In: *Class. Quant. Grav.* 38.11 (2021), p. 115011. arXiv: 2012.04507 [gr-qc].

[RF7] A. Baldazzi, K. Falls, and R. Ferrero. "Relational observables in asymptotically safe gravity". In: *Annals Phys.* 440 (2022), p. 168822. arXiv: 2112. 02118 [hep-th].

[RF8] R. Banerjee, M. Becker, and R. Ferrero. "N-cutoff regularization for fields on hyperbolic space". In: accepted in *Phys. Rev. D* (Feb. 2023). arXiv: 2302.03547 [hep-th]].

Bibliography

[1]   J. Stachel. "The Early History of Quantum Gravity (1916–1940)". In: *Fundam. Theor. Phys.* 100 (1999), pp. 525–534.

[2]   S. Carlip et al. "Quantum Gravity: A Brief History of Ideas and Some Prospects". In: *Int. J. Mod. Phys. D* 24.11 (2015), p. 1530028. arXiv: 1507.08194 [gr-qc].

[3]   R. Loll et al. "Quantum Gravity in 30 Questions". In: *PoS* CORFU2021 (2022), p. 316. arXiv: 2206.06762 [hep-th].

[4]   A. Einstein and M. Grossmann. *Entwurf einer verallgemeinerten Relativitätstheorie und einer Theorie der Gravitation.* Zeitschrift für Mathematik und Physik. Druck und Verlag von B.G. Teubner, 1914.

[5]   A. Einstein and M. Grossmann. "Kovarianzeigenschaften der Feldgleichungen der auf die verallgemeinerte Relativitätstheorie gegründeten Gravitationstheorie". In: *Zeitschrift für Mathematik und Physik* 63 (Jan. 1914), pp. 215–225.

[6]   A. Einstein. "Prinzipielles zur verallgemeinerten Relativitätstheorie und Gravitationstheorie". In: *Physikalische Zeitschrift* 15 (1914), pp. 176–180.

[7]   A. Einstein. "Die Grundlage der allgemeinen Relativitätstheorie". In: *Annalen der Physik* 354.7 (Jan. 1916), pp. 769–822.

[8]   A. Einstein. "Näherungsweise Integration der Feldgleichungen der Gravitation". In: *Sitzungsberichte der königlich-preußischen Akadademie der Wissenschaften zu Berlin.* 1916, 688–696.

[9]   L. Rosenfeld. "Über die Gravitationswirkungen des Lichts". In: *Zeitschrift für Physik* 65 (1930), 589–599.

[10] M. Fierz and W. Pauli. "On relativistic wave equations for particles of arbitrary spin in an electromagnetic field". In: *Proc. Roy. Soc. Lond. A* 173 (1939), pp. 211–232.

[11] M. P. Bronstein. "Quantification of gravitational waves". In: *Zhurnal Eksperimentalnoi i Teoreticheskoi Fiziki* 6 (Jan. 1930), p. 195.

[12] M. Bronstein. "Quantentheorie schwacher Gravitationsfelder". In: *Physikalische Zeitschrift der Sowjetunion* 9 (1936), 140–157.

[13] J. Solomon. "Gravitation et Quanta". In: *Journal de Physique et Le Radium* 9 (1938), 479–485.

[14] D. van Dantzig. "Some possibilities of the future development of the notions of space and time ". In: *Erkenntnis* 7 (1937), 142–146.

[15] B. S. DeWitt. "Quantum Theory of Gravity. 1. The Canonical Theory". In: *Phys. Rev.* 160 (1967). Ed. by L.-Z. Fang and R. Ruffini, pp. 1113–1148.

[16] B. S. DeWitt. "Quantum Theory of Gravity. II. The Manifestly Covariant Theory". In: *Phys. Rev.* 162 (5 1967), pp. 1195–1239.

[17] B. S. DeWitt. "Quantum Theory of Gravity. 3. Applications of the Covariant Theory". In: *Phys. Rev.* 162 (1967). Ed. by J.-P. Hsu and D. Fine, pp. 1239–1256.

[18] G. 't Hooft and M. J. G. Veltman. "One loop divergencies in the theory of gravitation". In: *Ann. Inst. H. Poincare Phys. Theor. A* 20 (1974), pp. 69–94.

[19] M. H. Goroff and A. Sagnotti. "Quantum Gravity at two loops". In: *Phys. Lett.* B160 (1985), p. 81.

[20] M. H. Goroff and A. Sagnotti. "The Ultraviolet Behavior of Einstein Gravity". In: *Nucl. Phys.* B266 (1986), p. 709.

[21] A. E. M. van de Ven. "Two loop quantum gravity". In: *Nucl. Phys. B* 378 (1992), pp. 309–366.

[22] C. Rovelli. *Quantum gravity.* Cambridge Monographs on Mathematical Physics. Cambridge, UK: Univ. Pr., 2004.

[23] C. Kiefer. *Quantum Gravity.* 2nd ed. New York: Oxford University Press, 2007.

[24] A. Ashtekar, M. Reuter, and C. Rovelli. "From General Relativity to Quantum Gravity". In: (Aug. 2014). arXiv: 1408.4336 [gr-qc].

[25] C. D. Hoyle et al. "Submillimeter tests of the gravitational inverse-square law". In: *Phys. Rev. D* 70 (4 2004), p. 042004.

[26] E. G. Adelberger et al. "Particle-Physics Implications of a Recent Test of the Gravitational Inverse-Square Law". In: *Phys. Rev. Lett.* 98 (13 2007), p. 131104.

[27] D. J. Kapner et al. "Tests of the gravitational inverse-square law below the dark-energy length scale". In: *Phys. Rev. Lett.* 98 (2007), p. 021101. arXiv: hep-ph/0611184.

[28] A. O. Sushkov et al. "New Experimental Limits on Non-Newtonian Forces in the Micrometer Range". In: *Phys. Rev. Lett.* 107 (2011), p. 171101. arXiv: 1108.2547 [quant-ph].

[29] D. Giulini. "Some remarks on the notions of general covariance and background independence". In: *Lect. Notes Phys.* 721 (2007), pp. 105–120. arXiv: gr-qc/0603087.

[30] C. J. Isham. "Prima facie questions in quantum gravity". In: *Lect. Notes Phys.* 434 (1994). Ed. by J. Ehlers and H. Friedrich, pp. 1–21. arXiv: gr-qc/9310031.

[31] C. Kiefer. *Why Quantum Gravity?* Approaches to Fundamental Physics. edited by E. Seiler and I.-O. Stamatescu, 2007.

[32] M. Becker and M. Reuter. "Background Independent Field Quantization with Sequences of Gravity-Coupled Approximants". In: *Phys. Rev. D* 102.12 (2020), p. 125001. arXiv: 2008.09430 [gr-qc].

[33] D. J. W. Giulini, C. Kiefer, and C. Lammerzahl, eds. *Proceedings, 271st WE-Heraeus Seminar on Aspects of Quantum Gravity: From Theory to Experiment Search: Bad Honnef, Germany, February 25-March 1, 2002.* Vol. 631. 2003, pp.1–242.

[34] B. P. Abbott et al. "Multi-messenger Observations of a Binary Neutron Star Merger". In: *Astrophys. J. Lett.* 848.2 (2017), p. L12. arXiv: 1710.05833 [astro-ph.HE].

[35] G. Aad et al. "Observation of a new particle in the search for the Standard Model Higgs boson with the ATLAS detector at the LHC". In: *Phys. Lett. B* 716 (2012), pp. 1–29. arXiv: 1207.7214 [hep-ex].

[36] S. Chatrchyan et al. "Observation of a New Boson at a Mass of 125 GeV with the CMS Experiment at the LHC". In: *Phys. Lett. B* 716 (2012), pp. 30–61. arXiv: 1207.7235 [hep-ex].

[37] B. P. Abbott et al. "GW170817: Observation of Gravitational Waves from a Binary Neutron Star Inspiral". In: *Phys. Rev. Lett.* 119.16 (2017), p. 161101. arXiv: 1710.05832 [gr-qc].

[38] C. Kiefer and M. Kraemer. "Quantum Gravitational Contributions to the CMB Anisotropy Spectrum". In: *Phys. Rev. Lett.* 108 (2012), p. 021301. arXiv: 1103.4967 [gr-qc].

[39] C. Kiefer and M. Kraemer. "Can effects of quantum gravity be observed in the cosmic microwave background?" In: *Int. J. Mod. Phys. D* 21 (2012), p. 1241001. arXiv: 1205.5161 [gr-qc].

[40] R. Loll. "Discrete approaches to quantum gravity in four-dimensions". In: *Living Rev. Rel.* 1 (1998), p. 13. arXiv: gr-qc/9805049.

[41] B. P. Abbott et al. "Search for Tensor, Vector, and Scalar Polarizations in the Stochastic Gravitational-Wave Background". In: *Phys. Rev. Lett.* 120.20 (2018), p. 201102. arXiv: 1802.10194 [gr-qc].

[42] N. E. J Bjerrum-Bohr, J. F. Donoghue, and B. R. Holstein. "Quantum gravitational corrections to the nonrelativistic scattering potential of two masses". In: *Phys. Rev. D* 67 (2003). [Erratum: Phys.Rev.D 71, 069903 (2005)], p. 084033. arXiv: hep-th/0211072.

[43] A. Buonanno et al. "Snowmass White Paper: Gravitational Waves and Scattering Amplitudes". In: *Snowmass 2021.* Apr. 2022. arXiv: 2204.05194 [hep-th].

[44] T. Thiemann. *Modern Canonical Quantum General Relativity.* Cambridge Monographs on Mathematical Physics. Cambridge University Press, 2007.

[45] J. M. Maldacena. "The Large N limit of superconformal field theories and supergravity". In: *Adv. Theor. Math. Phys.* 2 (1998), pp. 231–252. arXiv: hep-th/9711200.

[46] A. Ashtekar. *Lectures on nonperturbative canonical gravity*. Vol. 6. 1991.

[47] A. Ashtekar and J. Lewandowski. "Background independent quantum gravity: A Status report". In: *Class. Quant. Grav.* 21 (2004), R53. arXiv: gr-qc/0404018.

[48] K. Gawedzki and A. Kupiainen. "Renormalizing the Nonrenormalizable". In: *Phys. Rev. Lett.* 55 (1985), pp. 363–365.

[49] M. Reuter and F. Saueressig. *Quantum Gravity and the Functional Renormalization Group: The Road towards Asymptotic Safety*. Cambridge University Press, Jan. 2019.

[50] R. Percacci. *An Introduction to Covariant Quantum Gravity and Asymptotic Safety*. Vol. 3. 100 Years of General Relativity. World Scientific, 2017.

[51] F. Saueressig. "The Functional Renormalization Group in Quantum Gravity". In: (Feb. 2023). arXiv: 2302.14152 [hep-th].

[52] H. W. Hamber. "Phases of four-dimensional simplicial quantum gravity". In: *Phys. Rev. D* 45 (2 1992), pp. 507–512.

[53] H. W. Hamber. "Quantum Gravity on the Lattice". In: *Gen. Rel. Grav.* 41 (2009), pp. 817–876. arXiv: 0901.0964 [gr-qc].

[54] T. Regge and R. M. Williams. "Discrete structures in gravity". In: *J. Math. Phys.* 41 (2000), pp. 3964–3984. arXiv: gr-qc/0012035.

[55] J. Ambjorn, J. Jurkiewicz, and R. Loll. "Emergence of a 4-D world from causal quantum gravity". In: *Phys. Rev. Lett.* 93 (2004), p. 131301. arXiv: hep-th/0404156.

[56] J. Ambjorn, J. Jurkiewicz, and R. Loll. "Semiclassical universe from first principles". In: *Phys. Lett. B* 607 (2005), pp. 205–213. arXiv: hep-th/0411152.

[57] J. Ambjorn, J. Jurkiewicz, and R. Loll. "Reconstructing the universe". In: *Phys. Rev. D* 72 (2005), p. 064014. arXiv: hep-th/0505154.

[58] L. Bombelli et al. "Space-time as a causal set". In: *Phys. Rev. Lett.* 59 (5 1987), pp. 521–524.

[59] S. Surya. "The causal set approach to quantum gravity". In: *Living Rev. Rel.* 22.1 (2019), p. 5. arXiv: 1903.11544 [gr-qc].

[60] R. M. Wald. *Quantum Field Theory in Curved Space-Time and Black Hole Thermodynamics*. Chicago Lectures in Physics. Chicago, IL: University of Chicago Press, 1995.

[61] A. Connes. *Noncommutative Geometry*. Academic Press, San Diego, 1994.

[62] A. Ashtekar, L. Bombelli, and O. Reula. "The covariant phase space of asymptotically flat gravitational fields". In: (May 1990).

[63] I. V. Kanatchikov. "Precanonical perspective in quantum gravity". In: *Nucl. Phys. B Proc. Suppl.* 88 (2000). Ed. by V. de Alfaro et al., pp. 326–330. arXiv: gr-qc/0004066.

[64] R. B. Griffiths. "Consistent histories and the interpretation of quantum mechanics". In: *Journal of Statistical Physics* 36 (1984), pp. 219–272.

[65] K. S. Stelle. "Renormalization of Higher Derivative Quantum Gravity". In: *Phys. Rev. D* 16 (1977), pp. 953–969.

[66] K. S. Stelle. "Classical Gravity with Higher Derivatives". In: *Gen. Rel. Grav.* 9 (1978), pp. 353–371.

[67] M. Niedermaier and M. Reuter. "The Asymptotic Safety Scenario in Quantum Gravity". In: *Living Rev. Rel.* 9 (2006), pp. 5–173.

[68] M. Atance and J. L. Cortes. "Effective field theory of gravity, reduction of couplings and the renormalization group". In: *Phys. Rev. D* 54 (1996), pp. 4973–4981. arXiv: hep-ph/9605455.

[69] J. Kubo and M. Nunami. "Unrenormalizable theories are predictive". In: *Eur. Phys. J. C* 26 (2003), pp. 461–472. arXiv: hep-th/0112032.

[70] A. Ashtekar. "Quantum mechanics of geometry". In: (Jan. 1999). arXiv: gr-qc/9901023.

[71] R. Loll. "Quantum Gravity from Causal Dynamical Triangulations: A Review". In: *Class. Quant. Grav.* 37.1 (2020), p. 013002. arXiv: 1905.08669 [hep-th].

[72] R. Ferrero and M. Reuter. "Towards a Geometrization of Renormalization Group Histories in Asymptotic Safety". In: *Universe* 7.5 (2021), p. 125. arXiv: 2103.15709 [hep-th].

[73] R. Ferrero and M. Reuter. "On the possibility of a novel (A)dS/CFT relationship emerging in Asymptotic Safety". In: *JHEP* 12 (2022), p. 118. arXiv: 2205.12030 [hep-th].

[74] R. Ferrero and M. Reuter. "The spectral geometry of de Sitter space in asymptotic safety". In: *JHEP* 08 (2022), p. 040. arXiv: 2203.08003 [hep-th].

[75] R. Ferrero and C. Ripken. "De Sitter scattering amplitudes in the Born approximation". In: *SciPost Phys.* 13 (2022), p. 106. arXiv: 2112.03766 [hep-th].

[76] R. Ferrero and C. Ripken. "Quadratic gravity potentials in de Sitter spacetime from Feynman diagrams". In: *JHEP* 08 (2023), p. 199. arXiv: 2212.08052 [hep-th].

[77] R. Ferrero and R. Percacci. "Dynamical diffeomorphisms". In: *Class. Quant. Grav.* 38.11 (2021), p. 115011. arXiv: 2012.04507 [gr-qc].

[78] A. Baldazzi, K. Falls, and R. Ferrero. "Relational observables in asymptotically safe gravity". In: *Annals Phys.* 440 (2022), p. 168822. arXiv: 2112.02118 [hep-th].

[79] R. Banerjee, M. Becker, and R. Ferrero. "N-cutoff regularization for fields on hyperbolic space". In: (Feb. 2023). arXiv: 2302.03547 [hep-th].

[80] C. Pagani and M. Reuter. "Background Independent Quantum Field Theory and Gravitating Vacuum Fluctuations". In: *Annals Phys.* 411 (2019), p. 167972. arXiv: 1906.02507 [gr-qc].

[81] C. Pagani and M. Reuter. "Why the Cosmological Constant Seems to Hardly Care About Quantum Vacuum Fluctuations: Surprises From Background Independent Coarse Graining". In: *Front. in Phys.* 8 (2020), p. 214.

[82] C. G. Callan Jr. "Broken scale invariance in scalar field theory". In: *Phys. Rev. D* 2 (1970), pp. 1541–1547.

[83] K. Symanzik. "Small distance behavior in field theory and power counting". In: *Commun. Math. Phys.* 18 (1970), pp. 227–246.

[84] K. Symanzik. "Small distance behavior analysis and Wilson expansion". In: *Commun. Math. Phys.* 23 (1971), pp. 49–86.

[85] C. Wetterich. "Average Action and the Renormalization Group Equations". In: *Nucl. Phys. B* 352 (1991), pp. 529–584.

[86] K. G. Wilson and J. B. Kogut. "The Renormalization group and the epsilon expansion". In: *Phys. Rept.* 12 (1974), pp. 75–199.

[87] K. G. Wilson. "The Renormalization Group: Critical Phenomena and the Kondo Problem". In: *Rev. Mod. Phys.* 47 (1975), p. 773.

[88] L. P. Kadanoff. *Statistical physics: Statics, dynamics and renormalization.* 2000.

[89] T. R. Morris. "The Exact renormalization group and approximate solutions". In: *Int. J. Mod. Phys. A* 9 (1994), pp. 2411–2450. arXiv: hep-ph/9308265.

[90] M. Reuter and C. Wetterich. "Effective average action for gauge theories and exact evolution equations". In: *Nucl. Phys. B* 417 (1994), pp. 181–214.

[91] M. Reuter and F. Saueressig. "Asymptotic Safety, Fractals, and Cosmology". In: *Lect. Notes Phys.* 863 (2013). Ed. by G. Calcagni et al., pp. 185–223. arXiv: 1205.5431 [hep-th].

[92] M. Reuter and F. Saueressig. "Functional Renormalization Group Equations, Asymptotic Safety, and Quantum Einstein Gravity". In: *First Quantum Geometry and Quantum Gravity School.* 2010, pp. 288–329. arXiv: 0708.1317 [hep-th].

[93] M. Reuter and F. Saueressig. *Quantum Gravity and the Functional Renormalization Group.* Cambridge University Press, 2019.

[94] M. Fraaije, A. Platania, and F. Saueressig. "On the reconstruction problem in quantum gravity". In: *Phys. Lett. B* 834 (2022), p. 137399. arXiv: 2206.10626 [hep-th].

[95] M. Reuter. "Nonperturbative evolution equation for quantum gravity". In: *Phys.Rev. D57* (1998), pp. 971–985. arXiv: hep-th/9605030 [hep-th].

[96] S. Weinberg. "Ultraviolet divergences in quantum theories of gravitation". In: *General Relativity: An Einstein Centenary Survey.* 1980, pp. 790–831.

[97] M. Reuter and F. Saueressig. "Renormalization group flow of quantum gravity in the Einstein-Hilbert truncation". In: *Phys. Rev. D* 65 (2002), p. 065016. arXiv: hep-th/0110054.

[98] A. Bonanno et al. "Critical reflections on asymptotically safe gravity". In: *Front. in Phys.* 8 (2020), p. 269. arXiv: 2004.06810 [gr-qc].

[99] O. Lauscher and M. Reuter. "Is quantum Einstein gravity nonperturbatively renormalizable?" In: *Class. Quant. Grav.* 19 (2002), pp. 483–492. arXiv: hep-th/0110021.

[100] O. Lauscher and M. Reuter. "Fractal spacetime structure in asymptotically safe gravity". In: *JHEP* 10 (2005), p. 050. arXiv: hep-th/0508202.

[101] O. Lauscher and M. Reuter. "Towards nonperturbative renormalizability of quantum Einstein gravity". In: *Int. J. Mod. Phys. A* 17 (2002). Ed. by M. Bordag, pp. 993–1002. arXiv: hep-th/0112089.

[102] O. Lauscher and M. Reuter. "Flow equation of quantum Einstein gravity in a higher derivative truncation". In: *Phys. Rev. D* 66 (2002), p. 025026. arXiv: hep-th/0205062.

[103] E. Manrique and M. Reuter. "Bimetric Truncations for Quantum Einstein Gravity and Asymptotic Safety". In: *Annals Phys.* 325 (2010), pp. 785–815. arXiv: 0907.2617 [gr-qc].

[104] M. Demmel, F. Saueressig, and O. Zanusso. "RG flows of Quantum Einstein Gravity on maximally symmetric spaces". In: *JHEP* 06 (2014), p. 026. arXiv: 1401.5495 [hep-th].

[105] M. Demmel, F. Saueressig, and O. Zanusso. "Fixed-Functionals of three-dimensional Quantum Einstein Gravity". In: *JHEP* 11 (2012), p. 131. arXiv: 1208.2038 [hep-th].

[106] M. Demmel, F. Saueressig, and O. Zanusso. "A proper fixed functional for four-dimensional Quantum Einstein Gravity". In: *JHEP* 08 (2015), p. 113. arXiv: 1504.07656 [hep-th].

[107] P. Donà, A. Eichhorn, and R. Percacci. "Matter matters in asymptotically safe quantum gravity". In: *Phys. Rev. D* 89.8 (2014), p. 084035. arXiv: 1311.2898 [hep-th].

[108] D. Dou and R. Percacci. "The running gravitational couplings". In: *Class. Quant. Grav.* 15 (1998), pp. 3449–3468. arXiv: hep-th/9707239.

[109] K. Groh and F. Saueressig. "Ghost wave-function renormalization in Asymptotically Safe Quantum Gravity". In: *J. Phys. A* 43 (2010), p. 365403. arXiv: 1001.5032 [hep-th].

[110] A. Eichhorn, H. Gies, and M. M. Scherer. "Asymptotically free scalar curvature-ghost coupling in Quantum Einstein Gravity". In: *Phys. Rev. D* 80 (2009), p. 104003. arXiv: 0907.1828 [hep-th].

[111] A. Eichhorn and H. Gies. "Ghost anomalous dimension in asymptotically safe quantum gravity". In: *Phys. Rev. D* 81 (2010), p. 104010. arXiv: 1001.5033 [hep-th].

[112] A. Eichhorn et al. "Effective universality in quantum gravity". In: *SciPost Phys.* 5.4 (2018), p. 031. arXiv: 1804.00012 [hep-th].

[113] A. Eichhorn. "An asymptotically safe guide to quantum gravity and matter". In: *Front. Astron. Space Sci.* 5 (2019), p. 47. arXiv: 1810.07615 [hep-th].

[114] O. Lauscher and M. Reuter. "Ultraviolet fixed point and generalized flow equation of quantum gravity". In: *Phys. Rev. D* 65 (2002), p. 025013. arXiv: hep-th/0108040.

[115] E. Manrique, S. Rechenberger, and F. Saueressig. "Asymptotically Safe Lorentzian Gravity". In: *Phys. Rev. Lett.* 106 (2011), p. 251302. arXiv: 1102.5012 [hep-th].

[116] S. Rechenberger and F. Saueressig. "A functional renormalization group equation for foliated spacetimes". In: *JHEP* 03 (2013), p. 010. arXiv: 1212.5114 [hep-th].

[117] J. E. Daum and M. Reuter. "Renormalization Group Flow of the Holst Action". In: *Phys. Lett. B* 710 (2012), pp. 215–218. arXiv: 1012.4280 [hep-th].

[118] J.-E. Daum and M. Reuter. "Einstein-Cartan gravity, Asymptotic Safety, and the running Immirzi parameter". In: *Annals Phys.* 334 (2013), pp. 351–419. arXiv: 1301.5135 [hep-th].

[119] M. Reuter and F. Saueressig. "A Class of nonlocal truncations in quantum Einstein gravity and its renormalization group behavior". In: *Phys. Rev. D* 66 (2002), p. 125001. arXiv: hep-th/0206145.

[120] R. Percacci and D. Perini. "Asymptotic safety of gravity coupled to matter". In: *Phys. Rev. D* 68 (2003), p. 044018. arXiv: hep-th/0304222.

[121] R. Percacci and D. Perini. "Should we expect a fixed point for Newton's constant?" In: *Class. Quant. Grav.* 21 (2004), pp. 5035–5041. arXiv: hep-th/0401071.

[122] A. Bonanno and M. Reuter. "Proper time flow equation for gravity". In: *JHEP* 02 (2005), p. 035. arXiv: hep-th/0410191.

[123] G. P. Vacca and O. Zanusso. "Asymptotic Safety in Einstein Gravity and Scalar-Fermion Matter". In: *Phys. Rev. Lett.* 105 (2010), p. 231601. arXiv: 1009.1735 [hep-th].

[124] M. R. Niedermaier. "Gravitational Fixed Points from Perturbation Theory". In: *Phys. Rev. Lett.* 103 (2009), p. 101303.

[125] M. Niedermaier. "Gravitational fixed points and asymptotic safety from perturbation theory". In: *Nucl. Phys. B* 833 (2010), pp. 226–270.

[126] M. Reuter and H. Weyer. "Running Newton constant, improved gravitational actions, and galaxy rotation curves". In: *Phys. Rev. D* 70 (2004), p. 124028. arXiv: hep-th/0410117.

[127] M. Reuter and H. Weyer. "Background Independence and Asymptotic Safety in Conformally Reduced Gravity". In: *Phys. Rev. D* 79 (2009), p. 105005. arXiv: 0801.3287 [hep-th].

[128] M. Reuter and H. Weyer. "The Role of Background Independence for Asymptotic Safety in Quantum Einstein Gravity". In: *Gen. Rel. Grav.* 41 (2009), pp. 983–1011. arXiv: 0903.2971 [hep-th].

[129] M. Reuter and H. Weyer. "Conformal sector of Quantum Einstein Gravity in the local potential approximation: Non-Gaussian fixed point and a phase of unbroken diffeomorphism invariance". In: *Phys. Rev. D* 80 (2009), p. 025001. arXiv: 0804.1475 [hep-th].

[130] C. Pagani and R. Percacci. "Quantization and fixed points of non-integrable Weyl theory". In: *Class. Quant. Grav.* 31 (2014), p. 115005. arXiv: 1312.7767 [hep-th].

[131] A. Codello and R. Percacci. "Fixed points of higher derivative gravity". In: *Phys. Rev. Lett.* 97 (2006), p. 221301. arXiv: hep-th/0607128.

[132] A. Codello, R. Percacci, and C. Rahmede. "Investigating the Ultraviolet Properties of Gravity with a Wilsonian Renormalization Group Equation". In: *Annals Phys.* 324 (2009), pp. 414–469. arXiv: 0805.2909 [hep-th].

[133] A. Codello, R. Percacci, and C. Rahmede. "Ultraviolet properties of f(R)-gravity". In: *Int. J. Mod. Phys. A* 23 (2008), pp. 143–150. arXiv: 0705.1769 [hep-th].

[134] A. Codello and G. D'Odorico. "Scaling and Renormalization in two dimensional Quantum Gravity". In: *Phys. Rev. D* 92.2 (2015), p. 024026. arXiv: 1412.6837 [gr-qc].

[135] D. Benedetti, P. F. Machado, and F. Saueressig. "Asymptotic safety in higher-derivative gravity". In: *Mod. Phys. Lett. A* 24 (2009), pp. 2233–2241. arXiv: 0901.2984 [hep-th].

[136] D. Benedetti. "On the number of relevant operators in asymptotically safe gravity". In: *EPL* 102.2 (2013), p. 20007. arXiv: 1301.4422 [hep-th].

[137] D. Benedetti et al. "The Universal RG Machine". In: *JHEP* 06 (2011), p. 079. arXiv: 1012.3081 [hep-th].

[138] D. Benedetti and F. Caravelli. "The Local potential approximation in quantum gravity". In: *JHEP* 06 (2012). [Erratum: JHEP 10, 157 (2012)], p. 017. arXiv: 1204.3541 [hep-th].

[139] J.-E. Daum and M. Reuter. "Effective Potential of the Conformal Factor: Gravitational Average Action and Dynamical Triangulations". In: *Adv. Sci. Lett.* 2 (2009), pp. 255–260. arXiv: 0806.3907 [hep-th].

[140] J.-E. Daum, U. Harst, and M. Reuter. "Running Gauge Coupling in Asymptotically Safe Quantum Gravity". In: *JHEP* 01 (2010), p. 084. arXiv: 0910.4938 [hep-th].

[141] J.-E. Daum and M. Reuter. "The Effective Potential of the Conformal Factor in Quantum Einstein Gravity". In: *PoS* CLAQG08 (2011), p. 013. arXiv: 0910.5401 [hep-th].

[142] U. Harst and M. Reuter. "QED coupled to QEG". In: *JHEP* 05 (2011), p. 119. arXiv: 1101.6007 [hep-th].

[143] A. Nink and M. Reuter. "On the physical mechanism underlying Asymptotic Safety". In: *JHEP* 01 (2013), p. 062. arXiv: 1208.0031 [hep-th].

[144] D. Becker and M. Reuter. "Running boundary actions, Asymptotic Safety, and black hole thermodynamics". In: *JHEP* 07 (2012), p. 172. arXiv: 1205.3583 [hep-th].

[145] M. Reuter and F. Saueressig. "Quantum Einstein Gravity". In: *New J. Phys.* 14 (2012), p. 055022. arXiv: 1202.2274 [hep-th].

[146] D. Becker and M. Reuter. "Towards a C-function in 4D quantum gravity". In: *JHEP* 03 (2015), p. 065. arXiv: 1412.0468 [hep-th].

[147] D. Becker and M. Reuter. "En route to Background Independence: Broken split-symmetry, and how to restore it with bi-metric average actions". In: *Annals Phys.* 350 (2014), pp. 225–301. arXiv: 1404.4537 [hep-th].

[148] N. Ohta and R. Percacci. "Ultraviolet Fixed Points in Conformal Gravity and General Quadratic Theories". In: *Class. Quant. Grav.* 33 (2016), p. 035001. arXiv: 1506.05526 [hep-th].

[149] N. Ohta, R. Percacci, and G. P. Vacca. "Flow equation for $f(R)$ gravity and some of its exact solutions". In: *Phys. Rev. D* 92.6 (2015), p. 061501. arXiv: 1507.00968 [hep-th].

[150] N. Ohta, R. Percacci, and G. P. Vacca. "Renormalization Group Equation and scaling solutions for f(R) gravity in exponential parametrization". In: *Eur. Phys. J. C* 76.2 (2016), p. 46. arXiv: 1511.09393 [hep-th].

[151] H. Gies et al. "Gravitational Two-Loop Counterterm Is Asymptotically Safe". In: *Phys. Rev. Lett.* 116.21 (2016), p. 211302. arXiv: 1601.01800 [hep-th].

[152] Y. Kluth and D. F. Litim. "Fixed Points of Quantum Gravity and the Dimensionality of the UV Critical Surface". In: (Aug. 2020). arXiv: 2008.09181 [hep-th].

[153] K. Falls et al. "Further evidence for asymptotic safety of quantum gravity". In: *Phys. Rev. D* 93.10 (2016), p. 104022. arXiv: 1410.4815 [hep-th].

[154] K. Falls et al. "On de Sitter solutions in asymptotically safe $f(R)$ theories". In: *Class. Quant. Grav.* 35.13 (2018), p. 135006. arXiv: 1607.04962 [gr-qc].

[155] K. Falls and N. Ohta. "Renormalization Group Equation for $f(R)$ gravity on hyperbolic spaces". In: *Phys. Rev. D* 94.8 (2016), p. 084005. arXiv: 1607.08460 [hep-th].

[156] K. Falls et al. "Asymptotic safety of quantum gravity beyond Ricci scalars". In: *Phys. Rev. D* 97.8 (2018), p. 086006. arXiv: 1801.00162 [hep-th].

[157] J. A. Dietz and T. R. Morris. "Asymptotic safety in the f(R) approximation". In: *JHEP* 01 (2013), p. 108. arXiv: 1211.0955 [hep-th].

[158] P. Labus, T. R. Morris, and Z. H. Slade. "Background independence in a background dependent renormalization group". In: *Phys. Rev. D* 94.2 (2016), p. 024007. arXiv: 1603.04772 [hep-th].

[159] J. A. Dietz, T. R. Morris, and Z. H. Slade. "Fixed point structure of the conformal factor field in quantum gravity". In: *Phys. Rev. D* 94.12 (2016), p. 124014. arXiv: 1605.07636 [hep-th].

[160] T. R. Morris and D. Stulga. "The functional $f(R)$ approximation". In: (Oct. 2022). arXiv: 2210.11356 [hep-th].

[161] N. Alkofer and F. Saueressig. "Asymptotically safe $f(R)$-gravity coupled to matter I: the polynomial case". In: *Annals Phys.* 396 (2018), pp. 173–201. arXiv: 1802.00498 [hep-th].

[162] J. Daas et al. "Asymptotically safe gravity with fermions". In: *Phys. Lett. B* 809 (2020), p. 135775. arXiv: 2005.12356 [hep-th].

[163] N. Christiansen et al. "Fixed points and infrared completion of quantum gravity". In: *Phys. Lett. B* 728 (2014), pp. 114–117. arXiv: 1209.4038 [hep-th].

[164] N. Christiansen et al. "Global Flows in Quantum Gravity". In: *Phys. Rev. D* 93.4 (2016), p. 044036. arXiv: 1403.1232 [hep-th].

[165] N. Christiansen et al. "Curvature dependence of quantum gravity". In: *Phys. Rev. D* 97.4 (2018), p. 046007. arXiv: 1711.09259 [hep-th].

[166] N. Christiansen et al. "Asymptotic safety of gravity with matter". In: *Phys. Rev. D* 97.10 (2018), p. 106012. arXiv: 1710.04669 [hep-th].

[167] D. F. Litim. "Fixed points of quantum gravity". In: *Phys. Rev. Lett.* 92 (2004), p. 201301. arXiv: hep-th/0312114.

[168] A. Eichhorn et al. "Universal critical behavior in tensor models for four-dimensional quantum gravity". In: *JHEP* 02 (2020), p. 110. arXiv: 1912.05314 [gr-qc].

[169] A. Eichhorn, J. H. Kwapisz, and M. Schiffer. "Weak-gravity bound in asymptotically safe gravity-gauge systems". In: *Phys. Rev. D* 105.10 (2022), p. 106022. arXiv: 2112.09772 [gr-qc].

[170] A. Eichhorn and M. Schiffer. "Asymptotic safety of gravity with matter". In: (Dec. 2022). arXiv: 2212.07456 [hep-th].

[171] S. Sen, C. Wetterich, and M. Yamada. "Scaling solutions for asymptotically free quantum gravity". In: *JHEP* 02 (2023), p. 054. arXiv: 2211.05508 [hep-th].

[172] S. Sen, C. Wetterich, and M. Yamada. "Asymptotic freedom and safety in quantum gravity". In: *JHEP* 03 (2022), p. 130. arXiv: 2111.04696 [hep-th].

[173] B. Knorr, C. Ripken, and F. Saueressig. "Form Factors in Asymptotic Safety: conceptual ideas and computational toolbox". In: *Class. Quant. Grav.* 36.23 (2019), p. 234001. arXiv: 1907.02903 [hep-th].

[174] C. Laporte et al. "Scalar-tensor theories within Asymptotic Safety". In: *JHEP* 12 (2021), p. 001. arXiv: 2110.09566 [hep-th].

[175] A. Baldazzi and K. Falls. "Essential Quantum Einstein Gravity". In: *Universe* 7.8 (2021), p. 294. arXiv: 2107.00671 [hep-th].

[176] A. Ashtekar, M. Reuter, and C. Rovelli. "From General Relativity to Quantum Gravity". In: (Aug. 2014). arXiv: 1408.4336 [gr-qc].

[177] E. Manrique, S. Rechenberger, and F. Saueressig. "Asymptotically Safe Lorentzian Gravity". In: *Phys. Rev. Lett.* 106 (2011), p. 251302. arXiv: 1102.5012 [hep-th].

[178] S. Floerchinger. "Analytic Continuation of Functional Renormalization Group Equations". In: *JHEP* 05 (2012), p. 021. arXiv: 1112.4374 [hep-th].

[179] J. M. Pawlowski and N. Strodthoff. "Real time correlation functions and the functional renormalization group". In: *Phys. Rev. D* 92.9 (2015), p. 094009. arXiv: 1508.01160 [hep-ph].

[180] J. M. Pawlowski and M. Reichert. "Quantum Gravity: A Fluctuating Point of View". In: *Front. in Phys.* 8 (2021), p. 551848. arXiv: 2007.10353 [hep-th].

[181] A. Baldazzi, R. Percacci, and V. Skrinjar. "Wicked metrics". In: *Class. Quant. Grav.* 36.10 (2019), p. 105008. arXiv: 1811.03369 [gr-qc].

[182] A. Baldazzi, R. Percacci, and V. Skrinjar. "Quantum fields without Wick rotation". In: *Symmetry* 11.3 (2019), p. 373. arXiv: 1901.01891 [gr-qc].

[183] R. Banerjee and M. Niedermaier. "The spatial Functional Renormalization Group and Hadamard states on cosmological spacetimes". In: *Nucl. Phys. B* 980 (2022), p. 115814. arXiv: 2201.02575 [hep-th].

[184] E. D'Angelo et al. "Wetterich equation on Lorentzian manifolds". In: (Feb. 2022). arXiv: 2202.07580 [math-ph].

[185] J. F. Donoghue. "A Critique of the Asymptotic Safety Program". In: *Front. in Phys.* 8 (2020), p. 56. arXiv: 1911.02967 [hep-th].

[186] A. Bonanno et al. "Critical reflections on asymptotically safe gravity". In: *Front. in Phys.* 8 (2020), p. 269. arXiv: 2004.06810 [gr-qc].

[187] C. Rovelli. "What Is Observable in Classical and Quantum Gravity?" In: *Class. Quant. Grav.* 8 (1991), pp. 297–316.

[188] S. B. Giddings, D. Marolf, and J. B. Hartle. "Observables in effective gravity". In: *Phys. Rev. D* 74 (2006), p. 064018. arXiv: hep-th/0512200.

[189] M. Becker and C. Pagani. "Geometric Operators in the Einstein–Hilbert Truncation". In: *Universe* 5.3 (2019), p. 75.

[190] J. Ambjørn, B. Durhuus, and T. Jonsson. *Quantum Geometry: A Statistical Field Theory Approach*. Cambridge Monographs on Mathematical Physics. Cambridge, UK: Cambridge Univ. Press, Dec. 2005.

[191] H. W. Hamber. *Quantum gravitation: The Feynman path integral approach*. Berlin: Springer, 2009.

[192] M. Becker and C. Pagani. "Geometric operators in the asymptotic safety scenario for quantum gravity". In: *Phys. Rev. D* 99.6 (2019), p. 066002. arXiv: 1810.11816 [gr-qc].

[193] M. Becker, C. Pagani, and O. Zanusso. "Fractal Geometry of Higher Derivative Gravity". In: *Phys. Rev. Lett.* 124.15 (2020), p. 151302. arXiv: 1911.02415 [gr-qc].

[194] M. Reuter and C. Wetterich. "Quantum Liouville field theory as solution of a flow equation". In: *Nucl. Phys. B* 506 (1997), pp. 483–520. arXiv: hep-th/9605039.

[195] C. Pagani. "Note on scaling arguments in the effective average action formalism". In: *Phys. Rev. D* 94.4 (2016), p. 045001. arXiv: 1603.07250 [hep-th].

[196] G. Jona-Lasinio. "Collective Properties of Physical Systems". In: *Proc. Nobel Symp. 24*. Ed. by N. Foundation. Stockholm: Academic Press, May 1973, 38–44.

[197] S. Weinberg. Ed. by S. W. Hawking and W. Israel. Cambridge, UK: Univ. Pr., 1979, 790–831.

[198] D. Anselmi. "A General Field-Covariant Formulation Of Quantum Field Theory". In: *Eur. Phys. J. C* 73.3 (2013), p. 2338. arXiv: 1205.3279 [hep-th].

[199] A. Baldazzi, R. B. A. Zinati, and K. Falls. "Essential renormalisation group". In: *SciPost Phys.* 13 (2022), p. 085. arXiv: 2105.11482 [hep-th].

[200] F. J. Wegner. "Some invariance properties of the renormalization group". In: *Journal of Physics C: Solid State Physics* 7 (1974), pp. 2098–2108.

[201] J. S. R. Chisholm. "Change of variables in quantum field theories". In: *Nucl. Phys.* 26.3 (1961), pp. 469–479.

[202] S. Kamefuchi, L. O'Raifeartaigh, and A. Salam. "Change of variables and equivalence theorems in quantum field theories". In: *Nucl. Phys.* 28 (1961), pp. 529–549.

[203] R. D. Ball et al. "Scheme independence and the exact renormalization group". In: *Phys. Lett. B* 347 (1995), pp. 80–88. arXiv: hep-th/9411122.

[204] J. I. Latorre and T. R. Morris. "Exact scheme independence". In: *JHEP* 11 (2000), p. 004. arXiv: hep-th/0008123.

[205] S. Arnone, A. Gatti, and T. R. Morris. "Exact scheme independence at one loop". In: *JHEP* 05 (2002), p. 059. arXiv: hep-th/0201237.

[206] O. J. Rosten. "Scheme independence to all loops". In: *J. Phys. A* 39 (2006), pp. 8141–8156. arXiv: hep-th/0511107.

[207] J. A. Dietz and T. R. Morris. "Redundant operators in the exact renormalisation group and in the f(R) approximation to asymptotic safety". In: *JHEP* 07 (2013), p. 064. arXiv: 1306.1223 [hep-th].

[208] C. Wetterich. "Exact evolution equation for the effective potential". In: *Phys. Lett. B* 301 (1993), pp. 90–94. arXiv: 1710.05815 [hep-th].

[209] M. Reuter and C. Wetterich. "Average action for the Higgs model with Abelian gauge symmetry". In: *Nucl. Phys. B* 391 (1993), pp. 147–175.

[210] M. Reuter and C. Wetterich. "Exact evolution equation for scalar electrodynamics". In: *Nucl. Phys. B* 427 (1994), pp. 291–324.

[211] M. Reuter. "Renormalization of the topological charge in Yang-Mills theory". In: *Mod. Phys. Lett. A* 12 (1997), pp. 2777–2802. arXiv: hep-th/9604124.

[212] A. Codello, M. Demmel, and O. Zanusso. "Scheme dependence and universality in the functional renormalization group". In: *Phys. Rev. D* 90.2 (2014), p. 027701. arXiv: 1310.7625 [hep-th].

[213] A. Baldazzi, R. Percacci, and L. Zambelli. "Limit of vanishing regulator in the functional renormalization group". In: *Phys. Rev. D* 104.7 (2021), p. 076026. arXiv: 2105.05778 [hep-th].

[214] L. F. Abbott. "Introduction to the Background Field Method". In: *Acta Phys. Polon. B* 13 (1982), p. 33.

[215] E. Manrique and M. Reuter. "Bare versus Effective Fixed Point Action in Asymptotic Safety: The Reconstruction Problem". In: *PoS* CLAQG08 (2011), p. 001. arXiv: 0905.4220 [hep-th].

[216] B. S. DeWitt. *The global approach to quantum field theory. Vol. 1, 2*. Vol. 114. 2003.

[217] E. Manrique and M. Reuter. "Bimetric Truncations for Quantum Einstein Gravity and Asymptotic Safety". In: *Annals Phys.* 325 (2010), pp. 785–815. arXiv: 0907.2617 [gr-qc].

[218] K. G. Falls, D. F. Litim, and J. Schröder. "Aspects of asymptotic safety for quantum gravity". In: *Phys. Rev. D* 99.12 (2019), p. 126015. arXiv: 1810.08550 [gr-qc].

[219] M. Demmel, F. Saueressig, and O. Zanusso. "RG flows of Quantum Einstein Gravity in the linear-geometric approximation". In: *Annals Phys.* 359 (2015), pp. 141–165. arXiv: 1412.7207 [hep-th].

[220] M. Reuter and F. Saueressig. "Renormalization group flow of quantum gravity in the Einstein-Hilbert truncation". In: *Phys. Rev.* D65 (2002), p. 065016. arXiv: hep-th/0110054 [hep-th].

[221] A. Bonanno and M. Reuter. "Entropy signature of the running cosmological constant". In: *JCAP* 08 (2007), p. 024. arXiv: 0706.0174 [hep-th].

[222] A. L. Besse. *Einstein Manifolds*. New York: Springer, 1987.

[223] M. Becker and M. Reuter. "Background Independent Field Quantization with Sequences of Gravity-Coupled Approximants". In: *Phys. Rev. D* 102.12 (2020), p. 125001. arXiv: 2008.09430 [gr-qc].

[224] M. Becker and M. Reuter. "Background independent field quantization with sequences of gravity-coupled approximants. II. Metric fluctuations". In: *Phys. Rev. D* 104.12 (2021), p. 125008. arXiv: 2109.09496 [hep-th].

[225] J. Fehre et al. "Lorentzian quantum gravity and the graviton spectral function". In: (Nov. 2021). arXiv: 2111.13232 [hep-th].

[226] I. Steib, S. Nagy, and J. Polonyi. "Renormalization in Minkowski space–time". In: *Int. J. Mod. Phys. A* 36.05 (2021), p. 2150031. arXiv: 1908.11311 [hep-th].

[227] J. Louko and R. D. Sorkin. "Complex actions in two-dimensional topology change". In: *Class. Quant. Grav.* 14 (1997), pp. 179–204. arXiv: gr-qc/9511023.

[228] M. Kontsevich and G. Segal. "Wick Rotation and the Positivity of Energy in Quantum Field Theory". In: *Quart. J. Math. Oxford Ser.* 72.1-2 (2021), pp. 673–699. arXiv: 2105.10161 [hep-th].

[229] E. Witten. "Anti-de Sitter space and holography". In: *Adv. Theor. Math. Phys.* 2 (1998), pp. 253–291. arXiv: hep-th/9802150.

[230] M. Visser. "Feynman's iε prescription, almost real spacetimes, and acceptable complex spacetimes". In: *JHEP* 08 (2022), p. 129. arXiv: 2111.14016 [gr-qc].

[231] S. K. Asante, B. Dittrich, and J. Padua-Argüelles. "Complex actions and causality violations: Applications to Lorentzian quantum cosmology". In: (Dec. 2021). arXiv: 2112.15387 [gr-qc].

[232] J. Biemans, A. Platania, and F. Saueressig. "Quantum gravity on foliated spacetimes: Asymptotically safe and sound". In: *Phys. Rev. D* 95.8 (2017), p. 086013. arXiv: 1609.04813 [hep-th].

[233] A. Platania and F. Saueressig. "Functional Renormalization Group Flows on Friedman–Lemaître–Robertson–Walker backgrounds". In: *Found. Phys.* 48.10 (2018), pp. 1291–1304. arXiv: 1710.01972 [hep-th].

[234] B. Knorr. "Lorentz symmetry is relevant". In: *Phys. Lett. B* 792 (2019), pp. 142–148. arXiv: 1810.07971 [hep-th].

[235] S. Nagy, K. Sailer, and I. Steib. "Renormalization of Lorentzian conformally reduced gravity". In: *Class. Quant. Grav.* 36.15 (2019), p. 155004.

[236] J. Ambjorn, J. Jurkiewicz, and R. Loll. "A Nonperturbative Lorentzian path integral for gravity". In: *Phys. Rev. Lett.* 85 (2000), pp. 924–927. arXiv: hep-th/0002050.

[237] J. Ambjorn, J. Jurkiewicz, and R. Loll. "Dynamically triangulating Lorentzian quantum gravity". In: *Nucl. Phys. B* 610 (2001), pp. 347–382. arXiv: hep-th/0105267.

[238] R. Loll. "Quantum Gravity from Causal Dynamical Triangulations: A Review". In: *Class. Quant. Grav.* 37.1 (2020), p. 013002. arXiv: 1905.08669 [hep-th].

[239] J. Ambjorn, J. Jurkiewicz, and R. Loll. "Spectral dimension of the universe". In: *Phys. Rev. Lett.* 95 (2005), p. 171301. arXiv: hep-th/0505113.

[240] M. Reuter and F. Saueressig. "Fractal space-times under the microscope: A Renormalization Group view on Monte Carlo data". In: *JHEP* 12 (2011), p. 012. arXiv: 1110.5224 [hep-th].

[241] D. Benedetti, P. F. Machado, and F. Saueressig. "Asymptotic safety in higher-derivative gravity". In: *Mod. Phys. Lett. A* 24 (2009), pp. 2233–2241. arXiv: 0901.2984 [hep-th].

[242] P. F. Machado and F. Saueressig. "On the renormalization group flow of f(R)-gravity". In: *Phys. Rev. D* 77 (2008), p. 124045. arXiv: 0712.0445 [hep-th].

[243] K. Groh and F. Saueressig. "Ghost wave-function renormalization in Asymptotically Safe Quantum Gravity". In: *J. Phys. A* 43 (2010), p. 365403. arXiv: 1001.5032 [hep-th].

[244] M. Reuter and F. Saueressig. "Fractal space-times under the microscope: A Renormalization Group view on Monte Carlo data". In: *JHEP* 12 (2011), p. 012. arXiv: 1110.5224 [hep-th].

[245] C. Pagani and H. Sonoda. "Products of composite operators in the exact renormalization group formalism". In: *PTEP* 2018.2 (2018), 023B02. arXiv: 1707.09138 [hep-th].

[246] C. Pagani and M. Reuter. "Composite Operators in Asymptotic Safety". In: *Phys. Rev. D* 95.6 (2017), p. 066002. arXiv: 1611.06522 [gr-qc].

[247] J. M. Pawlowski. "Aspects of the functional renormalisation group". In: *Annals Phys.* 322 (2007), pp. 2831–2915. arXiv: hep-th/0512261.

[248] H. Gies and C. Wetterich. "Renormalization flow of bound states". In: *Phys. Rev. D* 65 (2002), p. 065001. arXiv: hep-th/0107221.

[249] S. Floerchinger and C. Wetterich. "Exact flow equation for composite operators". In: *Phys. Lett. B* 680 (2009), pp. 371–376. arXiv: 0905.0915 [hep-th].

[250] M. Mitter, J. M. Pawlowski, and N. Strodthoff. "Chiral symmetry breaking in continuum QCD". In: *Phys. Rev. D* 91 (2015), p. 054035. arXiv: 1411.7978 [hep-ph].

[251] J. Braun et al. "From Quarks and Gluons to Hadrons: Chiral Symmetry Breaking in Dynamical QCD". In: *Phys. Rev. D* 94.3 (2016), p. 034016. arXiv: 1412.1045 [hep-ph].

[252] K. Groh, F. Saueressig, and O. Zanusso. "Off-diagonal heat-kernel expansion and its application to fields with differential constraints". In: (Dec. 2011). arXiv: 1112.4856 [math-ph].

[253] R. Martini, D. Sauro, and O. Zanusso. "Composite higher derivative operators in $d = 2 + \epsilon$ dimensions and the spectrum of asymptotically safe gravity". In: (Feb. 2023). arXiv: 2302.14804 [hep-th].

[254] M. Reuter and C. Wetterich. "Running gauge coupling in three-dimensions and the electroweak phase transition". In: *Nucl. Phys. B* 408 (1993), pp. 91–132.

[255] S. Perlmutter et al. "Measurements of Ω and Λ from 42 high redshift supernovae". In: *Astrophys. J.* 517 (1999), pp. 565–586. arXiv: astro-ph/9812133.

[256] A. G. Riess et al. "Observational evidence from supernovae for an accelerating universe and a cosmological constant". In: *Astron. J.* 116 (1998), pp. 1009–1038. arXiv: astro-ph/9805201.

[257] N. Aghanim et al. "Planck 2018 results". In: *Astronomy and Astrophysics* 641 (2020), A6.

[258] J. E. Daum and M. Reuter. "Einstein-Cartan gravity, Asymptotic Safety, and the running Immirzi parameter". In: *Annals Phys.* 334 (2013), pp. 351–419. arXiv: 1301.5135 [hep-th].

[259] U. Harst and M. Reuter. "The 'Tetrad only' theory space: Nonperturbative renormalization flow and Asymptotic Safety". In: *JHEP* 05 (2012), p. 005. arXiv: 1203.2158 [hep-th].

[260] U. Harst and M. Reuter. "A new functional flow equation for Einstein–Cartan quantum gravity". In: *Annals Phys.* 354 (2015), pp. 637–704. arXiv: 1410.7003 [hep-th].

[261] U. Harst and M. Reuter. "On selfdual spin-connections and Asymptotic Safety". In: *Phys. Lett. B* 753 (2016), pp. 395–400. arXiv: 1509.09122 [hep-th].

[262] O. Lauscher and M. Reuter. "Fractal spacetime structure in asymptotically safe gravity". In: *JHEP* 10 (2005), p. 050. arXiv: hep-th/0508202.

[263] A. B. Zamolodchikov. "Irreversibility of the Flux of the Renormalization Group in a 2D Field Theory". In: *JETP Lett.* 43 (1986), pp. 730–732.

[264] A. B. Zamolodchikov. "Renormalization Group and Perturbation Theory Near Fixed Points in Two-Dimensional Field Theory". In: *Sov. J. Nucl. Phys.* 46 (1987), p. 1090.

[265] Z. Komargodski and A. Schwimmer. "On Renormalization Group Flows in Four Dimensions". In: *JHEP* 12 (2011), p. 099. arXiv: 1107.3987 [hep-th].

[266] S. S. Gubser, I. R. Klebanov, and A. M. Polyakov. "Gauge theory correlators from noncritical string theory". In: *Phys. Lett. B* 428 (1998), pp. 105–114. arXiv: hep-th/9802109.

[267] M. Ammon and J. Erdmenger. *Gauge/gravity duality: Foundations and applications*. Cambridge: Cambridge University Press, Apr. 2015.

[268] L. Nottale. "Scale Relativity and Fractal Space-Time: Theory and Applications". In: *Foundations of Science* 15.2 (2010), pp. 101–152.

[269] R. Percacci. "The Renormalization group, systems of units and the hierarchy problem". In: *J. Phys. A* 40 (2007), pp. 4895–4914. arXiv: hep-th/0409199.

[270] M. Reuter and J.-M. Schwindt. "A Minimal length from the cutoff modes in asymptotically safe quantum gravity". In: *JHEP* 01 (2006), p. 070. arXiv: hep-th/0511021.

[271] C. Pagani and M. Reuter. "Background Independent Quantum Field Theory and Gravitating Vacuum Fluctuations". In: *Annals Phys.* 411 (2019), p. 167972. arXiv: 1906.02507 [gr-qc].

[272] C. Pagani and M. Reuter. "Why the Cosmological Constant Seems to Hardly Care About Quantum Vacuum Fluctuations: Surprises From Background Independent Coarse Graining". In: *Front. in Phys.* 8 (2020), p. 214.

[273] C. Nash. *Differential topology and quantum field theory*. 1991.

[274] J. F. Donoghue. "Leading quantum correction to the Newtonian potential". In: *Phys. Rev. Lett.* 72 (1994), pp. 2996–2999. arXiv: gr-qc/9310024.

[275] H. W. Hamber and S. Liu. "On the quantum corrections to the Newtonian potential". In: *Phys. Lett. B* 357 (1995), pp. 51–56. arXiv: hep-th/9505182.

[276] J. F. Donoghue. "General relativity as an effective field theory: The leading quantum corrections". In: *Phys. Rev. D* 50 (1994), pp. 3874–3888. arXiv: gr-qc/9405057.

[277] I. J. Muzinich and S. Vokos. "Long range forces in quantum gravity". In: *Phys. Rev. D* 52 (1995), pp. 3472–3483. arXiv: hep-th/9501083.

[278] D. Neill and I. Z. Rothstein. "Classical Space-Times from the S Matrix". In: *Nucl. Phys. B* 877 (2013), pp. 177–189. arXiv: 1304.7263 [hep-th].

[279] N. C. Tsamis and R. P. Woodard. "The Structure of perturbative quantum gravity on a De Sitter background". In: *Commun. Math. Phys.* 162 (1994), pp. 217–248.

[280] S. Park, T. Prokopec, and R. P. Woodard. "Quantum Scalar Corrections to the Gravitational Potentials on de Sitter Background". In: *JHEP* 01 (2016), p. 074. arXiv: 1510.03352 [gr-qc].

[281] I. Antoniadis and E. Mottola. "Graviton Fluctuations in De Sitter Space". In: *J. Math. Phys.* 32 (1991), pp. 1037–1044.

[282] I. Antoniadis and E. T. Tomboulis. "Gauge Invariance and Unitarity in Higher Derivative Quantum Gravity". In: *Phys. Rev. D* 33 (1986), p. 2756.

[283] B. Allen and M. Turyn. "An evaluation of the graviton propagator in de sitter space". In: *Nuclear Physics* 292 (1987), pp. 813–852.

[284] E. G. Floratos, J. Iliopoulos, and T. N. Tomaras. "Tree Level Scattering Amplitudes in De Sitter Space Diverge". In: *Phys. Lett. B* 197 (1987), pp. 373–378.

[285] E. T. Akhmedov. "IR divergences and kinetic equation in de Sitter space. Poincare patch: Principal series". In: *JHEP* 01 (2012), p. 066. arXiv: 1110.2257 [hep-th].

[286] L. H. Ford and L. Parker. "Infrared divergences in a class of Robertson-Walker universes". In: *Phys. Rev. D* 16 (2 1977), pp. 245–250.

[287] I. Antoniadis and E. Mottola. "Four-dimensional quantum gravity in the conformal sector". In: *Phys. Rev. D* 45 (6 1992), pp. 2013–2025.

[288] B. Allen. "Graviton propagator in de Sitter space". In: *Physical review D: Particles and fields* 34 (Jan. 1987), pp. 3670–3675.

[289] B. Allen. "Gravitons in de sitter space". In: 1987.

[290] M. Turyn. "The graviton propagator in maximally symmetric spaces". In: *Journal of Mathematical Physics* 31.3 (1990), pp. 669–679. eprint: https://doi.org/10.1063/1.528903.

[291] S. P. Miao, N. C. Tsamis, and R. P. Woodard. "The Graviton Propagator in de Donder Gauge on de Sitter Background". In: *J. Math. Phys.* 52 (2011), p. 122301. arXiv: 1106.0925 [gr-qc].

[292] S. P. Miao, N. C. Tsamis, and R. P. Woodard. "Gauging away Physics". In: *Class. Quant. Grav.* 28 (2011), p. 245013. arXiv: 1107.4733 [gr-qc].

[293] J. P. Gazeau, J. Renaud, and M. V. Takook. "Gupta-Bleuler quantization for minimally coupled scalar fields in de Sitter space". In: *Class. Quant. Grav.* 17 (2000), pp. 1415–1434. arXiv: gr-qc/9904023.

[294] M. V. Takook. "Covariant two point function for minimally coupled scalar field in de Sitter space-time". In: *Mod. Phys. Lett. A* 16 (2001), pp. 1691–1698. arXiv: gr-qc/0005020.

[295] S. Rouhani and M. V. Takook. "Tree-level scattering amplitude in de Sitter space". In: *Europhys. Lett.* 68 (2004), p. 15. arXiv: gr-qc/0409120.

[296] M. V. Takook. "Negative norm states in de Sitter space and QFT without renormalization procedure". In: *Int. J. Mod. Phys. E* 11 (2002), pp. 509–518. arXiv: gr-qc/0006019.

[297] A. Higuchi and S. S. Kouris. "The Covariant graviton propagator in de Sitter space-time". In: *Class. Quant. Grav.* 18 (2001), pp. 4317–4328. arXiv: gr-qc/0107036.

[298] M. Faizal and A. Higuchi. "Physical equivalence between the covariant and physical graviton two-point functions in de Sitter spacetime". In: *Phys. Rev. D* 85 (2012), p. 124021. arXiv: 1107.0395 [gr-qc].

[299] B. Allen. "The graviton propagator in homogeneous and isotropic spacetimes". In: *Nuclear Physics* 287 (1987), pp. 743–756.

[300] E. T. Akhmedov. "Lecture notes on interacting quantum fields in de Sitter space". In: *Int. J. Mod. Phys. D* 23 (2014), p. 1430001. arXiv: 1309.2557 [hep-th].

[301] E. T. Akhmedov et al. "Propagators and Gaussian effective actions in various patches of de Sitter space". In: *Phys. Rev. D* 100.10 (2019), p. 105011. arXiv: 1905.09344 [hep-th].

[302] E. T. Akhmedov et al. "Quantum fields in the static de Sitter universe". In: *Phys. Rev. D* 102.8 (2020), p. 085003. arXiv: 2005.13952 [hep-th].

[303] K. Lochan et al. "Quantum correlators in Friedmann spacetimes: The omnipresent de Sitter spacetime and the invariant vacuum noise". In: *Phys. Rev. D* 98.10 (2018), p. 105015. arXiv: 1805.08800 [gr-qc].

[304] S. Singh, C. Ganguly, and T. Padmanabhan. "Quantum field theory in de Sitter and quasi–de Sitter spacetimes revisited". In: *Phys. Rev. D* 87.10 (2013), p. 104004. arXiv: 1302.7177 [gr-qc].

[305] S. P. Kim. "Vacuum Structure of de Sitter Space". In: (Aug. 2010). arXiv: 1008.0577 [hep-th].

[306] J. Bros, U. Moschella, and J. P. Gazeau. "Quantum field theory in the de Sitter universe". In: *Phys. Rev. Lett.* 73 (1994), pp. 1746–1749.

[307] J. Bros and U. Moschella. "Two point functions and quantum fields in de Sitter universe". In: *Rev. Math. Phys.* 8 (1996), pp. 327–392. arXiv: gr-qc/9511019.

[308] J. Bros, H. Epstein, and U. Moschella. "Analyticity properties and thermal effects for general quantum field theory on de Sitter space-time". In: *Commun. Math. Phys.* 196 (1998), pp. 535–570. arXiv: gr-qc/9801099.

[309] A. Higuchi, D. Marolf, and I. A. Morrison. "On the Equivalence between Euclidean and In-In Formalisms in de Sitter QFT". In: *Phys. Rev. D* 83 (2011), p. 084029. arXiv: 1012.3415 [gr-qc].

[310] M. Fukuma, S. Sugishita, and Y. Sakatani. "Propagators in de Sitter space". In: *Phys. Rev. D* 88.2 (2013), p. 024041. arXiv: 1301.7352 [hep-th].

[311] N. Arkani-Hamed and J. Maldacena. "Cosmological Collider Physics". In: (Mar. 2015). arXiv: 1503.08043 [hep-th].

[312] N. Arkani-Hamed et al. "The Cosmological Bootstrap: Inflationary Correlators from Symmetries and Singularities". In: *JHEP* 04 (2020), p. 105. arXiv: 1811.00024 [hep-th].

[313] S. Cacciatori et al. "Conservation laws and scattering for de Sitter classical particles". In: *Class. Quant. Grav.* 25 (2008). Ed. by K. Safarik, L. Sandor, and B. Tomasik, p. 075008. arXiv: 0710.0315 [hep-th].

[314] B. Allen. "Vacuum states in de Sitter space". In: *Phys. Rev. D* 32 (12 1985), pp. 3136–3149.

[315] N. D. Birrell and P. C. W. Davies. *Quantum Fields in Curved Space*. Cambridge Monographs on Mathematical Physics. Cambridge University Press, 1982.

[316] V. Mukhanov and S. Winitzki. *Introduction to quantum effects in gravity*. Cambridge University Press, June 2007.

[317] E. T. Akhmedov, U. Moschella, and F. K. Popov. "Characters of different secular effects in various patches of de Sitter space". In: *Phys. Rev. D* 99.8 (2019), p. 086009. arXiv: 1901.07293 [hep-th].

[318] N. Birrell. "Momentum Space Techniques for Curved Space-Time Quantum Field Theory". In: *Proceedings of The Royal Society A: Mathematical, Physical and Engineering Sciences* 367 (Aug. 1979), pp. 123–141.

[319] T. S. Bunch and L. Parker. "Feynman propagator in curved spacetime: A momentum-space representation". In: *Phys. Rev. D* 20 (10 1979), pp. 2499–2510.

[320] S. J. Avis, C. J. Isham, and D. Storey. "Quantum field theory in anti-de Sitter space-time". In: *Phys. Rev. D* 18 (10 1978), pp. 3565–3576.

[321] C. Burgess and C. Lütken. "Propagators and effective potentials in anti-de Sitter space". In: *Physics Letters B* 153.3 (1985), pp. 137–141.

[322] E. Witten. "Anti-de Sitter space and holography". In: *Adv. Theor. Math. Phys.* 2 (1998), pp. 253–291. arXiv: hep-th/9802150.

[323] W. Mueck and K. S. Viswanathan. "Conformal field theory correlators from classical scalar field theory on AdS(d+1)". In: *Phys. Rev. D* 58 (1998), p. 041901. arXiv: hep-th/9804035.

[324] D. Z. Freedman et al. "Correlation functions in the CFT(d) / AdS(d+1) correspondence". In: *Nucl. Phys. B* 546 (1999), pp. 96–118. arXiv: hep-th/9804058.

[325] M. Faizal. "Covariant Graviton Propagator in Anti-de Sitter Spacetime". In: *Class. Quant. Grav.* 29 (2012), p. 035007. arXiv: 1112.4369 [gr-qc].

[326] J. Bros et al. "Anti de Sitter quantum field theory and a new class of hypergeometric identities". In: *Commun. Math. Phys.* 309 (2012), pp. 255–291. arXiv: 1107.5161 [hep-th].

[327] M. Cadoni and P. Carta. "Tachyons in de Sitter space and analytical continuation from dS / CFT to AdS / CFT". In: *Int. J. Mod. Phys. A* 19 (2004), pp. 4985–5002. arXiv: hep-th/0211018.

[328] C. Sleight. "A Mellin Space Approach to Cosmological Correlators". In: *JHEP* 01 (2020), p. 090. arXiv: 1906.12302 [hep-th].

[329] C. Sleight and M. Taronna. "From AdS to dS Exchanges: Spectral Representation, Mellin Amplitudes and Crossing". In: (July 2020). arXiv: 2007.09993 [hep-th].

[330] E. Witten. "Quantum gravity in de Sitter space". In: *Strings 2001: International Conference*. June 2001. arXiv: hep-th/0106109.

[331] R. Bousso. "Cosmology and the S-matrix". In: *Phys. Rev. D* 71 (2005), p. 064024. arXiv: hep-th/0412197.

[332] D. Marolf, I. A. Morrison, and M. Srednicki. "Perturbative S-matrix for massive scalar fields in global de Sitter space". In: *Class. Quant. Grav.* 30 (2013), p. 155023. arXiv: 1209.6039 [hep-th].

[333] S. Mandal and S. Banerjee. "Local description of S-matrix in quantum field theory in curved spacetime using Riemann-normal coordinate". In: *Eur. Phys. J. Plus* 136.10 (2021), p. 1064. arXiv: 1908.06717 [hep-th].

[334] S. B. Giddings. "The gravitational S-matrix: Erice lectures". In: *arXiv: High Energy Physics - Theory* 48 (2013), pp. 93–147.

[335] A. M. Polyakov. "De Sitter space and eternity". In: *Nucl. Phys. B* 797 (2008), pp. 199–217. arXiv: 0709.2899 [hep-th].

[336] P. R. Anderson and E. Mottola. "Instability of global de Sitter space to particle creation". In: *Phys. Rev. D* 89 (2014), p. 104038. arXiv: 1310.0030 [gr-qc].

[337] P. R. Anderson, E. Mottola, and D. H. Sanders. "Decay of the de Sitter Vacuum". In: *Phys. Rev. D* 97.6 (2018), p. 065016. arXiv: 1712.04522 [gr-qc].

[338] T. Markkanen and A. Rajantie. "Massive scalar field evolution in de Sitter". In: *JHEP* 01 (2017), p. 133. arXiv: 1607.00334 [gr-qc].

[339] A. A. Starobinsky. "A New Type of Isotropic Cosmological Models Without Singularity". In: *Phys. Lett. B* 91 (1980). Ed. by I. M. Khalatnikov and V. P. Mineev, pp. 99–102.

[340] S. V. Ketov and A. A. Starobinsky. "Inflation and non-minimal scalar-curvature coupling in gravity and supergravity". In: *JCAP* 08 (2012), p. 022. arXiv: 1203.0805 [hep-th].

[341] A. S. Koshelev, K. Sravan Kumar, and A. A. Starobinsky. "R^2 inflation to probe non-perturbative quantum gravity". In: *JHEP* 03 (2018), p. 071. arXiv: 1711.08864 [hep-th].

[342] A. S. Koshelev et al. "Non-Gaussianities and tensor-to-scalar ratio in non-local R²-like inflation". In: *JHEP* 06 (2020), p. 152. arXiv: 2003.00629 [hep-th].

[343] A. Vilenkin. "Classical and Quantum Cosmology of the Starobinsky Inflationary Model". In: *Phys. Rev. D* 32 (1985), p. 2511.

[344] C. P. L. Berry and J. R. Gair. "Linearized f(R) Gravity: Gravitational Radiation and Solar System Tests". In: *Phys. Rev. D* 83 (2011). [Erratum: Phys.Rev.D 85, 089906 (2012)], p. 104022. arXiv: 1104.0819 [gr-qc].

[345] J. A. R. Cembranos. "Dark Matter from R2-gravity". In: *Phys. Rev. Lett.* 102 (2009), p. 141301. arXiv: 0809.1653 [hep-ph].

[346] B. L. Giacchini. "Experimental limits on the free parameters of higher-derivative gravity". In: *14th Marcel Grossmann Meeting on Recent Developments in Theoretical and Experimental General Relativity, Astrophysics, and Relativistic Field Theories*. Vol. 2. 2017, pp. 1340–1345. arXiv: 1612.01823 [gr-qc].

[347] M. V. Ostrogradsky. " Mémoires sur les équations différentielles, relatives au problème des isopérimètres". In: *Mem. Ac. St. Petersbourg* VI 4 (1850), p. 385.

[348] I. Antoniadis and E. T. Tomboulis. "Gauge invariance and unitarity in higher-derivative quantum gravity". In: *Phys. Rev. D* 33 (10 1986), pp. 2756–2779.

[349] J. F. Donoghue and G. Menezes. "On quadratic gravity". In: *Nuovo Cim. C* 45.2 (2022), p. 26. arXiv: 2112.01974 [hep-th].

[350] M. Milgrom. "A modification of the newtonian dynamics as a possible alternative to the hidden mass hypothesis". In: *The Astrophysical Journal* 270 (1983), pp. 365–370.

[351] M. Milgrom. "MOND–particularly as modified inertia". In: *Acta Phys. Polon. B* 42 (2011). Ed. by M. Biesiada, I. Bednarek, and J. Gluza, pp. 2175–2184. arXiv: 1111.1611 [astro-ph.CO].

[352] B. Famaey and S. McGaugh. "Modified Newtonian Dynamics (MOND): Observational Phenomenology and Relativistic Extensions". In: *Living Rev. Rel.* 15 (2012), p. 10. arXiv: 1112.3960 [astro-ph.CO].

[353] A. O. F. de Almeida, L. Amendola, and V. Niro. "Galaxy rotation curves in modified gravity models". In: *JCAP* 08 (2018), p. 012. arXiv: 1805.11067 [astro-ph.GA].

[354] M. M. Brouwer et al. "The weak lensing radial acceleration relation: Constraining modified gravity and cold dark matter theories with KiDS-1000". In: *Astron. Astrophys.* 650 (2021), A113. arXiv: 2106.11677 [astro-ph.GA].

[355] K. Sanders. "Static Symmetric Solutions of the Semi-Classical Einstein–Klein–Gordon System". In: *Annales Henri Poincare* 23.4 (2022), pp. 1321–1358. arXiv: 2007.14311 [math-ph].

[356] L. Blanchet and J. Novak. "Testing MOND in the Solar System". In: *46th Rencontres de Moriond on Gravitational Waves and Experimental Gravity*. May 2011, pp. 295–302. arXiv: 1105.5815 [astro-ph.CO].

[357] M. Reuter and J.-M. Schwindt. "A Minimal length from the cutoff modes in asymptotically safe quantum gravity". In: *JHEP* 01 (2006), p. 070. arXiv: hep-th/0511021.

[358] M. Reuter and J.-M. Schwindt. "Scale-dependent metric and causal structures in Quantum Einstein Gravity". In: *JHEP* 01 (2007), p. 049. arXiv: hep-th/0611294.

[359] P. S. Wesson. *Space - time - matter: Modern Kaluza-Klein theory*. World Scientific, 1999.

[360] P. S. Wesson. "The cosmological 'constant' and quantization in five dimensions". In: *Phys. Lett. B* 706 (2011), pp. 1–5.

[361] P. S. Wesson. "The status of modern five-dimensional gravity (A short review: Why physics needs the fifth dimension)". In: *Int. J. Mod. Phys. D* 24.01 (2014), p. 1530001. arXiv: 1412.6136 [gr-qc].

[362] G. S. Hall. *Symmetries and Curvature Structure in General Relativity*. World Scientific, 2004.

[363] K. Yano. *The Theory of Lie Derivatives and Its Applications,* Amsterdam: North-Holland Pub, 1957.

[364] B. J. Carr and A. A. Coley. "Selfsimilarity in general relativity". In: *Class. Quant. Grav.* 16 (1999), R31–R71. arXiv: gr-qc/9806048.

[365] E. Manrique, M. Reuter, and F. Saueressig. "Matter Induced Bimetric Actions for Gravity". In: *Annals Phys.* 326 (2011), pp. 440–462. arXiv: 1003.5129 [hep-th].

[366] E. Manrique, M. Reuter, and F. Saueressig. "Bimetric Renormalization Group Flows in Quantum Einstein Gravity". In: *Annals Phys.* 326 (2011), pp. 463–485. arXiv: 1006.0099 [hep-th].

[367] S. P. Kumar and V. Vaganov. "Probing crunching AdS cosmologies". In: *JHEP* 02 (2016), p. 026. arXiv: 1510.03281 [hep-th].

[368] A. Karch and L. Randall. "Geometries with mismatched branes". In: *JHEP* 09 (2020), p. 166. arXiv: 2006.10061 [hep-th].

[369] J. B. Griffiths and J. Podolsky. *Exact Space-Times in Einstein's General Relativity,* Cambridge: Cambridge University Press, 2012.

[370] In: ().

[371] M. Becker and M. Reuter. "Background Independent Field Quantization with Sequences of Gravity-Coupled Approximants". In: *Phys. Rev. D* 102.12 (2020), p. 125001. arXiv: 2008.09430 [gr-qc].

[372] S. B. Giddings. "The Boundary S matrix and the AdS to CFT dictionary". In: *Phys. Rev. Lett.* 83 (1999), pp. 2707–2710. arXiv: hep-th/9903048.

[373] J. de Boer, E. P. Verlinde, and H. L. Verlinde. "On the holographic renormalization group". In: *JHEP* 08 (2000), p. 003. arXiv: hep-th/9912012.

[374] I. Heemskerk and J. Polchinski. "Holographic and Wilsonian Renormalization Groups". In: *JHEP* 06 (2011), p. 031. arXiv: 1010.1264 [hep-th].

[375] B. Sathiapalan and H. Sonoda. "A Holographic form for Wilson's RG". In: *Nucl. Phys. B* 924 (2017), pp. 603–642. arXiv: 1706.03371 [hep-th].

[376] F. Gao and M. Yamada. "Determining holographic wave functions from Wilsonian renormalization group". In: (Feb. 2022). arXiv: 2202.13699 [hep-th].

[377] A. Nink and M. Reuter. "The unitary conformal field theory behind 2D Asymptotic Safety". In: *JHEP* 02 (2016), p. 167. arXiv: 1512.06805 [hep-th].

[378] K. Farnsworth, K. Hinterbichler, and O. Hulik. "Scale versus conformal invariance at the IR fixed point of quantum gravity". In: *Phys. Rev. D* 105.6 (2022), p. 066026. arXiv: 2110.10160 [hep-th].

[379] E. Manrique and M. Reuter. "Bare Action and Regularized Functional Integral of Asymptotically Safe Quantum Gravity". In: *Phys. Rev. D* 79 (2009), p. 025008. arXiv: 0811.3888 [hep-th].

[380] A. Strominger. "The dS / CFT correspondence". In: *JHEP* 10 (2001), p. 034. arXiv: hep-th/0106113.

[381] J. D. Brown and M. Henneaux. "Central Charges in the Canonical Realization of Asymptotic Symmetries: An Example from Three-Dimensional Gravity". In: *Commun. Math. Phys.* 104 (1986), pp. 207–226.

[382] S. de Haro, S. N. Solodukhin, and K. Skenderis. "Holographic reconstruction of space-time and renormalization in the AdS / CFT correspondence". In: *Commun. Math. Phys.* 217 (2001), pp. 595–622. arXiv: hep-th/0002230.

[383] U. Ellwanger and C. Wetterich. "Evolution equations for the quark - meson transition". In: *Nucl. Phys. B* 423 (1994), pp. 137–170. arXiv: hep-ph/9402221.

[384] E. T. Akhmedov. "A Remark on the AdS / CFT correspondence and the renormalization group flow". In: *Phys. Lett. B* 442 (1998), pp. 152–158. arXiv: hep-th/9806217.

[385] M. Bianchi, D. Z. Freedman, and K. Skenderis. "How to go with an RG flow". In: *JHEP* 08 (2001), p. 041. arXiv: hep-th/0105276.

[386] F. W. Olver et al. *NIST Handbook of Mathematical Functions*. 1st. USA: Cambridge University Press, 2010.

[387] J. S. Schwinger. "On gauge invariance and vacuum polarization". In: *Phys. Rev.* 82 (1951). Ed. by K. A. Milton, pp. 664–679.

[388] W. Dittrich and M. Reuter. *Effective Lagrangians in Quantum Electrodynamics*. Berlin: Springer, 1985.

[389] G. Gubitosi et al. "Consistent early and late time cosmology from the RG flow of gravity". In: *JCAP* 12 (2018), p. 004. arXiv: 1806.10147 [hep-th].

[390] G. Gubitosi, C. Ripken, and F. Saueressig. "Scales and hierachies in asymptotically safe quantum gravity: a review". In: *Found. Phys.* 49.9 (2019), pp. 972–990. arXiv: 1901.01731 [gr-qc].

[391] G. Landi. *An Introduction to Noncommutative Spaces and their Geometry*. Springer, 1994.

[392] T. Padmanabhan. "The Physical Principle that determines the Value of the Cosmological Constant". In: (Oct. 2012). arXiv: 1210.4174 [hep-th].

[393] T. Padmanabhan and H. Padmanabhan. "Cosmological Constant from the Emergent Gravity Perspective". In: *Int. J. Mod. Phys. D* 23.6 (2014), p. 1430011. arXiv: 1404.2284 [gr-qc].

[394] J. Julve and M. Tonin. "Quantum Gravity with Higher Derivative Terms". In: *Nuovo Cim. B* 46 (1978), pp. 137–152.

[395] L. Alvarez-Gaume et al. "Aspects of Quadratic Gravity". In: *Fortsch. Phys.* 64.2-3 (2016), pp. 176–189. arXiv: 1505.07657 [hep-th].

[396] B. Knorr and C. Ripken. "Scattering amplitudes in affine gravity". In: *Phys. Rev. D* 103.10 (2021), p. 105019. arXiv: 2012.05144 [hep-th].

[397] D. Brizuela, J. M. Martin-Garcia, and G. A. Mena Marugan. "xPert: Computer algebra for metric perturbation theory". In: *Gen. Rel. Grav.* 41 (2009), pp. 2415–2431. arXiv: 0807.0824 [gr-qc].

[398] J. M. Martín-García. "xPerm: fast index canonicalization for tensor computer algebra". In: *CoRR* abs/0803.0862 (2008). arXiv: 0803.0862.

[399] T. Nutma. "xTras : A field-theory inspired xAct package for mathematica". In: *Comput. Phys. Commun.* 185 (2014), pp. 1719–1738. arXiv: 1308.3493 [cs.SC].

[400] *xAct: Efficient tensor computer algebra for Mathematica.* http://xact.es/index.html.

[401] T. Garidi. "What is mass in de Sitterian physics?" In: (Sept. 2003). arXiv: hep-th/0309104.

[402] H. Pejhan et al. "Massless spin-2 field in de Sitter space". In: *Phys. Rev. D* 98.4 (2018), p. 045007. arXiv: 1803.02074 [gr-qc].

[403] E. Joung, J. Mourad, and R. Parentani. "Group theoretical approach to quantum fields in de Sitter space. I. The Principle series". In: *JHEP* 08 (2006), p. 082. arXiv: hep-th/0606119.

[404] E. Joung, J. Mourad, and R. Parentani. "Group theoretical approach to quantum fields in de Sitter space. II. The complementary and discrete series". In: *JHEP* 09 (2007), p. 030. arXiv: 0707.2907 [hep-th].

[405] G. Sengör and C. Skordis. "Unitarity at the Late time Boundary of de Sitter". In: *JHEP* 06 (2020), p. 041. arXiv: 1912.09885 [hep-th].

[406] J. P. Gazeau and M. Lachieze Rey. "Quantum field theory in de Sitter space: A Survey of recent approaches". In: *PoS* IC2006 (2006). Ed. by A. A. Bytsenko et al., p. 007. arXiv: hep-th/0610296.

[407] B. S. DeWitt. "Quantum Theory of Gravity. III. Applications of the Covariant Theory". In: *Phys. Rev.* 162 (5 1967), pp. 1239–1256.

[408] T. Draper et al. "Graviton-Mediated Scattering Amplitudes from the Quantum Effective Action". In: *JHEP* 11 (2020), p. 136. arXiv: 2007.04396 [hep-th].

[409] M. B. Fröb and E. Verdaguer. "Quantum corrections to the gravitational potentials of a point source due to conformal fields in de Sitter". In: *JCAP* 03 (2016), p. 015. arXiv: 1601.03561 [hep-th].

[410] M. B. Fröb and E. Verdaguer. "Quantum corrections for spinning particles in de Sitter". In: *JCAP* 04 (2017), p. 022. arXiv: 1701.06576 [hep-th].

[411] D. Glavan et al. "One-loop Graviton Corrections to Conformal Scalars on a de Sitter Background". In: *Phys. Rev. D* 103.10 (2021), p. 105022. arXiv: 2007.10395 [gr-qc].

[412] I. Agullo, W. Nelson, and A. Ashtekar. "Preferred instantaneous vacuum for linear scalar fields in cosmological space-times". In: *Phys. Rev. D* 91 (2015), p. 064051. arXiv: 1412.3524 [gr-qc].

[413] C. Moreno-Pulido and J. S. Peracaula. "Renormalizing the vacuum energy in cosmological spacetime: implications for the cosmological constant problem". In: (Jan. 2022). arXiv: 2201.05827 [gr-qc].

[414] W. Junker and E. Schrohe. "Adiabatic vacuum states on general space-time manifolds: Definition, construction, and physical properties". In: *Annales Henri Poincare* 3 (2002), pp. 1113–1182. arXiv: math-ph/0109010.

[415] C. Lueders and J. E. Roberts. "Local quasiequivalence and adiabatic vacuum states". In: *Commun. Math. Phys.* 134 (1990), pp. 29–63.

[416] H. Olbermann. "States of low energy on Robertson-Walker spacetimes". In: *Class. Quant. Grav.* 24 (2007), pp. 5011–5030. arXiv: 0704.2986 [gr-qc].

[417] S. A. Fulling. "Remarks on positive frequency and hamiltonians in expanding universes". In: *General Relativity and Gravitation* 10 (1979), pp. 807–824.

[418] S. A. Fulling and L. Parker. "Renormalization in the theory of a quantized scalar field interacting with a robertson-walker spacetime". In: *Annals Phys.* 87 (1974), pp. 176–204.

[419] S. A. Fulling. *Aspects of Quantum Field Theory in Curved Space-time.* Vol. 17. 1989.

[420] L. Parker. "Particle creation in expanding universes". In: *Phys. Rev. Lett.* 21 (1968), pp. 562–564.

[421] L. Parker. "Quantized fields and particle creation in expanding universes. 1." In: *Phys. Rev.* 183 (1969), pp. 1057–1068.

[422] L. Parker. "Quantized fields and particle creation in expanding universes. 2." In: *Phys. Rev. D* 3 (1971). [Erratum: Phys.Rev.D 3, 2546–2546 (1971)], pp. 346–356.

[423] L. Parker and S. A. Fulling. "Adiabatic regularization of the energy momentum tensor of a quantized field in homogeneous spaces". In: *Phys. Rev. D* 9 (1974), pp. 341–354.

[424] L. E. Parker and D. Toms. *Quantum Field Theory in Curved Spacetime: Quantized Field and Gravity.* Cambridge Monographs on Mathematical Physics. Cambridge University Press, Aug. 2009.

[425] N. D. Birrell. "The Application of Adiabatic Regularization to Calculations of Cosmological Interest". In: *Proceedings of the Royal Society of London Series A* 361.1707 (June 1978), pp. 513–526.

[426] T. S. Bunch. "Adiabatic regularisation for scalar fields with arbitrary coupling to the scalar curvature". In: *Journal of Physics A Mathematical General* 13 (Apr. 1980), pp. 1297–1310.

[427] T. S. Bunch, S. M. Christensen, and S. A. Fulling. "Massive Quantum Field Theory in Two-Dimensional Robertson-Walker Space-Time". In: *Phys. Rev. D* 18 (1978), pp. 4435–4459.

[428] J. Haro and E. Elizalde. "On particle creation in the flat FRW chart of de Sitter spacetime". In: *J. Phys. A* 41 (2008), p. 372003.

[429] S. Winitzki. "Cosmological particle production and the precision of the WKB approximation". In: *Phys. Rev. D* 72 (2005), p. 104011. arXiv: gr-qc/0510001.

[430] Y. Zel'Dovich and A. Starobinsky. "Particle Production and Vacuum Polarization in an Anisotropic Gravitational Field". In: *Soviet Journal of Experimental and Theoretical Physics* 34 (Jan. 1972), p. 1159.

[431] Y. B. Zel'dovich and A. A. Starobinsky. "Rate of particle production in gravitational fields". In: *JETP Lett.* 26.5 (1977), p. 252.

[432] J. de Boer and S. N. Solodukhin. "A Holographic reduction of Minkowski spacetime". In: *Nucl. Phys. B* 665 (2003), pp. 545–593. arXiv: hep-th/0303006.

[433] D. Colosi. "General boundary quantum field theory in de Sitter spacetime". In: (Oct. 2010). arXiv: 1010.1209 [hep-th].

[434] C. Cheung, A. de la Fuente, and R. Sundrum. "4D scattering amplitudes and asymptotic symmetries from 2D CFT". In: *JHEP* 01 (2017), p. 112. arXiv: 1609.00732 [hep-th].

[435] I. Park. "Foliation-Based Approach to Quantum Gravity and Applications to Astrophysics". In: *Universe* 5.3 (2019), p. 71. arXiv: 1902.03332 [hep-th].

[436] A. A. Saharian, T. A. Petrosyan, and V. S. Torosyan. "Mean field squared and energy–momentum tensor for the hyperbolic vacuum in dS spacetime". In: *Annals Phys.* 437 (2022), p. 168728. arXiv: 2110.06662 [hep-th].

[437] F. W. J. Olver et al. *The NIST Handbook of Mathematical Functions*. Cambridge Univ. Press, 2010.

[438] T. S. Bunch and P. C. W. Davies. "Quantum field theory in de Sitter space - Renormalization by point-splitting". In: *Proceedings of the Royal Society of London Series A* 360.1700 (Mar. 1978), pp. 117–134.

[439] H. Goodhew. "Rational Wavefunctions in de Sitter Spacetime". In: (Oct. 2022). arXiv: 2210.09977 [hep-th].

[440] G. Frobenius. "Ueber die Integration der linearen Differentialgleichungen durch Reihen." In: *Journal für die reine und angewandte Mathematik* 76 (1873), pp. 214–235.

[441] A. R. Miller. "The Mellin transform of a product of two hypergeometric functions". In: *Journal of Computational and Applied Mathematics* 137.1 (2001), pp. 77–82.

[442] T. Padmanabhan. "Topological interpretation of the horizon temperature". In: *Mod. Phys. Lett. A* 18 (2003), pp. 2903–2912. arXiv: hep-th/0302068.

[443] P. D. Mannheim and J. G. O'Brien. "Fitting galactic rotation curves with conformal gravity and a global quadratic potential". In: *Phys. Rev. D* 85 (2012), p. 124020. arXiv: 1011.3495 [astro-ph.CO].

[444] S. S. McGaugh, F. Lelli, and J. M. Schombert. "Radial Acceleration Relation in Rotationally Supported Galaxies". In: *Physical Review Letters* 117.20, 201101 (Nov. 2016), p. 201101. arXiv: 1609.05917 [astro-ph.GA].

[445] J. G. O'Brien, T. L. Chiarelli, and P. D. Mannheim. "Universal properties of galactic rotation curves and a first principles derivation of the Tully–Fisher relation". In: *Physics Letters B* 782 (2018), pp. 433–439.

[446] P. D. Mannheim and J. W. Moffat. "External field effect in gravity". In: *Int. J. Mod. Phys. D* 30.14 (2021), p. 2142009. arXiv: 2103.13972 [gr-qc].

[447] P. D. Mannheim. "Alternatives to dark matter and dark energy". In: *Progress in Particle and Nuclear Physics* 56.2 (2006), pp. 340–445.

[448] A. Bonanno and M. Reuter. "Renormalization group improved black hole spacetimes". In: *Phys. Rev. D* 62 (2000), p. 043008. arXiv: hep-th/0002196.

[449] J. D. Barrow and D. J. Shaw. "The Value of the Cosmological Constant". In: *Gen. Rel. Grav.* 43 (2011), pp. 2555–2560. arXiv: 1105.3105 [gr-qc].

[450] J. Martin. "Everything You Always Wanted To Know About The Cosmological Constant Problem (But Were Afraid To Ask)". In: *Comptes Rendus Physique* 13 (2012), pp. 566–665. arXiv: 1205.3365 [astro-ph.CO].

[451] M. Charles W. et al. *Gravitation*. First Edition. Physics Series. W. H. Freeman, 1973.

[452] A. Einstein. *Über die spezielle und die allgemeine Relativitätstheorie*. Springer Berlin Heidelberg, 2008.

[453] H. Westman and S. Sonego. "Coordinates, observables and symmetry in relativity". In: *Annals Phys.* 324 (2009), pp. 1585–1611. arXiv: 0711.2651 [gr-qc].

[454] H. Leutwyler. "Phonons as goldstone bosons". In: *Helv. Phys. Acta* 70 (1997), pp. 275–286. arXiv: hep-ph/9609466.

[455] S. Dubovsky et al. "Effective field theory for hydrodynamics: thermodynamics, and the derivative expansion". In: *Phys. Rev. D* 85 (2012), p. 085029. arXiv: 1107.0731 [hep-th].

[456] S. Endlich et al. "The Quantum mechanics of perfect fluids". In: *JHEP* 04 (2011), p. 102. arXiv: 1011.6396 [hep-th].

[457] C. G. Torre. "Gravitational observables and local symmetries". In: *Phys. Rev. D* 48 (1993), R2373–R2376. arXiv: gr-qc/9306030.

[458] C. G. Torre. "The Problems of time and observables: Some recent mathematical results". In: (Apr. 1994). arXiv: gr-qc/9404029.

[459] C. Rovelli. "Quantum reference systems". In: *Class. Quant. Grav.* 8 (1991), pp. 317–332.

[460] C. Rovelli. "Partial observables". In: *Phys. Rev. D* 65 (2002), p. 124013. arXiv: gr-qc/0110035.

[461] B. Dittrich. "Partial and complete observables for Hamiltonian constrained systems". In: *Gen. Rel. Grav.* 39 (2007), pp. 1891–1927. arXiv: gr-qc/0411013.

[462] B. Dittrich. "Partial and complete observables for canonical general relativity". In: *Class. Quant. Grav.* 23 (2006), pp. 6155–6184. arXiv: gr-qc/0507106.

[463] B. Dittrich et al. "Chaos, Dirac observables and constraint quantization". In: (Aug. 2015). arXiv: 1508.01947 [gr-qc].

[464] W. Donnelly and S. B. Giddings. "Observables, gravitational dressing, and obstructions to locality and subsystems". In: *Phys. Rev. D* 94.10 (2016), p. 104038. arXiv: 1607.01025 [hep-th].

[465] P. A. Hoehn, A. R. H. Smith, and M. P. E. Lock. "Equivalence of Approaches to Relational Quantum Dynamics in Relativistic Settings". In: *Front. in Phys.* 9 (2021), p. 181. arXiv: 2007.00580 [gr-qc].

[466] S. Gielen. "Group field theory and its cosmology in a matter reference frame". In: *Universe* 4.10 (2018), p. 103. arXiv: 1808.10469 [gr-qc].

[467] F. de Felice and D. Bini. *Classical Measurements in Curved Space-Times*. Cambridge Monographs on Mathematical Physics. Cambridge University Press, 2010.

[468] A. Komar. "Construction of a Complete Set of Independent Observables in the General Theory of Relativity". In: *Phys. Rev.* 111.4 (1958), p. 1182.

[469] P. G. Bergmann and A. B. Komar. "Poisson brackets between locally defined observables in general relativity". In: *Phys. Rev. Lett.* 4 (1960), pp. 432–433.

[470] P. G. Bergmann. "Observables in General Relativity". In: *Rev. Mod. Phys.* 33 (1961), pp. 510–514.

[471] K. V. Kuchar and C. G. Torre. "Gaussian reference fluid and interpretation of quantum geometrodynamics". In: *Phys. Rev. D* 43 (1991), pp. 419–441.

[472] J. D. Brown and K. V. Kuchar. "Dust as a standard of space and time in canonical quantum gravity". In: *Phys. Rev. D* 51 (1995), pp. 5600–5629. arXiv: gr-qc/9409001.

[473] I. Khavkine. "Local and gauge invariant observables in gravity". In: *Class. Quant. Grav.* 32.18 (2015), p. 185019. arXiv: 1503.03754 [gr-qc].

[474] R. Brunetti, K. Fredenhagen, and K. Rejzner. "Quantum gravity from the point of view of locally covariant quantum field theory". In: *Commun. Math. Phys.* 345.3 (2016), pp. 741–779. arXiv: 1306.1058 [math-ph].

[475] R. Brunetti et al. "Cosmological perturbation theory and quantum gravity". In: *JHEP* 08 (2016), p. 032. arXiv: 1605.02573 [gr-qc].

[476] M. B. Fröb and W. C. C. Lima. "Propagators for gauge-invariant observables in cosmology". In: *Class. Quant. Grav.* 35.9 (2018), p. 095010. arXiv: 1711.08470 [gr-qc].

[477] J. Tambornino. "Relational Observables in Gravity: a Review". In: *SIGMA* 8 (2012), p. 017. arXiv: 1109.0740 [gr-qc].

[478] C. Pagani and H. Sonoda. "Operator product expansion coefficients in the exact renormalization group formalism". In: *Phys. Rev. D* 101.10 (2020), p. 105007. arXiv: 2001.07015 [hep-th].

[479] W. Souma. "Nontrivial ultraviolet fixed point in quantum gravity". In: *Prog. Theor. Phys.* 102 (1999), pp. 181–195. arXiv: hep-th/9907027.

[480] W. Houthoff, A. Kurov, and F. Saueressig. "On the scaling of composite operators in asymptotic safety". In: *JHEP* 04 (2020), p. 099. arXiv: 2002.00256 [hep-th].

[481] A. Kurov and F. Saueressig. "On characterizing the Quantum Geometry underlying Asymptotic Safety". In: *Front. in Phys.* 8 (2020), p. 187. arXiv: 2003.07454 [hep-th].

[482] L. Amendola and S. Tsujikawa. *Dark Energy: Theory and Observations*. Cambridge University Press, Jan. 2015.

[483] C. Omero and R. Percacci. "Generalized nonlinear sigma models in curved space and spontaneous compactification". In: *Nucl. Phys. B* 165 (1980), pp. 351–364.

[484] M. Gell-Mann and B. Zwiebach. "Dimensional Reduction of Space-time Induced by Nonlinear Scalar Dynamics and Noncompact Extra Dimensions". In: *Nucl. Phys. B* 260 (1985), pp. 569–592.

[485] M. Gell-Mann and B. Zwiebach. "Space-time compactification due to scalars". In: *Phys. Lett. B* 141 (1984), pp. 333–336.

[486] K. Hinterbichler. "Theoretical Aspects of Massive Gravity". In: *Rev. Mod. Phys.* 84 (2012), pp. 671–710. arXiv: 1105.3735 [hep-th].

[487] E. C. G. Stueckelberg. "Theory of the radiation of photons of small arbitrary mass". In: *Helv. Phys. Acta* 30 (1957), pp. 209–215.

[488] N. Arkani-Hamed, H. Georgi, and M. D. Schwartz. "Effective field theory for massive gravitons and gravity in theory space". In: *Annals Phys.* 305 (2003), pp. 96–118. arXiv: hep-th/0210184.

[489] D. G. Boulware and S. Deser. "Can gravitation have a finite range?" In: *Phys. Rev. D* 6 (1972), pp. 3368–3382.

[490] P. Creminelli et al. "Ghosts in massive gravity". In: *JHEP* 09 (2005), p. 003. arXiv: hep-th/0505147.

[491] C. de Rham, G. Gabadadze, and A. J. Tolley. "Resummation of Massive Gravity". In: *Phys. Rev. Lett.* 106 (2011), p. 231101. arXiv: 1011.1232 [hep-th].

[492] C. de Rham, G. Gabadadze, and A. J. Tolley. "Ghost free Massive Gravity in the Stückelberg language". In: *Phys. Lett. B* 711 (2012), pp. 190–195. arXiv: 1107.3820 [hep-th].

[493] S. F. Hassan and R. A. Rosen. "Resolving the Ghost Problem in non-Linear Massive Gravity". In: *Phys. Rev. Lett.* 108 (2012), p. 041101. arXiv: 1106.3344 [hep-th].

[494] S. F. Hassan and R. A. Rosen. "On Non-Linear Actions for Massive Gravity". In: *JHEP* 07 (2011), p. 009. arXiv: 1103.6055 [hep-th].

[495] S. F. Hassan and R. A. Rosen. "Confirmation of the Secondary Constraint and Absence of Ghost in Massive Gravity and Bimetric Gravity". In: *JHEP* 04 (2012), p. 123. arXiv: 1111.2070 [hep-th].

[496] C. de Rham, A. J. Tolley, and S.-Y. Zhou. "The Λ_2 limit of massive gravity". In: *JHEP* 04 (2016), p. 188. arXiv: 1602.03721 [hep-th].

[497] V. A. Rubakov. "Lorentz-violating graviton masses: Getting around ghosts, low strong coupling scale and VDVZ discontinuity". In: (July 2004). arXiv: hep-th/0407104.

[498] S. L. Dubovsky. "Phases of massive gravity". In: *JHEP* 10 (2004), p. 076. arXiv: hep-th/0409124.

[499] D. Comelli, F. Nesti, and L. Pilo. "Massive gravity: a General Analysis". In: *JHEP* 07 (2013), p. 161. arXiv: 1305.0236 [hep-th].

[500] D. Comelli, F. Nesti, and L. Pilo. "Weak Massive Gravity". In: *Phys. Rev. D* 87.12 (2013), p. 124021. arXiv: 1302.4447 [hep-th].

[501] P. Horava. "Quantum Gravity at a Lifshitz Point". In: *Phys. Rev. D* 79 (2009), p. 084008. arXiv: 0901.3775 [hep-th].

[502] S. Endlich, A. Nicolis, and J. Wang. "Solid Inflation". In: *JCAP* 10 (2013), p. 011. arXiv: 1210.0569 [hep-th].

[503] D. Comelli, F. Nesti, and L. Pilo. "Cosmology in General Massive Gravity Theories". In: *JCAP* 05 (2014), p. 036. arXiv: 1307.8329 [hep-th].

[504] D. Comelli, F. Nesti, and L. Pilo. "Nonderivative Modified Gravity: a Classification". In: *JCAP* 11 (2014), p. 018. arXiv: 1407.4991 [hep-th].

[505] G. Ballesteros, D. Comelli, and L. Pilo. "Massive and modified gravity as self-gravitating media". In: *Phys. Rev. D* 94.12 (2016), p. 124023. arXiv: 1603.02956 [hep-th].

[506] M. Celoria, D. Comelli, and L. Pilo. "Fluids, Superfluids and Supersolids: Dynamics and Cosmology of Self Gravitating Media". In: *JCAP* 09 (2017), p. 036. arXiv: 1704.00322 [gr-qc].

[507] M. Celoria, D. Comelli, and L. Pilo. "Self-gravitating Λ-media". In: *JCAP* 01 (2019), p. 057. arXiv: 1712.04827 [gr-qc].

[508] M. Celoria et al. "Adiabatic Media Inflation". In: *JCAP* 12 (2019), p. 018. arXiv: 1907.11784 [gr-qc].

[509] J. Eells and L. Lemaire. "A Report on Harmonic Maps". In: *Bulletin of the London Mathematical Society* 10.1 (1978), pp. 1–68. eprint: https://londmathsoc.onlinelibrary.wiley.com/doi/pdf/10.1112/blms/10.1.1.

[510] E. Mazet. "La formule de la variation seconde de l'énergie au voisinage d'une application harmonique". In: *Journal of Differential Geometry* 8.2 (1973), pp. 279 –296.

[511] R. T. Smith. "The Second Variation Formula for Harmonic Mappings". In: *Proceedings of the American Mathematical Society* 47.1 (1975), pp. 229–236.

[512] B. Chow and P. Lu. "Harmonic maps near the identity of Sn". In: *Differential Geometry and its Applications* 42 (2015), pp. 31–36.

[513] A. M. Polyakov and A. A. Belavin. "Metastable States of Two-Dimensional Isotropic Ferromagnets". In: *JETP Lett.* 22 (1975), pp. 245–248.

[514] C. de Rham, A. J. Tolley, and S.-Y. Zhou. "Non-compact nonlinear sigma models". In: *Phys. Lett. B* 760 (2016), pp. 579–583. arXiv: 1512.06838 [hep-th].

[515] J. M. Cline et al. "Update on scalar singlet dark matter". In: *Phys. Rev. D* 88 (2013). [Erratum: Phys.Rev.D 92, 039906 (2015)], p. 055025. arXiv: 1306.4710 [hep-ph].

[516] R. D. Peccei and H. R. Quinn. "CP Conservation in the Presence of Instantons". In: *Phys. Rev. Lett.* 38 (1977), pp. 1440–1443.

[517] Z. Péli. "Derivative expansion for computing critical exponents of $O(N)$ symmetric models at next-to-next-to-leading order". In: *Phys. Rev. E* 103.3 (2021), p. 032135. arXiv: 2010.04020 [hep-th].

[518] J. Brunekreef and R. Loll. "Curvature profiles for quantum gravity". In: *Phys. Rev. D* 103.2 (2021), p. 026019. arXiv: 2011.10168 [gr-qc].

[519] J. Ambjørn et al. "Scalar fields in causal dynamical triangulations". In: *Class. Quant. Grav.* 38.19 (2021), p. 195030. arXiv: 2105.10086 [gr-qc].

[520] G. W. Gibbons and S. W. Hawking. "Cosmological event horizons, thermodynamics, and particle creation". In: *Phys. Rev. D* 15 (10 1977), pp. 2738–2751.

[521] S. Weinberg. *Gravitation and Cosmology: Principles and Applications of the General Theory of Relativity*. New York: John Wiley and Sons, 1972.

[522] A. Zee. *Einstein Gravity in a Nutshell*. New Jersey: Princeton University Press, May 2013.

[523] E. A. Coddington and N. Levinson. *Theory of ordinary differential equations [by] Earl A. Coddington [and] Norman Levinson*. English. McGraw-Hill New York, 1955, 429 p.

[524] K. Tomantschger. "Series solutions of coupled differential equations with one regular singular point". In: *Journal of Computational and Applied Mathematics* 140.1 (2002). Int. Congress on Computational and Applied Mathematics 2000, pp. 773–783.

[525] J. Mandelkern. "A matrix formulation of Frobenius power series solutions using products of 4X4 matrices". In: *Electronic Journal of Differential Equations* 2015 (Aug. 2015).

[526] E. Kausel and H. Gravenkamp. "On the numerical solution of matrix Bessel equations". In: *ZAMM Journal of applied mathematics and mechanics: Zeitschrift für angewandte Mathematik und Mechanik* 99 (June 2019), e201800288.

[527] C. F. Steinwachs and A. Y. Kamenshchik. "One-loop divergences for gravity non-minimally coupled to a multiplet of scalar fields: calculation in the Jordan frame. I. The main results". In: *Phys. Rev. D* 84 (2011), p. 024026. arXiv: 1101. 5047 [gr-qc].